J.F. MANWELL | J.G. MCGOWAN | A.L. ROGERS

WIND ENERGY
EXPLAINED

THEORY, DESIGN AND APPLICATION

SECOND EDITION

⊕WILEY

WIND ENERGY EXPLAINED

WIND ENERGY EXPLAINED

Theory, Design and Application
Second Edition

J. F. Manwell and J. G. McGowan

*Department of Mechanical and Industrial Engineering,
University of Massachusetts, USA*

A. L. Rogers

DNV – Global Energy Concepts, Washington, USA

Contents

About the Authors

James Manwell is a professor of Mechanical Engineering at the University of Massachusetts and the Director of the Wind Energy Center there. He holds an M.S. in Electrical and Computer Engineering and a Ph.D. in Mechanical Engineering. He has been involved with a wide range of wind energy research areas since the mid 1970's. These range from wind turbine dynamics to wind hybrid power systems. His most recent research has focused on the assessment of external conditions related to the design of offshore wind turbines. He has participated in activities of the International Energy Agency, the International Electrotechnical Commission and the International Science Panel on Renewable Energies. He lives in Conway, Massachusetts.

Jon McGowan is a professor of Mechanical Engineering at the University of Massachusetts and the co-Director of the Wind Energy Center there. He holds an M.S. and a Ph.D. in Mechanical Engineering. During his forty plus years at the University he has developed and taught a number of fundamental undergraduate/ graduate engineering courses in renewable energy and energy conversion. His research and graduate student supervision at UMass has produced approximately 200 technical papers in a wide range of energy conversion applications. His recent research interests in wind engineering have been concentrated in the areas of wind system siting, hybrid systems modeling, economics, and offshore wind engineering. Professor McGowan is a Fellow of the American Society of Mechanical Engineers (ASME) and editor of *Wind Engineering* journal. He lives in Northfield, Massachusetts.

Anthony Rogers holds both and M.S. and Ph.D. in Mechanical Engineering from the University of Massachusetts and was formerly a senior research engineer in the Renewable Energy Research Laboratory (now the Wind Energy Center) there. He is presently a senior engineer at DNV Global Energy Concepts. He has had a long career in the wind energy field, and has been involved with a wide range of topics. These have included wind turbine monitoring and control and the application of remote sensing devices. He lives in Amherst, Massachusetts.

Preface

The technology of extracting energy from the wind has evolved dramatically over the last few decades, and there have, up until now, been relatively few attempts to describe that technology in a single textbook. The lack of such a text, together with a perceived need, provided the impetus for writing this book.

The material in this text has evolved from course notes from Wind Energy Engineering, a course which has been taught at the University of Massachusetts since the mid-1970s. These notes were later substantially revised and expanded with the support of the US Department of Energy's National Renewable Energy Laboratory (NREL). In this, the second edition of this textbook, we have again added new material to reflect the rapid worldwide expansion of wind engineering in the 21st century.

This book provides a description of the topics which are fundamental to understanding the conversion of wind energy to electricity and its eventual use by society. These topics span a wide range, from meteorology through many fields of engineering to economics and environmental concerns. The book begins with an introduction which provides an overview of the technology, and explains how it came to take the form it has today. The next chapter describes the wind resource and how it relates to energy production. Chapter 3 discusses aerodynamic principles and explains how the wind's energy will cause a wind turbine's rotor to turn. Chapter 4 delves into the dynamic and mechanical aspects of the turbine in more detail, and considers the relation of the rotor to the rest of the machine. Chapter 5 provides a summary of the electrical aspects of wind energy conversion, particularly regarding the actual generation and conversion of the electricity. Next, Chapter 6 presents a summary of wind turbine materials and components. Chapter 7 discusses the design of wind turbines and the testing of wind turbines. Chapter 8 examines wind turbine and wind system control. Chapter 9 discusses siting of wind turbines and their integration into electrical systems both large and small. Next, Chapter 10 gives a detailed summary of wind turbine applications. Chapter 11 concerns the economics of wind energy. It describes economic analysis methods and shows how wind energy can be compared with conventional forms of generation. Chapter 12 describes the environmental aspects of wind energy generation. Finally, a new appendix (C) has been added. This appendix provides an overview of some of the data analysis techniques that are commonly used in wind turbine design and use.

This book is intended primarily as a textbook for engineering students and for professionals in related fields who are just getting into wind energy. It is also intended to be used by anyone with a good background in math and physics who wants to gain familiarity with the subject. It should be useful for those interested in wind turbine design *per se*. For others, it should provide

enough understanding of the underlying principles of wind turbine operation and design to appreciate more fully those aspects in which they have a particular interest. These areas include turbine siting, grid integration, environmental issues, economics, and public policy.

The study of wind energy spans such a wide range of fields. Since it is likely that many readers will not have a background in all of them, most of the chapters include some introductory material. Where appropriate, the reader is referred to other sources for more details.

Acknowledgments

1

Introduction: Modern Wind Energy and its Origins

The re-emergence of the wind as a significant source of the world's energy must rank as one of the significant developments of the late 20th century. The advent of the steam engine, followed by the appearance of other technologies for converting fossil fuels to useful energy, would seem to have forever relegated to insignificance the role of the wind in energy generation. In fact, by the mid 1950s that appeared to be what had already happened. By the late 1960s, however, the first signs of a reversal could be discerned, and by the early 1990s it was becoming apparent that a fundamental reversal was underway. That decade saw a strong resurgence in the worldwide wind energy industry, with installed capacity increasing over five-fold. The 1990s were also marked by a shift to large, megawatt-sized wind turbines, a reduction and consolidation in wind turbine manufacture, and the actual development of offshore wind power (see McGowan and Connors, 2000). During the start of the 21st century this trend has continued, with European countries (and manufacturers) leading the increase via government policies focused on developing domestic sustainable energy supplies and reducing pollutant emissions.

To understand what was happening, it is necessary to consider five main factors. First of all there was a need. An emerging awareness of the finiteness of the earth's fossil fuel reserves as well as of the adverse effects of burning those fuels for energy had caused many people to look for alternatives. Second, there was the potential. Wind exists everywhere on the earth, and in some places with considerable energy density. Wind had been widely used in the past, for mechanical power as well as transportation. Certainly, it was conceivable to use it again. Third, there was the technological capacity. In particular, there had been developments in other fields, which, when applied to wind turbines, could revolutionize they way they could be used. These first three factors were necessary to foster the re-emergence of wind energy, but not sufficient. There needed to be two more factors, first of all a vision of a new way to use the wind, and second the political will to make it happen. The vision began well before the 1960s with such individuals as Poul la Cour, Albert Betz, Palmer Putnam, and Percy Thomas. It was continued by Johannes Juul, E. W. Golding, Ulrich Hütter, and William Heronemus, but soon spread to others too numerous to mention. At the beginning of wind's re-emergence, the cost of energy

from wind turbines was far higher than that from fossil fuels. Government support was required to carry out research, development, and testing; to provide regulatory reform to allow wind turbines to interconnect with electrical networks; and to offer incentives to help hasten the deployment of the new technology. The necessary political will for this support appeared at different times and to varying degrees, in a number of countries: first in the United States, Denmark, and Germany, and now in much of the rest of the world.

The purpose of this chapter is to provide an overview of wind energy technology today, so as to set a context for the rest of the book. It addresses such questions as: What does modern wind technology look like? What is it used for? How did it get this way? Where is it going?

1.1 Modern Wind Turbines

A wind turbine, as described in this book, is a machine which converts the power in the wind into electricity. This is in contrast to a 'windmill', which is a machine which converts the wind's power into mechanical power. As electricity generators, wind turbines are connected to some electrical network. These networks include battery-charging circuits, residential scale power systems, isolated or island networks, and large utility grids. In terms of total numbers, the most frequently found wind turbines are actually quite small – on the order of 10 kW or less. In terms of total generating capacity, the turbines that make up the majority of the capacity are, in general, rather large – in the range of 1.5 to 5 MW. These larger turbines are used primarily in large utility grids, at first mostly in Europe and the United States and more recently in China and India. A typical modern wind turbine, in a wind farm configuration, connected to a utility network, is illustrated in Figure 1.1. The turbine shown is a General Electric 1.5 MW and this manufacturer had delivered over 10 000 units of this model at the time of writing of this text.

To understand how wind turbines are used, it is useful to briefly consider some of the fundamental facts underlying their operation. In modern wind turbines, the actual conversion process uses the basic aerodynamic force of lift to produce a net positive torque on a rotating shaft, resulting first in the production of mechanical power and then in its transformation to electricity in a generator. Wind turbines, unlike most other generators, can produce energy only in response to the resource that is immediately available. It is not possible to store the wind and

Figure 1.1   Modern utility-scale wind turbine. Reproduced by permission of General Electric

use it at a later time. The output of a wind turbine is thus inherently fluctuating and non-dispatchable. (The most one can do is to limit production below what the wind could produce.) Any system to which a wind turbine is connected must, in some way, take this variability into account. In larger networks, the wind turbine serves to reduce the total electrical load and thus results in a decrease in either the number of conventional generators being used or in the fuel use of those that are running. In smaller networks, there may be energy storage, backup generators, and some specialized control systems. A further fact is that the wind is not transportable: it can only be converted where it is blowing. Historically, a product such as ground wheat was made at the windmill and then transported to its point of use. Today, the possibility of conveying electrical energy via power lines compensates to some extent for wind's inability to be transported. In the future, hydrogen-based energy systems may add to this possibility.

1.1.1 Modern Wind Turbine Design

Today, the most common design of wind turbine, and the type which is the primary focus of this book, is the horizontal axis wind turbine (HAWT). That is, the axis of rotation is parallel to the ground. HAWT rotors are usually classified according to the rotor orientation (upwind or downwind of the tower), hub design (rigid or teetering), rotor control (pitch vs. stall), number of blades (usually two or three blades), and how they are aligned with the wind (free yaw or active yaw). Figure 1.2 shows the upwind and downwind configurations.

The principal subsystems of a typical (land-based) horizontal axis wind turbine are shown in Figure 1.3. These include:

- The rotor, consisting of the blades and the supporting hub.
- The drive train, which includes the rotating parts of the wind turbine (exclusive of the rotor); it usually consists of shafts, gearbox, coupling, a mechanical brake, and the generator.
- The nacelle and main frame, including wind turbine housing, bedplate, and the yaw system.
- The tower and the foundation.
- The machine controls.
- The balance of the electrical system, including cables, switchgear, transformers, and possibly electronic power converters.
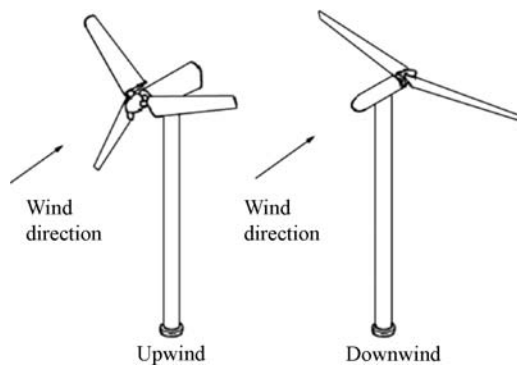
Figure 1.2　HAWT rotor configurations
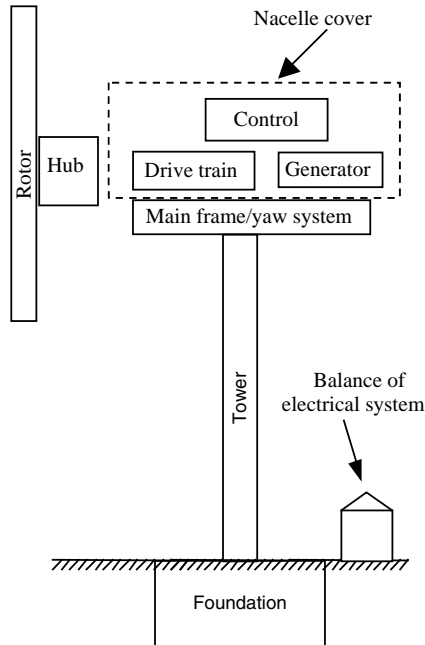
Figure 1.3   Major components of a horizontal axis wind turbine

The main options in wind turbine design and construction include:

- number of blades (commonly two or three);
- rotor orientation: downwind or upwind of tower;
- blade material, construction method, and profile;
- hub design: rigid, teetering, or hinged;
- power control via aerodynamic control (stall control) or variable-pitch blades (pitch control);
- fixed or variable rotor speed;
- orientation by self-aligning action (free yaw), or direct control (active yaw);
- synchronous or induction generator (squirrel cage or doubly fed);
- gearbox or direct drive generator.

A short introduction to and overview of some of the most important components follows. A more detailed discussion of the overall design aspects of these components, and other important parts of a wind turbine system, is contained in Chapters 3 through 9 of this book.

1.1.1.1 Rotor

The rotor consists of the hub and blades of the wind turbine. These are often considered to be the turbine's most important components from both a performance and overall cost standpoint.

Most turbines today have upwind rotors with three blades. There are some downwind rotors and a few designs with two blades. Single-blade turbines have been built in the past, but are no

longer in production. Some intermediate-sized turbines used fixed-blade pitch and stall control (described in Chapters 3, 6, 7 and 8). Most manufacturers use pitch control, and the general trend is the increased use of pitch control, especially in larger machines. The blades on the majority of turbines are made from composites, primarily fiberglass or carbon fiber reinforced plastics (GRP or CFRP), but sometimes wood/epoxy laminates are used. These subjects are addressed in more detail in the aerodynamics chapter (Chapter 3) and in Chapters 6 and 7.

1.1.1.2 Drive Train

The drive train consists of the other rotating parts of the wind turbine downstream of the rotor. These typically include a low-speed shaft (on the rotor side), a gearbox, and a high-speed shaft (on the generator side). Other drive train components include the support bearings, one or more couplings, a brake, and the rotating parts of the generator (discussed separately in the next section). The purpose of the gearbox is to speed up the rate of rotation of the rotor from a low value (tens of rpm) to a rate suitable for driving a standard generator (hundreds or thousands of rpm). Two types of gearboxes are used in wind turbines: parallel shaft and planetary. For larger machines (over approximately 500 kW), the weight and size advantages of planetary gearboxes become more pronounced. Some wind turbine designs use multiple generators, and so are coupled to a gearbox with more than one output shaft. Others use specially designed, low-speed generators requiring no gearbox.

While the design of wind turbine drive train components usually follows conventional mechanical engineering machine design practice, the unique loading of wind turbine drive trains requires special consideration. Fluctuating winds and the dynamics of large rotating rotors impose significant varying loads on drive train components.

1.1.1.3 Generator

Nearly all wind turbines use either induction or synchronous generators (see Chapter 5). These designs entail a constant or nearly constant rotational speed when the generator is directly connected to a utility network. If the generator is used with power electronic converters, the turbine will be able to operate at variable speed.

Many wind turbines installed in grid connected applications use squirrel cage induction generators (SQIG). A SQIG operates within a narrow range of speeds slightly higher than its synchronous speed (a four-pole generator operating in a 60 Hz grid has a synchronous speed of 1800 rpm). The main advantages of this type of induction generator are that it is rugged, inexpensive, and easy to connect to an electrical network. An increasingly popular option today is the doubly fed induction generator (DFIG). The DFIG is often used in variable-speed applications. It is described in more detail in Chapter 5.

An increasingly popular option for utility-scale electrical power generation is the variable-speed wind turbine. There are a number of benefits that such a configuration offers, including the reduction of wear and tear on the wind turbine and potential operation of the wind turbine at maximum efficiency over a wide range of wind speeds, yielding increased energy capture. Although there are a large number of potential hardware options for variable-speed operation of wind turbines, power electronic components are used in most variable-speed machines currently being designed. When used with suitable power electronic converters, either synchronous or induction generators of either type can run at variable speed.

1.1.1.4 Nacelle and Yaw System

This category includes the wind turbine housing, the machine bedplate or main frame, and the yaw orientation system. The main frame provides for the mounting and proper alignment of the drive train components. The nacelle cover protects the contents from the weather.

A yaw orientation system is required to keep the rotor shaft properly aligned with the wind. Its primary component is a large bearing that connects the main frame to the tower. An active yaw drive, used with upwind wind turbines and sometimes with downwind turbines, contains one or more yaw motors, each of which drives a pinion gear against a bull gear attached to the yaw bearing. This mechanism is controlled by an automatic yaw control system with its wind direction sensor usually mounted on the nacelle of the wind turbine. Sometimes yaw brakes are used with this type of design to hold the nacelle in position, when not yawing. Free yaw systems (meaning that they can self-align with the wind) are often used on downwind wind machines.

1.1.1.5 Tower and Foundation

This category includes the tower itself and the supporting foundation. The principal types of tower design currently in use are the free-standing type using steel tubes, lattice (or truss) towers, and concrete towers. For smaller turbines, guyed towers are also used. Tower height is typically 1 to 1.5 times the rotor diameter, but in any case is normally at least 20 m. Tower selection is greatly influenced by the characteristics of the site. The stiffness of the tower is a major factor in wind turbine system dynamics because of the possibility of coupled vibrations between the rotor and tower. For turbines with downwind rotors, the effect of tower shadow (the wake created by air flow around a tower) on turbine dynamics, power fluctuations, and noise generation must be considered. For example, because of the tower shadow, downwind turbines are typically noisier than their upwind counterparts.

1.1.1.6 Controls

The control system for a wind turbine is important with respect to both machine operation and power production. A wind turbine control system includes the following components:

- **sensors** – speed, position, flow, temperature, current, voltage, etc.;
- **controllers** – mechanical mechanisms, electrical circuits;
- **power amplifiers** – switches, electrical amplifiers, hydraulic pumps, and valves;
- **actuators** – motors, pistons, magnets, and solenoids;
- **intelligence** – computers, microprocessors.

The design of control systems for wind turbine application follows traditional control engineering practices. Many aspects, however, are quite specific to wind turbines and are discussed in Chapter 8. Wind turbine control involves the following three major aspects and the judicious balancing of their requirements:

- Setting upper bounds on and limiting the torque and power experienced by the drive train.

- Maximizing the fatigue life of the rotor drive train and other structural components in the presence of changes in the wind direction, speed (including gusts), and turbulence, as well as start–stop cycles of the wind turbine.
- Maximizing the energy production.

1.1.1.7 Balance of Electrical System

In addition to the generator, the wind turbine system utilizes a number of other electrical components. Some examples are cables, switchgear, transformers, power electronic converters, power factor correction capacitors, yaw and pitch motors. Details of the electrical aspects of wind turbines themselves are contained in Chapter 5. Interconnection with electrical networks is discussed in Chapter 9.

1.1.2 Power Output Prediction

The power output of a wind turbine varies with wind speed and every wind turbine has a characteristic power performance curve. With such a curve it is possible to predict the energy production of a wind turbine without considering the technical details of its various components. The power curve gives the electrical power output as a function of the hub height wind speed. Figure 1.4 presents an example of a power curve for a hypothetical wind turbine.

The performance of a given wind turbine generator can be related to three key points on the velocity scale:

- **Cut-in speed:** the minimum wind speed at which the machine will deliver useful power.
- **Rated wind speed:** the wind speed at which the rated power (generally the maximum power output of the electrical generator) is reached.
- **Cut-out speed:** the maximum wind speed at which the turbine is allowed to deliver power (usually limited by engineering design and safety constraints).

Power curves for existing machines can normally be obtained from the manufacturer. The curves are derived from field tests, using standardized testing methods. As is discussed in
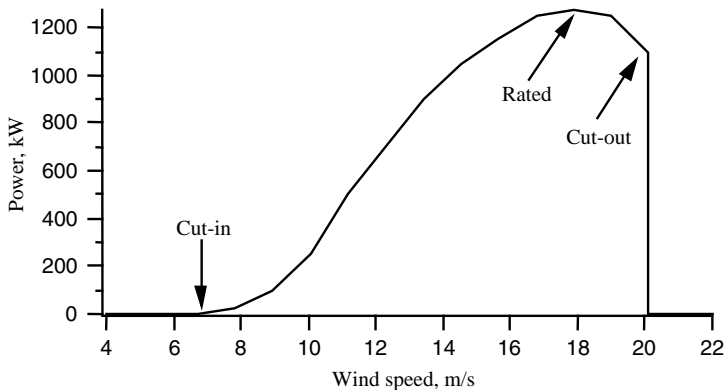
Figure 1.4   Typical wind turbine power curve

Chapter 7, it is also possible to estimate the approximate shape of the power curve for a given machine. Such a process involves determination of the power characteristics of the wind turbine rotor and electrical generator, gearbox gear ratios, and component efficiencies.

1.1.3 Other Wind Turbine Concepts

The wind turbine overview provided above assumed a topology of a basic type, namely one that employs a horizontal axis rotor, driven by lift forces. It is worth noting that a vast number of other topologies have been proposed, and in some cases built. None of these has met with the same degree of success as those with a horizontal-axis, lift-driven rotor. A few words are in order, however, to summarize briefly some of these other concepts. The closest runner up to the HAWT is the Darrieus vertical axis wind turbine (VAWT). This concept was studied extensively in both the United States and Canada in the 1970s and 1980s. An example of a VAWT wind turbine (Sandia 17 m design (SNL, 2009)) based on this concept is show in Figure 1.5.

Despite some appealing features, Darrieus wind turbines had some major reliability problems and were never able to match corresponding HAWTs in cost of energy. However, it is possible that the concept could emerge again for some applications. For a summary of past work on this turbine design and other VAWT wind turbine designs the reader is referred to Paraschivoiu (2002), Price (2006), and the summary of VAWT work carried out by Sandia National Laboratories (SNL) in the US (2009).

Another concept that appears periodically is the concentrator or diffuser augmented wind turbine (see van Bussel, 2007). In both types of design, the idea is to channel the wind to increase the productivity of the rotor. The problem is that the cost of building an effective concentrator or diffuser, which can also withstand occasional extreme winds, has always been more than the device was worth.
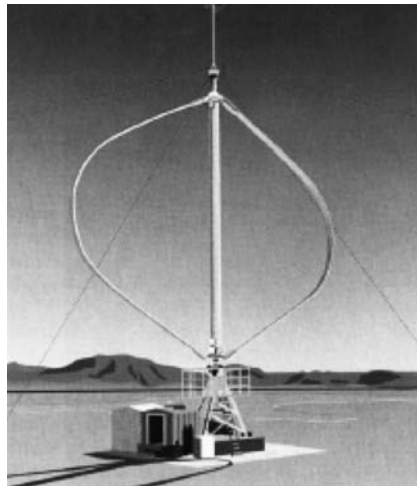
Figure 1.5   Sandia 17-meter Darrieus VAWT (Sandia National Laboratory, 2009)

Finally, a number of rotors using drag instead of lift have been proposed. One concept, the Savonius rotor, has been used for some small water-pumping applications. There are two fundamental problems with such rotors: (1) they are inherently inefficient (see comments on drag machines in Chapter 3), and (2) it is difficult to protect them from extreme winds. It is doubtful whether such rotors will ever achieve widespread use in wind turbines.

The reader interested in some of the variety of wind turbine concepts may wish to consult Nelson (1996). This book provides a description of a number of innovative wind systems. Reviews of various types of wind machines are given in Eldridge (1980) and Le Gourieres (1982). Some of the more innovative designs are documented in work supported by the US Department of Energy (1979, 1980). A few of the many interesting wind turbine concepts are illustrated in Figures 1.6 and 1.7.
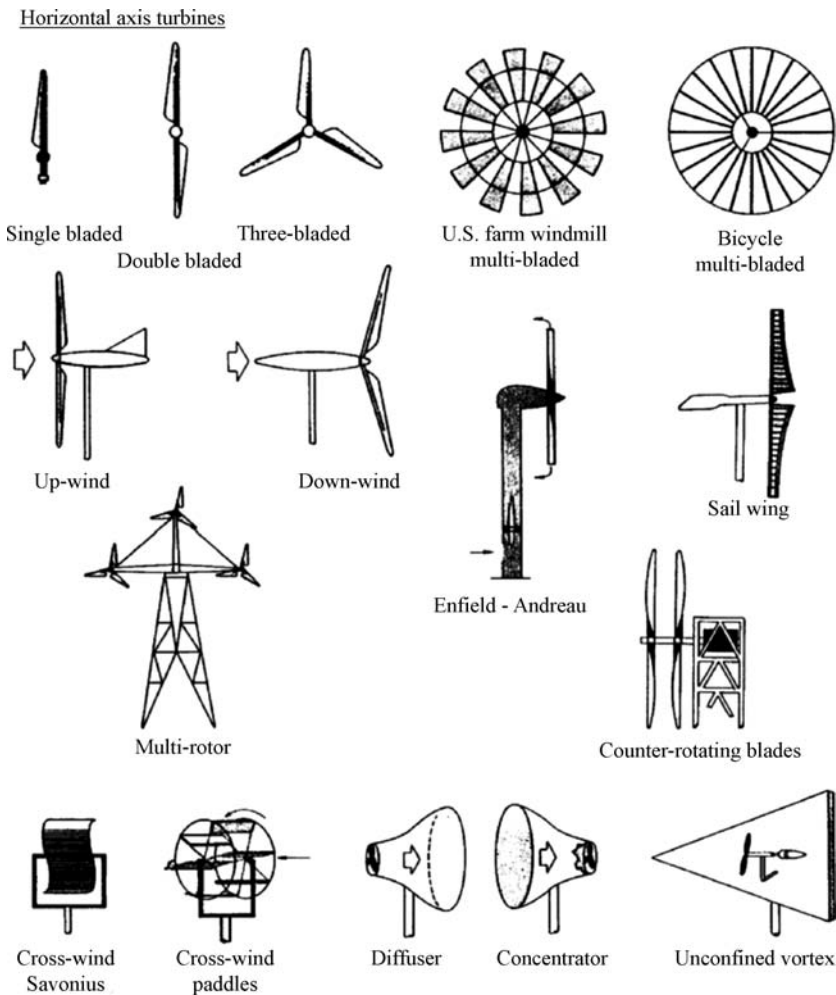
Figure 1.6 Various concepts for horizontal axis turbines (Eldridge, 1980)

Primarily drag-type

Savonius | Multi-bladed Savonius | Plates | Cupped

Shield

Primarily lift-type

φ-Darrieus | Δ-Darrieus | Giromill | Turbine

Combinations

Savonius /φ-Darrieus | Split Savonius | Magnus | Airfoil

Others

Deflector | Sunlight | Venturi | Confined Vortex
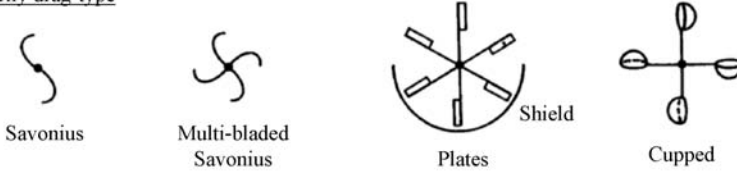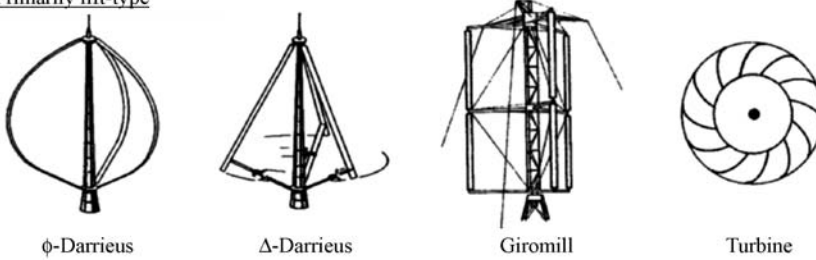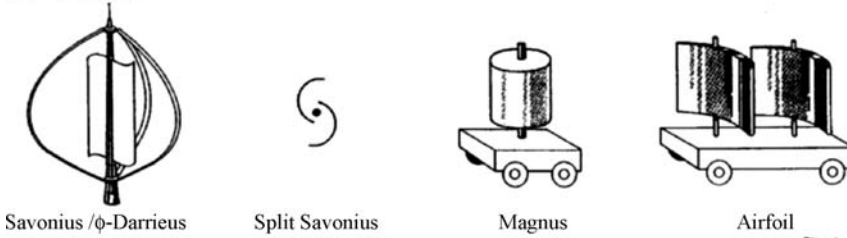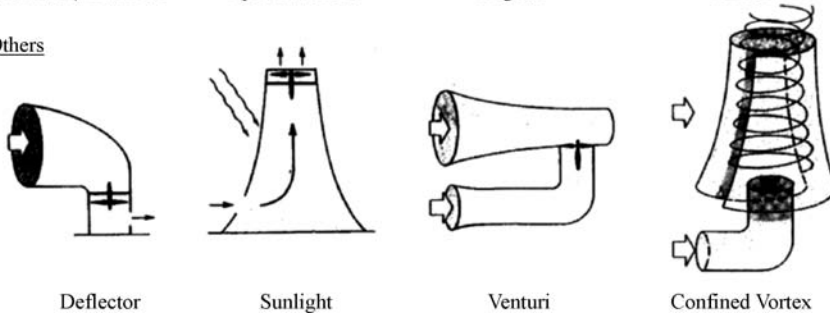
Figure 1.7   Various concepts for vertical axis turbines (Eldridge, 1980)

1.2 History of Wind Energy

It is worthwhile to consider some of the history of wind energy. The history serves to illustrate the issues that wind energy systems still face today, and provides insight into why turbines look the way they do. In the following summary, emphasis is given to those concepts which have particular relevance today.

The reader interested in a fuller description of the history of wind energy is referred to Park (1981), Eldridge (1980), Inglis (1978), Freris (1990), Shepherd (1990), Dodge (2009), and Ackermann and Soder (2002). Golding (1977) presents a history of wind turbine design from

the ancient Persians to the mid-1950s. In addition to a summary of the historic uses of wind power, Johnson (1985) presents a history of wind electricity generation, and the US research work of the 1970–85 period on horizontal axis, vertical axis, and innovative types of wind turbines. The most recent comprehensive historical reviews of wind energy systems and wind turbines are contained in the books of Spera (1994), Gipe (1995), Harrison *et al.* (2000), and Gasch and Twele (2002). Eggleston and Stoddard (1987) give a historical perspective of some of the key components of modern wind turbines. Berger (1997) provides a fascinating picture of the early days of wind energy's re-emergence, particularly of the California wind farms.

1.2.1 A Brief History of Windmills

The first known historical reference to a windmill is from Hero of Alexandria, in his work *Pneumatics* (Woodcroft, 1851). Hero was believed to have lived either in the 1st century B.C. or the 1st century A.D. His *Pneumatics* describes a device which provides air to an organ by means of a windmill. An illustration which accompanies Hero's description is shown in Figure 1.8.

There has been some debate about whether such a windmill actually existed and whether the illustration actually accompanied the original documents. See Shepherd (1990) and Drachman (1961). One of the primary scholars on the subject, however, H. P. Vowles, (Vowles, 1932) does consider Hero's description to be plausible. One of the arguments against the early Greeks having been familiar with windmills has to do with their presumed lack of technological sophistication. However, both mechanically driven grinding stones and gearing, which would generally be used with a wind-driven rotor, were known to exist at the time of Hero. For example, Reynolds (1983) describes water-powered grinding wheels at that time. In addition, the analysis of the Antikythera mechanism (Marchant, 2006) confirms that the early Greeks had a high degree of sophistication in the fabrication and use of gears.

Apart from Hero's windmill, the next reference on the subject dates from the 9th century A.D. (Al Masudi as reported by Vowles, 1932) Windmills were definitely in use in the Persian
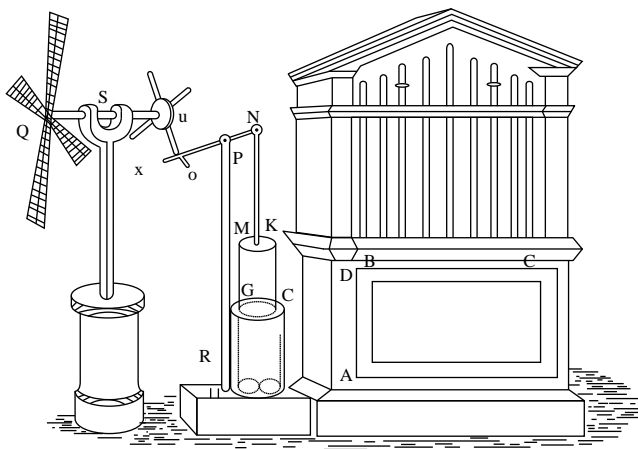
Figure 1.8   Hero's windmill (from Woodcroft, 1851)

Figure 1.9   Seistan windmill (Vowles, 1932)

region of Seistan (now eastern Iran) at that time. Al Masudi also related a story indicating that windmills were in use by 644 A.D. The Seistan windmills have continued to be used up to the present time. These windmills had vertical axis rotors, as illustrated in Figure 1.9.

Windmills made their first recorded appearance in northern Europe (England) in the 12th century but probably arrived in the 10th or 11th century (Vowles, 1930). Those windmills were considerably different in appearance to those of Seistan, and there has been considerable speculation as to if and how the Seistan mills might have influenced those that appeared later in Europe. There are no definite answers here, but Vowles 1930 has suggested that the Vikings, who traveled regularly from northern Europe to the Middle East, may have brought back the concept on one of their return trips.

An interesting footnote to this early evolution concerns the change in the design of the rotor from the Seistan windmills to those of northern Europe. The Seistan rotors had vertical axes and were driven by drag forces. As such they were inherently inefficient and particularly susceptible to damage in high winds. The northern European designs had horizontal axes and were driven by lift forces. How this transition came about is not well understood, but it was to be of great significance. It can be surmised, however, that the evolution of windmill rotor design paralleled the evolution of rigging on ships during the 1st millennium A.D., which moved progressively from square sails (primarily drag devices) to other types of rigging which used lift to facilitate tacking upwind. See, for example, Casson (1991).

The early northern European windmills all had horizontal axes. They were used for nearly any mechanical task, including water pumping, grinding grain, sawing wood, and powering tools. The early mills were built on posts, so that the entire mill could be turned to face the wind (or yaw) when its direction changed. These mills normally had four blades. The number and size of blades presumably was based on ease of construction as well as an empirically determined efficient solidity (ratio of blade area to swept area). An example of a post mill can be seen in Figure 1.10.

The wind continued to be a major source of energy in Europe through the period just prior to the Industrial Revolution, but began to recede in importance after that time. The reason that wind energy began to disappear is primarily attributable to its non-dispatchability and its non-transportability. Coal had many advantages which the wind did not possess. Coal could be transported to wherever it was needed and used whenever it was desired. When coal was used to fuel a steam engine, the output of the engine could be adjusted to suit the load. Water power,

Figure 1.10   Post mill (http://en.wikipedia.org/wiki/File:Oldland_Mill.jpg)

which has some similarities to wind energy, was not eclipsed so dramatically. This is no doubt because water power is, to some extent, transportable (via canals) and dispatchable (by using ponds as storage).

Prior to its demise, the European windmill had reached a high level of design sophistication. In the later mills (or 'smock mills'), such as the one shown in Figure 1.11, the majority of the mill was stationary. Only the top would be moved to face the wind. Yaw mechanisms included

Figure 1.11   European smock mill (Hills, 1994). Reproduced by permission of Cambridge University Press

both manually operated arms and separate yaw rotors. Blades had acquired somewhat of an airfoil shape and included some twist. The power output of some machines could be adjusted by an automatic control system. This was the forerunner of the system used by James Watt on steam engines. In the windmill's case a fly ball governor would sense when the rotor speed was changing. A linkage to a tentering mechanism would cause the upper millstone to move closer or farther away from the lower one, letting in more or less grain to grind. Increasing the gap would result in more grain being ground and thus a greater load on the rotor, thereby slowing it down and vice versa. See Stokhuyzen (1962) for details on this governor as well as other features of Dutch windmills.

One significant development in the 18th century was the introduction of scientific testing and evaluation of windmills. The Englishman John Smeaton, using such apparatus as illustrated in Figure 1.12, discovered three basic rules that are still applicable:

- The speed of the blade tips is ideally proportional to the speed of wind.
- The maximum torque is proportional to the speed of wind squared.
- The maximum power is proportional to the speed of wind cubed.

The 18th century European windmills represented the culmination of one approach to using wind for mechanical power and included a number of features which were later incorporated into some early electricity-generating wind turbines.

As the European windmills were entering their final years, another variant of windmill came into widespread use in the United States. This type of windmill, illustrated in Figure 1.13, was most notably used for pumping water, particularly in the west. They were used on ranches for cattle and to supply water for the steam railroads. These mills were distinctive for their multiple blades and are often referred to as 'fan mills'. One of their most significant features was a simple but effective regulating system. This allowed the turbines to run unattended for long periods. Such regulating systems foreshadowed the automatic control systems which are now an integral part of modern wind turbines.
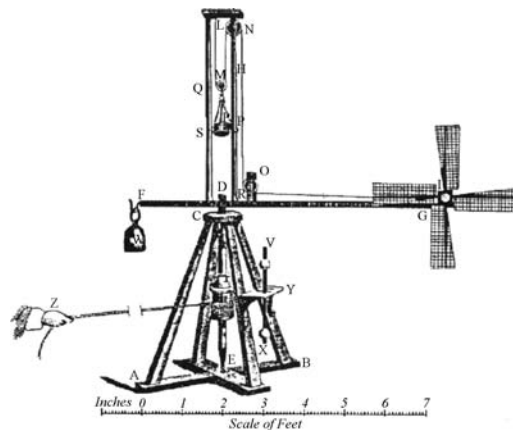
Figure 1.12   Smeaton's laboratory windmill testing apparatus

Figure 1.13   American water-pumping windmill design (US Department of Agriculture)

1.2.2 Early Wind Generation of Electricity

The initial use of wind for electricity generation, as opposed to mechanical power, included the successful commercial development of small wind generators and research and experiments using large wind turbines.

When electrical generators appeared towards the end of the 19th century, it was reasonable that people would try to turn them with a windmill rotor. In the United States, the most notable early example was built by Charles Brush in Cleveland, Ohio in 1888. The Brush turbine did not result in any trend, but in the following years, small electrical generators did become widespread. These small turbines, pioneered most notably by Marcellus Jacobs and illustrated in Figure 1.14, were, in some ways, the logical successors to the water-pumping fan mill. They were also significant in that their rotors had three blades with true airfoil shapes and began to resemble the turbines of today. Another feature of the Jacobs turbine was that it was typically incorporated into a complete, residential scale power system, including battery storage. The Jacobs turbine is considered to be a direct forerunner of such modern small turbines as the Bergey and Southwest Windpower machines. The expansion of the central electrical grid under the auspices of the Rural Electrification Administration during the 1930s marked the beginning of the end of the widespread use of small wind electric generators, at least for the time being.

The first half of the 20th century also saw the construction or conceptualization of a number of larger wind turbines which substantially influenced the development of today's technology. Probably the most important sequence of turbines was in Denmark. Between 1891 and 1918 Poul La Cour built more than 100 electricity generating turbines in the 20–35 kW size range. His design was based on the latest generation of Danish smock mills. One of the more remarkable features of the turbine was that the electricity that was generated was used to produce hydrogen, and the hydrogen gas was then used for lighting. La Cour's turbines were followed by a number of turbines made by Lykkegaard Ltd. and F. L. Smidth & Co prior to World War II. These ranged in size from 30 to 60 kW. Just after the war, Johannes

Figure 1.14   Jacobs turbine (Jacobs, 1961)

Juul erected the 200 kW Gedser turbine, illustrated in Figure 1.15, in southeastern Denmark. This three-bladed machine was particularly innovative in that it employed aerodynamic stall for power control and used an induction generator (squirrel cage type) rather than the more conventional (at the time) synchronous generator. This type of induction generator is much simpler to connect to the grid than is a synchronous generator. Stall is also a simple way to control power. These two concepts formed the core of the strong Danish presence in wind energy in the 1980s (see http://www.risoe.dk/ and http://www.windpower.dk for more details on wind energy in Denmark). One of the pioneers in wind energy in the 1950s was Ulrich Hütter in Germany (Dörner, 2002). His work focused on applying modern aerodynamic principles to wind turbine design. Many of the concepts he worked with are still in use in some form today.

   In the United States, the most significant early large turbine was the Smith–Putnam machine, built at Grandpa's Knob in Vermont in the late 1930s (Putnam, 1948). With a diameter of 53.3 m and a power rating of 1.25 MW, this was the largest wind turbine ever built up until that time and for many years thereafter. This turbine, illustrated in Figure 1.16, was also significant in that it was the first large turbine with two blades. In this sense it was a predecessor of the two-bladed turbines built by the US Department of Energy in the late 1970s and early 1980s. The turbine was also notable in that the company that built it, S. Morgan Smith, had long experience in hydroelectric generation and intended to produce a commercial line of wind machines. Unfortunately, the Smith–Putnam turbine was too large, too early, given the level of understanding of wind energy engineering. It suffered a blade failure in 1945, and the project was abandoned.

Figure 1.15 Danish Gedser wind turbine. Reproduced by permission of Danish Wind Turbine Manufacturers

1.2.3 The Re-Emergence of Wind Energy

The re-emergence of wind energy can be considered to have begun in the late 1960s. The book *Silent Spring* (Carson, 1962) made many people aware of the environmental consequences of industrial development. *Limits to Growth* (Meadows *et al.*, 1972) followed in the same vein, arguing that unfettered growth would inevitably lead to either disaster or change. Among the culprits identified were fossil fuels. The potential dangers of nuclear energy also became more public at this time. Discussion of these topics formed the backdrop for an environmental movement which began to advocate cleaner sources of energy.

In the United States, in spite of growing concern for environmental issues, not much new happened in wind energy development until the Oil Crises of the mid-1970s. Under the Carter administration, a new effort was begun to develop 'alternative' sources of energy, one of which was wind energy. The US Department of Energy (DOE) sponsored a number of projects to foster the development of the technology. Most of the resources were allocated to large machines, with mixed results. These machines ranged from the 100 kW (38 m diameter) NASA MOD-0 to the 3.2 MW Boeing MOD-5B with its 98 m diameter. Much interesting data was generated but none of the large turbines led to commercial projects. DOE also supported development of some small wind turbines and built a test facility for small machines at Rocky

Figure 1.16   Smith–Putnam wind turbine (Eldridge, 1980)

Flats, Colorado. A number of small manufacturers of wind turbines also began to spring up, but there was not a lot of activity until the late 1970s (see Dodge, 2009).

The big opportunities occurred as the result of changes in the utility regulatory structure and the provision of incentives. The US federal government, through the Public Utility Regulatory Policy Act of 1978, required utilities (1) to allow wind turbines to connect with the grid and (2) to pay the 'avoided cost' for each kWh the turbines generated and fed into the grid.

The actual avoided cost was debatable, but in many states utilities would pay enough that wind generation began to make economic sense. In addition, the federal government and some states provided investment tax credits to those who installed wind turbines. The state which provided the best incentives, and which also had regions with good winds, was California. It was now possible to install a number of small turbines together in a group ('wind farm'), connect them to the grid, and make some money.

The California wind rush was on. Over a period of a few years, thousands of wind turbines were installed in California, particularly in the Altamont Pass, San Gorgonio Pass, and Tehachipi. A typical installation is shown in Figure 1.17. The installed capacity reached approximately 1500 MW. The early years of the California wind rush were fraught with difficulties, however. Many of the machines were essentially still prototypes, and not yet up to the task. An investment tax credit (as opposed to a production tax credit) is arguably not the best way to encourage the development and deployment of productive machines, especially when there is no means for certifying that machines will actually perform as the manufacturer claims.

Figure 1.17 California wind farm (National Renewable Energy Laboratory)

When the federal tax credits were withdrawn by the Reagan administration in the early 1980s, the wind rush collapsed.

Wind turbines installed in California were not limited to those made in the United States. In fact, it was not long before Danish turbines began to have a major presence in the California wind farms. The Danish machines also had some teething problems in California, but in general they were closer to production quality than were their US counterparts. When all the dust had settled after the wind rush had ended, the majority of US manufacturers had gone out of business. The Danish manufacturers had restructured or merged, but had in some way survived.

During the 1990s, a decade which saw the demise (in 1996) of the largest US manufacturer, Kennetech Windpower, the focal point of wind turbine manufacturing definitively moved to Europe, particularly Denmark and Germany. Concerns about global warming and continued apprehension about nuclear power resulted in a strong demand for more wind generation there and in other countries as well. The 21st century has seen some of the major European suppliers establish manufacturing plants in other countries, such as China, India, and the United States.

In recent times, the size of the largest commercial wind turbines, as illustrated in Figure 1.18, has increased from approximately 25 kW to 6 MW, with machines up to 10 MW under design. The total installed capacity in the world as of the year 2009 was about 115 000 MW, with the majority of installations in Europe. Offshore wind energy systems were also under active development in Europe, with about 2000 MW installed as of 2008. Design standards and machine certification procedures have been established, so that the reliability and performance are far superior to those of the 1970s and 1980s. The cost of energy from wind has dropped to the point that in many sites it is nearly competitive with conventional sources, even without incentives. In those countries where incentives are in place, the rate of development is quite strong.

1.2.4 Technological Underpinnings of Modern Wind Turbines

Wind turbine technology, dormant for many years, awoke at the end of the 20th century to a world of new opportunities. Developments in many other areas of technology were adapted to
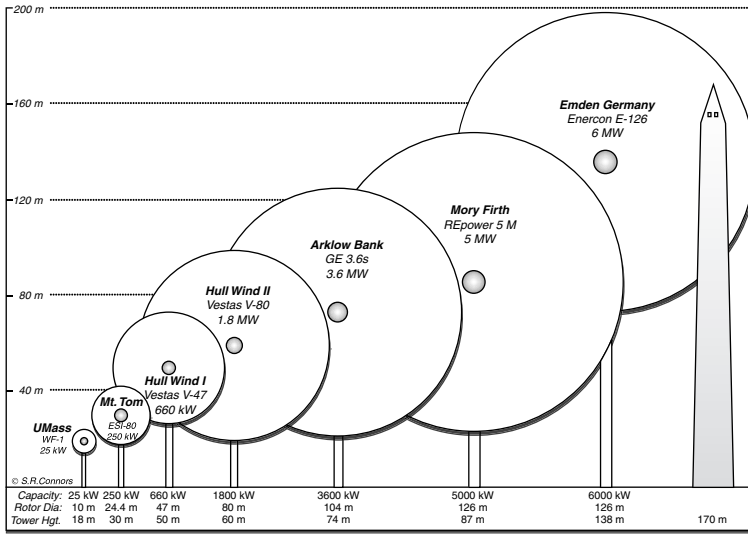
Figure 1.18   Representative size, height, and diameter of wind turbines (Steve Connors, MIT)

wind turbines and have helped to hasten their re-emergence. A few of the many areas which have contributed to the new generation of wind turbines include materials science, computer science, aerodynamics, analytical design and analysis methods, testing and monitoring, and power electronics. Materials science has brought new composites for the blades and alloys for the metal components. Developments in computer science facilitate design, analysis, monitoring, and control. Aerodynamic design methods, originally developed for the aerospace industry, have now been adapted to wind turbines. Analytical design and analysis methods have now developed to the point where it is possible to have a much clearer understanding of how a new design should perform than was previously possible. Testing and monitoring using a vast array of commercially available sensors and modern data collection and analysis equipment allow designers to better understand how the new turbines actually perform. Power electronics is now widely used with wind turbines. Power electronic devices can help connect the turbine's generator smoothly to the electrical network; allow the turbine to run at variable speed, producing more energy, reducing fatigue damage, and benefit the utility in the process; facilitate operation in a small, isolated network; and transfer energy to and from storage.

1.2.5 Trends

Wind turbines have evolved a great deal over the last 35 years. They are more reliable, more cost effective, and quieter. It cannot be concluded that the evolutionary period is over, however. It should still be possible to reduce the cost of energy at sites with lower wind speeds. Turbines for use in remote communities still remain to be made commercially viable. The world of offshore wind energy is just in its infancy. There are tremendous opportunities in offshore locations but many difficulties to be overcome. As wind energy comes to supply an ever larger fraction of the world's electricity, the issues of intermittency, transmission, and storage must be revisited.

There will be continuing pressure for designers to improve the cost effectiveness of turbines for all applications. Improved engineering methods for the analysis, design, and for mass-produced manufacturing will be required. Opportunities also exist for the development of new materials to increase wind turbine life. Increased consideration will need to be given to the requirements of specialized applications. In all cases, the advancement of the wind industry represents an opportunity and challenge for a wide range of disciplines, especially including mechanical, electrical, materials, aeronautical, controls, ocean and civil engineering as well as computer science.

References

Ackermann, T. and Soder, L. (2002) An overview of wind energy-status 2002. *Renewable and Sustainable Energy Reviews*, **6**, 67–127.

Berger, J. J. (1997) *Charging Ahead: The Business of Renewable Energy and What it Means for America*. University of California Press, Berkeley, CA.

Carson, R. (1962) *Silent Spring*. Houghton Mifflin, New York.

Casson, L. (1991) *The Ancient Mariners: Seafarers and Sea Fighters of the Mediterranean in Ancient Times*. Princeton University Press, Princeton, NJ.

Danish Wind Turbine Manufacturers (2001) http://www.windpower.dk.

Dodge, D. M. (2009) Illustrated history of wind power development, http://telosnet.com/wind.

Dörner, H. (2002) *Drei Welten- ein Leben: Prof. Dr Ulrich Hütter*. Heilbronn.

Drachman, A. G. (1961) Heron's windmill. *Centaurus*, **7**(2), 145–151.

Eggleston, D. M. and Stoddard, F. S. (1987) *Wind Turbine Engineering Design*. Van Nostrand Reinhold, New York.

Eldridge, F. R. (1980) *Wind Machines*, 2nd edition. Van Nostrand Reinhold, New York.

Freris, L. L. (1990) *Wind Energy Conversion Systems*. Prentice Hall, New York.

Gasch, R. and Twele, J. (2002) *Wind Power Plants*. James & James, London.

Gipe, P. (1995) *Wind Energy Comes of Age*. John Wiley & Sons, Inc., New York.

Golding, E. W. (1977) *The Generation of Electricity by Wind Power*. E. & F. N. Spon, London.

Harrison, R., Hau, E. and Snel, H. (2000) *Large Wind Turbines: Design and Economics*. John Wiley & Sons, Ltd, Chichester.

Hills, R. L. (1994) *Power from Wind*. Cambridge University Press, Cambridge, UK.

Inglis, D. R. (1978) *Windpower and Other Energy Options*. University of Michigan Press, Ann Arbor.

Jacobs, M. L. (1961) Experience with Jacobs wind-driven electric generating plant, 1931–1957. *Proc. of the United Nations Conference on New Sources of Energy*, **7**, 337–339.

Johnson, G. L. (1985) *Wind Energy Systems*. Prentice Hall, Englewood Cliffs, NJ.

Le Gourieres, D. (1982) *Wind Power Plants*. Pergamon Press, Oxford.

Marchant, J. (2006) In Search of Lost Time. *Nature*, **444**, 534–538.

McGowan, J. G. and Connors, S. R. (2000) Windpower: a turn of the century review. *Annual Review of Energy and the Environment*, **25**, 147–197.

Meadows, D. H., Meadows, D. L., Randers, J. and Behrens III, W. W. (1972) *The Limits to Growth*. Universe Books, New York.

Nelson, V. (1996) *Wind Energy and Wind Turbines*. Alternative Energy Institute, Canyon, TX.

Paraschivoiu, I. (2002) *Wind Turbine Design: With Emphasis on Darrieus Concept*. Polytechnic International Press, Montreal.

Park, J. (1981) *The Wind Power Book*. Cheshire Books, Palo Alto, CA.

Price, T. J. (2006) UK Large-scale wind power programme from 1970 to 1990: The Carmarthen Bay experiments and the Musgrove vertical-axis turbines. *Wind Engineering*, **30**(3), 225–242.

Putnam, P. C. (1948) *Power From the Wind*. Van Nostrand Reinhold, New York.

Reynolds, T. S. (1983) *Stronger than a Hundred Men: A History of the Vertical Water Wheel*. Johns Hopkins University Press, Baltimore.

Shepherd, D. G. (1990) *The Historical Development of the Windmill*, NASA Contractor Report 4337, DOE/NASA 52662.

SNL (2009) *VAWT Technology*, Sandia National Laboratories, http://sandia.gov/wind/topical.htm# VAWTARCHIVE.

Spera, D. A. (Ed.) (1994) *Wind Turbine Technology: Fundamental Concepts of Wind Turbine Engineering*. ASME Press, New York.

Stokhuyzen, F. (1962) *The Dutch Windmill*, available at http://www.nt.ntnu.no/users/haugwarb/DropBox/The Dutch Windmill Stokhuyzen 1962.htm.

US Department of Energy (1979) *Wind Energy Innovative Systems Conference Proceedings*. Solar Energy Research Institute (SERI).

US Department of Energy (1980), *SERI Second Wind Energy Innovative Systems Conference Proceedings*, Solar Energy Research Institute (SERI).

van Bussel, G. J. W. (2007) The science of making more torque from wind: diffuser experiments and theory revisited. *Journal of Physics: Conference Series*, **75**, 1–11.

Vowles, H. P. (1930) An inquiry into the origins of the windmill. *Journal of the Newcomen Society*, **11**, 1–14.

Vowles, H. P. (1932) Early evolution of power engineering. *Isis*, **17**(2), 412–420.

Woodcroft, B. (1851) Translation from the Greek of The Pneumatics of Hero of Alexandria. Taylor Walton and Maberly, London. Available at: http://www.history.rochester.edu/steam/hero/.

2

Wind Characteristics and Resources

2.1 Introduction

This chapter will review an important topic in wind energy: wind resources and characteristics. The material covered in this chapter can be of direct use to other aspects of wind energy which are discussed in the other sections of this book. For example, knowledge of the wind characteristics at a particular site is relevant to the following topics:

- **Systems design** – system design requires knowledge of representative average wind conditions, as well as information on the turbulent nature of the wind and extreme wind events. This information is used in the design and selection of a wind turbine intended for a particular site.
- **Performance evaluation** – performance evaluation requires determining the expected energy productivity and cost effectiveness of a particular wind energy system based on the wind resource.
- **Siting** – siting requirements can include the assessment or prediction of the relative desirability of candidate sites for one or more wind turbines.
- **Operations** – operation requirements include the need for wind resource information that can be used for load management, operational procedures (such as start-up and shutdown), and the prediction of maintenance or system life.

The chapter starts with a general discussion of wind resource characteristics, followed by a section on the characteristics of the atmospheric boundary layer that are directly applicable to wind energy applications. The next two sections present a number of topics that enable one to analyze wind data, make resource estimates, anticipate extreme wind speeds, and determine wind turbine power production from wind resource data, or from a limited amount of wind data (such as average wind speed). Next, a summary of available worldwide wind resource assessment data is given followed by a discussion of wind prediction and forecasting. The section after that reviews wind resource measurement techniques and instrumentation. The chapter concludes with a summary of a number of advanced topics in the area of wind resource characterization.

There are a number of other sources of information on wind characteristics as related to wind energy. These include the classic references Putnam (1948) as well as books by Eldridge (1980), Johnson (1985), Freris (1990), Spera (1994) and Burton *et al.* (2001). In addition, this text will refer to wind resource material included in several books devoted to this subject. These include the work of Justus (1978), Hiester and Pennell (1981), and the text of Rohatgi and Nelson (1994).

2.2 General Characteristics of the Wind Resource

In discussing the general characteristics of the wind resource it is important to consider such topics as the global origins of the wind resource, the general characteristics of the wind, and estimates of the wind resource potential.

2.2.1 Wind Resource: Global Origins

2.2.1.1 Overall Global Patterns

The original source of the renewable energy contained in the earth's wind resource is the sun. Global winds are caused by pressure differences across the earth's surface due to the uneven heating of the earth by solar radiation. For example, the amount of solar radiation absorbed at the earth's surface is greater at the equator than at the poles. The variation in incoming energy sets up convective cells in the lower layers of the atmosphere (the troposphere). In a simple flow model, air rises at the equator and sinks at the poles. The circulation of the atmosphere that results from uneven heating is greatly influenced by the effects of the rotation of the earth (at a speed of about 1670 kilometers per hour at the equator, decreasing to zero at the poles). In addition, seasonal variations in the distribution of solar energy give rise to variations in the circulation.

The spatial variations in heat transfer to the earth's atmosphere create variations in the atmospheric pressure field that cause air to move from high to low pressure. There is a pressure gradient force in the vertical direction, but this is usually cancelled by the downward gravitational force. Thus, the winds blow predominately in the horizontal plane, responding to horizontal pressure gradients. At the same time, there are forces that strive to mix the different temperature and pressure air masses distributed across the earth's surface. In addition to the pressure gradient and gravitational forces, inertia of the air, the earth's rotation, and friction with the earth's surface (resulting in turbulence), affect the atmospheric winds. The influence of each of these forces on atmospheric wind systems differs depending on the scale of motion considered.

As shown in Figure 2.1, worldwide wind circulation involves large-scale wind patterns which cover the entire planet. These affect prevailing near surface winds. It should be noted that this model is an oversimplification because it does not reflect the effect that land masses have on the wind distribution.

2.2.1.2 Mechanics of Wind Motion

In one of the simplest models for the mechanics of the atmosphere's wind motion, four atmospheric forces can be considered. These include pressure forces, the Coriolis force caused by the rotation of the earth, inertial forces due to large-scale circular motion, and frictional forces at the earth's surface.
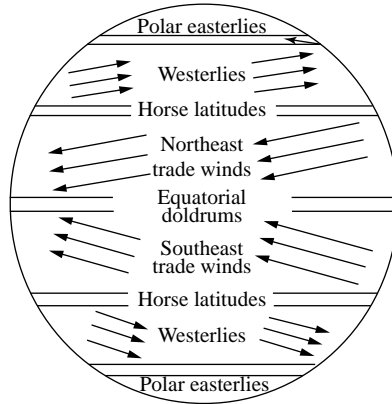
Figure 2.1   Surface winds of worldwide circulation pattern (Hiester and Pennell, 1981)

The pressure force on the air (per unit mass), F_p, is given by:

$$F_p = \frac{-1}{\rho} \frac{\partial p}{\partial n} \qquad (2.1)$$

where ρ is the density of the air and n is the direction normal to lines of constant pressure. Also, $\partial p / \partial n$ is defined as the pressure gradient normal to the lines of constant pressure, or isobars. The Coriolis force (per unit mass), F_c, a fictitious force caused by measurements with respect to a rotating reference frame (the earth), is expressed as:

$$F_c = fU \qquad (2.2)$$

where U is the wind speed and f is the Coriolis parameter [$f = 2\omega \sin(\phi)$]. ϕ represents the latitude and ω the angular rotation of the earth. Thus, the magnitude of the Coriolis force depends on wind speed and latitude. The direction of the Coriolis force is perpendicular to the direction of motion of the air. The resultant of these two forces, called the geostrophic wind, tends to be parallel to isobars (see Figure 2.2).
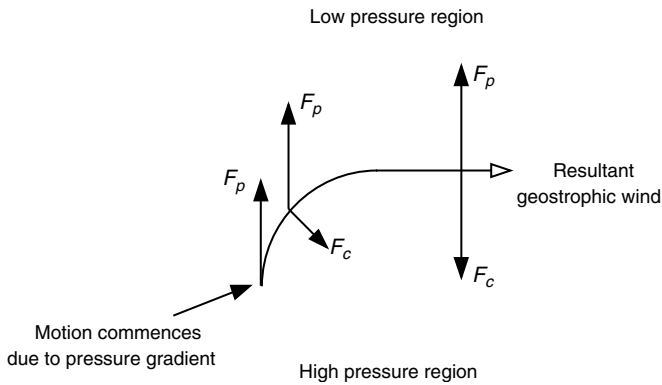
Figure 2.2   Illustration of the geostrophic wind; F_p, pressure force on the air; F_c, Coriolis force
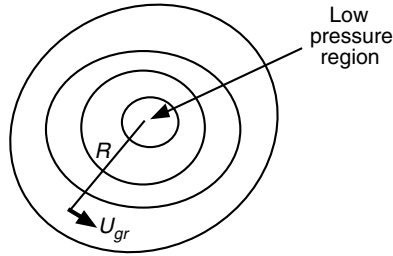
Figure 2.3   Illustration of the gradient wind U_{gr}; R, radius of curvature

The magnitude of the geostrophic wind, U_g, is a function of the balance of forces and is given by:

$$U_g = \frac{-1}{f\rho}\frac{\partial p}{\partial n} \tag{2.3}$$

This is an idealized case since the presence of areas of high and low pressure causes the isobars to be curved. This imposes a further force on the wind, a centrifugal force. The resulting wind, called a gradient wind, U_{gr}, is shown in Figure 2.3.

The gradient wind is also parallel to the isobars and is the result of the balance of the forces:

$$\frac{U_{gr}^2}{R} = -fU_{gr} - \frac{1}{\rho}\frac{\partial p}{\partial n} \tag{2.4}$$

where R is the radius of curvature of the path of the air particles, and substituting from Equation (2.3) for U_g gives:

$$U_g = U_{gr} + \frac{U_{gr}^2}{fR} \tag{2.5}$$

A final force on the wind is due to friction at the earth's surface. That is, the earth's surface exerts a horizontal force upon the moving air, the effect of which is to retard the flow. This force decreases as the height above the ground increases and becomes negligible above the boundary layer (defined as the near earth region of the atmosphere where viscous forces are important). Above the boundary layer, a frictionless wind balance is established and the wind flows with the gradient wind velocity along the isobars. Friction at the surface causes the wind to be diverted more toward the low-pressure region. More details concerning the earth's boundary layer and its characteristics will be given in later sections.

2.2.1.3 Other Atmospheric Circulation Patterns

The general circulation flow pattern described previously best represents a model for a smooth spherical surface. In reality, the earth's surface varies considerably, with large ocean and

land masses. These different surfaces can affect the flow of air due to variations in pressure fields, the absorption of solar radiation, and the amount of moisture available.

The oceans act as a large sink for energy. Therefore, the movement of air is often affected by the ocean circulation. All these effects lead to differential pressures which affect the global winds and many of the persistent regional winds, such as those occurring during monsoons. In addition, local heating or cooling may cause persistent local winds to occur on a seasonal or daily basis. These include sea breezes and mountain winds.

Smaller scale atmospheric circulation can be divided into secondary and tertiary circulation (see Rohatgi and Nelson, 1994). Secondary circulation occurs if the centers of high or low pressure are caused by heating or cooling of the lower atmosphere. Secondary circulations include the following:

- hurricanes;
- monsoon circulation;
- extratropical cyclones.

Tertiary circulations are small-scale, local circulations characterized by local winds. These include the following:

- land and sea breezes;
- valley and mountain winds;
- monsoon-like flow (example: flow in California passes);
- foehn winds (dry, high-temperature winds on the downwind side of mountain ranges);
- thunderstorms;
- tornadoes.

Examples of tertiary circulation, valley and mountain winds, are shown in Figure 2.4. During the day, the warmer air of the mountain slope rises and replaces the heavier cool air above it. The direction reverses at night, as cold air drains down the slopes and stagnates in the valley floor.

An understanding of these wind patterns, and other local effects, is important for the evaluation of potential wind energy sites.
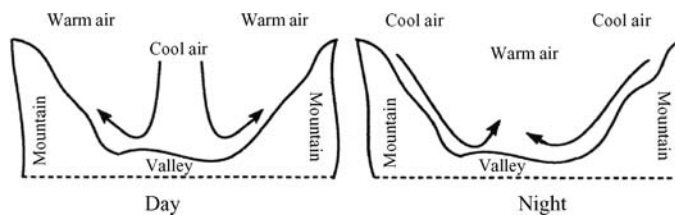
Figure 2.4   Diurnal valley and mountain wind (Rohatgi and Nelson, 1994). Reproduced by permission of Alternative Energy Institute
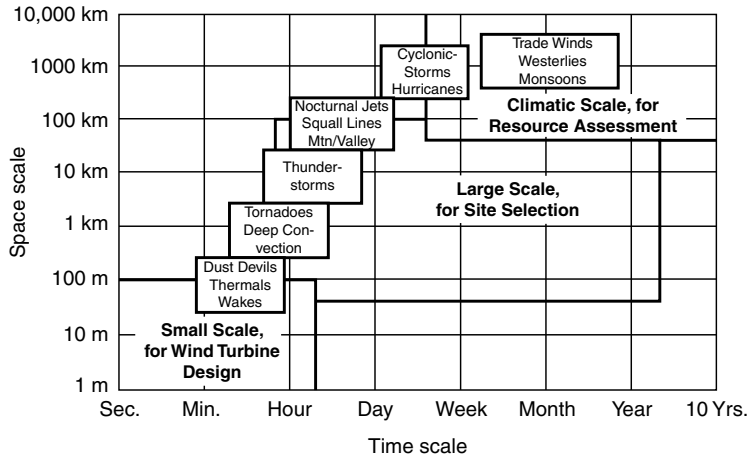
Figure 2.5 Time and space scales of atmospheric motion (Spera, 1994). Reproduced by permission of ASME

2.2.2 Temporal and Spatial Characteristics of Wind

Atmospheric motions vary in both time (seconds to months) and space (centimeters to thousands of kilometers). Figure 2.5 summarizes the time and space variations of atmospheric motion as applied to wind energy. As will be discussed in later sections, space variations are generally dependent on height above the ground and global and local geographical conditions.

2.2.2.1 Variations in Time

Following conventional practice, variations in wind speed in time can be divided into the following categories:

- inter-annual;
- annual;
- diurnal;
- short-term (gusts and turbulence).

   A review of each of these categories as well as comments on wind speed variation due to location and wind direction follows.

Inter-annual
Inter-annual variations in wind speed occur over time scales greater than one year. They can have a large effect on long-term wind turbine production. The ability to estimate the inter-annual variability at a given site is almost as important as estimating the long-term mean wind at a site. Meteorologists generally conclude that it takes 30 years of data to determine long-term values of weather or climate and that it takes at least five years to arrive at a reliable average annual wind speed at a given location. Nevertheless, shorter data records can be useful.
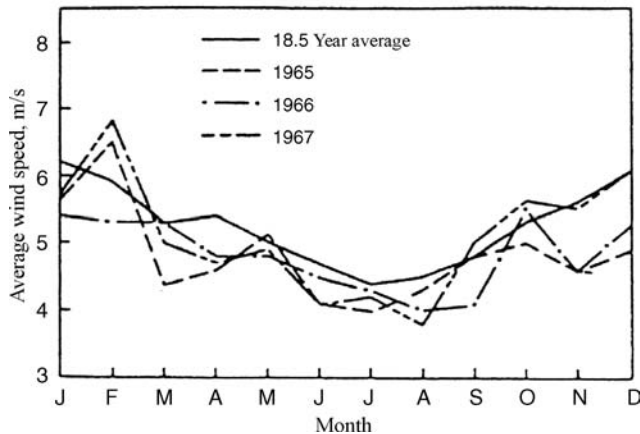
Figure 2.6 Seasonal changes in monthly average wind speeds (Hiester and Pennell, 1981)

Aspliden *et al.* (1986) note that one statistically developed rule of thumb is that one year of record data is generally sufficient to predict long-term seasonal mean wind speeds within an accuracy of 10% with a confidence level of 90%.

Researchers are still looking for reliable prediction models for long-term mean wind speed. The complexities of the interactions of the meteorological and topographical factors that cause its variation make the task difficult.

Annual

Significant variations in seasonal or monthly averaged wind speeds are common over most of the world. For example, for the eastern one-third of the United States, maximum wind speeds occur during the winter and early spring. Spring maxima occur over the Great Plains, the North Central States, the Texas Coast, in the basins and valleys of the West, and the coastal areas of Central and Southern California. Winter maxima occur over all US mountainous regions, except for some areas in the lower Southwest, where spring maxima occur. Spring and summer maxima occur in the wind corridors of Oregon, Washington, and California.

Figure 2.6 illustrates seasonal changes in monthly wind speed for Billings, Montana. It is interesting to note that this figure clearly shows that the typical behavior of monthly variation is not defined by a single year of data.

Similarly, Figure 2.7 provides an illustration of the importance of annual wind speed variation and its effect on available wind power (error bars show the standard deviation).

Diurnal (Time of Day)

In both tropical and temperate latitudes, large wind variations also can occur on a diurnal or daily time scale. This type of wind speed variation is due to differential heating of the earth's surface during the daily radiation cycle. A typical diurnal variation is an increase in wind speed during the day with the wind speeds lowest during the hours from midnight to sunrise. Daily variations in solar radiation are responsible for diurnal wind variations in temperate latitudes over relatively flat land areas. The largest diurnal changes generally occur in spring and summer, and the smallest in winter. Furthermore, the diurnal variation in wind speed may
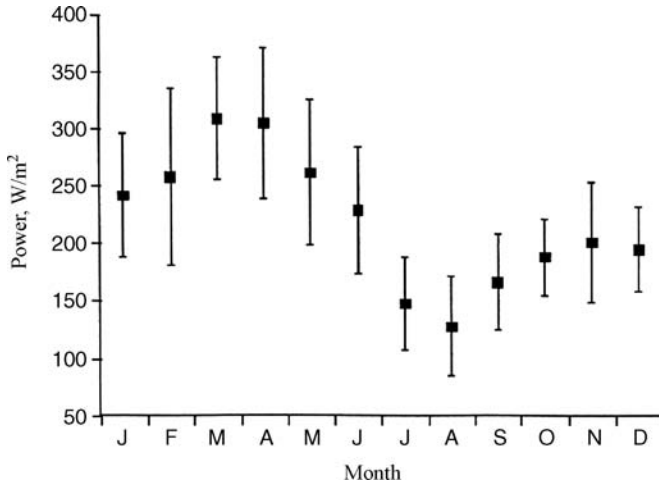
Figure 2.7 Seasonal variation in available wind power per unit area for Amarillo, Texas (Rohatgi and Nelson, 1994). Reproduced by permission of Alternative Energy Institute

vary with location and altitude above sea level. For example, at altitudes high above surrounding terrain, e.g., mountains or ridges, the diurnal pattern may be very different. This variation can be explained by mixing or transfer of momentum from the upper air to the lower air.

As illustrated in Figure 2.8, there may be significant year-to-year differences in diurnal behavior, even at fairly windy locations. Although gross features of the diurnal cycle can be established with a single year of data, more detailed features such as the amplitude of the diurnal oscillation and the time of day that the maximum winds occur cannot be determined precisely.

Short-term

Short-term wind speed variations of interest include turbulence and gusts. Figure 2.9, output from an anemometer (described later), shows the type of short-term wind speed variations that normally exist.

Short-term variations usually mean variations over time intervals of ten minutes or less. Ten-minute averages are typically determined using a sampling rate of about 1 second. It is generally accepted that variations in wind speed with periods from less than a second to ten minutes and that have a stochastic character are considered to represent turbulence. For wind energy applications, turbulent fluctuations in the flow need to be quantified. For example, turbine design considerations can include maximum load and fatigue prediction, structural excitations, control, system operation, and power quality. More details on these factors as related to turbine design are discussed in Chapters 6 and 7 of this text.

Turbulence can be thought of as random wind speed fluctuations imposed on the mean wind speed. These fluctuations occur in all three directions: longitudinal (in the direction of the wind), lateral (perpendicular to the average wind), and vertical. Turbulence and its effects will be discussed in later sections of this chapter.
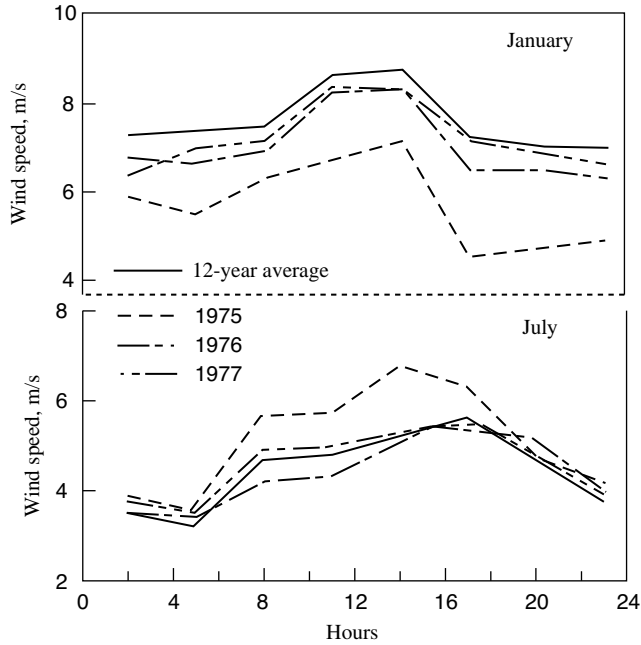
Figure 2.8   Monthly mean diurnal wind speeds for January and July for Casper, Wyoming (Hiester and Pennell, 1981)

A gust is a discrete event within a turbulent wind field. As illustrated in Figure 2.10, one way to characterize a gust is to determine: (a) amplitude, (b) rise time, (c) maximum gust variation, and (d) lapse time. Wind turbine structural loads caused by gusts are affected by these four factors.
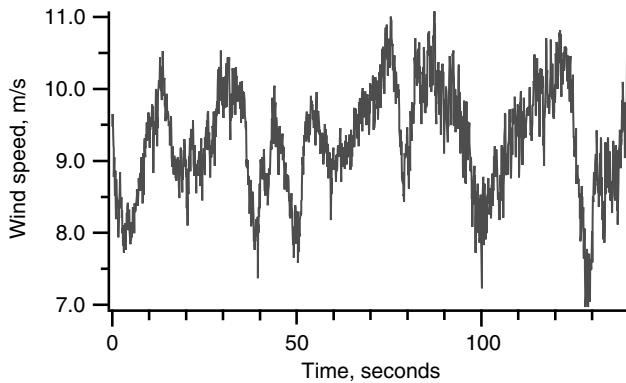
Figure 2.9   Typical plot of wind speed vs. time for a short period
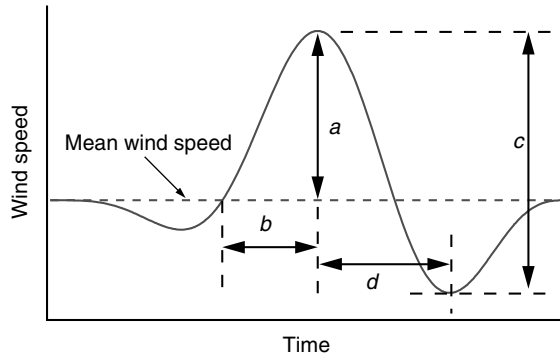
Figure 2.10 Illustration of a discrete gust event; *a*, amplitude; *b*, rise time; *c*, maximum gust variation; *d*, lapse time

2.2.2.2 Variations due to Location and Wind Direction

Variations due to Location

Wind speed is also very dependent on local topographical and ground cover variations. For example, as shown in Figure 2.11 (Hiester and Pennell, 1981), differences between two sites close to each other can be significant. The graph shows monthly and five-year mean wind speeds for two sites 21 km apart. The five-year average mean wind speeds differ by about 12% (4.75 and 4.25 m/s annual averages).

Variations in Wind Direction

Wind direction also varies over the same time scales over which wind speeds vary. Seasonal variations may be small, on the order of 30 degrees, or the average monthly winds may change direction by 180 degrees over a year. Short-term direction variations are the result of the turbulent nature of the wind. These short-term variations in wind direction need to be
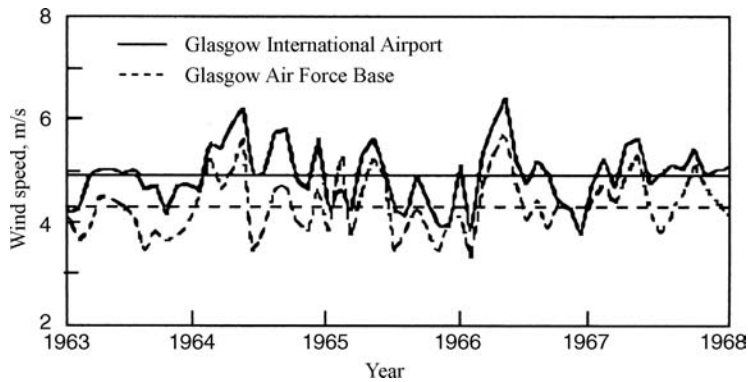
Figure 2.11 Time series of monthly wind speeds for Glasgow, Montana International Airport and Air Force Base (AFB) (Hiester and Pennell, 1981)

considered in wind turbine design and siting. Horizontal axis wind turbines must rotate (yaw) with changes in wind direction. Yawing causes gyroscopic loads throughout the turbine structure and exercises any mechanism involved in the yawing motion. Crosswinds due to changes in wind direction affect blade loads. Thus, as will be discussed later, short-term variations in wind direction and the associated motion affect the fatigue life of components such as blades and yaw drives.

2.2.3 Estimation of Potential Wind Resource

In this section the available potential of the wind resource and its power production capabilities via wind turbines will be summarized.

2.2.3.1 Available Wind Power

As illustrated in Figure 2.12, one can determine the mass flow of air, dm/dt, through a rotor disc of area A. From the continuity equation of fluid mechanics, the mass flow rate is a function of air density, ρ, and air velocity (assumed uniform), U, and is given by:

$$\frac{dm}{dt} = \rho A U \tag{2.6}$$

The kinetic energy per unit time, or power, of the flow is given by:

$$P = \frac{1}{2}\frac{dm}{dt}U^2 = \frac{1}{2}\rho A U^3 \tag{2.7}$$

The wind power per unit area, P/A or wind power density is:

$$\frac{P}{A} = \frac{1}{2}\rho U^3 \tag{2.8}$$

One should note that:

- The wind power density is proportional to the density of the air. For standard conditions (sea-level, $15\,^{\circ}C$) the density of air is 1.225 kg/m^3.
- Power from the wind is proportional to the area swept by the rotor (or the rotor diameter squared for a conventional horizontal axis wind machine).
- The wind power density is proportional to the cube of the wind velocity.

The actual power production potential of a wind turbine must take into account the fluid mechanics of the flow passing through a power-producing rotor, and the aerodynamics and
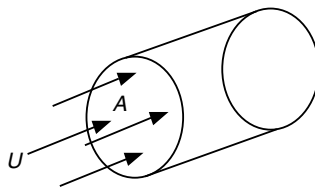
Figure 2.12 Flow of air through a rotor disc; A, area; U, wind velocity

Table 2.1 Power per unit area available from steady wind (air density $= 1.225 \, \text{kg/m}^3$)

Wind speed (m/s)	Power/area (W/m^2)
0	0
5	80
10	610
15	2070
20	4900
25	9560
30	16 550

efficiency of the rotor/generator combination. In practice, a maximum of about 45% of the available wind power is harvested by the best modern horizontal axis wind turbines (this will be discussed in Chapter 3).

Table 2.1 shows that the wind velocity is an important parameter and significantly influences the power per unit area available from the wind.

If annual average wind speeds are known for certain regions, one can develop maps that show average wind power density over these regions. More accurate estimates can be made if hourly averages, U_i, are available for a year. Then, the average of power estimates for each hour can be determined. The average wind power density, based on hourly averages, is:

$$\overline{P}/A = \frac{1}{2} \rho \overline{U}^3 K_e \tag{2.9}$$

where $\overline{U}$ is the annual average wind speed and K_e is called the energy pattern factor. The energy pattern factor is calculated from:

$$K_e = \frac{1}{N\overline{U}^3} \sum_{i=1}^{N} U_i^3 \tag{2.10}$$

where N is the number of hours in a year, 8760.

Some sample qualitative magnitude evaluations of the wind resource are:

$$\overline{P}/A < 100 \, \text{W/m}^2 - \text{low}$$
$$\overline{P}/A \approx 400 \, \text{W/m}^2 - \text{good}$$
$$\overline{P}/A > 700 \, \text{W/m}^2 - \text{great}$$

2.2.3.2 Estimates of Worldwide Resource

Based on wind resource data and an estimate of the real efficiency of actual wind turbines, numerous investigators have made estimates of the wind power potential of regions of the earth and of the entire earth itself. It will be shown in Chapter 3 that the maximum power-producing potential that can be theoretically realized from the kinetic energy contained in the wind is about 60% of the available power.

Using estimates for regional wind resources, one can estimate the (electrical) power-producing potential of wind energy. It is important to distinguish between the different types

of wind energy potential that can be estimated. One such estimate (World Energy Council, 1993) identified the following five categories:

(1) **Meteorological potential.** This is equivalent to the available wind resource.
(2) **Site potential.** This is based on the meteorological potential, but is restricted to those sites that are geographically available for power production.
(3) **Technical potential.** The technical potential is calculated from the site potential, accounting for the available technology.
(4) **Economic potential.** The economic potential is the technical potential that can be realized economically.
(5) **Implementation potential.** Implementation potential takes into account constraints and incentives to assess the wind turbine capacity that can be implemented within a certain time frame.

For worldwide wind resource assessments, at least the first three categories have been considered. For example, one of the earliest global wind energy resource assessments was carried out by Gustavson (1979). In this study Gustavson based his resource estimate on the input of the solar energy reaching the earth and how much of this energy was transformed into useful wind energy. On a global basis, his estimate was that the global resource was about 1000×10^{12} kWh/yr. In comparison, the global consumption of electricity at that time was about 55×10^{12} kWh/yr.

The World Energy Council (1993), using a world average estimate for the meteorological potential of wind energy and including machine efficiency and availability (percentage of time on line), made a global estimate of the wind resource. They estimated that the onshore wind power resource was about 20×10^{12} kWh/yr, still a considerable resource. More recent work on the world technical and economic potential of onshore wind energy is summarized in the paper of Hoogwijk *et al.* (2004). These authors conclude that, with present technology, the onshore technical potential of wind is about 6–7 times the world's electrical consumption (in 2001).

Numerous wind resource estimates have been made for the potential of wind energy in the United States. The estimates published in the 1990s are much more realistic than earlier ones, since they feature practical assumptions about machine characteristics and land exclusions (technical and site potential considerations). They also feature expanded data collection methods and improved analysis techniques. Elliot *et al.* (1991) used this type of improved analysis in conjunction with US wind resource data (Elliot *et al.* 1987). Their work concluded that wind energy could supply at least 20% of the US electrical needs, assuming that wind energy could be exploited in locations where the average wind speed was at least 7.3 m/s (16 mph) at a height of 30 m. In order to provide this fraction of the US electrical demand (about 600 billion kWh per year), 0.6% of the land (about 18 000 square miles) in the lower 48 states would have to be developed. The majority of this land was in the West, however, and far from major population centers. Therefore, the actual use of this land involves other siting considerations such as transmission line access.

As noted in Volume 1 of *Wind Energy: The Facts* (EWEA, 2004), there are a few estimates of the onshore wind potential of Europe, and those that exist make assumptions which are conservative in light of present wind system technology. For example, EWEA estimated (based on a 1993 study) that the technical potential for Europe (EU-15 and Norway) was about 0.65×10^{12} kWh/yr. For offshore wind farms, they also summarize predictions that range from

0.5 to about 3×10^{12} kWh/yr. Furthermore, this reference noted that an estimate of the potential wind resource is not a fixed quantity and that it changes over time as the technology develops and also as more is learned about the environmental and social considerations which influence the density and location of turbine deployment. As an example of this statement they show that (primarily due to increases in turbine size) one estimate of the 'practical' resource for Europe almost doubled from 1994 to 1997.

2.3 Characteristics of the Atmospheric Boundary Layer

The atmospheric boundary layer, also known as the planetary boundary layer, is the lowest part of the atmosphere and its characteristics are directly influenced by contact with the earth's surface. Here, physical quantities such as velocity, temperature, and relative humidity can change rapidly in space and time. For example, an important parameter in the characterization of the wind resource is the variation of horizontal wind speed with height above the ground. One would expect the horizontal wind speed to be zero at the earth's surface and to increase with height in the atmospheric boundary layer. This variation of wind speed with elevation is called the vertical profile of the wind speed or vertical wind shear. In wind energy engineering the determination of vertical wind shear is an important design parameter since: (1) it directly determines the productivity of a wind turbine on a tower of certain height, and (2) it can strongly influence the lifetime of a turbine rotor blade . Rotor blade fatigue life is influenced by the cyclic loads resulting from rotation through a wind field that varies in the vertical direction.

There are at least two basic problems of interest with the determination of vertical wind profiles for wind energy applications:

- Instantaneous variation in wind speeds as a function of height (e.g., time scale on the order of seconds).
- Seasonal variation in average wind speeds as a function of height (e.g., monthly or annual averages).

It should be noted that these are separate and distinct problems, and it is often erroneously assumed that a single methodology can be applied to both of them. That is, the variation of 'instantaneous' profiles is related via the similarity theory of boundary layers (Schlichting, 1968). On the other hand, the changes in long-term averages as a function of height are related to the statistics of occurrence of various influencing factors, such as atmospheric stability (discussed next), and must rely on a more empirical approach (Justus, 1978).

In addition to variations due to the atmospheric stability, the variation of wind speed with height depends on surface roughness and terrain. These factors will be discussed in the next sections.

2.3.1 Atmospheric Density and Pressure

As demonstrated in Equation (2.8), the power in the wind is a function of air density. Air density, ρ, is a function of temperature, T, and pressure, p, both of which vary with height. The density of dry air can be determined by applying the ideal gas law, which can be expressed as:

$$\rho = \frac{p}{RT} = 3.4837 \frac{p}{T} \qquad (2.11)$$

where the density is in kg/m^3, the pressure is in kPa (kN/m^2), and the temperature is in Kelvin. Moist air is slightly less dense than dry air, but corrections for air moisture are rarely used. Air density as a function of moisture content can be found in numerous books on thermodynamics such as Balmer (1990).

The international standard atmosphere assumes that the sea-level temperature and pressure are 288.15 K and 101.325 kPa, resulting in a standard sea-level density of 1.225 kg/m^3 (see Avallone and Baumeister, 1978). Air pressure decreases with elevation above sea level. The pressure in the international standard atmosphere up to an elevation of 5000 m is very closely approximated by:

$$p = 101.29 - (0.011837)\,z + \left(4.793 \times 10^{-7}\right)z^2 \tag{2.12}$$

where z is the elevation in meters and the pressure is in kPa. Of course, the actual pressure may vary about the standard pressure as weather patterns change. In practice, at any location, the daily and seasonal temperature fluctuations have a much greater effect on air density than do daily and seasonal changes in pressure and air moisture.

2.3.2 Stability of the Atmospheric Boundary Layer

A particularly important characteristic of the atmosphere is its stability – the tendency to resist vertical motion or to suppress existing turbulence. The stability of the atmospheric boundary layer is a determining factor for the wind speed gradients (e.g. wind shear) that are experienced in the first few hundred meters above the ground. Atmospheric stability is usually classified as stable, neutrally stable, or unstable. The stability of the earth's atmosphere is governed by the vertical temperature distribution resulting from the radiative heating or cooling of its surface and the subsequent convective mixing of the air adjacent to the surface. A summary of how the atmospheric temperature changes with elevation (assuming an adiabatic expansion) follows.

2.3.2.1 Lapse Rate

The lapse rate of the atmosphere is generally defined as the rate of change of temperature with height. As will be shown in the following analysis, it is easier to determine the lapse rate by calculating the change in pressure with height and using conventional thermodynamic relationships. If the atmosphere is approximated as a dry (no water vapor in the mixture) ideal gas, the relationship between a change in pressure and a change in elevation for a fluid element in a gravitational field is given by:

$$dp = -\rho g \, dz \tag{2.13}$$

where p = atmospheric pressure, ρ = atmospheric density, z = elevation above ground, and g = local gravitational acceleration (assumed constant here).

The negative sign results from the convention that height, z, is measured positively upward, and that the pressure, p, decreases in the positive z direction.

The first law of thermodynamics for an ideal gas closed system of unit mass undergoing a quasi-static change of state is given by:

$$dq = du + p\,dv = dh - v\,dp = c_p dT - \frac{1}{\rho}dp \tag{2.14}$$

where T = temperature, q = heat transferred, u = internal energy, h = enthalpy, v = specific volume, c_p = constant pressure specific heat.

For an adiabatic process (no heat transfer) $dq = 0$, and Equation (2.12) becomes:

$$c_p dT = \frac{1}{\rho} dp \tag{2.15}$$

Substitution for dp in Equation (2.13) and rearrangement gives:

$$\left(\frac{dT}{dz}\right)_{Adiabatic} = g\frac{1}{c_p} \tag{2.16}$$

If the changes in g and c_p with elevation are assumed negligible, then the change in temperature, under adiabatic conditions, is a constant. Using $g = 9.81$ m/s^2 and $c_p = 1.005$ kJ/kg K yields:

$$\left(\frac{dT}{dz}\right)_{Adiabatic} = -\frac{0.0098\,^{\circ}C}{m} \tag{2.17}$$

Thus, the rate that temperature decreases with an increase in height for a system with no heat transfer is about 1 °C per 100 m and is known as the dry adiabatic lapse rate. Using conventional nomenclature, the lapse rate, Γ, is defined as the negative of the temperature gradient in the atmosphere. Therefore, the dry adiabatic lapse rate is given by:

$$\Gamma = -\left(\frac{dT}{dz}\right)_{Adiabatic} \approx \frac{1\,^{\circ}C}{100\,m} \tag{2.18}$$

The dry adiabatic lapse rate is extremely important in meteorological studies since a comparison of its value to the actual lapse rate in the lower atmosphere is a measure of the stability of the atmosphere.

For comparative purposes, the international standard atmospheric lapse rate, based on meteorological data, has been defined and adopted. Specifically, on the average, in the middle latitudes, the temperature decreases linearly with elevation up to about 10 000 m (for definition purposes 10.8 km). The temperature averages 288 °K at sea level and decreases to 216.7 °K at 10.8 km, giving the standard temperature gradient as:

$$\left(\frac{dT}{dz}\right)_{Standard} = \frac{(216.7 - 288)\,^{\circ}C}{10\,800\,m} = -\frac{0.0066\,^{\circ}C}{m} \tag{2.19}$$

Thus, the standard lapse rate, based on international convention, is 0.66 °C/100 m.

Different temperature gradients create different stability states in the atmosphere. Figure 2.13 illustrates that the temperature profiles change from day to night due to heating of the earth's surface. The temperature profile before sunrise (the solid line) decreases with increasing height near the ground and reverses after sunrise (dashed line). The air is heated near the ground, and the temperature gradient close to the earth's surface increases with height, up to height z_i (called the inversion height). The surface layer of air extending to z_i is called the convective or mixing layer. Above z_i the temperature profile reverses.

The concept of atmospheric stability is illustrated by considering the upward displacement of a small element of air to an altitude with a lower ambient pressure. Assume the standard rate of 0.66 °C/100 m. The small element of air being lifted in this example will cool at the dry
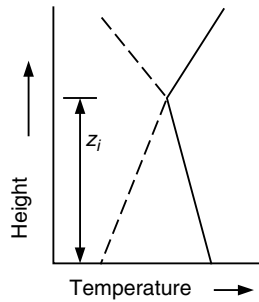
Figure 2.13 Temperature profile above the earth's surface, before (solid) and after (dashed) sunrise

adiabatic lapse rate (1 °C per 100 m). If the test element of air had the same temperature as the surrounding air at the start, then after it had been raised 100 m, it would have cooled faster than the surrounding air and would be 0.34 °C cooler than its surroundings. The sample would be denser and would tend to return to its original level. This atmospheric state is called stable.

To generalize, any atmosphere whose dT/dz is greater than $(dT/dz)_{adiabatic}$ is a stable one. One should note that the standard international lapse rate seldom occurs in nature. This explains the need for the daily balloon soundings taken at major airports worldwide to determine the actual lapse rate. Also, in order to have stability, it is not necessary for an inversion (increase of temperature with height) to exist. When one does exist, however, the atmosphere is even more stable.

2.3.3 Turbulence

Turbulence in the wind is caused by dissipation of the wind's kinetic energy into thermal energy via the creation and destruction of progressively smaller eddies (or gusts). Turbulent wind may have a relatively constant mean over time periods of an hour or more, but over shorter times (minutes or less) it may be quite variable. The wind's variability superficially appears to be quite random, but actually it has distinct features. These features are characterized by a number of statistical properties:

- turbulence intensity;
- wind speed probability density function;
- autocorrelation;
- integral time scale/length scale;
- power spectral density function.

A summary and examples of these properties follows. More details concerning them are given in Appendix C and in the texts of Rohatgi and Nelson (1994) and Bendat and Piersol (1993).

Turbulent wind consists of longitudinal, lateral, and vertical components. The longitudinal component, in the prevailing wind direction, is designated $u(z,t)$. The lateral component (perpendicular to U) is $v(z,t)$ and the vertical component is $w(z,t)$. Each component is frequently conceived of as consisting of a short-term mean wind, for example, U, with a

superimposed fluctuating wind of zero mean, $\tilde{u}$, added to it, thus:

$$u = U + \tilde{u} \tag{2.20}$$

where $u =$ instantaneous longitudinal wind speed, $z =$ height above ground, and $t =$ time. The lateral and vertical components can be decomposed into a mean and a fluctuating component in a similar manner. For the sake of clarity, the dependency on height above ground and time will not be shown explicitly in subsequent equations.

Note that the short-term mean wind speed, in this case U, refers to mean wind speed averaged over some (short) time period, Δt, longer than the characteristic time of the fluctuations in the turbulence. This time period is usually taken to be ten minutes, but can be as long as an hour. In equation form:

$$U = \frac{1}{\Delta t} \int_0^{\Delta t} u \, dt \tag{2.21}$$

Instantaneous turbulent wind is not actually observed continuously; it is actually sampled at some relatively high rate. Assuming that the sample interval is δt, such that $\Delta t = N_s \delta t$ where $N_s =$ number of samples during each short-term interval, then turbulent wind can be expressed as a sequence, u_i. The short-term mean wind speed can then be expressed in sampled form as:

$$U = \frac{1}{N_s} \sum_{i=1}^{N_s} u_i \tag{2.22}$$

The short-term average longitudinal wind speed, U, is the one most often used in time series observations and will be used henceforth in this text in that way.

2.3.3.1 Turbulence Intensity

The most basic measure of turbulence is the turbulence intensity. It is defined by the ratio of the standard deviation of the wind speed to the mean wind speed. In this calculation both the mean and standard deviation are calculated over a time period longer than that of the turbulent fluctuations, but shorter than periods associated with other types of wind speed variations (such as diurnal effects). The length of this time period is normally no more than an hour, and by convention in wind energy engineering it is usually equal to ten minutes. The sample rate is normally at least once per second (1 Hz). The turbulence intensity, TI, is defined by:

$$TI = \frac{\sigma_u}{U} \tag{2.23}$$

where σ_u is the standard deviation, given in sampled form by:

$$\sigma_u = \sqrt{\frac{1}{N_s - 1} \sum_{i=1}^{N_s} (u_i - U)^2} \tag{2.24}$$

Turbulence intensity is frequently in the range of 0.1 to 0.4. In general, the highest turbulence intensities occur at the lowest wind speeds, but the lower limiting value at a given location will depend on the specific terrain features and surface conditions at the site. Figure 2.14 illustrates a graph of a typical segment of wind data sampled at 8 Hz. The data
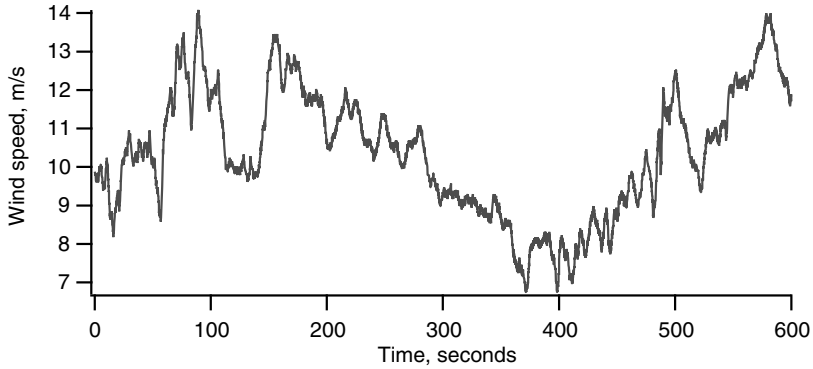
Figure 2.14   Sample wind data

has a mean of 10.4 m/s and a standard deviation of 1.63 m/s. Thus, the turbulence intensity, over the ten-minute period, is 0.16.

2.3.3.2 Wind Speed Probability Density Functions

The likelihood that the wind speed has a particular value can be described in terms of a probability density function (pdf). Experience has shown that the wind speed is more likely to be close to the mean value than far from it, and that it is nearly as likely to be below the mean as above it. The probability density function that best describes this type of behavior for turbulence is the Gaussian, or normal, distribution. The normal probability density function for continuous data in terms of the variables used here is given by:

$$p(u) = \frac{1}{\sigma_u \sqrt{2\pi}} \exp\left[-\frac{(u-U)^2}{2\sigma_u^2} \right] \tag{2.25}$$

Figure 2.15 illustrates a histogram of the wind speeds about the mean wind speed in the sample data above (Figure 2.14). The Gaussian probability density function that represents the
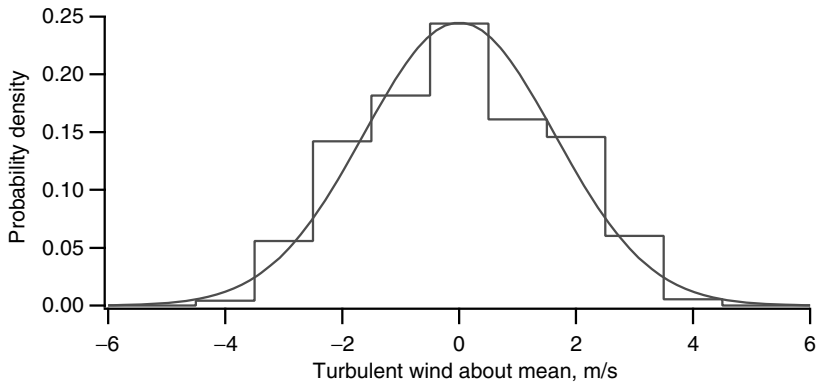
Figure 2.15   Gaussian probability density function and histogram of wind data
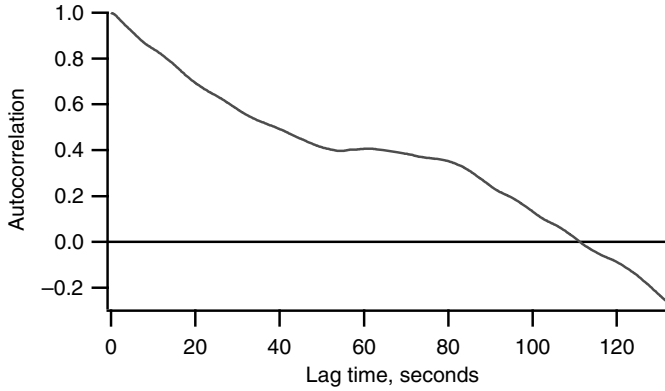
Figure 2.16   Autocorrelation function of sample wind data

data is superimposed on the histogram. (Note: see Section 2.5 for general discussion of histograms and statistical analysis of wind data.)

2.3.3.3 Autocorrelation

The probability density function of the wind speed provides a measure of the likelihood of particular values of wind speed. As described in Appendix C, the normalized autocorrelation function for sampled turbulent wind speed data is given by:

$$R(r\,\delta t) = \frac{1}{\sigma_u^2(N_s-r)} \sum_{i=1}^{N_s-r} u_i\, u_{i+r} \tag{2.26}$$

where $r=$ lag number. Figure 2.16 shows a graph of the autocorrelation function of the data presented above in Figure 2.14.

The autocorrelation function can be used to determine the integral time scale of turbulence as described below.

2.3.3.4 Integral Time Scale/Length Scale

The autocorrelation function will, if any trends are removed before starting the process, decay from a value of 1.0 at a lag of zero to a value of zero, and will then tend to take on small positive or negative values as the lag increases. A measure of the average time over which wind speed fluctuations are correlated with each other is found by integrating the autocorrelation from zero lag to the first zero crossing. The single resulting value is known as the integral time scale of the turbulence. While typical values are less than ten seconds, the integral time scale is a function of the site, atmospheric stability, and other factors and may be significantly greater than ten seconds. Gusts are relatively coherent (well correlated) rises and falls in the wind, and have characteristic times on the same order as the integral time scale.

Multiplying the integral time scale by the mean wind velocity gives the integral length scale. The integral length scale tends to be more constant over a range of wind speeds than is the integral time scale, and thus is somewhat more representative of a site.

Based on the autocorrelation function illustrated above, the integral time scale is 50.6 seconds. The mean wind velocity is 10.4 m/s. Thus, the size of the turbulent eddies in the mean flow, or the integral length scale, is on the order of 526 m.

2.3.3.5 Power Spectral Density Function

The fluctuations in the wind can be thought of as resulting from a composite of sinusoidally varying winds superimposed on the mean steady wind. These sinusoidal variations will have a variety of frequencies, amplitudes, and phases. The term 'spectrum' is used to describe functions of frequency. Thus, the function that characterizes turbulence as a function of frequency is known as a 'spectral density' function. Since the average value of any sinusoid is zero, the amplitudes are characterized in terms of their mean square values. This type of analysis originated in electrical power applications, where the square of the voltage or current is proportional to the power. The complete name for the function describing the relation between frequency and amplitudes of sinusoidally varying waves making up the fluctuating wind speed is therefore 'power spectral density'.

There are two points of particular importance to note regarding power spectral densities (psds). The first is that the average power in the turbulence over a range of frequencies may be found by integrating the psd between the two frequencies. Secondly, the integral over all frequencies is equal to the total variance.

Power spectral densities are often used in dynamic analyses. A number of power spectral density functions are used as models in wind energy engineering when representative turbulence power spectral densities are unavailable for a given site. A suitable model that is similar to the one developed by von Karman for turbulence in wind tunnels (Freris, 1990) is given by Equation (2.27). This is referred to as the von Karman psd elsewhere in this text.

$$S(f) = \frac{\sigma_u^2 4(L/U)}{\left[1 + 70.8(f\,L/U)^2\right]^{5/6}} \tag{2.27}$$

where f is the frequency (Hz), L is the integral length scale, and U is the mean wind speed at the height of interest. Other psds are also used in wind engineering applications (see the discussion of standards in Chapter 7). In addition, Appendix C gives details of how to determine psds.

The power spectral density of the sample wind data above is illustrated in Figure 2.17. The graph also includes the von Karman power spectral density function described above for comparison.

2.3.4 The Steady Wind: Wind Speed Variation with Height

As shown in Figure 2.18 (van der Tempel, 2006), real wind velocity varies in space and time. The actual wind speed, at any location, also varies in time and direction around its mean value due to the effect of turbulence. Of most importance here, this figure clearly shows that the mean wind speed increases with height, which defines the phenomenon called wind shear.
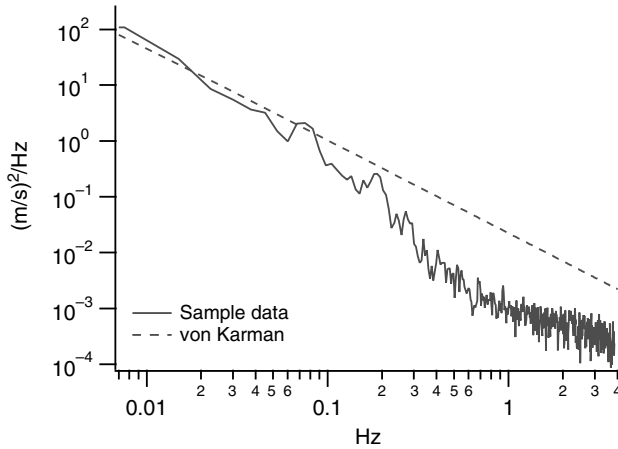
Figure 2.17   Wind data power spectral density functions

Wind shear influences both the assessment of wind resources and the design of wind turbines. First, the assessment of wind resources over a wide geographical area might require that the anemometer data from a number of sources be corrected to a common elevation. Second, from a design aspect, rotor blade fatigue life will be influenced by the cyclic loads resulting from rotation through a wind field that varies in the vertical direction. Thus, a model of the wind speed variation with height is required in wind energy applications. The summary that follows will present some of the current models that are used to predict the variation in wind speed with elevation above ground.

In wind energy studies, two mathematical models or 'laws' have generally been used to model the vertical profile of wind speed over regions of homogenous, flat terrain (e.g., fields, deserts, and prairies). The first approach, the log law, has its origins in boundary layer flow in fluid mechanics and in atmospheric research. It is based on a combination of theoretical and
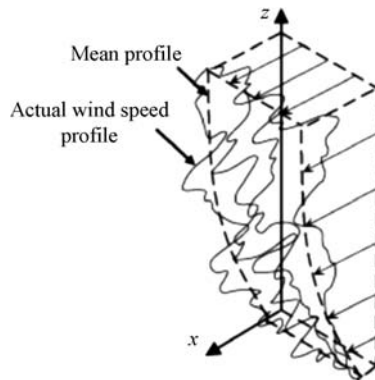
Figure 2.18   Experimental speed profile (van der Tempel, 2006)

empirical research. The second approach, used by many wind energy researchers, is the power law. Both approaches are subject to uncertainty caused by the variable, complex nature of turbulent flows (Hiester and Pennell, 1981). A summary of each of these laws and their general application follows.

2.3.4.1 Logarithmic Profile (Log Law)

Although there are a number of ways to arrive at a prediction of a logarithmic wind profile (e.g., mixing length theory, eddy viscosity theory, and similarity theory), a mixing length type analysis given by Wortman (1982) is summarized here.

Near the surface of the earth the momentum equation reduces to:

$$\frac{\partial p}{\partial x} = \frac{\partial}{\partial z} \tau_{xz} \tag{2.28}$$

where x and z are the horizontal and vertical coordinates, p is the pressure, and τ_{xz} is the shear stress in the direction of x whose normal coincides with z.

In this region the pressure is independent of z and integration yields:

$$\tau_{xz} = \tau_0 + z \frac{\partial p}{\partial x} \tag{2.29}$$

where τ_0 is the surface value of the shear stress. Near the surface the pressure gradient is small, so the second term on the right-hand side may be neglected. Also, using the Prandtl mixing length theory, the shear stress may be expressed as:

$$\tau_{xz} = \rho \ell^2 \left(\frac{\partial U}{\partial z}\right)^2 \tag{2.30}$$

where ρ is the density of the air, U the horizontal component of velocity, and ℓ the mixing length. Note that U is used here, signifying that the effects of turbulence have been averaged out.

Combining Equations (2.29) and (2.30) gives:

$$\frac{\partial U}{\partial z} = \frac{1}{\ell} \sqrt{\frac{\tau_0}{\rho}} = \frac{U^*}{\ell} \tag{2.31}$$

where $U^* = \sqrt{\frac{\tau_0}{\rho}}$ is defined as the friction velocity.

If one assumes a smooth surface, $\ell = k\,z$, with $k = 0.4$ (von Karman's constant), then Equation (2.31) can be integrated directly from z_0 to z where z_0 is the surface roughness length, which characterizes the roughness of the ground terrain. This yields:

$$U(z) = \frac{U^*}{k} \ln\left(\frac{z}{z_0}\right) \tag{2.32}$$

This equation is known as the logarithmic wind profile.

The integration is from the lower limit of z_0 instead of 0 because natural surfaces are never uniform and smooth. Table 2.2 gives some approximate surface roughness lengths for various terrain types.

Table 2.2 Values (approximate) of surface roughness length for various types of terrain

Terrain description	z_0 (mm)
Very smooth, ice or mud	0.01
Calm open sea	0.20
Blown sea	0.50
Snow surface	3.00
Lawn grass	8.00
Rough pasture	10.00
Fallow field	30.00
Crops	50.00
Few trees	100.00
Many trees, hedges, few buildings	250.00
Forest and woodlands	500.00
Suburbs	1500.00
Centers of cities with tall buildings	3000.00

Equation (2.32) can also be written as:

$$\ln(z) = \left(\frac{k}{U^*}\right)U(z) + \ln(z_0) \tag{2.33}$$

This equation can be plotted as a straight line on a semilog graph. The slope of this graph is k/U^*, and from a graph of experimental data, U^* and z_0 can be calculated. The log law is often used to extrapolate wind speed from a reference height, z_r, to another level using the following relationship:

$$U(z)/U(z_r) = \ln\left(\frac{z}{z_0}\right) \bigg/ \ln\left(\frac{z_r}{z_0}\right) \tag{2.34}$$

Sometimes, the log law is modified to consider mixing at the earth's surface, by expressing the mixing length as $\ell = k(z + z_0)$. When this is used, the log profile becomes:

$$U(z) = \frac{U^*}{k}\ln\left(\frac{z + z_0}{z_0}\right) \tag{2.35}$$

2.3.4.2 Power Law Profile

The power law represents a simple model for the vertical wind speed profile. Its basic form is:

$$\frac{U(z)}{U(z_r)} = \left(\frac{z}{z_r}\right)^\alpha \tag{2.36}$$

where $U(z)$ is the wind speed at height z, $U(z_r)$ is the reference wind speed at height z_r, and α is the power law exponent.

Early work on this subject showed that under certain conditions α is equal to 1/7, indicating a correspondence between wind profiles and flow over flat plates (see Schlichting, 1968). In practice, the exponent α is a highly variable quantity.

Table 2.3 Effect of α on estimates of wind power density at higher elevations

	$\alpha = 0.1$	1/7	0.3
U_{30m} (m/s)	5.58	5.85	6.95
P/A (W/m^2)	106.4	122.6	205.6
% increase over 10 m	39.0	62.2	168.5

The following example emphasizes the importance of a variation in α.

If $U_0 = 5$ m/s at 10 m, what are U and P/A at 30 m? Note that at 10 m, $P/A = 75.6$ W/m^2. The wind velocity at 30 m is set out in Table 2.3 for three different values of α, and P/A is calculated assuming $\rho = 1.225$ kg/m^3.

It has been found that α varies with such parameters as elevation, time of day, season, nature of the terrain, wind speed, temperature, and various thermal and mechanical mixing parameters. Some researchers have developed methods for calculating α from the parameters in the log law. Many researchers, however, feel that these complicated approximations reduce the simplicity and applicability of the general power law and that wind energy specialists should accept the empirical nature of the power law and choose values of α that best fit available wind data. A review of a few of the more popular empirical methods for determining representative power law exponents follows.

Correlation for the Power Law Exponent as a Function of Velocity and Height

One way of handling this type of variation was proposed by Justus (1978). His expression has the form:

$$\alpha = \frac{0.37 - 0.088 \ln\left(U_{ref}\right)}{1 - 0.088 \ln\left(\frac{z_{ref}}{10}\right)} \tag{2.37}$$

where U is given in m/s and z_{ref} in m.

Correlation Dependent on Surface Roughness

The following form for this type of correlation was proposed by Counihan (1975):

$$\alpha = 0.096 \log_{10} z_0 + 0.016 (\log_{10} z_0)^2 + 0.24 \tag{2.38}$$

for 0.001 m $< z_0 < 10$ m, where z_0 represents the surface roughness in m (see Table 2.2 for example values).

Correlations Based on Both Surface Roughness (z_0) and Velocity

Wind researchers at NASA proposed equations for α based on both surface roughness and the wind speed at the reference elevation, U_{ref} (see Spera, 1994).

2.3.4.3 Comparison of Predicted Velocity Profiles with Actual Data

The importance of characterizing the variation in wind speed with elevation, or wind shear, at a given site for a utility-scale wind turbine cannot be overemphasized. That is, such a characterization is needed for an accurate prediction of power output, and it is essential for

wind power developers to accurately know the wind speed characteristics at turbine hub height (generally between 60 to 100 m) – and across the rotor.

Recent work on this subject (e.g., see Elkinton *et al.*, 2006), which has included the use of tall-tower wind data sets, has shown that there is no significant difference between the performance of the log and power laws to predict wind shear; and, under some circumstances, using either may give inaccurate predictions of hub-height mean wind speeds. This conclusion was based on the use of experimental data sets from: (1) flat terrain with no trees, (2) hilly terrain with no trees, and (3) forested terrain . For these three types of terrain, these investigators found that the difference between the predicted hub-height (50 m) wind speed and the experimentally measured value ranged from about 1% to a maximum value of 13%.

In practice, one should recognize that wind shear changes with a number of variables including:

- atmospheric stability;
- surface roughness;
- changes in surface conditions;
- terrain shape.

Thus, wind shear extrapolation may have a large uncertainty because the wind shear models do not always characterize reality.

2.3.5 *Effect of Terrain on Wind Characteristics*

The importance of terrain features on wind characteristics is discussed in various siting handbooks for wind systems (see Troen and Petersen, 1989; Hiester and Pennell, 1981; and Wegley *et al.*, 1980). Some of the effects of terrain include velocity deficits, unusual wind shear, and wind acceleration. The influence of terrain features on the energy output from a turbine may be so great that the economics of the whole project may depend on the proper selection of the site.

In the previous section, two methods were described (log profile and power law profile laws) for modeling the vertical wind speed profile. These were developed for flat and homogenous terrain. One can expect that any irregularities on the earth's surface will modify the wind flow, thus compromising the applicability of these prediction tools. This section presents a qualitative discussion of a few of the more important areas of interest on the subject of terrain effects.

2.3.5.1 Classification of Terrain

The most basic classification of terrain divides it into flat and non-flat terrain. Many authors define non-flat terrain as complex terrain (this is defined as an area where terrain effects are significant on the flow over the land area being considered). Flat terrain is terrain with small irregularities such as forest, shelter belts, etc. (see Wegley *et al.*, 1980). Non-flat terrain has large-scale elevations or depressions such as hills, ridges, valleys, and canyons. To qualify as flat terrain, the following conditions must hold. Note that some of these rules include wind turbine geometry:

- Elevation differences between the wind turbine site and the surrounding terrain are not greater than about 60 m anywhere in an 11.5 km diameter circle around the turbine site.
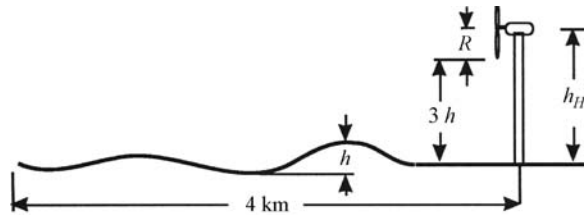
Figure 2.19 Determination of flat terrain (Wegley *et al.*, 1980)

- No hill has an aspect ratio (height to width) greater than 1/50 within 4 km upstream and downstream of the site.
- The elevation difference between the lower end of the rotor disc and the lowest elevation on the terrain is greater than three times the maximum elevation difference (h) within 4 km upstream (see Figure 2.19).

Non-flat or complex terrain, according to Hiester and Pennell (1981), consists of a great variety of features, and one generally uses the following subclassifications: (1) isolated elevation or depression, and (2) mountainous terrain. Flow conditions in mountainous terrain are complex because the elevations and depressions occur in a random fashion. Flow in such terrain is divided into two classifications: small and large scales. The distinction between the two is made with comparison to the planetary boundary layer, which is assumed to be about 1 km. That is, a hill of a height which is a small fraction of the planetary boundary layer (approximately 10%) is considered to have small-scale terrain features.

An important point to be made here is that information on wind direction should be considered when defining the terrain classification. For example, if an isolated hill (200 m high and 1000 m wide) were situated 1 km south of a proposed site, the site could be classified as non-flat. If, however, the wind blows only 5% of the time from this direction with a low average speed, say 2 m/s, then this terrain should be classified as flat.

2.3.5.2 Flow Over Flat Terrain with Obstacles

Flow over flat terrain with man-made and natural obstacles has been studied extensively. Man-made obstacles are defined as buildings, silos, etc. Natural obstacles include rows of trees, shelter belts, etc. For man-made obstacles, a common approach is to consider the obstacle to be a rectangular block and to consider the flow to be two-dimensional. This type of flow, shown in Figure 2.20, produces a momentum wake, and, as illustrated, a free shear layer that
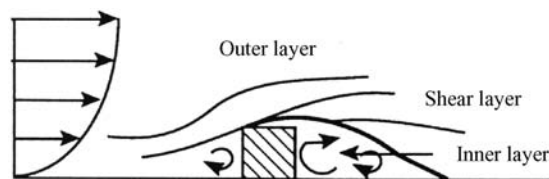
Figure 2.20 Schematic of a momentum wake (Rohatgi and Nelson, 1994). Reproduced by permission of Alternative Energy Institute
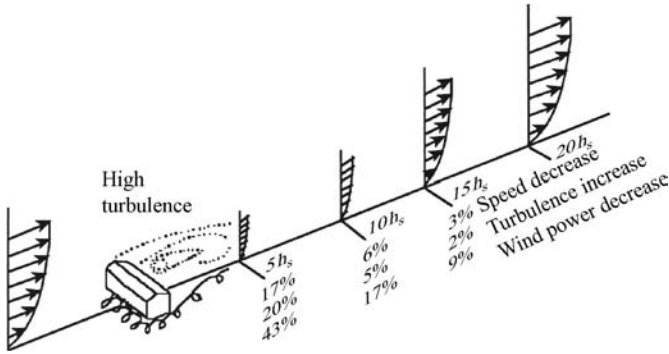
Figure 2.21   Speed, power, and turbulence effects downstream of a building (Wegley *et al.*, 1980)

separates from the leading edge and reattaches downwind, forming a boundary between an inner recirculating flow region (eddy) and the outer flow region.

The results of an attempt to quantify data from man-made obstacles are shown in Figure 2.21, where the change in available power and turbulence is shown in the wake of a sloped-roof building. Note that the estimates in the figure apply at a level equal to one building height, h_S, above the ground, and that power losses become small downwind of the building after a distance equal to 15 h_S.

2.3.5.3 Flow in Flat Terrain with a Change in Surface Roughness

In most natural terrain, the surface of the earth is not uniform and changes significantly from location to location. This affects the local wind profile. For example, Figure 2.22 shows that the downwind profile changes significantly in going from a smooth to a rough surface.

2.3.5.4 Characteristics of Non-flat Terrain: Small-scale Features

Researchers (Hiester and Pennell, 1981) have divided non-flat terrain into isolated and mountainous terrain, in which the first refers to terrain of small-scale features and the latter refers to large-scale features. For small-scale flows this classification is further divided into elevations and depressions. A summary of each follows.
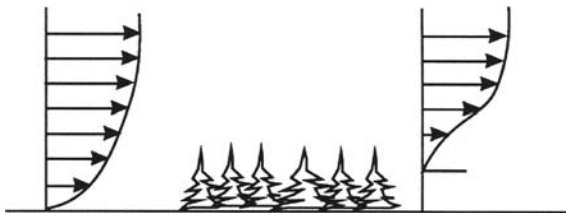
Figure 2.22   Effect of change in surface roughness from smooth to rough (Wegley *et al.*, 1980)

Perpendicular (best) Oblique (good)   Parallel (fair)

Concave (good)   Convex (less desirable)
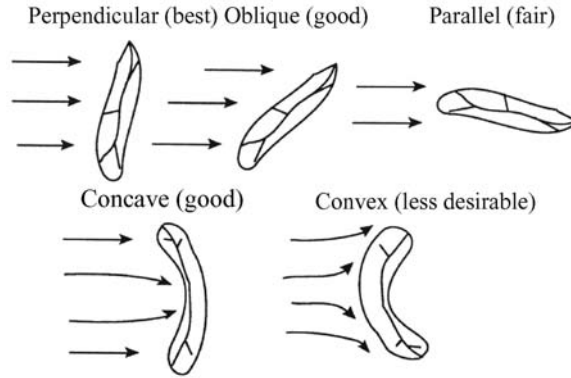
Figure 2.23   Effect of ridge orientation and shape on site suitability (Wegley *et al.*, 1980)

Elevations

Flow over elevated terrain features resembles flow around obstacles. Characterization studies of this type of flow in water and wind tunnels, especially for ridges and small cliffs, have been carried out. Examples of the results for ridges follow.

Ridges are elongated hills that are less than or equal to 600 m above the surrounding terrain and have little or no flat area on the summit. The ratio of length to height should be at least 10. Figure 2.23 illustrates that, for wind turbine siting, the ideal prevailing wind direction should be perpendicular to the ridge axis. When the prevailing wind is not perpendicular, the ridge will not be as attractive a site. Also, as shown in this figure, concavity in the windward direction enhances speed-up, and convexity reduces speed-up by deflecting the wind flow around the ridge.

The slope of a ridge is also an important parameter. Steeper slopes give rise to stronger wind flow, but on the lee of ridges steeper slopes give rise to high turbulence. Furthermore, as shown in Figure 2.24, a flat-topped ridge creates a region of high wind shear due to the separation of the flow.

Depressions

Depressions are characterized by a terrain feature lower than the surroundings. The change in speed of the wind is greatly increased if depressions can effectively channel the wind. This classification includes features such as valleys, canyons, basins, and passes. In addition to diurnal flow variations in certain depressions, there are many factors that influence the flow in

High wind shear
and turbulence
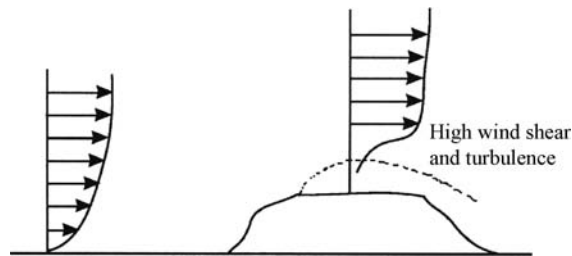
Figure 2.24   Region of high wind shear over a flat-topped ridge (Wegley *et al.*, 1980)

depressions. These include orientation of the wind in relation to the depression, atmospheric stability, the width, length, slope, and roughness of the depression, and the regularity of the section of valley or canyon.

Shallow valleys and canyons (<50 m) are considered small-scale depressions, and other features such as basins, gaps, etc. are considered large-scale depressions. The large number of parameters affecting the wind characteristics in a valley, along with the variability of these parameters from valley to valley, make it almost impossible to draw specific conclusions valid for flow characterization.

2.3.5.5 Characteristics of Non-flat Terrain: Large-scale Features

Large-scale features are ones for which the vertical dimension is significant in relation to the planetary boundary layer. They include mountains, ridges, high passes, large escarpments, mesas, deep valleys, and gorges. The flow over these features is the most complex, and flow predictions for this category of terrain classification are the least quantified. The following types of large depressions have been studied under this terrain classification:

- valley and canyons;
- slope winds;
- prevailing winds in alignment;
- prevailing winds in non-alignment;
- gaps and gorges;
- passes and saddles;
- large basins.

An example of a large depression with the prevailing winds in alignment is shown in Figure 2.25. This occurs when moderate to strong prevailing winds are parallel to or in alignment (within about 35 degrees) with the valley or canyon. Here the mountains can effectively channel and accelerate the flow.
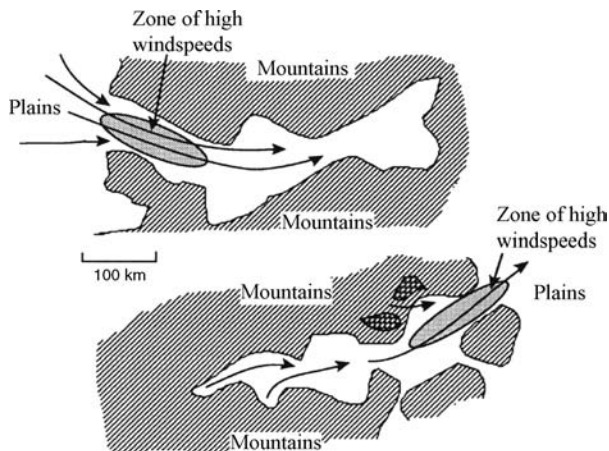
Figure 2.25 Increased wind speeds due to channeling of prevailing winds by mountains (Rohatgi and Nelson, 1994). Reproduced by permission of Alternative Energy Institute

2.4 Wind Data Analysis and Resource Estimation

In this section it is assumed that a large quantity of wind data has been collected. (Wind measurements and instrumentation are discussed in a later section of this chapter.) This data could include direction data as well as wind speed data. There are a number of ways to summarize the data in a compact form so that one may evaluate the wind resource or wind power production potential of a particular site. These include both direct and statistical techniques. Furthermore, some of these techniques can be used with a limited amount of wind data (e.g., average wind speed only) from a given site. This section will review the following topics:

- wind turbine energy production in general;
- direct (non-statistical) methods of data analysis and resource characterization;
- statistical analysis of wind data and resource characterization;
- statistically based wind turbine productivity estimates.

2.4.1 General Aspects of Wind Turbine Energy Production

In this section we will determine the productivity (both maximum energy potential and machine power output) of a given wind turbine at a given site in which wind speed information is available in either time series format or in a summary format (average wind speed, standard deviation, etc.)

The power available from wind is $P = (1/2)\rho A U^3$ as shown in Section 2.2 (Equation 2.7). In practice, the power available from a wind turbine, P_w, can be shown by a machine power curve, as was introduced in Chapter 1. Two typical curves, $P_w(U)$, simplified for purposes of illustration, are shown in Figure 2.26. Later sections of this text will describe how such curves can be estimated from analytical models of the wind turbine system. Normally these curves are based on test data, as described in IEC (2005) or AWEA (1988).
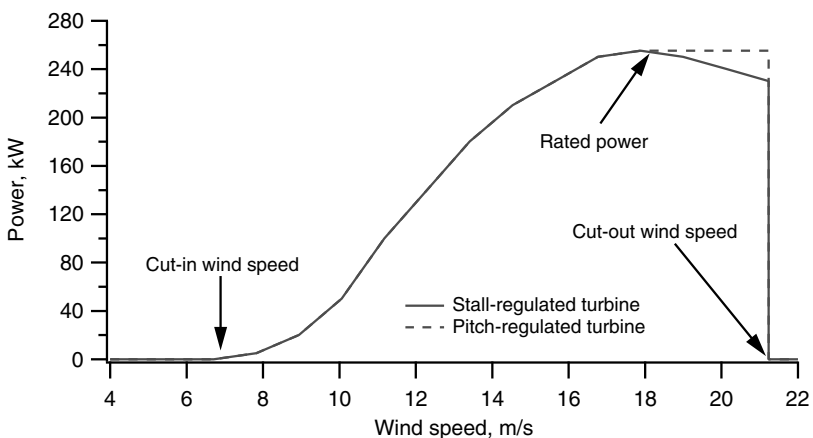
Figure 2.26 Power output curve for wind turbine

As also discussed in Chapter 1, the power curve illustrates three important characteristic velocities: (1) the cut-in velocity, (2) the rated velocity, and (3) the cut-out velocity.

In the following sections, methods for the determination of machine production will be analyzed, as well as methods to summarize wind speed information from a given site. The following four approaches will be considered:

- direct use of data averaged over a short time interval;
- the method of bins;
- development of velocity and power curves from data;
- statistical analysis using summary measures.

The next section summarizes the use of the three non-statistical methods.

2.4.2 Direct Methods of Data Analysis, Resource Characterization, and Turbine Productivity

2.4.2.1 Direct Use of Data

Suppose one is given a series of N wind speed observations, U_i, each averaged over the time interval Δt. These data can be used to calculate the following useful parameters:

(1) The long-term average wind speed, $\overline{U}$, over the total period of data collection is:

$$\overline{U} = \frac{1}{N} \sum_{i=1}^{N} U_i \tag{2.39}$$

(2) The standard deviation of the individual wind speed averages, σ_U is:

$$\sigma_U = \sqrt{\frac{1}{N-1} \sum_{i=1}^{N} (U_i - \overline{U})^2} = \sqrt{\frac{1}{N-1} \left\{ \sum_{i=1}^{N} U_i^2 - N\overline{U}^2 \right\}} \tag{2.40}$$

(3) The average wind power density, $\overline{P}/A$, is the average available wind power per unit area and is given by:

$$\overline{P}/A = (1/2)\rho \frac{1}{N} \sum_{i=1}^{N} U_i^3 \tag{2.41}$$

Similarly, the wind energy density per unit area for a given extended time period $N\Delta t$ long is given by:

$$\overline{E}/A = (1/2)\rho \Delta t \sum_{i=1}^{N} U_i^3 = (\overline{P}/A)(N\Delta t) \tag{2.42}$$

(4) The average wind machine power, $\overline{P}_w$, is:

$$\overline{P}_w = \frac{1}{N} \sum_{i=1}^{N} P_w(U_i) \tag{2.43}$$

where $P_w(U_i)$ is the power output defined by a wind machine power curve.

(5) The energy from a wind machine, E_w, is:

$$E_w = \sum_{i=1}^{N} P_w(U_i)(\Delta t) \tag{2.44}$$

2.4.2.2 Method of Bins

The method of bins also provides a way to summarize wind data and to determine expected turbine productivity. The data must first be separated into the wind speed intervals or bins in which they occur. It is most convenient to use the same size bins. Suppose that the data are separated into N_B bins of width w_j, with midpoints m_j, and with f_j, the number of occurrences in each bin or frequency, such that:

$$N = \sum_{j=1}^{N_B} f_j \tag{2.45}$$

The values found from Equations (2.39)–(2.41), (2.43), and (2.44) can be determined from the following:

$$\overline{U} = \frac{1}{N} \sum_{j=1}^{N_B} m_j f_j \tag{2.46}$$

$$\sigma_U = \sqrt{\frac{1}{N-1} \left\{ \sum_{j=1}^{N_B} m_j^2 f_j - N(\overline{U})^2 \right\}} = \sqrt{\frac{1}{N-1} \left\{ \sum_{j=1}^{N_B} m_j^2 f_j - N \left(\frac{1}{N} \sum_{j=1}^{N_B} m_j f_j \right)^2 \right\}} \tag{2.47}$$

$$\overline{P}/A = (1/2)\rho \frac{1}{N} \sum_{j=1}^{N_B} m_j^3 f_j \tag{2.48}$$

$$\overline{P}_w = \frac{1}{N} \sum_{j=1}^{N_B} P_w(m_j) f_j \tag{2.49}$$

$$E_w = \sum_{j=1}^{N_B} P_w(m_j) f_j \, \Delta t \tag{2.50}$$

A histogram (bar graph) showing the number of occurrences and bin widths is usually plotted when using this method. Figure 2.27 illustrates a typical histogram. This histogram was derived from one year of hourly data, for which the mean was 5.91 m/s and the standard deviation was 2.95 m/s.

2.4.2.3 Velocity and Power Duration Curves from Data

Velocity and power duration curves can be useful when comparing the energy potential of candidate wind sites. As defined in this text, the velocity duration curve is a graph with wind speed on the y axis and the number of hours in the year for which the speed equals or exceeds each particular value on the x axis. An example of velocity duration curves
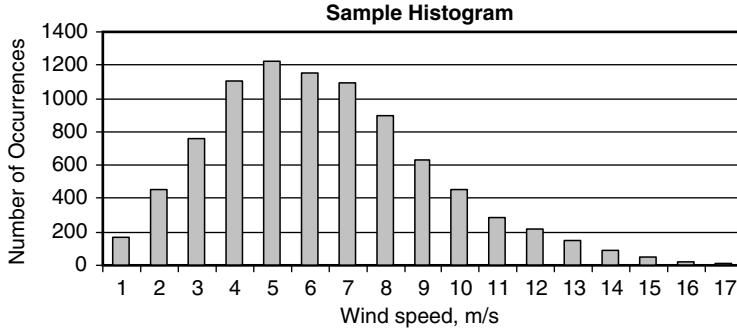
Figure 2.27   Typical histogram

(Rohatgi and Nelson, 1994) for various parts of the world (with average wind speeds varying from about 4 to 11 m/s) is shown in Figure 2.28. This type of figure gives an approximate idea about the nature of the wind regime at each site. The total area under the curve is a measure of the average wind speed. In addition, the flatter the curve, the more constant are the wind speeds (e.g., characteristic of the trade-wind regions of the earth). The steeper the curve, the more variable is the wind regime.

A velocity duration curve can be converted to a power duration curve by cubing the ordinates, which are then proportional to the available wind power for a given rotor swept area. The difference between the energy potential of different sites is visually apparent, because the areas under the curves are proportional to the annual energy available from the wind. The following steps must be carried out to construct velocity and power duration curves from data:

- arrange the data in bins;
- find the number of hours that a given velocity (or power per unit area) is exceeded;
- plot the resulting curves.
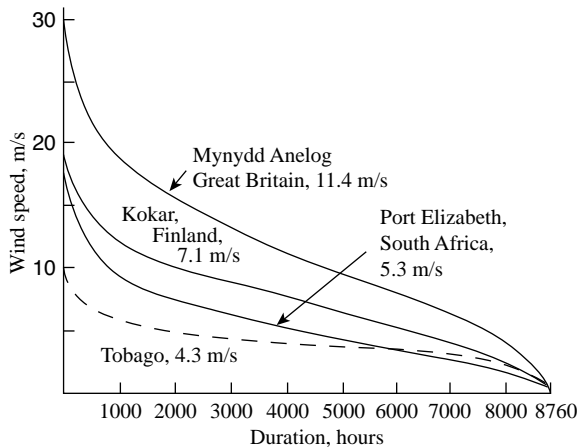
Figure 2.28   Velocity duration curve example (Rohatgi and Nelson, 1994). Reproduced by permission of Alternative Energy Institute
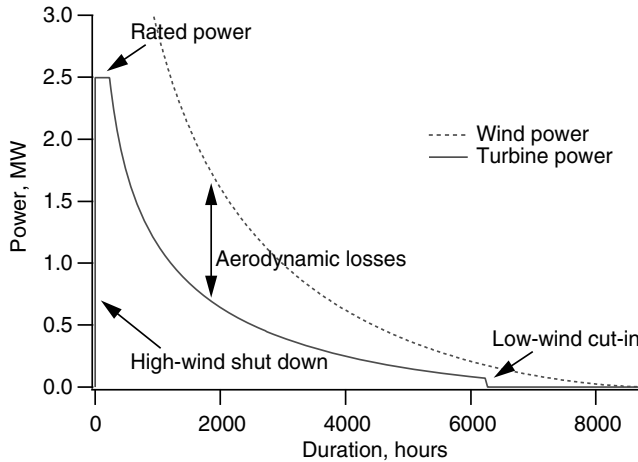
Figure 2.29   Turbine power duration curve

A turbine power duration curve for a particular wind turbine at a given site may be constructed using the power duration curve in conjunction with a power curve for a given wind turbine. An example of a curve of this type is shown in Figure 2.29. Note that the losses in energy production with the use of an actual wind turbine at this site can be identified.

2.4.3 Statistical Analysis of Wind Data

Statistical analysis can be used to determine the wind energy potential of a given site and to estimate the energy output from a wind turbine installed there. These techniques have been discussed by a number of authors including Justus (1978), Johnson (1985), and Rohatgi and Nelson (1994). If time series measured data are available at the desired location and height, there may be little need for a data analysis in terms of probability distributions and statistical techniques. That is, the previously described techniques may be all that are needed. On the other hand, if projection of measured data from one location to another is required, or when only summary data are available, then there are distinct advantages to the use of analytical representations for the probability distribution of wind speed.

For statistical analysis, a probability distribution is a term that describes the likelihood that certain values of a random variable (such as wind speed) will occur. As discussed next, probability distributions are typically characterized by a probability density function or a cumulative density function.

2.4.3.1 Probability Density Function

The frequency of occurrence of wind speeds may be described by the probability density function, *p(U)*, of wind speed. This mathematical function was previously mentioned as a means of characterizing turbulence (see Section 2.3.3.2). The probability density function may be used to express the probability of a wind speed occurring between U_a and U_b:

$$p(U_a \leq U \leq U_b) = \int_{U_a}^{U_b} p(U)\mathrm{d}U \qquad (2.51)$$

Also, the total area under the probability density curve is given by:

$$\int_0^\infty p(U)\mathrm{d}U = 1 \tag{2.52}$$

If $p(U)$ is known, the following parameters can be calculated:

Mean wind speed, $\overline{U}$:

$$\overline{U} = \int_0^\infty U p(U)\mathrm{d}U \tag{2.53}$$

Standard deviation of wind speed, σ_U:

$$\sigma_U = \sqrt{\int_0^\infty \left(U-\overline{U}\right)^2 p(U)\,\mathrm{d}U} \tag{2.54}$$

Mean available wind power density, $\overline{P}/A$

$$\overline{P}/A = (1/2)\rho \int_0^\infty U^3 p(U)\mathrm{d}U = (1/2)\rho \overline{U^3} \tag{2.55}$$

where $\overline{U^3}$ is the expected value for the cube of the wind speed.

It should also be noted that the probability density function can be superimposed on a wind velocity histogram by scaling it to the area of the histogram.

2.4.3.2 Cumulative Distribution Function

The cumulative distribution function $F(U)$ represents the time fraction or probability that the wind speed is smaller than or equal to a given wind speed, U. That is: $F(U) =$ Probability $(U' \leq U)$ where U' is a dummy variable. It can be shown that:

$$F(U) = \int_0^U p(U')\mathrm{d}U' \tag{2.56}$$

Also, the derivative of the cumulative distribution function is equal to the probability density function, i.e.:

$$p(U) = \frac{\mathrm{d}F(U)}{\mathrm{d}U} \tag{2.57}$$

Note that the velocity duration curve is closely related to the cumulative distribution function. In fact, the velocity duration curve $= 8760 \times (1 - F(u))$, but with the x and y axes reversed.

2.4.3.3 Commonly Used Probability Distributions

Two probability distributions are commonly used in wind data analysis: (1) the Rayleigh and (2) the Weibull. The Rayleigh distribution uses one parameter: the mean wind speed. The Weibull distribution is based on two parameters and, thus, can better represent a wider variety of wind regimes. Both the Rayleigh and Weibull distributions are called 'skew' distributions in that they are defined only for values greater than 0.
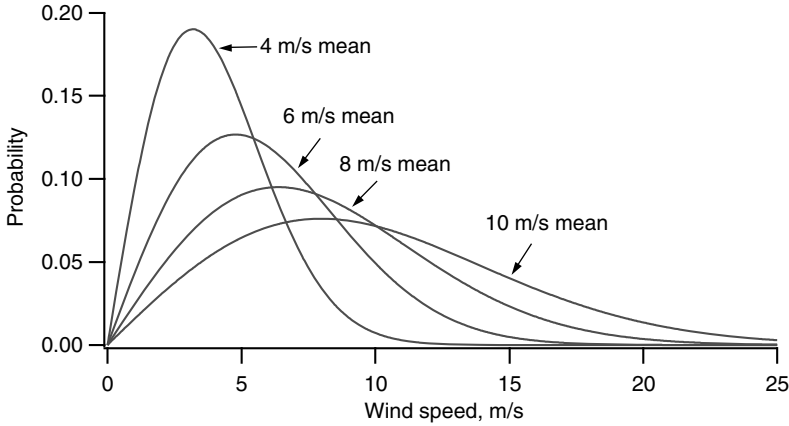
Figure 2.30   Example of Rayleigh probability density function

Rayleigh Distribution

This is the simplest velocity probability distribution to represent the wind resource since it requires only a knowledge of the mean wind speed, $\overline{U}$. The probability density function and the cumulative distribution function are given by:

$$p(U) = \frac{\pi}{2} \left(\frac{U}{\overline{U}^2} \right) \exp \left[-\frac{\pi}{4} \left(\frac{U}{\overline{U}} \right)^2 \right] \tag{2.58}$$

$$F(U) = 1 - \exp \left[-\frac{\pi}{4} \left(\frac{U}{\overline{U}} \right)^2 \right] \tag{2.59}$$

Figure 2.30 illustrates a Rayleigh probability density function for different mean wind speeds. As shown, a larger value of the mean wind speed gives a higher probability of higher wind speeds.

Weibull Distribution

Use of the Weibull probability density function requires knowledge of two parameters: k, a shape factor, and c, a scale factor. Both of these parameters are functions of $\overline{U}$ and σ_U. The Weibull probability density function and the cumulative distribution function are given by:

$$p(U) = \left(\frac{k}{c} \right) \left(\frac{U}{c} \right)^{k-1} \exp \left[-\left(\frac{U}{c} \right)^k \right] \tag{2.60}$$

$$F(U) = 1 - \exp \left[-\left(\frac{U}{c} \right)^k \right] \tag{2.61}$$

Examples of a Weibull probability density function, for various values of k, are given in Figure 2.31. As shown, as the value of k increases, the curve has a sharper peak, indicating that there is less wind speed variation. Methods to determine k and c from $\overline{U}$ and σ_U are presented below.
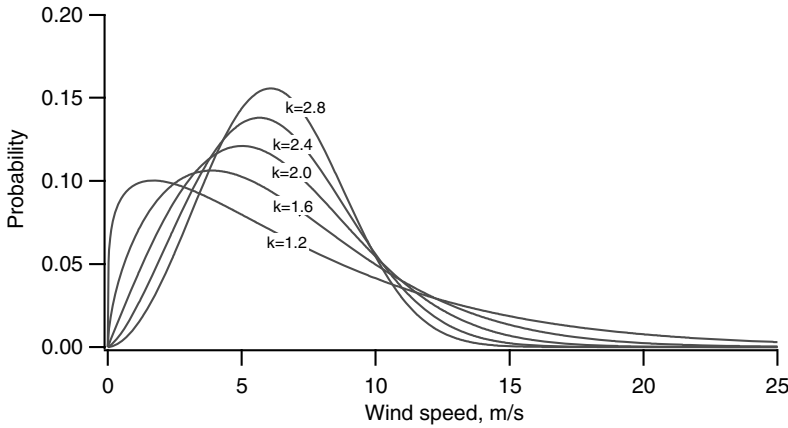
Figure 2.31 Example of Weibull probability density function for $\overline{U} = 6\,\text{m/s}$

Using Equation (2.60) for the Weibull distribution, it is possible to determine the average velocity as follows:

$$\overline{U} = c\,\Gamma\left(1 + \frac{1}{k}\right) \tag{2.62}$$

where $\Gamma(x) = $ gamma function $= \int_0^\infty e^{-t}t^{x-1}\,\mathrm{d}t$

The gamma function can be approximated by (Jamil, 1994):

$$\Gamma(x) = \left(\sqrt{2\pi x}\right)\left(x^{x-1}\right)\left(e^{-x}\right)\left(1 + \frac{1}{12x} + \frac{1}{288x^2} - \frac{139}{51840x^3} + \ldots\right) \tag{2.63}$$

It can also be shown that for the Weibull distribution:

$$\sigma_u^2 = \overline{U}^2\left[\frac{\Gamma(1+2/k)}{\Gamma^2(1+2/k)} - 1\right] \tag{2.64}$$

It is not a straightforward process to get c and k in terms of $\overline{U}$ and σ_u. However, there are a number of approximations that can be used. For example:

(i) Analytical/Empirical (Justus, 1978)

For $1 \leq k < 10$, a good approximation for k is:

$$k = \left(\frac{\sigma_U}{\overline{U}}\right)^{-1.086} \tag{2.65}$$

Equation (2.62) can then be used to solve for c:

$$c = \frac{\overline{U}}{\Gamma(1+1/k)} \tag{2.66}$$

This method still requires use of the gamma function.

(ii) Empirical (Lysen, 1983)

Use Equation (2.65) to find k. Then, find c from the following approximation:

$$\frac{c}{\overline{U}} = (0.568 + 0.433/k)^{-\frac{1}{k}} \tag{2.67}$$

(iii) Graphical: Log–Log Plot (Rohatgi and Nelson, 1994)

Using this method, a straight line is drawn through a plot of wind speed, U, on the x-axis and log $F(U)$ on the y-axis of log–log paper. The slope of the straight line gives k. Then, the intersection of a horizontal line with $F(U) = 0.632$ gives an estimate of c on the x-axis.

Using the Weibull distribution and assuming that c and k are known, the expected value of the cube of the wind speed, $\overline{U^3}$, may be found as follows:

$$\overline{U^3} = \int_0^\infty U^3 p(U) \mathrm{d}U = c^3 \Gamma(1 + 3/k) \tag{2.68}$$

One should note that normalized values of $\overline{U^3}$ depend only on the shape factor k. For example, the energy pattern factor, K_e (defined as the total amount of power available in the wind divided by the power calculated from cubing the average wind speed) is given by:

$$K_e = \frac{\overline{U^3}}{\left(\overline{U}\right)^3} = \frac{\Gamma(1 + 3/k)}{\Gamma^3(1 + 1/k)} \tag{2.69}$$

Examples of some parameters of interest are given in Table 2.4.

It should also be noted that a Weibull distribution for which $k = 2$ is a special case of the Weibull distribution. It equals the Rayleigh distribution. That is, for $k = 2$, $\Gamma^2(1 + 1/2) = \pi/4$. One can also note that $\sigma_u/\overline{U} = 0.523$ for a Rayleigh distribution.

2.4.4 Extreme Wind Speeds

The primary meteorological factor in evaluating a prospective wind turbine site is the mean wind speed. Another important consideration is the anticipated extreme wind speed. This is the highest wind speed expected over some relatively long period of time. Extreme wind speeds are of particular concern in the design process, since the turbine must be designed in order to withstand those likely but infrequent conditions.

Extreme winds are normally described in terms of recurrence (or return) period. Specifically, an extreme wind is the value of the highest wind speed, averaged over some appropriate time

Table 2.4 Variation of parameters with Weibull k shape factor

k	$\sigma_U/\overline{U}$	K_e
1.2	0.837	3.99
2	0.523	1.91
3	0.363	1.40
5.0	0.229	1.15

interval, with an annual probability of occurrence of $1/N$ years. For example, the highest 10 min average wind with 50 year recurrence period, would have a probability of occurrence of $1/(6 \times 8760 \times 50) = 3.8 \times 10^{-7}$.

Determination of extreme wind speeds by actual measurement is difficult, since it would require measurements over a long period of time. It is possible to estimate extreme wind speeds, however, by using extremes over some shorter period of time, together with a suitable statistical model.

The most common statistical model for estimating extreme wind speeds is the Gumbel distribution. The probability density function for the Gumbel distribution is shown in Equation (2.70) and the cumulative distribution function is shown in Equation (2.71).

$$p(U_e) = \frac{1}{\beta} \exp\left(\frac{-(U_e - \mu)}{\beta}\right) \exp\left(-\exp\left(\frac{-(U_e - \mu)}{\beta}\right)\right) \tag{2.70}$$

where U_e = extreme wind over some as yet unspecified time period, $\beta = \left(\sigma_e \sqrt{6}\right)/\pi$, $\mu = \overline{U}_e - 0.577\beta$, $\overline{U}_e$ = the mean of a set of extreme values, and σ_e = the standard deviation of that set.

$$F(U_e) = \exp\left(-\exp\left(\frac{-(U_e - \mu)}{\beta}\right)\right) \tag{2.71}$$

A Gumbel probability density function is illustrated in Figure 2.32 for the case of a mean of 10 m/s and a standard deviation of 4 m/s.

Example: The highest 10 min wind speed with a recurrence period of 50 yrs, U_{e50}, could be estimated by finding the highest 10 min wind speed every year for a series of years, say ten years. The average and standard deviation of the resulting set would be used to find the parameters β and μ. The cumulative distribution function, $F(U_e)$, would then be used to find the expected maximum. The maximum would be that wind speed U_e corresponding to $1 - F(U_e) = 1/50 = 0.02$. In the case of the values used in Figure 2.32, the 50 yr maximum would be approximately 20.4 m/s. Note an additional subscript, in this case '50', has been added to indicate the recurrence period of the extreme wind.
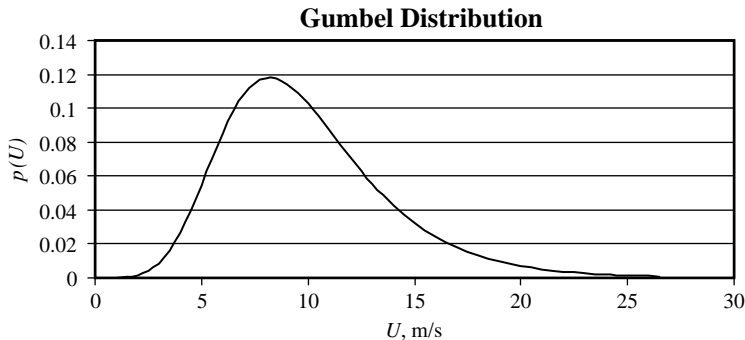
Figure 2.32 Illustration of Gumbel distribution

2.5 Wind Turbine Energy Production Estimates Using Statistical Techniques

For a given wind regime probability density function, $p(U)$, and a known turbine power curve, $P_w(U)$, the average wind turbine power, $\bar{P}_w$, is given by:

$$\overline{P}_w = \int_0^\infty P_w(U)\, p(U)\, \mathrm{d}U \qquad (2.72)$$

The average wind turbine power, $\bar{P}_w$, can also be used to calculate a related performance parameter, the capacity factor, CF. The capacity factor of a wind turbine at a given site is defined as the ratio of the energy actually produced by the turbine to the energy that could have been produced if the machine ran at its rated power, P_R, over a given time period. Thus:

$$CF = \overline{P}_w / P_R \qquad (2.73)$$

As will be discussed in Chapter 7, it is possible to determine a turbine power curve based on the power available in the wind and the rotor power coefficient, C_P. The result is the following expression for $P_w(U)$:

$$P_w(U) = \tfrac{1}{2}\rho A\, C_p \eta\, U^3 \qquad (2.74)$$

where η is the drive train efficiency (generator power/rotor power) and A and ρ have been previously defined. The rotor power coefficient is defined by:

$$C_p = \frac{\text{Rotor power}}{\text{Power in the wind}} = \frac{P_{rotor}}{\tfrac{1}{2}\rho\, A\, U^3} \qquad (2.75)$$

In the next chapter, it will be shown that C_P can generally be expressed as a function of the tip speed ratio, λ, defined by:

$$\lambda = \frac{\text{Blade tip speed}}{\text{Wind speed}} = \frac{\Omega R}{U} \qquad (2.76)$$

where Ω is the angular velocity (in radians/sec) of the wind turbine rotor and R is the radius of the wind rotor.

Therefore, assuming a constant value for drive train efficiency, another expression for the average wind machine power is given by:

$$\overline{P}_w = \tfrac{1}{2}\rho\, \pi R^2 \eta \int_0^\infty C_p(\lambda)\, U^3 p(U)\, \mathrm{d}U \qquad (2.77)$$

We are now in a position to use statistical methods for the estimation of the energy productivity of a specific wind turbine at a given site with a minimum of information. Two examples using Rayleigh and Weibull distributions form a basis for the analysis that follows.

2.5.1 Idealized Machine Productivity Calculations using Rayleigh Distribution

A measure of the maximum possible average power from a given rotor diameter can be calculated assuming an ideal wind machine and using a Rayleigh probability density function.

The analysis, based on the work of Carlin (1997), assumes the following:

- Idealized wind turbine, no losses, machine power coefficient, C_P, equal to the Betz limit ($C_{P,Betz} = 16/27$). As will be discussed in the next chapter, the Betz limit is the theoretical maximum possible power coefficient.
- Wind speed probability is given by a Rayleigh distribution.

The average wind machine power, $\overline{P}_w$, is given by Equation (2.77), and, for a Rayleigh distribution, is given by:

$$\overline{P}_w = \tfrac{1}{2}\rho\pi R^2\eta\int_0^\infty C_p(\lambda)U^3\left\{\frac{2U}{U_c^2}\exp\left[-\left(\frac{U}{U_c}\right)^2\right]\right\}dU \tag{2.78}$$

where U_c is a characteristic wind velocity given by: $U_c = 2\overline{U}/\sqrt{\pi}$.

For an ideal machine, $\eta = 1$, and the power coefficient can be replaced with the Betz value of $C_{P,Betz} = 16/27$, thus:

$$\overline{P}_w = \tfrac{1}{2}\rho\,\pi R^2\,U_c^3 C_{p,Betz}\int_0^\infty\left(\frac{U}{U_c}\right)^3\left\{\frac{2U}{U_c}\exp\left[-\left(\frac{U}{U_c}\right)^2\right]\right\}dU/U_c \tag{2.79}$$

One can now normalize the wind speed by defining a dimensionless wind speed, x, such that: $x = U/U_c$. This simplifies the previous integral as follows:

$$\overline{P}_w = \tfrac{1}{2}\rho\,\pi R^2\,U_c^3\,C_{p,Betz}\int_0^\infty (x)^3\left\{2x\exp\left[-(x)^2\right]\right\}dx \tag{2.80}$$

Note that the wind machine constants have been removed from the integral. The integral can now be evaluated over all wind speeds. Its value is $(3/4)\sqrt{\pi}$. Thus:

$$\overline{P}_w = \tfrac{1}{2}\rho\,\pi R^2\,U_c^3(16/27)(3/4)\sqrt{\pi} \tag{2.81}$$

Using the diameter, D, divided by 2 instead of the radius and substituting for the characteristic velocity, U_c, the equation for average power is further simplified to:

$$\overline{P}_w = \rho\left(\frac{2}{3}D\right)^2\overline{U}^3 \tag{2.82}$$

Carlin called this the one-two-three equation! (The density is raised to the first power).

For a numerical example, one could calculate the average annual production of an 18 meter diameter 'Rayleigh–Betz' turbine at sea level in a 6 m/s average annual wind velocity regime. For this example:

$$\overline{P}_w = \left(1.225\,kg/m^3\right)\left(\frac{2}{3}\times 18\,m\right)^2(6\,m/s)^3 = 38.1\,kW$$

Multiplication of this by 8760 hr/yr yields an expected annual energy production of 334 000 kWhr.

2.5.2 Productivity Calculations for a Real Wind Turbine using a Weibull Distribution

Similar to the previous example, the average wind machine power is calculated using Equation (2.72):

$$\overline{P}_w = \int_0^\infty P_w(U)\, p(U)\mathrm{d}U \tag{2.83}$$

Based on Equation (2.56), it is also possible to rewrite this equation using the cumulative distribution function, thus:

$$\overline{P}_w = \int_0^\infty P_w(U)\mathrm{d}F(U) \tag{2.84}$$

For a Weibull distribution, Equation (2.61) gives the following expression for $F(U)$:

$$F(U) = 1 - \exp\left[-\left(\frac{U}{c}\right)^k\right] \tag{2.85}$$

Therefore, replacing the integral in Equation (2.84) with a summation over N_B bins, the following expression can be used to find the average wind machine power:

$$\overline{P}_w = \sum_{j=1}^{N_B}\left\{\exp\left[-\left(\frac{U_{j-1}}{c}\right)^k\right] - \exp\left[-\left(\frac{U_j}{c}\right)^k\right]\right\} P_w\left(\frac{U_{j-1}+U_j}{2}\right) \tag{2.86}$$

Note that Equation (2.86) is the statistical method's equivalent to Equation (2.49). In particular, the relative frequency, f_j/N, corresponds to the term in brackets and the wind turbine power is calculated at the midpoint between U_{j-1} and U_j.

2.6 Regional Wind Resource Assessment

2.6.1 Overview

Many researchers have noted that a major barrier to deployment in many regions of the world is a lack of reliable and detailed wind resource data, e.g., Elliot (2002). Thus, one of the first steps required for a regional wind energy feasibility study is an estimate of the available wind resource. As summarized in the review of Landberg *et al.* (2003a), there are many methods for estimating the wind resource of an area. This review summarized the following methods:

(1) Folklore.
(2) Measurements only.
(3) Measure–correlate–predict.
(4) Global databases.
(5) Wind atlas methodology.
(6) Site data based modeling.
(7) Mesoscale modeling.
(8) Combined meso/microscale modeling.

A detailed review of all of these methods is beyond the scope of this text, although some of them will be discussed in various sections of the book. In this section, a review of worldwide wind resource data that is readily available (based on methods 4 and 5 of the above list) will be presented.

The use of available wind resource data is an important part of any resource assessment activity. In evaluating available wind data, however, it is important to realize the data's limitations. That is, not all of this type of information has been collected for the purpose of wind energy assessment, and many data collection stations were located near or in cities, in relatively flat terrain or areas with low elevation (e.g., airports). Studies (e.g., in the United States and Europe) resulted in the completion of detailed wind atlases. These are documents that contain data on the wind speeds and direction in a region. These original atlases provided a general description of the wind resource within a large area (mesoscale), but typically were not able to provide enough information for the detailed examination of candidate sites for wind development (microscale). In recent times, however, wind atlases with high resolution (as fine as 200 m) have been produced. These are designed to quantify a particular location's wind resource (also at various above-ground heights).

2.6.2 United States Resource Information

In the 1970s, a preliminary wind resource assessment of the United States was carried out that produced 12 regional wind energy atlases. The atlases depicted the annual and seasonal wind resource on a state and regional level. They also included the wind resource's certainty rating (an indication of the reliability of the data) and an estimate for the percentage of land suitable for wind energy development based on variations in land-surface form.

These data were used to produce a general wind power potential map that gave an indication of the wind resource (in W/m^2) for all locations in the United States in one map (see Figure 2.33). Almost as soon as these results were published, however, it was realized that these resource maps were not adequate. An intensive program was therefore initiated by the Pacific Northwest Laboratories (PNL) to better characterize the wind energy potential in the United States. This work resulted in the publication of a new wind energy resource atlas in 1987 (Elliot *et al.*, 1987).

The 1987 wind atlas integrated the pre-1979 wind measurements with topography and land form characteristics to determine US wind resource estimates. The updated wind resource values are depicted on gridded maps, $1/4°$ latitude by $1/3°$ longitude resolution (about $120\,km^2$), on both a national scale and a state-by-state basis. In the 1987 atlas, the magnitude of the wind resource was expressed in terms of seven wind power classes, rather than as a function of wind speed. The wind power classes range from Class 1 (for winds containing the least energy) to Class 7 (for winds containing the most energy). Each class represents a range of mean power density (W/m^2) or equivalent mean wind speed at specified heights above the ground. Table 2.5 shows the wind power classes in terms of their mean wind power density and the mean wind speed at 10, 30, and 50 m above the ground. Note that the 30 and 50 m heights correspond to the range of hub heights of many wind turbines then operating or under development. This table was constructed using the following assumptions:

- Vertical extrapolation of wind power density and wind speed were based on the 1/7 power law.
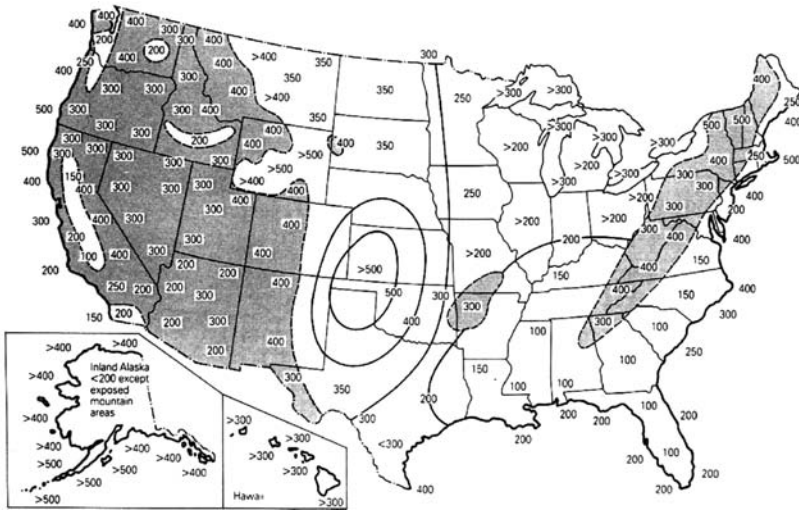
Figure 2.33 Initial wind power potential map of the United States (Elliot, 1977)

- Mean wind speed was estimated assuming a Rayleigh distribution of wind speeds and standard sea-level air density.

Areas designated as class 4 or greater are generally considered to be suitable for most wind turbine applications. Class 3 areas are suitable for wind energy development if tall towers are used. Class 2 areas are marginal and class 1 areas are unsuitable for wind energy development. It should be noted that the results of this categorization also indicate the certainty of the wind resource based on data reliability and their area distribution. They do not account, however, for the variability in mean wind speed on a local scale; rather, they indicate regions where a high wind resource is likely to exist. An example of the type of data summary contained in this atlas is given in Figure 2.34, which presents the average wind power

Table 2.5 Wind power density classes

Wind power class	10 m		30 m		50 m	
	Power density W/m^2	Speed m/s	Power density W/m^2	Speed m/s	Power density W/m^2	Speed m/s
1	0–100	0–4.4	0–160	0–5.1	0–200	0–5.6
2	100–150	4.4–5.1	160–240	5.1–5.8	200–300	5.6–6.4
3	150–200	5.1–5.6	240–320	5.8–6.5	300–400	6.4–7.0
4	200–250	5.6–6.0	320–400	6.5–7.0	400–500	7.0–7.5
5	250–300	6.0–6.4	400–480	7.0–7.4	500–600	7.5–8.0
6	300–400	6.4–7.0	480–640	7.4–8.2	600–800	8.0–8.8
7	400–1000	7.0–9.4	640–1600	8.2–11.0	800–2000	8.8–11.9
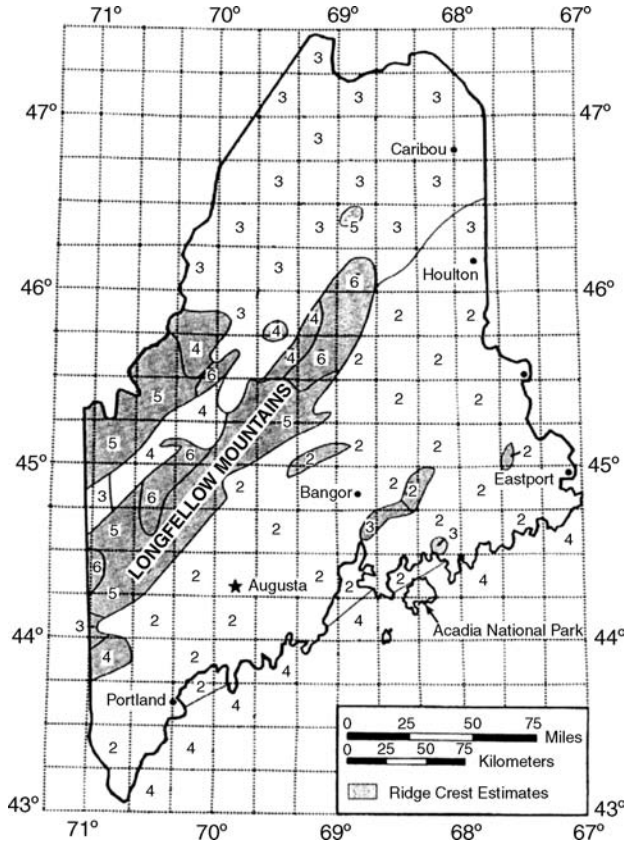
Figure 2.34 Average annual wind power for Maine (Elliot *et al.*, 1987)

(by class) for the state of Maine. The work of Elliot *et al.* (1991) illustrates how the data contained in this wind atlas can be used. This report contains, for example, detailed estimates of land areas with various levels of wind energy resource and resultant wind energy potential for each state in the United States.

In the most recent work on this subject, under the support of the National Renewable Energy Laboratory (NREL) and the Wind Powering America initiative, high-resolution (digital-based) wind resource maps have been produced for most of the US (Elliot and Schwartz, 2005). The approach for developing these maps consisted of three steps:

(1) Use of a numerical mesoscale weather prediction model for development of preliminary maps.
(2) Review and validation of the preliminary maps by NREL and meteorological consultants.
(3) Revisions to create the final maps.

Details of this process (and validation of the maps) are summarized by Elliot and Schwartz (2004). Various versions of wind resource maps for individual states are readily

available on the Internet (see http://www.eere.energy.gov/windandhydro/windpoweringamerica/wind_maps.asp). In most cases, the high resolution digital data for 200 m grids can be obtained. Figure 2.35 shows the overall results for the state of Maine (wind resource at 50 m). The increased detail as compared to the 1987 wind atlas work is readily apparent, especially when the maps are viewed in color.
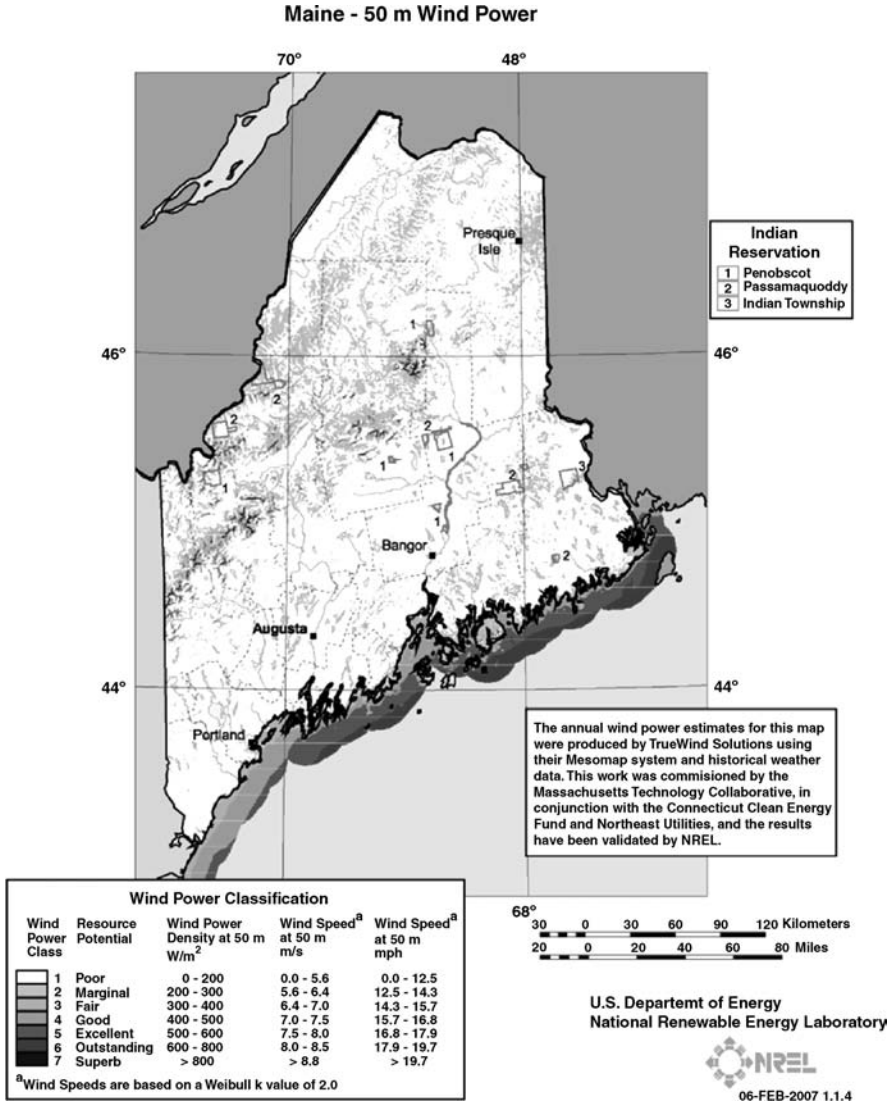
Figure 2.35 Wind resource map for Maine

2.6.3 European Resource Information

The wind energy resources vary considerably over Europe and are influenced by:

- Large temperature differences between the polar air in the north and subtropical air in the south.
- The distribution of land and sea with the Atlantic Ocean to the west, Asia to the east, and the Mediterranean Sea and Africa to the south.
- Major orographic barriers such as the Alps, the Pyrenees, and the Scandinavian mountain chain.

In order to characterize these resources, the European Community developed a detailed wind resource atlas for Europe (Troen and Petersen, 1989). The atlas is divided into the following three parts:

- **Wind resource.** This section, via graphs and tables, gives an overall view of the wind climate and magnitude and distribution of wind resources in the European Union.
- **Determining the wind resource.** This section provides information for regional wind resource assessments. It also gives a methodology for the local estimation of the mean power produced by a specific wind turbine at a specific site.
- **The models and the analysis.** This section contains the documentation (meteorological and statistical) part of the atlas.

It should be noted that the methodology for characterizing the wind resource was different than that used by PNL for the US wind atlases. As shown in Table 2.6, the maps of the European wind atlas are divided into five categories of wind speed, indicated by colors on the maps, instead of the seven classes used in the United States.

Additionally, as shown in Table 2.6, wind speed criteria for each category are subdivided into estimates of the wind speed for five topographical conditions. The different terrains have been divided into four types, each characterized by its roughness elements. Each terrain type was also associated with a roughness class. The five topographical conditions are:

- **Sheltered terrain.** This includes such terrain as urban districts, forest, and farm land with many windbreaks (roughness class 3).
- **Open plain.** This is described as flat land with a few windbreaks (roughness class 1).
- **Sea coast.** This describes a location with a uniform wind direction and land surface with a few windbreaks (roughness class 3).
- **Open sea.** This condition defines a sea location 10 km offshore (roughness class 0).
- **Hills and ridges.** These are characterized by the summit of a single axisymmetric hill with a height of 400 m and a base diameter of 4 km.

2.6.4 Wind Resource Information for Other Parts of the World

There are numerous technical publications that summarize wind resource information for other parts of the world. There is no one publication, or wind atlas, however, that summarizes all of this work. In 1981 the US Department of Energy's Pacific Northwest Laboratory (PNL) created a world resource map based on ship data, national weather data,

Table 2.6 European wind atlas classification of wind resource at 50 m

Map color	Sheltered terrain		Open plain		Sea coast		Open sea		Hills and ridges	
	m/s	W/m^2	m/s	W/m^2	m/s	W/m^2	m/s	W/m^2	m/s	W/m^2
Blue	0–3.5	<50	0–4.5	<100	0–5.0	<150	0–5.5	0–200	0–7.0	0–400
Green	3.5–4.5	50–100	4.5–5.5	100–200	5.0–6.0	150–250	5.5–7.0	200–400	7.0–8.5	400–700
Orange	4.5–5.0	100–150	5.5–6.5	200–300	6.0–7.0	250–400	7.0–8.0	400–600	8.5–10.0	700–1200
Red	5.0–6.0	150–250	6.5–7.5	300–500	7.0–8.5	400–700	8.0–9.0	600–800	10.0–11.5	1200–1800
Purple	>6.0	250	7.5	>500	>8.5	700	9.0	800	11.5	>1800

Figure 2.36   Worldwide status of wind atlas studies (Landberg *et al.*, 2003)

and terrain (Cherry *et al.*, 1981). Landberg *et al.* (2003a) note that the European Wind Atlas method, usually in combination with the micro-scale modeling tool WA^{S}P (Mortensen *et al.*, 2003) has been used for wind resource studies in a large portion of the world. The scope of this work as of 2003 is shown in Figure 2.36. For this figure national wind atlases have been published for the countries marked in dark gray, and regional and/or local wind resource studies exist for the countries marked in black.

In a summary of world wind energy resource assessment technology, Singh *et al.* (2006) state that the (previously discussed) methods of the National Renewable Energy Laboratory (NREL) have been used in large number to produce international wind resource atlases. Other world country-by-country wind data maps have been produced by the UN's SWEARA program (see http://swera.unep.net/index.php?id=7). Also, numerous international wind resource maps can be found from other sources on the Internet (see http://www.nrel.gov/wind/international_wind_resources.html).

Furthermore, US-based organizations such as the National Renewable Energy Laboratory, PNL, Sandia National Laboratory, the US DOE, the Agency for International Development, and the American Wind Energy Association, and numerous European research and development agencies have provided technical assistance for wind resource assessment in developing countries. These have included Mexico, Indonesia, the Caribbean Islands, the former Soviet Union, and various South American countries. Resource assessments in these countries have focused on the development of rural wind power applications.

As more countries measure the wind resource for determining energy or power potential, the resource maps will become more detailed. It is expected that they will enable wind energy researchers to better predict locations suitable for wind power sites.

2.7 Wind Prediction and Forecasting

With the inherent variability of the wind resource, it is often valuable to be able to predict, or forecast, the wind speed for some time ahead. For example, it may be useful, from a controls standpoint, to be able to predict the very short-term turbulent variations from a few seconds to a few minutes. Or, in the case of a wind turbine or wind farm operator, the capacity to effectively integrate the wind energy into a grid may be affected by the predictability of the output of the wind turbine(s). In this case, wind speed, or power production forecasts, might be needed for the next few hours or one to two days.

Recent work in wind energy forecasting has been concentrated on the next few hours or one to two day timeframe, and is generally defined as short-term wind energy forecasting. In this area, an excellent source of information is contained in the European-based ANEMOS project work (see Kariniotakis *et al.*, 2006) for a review of this project). The overall aim of this project is to develop accurate and robust models that substantially outperform current state-of-the-art forecasting models for both onshore and offshore applications.

Most short-term forecasting techniques are based on statistical time series models or numerical weather prediction models (physical/meteorological models) or a combination of both. A detailed review of these models is beyond the scope of this chapter, but Giebel (2003) and Landberg *et al.* 2003b) give an overview of the models used in wind energy resource prediction for wind systems. Most of the currently used forecasting models consist of all or most of the following (Landberg *et al.*, 2003b):

- numerical weather prediction (NWP) model output;
- input of observations;
- a numerical forecasting model and output.

Forecasting models require a basic set of inputs. For physical models these include the layout of the wind farm and the power curves of the wind turbines. Sometimes measurements of the production of individual turbines or the wind farm are used. Microscale and mesoscale models also require information about the terrain (i.e., height variation and roughness).

Short-term forecasting models usually estimate the energy production of a wind farm from one hour up to 48 hours ahead. Generally an estimate of the error (i.e., standard deviation or confidence interval) is also calculated. In addition, the forecasting model can be used to predict extreme events such as storms. Figure 2.37 shows the results of such a simulation compared to actual data (Landberg *et al.*, 2003b).
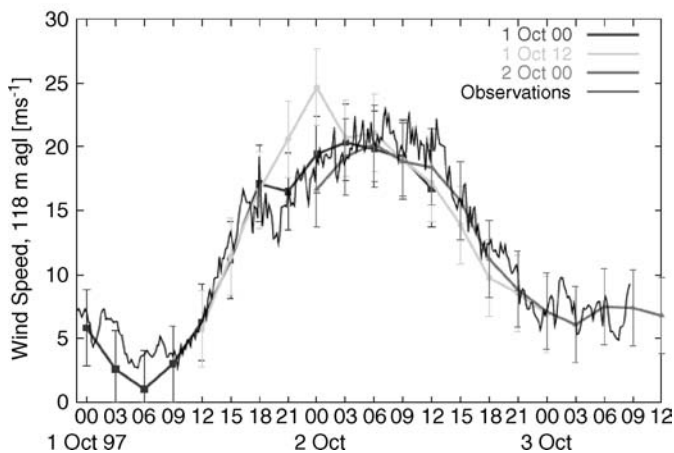
Figure 2.37 Example of forecasting results under storm conditions. The black line is the observed wind speed at the 118 m tall Risø mast; the gray lines are the twice-daily predictions of the Prediktor forecasting model (Landberg *et al.*, 2003b)

2.8 Wind Measurement and Instrumentation

2.8.1 Overview

So far in this chapter it has been assumed that one has perfectly reliable meteorological wind speed data for the location of interest. In most wind energy applications such information is not available, however, and measurements must be made specifically for determining the wind resource at the candidate location.

There are three types of instrument systems used for wind measurements:

- instruments used by national meteorological services;
- instruments designed specifically for measuring and characterizing the wind resource;
- instruments specially designed for high sampling rates for determining gust, turbulence, and inflow wind information for analyzing wind turbine response.

For each wind energy application, the type and amount of instrumentation required varies widely. For example, this can vary from a simple system just containing one wind speed anemometer/recorder to a very complex system designed to characterize turbulence across the rotor plane. Figure 2.38 shows an example of the latter type of system developed by PNL. This system consisted of two towers and eight anemometers, with data sampled at a rate of 5 Hz.

Instrumentation for wind energy applications is an important subject and has been discussed in detail by numerous authors. These include the early work of Putnam (1948) and
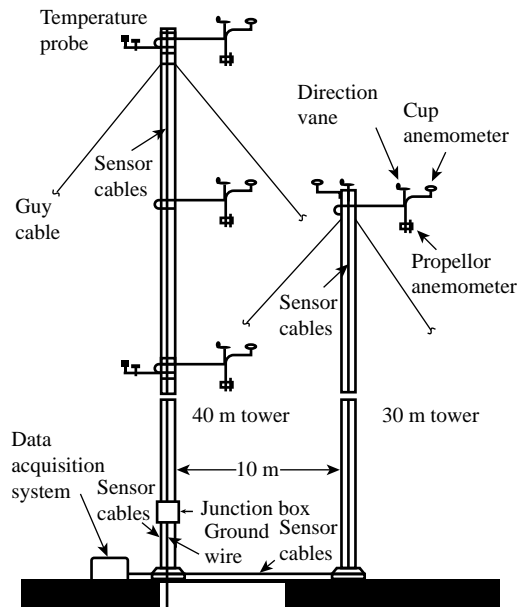
Figure 2.38 Turbulence characterization system of Pacific Northwest Laboratories (Wendell *et al.*, 1991)

Golding (1977) as well as the books of Hiester and Pennell (1981), Johnson (1985), Freris (1990), and Rohatgi and Nelson (1994). In addition, the performance test codes for wind turbines of the American Society of Mechanical Engineers (ASME, (1988)) and the measurement standards of the American Wind Energy Association (AWEA, (1986)) contain much useful information on wind instrumentation equipment and procedures.

Wind energy applications use the following types of meteorological sensors:

- anemometers to measure wind velocity;
- wind vanes to measure wind direction;
- thermometers to measure the ambient air temperature;
- barometers to measure the air pressure.

In this section the discussion will be limited to the first two types of sensor. For more detail on the use of the third and fourth sensor types, one should refer to the wind resource assessment handbook of Bailey *et al.* (1996). Furthermore, wind instrumentation systems consist of three major components: sensors, signal conditioners, and recorders. In the following review, these components will be discussed in more detail.

2.8.2 General Characteristics of Instruments

Before discussing instrumentation systems, it is important to review some basics of measurement systems. The important parameters and concepts of instrumentation and measurement systems are reviewed below. This review is divided into three sections:

- system components;
- characterization of measurements;
- instrument characteristics.

2.8.2.1 System Components

Sensors
A sensor is a device, such as a cup of an anemometer or a hot wire, which reacts to changes in the environment. For example, the cup reacts to the force of the wind, whereas the hot wire reacts to the wind flow via a temperature response.

Transducers
A transducer is a device which converts energy from one form to another. In the case of wind measurement, it usually refers to the device that converts a mechanical motion to an electrical signal.

Signal Conditioners
Signal conditioners supply power to the sensor when required, receive the signal from the sensor, and convert it to a form that can be used by a recorder for display.

Recorders
Recorders are devices that store and/or display the data obtained by the sensor/transducer/ signal conditioner combination.

2.8.2.2 Characterization of Measurements

Accuracy and Precision
Accuracy and precision are two measures of instrument system performance that are often treated ambiguously. The accuracy of an instrument refers to the mean difference between the output of the instrument and the true value of the measured variable. Precision refers to the dispersion about that mean. For example, an instrument may produce the same measured value every time, but that value may be 50% off. Thus, that system has high precision, but low accuracy. Another instrument measuring a variable may produce measurements with no mean error, but the dispersion of a single measurement may vary widely about the mean. This instrument has high accuracy, but low precision. In general, for wind measurement systems, the precision is usually high, so that accuracy is the principal concern.

Error
Error is the difference between the indication and the true value of the measured signal.

Reliability
The reliability of an instrument is a measure of the likelihood that it will continue to perform within specified limits of error for a specified time under specified conditions. The best indicator of reliability is the past performance of similar instruments. In general, simple and rugged instruments with fewer parts are more reliable than those with a large number of parts.

Repeatability
The repeatability of an instrument is the closeness of agreement among a number of consecutive measurements of output for the same input value, provided the measurements are made under the same conditions.

Reproducibility
The closeness of agreement among measurements of the same quantity where the individual measurements are made under different conditions defines measurement reproducibility.

2.8.2.3 Instrument Characteristics

Time Constant
The period required for a sensor to respond to 63.2% $(1 - 1/e)$ of a stepwise change in an input signal defines its time constant.

Distance Constant
The distance constant is the length of air flow past a sensor required to cause it to respond to 63.2% of a step change in speed. It is calculated by multiplying the sensor time constant by the average speed of the wind. Standard cup anemometers can have distance constants as high as 10 m, depending on their size and weight. Small, lightweight cup anemometers, used for turbulence measurements, have distance constants between 1.5 and 3 m. For lightweight propeller anemometers, the distance constant is close to 1 m.

Response Time
The response time is the time required for an instrument to register a designated percentage (usually 90% or 95%) of a step change in the variable being measured.

Sampling Rate

The sampling rate is the frequency (Hz) at which the signal is measured. It can be a function of the data collection system.

Resolution

Resolution is defined as the smallest unit of a variable that is detectable by the sensor. As an example, a sensor may have a resolution of $\pm$ 0.1 m/s or $\pm$ 1 m/s depending on the instrument. The type of recorder used may also limit the resolution.

Sensitivity

The sensitivity of an instrument is the ratio of the full-scale output of an instrument to the full-scale input value.

2.8.3 Wind Speed Measuring Instrumentation

The sensors of wind-measuring instrumentation can be classified according to their principle of operation via the following (ASME, 1988):

- **momentum transfer** – cups, propellers, and pressure plates;
- **pressure on stationary sensors** – pitot tubes and drag spheres;
- **heat transfer** – hot wires and hot films;
- **Doppler effects** – acoustics and laser;
- **special methods** – ion displacement, vortex shedding, etc.

Despite the number of potential instruments available for wind speed measurements, in most wind energy applications four different systems have been used. As discussed below, they include:

- cup anemometers;
- propeller anemometers;
- sonic anemometers;
- acoustic Doppler sensors (SODAR);
- acoustic Doppler sensors (LIDAR).

2.8.3.1 Cup Anemometers

The cup anemometer is probably the most common instrument for measuring the wind speed (Kristensen, 1999). Cup anemometers use their rotation, which varies in proportion to the wind speed, to generate a signal. Today's most common designs feature three cups mounted on a small shaft. The rate of rotation of the cups can be measured by:

- mechanical counters registering the number of rotations;
- electrical or electronic voltage changes (AC or DC);
- a photoelectric switch.

The mechanical-type anemometers indicate the wind flow in distance. The mean wind speed is obtained by dividing the wind flow by time (this type is also called a wind-run anemometer). For remote sites, this type of anemometer has the advantage of not requiring a power source.

Some of the earliest types of mechanical anemometers also drove a pen recorder directly. However, these systems were expensive and difficult to maintain.

An electronic cup anemometer gives a measurement of instantaneous wind speed. The lower end of the rotating spindle is connected to a miniature AC or DC generator and the analog output is converted to wind speed via a variety of methods.

The photoelectric switch type has a disc containing up to 120 slots and a photocell. The periodic passage of the slots produces pulses during each revolution of the cup.

The response and accuracy of a cup anemometer are determined by its weight, physical dimensions, and internal friction. By changing any of these parameters, the response of the instrument will vary. If turbulence measurements are desired, small, lightweight, low-friction sensors should be used. Typically, the most responsive cups have a distance constant of about 1 m. Where turbulence data are not required, the cups can be larger and heavier, with distance constants from 2 to 5 m. This limits the maximum usable data sampling rate to no greater than once every few seconds. Typical accuracy values (based on wind tunnel tests) for cup anemometers are about $\pm 2\%$.

Environmental factors can affect cup anemometers and reduce their reliability. These include ice or blowing dust. Dust can lodge in the bearings, causing an increase in friction and wear and reducing anemometer wind speed readings. If an anemometer ices up, its rotation will slow, or completely stop, causing erroneous wind speed signals, until the sensor thaws completely. Heated cup anemometers can be used, but they require a significant source of power. Because of these problems, the assurance of reliability for cup anemometers depends on calibration and service visits. The frequency of these visits depends on the site environment and the value of the data.

One commonly used anemometer in the US wind industry is the Maximum cup anemometer. The sensor is about 15 cm in diameter (see Figure 2.39). This anemometer has a generator that provides a sine wave voltage output. It has a Teflon® sleeve bushing bearing system that is not supposed to be affected by dust, water, or lack of lubrication. The frequency of the sine wave is related to the wind speed. Special anemometers based on this design (16 pole magnet) can be used for some turbulence measurements with a 1 Hz sampling rate.

Figure 2.39   Maximum cup anemometer

In Europe, a widely used cup anemometer is the RISØ P2546 cup anemometer developed at Risø National Laboratories (Pedersen, 2004).

2.8.3.2 Propeller Anemometers

Propeller anemometers use the wind blowing into a propeller to turn a shaft that drives an AC or DC (most common) generator, or a light chopper to produce a pulse signal. The designs used for wind energy applications have a fast response and behave linearly in changing wind speeds. In a typical horizontal configuration, the propeller is kept facing the wind by a tail-vane, which also can be used as a direction indicator. The accuracy of this design is about $\pm 2\%$, similar to the cup anemometer. The propeller is usually made of polystyrene foam or polypropylene. The problems of reliability of propeller anemometers are similar to those discussed for cup anemometers.

When mounted on a fixed vertical arm, the propeller anemometer may be used for measuring the vertical wind component. A configuration for measuring three components of wind velocity is shown in Figure 2.40. The propeller anemometer responds primarily to wind parallel to its axis, and the wind perpendicular to the axis has no effect.

2.8.3.3 Sonic Anemometers

Sonic anemometers were initially developed in the 1970s. They use ultrasonic sound waves to measure wind speed and direction. Wind velocity is measured based on the time of flight of sonic pulses between pairs of transducers. A review of their theory of operation is given by Cuerva and Sanz-Andres (2000).

One-, two-, or three-dimensional flow can be measured via signals from pairs of transducers. Typical wind engineering applications use two- or three-dimensional sonic

Figure 2.40 Propeller-type anemometer for measuring three wind velocity components

anemometers. The spatial resolution is determined by the path length between transducers (typically 10 to 20 cm). Sonic anemometers can be used for turbulence measurements with fine temporal resolution (20 Hz or better). A summary review of the state of the art of sonic anemometry in wind engineering applications is given by Pedersen *et al.* (2006).

2.8.3.4 Acoustic Doppler Sensors (SODAR)

SODAR (standing for SOund Detection And Ranging) is classified as a remote sensing system, since it can make measurements without placing an active sensor at the point of measurement. Since such devices do not need tall (and expensive) towers for their use, the potential advantages of their use are obvious. Remote sensing is used extensively for meteorological and aerospace purposes, but only in recent times has it been used for wind siting and performance measurements.

SODAR is based on the principle of acoustic backscattering. In order to measure the wind profile with SODAR, acoustic pulses are sent vertically and at a small angle to the vertical. For measurement of three-dimensional wind velocity, at least three beams in different directions are needed. The acoustic pulse transmitted into the air experiences backscattering from particles or fluctuations in the refractive index of air. These fluctuations can be caused by wind shear as well as by temperature and humidity gradients. The acoustic energy scattered back to the ground is then collected by microphones. Assuming that the sender and the receiver are not separated, the SODAR configuration is referred to as a monostatic SODAR. At the present time all commercial SODARs used for wind energy applications are monostatic (simplifying the system design and reducing its size).

If the local speed of sound is known, the travel time between emission and reception determines the height the signal represents. A change in the acoustic frequency of the echo (Doppler shift) occurs if the scattering medium has a component of motion parallel to the beam motion. Thus, estimation of the speed of the wind speed parallel to the beam as a function of height can be carried out via frequency spectrum analysis of the received back-scattered signal.

SODARs have been used for both onshore (e.g., Hansen *et al.*, 2006) and offshore (e.g., Antoniou *et al.*, 2006) wind siting studies with measurement of wind speed up to 300 m above the device. There has been a great deal of development on these devices over the last several years, and they are now commercially available from a number of sources. A detailed review and evaluation of SODAR for wind energy applications has been sponsored under the WISE (Wind Energy SODAR Evaluation) program (see de Noord *et al.*, 2005). These authors point out that, although SODAR systems can be commercially purchased, the following issues have arisen:

- For wind energy applications, stricter requirements exist for uncertainty, reliability, and validity of the data than for other SODAR applications. For example, more work is needed on filtering techniques for data analysis.
- A general procedure for calibration of SODAR systems has not been established.
- Low wind speeds (below 4 m/s), high wind speeds (above 18 m/s), and other atmospheric phenomena can cause difficulty with SODAR measurements. This is especially important because power curve determination requires measurement of wind speeds up to the cut-out wind speed, typically around 25 m/s.
- SODAR systems have been designed for use on land. For offshore applications problems associated with vibrations from supporting structures and an increased level of background noise have to be addressed.

- SODAR is designed to send a nearly vertical beam, and to use SODAR for the detection of oncoming gusts will require a near horizontal beam.
- SODAR systems have primarily been used at sites with easy access for maintenance and non-complex terrain. For wind energy applications at remote sites, and in complex terrain, autonomous SODAR systems will need further development, especially in areas of power supply and data communication.

Despite these problems, and others (such as noise issues in populated sites), it is expected that the use of SODAR in wind energy applications will increase rapidly in the future.

2.8.3.5 Laser Doppler Sensors (LIDAR)

LIDAR (LIght Detection And Ranging), similar to SODAR, is also classified as a remote sensing device, and can similarly be used to make measurements of a three-dimensional wind field. In this device, a beam of light is emitted, the beam interacts with the air and some of the light is scattered back to the LIDAR. The returned light is analyzed to determine the speed and distances to the particles from which it was scattered. In addition, the basic LIDAR principle relies on the measurement of the Doppler shift of radiation scattered by natural aerosols that are carried by the wind.

LIDARs have been used extensively in meteorological and aerospace applications (see Weitkamp, 2005), with the cost of meteorological LIDAR systems being quite high. However, developments in commercially available LIDAR systems have produced lower cost systems for wind speed determination at heights of interest in wind energy applications. In addition, eye safety concerns have been overcome since the majority of LIDAR lasers emit at the eye-safe wavelength of 1.5 microns. Using these new systems, LIDAR has most recently been applied to both onshore (Smith *et al.*, 2006; Jorgensen *et al.*, 2004) and offshore (Antoniou *et al.*, 2006) wind system applications.

At the present time, there are two types of commercial LIDAR device available for wind engineering applications: (1) a constant wave, variable focus design, and (2) a pulsed LIDAR with a fixed focus. Wind speeds at heights up to 200 m have been measured by both types of LIDAR system. The reader is referred to the work of Courtney *et al.* (2008) for a comparative review of these different systems.

As an example of an application of a constant wave LIDAR system, a portable and compact LIDAR system was used (Smith *et al.*, 2006) to determine horizontal and vertical wind speed and direction at heights up to 200 m. As shown in Figure 2.41, the LIDAR beam is offset at 30 degrees to the vertical. The beam scans as it revolves at one revolution per second. As the beam rotates it intercepts the wind at different angles, thereby building up a wind speed map around a disc of air. In a typical operation, three scans are performed at each height, and wind measurements are taken at five heights.

Because of the need for more cost-effective wind measurement systems at the higher heights required by larger wind turbines, it is expected that there will be more research and development on LIDAR systems for wind energy applications.

2.8.4 Wind Direction Instrumentation

Wind direction is normally measured via the use of a wind vane. A conventional wind vane consists of a broad tail that the wind keeps on the downwind side of a vertical shaft.
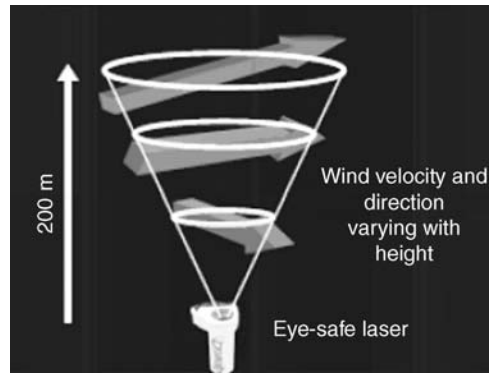
Figure 2.41   Schematic of conically scanned LIDAR system (Smith *et al.*, 2006)

A counterweight at the upwind end provides balance at the junction of the vane and shaft. Friction at the shaft is reduced with bearings, and so the vane requires a minimum force to initiate movement. For example, the usual threshold of this force occurs at wind speeds on the order of 1 m/s.

Wind vanes usually produce signals by contact closures or by potentiometers. Details of the circuitry required for these designs, and the overall design considerations (i.e., turning moment analysis) of such devices are given by Johnson (1985). The accuracy obtained from potentiometers is higher than that from contact closures, but the potentiometer-based wind vanes usually cost more. As with cup and propeller anemometers, environmental problems (blowing dust, salt, and ice) affect the reliability of wind vanes.

2.8.5 Instrumentation Towers

Since it is desirable to collect wind data at the hub height of turbines, one needs to use towers that can reach from a minimum of 20 m up to (or above) 150 m. Sometimes communications towers are available near the site under consideration. In most cases, however, towers must be installed specifically for wind measurement systems.

Instrumentation towers come in many styles: self-supporting, lattice or tubular towers, guyed lattice towers, and guyed tilt-up towers. Guyed tilt-up towers that can be erected from the ground are the type most commonly used today. These towers have been designed specifically for wind measurements and they are lightweight and can be moved easily. They require small foundations and can usually be installed in less than a day.

More details on this subject are included in the wind resource assessment handbook of Bailey *et al.* (1996).

2.8.6 Data Recording Systems

In the development of a wind measurement program one must select some type of data recording system in order to display, record, and analyze the data obtained from the sensors and transducers. The types of displays used for wind instruments are either of the analog type

(meters) or of the digital type (LED, LCD) and supply one with current information. Typical displays use dials, lights, and digital counters. Recorders can provide past information and also may provide current information. Today, the recorders used in wind instrumentation systems generally are based on solid-state devices.

In general, the favored method of handling the large amount of data needed for complete analysis is the use of data loggers or data acquisition using personal computers. A number of data logging systems are available on the market that record wind speed and direction averages and standard deviations, as well as maximum wind speed during the averaging interval. These systems often record the data on removable storage cards. Some allow the data to be downloaded via modem and a cell phone.

The choices of methods and data recording systems are large, and each has its own advantages and disadvantages. The particular situation will define the data requirements, which, in turn, will dictate the choice of recording methods.

2.8.7 Wind Data Analysis

The data produced by a wind monitoring system can be analyzed in a number of ways. These may include, but are not limited to:

- average horizontal wind speeds over specified time intervals;
- variations in the horizontal wind speed over the sampling intervals (standard deviation, turbulence intensity, maxima);
- average horizontal wind direction;
- variations in the horizontal wind direction over the sampling intervals (standard deviation);
- speed and direction distributions;
- persistence;
- determining gust parameters;
- statistical analysis, including autocorrelation, power spectral density, length and time scales, and spatial and time correlations with nearby measurements;
- steady and fluctuating u, v, w wind components;
- diurnal, seasonal, annual, inter-annual and directional variations of any of the above parameters.

Some mention has been made of each of these measures of wind data, except for persistence. Persistence is the duration of the wind speed within a given wind speed range. Also, histograms of the frequency of continuous periods of wind between the cut-in and cut-out wind speeds would provide information on the expected length of periods of continuous turbine operation.

A wind rose is a diagram showing the temporal distribution of wind direction and azimuthal distribution of wind speed at a given location. A wind rose (an example of which is shown in Figure 2.42) is a convenient tool for displaying anemometer data (wind speed and direction) for siting analysis. This figure illustrates the most common form, which consists of equally spaced concentric circles with 16 equally spaced radial lines (each represents a compass point). The line length is proportional to the frequency of the wind from the compass point, with the circles forming a scale. The frequency of calm conditions is indicated in the center. The longest lines identify the prevailing wind directions. Wind roses generally are used to represent annual, seasonal, or monthly data.
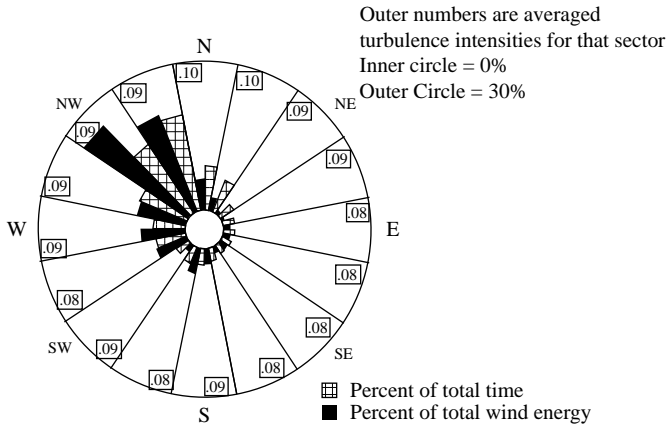
Figure 2.42   Example of a wind rose diagram

2.8.8 Overview of a Wind Monitoring Program

This section presents an outline of the procedure for conducting a successful wind monitoring program. It relies on the application of the fundamentals of wind characteristics, resource measurement and evaluation, and wind energy measurement systems.

In the United States much work has been carried out on this, and the researchers and wind engineers involved in this subject have carefully documented their work. More specifically, under the auspices of the US Department of Energy and their subcontractor, the National Renewable Energy Laboratory (NREL), a detailed handbook on this subject was prepared by AWS Scientific (Bailey *et al.*, 1996). The handbook, which has been designed for use in wind energy training seminars, contains ten chapters and an appendix. Following the approach of this handbook, a wind assessment and monitoring program includes the following components:

- review of guiding principles of a wind resource assessment program;
- determination of costs and labor requirements for a wind monitoring program;
- siting of monitoring systems;
- determination of measurement parameters;
- selection of monitoring station instrumentation;
- installation of monitoring systems;
- station operation and maintenance;
- data collection and handling;
- data validation, processing, and reporting.

2.9 Advanced Topics

There are some important topics in the area of wind characterization that are beyond the scope of this chapter, but they will be summarized briefly here.

- application of stochastic processes to wind energy;
- analysis and characterization of wind turbulence;
- use of numerical or computational fluid dynamic (CFD) models for flow characterization;
- micrositing;
- statistically based resource assessment techniques.

A short description of each of these advanced topics follows.

2.9.1 Application of Stochastic Processes to Wind Energy

In Section 2.4.3, statistical functions such as the Weibull and Rayleigh distributions were used to characterize wind speed variation. The variation in wind speed is a random process, however, and it is not possible to predict what will happen in the future, even with extensive wind speed data at the same site. Thus, one must find the likelihood, or probability, that the wind speed will be within certain limits. This type of variation is called a stochastic, probabilistic, or a random process.

Stochastic models are based on the concept that turbulence is made up of sinusoidal waves, or eddies with periods and random amplitudes. These types of models may also use probability distribution or other statistical parameters. Stochastic analysis can be invaluable in developing models of the wind inflow, because it facilitates the following critical engineering analysis or design tasks:

- representation of many data points taken in field tests;
- evaluation of fatigue loads;
- comparison of model field data with historical field data.

This subject is discussed in more detail in Appendix C. Also, more information on these types of models as applied to wind energy may be found in Spera (1994) and Rohatgi and Nelson (1994). For information on the analytical methods for stochastic process analysis see Bendat and Piersol (1993).

2.9.2 Analysis and Characterization of Wind Turbulence

Knowledge of the fundamentals of turbulence is important because turbulence causes random, fluctuating loads and power output, and stresses over the whole turbine and tower structure. It is important to consider turbulence for the following purposes:

- maximum load prediction;
- structural excitation;
- fatigue;
- control;
- power quality.

Turbulence is a complex subject, considered in many advanced fluid mechanics textbooks. There has been considerable progress made in the application of turbulence research to wind energy applications. See, for example, the discussions of this subject in the texts of Spera (1994) and Rohatgi and Nelson (1994). Also see Appendix C.

1 *u-v-w* sonic anemometer
2 Hot film anemometer
3 *u-v-w* Gill anemometer
4 Propellor vane anemometer
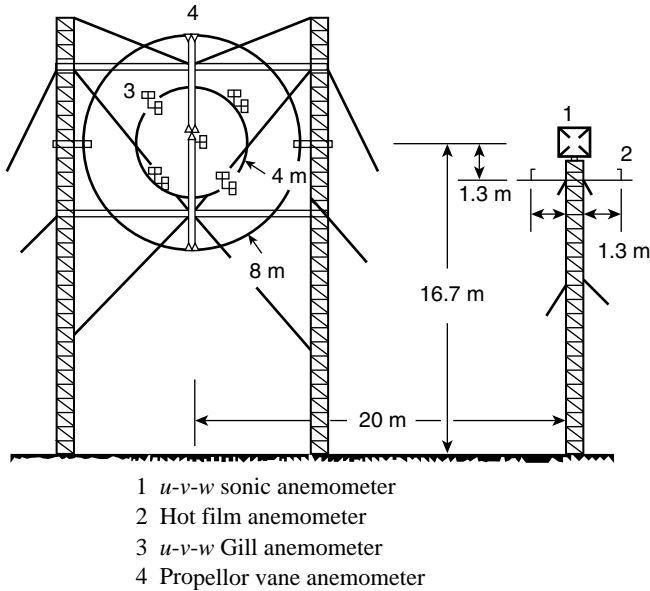
Figure 2.43 National Renewable Energy Laboratory combined experiment anemometry system (Butterfield, 1989)

To illustrate the instrumentation required for a detailed turbulence study, Figure 2.43 shows the turbulence characterization scheme used by NREL for their 'combined experiment' test program. This system consisted of a plane array of 13 anemometers used to measure the wind inflow. The system could collect a large amount of data in a very short time.

2.9.3 Use of Numerical or Computational Fluid Dynamic Models for Flow Characterization

The progress in computational or numerical modeling of complex flow fields has spread to the field of wind energy. For example, since many potential locations for wind turbines involve siting in complex terrain, it is useful to have analytical tools that can characterize the wind fields in these locations.

Today, the use of computational fluid dynamic (CFD) modeling is one of the most rapidly expanding areas in fluid mechanics (see Anderson, 1995). The rapid progress in CFD models and the ability to analyze complex flows are expected to expand with the ever-increasing power of digital computers, and the associated graphical routines.

2.9.4 Micrositing

Micrositing is defined as a resource assessment tool used to determine the exact position of one or more wind turbines on a parcel of land to optimize the power production. An objective of micrositing is to locate the wind turbines in the wind farm to maximize annual energy production or to yield the largest financial return for the owners of the wind farm.

   Effective micrositing depends on a combination of detailed wind resource information for the specific site and, generally, the use of CFD models to predict the detailed flow field in the wind farm (including machine wake effects). The output is then combined in another model that gives a prediction of the energy output of the wind farm. Some micrositing models are even able to give the optimized location for wind turbine placement. Some examples of micrositing models are summarized by Rohatgi and Nelson (1994).

2.9.5 Advanced Statistically-based Resource Assessment Techniques

For an estimate of the wind resource potential at a site with little or no wind resource measurement, one approach may be to link this site to a nearby site that has long duration wind resource measurements. Landberg and Mortensen (1993) note that this link can be accomplished using either physical methods (using CFD models) or via the use of statistical methods (based on statistical correlations between the two time series of data). A statistically based technique that has been widely used is the Measure–Correlate–Predict (MCP) approach.

   The basic idea behind the MCP approach is to establish relations between wind speed and direction at a potential wind site and a site where wind speed and direction have been measured over a long period of time. More information on this subject is presented in Chapter 9.

References

Anderson, J. D. (1995) *Computational Fluid Dynamics: The Basics with Applications*. McGraw-Hill, New York.

Antoniou, I. *et al.* (2006) Offshore wind profile measurements from remote sensing instruments. *Proc. 2006 European Wind Energy Conference. Athens.*

ASME (1988) *Performance Test Code for Wind Turbines*. ASME/ANSI PTC 42-1988. American Society of Mechanical Engineers, New York.

Aspliden, C. I., Elliot, D. L. and Wendell, L. L. (1986) Resource Assessment Methods, Siting, and Performance Evaluation. in *Physical Climatology for Solar and Wind Energy* (eds R. Guzzi and C. G. Justus) World Scientific, New Jersey.

Avallone, E. A. and Baumeister, T. III, (Eds.) (1978) *Mark's Standard Handbook for Mechanical Engineers*. McGraw-Hill, New York.

AWEA (1986) *Standard Procedures for Meteorological Measurements at a Potential Wind Site*. AWEA Standard 8.1. American Wind Energy Association, Washington, DC.

AWEA (1988) *Standard Performance Testing of Wind Energy Conversion Systems*. AWEA Standard 1.1. American Wind Energy Association, Washington, DC.

Bailey, B. H., McDonald, S. L., Bernadett, D. W., Markus, M. J. and Elsholtz, K. V. (1996) *Wind Resource Assessment Handbook*. AWS Scientific Report. (NREL Subcontract No. TAT-5-15283-01).

Balmer, R. T. (1990) *Thermodynamics*. West Publishing, St Paul, MN.

Bendat, J. S. and Piersol, A. G. (1993) *Engineering Applications of Correlation and Spectral Analysis*. John Wiley & Sons, Inc., New York.

Burton, T., Sharpe, D., Jenkins, N. and Bossanyi, E. (2001) *Wind Energy Handbook*. John Wiley & Sons, Ltd, Chichester.

Butterfield, C. P. (1989) Aerodynamic pressure and flow-visualization measurement from a rotating wind turbine blade. *Proc. 8th ASME Wind Energy Symposium*, 245–256.

Carlin, P. W. (1997) Analytic expressions for maximum wind turbine average power in a Rayleigh wind regime. *Proc. of the 1997 ASME/AIAA Wind Symposium*, 255–263.

Cherry, N. J., Elliot, D. L. and Aspliden, C. I. (1981) World-wide wind resource assessment. *Proc. AWEA Wind Workshop V,* American Wind Energy Association, Washington, DC.

Counihan, J. (1975) Adiabatic atmospheric boundary layers: a review and analysis of data collected from the period 1880–1972. *Atmospheric Environment*, **9**, 871–905.

Courtney, M., Wagner, R. and Lindelow, P. (2008) Commercial LIDAR profilers for wind energy: a comparative guide, *Proc. of the 2008 European Wind Energy Conference. Brussels.*

Cuerva, A. and Sanz-Andres, A. (2000) On sonic anemometer measurement theory. *Journal of Wind Engineering and Industrial Aerodynamics*, **88**(1), 25–55.

de Noord, M., Curvers, A., Eecen, P., Antoniou, I., Jørgensen, H. E., Pedersen, T. F., Bradley, S., Hünerbein S. and von Kindler D. (2005) *WISE Wind Energy SODAR Evaluation Final Report*, ECN Report, ECN-C-05-044.

Eldridge, F. R. (1980) *Wind Machines*, 2nd edition. Van Nostrand Reinhold, New York.

Elkinton, M. R., Rogers, A. L. and McGowan, J. G. (2006) An Investigation of Wind-shear Models and Experimental Data Trends for Different Terrains. *Wind Engineering*, **30**(4), 341–350.

Elliot, D. L. (1977) Adjustment and analysis of data for regional wind energy assessments. *Proc. of the Workshop on Wind Climate.* Ashville, NC.

Elliot, D. L. (2002) Assessing the world wind resource. Power Engineering Review, *IEEE*, **22**(9), 4–9.

Elliot, D. L. and Schwartz, M. (2004) *Validation of Updated State Wind Resource Maps for the United States.* National Renewable Energy Laboratory Report: NREL/CP-500-36200.

Elliot, D. L. and Schwartz, M. (2005) *Development and Validation of High-Resolution State Wind Resource Maps for the United States.* National Renewable Energy Laboratory Report: NREL/TP-500-38127.

Elliot, D. L., Wendell, L. L. and Gower, G. L. (1991) *An Assessment of the Available Windy Land Area and Wind Energy Potential in the Contiguous United States.* Pacific National Laboratories Report PNL-7789, NTIS.

Elliot, D. L., Holladay, C. G., Barchet, W. R., Foote, H. P. and Sandusky, W. F. (1987) *Wind Energy Resource Atlas of the United States.* Pacific Northwest Laboratories Report DOE/CH10094-4, NTIS.

EWEA (2004) *Wind Energy, The Facts, Vols. 1–5.* European Wind Energy Association, Brussels.

Freris, L. L. (1990) *Wind Energy Conversion Systems.* Prentice Hall, London.

Giebel, G. (2003) *The State-Of-The-Art in Short Term Prediction of Wind Power: A Literature Overview.* Project ANEMOS Report, European Commission.

Golding, E. W. (1977) *The Generation of Electricity by Wind Power*, E. & F. N. Spon, London.

Gustavson, M. R. (1979) Limits to wind power utilization. *Science*, **204**, 13–18.

Hansen, K. S. *et al.* (2006) Validation of SODAR measurements for wind power assessments, *Proc. of the 2006 European Wind Energy Conference.* Athens.

Hiester, T. R. and Pennell, W. T. (1981) *The Meteorological Aspects of Siting Large Wind Turbines.* Pacific Northwest Laboratories Report PNL- 2522, NTIS.

Hoogwijk, M., de Vries, B. and Turkenburg, W. (2004) Assessment of the global and regional geographical, technical and economic potential of onshore wind energy. *Energy Economics*, **26**, 889–919.

IEC (2005) *Wind Turbines – Part 12: Power Performance Measurements, IEC 61400-12 Ed. 1*, International Electrotechnical Commission, Geneva.

Jamil, M. (1994) Wind power statistics and evaluation of wind energy density. *Wind Engineering*, **18**(5), 227–240.

Johnson, G. L. (1985) *Wind Energy Systems.* Prentice Hall, Englewood Cliffs, NJ.

Jorgensen, H. *et al.* (2004) Site wind field determination using a cw Doppler LIDAR- comparison with cup anemometers at Riso, *Proc. The Science of Making Torque from Wind,* Delft.

Justus, C. G. (1978) *Winds and Wind System Performance.* Franklin Institute Press, Philadelphia, PA.

Kariniotakis, G. *et al.* (2006) Next generation short-term forecasting of wind power – overview of the ANEMOS project. *Proc. of the 2006 European Wind Energy Conference,* Athens.

Kristensen, L. (1999) The perennial cup anemometer. *Wind Energy*, **2** 59–75.

Landberg, L. and Mortensen, N. G. (1993) A comparison of physical and statistical methods for estimating the wind resource at a site. *Proc. 15th British Wind Energy Association Conference*, 119–125.

Landberg, L. *et al.* (2003a) Wind resource estimation – an overview. *Wind Energy*, **6**, 261–271.

Landberg, L. *et al.* (2003b) Short-term prediction – an overview. *Wind Energy*, **6**, 273–280.

Lysen, E. H. (1983) *Introduction to Wind Energy*, SWD Publication SWD 82-1, Amersfoort, NL.

Mortensen, N. G. *et al.* (2003) *Wind Atlas Analysis and Application Program: WAsP 8.0 Help Facility.* Risø National Laboratory. Roskilde.

Pedersen, T. F. (2004) *Characterisation and Classification of RISØ P2546 Cup Anemometer*, Risø National Laboratory Report: Riso-R-1366 (ed.2)(EN).

Pedersen, T. F. *et al.* (2006) ACCUWIND – *Accurate Wind Speed Measurements in Wind Energy: Summary Report.* Risø National Laboratory Report: Risø-R-1563(EN).

Putnam, P. C. (1948) *Power from the Wind.* Van Nostrand Reinhold, New York.

Rohatgi, J. S. and Nelson, V. (1994) *Wind Characteristics: An Analysis for the Generation of Wind Power*. Alternative Energy Institute, Canyon, TX.

Schlichting H. (1968) *Boundary Layer Theory*. 6th edition. McGraw-Hill, New York.

Singh, S., Bhatti, T. S. and Kothari, D. P. (2006) A Review of Wind-Resource-Assessment Technology. *Journal of Energy Engineering*, **132**(1), 8–14.

Smith, D. A., Harris, M. and Coffey, A. (2006) Wind LIDAR evaluation at the Danish wind test site in Hovsore. *Wind Energy*, **9** 87–93.

Spera, D. A. (Ed.) (1994) *Wind Turbine Technology: Fundamental Concepts of Wind Turbine Engineering*. ASME Press, New York.

Troen, I. and Petersen, E. L. (1989) *European Wind Atlas*. Risø National Laboratory, Denmark.

van der Tempel, J. (2006) *Design of Support Structures for Offshore Wind Turbines*. PhD Thesis, TU Delft, NL.

Wegley, H. L., Ramsdell, J. V., Orgill M. M. and Drake R. L. (1980) *A Siting Handbook for Small Wind Energy Conversion Systems*, Battelle Pacific Northwest Lab., PNL-2521, Rev. 1, NTIS.

Weitkamp, C. (Ed) (2005) *Lidar: Range-Resolved Optical Remote Sensing of the Atmosphere*, Springer.

Wendell, L. L., Morris, V. R., Tomich, S. D. and Gower, G. L. (1991) Turbulence Characterization for Wind Energy Development. *Proc. of the 1991 American Wind Energy Association Conference*, 254–265.

World Energy Council (1993) *Renewable Energy Resources: Opportunities and Constraints 1990–2020*. World Energy Council, London.

Wortman, A. J. (1982) *Introduction to Wind Turbine Engineering*. Butterworth, Boston, MA.

3

Aerodynamics of Wind Turbines

3.1 General Overview

Wind turbine power production depends on the interaction between the rotor and the wind. As discussed in Chapter 2, the wind may be considered to be a combination of the mean wind and turbulent fluctuations about that mean flow. Experience has shown that the major aspects of wind turbine performance (mean power output and mean loads) are determined by the aerodynamic forces generated by the mean wind. Periodic aerodynamic forces caused by wind shear, off-axis winds, and rotor rotation and randomly fluctuating forces induced by turbulence and dynamic effects are the source of fatigue loads and are a factor in the peak loads experienced by a wind turbine. These are, of course, important, but can only be understood once the aerodynamics of steady state operation have been understood. Accordingly, this chapter focuses primarily on steady state aerodynamics. An overview of the complex phenomena of unsteady aerodynamics and how they are addressed in the analysis of rotor performance is presented at the end of the chapter.

Practical horizontal axis wind turbine designs use airfoils to transform the kinetic energy in the wind into useful energy. The material in this chapter provides the background to enable the reader to understand power production with the use of airfoils, to calculate an optimum blade shape for the start of a blade design and to analyze the aerodynamic performance of a rotor with a known blade shape and airfoil characteristics. A number of authors have derived methods for predicting the steady state performance of wind turbine rotors. The classical analysis of the wind turbine was originally developed by Betz and Glauert (Glauert, 1935) in the 1930s. Subsequently, the theory was expanded and adapted for solution by digital computers (see Wilson and Lissaman, 1974; Wilson *et al.*, 1976; de Vries, 1979). In all of these methods, momentum theory and blade element theory are combined into a strip theory that enables calculation of the performance characteristics of an annular section of the rotor. The characteristics for the entire rotor are then obtained by integrating, or summing, the values obtained for each of the annular sections. This approach is the one used in this chapter.

The chapter starts with the analysis of an idealized wind turbine rotor. The discussion introduces important concepts and illustrates the general behavior of wind turbine rotors and the air flow over them. The analyses are also used to determine theoretical performance limits for wind turbines.

General aerodynamic concepts and the operation of airfoils are introduced next. This information is then used to consider the advantages of using airfoils for power production over other approaches.

The majority of the chapter (Sections 3.5 through 3.11) details the classical analytical approach to the analysis of horizontal axis wind turbines, as well as some applications and examples of its use. First the details of momentum theory and blade element theory are developed and used to calculate the optimum blade shape for simplified, ideal operating conditions. The results illustrate the derivation of the general blade shape used in wind turbines. The combination of the two approaches, called strip theory or blade element momentum (BEM) theory, is then used to outline a procedure for the aerodynamic design and performance analysis of a wind turbine rotor. Aerodynamic losses and off-design performance are discussed as well as an optimum blade design which takes the effects of wake rotation into account. A simplified design procedure is then presented that can be used for quick analyses.

The next two sections of the chapter, Sections 3.12 and 3.13, discuss limitations on the maximum theoretical performance of a wind turbine and introduce modifications to steady state BEM theory that address issues related to non-ideal steady state aerodynamics, turbine wakes, and unsteady aerodynamics. Section 3.13 also addresses other theoretical approaches to rotor performance analysis and the validation of computer codes used for analyzing rotor performance.

Finally, Section 3.14 covers the basics of vertical axis aerodynamic rotor performance calculations.

Every attempt has been made to make the material in this chapter accessible to readers without a fluid dynamics background. Nevertheless, it would be helpful to be familiar with a variety of concepts including Bernoulli's equation, streamlines, control volume analyses, and the concepts of laminar and turbulent flow. The material does require an understanding of basic physics.

3.2 One-dimensional Momentum Theory and the Betz Limit

A simple model, generally attributed to Betz (1926), can be used to determine the power from an ideal turbine rotor, the thrust of the wind on the ideal rotor, and the effect of the rotor operation on the local wind field. This simple model is based on a linear momentum theory developed over 100 years ago to predict the performance of ship propellers.

The analysis assumes a control volume, in which the control volume boundaries are the surface of a stream tube and two cross-sections of the stream tube (see Figure 3.1). The only flow is across the ends of the stream tube. The turbine is represented by a uniform 'actuator disc' which creates a discontinuity of pressure in the stream tube of air flowing through it. Note that this analysis is not limited to any particular type of wind turbine.

This analysis uses the following assumptions:

- homogenous, incompressible, steady state fluid flow;
- no frictional drag;
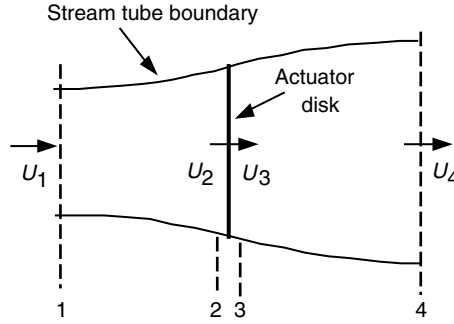
Figure 3.1   Actuator disc model of a wind turbine; U, mean air velocity; 1, 2, 3, and 4 indicate locations

- an infinite number of blades;
- uniform thrust over the disc or rotor area;
- a non–rotating wake;
- the static pressure far upstream and far downstream of the rotor is equal to the undisturbed ambient static pressure

Applying the conservation of linear momentum to the control volume enclosing the whole system, one can find the net force on the contents of the control volume. That force is equal and opposite to the thrust, T, which is the force of the wind on the wind turbine. From the conservation of linear momentum for a one-dimensional, incompressible, time-invariant flow, the thrust is equal and opposite to the rate of change of momentum of the air stream:

$$T = U_1(\rho A U)_1 - U_4(\rho A U)_4 \tag{3.1}$$

where ρ is the air density, A is the cross-sectional area, U is the air velocity, and the subscripts indicate values at numbered cross-sections in Figure 3.1.

For steady state flow, $(\rho A U)_1 = (\rho A U)_4 = \dot{m}$, where $\dot{m}$ is the mass flow rate. Therefore:

$$T = \dot{m}(U_1 - U_4) \tag{3.2}$$

The thrust is positive so the velocity behind the rotor, U_4, is less than the free stream velocity, U_1. No work is done on either side of the turbine rotor. Thus the Bernoulli function can be used in the two control volumes on either side of the actuator disc. In the stream tube upstream of the disc:

$$p_1 + \tfrac{1}{2}\rho U_1^2 = p_2 + \tfrac{1}{2}\rho U_2^2 \tag{3.3}$$

In the stream tube downstream of the disc:

$$p_3 + \tfrac{1}{2}\rho U_3^2 = p_4 + \tfrac{1}{2}\rho U_4^2 \tag{3.4}$$

where it is assumed that the far upstream and far downstream pressures are equal ($p_1 = p_4$) and that the velocity across the disc remains the same ($U_2 = U_3$).

The thrust can also be expressed as the net sum of the forces on each side of the actuator disc:

$$T = A_2(p_2 - p_3) \tag{3.5}$$

If one solves for $(p_2 - p_3)$ using Equations (3.3) and (3.4) and substitutes that into Equation (3.5), one obtains:

$$T = \tfrac{1}{2}\rho A_2(U_1^2 - U_4^2) \tag{3.6}$$

Equating the thrust values from Equations (3.2) and (3.6) and recognizing that the mass flow rate is also $\rho A_2 U_2$, one obtains:

$$U_2 = \frac{U_1 + U_4}{2} \tag{3.7}$$

Thus, the wind velocity at the rotor plane, using this simple model, is the average of the upstream and downstream wind speeds.

If one defines the axial induction factor, a, as the fractional decrease in wind velocity between the free stream and the rotor plane, then

$$a = \frac{U_1 - U_2}{U_1} \tag{3.8}$$

$$U_2 = U_1(1 - a) \tag{3.9}$$

and

$$U_4 = U_1(1 - 2a) \tag{3.10}$$

The quantity $U_1 a$ is often referred to as the induced velocity at the rotor, in which case the velocity of the wind at the rotor is a combination of the free stream velocity and the induced wind velocity. As the axial induction factor increases from 0, the wind speed behind the rotor slows more and more. If $a = 1/2$, the wind has slowed to zero velocity behind the rotor and the simple theory is no longer applicable.

The power out, P, is equal to the thrust times the velocity at the disc:

$$P = \tfrac{1}{2}\rho A_2(U_1^2 - U_4^2)U_2 = \tfrac{1}{2}\rho A_2 U_2(U_1 + U_4)(U_1 - U_4) \tag{3.11}$$

Substituting for U_2 and U_4 from Equations (3.9) and (3.10) gives:

$$P = \tfrac{1}{2}\rho A U^3 4a(1 - a)^2 \tag{3.12}$$

where the control volume area at the rotor, A_2, is replaced by A, the rotor area, and the free stream velocity U_1 is replaced by U.

Wind turbine rotor performance is usually characterized by its power coefficient, C_P:

$$C_P = \frac{P}{\tfrac{1}{2}\rho U^3 A} = \frac{\text{Rotor power}}{\text{Power in the wind}} \tag{3.13}$$

The non-dimensional power coefficient represents the fraction of the power in the wind that is extracted by the rotor. From Equation (3.12), the power coefficient is:

$$C_P = 4a(1-a)^2 \tag{3.14}$$

The maximum C_P is determined by taking the derivative of the power coefficient (Equation (3.14)) with respect to a and setting it equal to zero, yielding $a = 1/3$. Thus:

$$C_{P,\mathrm{max}} = 16/27 = 0.5926 \tag{3.15}$$

when $a = 1/3$. For this case, the flow through the disc corresponds to a stream tube with an upstream cross-sectional area of $2/3$ the disc area that expands to twice the disc area downstream. This result indicates that, if an ideal rotor were designed and operated such that the wind speed at the rotor were $2/3$ of the free stream wind speed, then it would be operating at the point of maximum power production. Furthermore, given the basic laws of physics, this is the maximum power possible.

From Equations (3.6), (3.9) and (3.10), the axial thrust on the disc is:

$$T = \tfrac{1}{2}\rho A U^2 \left[4a(1-a) \right] \tag{3.16}$$

Similarly to the power, the thrust on a wind turbine can be characterized by a non-dimensional thrust coefficient:

$$C_T = \frac{T}{\tfrac{1}{2}\rho U^2 A} = \frac{\text{Thrust force}}{\text{Dynamic force}} \tag{3.17}$$

From Equation (3.16), the thrust coefficient for an ideal wind turbine is equal to $4a(1-a)$. C_T has a maximum of 1.0 when $a = 0.5$ and the downstream velocity is zero. At maximum power output ($a = 1/3$), C_T has a value of $8/9$. A graph of the power and thrust coefficients for an ideal Betz turbine and the non-dimensionalized downstream wind speed are illustrated in Figure 3.2.

As mentioned above, this idealized model is not valid for axial induction factors greater than 0.5. In practice (Wilson *et al.*, 1976), as the axial induction factor approaches and exceeds 0.5, complicated flow patterns that are not represented in this simple model result in thrust
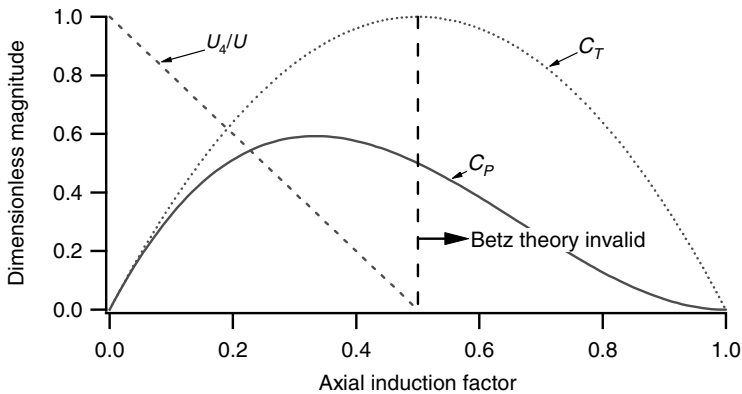
Figure 3.2 Operating parameters for a Betz turbine; U, velocity of undisturbed air; U_4, air velocity behind the rotor; C_P, power coefficient; C_T, thrust coefficient

coefficients that can go as high as 2.0. The details of wind turbine operation at these high axial induction factors appear in Section 3.8.

The Betz limit, $C_{P,\max} = 16/27$, is the maximum theoretically possible rotor power coefficient. In practice, three effects lead to a decrease in the maximum achievable power coefficient:

- rotation of the wake behind the rotor;
- finite number of blades and associated tip losses;
- non-zero aerodynamic drag.

Note that the overall turbine efficiency is a function of both the rotor power coefficient and the mechanical (including electrical) efficiency of the wind turbine:

$$\eta_{overall} = \frac{P_{out}}{\frac{1}{2}\rho A U^3} = \eta_{mech} C_P \qquad (3.18)$$

Thus:

$$P_{out} = \frac{1}{2}\rho A U^3 (\eta_{mech} C_P) \qquad (3.19)$$

3.3 Ideal Horizontal Axis Wind Turbine with Wake Rotation

In the previous analysis using linear momentum theory, it was assumed that no rotation was imparted to the flow. The previous analysis can be extended to the case where the rotating rotor generates angular momentum, which can be related to rotor torque. In the case of a rotating wind turbine rotor, the flow behind the rotor rotates in the opposite direction to the rotor, in reaction to the torque exerted by the flow on the rotor. An annular stream tube model of this flow, illustrating the rotation of the wake, is shown in Figure 3.3.
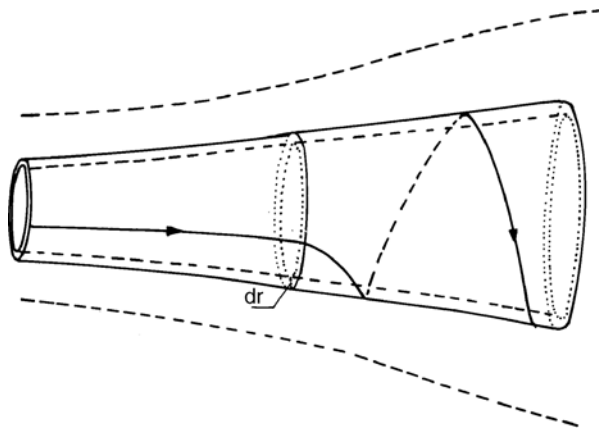
Figure 3.3 Stream tube model of flow behind rotating wind turbine blade. Picture of stream tube with wake rotation, from Lysen (1982) Reproduced by permission of the author
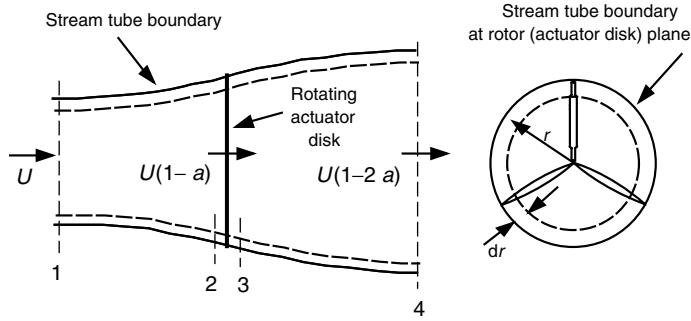
Figure 3.4   Geometry for rotor analysis; U, velocity of undisturbed air; a, induction factor; r, radius

The generation of rotational kinetic energy in the wake results in less energy extraction by the rotor than would be expected without wake rotation. In general, the extra kinetic energy in the wind turbine wake will be higher if the generated torque is higher. Thus, as will be shown here, slow-running wind turbines (with a low rotational speed and a high torque) experience more wake rotation losses than high-speed wind machines with low torque.

Figure 3.4 gives a schematic of the parameters involved in this analysis. Subscripts denote values at the cross-sections identified by numbers. If it is assumed that the angular velocity imparted to the flow stream, ω, is small compared to the angular velocity, Ω, of the wind turbine rotor, then it can also be assumed that the pressure in the far wake is equal to the pressure in the free stream (see Wilson *et al.*, 1976). The analysis that follows is based on the use of an annular stream tube with a radius r and a thickness dr, resulting in a cross-sectional area equal to $2\pi r \mathrm{d}r$ (see Figure 3.4). The pressure, wake rotation, and induction factors are all assumed to be functions of radius.

If one uses a control volume that moves with the angular velocity of the blades, the energy equation can be applied in the sections before and after the blades to derive an expression for the pressure difference across the blades (see Glauert, 1935 for the derivation). Note that across the flow disc, the angular velocity of the air relative to the blade increases from Ω to $\Omega + \omega$, while the axial component of the velocity remains constant. The results are:

$$p_2 - p_3 = \rho(\Omega + \tfrac{1}{2}\omega)\omega r^2 \tag{3.20}$$

The resulting thrust on an annular element, dT, is:

$$\mathrm{dT} = (p_2 - p_3)\mathrm{d}A = \left[\rho(\Omega + \tfrac{1}{2}\omega)\omega r^2\right]2\pi r \mathrm{d}r \tag{3.21}$$

An angular induction factor, a', is then defined as:

$$a' = \omega/2\Omega \tag{3.22}$$

Note that when wake rotation is included in the analysis, the induced velocity at the rotor consists of not only the axial component, Ua, but also a component in the rotor plane, $r\Omega a'$.

The expression for the thrust becomes:

$$\mathrm{dT} = 4a'(1 + a')\tfrac{1}{2}\rho\Omega^2 r^2 2\pi r \mathrm{d}r \tag{3.23}$$

Following the previous linear momentum analysis, the thrust on an annular cross-section can also be determined by the following expression that uses the axial induction factor, a, (note that U_1, the free stream velocity, is designated by U in this analysis):

$$dT = 4a(1-a)\tfrac{1}{2}\rho U^2 2\pi r dr \tag{3.24}$$

Equating the two expressions for thrust gives:

$$\frac{a(1-a)}{a'(1+a')} = \frac{\Omega^2 r^2}{U^2} = \lambda_r^2 \tag{3.25}$$

where λ_r is the local speed ratio (see below). This result will be used later in the analysis.

The tip speed ratio, λ, defined as the ratio of the blade tip speed to the free stream wind speed, is given by:

$$\lambda = \Omega R / U \tag{3.26}$$

The tip speed ratio often occurs in the aerodynamic equations for the rotor. The local speed ratio is the ratio of the rotor speed at some intermediate radius to the wind speed:

$$\lambda_r = \Omega r / U = \lambda r / R \tag{3.27}$$

Next, one can derive an expression for the torque on the rotor by applying the conservation of angular momentum. For this situation, the torque exerted on the rotor, Q, must equal the change in angular momentum of the wake. On an incremental annular area element this gives:

$$dQ = d\dot{m}(\omega\, r)(r) = (\rho U_2 2\pi r dr)(\omega\, r)(r) \tag{3.28}$$

Since $U_2 = U(1-a)$ and $a' = \omega/2\Omega$, this expression reduces to

$$dQ = 4a'(1-a)\tfrac{1}{2}\rho U\Omega r^2 2\pi r dr \tag{3.29}$$

The power generated at each element, dP, is given by:

$$dP = \Omega dQ \tag{3.30}$$

Substituting for dQ in this expression and using the definition of the local speed ratio, λ_r, (Equation (3.27)), the expression for the power generated at each element becomes:

$$dP = \tfrac{1}{2}\rho A U^3 \left[\frac{8}{\lambda^2} a'(1-a)\lambda_r^3 d\lambda_r\right] \tag{3.31}$$

It can be seen that the power from any annular ring is a function of the axial and angular induction factors and the tip speed ratio. The axial and angular induction factors determine the magnitude and direction of the air flow at the rotor plane. The local speed ratio is a function of the tip speed ratio and radius.

The incremental contribution to the power coefficient, dC_P, from each annular ring is given by:

$$dC_P = \frac{dP}{^{1}/_{2}\,\rho A U^3} \tag{3.32}$$

Thus

$$C_P = \frac{8}{\lambda^2} \int_0^\lambda a'(1-a)\lambda_r^3 d\lambda_r \qquad (3.33)$$

In order to integrate this expression, one needs to relate the variables a, a', and λ_r, (see Glauert, 1948; Sengupta and Verma, 1992). Solving Equation (3.25) to express a' in terms of a, one gets:

$$a' = -\tfrac{1}{2} + \tfrac{1}{2}\sqrt{\left[1 + \frac{4}{\lambda_r^2}a(1-a)\right]} \qquad (3.34)$$

The aerodynamic conditions for the maximum possible power production occur when the term $a'(1-a)$ in Equation (3.33) is at its greatest value. Substituting the value for a' from Equation (3.34) into $a'(1-a)$ and setting the derivative with respect to a equal to zero yields:

$$\lambda_r^2 = \frac{(1-a)(4a-1)^2}{1-3a} \qquad (3.35)$$

This equation defines the axial induction factor for maximum power as a function of the local tip speed ratio in each annular ring. Substituting into Equation (3.25), one finds that, for maximum power in each annular ring:

$$a' = \frac{1-3a}{4a-1} \qquad (3.36)$$

If Equation (3.35) is differentiated with respect to a, one obtains a relationship between $d\lambda_r$ and da at those conditions that result in maximum power production:

$$2\lambda_r d\lambda_r = \left[6(4a-1)(1-2a)^2/(1-3a)^2\right]da \qquad (3.37)$$

Now, substituting the Equations (3.35)–(3.37) into the expression for the power coefficient (Equation (3.33)) gives:

$$C_{P,\text{max}} = \frac{24}{\lambda^2}\int_{a_1}^{a_2}\left[\frac{(1-a)(1-2a)(1-4a)}{(1-3a)}\right]^2 da \qquad (3.38)$$

Here the lower limit of integration, a_1, corresponds to the axial induction factor for $\lambda_r = 0$ and the upper limit, a_2, corresponds to the axial induction factor at $\lambda_r = \lambda$. Also, from Equation (3.35):

$$\lambda^2 = (1-a_2)(1-4a_2)^2/(1-3a_2) \qquad (3.39)$$

Note that from Equation (3.35), $a_1 = 0.25$ gives λ_r a value of zero.

Equation (3.39) can be solved for the values of a_2 that correspond to operation at tip speed ratios of interest. Note also from Equation (3.39), $a_2 = 1/3$ is the upper limit of the axial induction factor, a, giving an infinitely large tip speed ratio.

Table 3.1   Power coefficient,$C_{P,\max}$, as a function of tip speed ratio, λ; a_2 = axial induction factor when the tip speed ratio equals the local speed ratio

λ	a_2	$C_{P,\max}$
0.5	0.2983	0.289
1.0	0.3170	0.416
1.5	0.3245	0.477
2.0	0.3279	0.511
2.5	0.3297	0.533
5.0	0.3324	0.570
7.5	0.3329	0.581
10.0	0.3330	0.585

The definite integral can be evaluated by changing variables: substituting x for $(1 - 3a)$ in Equation (3.38). The result is:

$$C_{P,\max} = \frac{8}{729\lambda^2} \left\{ \frac{64}{5}x^5 + 72x^4 + 124x^3 + 38x^2 - 63x - 12[\ln(x)] - 4x^{-1} \right\}_{x=(1-3a_2)}^{x=0.25}$$

(3.40)

Table 3.1 presents a summary of numerical values for $C_{P,\max}$ as a function of λ, with corresponding values for the axial induction factor at the tip, a_2.

The results of this analysis are graphically represented in Figure 3.5, which also shows the Betz limit of the ideal turbine based on the previous linear momentum analysis. The results show that, the higher the tip speed ratio, the closer the C_P can approach the theoretical maximum.

These equations can be used to look at the operation of an ideal wind turbine, assuming wake rotation. For example, Figure 3.6 shows the axial and angular induction factors for a turbine with a tip speed ratio of 7.5. It can be seen that the axial induction factors are close to the ideal of
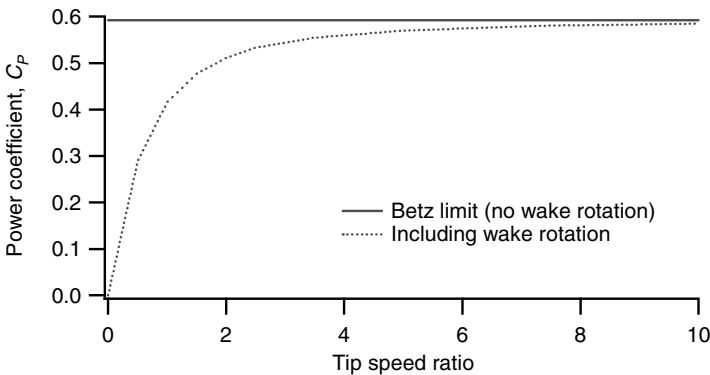
Figure 3.5   Theoretical maximum power coefficient as a function of tip speed ratio for an ideal horizontal axis wind turbine, with and without wake rotation
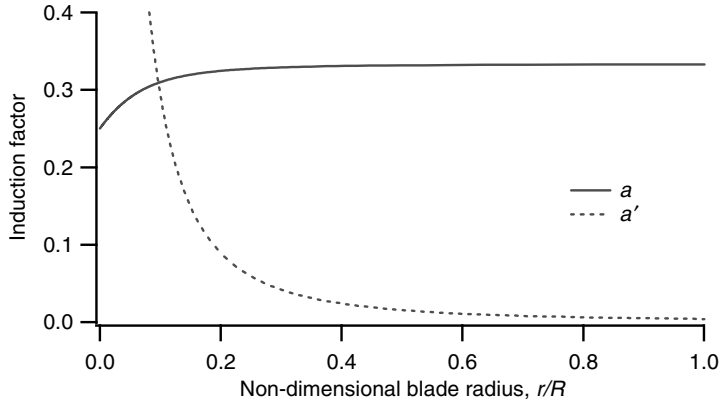
Figure 3.6 Induction factors for an ideal wind turbine with wake rotation; tip speed ratio, $\lambda = 7.5$; a, axial induction factor; a', angular induction factor; r, radius; R rotor radius

1/3 until one gets near the hub. Angular induction factors are close to zero in the outer parts of the rotor, but increase significantly near the hub.

   In the previous two sections, basic physics has been used to determine the nature of the air flow around a wind turbine and theoretical limits on the maximum power that can be extracted from the wind. The rest of the chapter explains how airfoils can be used to approach this theoretically achievable power extraction.

3.4 Airfoils and General Concepts of Aerodynamics

Airfoils are structures with specific geometric shapes that are used to generate mechanical forces due to the relative motion of the airfoil and a surrounding fluid. Wind turbine blades use airfoils to develop mechanical power. The cross-sections of wind turbine blades have the shape of airfoils. The width and length of the blade are functions of the desired aerodynamic performance, the maximum desired rotor power, the assumed airfoil properties, and strength considerations. Before the details of wind turbine power production are explained, aerodynamic concepts related to airfoils need to be discussed.

3.4.1 Airfoil Terminology

A number of terms are used to characterize an airfoil, as shown in Figure 3.7. The mean camber line is the locus of points halfway between the upper and lower surfaces of the airfoil. The most forward and rearward points of the mean camber line are on the leading and trailing edges, respectively. The straight line connecting the leading and trailing edges is the chord line of the airfoil, and the distance from the leading to the trailing edge measured along the chord line is designated the chord, c, of the airfoil. The camber is the distance between the mean camber line and the chord line, measured perpendicular to the chord line. The thickness is the distance between the upper and lower surfaces, also measured perpendicular to the chord line. Finally, the angle of attack, α, is defined as the angle between the relative wind (U_{rel}) and the chord line.
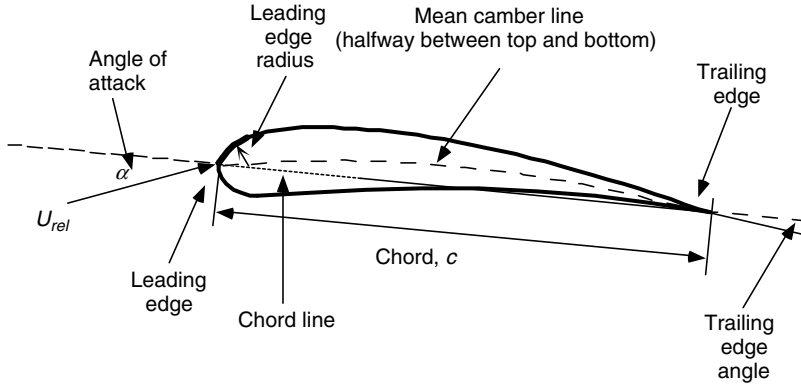
Figure 3.7   Airfoil nomenclature

Not shown in the figure is the span of the airfoil, which is the length of the airfoil perpendicular to its cross-section. The geometric parameters that have an effect on the aerodynamic performance of an airfoil include: the leading edge radius, mean camber line, maximum thickness and thickness distribution of the profile, and the trailing edge angle.

There are many types of airfoils (see Abbott and von Doenhoff, 1959; Althaus and Wortmann, 1981; Althaus, 1996; Miley, 1982; Tangler, 1987). A few examples of ones that have been used in wind turbine designs are shown in Figure 3.8. The NACA 0012 is a 12% thick symmetric airfoil. The NACA 63(2)-215 is a 15% thick airfoil with a slight camber, and the LS(1)-0417 is a 17% thick airfoil with a larger camber.

3.4.2 Lift, Drag and Non-dimensional Parameters

Air flow over an airfoil produces a distribution of forces over the airfoil surface. The flow velocity over airfoils increases over the convex surface resulting in lower average pressure on the 'suction' side of the airfoil compared with the concave or 'pressure' side of the airfoil. Meanwhile, viscous friction between the air and the airfoil surface slows the air flow to some extent next to the surface.
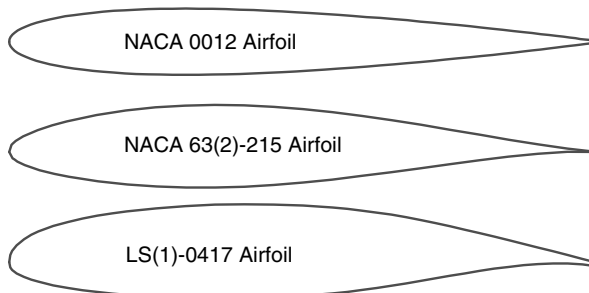
Figure 3.8   Sample airfoils
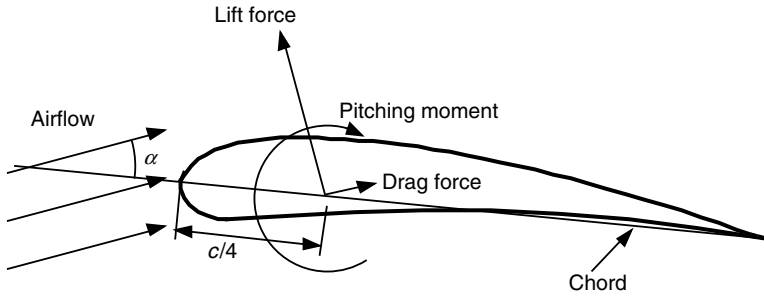
Figure 3.9 Forces and moments on an airfoil section, α angle of attack; c, chord. The direction of positive forces and moments is indicated by the direction of the arrow

As shown in Figure 3.9, the resultant of all of these pressure and friction forces is usually resolved into two forces and a moment that act along the chord at a distance of $c/4$ from the leading edge (at the 'quarter chord'):

- **Lift force** – defined to be perpendicular to direction of the oncoming air flow. The lift force is a consequence of the unequal pressure on the upper and lower airfoil surfaces.
- **Drag force** – defined to be parallel to the direction of the oncoming air flow. The drag force is due both to viscous friction forces at the surface of the airfoil and to unequal pressure on the airfoil surfaces facing toward and away from the oncoming flow.
- **Pitching moment** – defined to be about an axis perpendicular to the airfoil cross-section.

Theory and research have shown that many flow problems can be characterized by non-dimensional parameters. The most important non-dimensional parameter for defining the characteristics of fluid flow conditions is the Reynolds number. The Reynolds number, Re, is defined by:

$$Re = \frac{UL}{v} = \frac{\rho UL}{\mu} = \frac{\text{Inertial force}}{\text{Viscous force}} \tag{3.41}$$

where ρ is the fluid density, μ is fluid viscosity, $v = \mu/\rho$ is the kinematic viscosity, and U and L are a velocity and length that characterize the scale of the flow. These might be the incoming stream velocity, U_{wind}, and the chord length on an airfoil. For example, if U_{wind} is 65 m/s, v is 0.000013 m^2/s and the chord length is 2 m, the Reynolds number is 10 million.

Additional non-dimensionalized force and moment coefficients, which are functions of the Reynolds number, can be defined for two- or three-dimensional objects, based on wind tunnel tests. Three-dimensional airfoils have a finite span and force and moment coefficients are affected by the flow around the end of the airfoil. Two-dimensional airfoil data, on the other hand, are assumed to have an infinite span (no end effects). Two-dimensional data are measured in such a way that there is indeed no air flow around the end of the airfoil in the test section. Force and moment coefficients for flow around two-dimensional objects are usually designated with a lower case subscript, as in C_d for the two-dimensional drag coefficient. In that case, the forces measured are forces per unit span. Lift and drag coefficients that are measured for flow around three-dimensional objects are usually designated with an upper case subscript, as

in C_D. Rotor design usually uses two-dimensional coefficients, determined for a range of angles of attack and Reynolds numbers, in wind tunnel tests. The two-dimensional lift coefficient is defined as:

$$C_l = \frac{L/l}{\frac{1}{2}\rho U^2 c} = \frac{\text{Lift force/unit length}}{\text{Dynamic force/unit length}} \tag{3.42}$$

The two-dimensional drag coefficient is defined as:

$$C_d = \frac{D/l}{\frac{1}{2}\rho U^2 c} = \frac{\text{Drag force/unit length}}{\text{Dynamic force/unit length}} \tag{3.43}$$

and the pitching moment coefficient is:

$$C_m = \frac{M}{\frac{1}{2}\rho U^2 A c} = \frac{\text{Pitching moment}}{\text{Dynamic moment}} \tag{3.44}$$

where ρ is the density of air, U is the velocity of undisturbed air flow, A is the projected airfoil area (chord $\times$ span), c is the airfoil chord length, and l is the airfoil span.

Other dimensionless coefficients that are important for the analysis and design of wind turbines include the power and thrust coefficients and the tip speed ratio (mentioned above), the pressure coefficient:

$$C_p = \frac{p - p_\infty}{\frac{1}{2}\rho U^2} = \frac{\text{Static pressure}}{\text{Dynamic pressure}} \tag{3.45}$$

which is used to analyze airfoil flow, and the surface roughness ratio:

$$\frac{\varepsilon}{L} = \frac{\text{Surface roughness height}}{\text{Body length}} \tag{3.46}$$

3.4.3 Flow Over an Airfoil

The lift, drag, and pitching moment coefficients of an airfoil are generated by the pressure variation over the airfoil surface and the friction between the air and the airfoil.

The pressure variations are caused by changes in air velocity that can be understood using Bernoulli's principle, which states that the sum of the static pressure and the dynamic pressure (assuming frictionless flow) are constant:

$$p + \tfrac{1}{2}\rho U^2 = \text{constant} \tag{3.47}$$

where p is the static pressure and U is the local velocity along the airfoil surface.

As the air flow accelerates around the rounded leading edge, the pressure drops, resulting in a negative pressure gradient. As the air flow approaches the trailing edge, it decelerates and the surface pressure increases, resulting in a positive pressure gradient. If, given the airfoil design and the angle of attack, the air speeds up more over the upper surface than over the lower surface of the airfoil, then there is a net lift force. Similarly, the pitching moment is a function of the integral of the moments of the pressure forces about the quarter chord over the surface of the airfoil.

Drag forces are a result of both the pressure distribution over the airfoil and the friction between the air flow and the airfoil. The component of the net pressure distribution in the direction of the air flow results in the drag due to the pressure. Drag due to friction is a function of the viscosity of the fluid and dissipates energy into the flow field.

Drag also causes the development of two different regions of flow: one farther from the airfoil surface, where frictional effects are negligible and the boundary layer, immediately next to the airfoil surface, where frictional effects dominate. In the boundary layer, the velocity increases from zero at the airfoil surface to that of the friction-free flow outside of the boundary layer. The boundary layer on a wind turbine blade may vary in thickness from a millimeter to tens of centimeters.

The flow in the boundary layer may be laminar (smooth and steady) or turbulent (irregular with three-dimensional vortices). At the leading edge of the airfoil, the flow is laminar. Usually at some point downstream, the flow in the boundary layer becomes turbulent as the interaction between viscosity and nonlinear inertial forces causes a 'transition' to chaotic, turbulent flow. Laminar boundary layers result in much lower frictional forces than do turbulent boundary layers.

The pressure gradient of the flow has a significant effect on the boundary layer, as illustrated in Figure 3.10. That pressure gradient may be a favorable pressure gradient (positive in the direction of the flow) or an adverse pressure gradient (against the flow). Flow in the boundary layer is accelerated or decelerated by the pressure gradient. In the boundary layer, the flow is also slowed by surface friction. Thus, in an adverse pressure gradient and with the help of surface friction, the flow in the boundary layer may be stopped or it may reverse direction. This results in the flow separating from the airfoil, causing a condition called stall. Boundary layers that have already transitioned to turbulent flow are less sensitive to an adverse pressure gradient than are laminar boundary layers, but once the laminar or turbulent boundary layer has separated from the airfoil, the lift drops. An airfoil can only efficiently produce lift as long as the surface pressure distributions can be supported by the boundary layer.
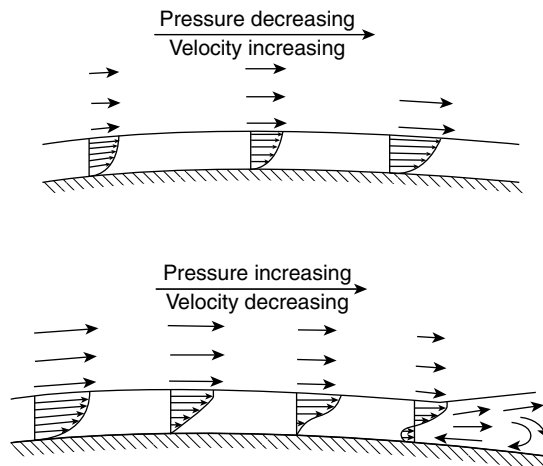
Figure 3.10 Effects of favorable (decreasing) and adverse (increasing) pressure gradients on the boundary layer (Miley, 1982)

It is important to distinguish the effects of the turbulence in the atmosphere from that in the boundary layer of the airfoil. Wind turbine airfoils operate in the turbulent planetary boundary layer but the scale of the turbulent fluctuations in the atmosphere is much larger than the scale of the turbulence in the boundary layer of a wind turbine airfoil. The flow in the boundary layer is only sensitive to fluctuations on the order of the size of the boundary layer itself. Thus, the atmospheric turbulence does not affect the airfoil boundary layer directly. It may affect it indirectly through changing angles of attack, which will change the flow patterns and pressure distributions over the blade surface.

3.4.4 Airfoil Behavior

It is useful to consider flow around a cylinder as a starting point for looking at airfoils. The flow can be best visualized with the help of streamlines. A streamline can be thought of as the path that a particle would take if placed in a flowing fluid. A flow field can then be depicted in terms of a number of streamlines. Streamlines have a few visually interesting properties. For example, streamlines which converge indicate an increase in velocity and a decrease in pressure. The opposite is the case for diverging streamlines. It is also the case that Bernoulli's equation is only strictly applicable along streamlines. Figure 3.11(a) illustrates a flow around a stationary cylinder. In this case the flow assumes that there is no drag and no inertia. It can be seen that the streamlines move closer together as they pass the cylinder. This indicates that the velocity is increasing and the pressure is decreasing. The pattern is symmetrical on both sides of the cylinder, so there is no net lift on the cylinder. In fact, in the absence of viscous drag there is no net force at all on the cylinder in this situation.

When there is rotational flow, however, the situation changes. The fluid rotation may be brought about either by rotation of an object in the flow, or it may result from the shape of the object (such as an airfoil), which imparts a rotational motion to the fluid.
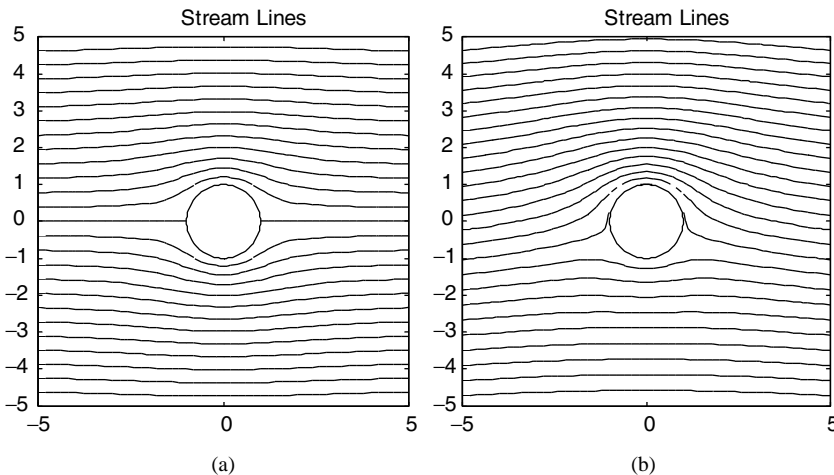
Figure 3.11   (a) Flow around stationary cylinder; (b) flow around rotating (CCW) cylinder

Rotational flow is described in terms of vorticity and circulation. If an element of fluid is rotating, its angular velocity is characterized by its vorticity, ζ, which is given by:

$$\zeta = \frac{\partial u}{\partial y} - \frac{\partial v}{\partial x} \qquad (3.48)$$

where u is the velocity component in the direction of the flow (x) and v is the component perpendicular to the flow (y). The vorticity is also equal to twice the angular velocity of the fluid element.

Circulation, Γ, is the integral of the vorticity of the elements, multiplied by their respective incremental areas, over the region of interest, as shown in Equation (3.49).

$$\Gamma = \iint \left(\frac{\partial u}{\partial y} - \frac{\partial v}{\partial x} \right) dx \, dy \qquad (3.49)$$

It can be shown that, in general, the lift per unit length, L/l, on a body is given by $L/l = \rho U_\infty \Gamma$, where U_∞ = free stream velocity. For a cylinder radius of r the maximum value of the circulation is $\Gamma = 4\pi U_\infty r$. The maximum lift coefficient is correspondingly $= 4\pi$. Figure 3.11(b) illustrates the flow about a rotating cylinder. Note that in this case the streamlines are closer together at the top than they are at the bottom, indicating that there is a net lower pressure, and hence lift, in the vertical direction. This phenomenon is known as the Magnus effect. The Magnus effect is the physical basis of the Flettner rotor, which has been used successfully in ship propulsion (Flettner, 1926).

The method outlined above can be used to predict pressure distributions about an airfoil. The first step in doing this is transforming the coordinate system of the cylinder in the flow so that the resulting shape resembles the airfoil of interest. Figure 3.12 illustrates a symmetrical airfoil derived from a cylinder in this way. The resulting airfoil shape is the locus of points ξ resulting from the transformation given by the Equation (3.50).

$$\xi = z + r^2/z \qquad (3.50)$$
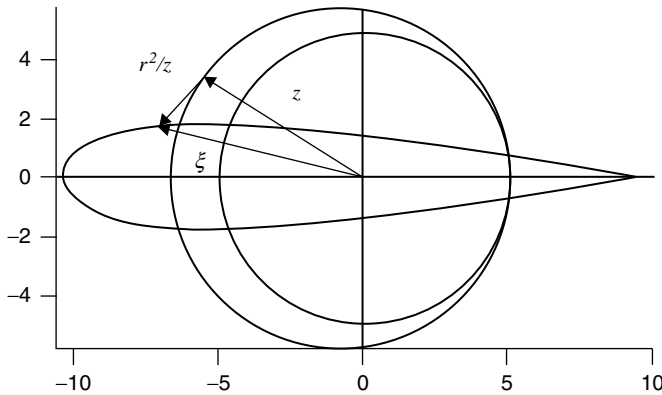
Figure 3.12   Airfoil derived from a transformed cylinder

where z is the vector to a circle offset from the origin. In the example shown, the radius of the circle is 5.5 and the offset is 0.8. A circle of radius 5 centered at the origin is included for comparison.

This method of analysis (i.e. the application of transformations of shapes, streamlines, and pressure distributions) provides the foundation of thin airfoil theory, which is used to predict the characteristics of most commonly used airfoils. Thin airfoil theory shows, for example, that the lift coefficient of a symmetrical airfoil at low angles of attack is equal to $2\pi\alpha$ (when the angle α is measured in radians), as shown in Equation (3.51). Details on the theory of lift and circulation, as well as on the use of transformations, are given in Abbott and von Doenhoff (1959) and most aerodynamics textbooks, such as Bertin and Smith (2008).

$$C_l = 2\pi\alpha \tag{3.51}$$

Under ideal conditions, all symmetric airfoils of finite thickness would have similar theoretical lift coefficients. This means that lift coefficients would increase with increasing angles of attack and continue to increase until the angle of attack reached 90 degrees. The behavior of real symmetric airfoils does indeed approximate this theoretical behavior at low angles of attack, although not for higher angles of attack. For example, typical lift and drag coefficients for a symmetric airfoil, the NACA 0012 airfoil, the profile of which was shown in Figure 3.8, are shown in Figure 3.13 as a function of angle of attack and Reynolds number. The lift coefficient for a flat plate under ideal conditions is also shown for comparison.

Note that, in spite of the very good correlation at low angles of attack, there are significant differences between actual airfoil operation and the theoretical performance at higher angles of attack. The differences are due primarily to the assumption, in the theoretical estimate of the lift coefficient, that air has no viscosity. As mentioned earlier, surface friction due to viscosity slows the air flow next to the airfoil surface, resulting in a separation of the flow from the surface at higher angles of attack and a rapid decrease in lift.

Airfoils for horizontal axis wind turbines (HAWTs) often are designed to be used at low angles of attack, where lift coefficients are fairly high and drag coefficients are fairly low. The lift coefficient for a symmetrical airfoil is zero at an angle of attack of zero and increases to
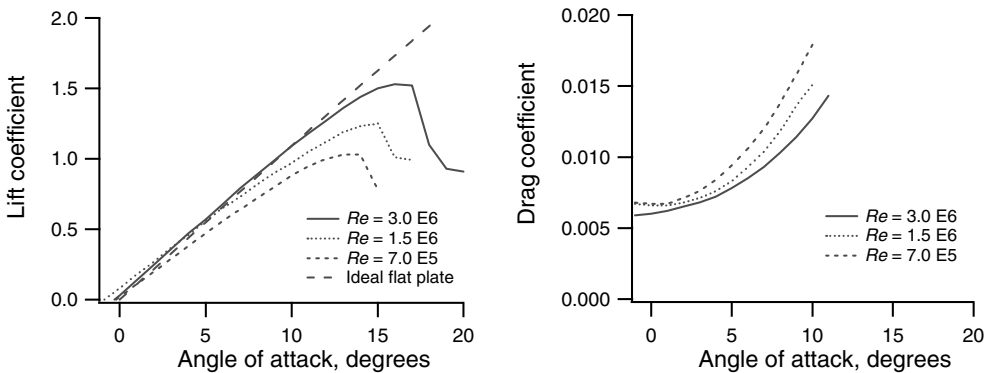
Figure 3.13 Lift and drag coefficients for the NACA 0012 symmetric airfoil (Miley, 1982); *Re*, Reynolds number
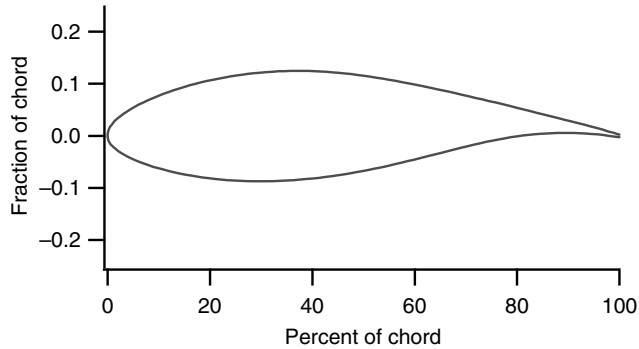
Figure 3.14   DU-93-W-210 airfoil shape

over 1.0 before decreasing at higher angles of attack. The drag coefficient is usually much lower than the lift coefficient at low angles of attack. It increases at higher angles of attack.

Note, also, that there are significant differences in airfoil behavior at different Reynolds numbers. For example, as Reynolds numbers decrease, viscous forces increase in magnitude compared to inertial forces. This increases the effects of surface friction, affecting velocities, the pressure gradient, and the lift generated by the airfoil. Rotor designers must make sure that appropriate Reynolds number data are available for the detailed analysis of a wind turbine rotor system.

The lift coefficient at low angles of attack can be increased and drag can often be decreased by using a cambered airfoil (Eggleston and Stoddard, 1987; Miley, 1982). For example, the DU-93-W-210 airfoil is used in some European wind turbines. Its cross-sectional profile is shown in Figure 3.14. The lift, drag, and pitching moment coefficients for this same airfoil are shown in Figures 3.15 and 3.16 for a Reynolds number of 3 million.

In a manner similar to the behavior of the symmetric airfoil, the lift coefficient for the DU-93-W-210 airfoil increases to about 1.35 but then decreases as the angle of attack increases.
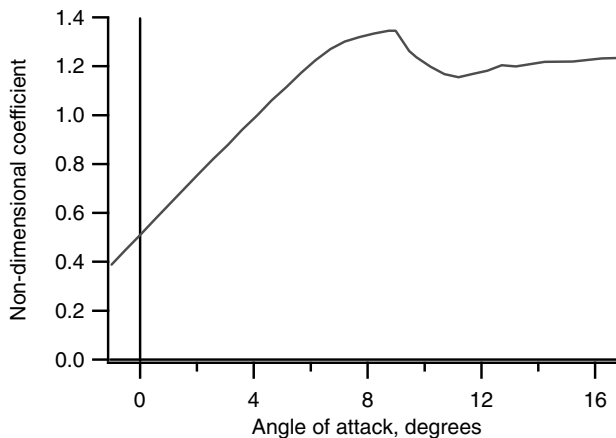
Figure 3.15   Lift coefficients for the DU-93-W-210 airfoil
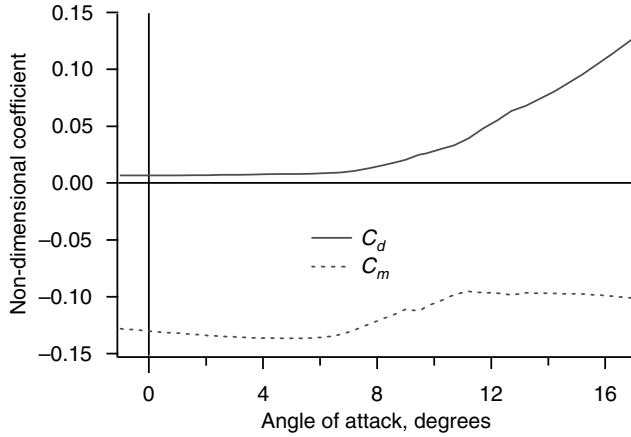
Figure 3.16 Drag and pitching moment coefficients for the DU-93-W-210 airfoil; C_d and C_m, respectively

Similarly, the drag coefficient starts out very low, but increases at about the same angle of attack that the lift coefficient decreases. This behavior is common to most airfoils. This cambered airfoil also has a non-zero lift coefficient at an angle of attack of zero.

Airfoil behavior can be categorized into three flow regimes: the attached flow regime, the high lift/stall development regime, and the flat plate/fully stalled regime (Spera, 1994). These flow regimes are described below and can be seen in the lift curves above and in Figure 3.17. Figure 3.17 shows the lift and drag coefficients for the S809 airfoil, which has also been used in wind turbines.
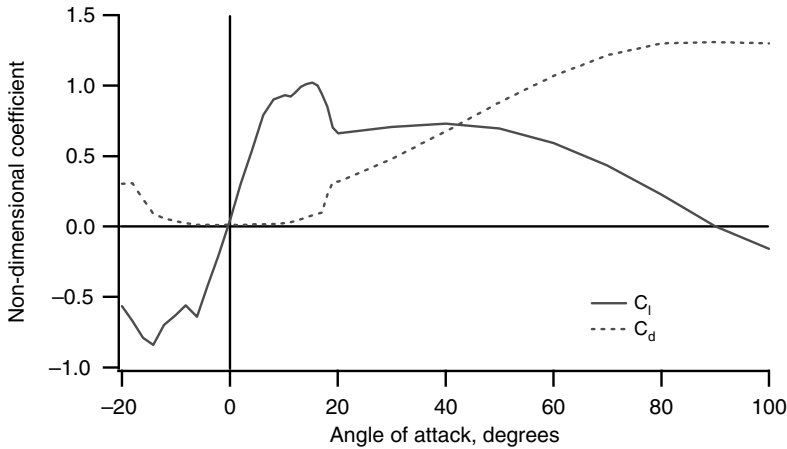
Figure 3.17 Lift and drag coefficients, C_l and C_d, respectively, for the S809 airfoil; Reynolds number $Re = 75\,000\,000$
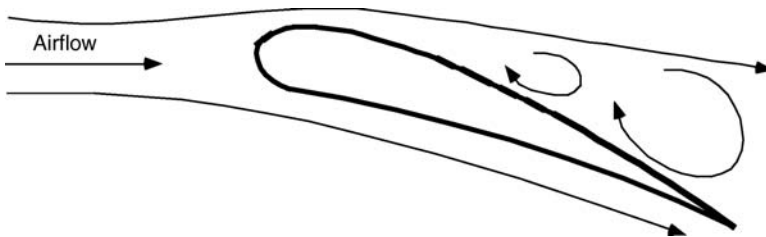
Figure 3.18   Illustration of airfoil stall

3.4.4.1 Attached Flow Regime

At low angles of attack (up to about 7 degrees for the DU-93-W-210 airfoil), the flow is attached to the upper surface of the airfoil. In this attached flow regime, lift increases with the angle of attack and drag is relatively low.

3.4.4.2 High Lift/Stall Development Regime

In the high lift/stall development regime (from about 7 to 11 degrees for the DU-93-W-210 airfoil), the lift coefficient peaks as the airfoil becomes increasingly stalled. Stall occurs when the angle of attack exceeds a certain critical value (say 10 to 16 degrees, depending on the Reynolds number) and separation of the boundary layer on the upper surface takes place, as shown in Figure 3.18. This causes a wake to form above the airfoil, which reduces lift and increases drag.

This condition can occur at certain blade locations or conditions of wind turbine operation. It is sometimes used to limit wind turbine power in high winds. For example, many wind turbine designs using fixed pitch blades rely on power regulation control via aerodynamic stall of the blades. That is, as wind speed increases, stall progresses outboard along the span of the blade (toward the tip), causing decreased lift and increased drag. In a well-designed, stall-regulated machine, this results in nearly constant power output as wind speeds increase above a certain value.

3.4.4.3 Flat Plate/Fully Stalled Regime

In the flat plate/fully stalled regime, at larger angles of attack up to 90 degrees, the airfoil acts increasingly like a simple flat plate with approximately equal lift and drag coefficients at an angle of attack of 45 degrees and zero lift at 90 degrees.

3.4.4.4 Modeling of Post-stall Airfoil Characteristics

Measured wind turbine airfoil data are used to design wind turbine blades. Wind turbine blades may often operate in the stalled region of operation, but data at high angles of attack are sometimes unavailable. Because of the similarity of stalled behavior to flat plate behavior, models have been developed to model lift and drag coefficients for stalled operation. Information on modeling post stall behavior of wind turbine airfoils can be found in Viterna

and Corrigan (1981). Summaries of the Viterna and Corrigan model can be found in Spera (1994) and Eggleston and Stoddard (1987).

3.4.5 Airfoils for Wind Turbines

Modern HAWT blades have been designed using airfoil 'families' (Hansen and Butterfield, 1993). That is, the blade tip is designed using a thin airfoil, for high lift to drag ratio, and the root region is designed using a thick version of the same airfoil for structural support. Typical Reynolds numbers found in wind turbine operation are in the range of 500 000 and 10 million. A catalog of airfoil data at these 'low' Reynolds numbers was compiled by Miley (1982).

Generally, in the 1970s and early 1980s, wind turbine designers felt that minor differences in airfoil performance characteristics were far less important than optimizing blade twist and taper. For this reason, little attention was paid to the task of airfoil selection. Thus, airfoils that were in use by the aircraft industry were chosen because aircraft were viewed as similar applications. Aviation airfoils such as the NACA 44xx and NACA 230xx (Abbott and von Doenhoff, 1959) were popular airfoil choices because they had high maximum lift coefficients, low pitching moment, and low minimum drag.

The NACA classification has 4, 5, and 6 series wing sections. For wind turbines, four-digit series were generally used, for example NACA 4415. The first integer indicates the maximum value of the mean camber line ordinate in percent of the chord. The second integer indicates the distance from the leading edge to the maximum camber in tenths of the chord. The last two integers indicate the maximum section thickness in percent of the chord.

In the early 1980s wind turbine designers became aware of airfoils such as the NASA LS(1) MOD, and this airfoil was chosen by US and British designers for its reduced sensitivity to leading edge roughness, compared to the NACA 44xx and NACA 230xx series airfoils (Tangler *et al.*, 1990). Danish wind turbine designers began to use the NACA 63(2)-xx instead of the NACA 44xx airfoils for the same reasons.

The experience gained from operating these traditional airfoils highlighted the shortcomings of such airfoils for wind turbine applications. Specifically, stall-controlled HAWTs commonly produced too much power in high winds. This caused generator damage. Stall-controlled turbines were operating with some part of the blade in deep stall for more than 50% of the life of the machine. Peak power and peak blade loads all occurred while the turbine was operating with most of the blade stalled, and predicted loads were only 50% to 70% of the measured loads. Designers began to realize that a better understanding of airfoil stall performance was important. In addition, leading edge roughness affected rotor performance. For example, with the early airfoil designs, when the blades accumulated insects and dirt along the leading edge, power output could drop as much as 40% of its clean value. Even the LS(1) MOD airfoils, which were designed to tolerate surface roughness, experienced a loss of power in the field once blades became soiled. Meanwhile, pitch-controlled wind turbines, in which the blades are rotated along their axis to control loads, often experienced excessive loads or load fluctuations during gusts, before the pitch system could rotate the blade. These occurred when the lift increased significantly as the gust occurred or the blade flow stalled before the pitch system could react.

As a consequence of these experiences, airfoil selection criteria and the designs for wind turbine airfoils and blades have had to change to achieve high and reliable performance. New

airfoil design codes have been used by wind energy engineers to design airfoils specifically for HAWTs. One of the most used codes in wind energy engineering was developed by Eppler and Somers (1980). Others were XFOIL and RFOIL (see Timmer and van Rooij, 2003) and PROFOIL (Selig and Tangler, 1995). These codes combine a variety of techniques to optimize boundary layer characteristics and airfoil shapes to achieve specified performance criteria.

Using the Eppler code, researchers at the National Renewable Energy Laboratory (Spera, 1994) have developed 'special purpose families' of airfoils for three different classes of wind turbines (the SERI designated classification of airfoils). As reported by Tangler *et al.* (1990) these S-Series airfoils have been tested on 8 m long blades and have been shown to be relatively insensitive to leading edge surface roughness and contributed to increased annual energy production by allowing a larger rotor diameter without increased peak power. These airfoils are now used on some commercial wind turbines.

Similar efforts in Europe attempted to address the same concerns. For example, the XFOIL and RFOIL codes were used at the Delft University of Technology (DUT) during the 1990s to design a number of airfoils specifically for wind turbine applications (Timmer and van Rooij, 2003). The primary design driver was low sensitivity to leading edge surface roughness. Low sensitivity to surface roughness was ensured by locating the point of transition to turbulent flow near the leading edge, as the flow approached stall. DUT also designed airfoils for the blade tips of pitch-controlled rotors with the design lift coefficient (the lift coefficient at the maximum lift–drag ratio) close enough to the peak lift coefficient to minimize changes in lift and, thus, peak loads as gusts occurred, but with a design angle of attack far enough from stall to minimize the fluctuating loads from stall before the pitch system could react.

Larger wind turbines that were built in the later 1990s required even thicker airfoils for structural strength. To deliver sufficient torque at low wind speeds, without significantly large chords, the maximum lift coefficients need to be high on these inboard airfoils. Some compromises needed to be made, as high maximum lift coefficients often accompany sensitivity to leading edge roughness. An additional complication is that the inner portion of the blade is more subject to flow distortions due to the rotation of the blades. These flow distortions affect the operating airfoil characteristics (see Section 3.13). In the last half of the 1990s and into 2000, the Delft University of Technology addressed these issues by using an updated version of XFOIL – RFOIL – to design a number of thick airfoils for wind turbines that met their design criteria while operating in the flow field in the inner portion of the blade (Timmer and van Rooij, 2003).

3.4.6 Lift Versus Drag Machines

Wind energy converters that have been built over the centuries can be divided into lift machines and drag machines. Lift machines use lift forces to generate power. Drag machines use drag forces. The horizontal axis wind turbines that are the primary topic of this book (and almost all modern wind turbines) are lift machines, but many useful drag machines have been developed. The advantages of lift over drag machines are described in this section through the use of a few simple examples.

As discussed in Chapter 1, drag-driven windmills, shown in Figure 3.19, were used in the Middle East over a thousand years ago. They included a vertical axis rotor consisting of flat surfaces in which half of the rotor was shielded from the wind. The simplified model on the right in Figure 3.19 is used to analyze the performance of this drag machine.
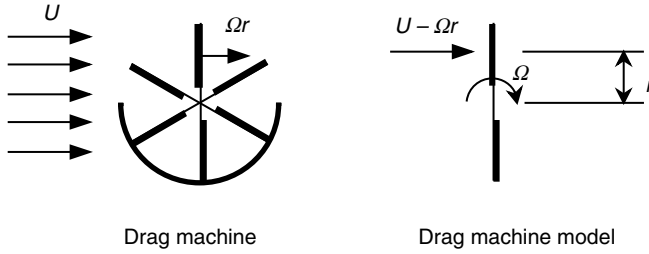
Figure 3.19   Simple drag machine and model; U, velocity of the undisturbed air flow; Ω, angular velocity of wind turbine rotor; r, radius

The drag force, F_D, is a function of the relative wind velocity at the rotor surface (the difference between the wind speed, U, and the speed of the surface, Ωr):

$$F_D = C_D \left[\tfrac{1}{2} \rho (U - \Omega r)^2 A \right] \tag{3.52}$$

where A is the drag surface area and where the three-dimensional drag coefficient, C_D, for a square plate is assumed to be 1.1.

The rotor power is the product of the torque due to the drag force and rotational speed of the rotor surfaces:

$$P = C_D \left[\tfrac{1}{2} \rho A (U - \Omega r)^2 \right] \Omega r = (\rho A U^3) \left[\tfrac{1}{2} C_D \lambda (1 - \lambda)^2 \right] \tag{3.53}$$

The power coefficient, shown in Figure 3.20, is a function of λ, the ratio of the surface velocity to the wind speed, and is based on an assumed total machine area of $2A$:

$$C_P = \left[\tfrac{1}{2} C_D \lambda (1 - \lambda)^2 \right] \tag{3.54}$$

The power coefficient is zero at speed ratios of zero (no motion) and 1.0 (the speed at which the surface moves at the wind speed and experiences no drag force). The peak power coefficient of 0.08 occurs at a speed ratio of $1/3$. This power coefficient is significantly lower than the
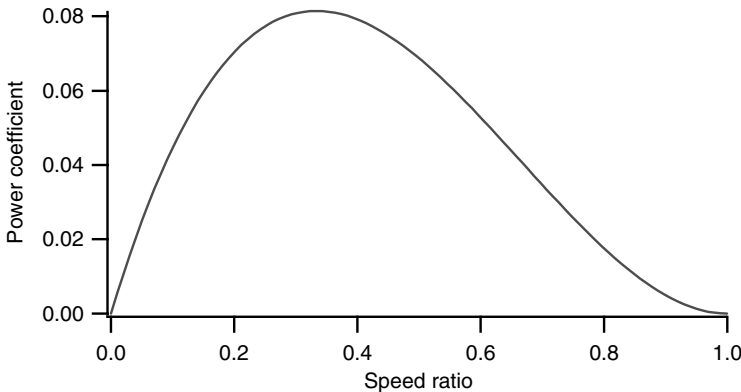
Figure 3.20   Power coefficient of flat plate drag machine
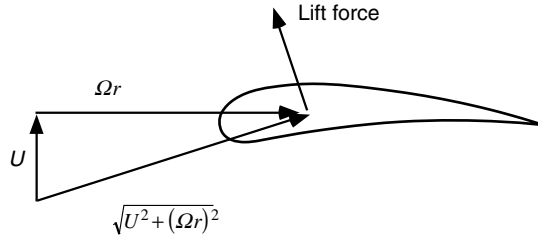
Figure 3.21 Relative velocity of a lift machine; for notation, see Figure 3.19

Betz limit of 0.593. This example also illustrates one of the primary disadvantages of a pure drag machine: the rotor surface cannot move faster than the wind speed. Thus, the wind velocity relative to the power-producing surfaces of the machine, U_{rel}, is limited to the free stream velocity:

$$U_{rel} = U(1-\lambda) \quad \lambda < 1 \tag{3.55}$$

The forces in lift machines are also a function of the relative wind velocity and of the lift coefficient:

$$F_L = C_L(\tfrac{1}{2}\rho A U_{rel}^2) \tag{3.56}$$

The maximum lift and drag coefficients of airfoils are of similar magnitude. One significant difference in the performance between lift and drag machines is that much higher relative wind velocities can be achieved with lift machines. Relative velocities are always greater than the free stream wind speed, sometimes by an order of magnitude. As illustrated in Figure 3.21, the relative wind velocity at the airfoil of a lift machine is:

$$U_{rel} = \sqrt{U^2 + (\Omega r)^2} = U\sqrt{1+\lambda^2} \tag{3.57}$$

With speed ratios of up to 10, and forces that are a function of the square of the relative speed, it can be seen that the forces that can be developed by a lift machine are significantly greater than those achievable with a drag machine with the same surface area. The larger forces allow for much greater power coefficients.

It should be pointed out that some drag-based machines, such as the Savonius rotor, may achieve maximum power coefficients of greater than 0.2 and may have tip speed ratios greater than 1.0. This is primarily due to the lift developed when the rotor surfaces turn out of the wind as the rotor rotates (Wilson *et al.*, 1976). Thus, the Savonius rotor and many other drag-based devices may also experience some lift forces.

3.5 Blade Design for Modern Wind Turbines

3.5.1 Blade Operational Environment

Wind turbine blades must be designed to convert the kinetic energy in the wind into torque, while having structural properties that ensure the required static and fatigue strength for a long operational life. In addition, they must have low enough material and manufacturing costs that the total wind turbine system can be accepted in the marketplace.

The starting point for wind turbine blade design assumes uniform axial flow upstream of the wind turbine two-dimensional flow over the blades and steady state operating conditions, all under specific design aerodynamic conditions defined by the relationship between the rotor rotational speed and the incoming wind speed. For example, a rotor might be designed for operation at a wind speed of 12 m/s and a rotational speed of 20 revolutions per minute. The blades will also operate at many other conditions, including off-design conditions, with non-uniform flow and in non-steady state conditions. Off-design operating conditions include operation at other ratios of rotational speed and wind speed. Depending on the control system, it might operate at 15 revolutions per second under some conditions at a wind speed of 5 m/s or at 20 revolutions per minute with an incoming wind speed of 22 m/s. The rotation of the rotor also induces flow along the blade, making the flow three-dimensional, especially near the hub. Non-uniform flow conditions include operation with wind shear across the rotor, or with the rotor yawed partially out of the wind or under inclined flow conditions on a mountain side (examples of off-axis flows). Non-steady states of operation include operation in the turbulent boundary layer in which the wind speed and direction at the rotor are varying in time and space. Additional non-steady conditions are induced by the rotation of the rotor which causes time-varying aerodynamics due to shear, off-axis flows.

3.5.2 Trends in Approaches to Rotor Design

An HAWT rotor consists of one or more blades, each with a series of airfoil shapes along the blade. The choice of airfoil, chord length, and twist along the blade determine the performance of the rotor under a variety of flow conditions. The approach to the choice of airfoil, chord length, and twist along the blade has changed over the years (Snel, 2002). In the 1980s rotors were typically designed to maximize the design power coefficient of the rotor, given some choice of airfoils. This can be done using the approach described in Section 3.6. This approach provided an optimally aerodynamically efficient rotor under certain conditions, but resulted in less than optimal efficiency under off-design conditions, of which there are many.

This initial approach gave way in the 1990s to maximizing the energy capture of the rotor. The approach starts with a choice of airfoils and a rotor designed for a maximum power coefficient, as described above. The blades' characteristics can then be modified to maximize energy capture, given the range of types of operating conditions that would be found at a site. This approach requires designing the rotor with a specific wind speed distribution and control system in mind.

Recently, rotors have been designed for minimum cost of energy (see Chapter 11 for more details on cost of energy calculations). This approach also starts with a rotor that is as aerodynamically efficient as possible. The rotor design is then optimized using a multidisciplinary approach that includes wind characteristics, an aerodynamic model, a structural model of the blades, and cost models for the blades and all major wind turbine components (Tangler, 2000). Such approaches have resulted in slightly lower energy capture than previous designs, but lower loads (by about 10%) and lower overall cost of energy.

3.5.3 Current Rotor Design Practice

The complex operating environment that wind turbine blades experience and the interaction between (1) the boundary layers around the airfoils, (2) the production of

power, and (3) the flow field around the wind turbine necessitate the use of computer codes for blade design. These computer codes may calculate some or all of the following: overall steady state rotor performance (energy yield), fluctuating aerodynamic loads along the blade, the flow field around the wind turbine, and noise emissions generated by aerodynamic effects.

Codes which calculate the fluctuating loads along the blade are referred to as aeroelastic codes, as they must model not only the aerodynamics of the rotor, but also the motions of the elastically deforming blades and the interactions between these blade motions and the flow. Manufacturers use these results to improve the performance of their wind turbines and to get their wind turbine design certified. Wind turbine designs need to be certified according to international standards (see Chapter 7) in order to be sold in many countries. Many load conditions need to be analyzed to obtain certification. These requirements demand modeling codes that provide accurate answers in a timely manner and from codes whose results have been validated against test data under realistic operating conditions.

There are a variety of aeroelastic codes used in the industry and in research to analyze wind turbine rotor behavior. The codes used on a daily basis in the industry for rotor design are referred to as engineering models (see Snel, 2002). These models are based on blade element momentum (BEM) theory, which describes the steady state behavior of a wind turbine rotor, with extensions to address unsteady operation. Sections 3.6 to 3.10 describe the basic equations of BEM models. BEM models have significant limitations and there are numerous more complicated modeling tools that are being developed to more accurately model the rotor aerodynamics. Some of these are described in Section 3.12.

3.6 Momentum Theory and Blade Element Theory

3.6.1 Overview

The calculation of rotor performance and aerodynamically effective blade shapes is presented in this and the following sections. The analysis builds on the foundation presented in the previous sections. A wind turbine rotor consists of airfoils that generate lift by virtue of the pressure difference across the airfoil, producing the same step change in pressure seen in the actuator disc type of analysis. In Sections 3.2 and 3.3, the flow field around a wind turbine rotor, represented by an actuator disc, was determined using the conservation of linear and angular momentum. That flow field, characterized by axial and angular induction factors that are a function of the rotor power extraction and thrust, will be used to define the air flow at the rotor airfoils. The geometry of the rotor and the lift and drag characteristics of the rotor airfoils, described in Section 3.4, can then be used to determine either the rotor shape, if certain performance parameters are known, or rotor performance, if the blade shape has already been defined.

The analysis here uses momentum theory and blade element theory. Momentum theory refers to a control volume analysis of the forces at the blade based on the conservation of linear and angular momentum. Blade element theory refers to an analysis of forces at a section of the blade, as a function of blade geometry. The results of these approaches can be combined into what is known as strip theory or blade element momentum (BEM) theory. This theory can be

used to relate blade shape to the rotor's ability to extract power from the wind. The analysis in this and the following sections covers:

- Momentum and blade element theory.
- The simplest 'optimum' blade design with an infinite number of blades and no wake rotation.
- Performance characteristics (forces, rotor air flow characteristics, power coefficient) for a general blade design of known chord and twist distribution, including wake rotation, drag, and losses due to a finite number of blades.
- A simple 'optimum' blade design including wake rotation and a finite number of blades. This blade design can be used as the start for a general blade design analysis.

3.6.2 Momentum Theory

The forces on a wind turbine blade and flow conditions at the blades can be derived by considering conservation of momentum since force is the rate of change of momentum. The necessary equations have already been developed in the derivation of the performance of an ideal wind turbine including wake rotation. The present analysis is based on the annular control volume shown in Figure 3.4. In this analysis, the axial and angular induction factors are assumed to be functions of the radius, r.

The result, from Section 3.3, of applying the conservation of linear momentum to the control volume of radius r and thickness $\mathrm{d}r$ (Equation (3.24)) is an expression for the differential contribution to the thrust:

$$\mathrm{d}T = \rho U^2 4a(1-a)\pi r \mathrm{d}r \tag{3.58}$$

Similarly, from the conservation of angular momentum equation, Equation (3.29), the differential torque, Q, imparted to the blades (and equally, but oppositely, to the air) is:

$$\mathrm{d}Q = 4a'(1-a)\rho U \pi r^3 \Omega \mathrm{d}r \tag{3.59}$$

Thus, from momentum theory one gets two equations, Equations (3.58) and (3.59), that define the thrust and torque on an annular section of the rotor as a function of the axial and angular induction factors (i.e. of the flow conditions).

3.6.3 Blade Element Theory

The forces on the blades of a wind turbine can also be expressed as a function of lift and drag coefficients and the angle of attack. As shown in Figure 3.22, for this analysis, the blade is assumed to be divided into N sections (or elements). Furthermore, the following assumptions are made:

- There is no aerodynamic interaction between elements (thus, no radial flow).
- The forces on the blades are determined solely by the lift and drag characteristics of the airfoil shape of the blades.

In analyzing the forces on the blade section, it must noted that the lift and drag forces are perpendicular and parallel, respectively, to an effective, or relative, wind. The relative wind is
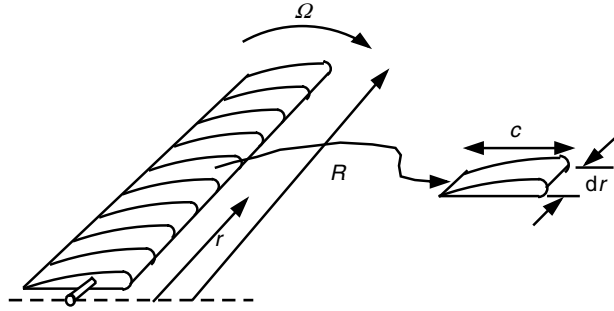
Figure 3.22   Schematic of blade elements; c, airfoil chord length; dr, radial length of element; r, radius; R, rotor radius; Ω, angular velocity of rotor

the vector sum of the wind velocity at the rotor, $U(1-a)$, and the wind velocity due to rotation of the blade. This rotational component is the vector sum of the blade section velocity, Ωr, and the induced angular velocity at the blades from conservation of angular momentum, $\omega r/2$, or

$$\Omega r + (\omega/2)r = \Omega r + \Omega a' r = \Omega r(1 + a') \tag{3.60}$$

The overall flow situation is shown in Figure 3.23 and the relationships of the various forces, angles, and velocities at the blade, looking down from the blade tip, are shown in Figure 3.24.

Here, θ_p is the section pitch angle, which is the angle between the chord line and the plane of rotation; $\theta_{p,0}$ is the blade pitch angle at the tip; θ_T is the blade twist angle; α is the angle of attack (the angle between the chord line and the relative wind); φ is the angle of relative wind; dF_L is the incremental lift force; dF_D is the incremental drag force; dF_N is the incremental force normal to the plane of rotation (this contributes to thrust); and dF_T is the incremental force tangential to the circle swept by the rotor. This is the force creating useful torque. Finally, U_{rel} is the relative wind velocity.

Note also that, here, the blade twist angle, θ_T, is defined relative to the blade tip (it could be defined otherwise). Therefore:

$$\theta_T = \theta_p - \theta_{p,0} \tag{3.61}$$
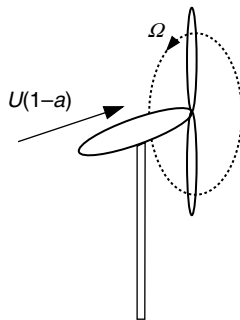
Figure 3.23   Overall geometry for a downwind horizontal axis wind turbine analysis; a, axial induction factor; U, velocity of undisturbed flow; Ω, angular velocity of rotor
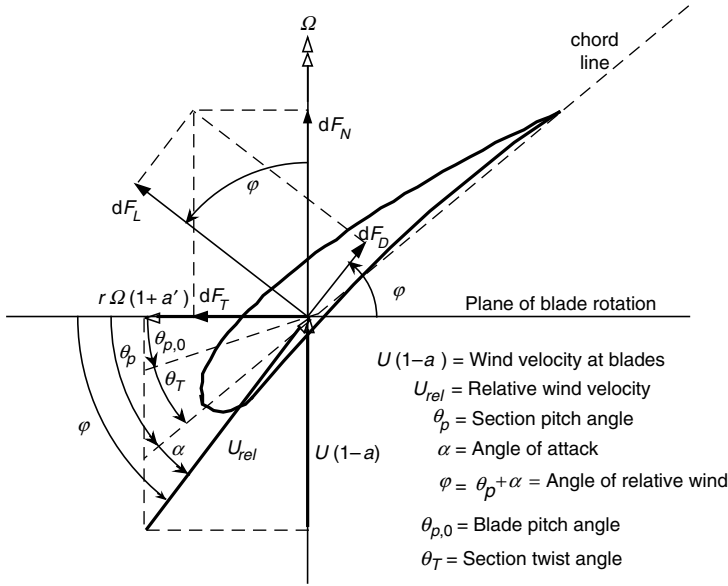
Figure 3.24   Blade geometry for analysis of a horizontal axis wind turbine. For definition of variables, see text

where $\theta_{p,0}$ is the blade pitch angle at the tip. The twist angle is, of course, a function of the blade geometry, whereas θ_p changes if the position of the blade, $\theta_{p,0}$, is changed. Note, also, that the angle of the relative wind is the sum of the section pitch angle and the angle of attack:

$$\varphi = \theta_p + \alpha \tag{3.62}$$

From Figure 3.24, one can determine the following relationships:

$$\tan \varphi = \frac{U(1-a)}{\Omega r(1+a')} = \frac{1-a}{(1+a')\lambda_r} \tag{3.63}$$

$$U_{rel} = U(1-a)/\sin \varphi \tag{3.64}$$

$$\mathrm{d}F_L = C_l \tfrac{1}{2}\rho U_{rel}^2 c\mathrm{d}r \tag{3.65}$$

$$\mathrm{d}F_D = C_d \tfrac{1}{2}\rho U_{rel}^2 c\mathrm{d}r \tag{3.66}$$

$$\mathrm{d}F_N = \mathrm{d}F_L \cos \varphi + \mathrm{d}F_D \sin \varphi \tag{3.67}$$

$$\mathrm{d}F_T = \mathrm{d}F_L \sin \varphi - \mathrm{d}F_D \cos \varphi \tag{3.68}$$

If the rotor has B blades, the total normal force on the section at a distance, r, from the center is:

$$\mathrm{d}F_N = B\tfrac{1}{2}\rho U_{rel}^2(C_l \cos\varphi + C_d \sin \varphi)c\mathrm{d}r \tag{3.69}$$

The differential torque due to the tangential force operating at a distance, r, from the center is given by:

$$dQ = Br\,dF_T \tag{3.70}$$

so

$$dQ = B\tfrac{1}{2}\rho U_{rel}^2 (C_l \sin \varphi - C_d \cos \varphi) cr\,dr \tag{3.71}$$

Note that the effect of drag is to decrease torque and hence power, but to increase the thrust loading.

Thus, from blade element theory, one also obtains two equations (Equations (3.69) and (3.71)) that define the normal force (thrust) and tangential force (torque) on the annular rotor section as a function of the flow angles at the blades and airfoil characteristics. These equations will be used below, with additional assumptions or equations, to determine ideal blade shapes for optimum performance and to determine rotor performance for any arbitrary blade shape.

3.7 Blade Shape for Ideal Rotor without Wake Rotation

As mentioned above, one can combine the momentum theory relations with those from blade element theory to relate blade shape to performance. Because the algebra can get complex, a simple, but useful, example will be presented here to illustrate the method.

In the first example of this chapter, the maximum possible power coefficient from a wind turbine, assuming no wake rotation or drag, was determined to occur with an axial induction factor of $1/3$. If the same simplifying assumptions are applied to the equations of momentum and blade element theory, the analysis becomes simple enough that an ideal blade shape can be determined. The blade shape approximates one that would provide maximum power at the design tip speed ratio of a real wind turbine. This will be called the 'Betz optimum rotor.'

In this analysis, the following assumptions will be made:

- There is no wake rotation; thus $a' = 0$.
- There is no drag; thus $C_d = 0$.
- There are no losses due to a finite number of blades (i.e. no tip loss).
- The axial induction factor, a, is $1/3$ in each annular stream tube.

First, a design tip speed ratio, λ, the desired number of blades, B, the radius, R, and an airfoil with known lift and drag coefficients as a function of angle of attack need to be chosen. An angle of attack (and, thus, a lift coefficient at which the airfoil will operate) is also chosen. This angle of attack should be selected where C_d/C_l is minimal in order to most closely approximate the assumption that $C_d = 0$. These choices allow the twist and chord distribution of a blade that would provide Betz limit power production (given the input assumptions) to be determined. With the assumption that $a = 1/3$, one gets from momentum theory (Equation (3.58)):

$$dT = \rho U^2 4\left(\tfrac{1}{3}\right)\left(1 - \tfrac{1}{3}\right)\pi r\,dr = \rho U^2 \left(^8/_9\right)\pi r\,dr \tag{3.72}$$

and, from blade element theory (Equation (3.69)), with $C_d = 0$:

$$dF_N = B\frac{1}{2}\rho U_{rel}^2 (C_l \cos \varphi)c\,dr \tag{3.73}$$

A third equation, Equation (3.64), can be used to express U_{rel} in terms of other known variables:

$$U_{rel} = U(1-a)/\sin\varphi = \frac{2U}{3\sin\varphi} \tag{3.74}$$

BEM theory or strip theory refers to the determination of wind turbine blade performance by combining the equations of momentum theory and blade element theory. In this case, equating Equations (3.72) and (3.73) and using Equation (3.74), yields:

$$\frac{C_l Bc}{4\pi r} = \tan\varphi \sin\varphi \tag{3.75}$$

A fourth equation, Equation (3.63), which relates a, a', and φ based on geometrical considerations, can be used to solve for the blade shape. Equation (3.63), with $a' = 0$ and $a = 1/3$, becomes:

$$\tan\varphi = \frac{2}{3\lambda_r} \tag{3.76}$$

Therefore

$$\frac{C_l Bc}{4\pi r} = \left(\frac{2}{3\lambda_r}\right)\sin\varphi \tag{3.77}$$

Rearranging, and noting that $\lambda_r = \lambda(r/R)$, one can determine the angle of the relative wind and the chord of the blade for each section of the ideal rotor:

$$\varphi = \tan^{-1}\left(\frac{2}{3\lambda_r}\right) \tag{3.78}$$

$$c = \frac{8\pi r \sin\varphi}{3BC_l\lambda_r} \tag{3.79}$$

These relations can be used to find the chord and twist distribution of the Betz optimum blade. As an example, suppose: $\lambda = 7$, the airfoil has a lift coefficient of $C_l = 1$, C_d/C_l has a minimum at $\alpha = 7°$ and, finally, that there are three blades, so $B = 3$. Then, from Equations (3.78) and (3.79) we get the results shown in Table 3.2. Here the chord and radius have been non-dimensionalized by dividing by the rotor radius. In this process, Equations (3.61) and (3.62) are also used to relate the various blade angles to each other (see Figure 3.24). The twist angle is assumed to start at 0 at the tip. The chord and twist of this blade are illustrated in Figures 3.25 and 3.26.

It can be seen that blades designed for optimum power production have an increasingly large chord and twist angle as one gets closer to the blade root. One consideration in blade design is the cost and difficulty of fabricating the blade. An optimum blade would be very difficult to manufacture at a reasonable cost, but the design provides insight into the blade shape that might be desired for a wind turbine.

Table 3.2 Twist and chord distribution for the example Betz optimum blade; r/R, fraction of rotor radius; c/R, non-dimensionalized chord

r/R	c/R	Twist angle (deg)	Angle of rel. wind (deg)	Section pitch (deg)
0.1	0.275	38.2	43.6	36.6
0.2	0.172	20.0	25.5	18.5
0.3	0.121	12.2	17.6	10.6
0.4	0.092	8.0	13.4	6.4
0.5	0.075	5.3	10.8	3.8
0.6	0.063	3.6	9.0	2.0
0.7	0.054	2.3	7.7	0.7
0.8	0.047	1.3	6.8	−0.2
0.9	0.042	0.6	6.0	−1.0
1	0.039	0	5.4	−1.6
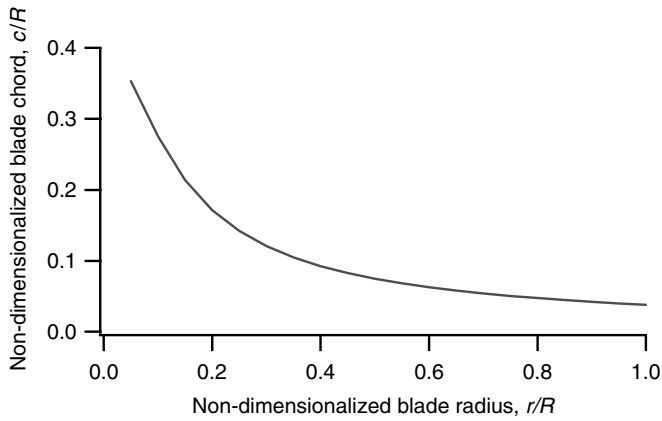
Figure 3.25 Blade chord for the example Betz optimum blade
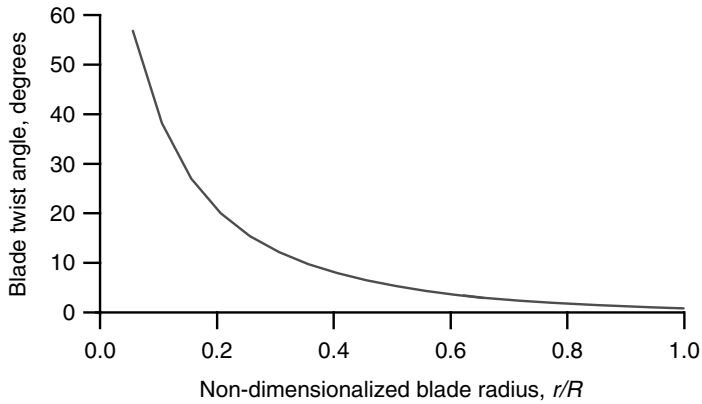
Figure 3.26 Blade twist angle for sample Betz optimum blade

3.8 General Rotor Blade Shape Performance Prediction

In general, a rotor is not of the optimum shape because of fabrication difficulties. Furthermore, when an 'optimum' blade is run at a different tip speed ratio than the one for which it is designed, it is no longer 'optimum'. Thus, blade shapes must be designed for easy fabrication and for overall performance over the range of wind and rotor speeds that they will encounter. In considering non-optimum blades, one generally uses an iterative approach. That is, one can assume a blade shape and predict its performance, try another shape and repeat the prediction until a suitable blade has been chosen.

So far, the blade shape for an ideal rotor without wake rotation has been considered. In this section, the analysis of arbitrary blade shapes is considered. The analysis includes wake rotation, drag, losses due to a finite number of blades, and off-design performance. In subsequent sections these methods will be used to determine an optimum blade shape, including wake rotation, and as part of a complete rotor design procedure.

3.8.1 Strip Theory for a Generalized Rotor, Including Wake Rotation

The analysis of a blade that includes wake rotation builds on the analysis used in the previous section. Here we also consider the nonlinear range of the lift coefficient versus angle of attack curve, i.e. stall. The analysis starts with the four equations derived from momentum and blade element theories. In this analysis, it is assumed that the chord and twist distributions of the blade are known. The angle of attack is not known, but additional relationships can be used to solve for the angle of attack and performance of the blade.

The forces and moments derived from momentum theory and blade element theory must be equal. Equating these, one can derive the flow conditions for a turbine design.

3.8.1.1 Momentum Theory

From axial momentum (Equation (3.58)) we already have:

$$dT = \rho U^2 4a(1-a)\pi r\, dr$$

From angular momentum (Equation (3.59)) we have:

$$dQ = 4a'(1-a)\rho U\pi r^3 \Omega\, dr$$

3.8.1.2 Blade Element Theory

From blade element theory (Equations (3.69) and (3.71)) we already have:

$$dF_N = B\tfrac{1}{2}\rho U_{rel}^2 (C_l \cos\varphi + C_d \sin\varphi)c\,dr$$

$$dQ = B\tfrac{1}{2}\rho U_{rel}^2 (C_l \sin\varphi - C_d \cos\varphi)cr\,dr$$

where the thrust, dT, is the same force as the normal force, dF_N. The relative velocity can be expressed as a function of the free stream wind using Equation (3.64). Thus, Equations (3.69)

and (3.71) from blade element theory can be written as:

$$dF_N = \sigma' \pi \rho \frac{U^2(1-a)^2}{\sin^2 \varphi}(C_l \cos \varphi + C_d \sin \varphi)r \, dr \tag{3.80}$$

$$dQ = \sigma' \pi \rho \frac{U^2(1-a)^2}{\sin^2 \varphi}(C_l \sin \varphi - C_d \cos \varphi)r^2 dr \tag{3.81}$$

where σ' is the local solidity, defined by:

$$\sigma' = Bc/2\pi r \tag{3.82}$$

3.8.1.3 Blade Element Momentum Theory

In the calculation of induction factors, a and a', accepted practice is to set C_d equal to zero (see Wilson and Lissaman, 1974). For airfoils with low drag coefficients, this simplification introduces negligible errors. So, when the torque equations from momentum and blade element theory are equated (Equations (3.59) and (3.81)), with $C_d = 0$, one gets:

$$a'/(1-a) = \sigma' C_l/(4\lambda_r \sin \varphi) \tag{3.83}$$

By equating the normal force equations from momentum and blade element theory (Equations (3.58) and (3.80)), one obtains:

$$a/(1-a) = \sigma' C_l \cos \varphi/(4 \sin^2 \varphi) \tag{3.84}$$

After some algebraic manipulation using Equation (3.63) (which relates a, a', φ and λ_r, based on geometric considerations) and Equations (3.83) and (3.84), the following useful relationships result:

$$C_l = 4 \sin \varphi \, \frac{(\cos \varphi - \lambda_r \sin \varphi)}{\sigma'(\sin \varphi + \lambda_r \cos \varphi)} \tag{3.85}$$

$$a'/(1+a') = \sigma' C_l/(4 \cos \varphi) \tag{3.86}$$

Other useful relationships that may be derived include:

$$a/a' = \lambda_r/\tan \varphi \tag{3.87}$$

$$a = 1/[1 + 4 \sin^2 \varphi/(\sigma' C_l \cos \varphi)] \tag{3.88}$$

$$a' = 1/[(4 \cos \varphi/(\sigma' C_l)) - 1] \tag{3.89}$$

3.8.1.4 Solution Methods

Two solution methods will be proposed using these equations to determine the flow conditions and forces at each blade section. The first one uses the measured airfoil characteristics and the BEM equations to solve directly for C_l and a. This method can be solved numerically, but it also lends itself to a graphical solution that clearly shows the flow conditions at the blade and the
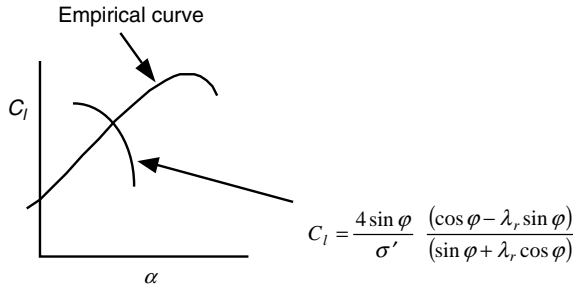
Figure 3.27 Angle of attack – graphical solution method; C_l, two-dimensional lift coefficient; α, angle of attack; λ_r, local speed ratio; φ, angle of relative wind; σ', local rotor solidity

existence of multiple solutions (see Section 3.8.4). The second solution is an iterative numerical approach that is most easily extended for flow conditions with large axial induction factors.

Method 1 – Solving for C_l and α

Since $\varphi = \alpha + \theta_p$, for a given blade geometry and operating conditions, there are two unknowns in Equation (3.85), C_l and α at each section. In order to find these values, one can use the empirical C_l vs. α curves for the chosen airfoil (see de Vries, 1979). One then finds the C_l and α from the empirical data that satisfy Equation (3.85). This can be done either numerically or graphically (as shown in Figure 3.27). Once C_l and α have been found, a' and a can be determined from any two of Equations (3.86) through (3.89). It should be verified that the axial induction factor at the intersection point of the curves is less than 0.5 to ensure that the result is valid.

Method 2 – Iterative Solution for a and a'

Another equivalent solution method starts with guesses for a and a', from which flow conditions and new induction factors are calculated. Specifically:

1. Guess values of a and a'.
2. Calculate the angle of the relative wind from Equation (3.63).
3. Calculate the angle of attack from $\theta = \alpha + \theta_p$ and then C_l and C_d.
4. Update a and a' from Equations (3.83) and (3.84) or (3.88) and (3.89).

The process is then repeated until the newly calculated induction factors are within some acceptable tolerance of the previous ones. This method is especially useful for highly loaded rotor conditions, as described in Section 3.8.4.3.

3.8.2 Calculation of Power Coefficient

Once a has been obtained from each section, the overall rotor power coefficient may be calculated from the following equation (Wilson and Lissaman, 1974):

$$C_P = (8/\lambda^2) \int_{\lambda_h}^{\lambda} \lambda_r^3 a'(1-a)[1 - (C_d/C_l)\cot \varphi]\mathrm{d}\lambda_r \tag{3.90}$$

where λ_h is the local speed ratio at the hub. Equivalently (de Vries, 1979):

$$C_P = (8/\lambda^2) \int_{\lambda_h}^{\lambda} \sin^2 \varphi (\cos \varphi - \lambda_r \sin \varphi)(\sin \varphi + \lambda_r \cos \varphi)[1 - (C_d/C_l) \cot \varphi]\lambda_r^2 d\lambda_r \quad (3.91)$$

Usually these equations are solved numerically, as will be discussed later. Note that even though the axial induction factors were determined assuming $C_d = 0$, the drag is included here in the power coefficient calculation.

The derivation of Equation (3.90) follows. The power contribution from each annulus is

$$dP = \Omega dQ \quad (3.92)$$

where Ω is the rotor rotational speed. The total power from the rotor is:

$$P = \int_{r_h}^{R} dP = \int_{r_h}^{R} \Omega dQ \quad (3.93)$$

where r_h is the rotor radius at the hub of the blade. The power coefficient, C_P, is

$$C_P = \frac{P}{P_{wind}} = \frac{\int_{r_h}^{R} \Omega \, dQ}{\frac{1}{2}\rho \pi R^2 U^3} \quad (3.94)$$

Using the expression for the differential torque from Equation (3.81) and the definition of the local tip speed ratio (Equation (3.27)):

$$C_P = \frac{2}{\lambda^2} \int_{\lambda_h}^{\lambda} \sigma' C_l (1-a)^2 (1/\sin \varphi)[1 - (C_d/C_l)\cot \varphi]\lambda_r^2 d\lambda_r \quad (3.95)$$

where λ_h is the local tip speed ratio at the hub. From Equations (3.84) and (3.87):

$$\sigma' C_l (1-a) = 4a \sin^2 \varphi / \cos \varphi \quad (3.96)$$

$$a \tan \varphi = a' \lambda_r \quad (3.97)$$

Substituting these into Equation (3.95), one gets the desired result, that is, Equation (3.90):

$$C_P = (8/\lambda^2) \int_{\lambda_h}^{\lambda} \lambda_r^3 a'(1-a)[1 - (C_d/C_l)\cot \varphi]d\lambda_r$$

Note that when $C_d = 0$, this equation for C_P is the same as the one derived from momentum theory, including wake rotation, Equation (3.33). The derivation of Equation (3.91) is algebraically complex and is left as an exercise for the interested reader.

3.8.3 Tip Loss: Effect on Power Coefficient of Number of Blades

Because the pressure on the suction side of a blade is lower than that on the pressure side, air tends to flow around the tip from the lower to upper surface, reducing lift and hence power production near the tip. This effect is most noticeable with fewer, wider blades.

A number of methods have been suggested for including the effect of the tip loss. The most straightforward approach to use is one developed by Prandtl (see de Vries, 1979). According to this method, a correction factor, F, must be introduced into the previously discussed equations. This correction factor is a function of the number of blades, the angle of relative wind, and the position on the blade. Based on Prandtl's method:

$$F = \left(\frac{2}{\pi}\right)\cos^{-1}\left[\exp\left(-\left\{\frac{(B/2)[1-(r/R)]}{(r/R)\sin\varphi}\right\}\right)\right] \tag{3.98}$$

where the angle resulting from the inverse cosine function is assumed to be in radians. If the inverse cosine function is in degrees, then the initial factor, $2/\pi$, is replaced by $1/90$. Note, also, that F is always between 0 and 1. This tip loss correction factor characterizes the reduction in the forces at a radius r along the blade that is due to the tip loss at the end of the blade.

The tip loss correction factor affects the forces derived from momentum theory. Thus Equations (3.58) and (3.59) become:

$$dT = F\rho U^2 4a(1-a)\pi r\,dr \tag{3.58a}$$

and

$$dQ = 4Fa'(1-a)\rho U\pi r^3\Omega\,dr \tag{3.59a}$$

Note that in this subsection, modifications of previous equations use the original equation numbers followed by an 'a' for easy comparison with the original equations.

Equations (3.61) through (3.71) are all based on the definition of the forces used in the blade element theory and remain unchanged. When the forces from momentum theory and from blade element theory are set equal, using the methods of strip theory, the derivation of the flow conditions is changed, however. Carrying the tip loss factor through the calculations, one finds these changes:

$$a'/(1-a) = \sigma' C_l/4F\lambda_r\sin\varphi \tag{3.83a}$$

$$a/(1-a) = \sigma' C_l\cos\varphi/4F\sin^2\varphi \tag{3.84a}$$

$$C_l = 4F\sin\varphi\,\frac{(\cos\varphi - \lambda_r\sin\varphi)}{\sigma'(\sin\varphi + \lambda_r\cos\varphi)} \tag{3.85a}$$

$$a'/(1+a') = \sigma' C_l/4F\cos\varphi \tag{3.86a}$$

$$a = 1/[1 + 4F\sin^2\varphi/(\sigma' C_l\cos\varphi\}] \tag{3.88a}$$

$$a' = 1/[(4F\cos\varphi/(\sigma' C_l)) - 1] \tag{3.89a}$$

and

$$U_{rel} = \frac{U(1-a)}{\sin\varphi} = \frac{U}{(\sigma' C_l/4F)\cot\varphi + \sin\varphi} \tag{3.99}$$

Note that Equation (3.87) remains unchanged. The power coefficient can be calculated from

$$C_P = 8/\lambda^2 \int_{\lambda_h}^{\lambda} F\lambda_r^3 a'(1-a)[1-(C_d/C_l)\cot\theta]d\lambda_r \qquad (3.90a)$$

or:

$$C_P = (8/\lambda^2)\int_{\lambda_h}^{\lambda} F\sin^2\varphi(\cos\varphi - \lambda_r\sin\varphi)(\sin\varphi + \lambda_r\cos\varphi)[1-(C_d/C_l)\cot\varphi]\lambda_r^2 d\lambda_r \quad (3.91a)$$

3.8.4 Off-design Performance Issues

When a section of blade has a pitch angle or flow conditions very different from the design conditions, a number of complications can affect the analysis. These include multiple solutions in the region of transition to stall and solutions for highly loaded conditions with values of the axial induction factor approaching and exceeding 0.5.

3.8.4.1 Multiple Solutions to Blade Element Momentum Equations

In the stall region, as shown in Figure 3.28, there may be multiple solutions for C_l. Each of these solutions is possible. The correct solution should be that which maintains the continuity of the angle of attack along the blade span.

3.8.4.2 Wind Turbine Flow States

Measured wind turbine performance closely approximates the results of BEM theory at low values of the axial induction factor. Momentum theory is no longer valid at axial induction factors greater than 0.5, because the wind velocity in the far wake would be negative. In practice, as the axial induction factor increases above 0.5, the flow patterns through the wind turbine become much more complex than those predicted by momentum theory. A number of operating states for a rotor have been identified (see Eggleston and Stoddard, 1987). The operating states relevant to wind turbines are designated the windmill state and the turbulent wake state. The windmill state is the normal wind turbine operating state. The turbulent wake state occurs under operation in high winds. Figure 3.29 illustrates fits to measured thrust coefficients for these operating states. The windmill state is characterized by the flow
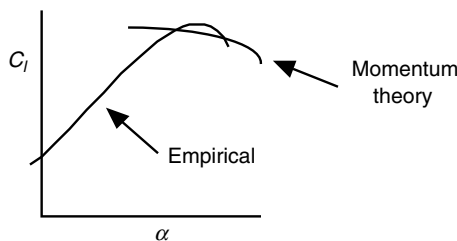
Figure 3.28 Multiple solutions: α, angle of attack; C_l, two-dimensional lift coefficient
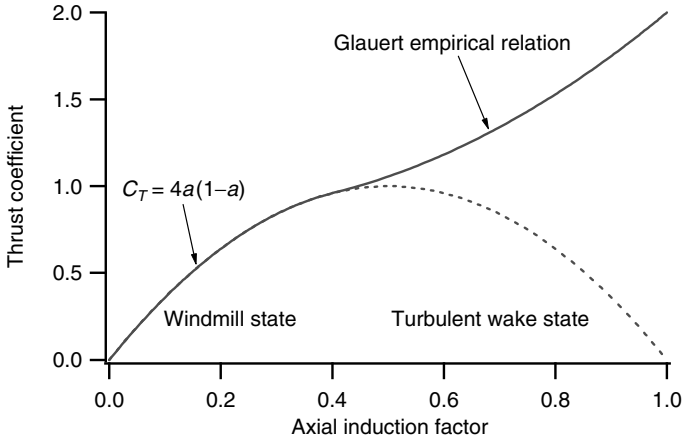
Figure 3.29 Fits to measured wind turbine thrust coefficients

conditions described by momentum theory for axial induction factors less than about 0.5. Above $a = 0.5$, in the turbulent wake state, measured data indicate that thrust coefficients increase up to about 2.0 at an axial induction factor of 1.0. This state is characterized by a large expansion of the slipstream, turbulence and recirculation behind the rotor. While momentum theory no longer describes the turbine behavior, empirical relationships between C_T and the axial induction factor are often used to predict wind turbine behavior.

3.8.4.3 Rotor Modeling for the Turbulent Wake State

The rotor analysis discussed so far uses the equivalence of the thrust forces determined from momentum theory and from blade element theory to determine the angle of attack at the blade. In the turbulent wake state the thrust determined by momentum theory is no longer valid. In these cases, the previous analysis can lead to a lack of convergence to a solution or a situation in which the curve defined by Equation (3.85a) or (3.85) would lie below the airfoil lift curve.

In the turbulent wake state, a solution can be found by using the empirical relationship between the axial induction factor and the thrust coefficient in conjunction with blade element theory. The empirical relationship developed by Glauert, and shown in Figure 3.29, (see Eggleston and Stoddard, 1987), including tip losses, is:

$$a = (1/F)\left[0.143 + \sqrt{0.0203 - 0.6427(0.889 - C_T)}\right] \qquad (3.100)$$

This equation is valid for $a > 0.4$ or, equivalently for $C_T > 0.96$.

The Glauert empirical relationship was determined for the overall thrust coefficient for a rotor. It is customary to assume that it applies equally to equivalent local thrust coefficients for each blade section. The local thrust coefficient, C_T, can be defined for each annular rotor section as (Wilson *et al.*, 1976):

$$C_{T_r} = \frac{dF_N}{\frac{1}{2}\rho U^2 2\pi r dr} \qquad (3.101)$$

From the equation for the normal force from blade element theory, Equation (3.80), the local thrust coefficient is:

$$C_{T_r} = \sigma'(1-a)^2(C_l \cos \varphi + C_d \sin \varphi)/\sin^2 \varphi \qquad (3.102)$$

The solution procedure can then be modified to include heavily loaded turbines. The easiest procedure to use is the iterative procedure (Method 2) that starts with the selection of possible values for a and a'. Once the angle of attack and C_l and C_d have been determined, the local thrust coefficient can be calculated according to Equation (3.102). If $C_T < 0.96$ then the previously derived equations can be used. If $C_T > 0.96$ then the next estimate for the axial induction factor should be determined using the local thrust coefficient and Equation (3.100). The angular induction factor, a', can be determined from Equation (3.89a).

3.8.4.4 Off-axis Flows and Blade Coning

The analysis in this chapter assumes that the prevailing wind is uniform and aligned with the rotor axis and that the blades rotate in a plane perpendicular to the rotor axis. These assumptions are rarely the case because of wind shear, yaw error, vertical wind components, turbulence, and blade coning. Wind shear will result in wind speeds that vary with height across the rotor disc. Wind turbines often operate with a steady state or transient yaw error (misalignment of the rotor axis and the wind direction about the vertical yaw axis of the turbine). Yaw error results in a flow component perpendicular to the rotor disc. The winds at the rotor may also have a vertical component, especially at sites in complex terrain. Turbulence results in a variety of wind conditions over the rotor. The angular position of the blade in the rotor plane is called the azimuth angle and is measured from some suitable reference. Each of the effects mentioned above results in conditions at the blade varying with blade azimuth angle. Finally, blades are also often attached to the hub at a slight angle to the plane perpendicular to the rotor axis. This blade coning may be done to reduce bending moments in the blades or to keep the blades from striking the tower.

In a rotor analysis, each of these situations is usually handled with appropriate geometrical transformations. Blade coning is handled by resolving the aerodynamic forces into components that are perpendicular and parallel to the rotor plane. Off-axis flow is also resolved into the flow components that are perpendicular and parallel to the rotor plane. Rotor performance is then determined for a variety of rotor azimuth angles. The axial and in-plane components of the flow that depend on the blade position result in angles of attack and aerodynamic forces that fluctuate cyclically as the blades rotate. BEM equations that include terms for blade coning are provided by Wilson *et al.* (1976). Linearized methods for dealing with small off-axis flows and blade coning are discussed in Chapter 4.

3.9 Blade Shape for Optimum Rotor with Wake Rotation

The blade shape for an ideal rotor that includes the effects of wake rotation can be determined using the analysis developed for a general rotor. This optimization includes wake rotation, but ignores drag ($C_D = 0$) and tip losses ($F = 1$). One can perform the optimization by taking the partial derivative of that part of the integral for C_P (Equation (3.91)) which is a function of the angle of the relative wind, φ, and setting it equal to zero, i.e.:

$$\frac{\partial}{\partial \varphi} \left[\sin^2 \varphi (\cos \varphi - \lambda_r \sin \varphi)(\sin \varphi + \lambda_r \cos \varphi) \right] = 0 \qquad (3.103)$$

This yields:

$$\lambda_r = \sin \varphi (2 \cos \varphi - 1)/[(1 - \cos \varphi)(2 \cos \varphi + 1)] \qquad (3.104)$$

Some more algebra (see the homework problems) reveals that:

$$\varphi = (^2/_3) \tan^{-1}(1/\lambda_r) \qquad (3.105)$$

$$c = \frac{8\pi r}{BC_l}(1 - \cos \varphi) \qquad (3.106)$$

Induction factors can be calculated from Equations (3.88) and (3.36):

$$a = 1/[1 + 4\sin^2 \varphi/(\sigma' C_l \cos \varphi)]$$

$$a' = \frac{1 - 3a}{4a - 1}$$

These results can be compared with the result for an ideal blade without wake rotation, for which, from Equations (3.78) and (3.79):

$$\varphi = \tan^{-1}\left(\frac{2}{3\lambda_r}\right)$$

$$c = \frac{8\pi r}{BC_l}\left(\frac{\sin \varphi}{3\lambda_r}\right)$$

Note, that the optimum values for φ and c, including wake rotation, are often similar to, but could be significantly different from, those obtained without assuming wake rotation. Also, as before, select α where C_d/C_l is minimal.

Solidity is the ratio of the planform area of the blades to the swept area, thus:

$$\sigma = \frac{1}{\pi R^2}\int_{r_h}^{R} c \, dr \qquad (3.107)$$

The optimum blade rotor solidity can be found from methods discussed above. When the blade is modeled as a set of N blade sections of equal span, the solidity can be calculated from:

$$\sigma \cong \frac{B}{N\pi}\left(\sum_{i=1}^{N} c_i/R\right) \qquad (3.108)$$

The blade shapes for three sample optimum rotors, assuming wake rotation, are given in Table 3.3. Here C_{l1} is assumed to be 1.00 at the design angle of attack. In these rotors, the blade twist is directly related to the angle of the relative wind because the angle of attack is assumed to be constant (see Equations (3.61) and (3.62)). Thus, changes in blade twist would mirror

Table 3.3 Three optimum rotors

r/R	$\lambda = 1$ $B = 1/2$		$\lambda = 6$ $B = 3$		$\lambda = 10$ $B = 2$	
	φ	c/R	φ	c/R	φ	c/R
0.95	31	0.284	6.6	0.053	4.0	0.029
0.85	33.1	0.289	7.4	0.059	4.5	0.033
0.75	35.4	0.291	8.4	0.067	5.1	0.037
0.65	37.9	0.288	9.6	0.076	5.8	0.042
0.55	40.8	0.280	11.2	0.088	6.9	0.050
0.45	43.8	0.263	13.5	0.105	8.4	0.060
0.35	47.1	0.234	17.0	0.128	10.6	0.075
0.25	50.6	0.192	22.5	0.159	14.5	0.100
0.15	54.3	0.131	32.0	0.191	22.5	0.143
Solidity, σ		0.86		0.088		0.036

Note: B, number of blades; c, airfoil chord length; r, blade section radius; R, rotor radius; λ, tip speed ratio; φ, angle of relative wind

the changes in the angle of the relative wind shown in Table 3.3. It can be seen that the slow 12-bladed machine would have blades that had a roughly constant chord over the outer half of the blade and smaller chords closer to the hub. The blades would also have a significant twist. The two faster machines would have blades with an increasing chord as one went from the tip to the hub. The blades would also have significant twist, but much less than the 12-bladed machine. The fastest machine would have the least twist, which is a function of local speed ratio only. It would also have the smallest chord because of the low angle of the relative wind and only two blades (see Equations (3.105) and (3.106)).

3.10 Generalized Rotor Design Procedure

3.10.1 Rotor Design for Specific Conditions

The previous analysis can be used in a generalized rotor design procedure. The procedure begins with the choice of various rotor parameters and the choice of an airfoil. An initial blade shape is then determined using the optimum blade shape assuming wake rotation. The final blade shape and performance are determined iteratively considering drag, tip losses, and ease of manufacture. The steps in determining a blade design follow.

3.10.1.1 Determine Basic Rotor Parameters

1. Begin by deciding what power, P, is needed at a particular wind velocity, U. Include the effect of a probable C_P and efficiencies, η, of various other components (e.g., gearbox, generator, pump, etc.). The radius, R, of the rotor may be estimated from:

$$P = C_P \eta \left(\frac{1}{2} \right) \rho \pi R^2 U^3 \tag{3.109}$$

2. According to the type of application, choose a tip speed ratio, λ. For a water-pumping windmill, for which greater torque is needed, use $1 < \lambda < 3$. For electrical power generation,

Table 3.4   Suggested blade number, B, for different tip speed ratios, λ

λ	B
1	8–24
2	6–12
3	3–6
4	3–4
>4	1–3

use $4 < \lambda < 10$. The higher speed machines use less material in the blades and have smaller gearboxes, but require more sophisticated airfoils.

3. Choose the number of blades, B, from Table 3.4. Note: if fewer than three blades are selected, there are a number of structural dynamic problems that must be considered in the hub design. One solution is a teetered hub (see Chapter 7).

4. Select an airfoil. If $\lambda < 3$, curved plates can be used. If $\lambda > 3$, use a more aerodynamic shape.

3.10.1.2 Define the Blade Shape

5. Obtain and examine the empirical curves for the aerodynamic properties of the airfoil at each section (the airfoil may vary from the root to the tip), i.e. C_l vs. α, C_d vs. α. Choose the design aerodynamic conditions, $C_{l,design}$ and α_{design}, such that $C_{d,design}/C_{l,design}$ is at a minimum for each blade section.

6. Divide the blade into N elements (usually 10–20). Use the optimum rotor theory to estimate the shape of the ith blade with a midpoint radius of r_i:

$$\lambda_{r,i} = \lambda(r_i/R) \tag{3.110}$$

$$\varphi_i = (^2/_3)\tan^{-1}(1/\lambda_{r,i}) \tag{3.111}$$

$$c_i = \frac{8\pi r_i}{BC_{l,design,i}}(1 - \cos\varphi_i) \tag{3.112}$$

$$\theta_{T,i} = \theta_{p,i} - \theta_{p,0} \tag{3.113}$$

$$\varphi_i = \theta_{p,i} + \alpha_{design,i} \tag{3.114}$$

7. Using the optimum blade shape as a guide, select a blade shape that promises to be a good approximation. For ease of fabrication, linear variations of chord, thickness, and twist might be chosen. For example, if a_1, b_1, and a_2 are coefficients for the chosen chord and twist distributions, then the chord and twist can be expressed as:

$$c_i = a_1 r_i + b_1 \tag{3.115}$$

$$\theta_{T,i} = a_2(R - r_i) \tag{3.116}$$

3.10.1.3 Calculate Rotor Performance and Modify Blade Design

8. As outlined above, one of two methods might be chosen to solve the equations for the blade performance.

Method 1 – Solving for C_l and α
Find the actual angle of attack and lift coefficients for the center of each element, using the following equations and the empirical airfoil curves:

$$C_{l,i} = 4F_i \sin \varphi_i \frac{(\cos \varphi_i - \lambda_{r,i} \sin \varphi_i)}{\sigma'_i(\sin \varphi_i + \lambda_{r,i} \cos \varphi_i)} \tag{3.117}$$

$$\sigma'_i = Bc_i/2\pi r_i \tag{3.118}$$

$$\varphi_i = \alpha_i + \theta_{T,i} + \theta_{P,0} \tag{3.119}$$

$$F_i = \left(\frac{2}{\pi}\right) \cos^{-1} \left[\exp\left(- \left\{ \frac{(B/2)[1 - (r_i/R)]}{(r_i/R)\sin \varphi_i} \right\} \right) \right] \tag{3.120}$$

The lift coefficient and angle of attack can be found by iteration or graphically. A graphical solution is illustrated in Figure 3.30. The iterative approach requires an initial estimate of the tip loss factor. To find a starting F_i, start with an estimate for the angle of the relative wind of:

$$\varphi_{i,1} = (2/3)\tan^{-1}(1/\lambda_{r,i}) \tag{3.121}$$

For subsequent iterations, find F_i using:

$$\varphi_{i,j+1} = \theta_{P,i} + \alpha_{i,j} \tag{3.122}$$

where j is the number of the iteration. Usually, only a few iterations are needed.
Finally, calculate the axial induction factor:

$$a_i = 1/[1 + 4 \sin^2 \varphi_i/(\sigma'_i C_{l,i} \cos \varphi_i)] \tag{3.123}$$

If a_i is greater than 0.4, use Method 2.
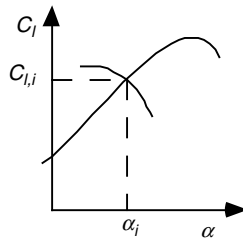
Figure 3.30 Graphical solution for angle of attack, α; C_l, two-dimensional lift coefficient; $C_{l,i}$ and α_i, C_l and α, respectively, for blade section, i

Method 2 – Iterative Solution for a and a'

Iterating to find the axial and angular induction factors using Method 2 requires initial guesses for their values. To find initial values, start with values from an adjacent blade section, values from the previous blade design in the iterative rotor design process, or use an estimate based on the design values from the starting optimum blade design:

$$\varphi_{i,1} = (^2/_3)\tan^{-1}(1/\lambda_{r,i}) \tag{3.124}$$

$$a_{i,1} = \frac{1}{\left[1 + \dfrac{4\sin^2(\varphi_{i,1})}{\sigma'_{i,design}C_{l,design}\cos\varphi_{i,1}}\right]} \tag{3.125}$$

$$a'_{i,1} = \frac{1 - 3a_{i,1}}{(4a_{i,1}) - 1} \tag{3.126}$$

Having guesses for $a_{i,1}$ and $a'_{i,1}$, start the iterative solution procedure for the jth iteration. For the first iteration $j = 1$. Calculate the angle of the relative wind and the tip loss factor:

$$\tan\varphi_{i,j} = \frac{U(1 - a_{i,j})}{\Omega r(1 + a'_{i,j})} = \frac{1 - a_{i,j}}{(1 + a'_{i,j})\lambda_{r,i}} \tag{3.127}$$

$$F_{i,j} = \left(\frac{2}{\pi}\right)\cos^{-1}\left[\exp\left(-\left\{\frac{(B/2)[1 - (r_i/R)]}{(r_i/R)\sin\varphi_{i,j}}\right\}\right)\right] \tag{3.128}$$

Determine $C_{l,i,j}$ and $C_{d,i,j}$ from the airfoil lift and drag data, using:

$$\alpha_{i,j} = \varphi_{i,j} - \theta_{p,i} \tag{3.129}$$

Calculate the local thrust coefficient:

$$C_{Tr,i,j} = \frac{\sigma'_i(1 - a_{i,j})^2(C_{l,i,j}\cos\varphi_{i,j} + C_{d,i,j}\sin\varphi_{i,j})}{\sin^2\varphi_{i,j}} \tag{3.130}$$

Update a and a' for the next iteration. If $C_{Tr,i,j} < 0.96$:

$$a_{i,j+1} = \frac{1}{\left[1 + \dfrac{4F_{i,j}\sin^2(\varphi_{i,j})}{\sigma'_iC_{l,i,j}\cos\varphi_{i,j}}\right]} \tag{3.131}$$

If $C_{Tr,i,j} > 0.96$:

$$a_{i,j} = (1/F_{i,j})\left[0.143 + \sqrt{0.0203 - 0.6427(0.889 - C_{Tr,i,j})}\right] \tag{3.132}$$

$$a'_{i,j+1} = \frac{1}{\dfrac{4F_{i,j}\cos\varphi_{i,j}}{\sigma'C_{l,i,j}} - 1} \tag{3.133}$$

If the newest induction factors are within an acceptable tolerance of the previous guesses, then the other performance parameters can be calculated. If not, then the procedure starts again at Equation (3.127) with $j = j + 1$.

9. Having solved the equations for the performance at each blade element, the power coefficient is determined using a sum approximating the integral in Equation (3.91a):

$$C_P = \sum_{i=1}^{N} \left(\frac{8\Delta\lambda_r}{\lambda^2}\right) F_i \sin^2 \varphi_i (\cos\varphi_i - \lambda_{ri}\sin\varphi_i)(\sin\varphi_i + \lambda_{ri}\cos\varphi_i)\left[1 - \left(\frac{C_d}{C_l}\right)\cot\varphi_i\right]\lambda_{ri}^2 \tag{3.134}$$

If the total length of the hub and blade is assumed to be divided into N equal length blade elements, then:

$$\Delta\lambda_r = \lambda_{ri} - \lambda_{r(i-1)} = \lambda/N \tag{3.135}$$

$$C_P = \frac{8}{\lambda N} \sum_{i=k}^{N} F_i \sin^2 \varphi_i (\cos\varphi_i - \lambda_{ri}\sin\varphi_i)(\sin\varphi_i + \lambda_{ri}\cos\varphi_i)\left[1 - \left(\frac{C_d}{C_l}\right)\cot\varphi_i\right]\lambda_{ri}^2 \tag{3.136}$$

where k is the index of the first 'blade' section consisting of the actual blade airfoil.

10. Modify the design if necessary and repeat steps 8–10 in order to find the best design for the rotor, given the limitations of fabrication.

3.10.2 C_P–λ Curves

Once the blade has been designed for optimum operation at a specific design tip speed ratio, the performance of the rotor over all expected tip speed ratios needs to be determined. This can be done using the methods outlined in Section 3.8. For each tip speed ratio, the aerodynamic conditions at each blade section need to be determined. From these, the performance of the total rotor can be determined. The results are usually presented as a graph of power coefficient versus tip speed ratio, called a $C_P - \lambda$ curve, as shown in Figure 3.31.
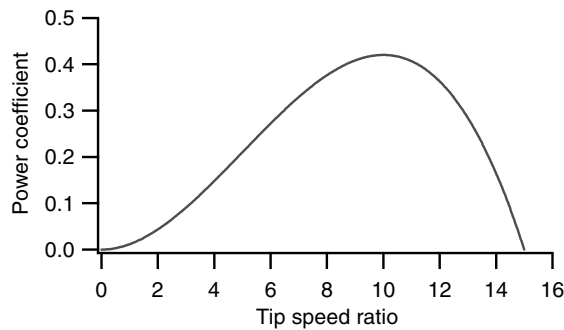
Figure 3.31 Sample $C_P - \lambda$ curve for a high tip speed ratio wind turbine

$C_P - \lambda$ curves can be used in wind turbine design to determine the rotor power for any combination of wind and rotor speed. They provide immediate information on the maximum rotor power coefficient and optimum tip speed ratio. Care must be taken in using $C_P - \lambda$ curves. The data for such a relationship can be found from turbine tests or from modeling. In either case, the results depend on the lift and drag coefficients of the airfoils, which may vary as a function of the flow conditions. Variations in airfoil lift and drag coefficients depend on the airfoil and the Reynolds numbers being considered, but, as shown in Figure 3.13, airfoils can have remarkably different behavior when the Reynolds number changes by as little as a factor of 2.

3.11 Simplified HAWT Rotor Performance Calculation Procedure

Manwell (1990) proposed a simplified method for calculating the performance of a horizontal axis wind turbine rotor that is particularly applicable for an unstalled rotor, but may also be useful under certain stall conditions. The method uses the previously discussed blade element theory and incorporates an analytical method for finding the blade angle of attack. Depending on whether tip losses are included, few or no iterations are required. The method assumes that two conditions apply:

- The airfoil section lift coefficient vs. angle of attack relation must be linear in the region of interest.
- The angle of attack must be small enough that the small-angle approximations may be used.

These two requirements normally apply if the section is unstalled. They may also apply under certain partially stalled conditions for moderate angles of attack if the lift curve can be linearized.

The simplified method is the same as Method 1 outlined above, with the exception of a simplification for determining the angle of attack and the lift coefficient for each blade section. The essence of the simplified method is the use of an analytical (closed-form) expression for finding the angle of attack of the relative wind at each blade element. It is assumed that the lift and drag curves can be approximated by:

$$C_l = C_{l,0} + C_{l,\alpha}\alpha \tag{3.137}$$

$$C_d = C_{d,0} + C_{d,\alpha 1}\alpha + C_{d,\alpha 2}\alpha^2 \tag{3.138}$$

When the lift curve is linear and when small-angle approximations can be used, it can be shown that the angle of attack is given by:

$$\alpha = \frac{-q_2 \pm \sqrt{q_2^2 - 4q_1 q_3}}{2q_3} \tag{3.139}$$

where:

$$q_1 = C_{l,0}d_2 - \frac{4F}{\sigma'}d_1 \sin\theta_p \tag{3.140}$$

$$q_2 = C_{l,\alpha}d_2 + d_1 C_{l,0} - \frac{4F}{\sigma'}(d_1 \cos\theta_p - d_2 \sin\theta_p) \tag{3.141}$$
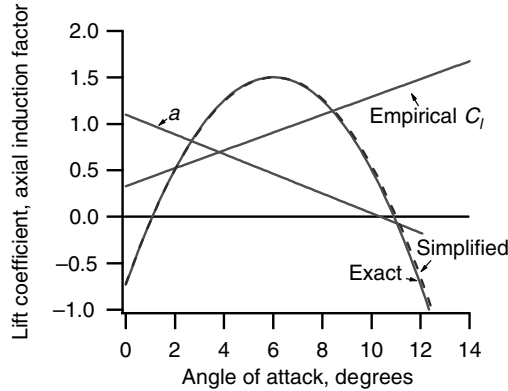
Figure 3.32 Comparison of calculation methods for one blade element; a, axial induction factor; C_l, two-dimensional lift coefficient

$$q_3 = C_{l,\alpha}d_1 + \frac{4F}{\sigma'}d_2\cos\theta_p \qquad (3.142)$$

$$d_1 = \cos\theta_p - \lambda_r\sin\theta_p \qquad (3.143)$$

$$d_2 = \sin\theta_p + \lambda_r\cos\theta_p \qquad (3.144)$$

Using this approach, the angle of attack can be calculated from Equation (3.139) once an initial estimate for the tip loss factor is determined. The lift and drag coefficients can then be calculated from Equations (3.137) and (3.138), using Equation (3.122). Iteration with a new estimate of the tip loss factor may be required.

The simplified method provides angles of attack very close to those of the more detailed method for many operating conditions. For example, results for the analysis of one blade of the University of Massachusetts WF-1 wind turbine are shown in Figure 3.32. This was a three-bladed turbine with a 10 m rotor, using near optimum tapered and twisted blades. The lift curve of the NACA 4415 airfoil was approximated by $C_l = 0.368 + 0.0942\alpha$. The drag coefficient equation constants were 0.00994, 0.000259, and 0.0001055. Figure 3.32 compares the results from the simplified method and the conventional strip theory method for the angle of attack for one of the blade elements. The point at which the curves cross the empirical lift line determines the angle of attack and the lift coefficient. Also plotted on Figure 3.32 is the axial induction factor, a, for the section. Note that it is the right-hand intersection point which gives a value of $a < 1/2$, as is normally the case.

3.12 Effect of Drag and Blade Number on Optimum Performance

At the beginning of the chapter, the maximum theoretically possible power coefficient for wind turbines was determined as a function of tip speed ratio. As explained in this chapter, airfoil drag and tip losses that are a function of the total number of blades reduce the power coefficients of wind turbines. The maximum achievable power coefficient for turbines with an optimum blade shape but a finite number of blades and aerodynamic drag has been calculated by Wilson
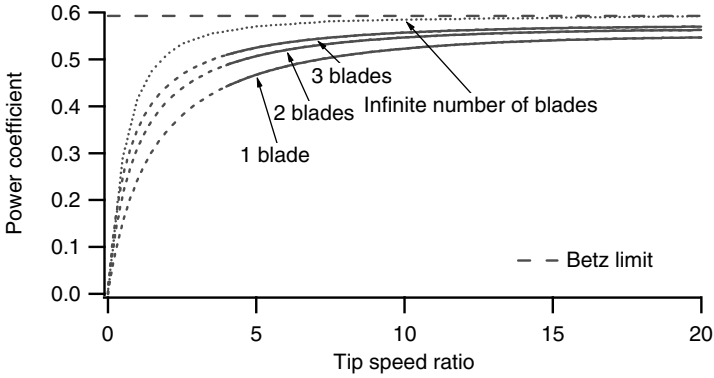
Figure 3.33 Maximum achievable power coefficients as a function of number of blades, no drag

et al. (1976). Their fit to the data is accurate to within 0.5% for tip speed ratios from 4 to 20, lift to drag ratios (C_l/C_d) from 25 to infinity, and from one to three blades (B):

$$C_{p,\max} = \left(\frac{16}{27}\right)\lambda\left[\lambda + \frac{1.32 + \left(\frac{\lambda - 8}{20}\right)^2}{B^{\frac{2}{3}}}\right]^{-1} - \frac{(0.57)\lambda^2}{\frac{C_l}{C_d}\left(\lambda + \frac{1}{2B}\right)} \tag{3.145}$$

Figure 3.33, based on this equation, shows the maximum achievable power coefficients for a turbine with one, two, and three optimum blades and no drag. The performance for ideal conditions including wake rotation (an infinite number of blades) is also shown. It can be seen that the fewer blades there are, the lower the possible C_p at the same tip speed ratio. Most wind turbines use two or three blades and, in general, most two-bladed wind turbines use a higher tip speed ratio than most three-bladed wind turbines. Thus, there is little practical difference in the maximum achievable C_P between typical two- and three-bladed designs, assuming no drag. The effect of the lift to drag ratio on maximum achievable power coefficients for a three-bladed rotor is shown in Figure 3.34. There is clearly a significant reduction in maximum achievable
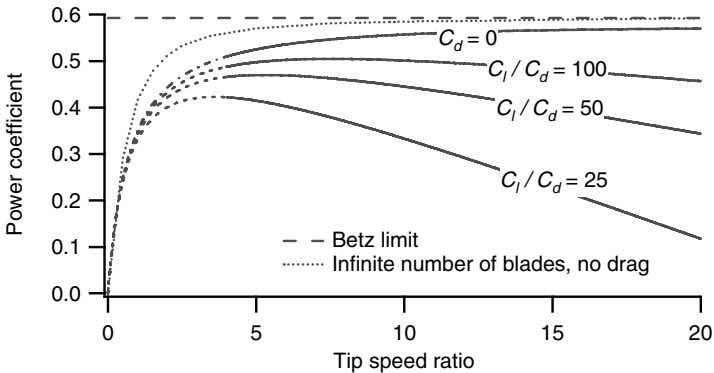
Figure 3.34 Maximum achievable power coefficients of a three-bladed optimum rotor as a function of the lift to drag ratio, C_l/C_d

power as the airfoil drag increases. For reference, the DU-93-W-210 airfoil has a maximum C_l/C_d ratio of 140 at an angle of attack of 6 degrees, and the 19% thick LS(1) airfoil has a maximum C_l/C_d ratio of 85 at an angle of attack of 4 degrees. It can be seen that it clearly benefits the blade designer to use airfoils with high lift to drag ratios. In practice, rotor power coefficients may be further reduced as a result of (1) non-optimum blade designs that are easier to manufacture, (2) the lack of airfoils at the hub and (3) aerodynamic losses at the hub end of the blade.

3.13 Computational and Aerodynamic Issues in Aerodynamic Design

As mentioned at the beginning of this chapter, the aerodynamic performance of wind turbines is primarily a function of the steady state aerodynamics discussed above. The analysis presented in this chapter provides a method for determining average loads on a wind turbine. There are, however, a number of important steady state and dynamic effects that cause increased loads or decreased power production from those expected with the BEM theory presented here, especially increased transient loads. An overview of these effects is provided in this section, including non-ideal steady state effects, the influence of turbine wakes, and unsteady aerodynamics. This section also includes comments on computer programs that can be used for rotor performance modeling and approaches to modeling rotor aerodynamics other than BEM methods.

3.13.1 Non-ideal Steady State Aerodynamic Issues

Steady state effects that influence wind turbine behavior include the degradation of blade performance due to surface roughness, the effects of stall on blade performance, and blade rotation.

As mentioned in Section 3.4.5, blade surfaces roughened by damage and debris can significantly increase drag and decrease the lift of an airfoil. This has been shown to decrease power production by as much as 40% on certain airfoils. The only solution is frequent blade repair and cleaning or the use of airfoils that are less sensitive to surface roughness.

Additionally, when parts of a blade operate in the stall region, fluctuating loads may result. On stall-controlled horizontal axis rotors, much of the blade may be stalled under some conditions. Stalled airfoils do not always exhibit the simple relationship between the angle of attack and aerodynamic forces that are evident in lift and drag coefficient data. The turbulent separated flow occurring during stall can induce rapidly fluctuating flow conditions and rapidly fluctuating loads on the wind turbine.

Finally, the lift and drag behavior of airfoils is measured in wind tunnels under non-rotating conditions. Investigation has shown that the same airfoils, when used on a horizontal axis wind turbine, may exhibit delayed stall and may produce more power than expected. The resulting unexpectedly high loads at high wind speeds can reduce turbine life. This behavior has been linked to spanwise pressure gradients that result in a spanwise velocity component along the blade that helps keep the flow attached to the blade, delaying stall and increasing lift.

3.13.2 Turbine Wakes

Many of the primary features of the air flow into and around wind turbines are described by the results of BEM theory: the induced velocities due to power production and the rotation of the turbine wake and the expanding wake downwind of the turbine. The actual flow field, however, is much more complicated. Some of the details of flow around and behind a horizontal axis wind turbine are described here. The consequences of these flow patterns affect downwind turbines and may result in a 'skewed wake,' which causes increased fluctuating loads which are not predicted by BEM theory. Before considering their consequences, the essential features of turbine wakes are described in the following paragraph.

Wind turbine wakes are often thought of as consisting of a near wake and a far wake (Voutsinas *et al.*, 1993). The difference between the near and far wakes is a function of the spatial distribution and the intensity of the turbulence in the flow field. Fluid flow modeling and experiments have shown that each blade generates a sheet of vortices that is transported through the wake by the mean axial and rotational flow in the wake. In addition to the vortex sheet from the trailing edge of the blades, vortices generated at the hub, and especially strong vortices generated at the blade tips, are also convected downstream. The tip vortices cause the tip losses mentioned in Section 3.8. All of these vortices and mechanically generated turbulence are dissipated and mixed in the near wake (within one to three rotor diameters downstream of the rotor). The stream of tip vortices from each blade merge in the near wake into a cylindrical sheet of rotating turbulence as they mix and diffuse through the flow (Sorensen and Shen, 1999). Much of the periodic nature of the flow is lost in the near wake (Ebert and Wood, 1994). Thus, turbulence and vorticity generated at the rotor are diffused in the near wake, resulting in more evenly distributed turbulence and velocity profiles in the far wake. Meanwhile, the mixing of the slower axial flow of the turbine wake with the free stream flow slowly re-energizes the flow. The vortex sheet from the tip vortices results in an annular area in the far wake of higher relative turbulence surrounding the less turbulent core of the wake. Mixing and diffusion continue in the far wake until the turbine-generated turbulence and velocity deficit with respect to the free stream flow have disappeared.

The consequences of the vorticity and turbulence in turbine wakes are increased loads and fatigue. The most obvious effect is the increased turbulence in the flow at turbines that are downwind of other turbines in a wind farm (see Chapter 9). The turbine wakes also affect the loads on the turbine producing the wake. For example, tip and hub vortices reduce the energy capture from the rotor.

Another important effect occurs with off-axis winds, i.e. those whose direction is not perpendicular to the plane of the rotor. Off-axis flows, whether due to yaw error or vertical wind components, result in a skewed wake in which the wake is not symmetric with the turbine axis. Skewed wakes result in the downwind side of the rotor being closer to the tip vortices being transported downstream than the upwind side of the rotor. The result is higher induced velocities on the downwind side of the rotor than the upwind side. This effect has been shown to result in higher turbine forces than otherwise would be expected (Hansen, 1992). One commonly used approach to modeling the effects of a skewed wake is the Pitt and Peters model (Pitt and Peters, 1981; Goankar and Peters, 1986). The model applies a multiplicative correction factor to the axial induction factor that is a function of yaw angle, radial position, and blade azimuth angle. For more information on its use in wind turbine modeling, see Hansen (1992).

3.13.3 Unsteady Aerodynamic Effects

There are a number of unsteady aerodynamic phenomena that have a large effect on wind turbine operation. The turbulent eddies carried along with the mean wind cause rapid changes in speed and direction over the rotor disc. These changes cause fluctuating aerodynamic forces, increased peak forces, blade vibrations, and significant material fatigue. Additionally, the transient effects of tower shadow, dynamic stall, dynamic inflow, and rotational sampling (all explained below) change turbine operation in unexpected ways. Many of these effects occur at the rotational frequency of the rotor or at multiples of that frequency. Effects that occur once per revolution are often referred to as having a frequency of $1P$. Similarly, effects that occur at three or n times per revolution of the rotor are referred to as occurring at a frequency of $3P$ or nP.

Tower shadow refers to the wind speed deficit behind a tower caused by the tower obstruction. The blades of a downwind rotor with B blades will encounter the tower shadow once per revolution, causing a rapid drop in power and BP vibrations in the turbine structure.

Dynamic stall refers to rapid aerodynamic changes that may bring about or delay stall behavior. Rapid changes in wind speed (for example, when the blades pass through the tower shadow) cause a sudden detachment and then reattachment of air flow along the airfoil. Such effects at the blade surface cannot be predicted with steady state aerodynamics, but may affect turbine operation, not only when the blades encounter tower shadow, but also during operation in turbulent wind conditions. Dynamic stall effects occur on time scales of the order of the time for the relative wind at the blade to traverse the blade chord, approximately $c/\Omega r$. For large wind turbines, this might be on the order of 0.2 seconds at the blade root to 0.01 seconds at the blade tip (Snel and Schepers, 1991). Dynamic stall can result in high transient forces as the wind speed increases, but stall is delayed. A variety of dynamic stall models have been used in computer rotor performance codes including those of Gormont (1973) and Beddoes (Björck *et al.*, 1999). The Gormont model, for example, modifies the angle of attack calculated with the BEM theory by adding a factor that depends on the rate of change of the angle of attack.

Dynamic inflow refers to the response of the larger flow field to turbulence and changes in rotor operation (pitch or rotor speed changes, for example). Steady state aerodynamics suggest that increased wind speed and, thus, increased power production should result in an instantaneous increase in the axial induction factor and changes in the flow field upstream and downstream of the rotor. During rapid changes in the flow and rapid changes in rotor operation, the larger field cannot respond quickly enough to instantly establish steady state conditions. Thus, the aerodynamic conditions at the rotor are not necessarily the expected conditions, but an ever-changing approximation as the flow field changes. The time scale of dynamic flow effects is on the order of D/U, the ratio of the rotor diameter to the mean ambient flow velocity. This might be as much as ten seconds (Snel and Schepers, 1991). Phenomena occurring slower than this can be considered using a steady state analysis. For more information on dynamic inflow see Snel and Schepers (1991, 1993) and Pitt and Peters (1981).

Finally, *rotational sampling* (see Connell, 1982) causes some unsteady aerodynamic effects and increases fluctuating loads on the wind turbine. The wind as seen by the rotor is constantly changing as the rotor rotates. The general flow turbulence may bring wind speed changes on a time scale of about five seconds. The turbulent eddies may be smaller than the rotor disc, resulting in different winds at different parts of the disc. If the blades are rotating once a second,

the blades 'sample' different parts of the flow field at a much faster rate than the general changes in the wind field itself, causing rapidly changing flow at the blade.

3.13.4 Other Computational Approaches to Aerodynamic Design

In this chapter, the BEM theory approach has been used to predict rotor performance. An iterative approach to blade design has also been outlined based on the analysis methods detailed in the text. There are other approaches to predicting blade performance and to designing blades that may be more applicable in some situations. Some of the disadvantages of the BEM theory include errors under conditions with large induced velocities (Glauert, 1948) or yawed flow and inability to predict delayed stall due to rotational effects.

Vortex wake methods have been used in the helicopter industry in addition to BEM methods. Vortex wake methods calculate the induced velocity field by determining the distribution of vorticity in the wake. This method is computationally intensive, but has advantages for yawed flow and operation subject to three-dimensional boundary layer effects (Hansen and Butterfield, 1993).

There are also other possible theoretical approaches. Researchers at Delft University of Technology have reported initial work on a model employing asymptotic acceleration potential methods (Hansen and Butterfield, 1993). Cascade theory, often used in turbomachinery design, has also been used to analyze wind turbine performance. Cascade theory takes into consideration the aerodynamic interactions between blades. Although it is more computationally intensive, cascade theory has been shown to provide better results than BEM theory for high-solidity, low tip speed rotors (Islam and Islam, 1994). Computational fluid dynamics (CFD), while also computationally intensive, has been applied to wind turbine rotors in some situations (see, for example, Sorensen *et al.*, 2002 and Duque *et al.*, 1999).

3.13.5 Model Validation and Modeling Issues

Numerous efforts have been made to validate rotor performance models. This is difficult because most test programs have instrumented wind turbines in typical operating environments with shear and turbulence. Sensors to measure the incoming wind field must be upwind of the rotor to ensure that the data is undisturbed by the wind turbine itself. By the time the turbulent flow field reaches the wind turbine, the instantaneous wind speeds across the rotor have changed from the values measured upwind. Thus, it is difficult to compare specific wind conditions with measured loads and with model outputs. Inflow conditions, measurements, and results can only be compared statistically. Nevertheless, field tests have provided important insights and measurements have highlighted aerodynamic issues to be considered in modeling codes.

Wind tunnels provide a more controlled environment for testing, but large wind tunnels and large wind turbines are needed to achieve the Reynolds numbers at the operating conditions of wind turbines. Recent tests of a wind turbine with a 10 m diameter rotor were performed at the NASA AMES wind tunnel in California (Fingersh *et al.*, 2001). The wind tunnel has a 25 m by 36 m test section and can achieve flows up to 50 m/s and Reynolds numbers approaching those of large wind turbines with high repeatability and very low turbulence. Tests included conditions with a variety of wind speeds, yaw angles, blade pitch settings, and rotor
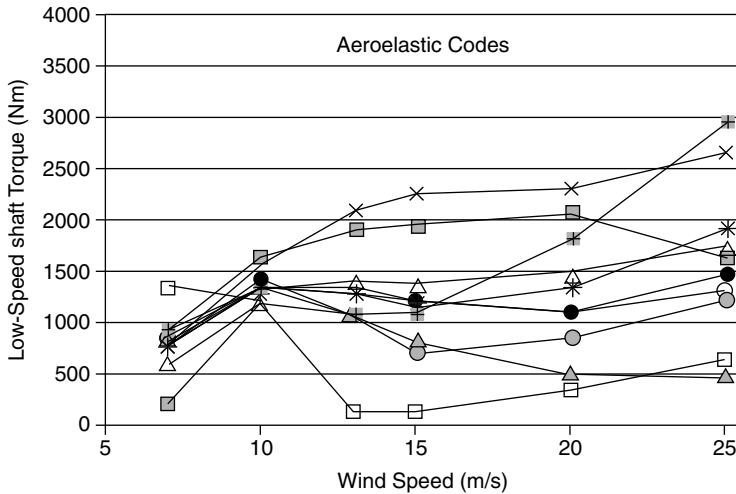
Figure 3.35   Low-speed shaft torque predictions from modeling codes compared with measured data from NASA AMES wind tunnel tests for axial flow (Simms *et al.*, 2001)

configurations (teetered, rigid, and upwind and downwind of the tower). Measurements included pressures over the blades, angle of attack, loads and moments, and output power. After the tests were completed, the measured input data, airfoil data, and operational conditions were provided to a number of modelers around the world. Nineteen modelers, using a variety of aerodynamic modeling programs (some used the same program) provided predictions of rotor performance, loads and pressure coefficients for 20 different operating conditions. The results were most surprising and have highlighted many areas that still need to be addressed.

The results of the modeling efforts were categorized by the type of model used to do the analysis: performance codes (steady state aerodynamics), aeroelastic codes (engineering codes using BEM methods with modifications and blade motions), wake codes, and full CFD codes. An example of the modeling results of the aeroelastic codes is provided in Figure 3.35. The graph shows the low-speed shaft torque as a function of wind speed with the rotor upwind of the tower and the rotor directly facing the incoming flow (a yaw angle of zero). The thick line with the solid symbol is the measured data. The thinner lines indicate the predictions of the low-speed shaft torque of nine aeroelastic modelers. Even at 7 m/s, a condition under which no part of the blade is stalled and which should be relatively easy to predict, predictions range from 25% to 175% of the measured values. It appears that most of the differences, in this case, are due to different approaches to using the 2-D airfoil data in the codes. At wind speeds above 10 m/s, more and more of each blade is stalled. These conditions results in fluctuating loads, but the estimation of the average of these loads clearly needs to be improved!

3.14 Aerodynamics of Vertical Axis Wind Turbines

3.14.1 General Overview

As previously discussed in Chapter 1, wind turbine rotors may rotate about either a horizontal or a vertical axis. Although most wind turbines have historically been of the horizontal axis

type, vertical axis machines have been used in some situations of interest. This section gives a brief overview of vertical axis turbines and summarizes key aspects of their aerodynamics.

Vertical axis wind turbines (VAWTs) may have either drag-driven or lift-driven rotors. The most common drag-driven vertical axis turbine is the Savonius rotor. It has been used for water pumping and other high-torque applications. The argument in favor of Savonius rotor turbines is that they can be relatively inexpensive to build. In practice, by virtue of being a drag-driven machine, they have intrinsically low power coefficients. In addition, they have a solidity approaching 1.0, so they are very heavy relative to the power that they produce. They are also difficult to protect from damage in high winds.

When vertical axis turbines have been used for electrical power generation they have nearly always used lift-driven rotors. Typically these rotors have had one of two types of configuration: (1) straight blades or (2) curved blades with a troposkein shape. The latter type of rotor is known as the Darrieus rotor. Some rotors with straight blades have incorporated a pitching mechanism, but most lift-driven vertical axis turbines have fixed pitch blades. Thus, power limitation at high winds is accomplished by stalling.

The principal advantage of vertical axis rotors is that they do not require any special mechanisms for yawing into wind. Another advantage is that, since the blades are generally untwisted and of constant chord, the blades can be made by mass production extrusion.

In practice, vertical axis turbines have not been used nearly as widely as have horizontal axis turbines. The reasons have to do with the balance between some of the intrinsic benefits and limitations. By the nature of the aerodynamics of the rotor, the structural loads on each blade vary greatly during each rotation. Such loads contribute to high fatigue damage, and require that the blades and joints themselves have a very long cycle life. In addition, the vertical axis turbines do not lend themselves to being supported by a separate, tall tower. This means that a large fraction of the rotor tends be located close to the ground in a region of relatively low wind. Productivity may then be less than that of a horizontal axis machine of equivalent rated power, but on a taller tower.

3.14.2 Aerodynamics of a Straight-blade Vertical Axis Wind Turbine

The following analysis applies to a straight-blade vertical axis wind turbine. The first section concerns a single stream tube method of analysis and follows the approach of de Vries (1979). The second section summarizes the multiple stream tube method. This is followed by a brief discussion of the double multiple stream tube method. The Darrieus rotor can be modeled with a modification of the straight-blade methods. In that case, the blades are divided into sections, and the effects of the different distances of the sections from axis of rotation are accounted for. See Section 3.14.3.

3.14.2.1 Single Stream Tube Analysis

A single blade of a vertical axis wind turbine, viewed from above, is illustrated in Figure 3.36. In the figure the blade is shown rotating in the counter-clockwise direction, and the wind is seen impinging on the rotor from left to right. As is typical in vertical axis wind turbines, the airfoil is symmetric. The blade is oriented so that the chord line is perpendicular to the radius of the circle of rotation. The radius defining the angular position of the blade (normally meeting the chord line at the quarter chord) makes an angle of ϕ with the wind direction, as shown in the figure.
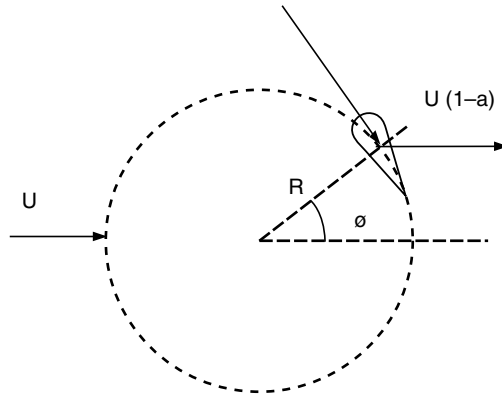
Figure 3.36   Geometry of a vertical axis turbine

Figure 3.37 illustrates the components of the wind acting on the blade. As can be seen, a component due to rotation is tangential to the circle of rotation, and thus parallel to the chord line of the airfoil. One component of the wind also acts tangentially. Another wind component is normal to the circle, and so perpendicular to the airfoil. An induction factor, a, accounts for the deceleration in the wind as it passes through the rotor.

The velocity relative to the blade element, by Pythagoras's Theorem, is:

$$U_{rel}^2 = \{\Omega R + (1-a)U\sin(\phi)\}^2 + \{(1-a)U\cos(\phi)\}^2 \tag{3.146}$$

This can be rewritten as:

$$\frac{U_{rel}}{U} = \sqrt{\{\lambda + (1-a)\sin(\phi)\}^2 + \{(1-a)\cos(\phi)\}^2} \tag{3.147}$$
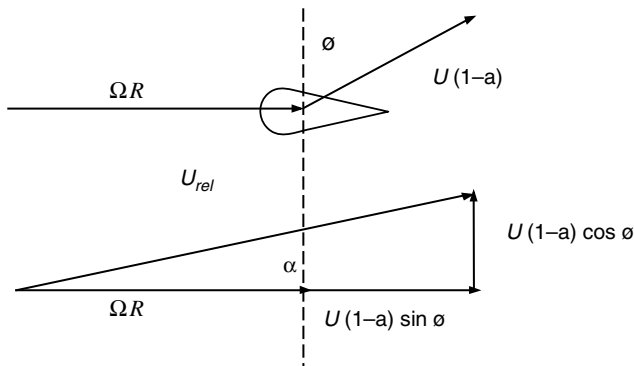
Figure 3.37   Components of wind acting on a vertical axis turbine blade

where:

$$\lambda = \frac{\Omega R}{U}$$

Note that at high tip speed ratios, the second term under the square root becomes small, so that:

$$\frac{U_{rel}}{U} \approx \lambda + (1 - a)\sin(\phi) \tag{3.148}$$

Since the chord is perpendicular to the radius of the circle, the angle of attack is:

$$\alpha = \tan^{-1}\left[\frac{(1 - a)\cos(\phi)}{\lambda + (1 - a)\sin(\phi)}\right] \tag{3.149}$$

At higher tip speed ratios, the second term in the denominator is small relative to the tip speed ratio and the tangent of α is approximately equal to α itself. Therefore:

$$\alpha \approx \frac{(1 - a)\cos(\phi)}{\lambda} \tag{3.150}$$

By analogy with momentum theory for horizontal axis rotors, the forces on the blade can be related to the change in momentum in the air stream. It is assumed, as before, that in the far wake the velocity is reduced to $U(1 - 2a)$, so that at the rotor it is $U(1 - a)$, as indicated in the figures.

The change in velocity is:

$$\Delta U = U - U(1 - 2a) = 2aU \tag{3.151}$$

The force per unit height, $\tilde{F}_D$, in the wind direction is found from:

$$\tilde{F}_D = \tilde{m}\Delta U \tag{3.152}$$

where $\tilde{m}$ is the mass flow rate per unit height. This is given by:

$$\tilde{m} = \rho 2RU(1 - a) \tag{3.153}$$

where R is the rotor radius and ρ is the density of the air. The force is thus:

$$\tilde{F}_D = 4R\rho a(1 - a)U^2 \tag{3.154}$$

That force must be equal to the average force on all the blades during a complete revolution. This is found using blade element theory by integrating around the circle, taking into account the contribution from each of the B blades:

$$\tilde{F}_D = \frac{B}{2\pi}\int_0^{2\pi} \frac{1}{2}\rho U_{rel}^2 cC_l \cos(\alpha + \phi)\mathrm{d}\phi \tag{3.155}$$

where $B = $ number of blades and $C_l = $ lift coefficient.

By equating Equations (3.154) and (3.155), the following relation may be obtained:

$$a(1-a) = \frac{1}{8}\frac{Bc}{R}\frac{1}{2\pi}\int_0^{2\pi}\left[\frac{U_{rel}}{U}\right]^2 C_l\cos(\alpha+\phi)\mathrm{d}\phi \tag{3.156}$$

This equation cannot be solved directly, so an iteration technique must be used. To do this, let $y = \lambda/(1-a)$. Dividing both sides of Equation (3.156) by $(1-a)^2$, using Equation (3.149) for the angle of attack, adding 1 to both sides and making the appropriate substitutions, one obtains the following:

$$\frac{1}{1-a} = 1 + \frac{1}{8}\frac{Bc}{R}\frac{1}{2\pi}\int_0^{2\pi}\left\{(y+\sin(\phi))^2 + \cos^2(\phi)\right\}C_l\cos\left\{\phi+\tan^{-1}\left(\frac{\cos(\phi)}{y+\sin(\phi)}\right)\right\}\mathrm{d}\phi \tag{3.157}$$

For a given geometry, Bc/R is fixed. A value for y can be assumed and $(1-a)$ can be calculated. From that the corresponding tip speed ratio can be found from:

$$\lambda = y(1-a) \tag{3.158}$$

The calculation is repeated until the desired tip speed ratio is found.

The power produced by the rotor is found, as usual, from the product of the average torque and the rotational speed. The torque varies with angular position, so the expression for power is:

$$P = \Omega\frac{1}{2\pi}\int_0^{2\pi}Q\mathrm{d}\phi \tag{3.159}$$

The torque is the product of the radius and the tangential force. The tangential force per unit length on each blade, $\tilde{F}_T$, (which varies with ϕ) is:

$$\tilde{F}_T = \frac{1}{2}\rho U_{rel}^2 c(C_l\sin(\alpha) - C_d\cos(\alpha)) \tag{3.160}$$

The total torque, assuming B blades and a rotor of height H, is:

$$Q = BHF_T \tag{3.161}$$

The average rotor power over one revolution is then:

$$P = \Omega RH\frac{Bc}{2\pi}\frac{1}{2}\rho\int_0^{2\pi}U_{rel}^2(C_l\sin(\alpha) - C_d\cos(\alpha))\mathrm{d}\phi \tag{3.162}$$

The power coefficient is given by the power divided by the power in the wind passing through an area defined by the projected area of the rotor, $2RH$:

$$C_P = \frac{P}{\frac{1}{2}\rho 2RHU^3} \tag{3.163}$$

Therefore:

$$C_P = \frac{\lambda}{4\pi} \frac{Bc}{R} \int_0^{2\pi} \left[\frac{U_{rel}}{U}\right]^2 C_l \sin(\alpha) \left[1 - \frac{C_d}{C_l \tan(\alpha)}\right] d\phi \tag{3.164}$$

This formula can be solved numerically, but it is also of interest to consider some idealized conditions. In particular, for high tip speed ratios ($\lambda \gg 1$), the angle of attack will be relatively small. For small angles of attack (below stall), the lift coefficient is linearly related to the angle of attack and since a symmetrical airfoil is assumed, the lift coefficient may be written as:

$$C_l = C_{l,\alpha}\alpha \tag{3.165}$$

where $C_{l,\alpha}$ = slope of the lift curve

Thus, the angle of attack as given in Equation (3.150) is the appropriate form and, in addition, $\cos(\phi + \alpha) \approx \cos(\phi)$. Equation (3.157) can be approximated as:

$$\frac{1}{1-a} = 1 + \frac{1}{8}\frac{Bc}{R}\frac{1}{2\pi}\int_0^{2\pi}\left\{(y + \sin(\phi))^2 + \cos^2(\phi)\right\}C_{l,\alpha}\alpha\cos(\phi)d\phi \tag{3.166}$$

The term in brackets can be expanded and, using Equation (3.150), Equation (3.166) can be written as:

$$\frac{1}{1-a} = 1 + \frac{1}{16}\frac{Bc}{R}\frac{1}{\pi}\int_0^{2\pi}\left\{y^2 + 2y\sin(\phi) + \sin^2(\phi) + \cos^2(\phi)\right\}C_{l,\alpha}\frac{1}{y}\cos^2(\phi)d\phi \tag{3.167}$$

Taking advantage of the identity $\sin^2(\phi) + \cos^2(\phi) = 1$, Equation (3.167) yields:

$$\frac{1}{1-a} = 1 + \frac{1}{16}\frac{Bc}{R}\frac{1}{\pi}\int_0^{2\pi}\left\{y + 2\sin(\phi) + \frac{1}{y}\right\}C_{l\alpha}\cos^2(\phi)d\phi \tag{3.168}$$

Performing the integration, the sine term becomes zero and the cosine squared terms integrate to π. Thus:

$$\frac{1}{1-a} = 1 + \frac{1}{16}\frac{Bc}{R}C_{l,\alpha}\left(y + \frac{1}{y}\right) \approx 1 + \frac{1}{16}\frac{Bc}{R}C_{l,\alpha}y \tag{3.169}$$

or

$$a \approx \frac{1}{16}\frac{Bc}{R}C_{l,\alpha}\lambda \tag{3.170}$$

The expression for the power coefficient may also be simplified by using small-angle approximations and by assuming the drag coefficient to be constant. That is:

$$C_d(\alpha) \approx C_{d,0} \tag{3.171}$$

where $C_{d,0}$ is a constant drag term.

Equation (3.164) can then be integrated to give:

$$C_P = \frac{1}{4\pi}\frac{Bc}{R}C_{l,\alpha}\frac{(1-a)^4}{\lambda}(y^2+1) - \frac{1}{2}\frac{Bc}{R}C_{d,0}\lambda(1-a)^2(y^2+1) \qquad (3.172)$$

Equation (3.172) can be further simplified by noting that since $y \gg 1$, it is also true that $y^2 + 1 \approx y^2$ and also that $(1-a)^2 y^2 = \lambda^2$. The expression for C_P can then be approximated as:

$$C_P \approx 4a(1-a)^2 - \frac{1}{2}\frac{Bc}{R}C_{d,0}\lambda^3 \qquad (3.173)$$

When there is no drag, the optimum C_P from this equation occurs when $a = 1/3$. Thus this vertical axis wind turbine has the same the Betz limit as do horizontal axis wind turbines. Therefore:

$$C_{P,\text{max}} = \frac{16}{27} = 0.5926 \qquad (3.174)$$

The same minimum limit on the induction factor, a, applies is it does for horizontal axis wind turbines, namely $a < 0.5$.

3.14.2.2 Multiple Stream Tube Momentum Theory

Another approach, known as the multiple stream tube theory, is sometimes used for the analysis of vertical axis wind turbines. In this approach it is assumed that the induction factor may vary in the direction perpendicular to the wind, but is constant in the direction of the wind. Each stream tube of constant a is parallel to the wind, as shown in Figure 3.38. The force on a stream tube of width $R\cos(\phi)\Delta\phi$ can be related to the change in momentum of the wind passing through it. The equation for force per unit height, analogous to Equation (3.152), is given by:

$$\Delta\tilde{F}_D = R\cos(\phi)(\Delta\phi)\rho 2a(1-a)U^2 \qquad (3.175)$$
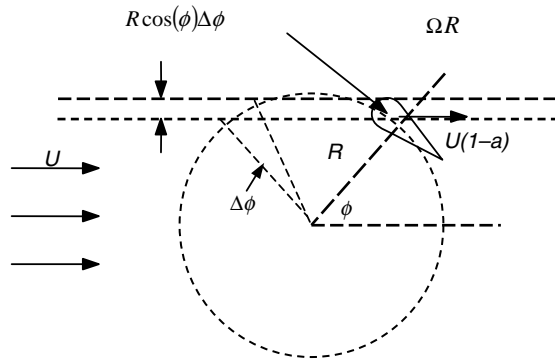
Figure 3.38 Multiple stream tube geometry

During any given rotation, the blade will pass through the stream tube twice. The force on the blade is found from blade element theory. It turns out that the force on the blade at both the upwind and downwind crossing position is the same. The equation for force, analogous to Equation (3.154), is accordingly given by:

$$\Delta \tilde{F}_D = B \frac{2}{2\pi} \int\limits_{\phi}^{\phi + \Delta\phi} \frac{1}{2}\rho U_{rel}^2 cC_l \cos(\phi + \alpha) \mathrm{d}\phi \qquad (3.176)$$

The two equations above may be equated and an expression for a may be found for each stream tube. The integral in Equation (3.176) is given approximately by:

$$\int\limits_{\phi}^{\phi + \Delta\phi} \frac{1}{2}\rho U_{rel}^2 cC_l \cos(\phi + \alpha) \mathrm{d}\phi = \frac{1}{2}\rho U_{rel}^2 cC_l \cos(\phi + \alpha)\Delta\phi \qquad (3.177)$$

By using Equations (3.175) and (3.176), and taking advantage of Equation (3.177), it may be shown that:

$$a(1 - a) = \left(\frac{1}{4\pi}\right)\left(\frac{Bc}{R}\right)\left(\frac{U_{rel}}{U}\right)^2 C_l \frac{\cos(\phi + \alpha)}{\cos(\phi)} \qquad (3.178)$$

The power coefficient can be solved as before with Equation (3.172), but in this case an iterative method must be used since a is now a function of the angle of attack. Detailed analysis of this method is beyond the scope of this book. More information may be found in de Vries (1979) and Paraschivoiu (2002).

3.14.2.3 Double Multiple Stream Tube Momentum Theory

An extension of the multiple stream tube theory is known as the 'double multiple stream tube theory.' The approach is similar to that of the multiple stream tube theory described above. The main difference is that the induction factors in the upwind and downwind positions need not be the same. Simulation models for vertical axis wind turbines developed by Sandia National Laboratory are based on the double multiple stream tube theory. Detailed discussion of this model is beyond the scope of this book. References such as Spera (1994) should be consulted for further information.

3.14.3 Aerodynamics of the Darrieus Rotor

The Darrieus rotor may be analyzed with either the single or multiple stream tube methods discussed above. The main differences have to do with (1) the orientation of the blade elements, which are now different from one another, and (2) the distance of the blade elements from the axis of rotation, which is not constant over the length of the blades. Further discussion of Darrieus rotor aerodynamics is beyond the scope of this book. The reader is referred to Paraschivoiu (2002) for references that give a more in-depth coverage of this topic.
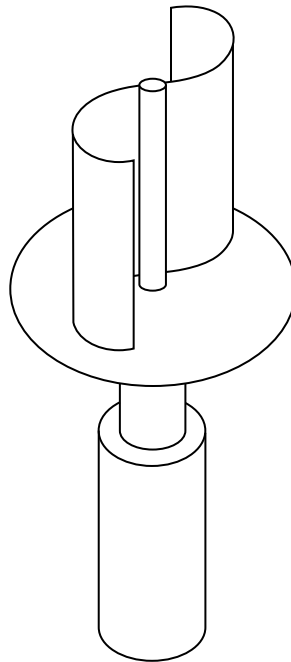
Figure 3.39   Savonius rotor (S. Kuntoff, reproduced under Creative Commons license)

3.14.4 Savonius Rotor

The Savonius rotor is a vertical axis wind turbine with an S-shaped cross-section when viewed from above. A schematic is illustrated in Figure 3.39. It is primarily a drag-type device, but there may be some amount of lift contributing to the power as well.

The power from the Savonius is based on the difference in pressure across the blade retreating from the wind and that advancing into the wind. This is in turn related to the difference in the drag coefficients associated with the convex side of the blade and the concave side of the blades. A detailed discussion of the aerodynamics of the Savonius rotor may be found in Paraschivoiu (2002).

Savonius rotors have, in general, fairly low efficiencies, although power coefficients close to 0.30 have been measured (see Blackwell *et al.*, 1977). The peak power coefficient for any Savonius rotor occurs at a tip speed ratio less than 1.0.

References

Abbott, I. A. and von Doenhoff, A. E. (1959) *Theory of Wing Sections*. Dover Publications, New York.

Althaus, D. (1996) *Airfoils and Experimental Results from the Laminar Wind Tunnel of the Institute for Aerodynamik and Gasdynamik of the University of Stuttgart*. University of Stuttgart.

Althaus, D. and Wortmann, F. X. (1981) *Stuttgarter Profilkatalog*. Friedr. Vieweg und Sohn, Braunschweig/ Wiesbaden.

Bertin, J. J. And Smith, M. L. (2008) *Aerodynamics for Engineers*, 5th edition. Prentice Hall, Inc., Upper Saddle River, New Jersey.

Betz, A. (1926) *Windenergie und Ihre Ausnutzung durch Windmüllen*. Vandenhoeck and Ruprecht, Göttingen.

Björck, A., Mert, M. and Madsen, H. A. (1999) Optimal parameters for the FFA-Beddoes dynamic stall model. *Proc. of 1999 European Wind Energy Conference, Nice*, pp. 125–129.

Blackwell, B. F., Sheldahl, R. E. and Feltz, L. V. (1977) *Wind Tunnel Performance Data for Two- and Three-Bucket Savonius Rotors*, SAND76-0131, Sandia National Laboratories, (also available as http://www.prod.sandia.gov/cgi-bin/techlib/access-control.pl/1976/760131.pdf)

Connell, J. R. (1982) The spectrum of wind speed fluctuations encountered by a rotating blade of a wind energy conversion system. *Solar Energy*, **29**(5), 363–375.

de Vries, O. (1979) *Fluid Dynamic Aspects of Wind Energy Conversion*. Advisory Group for Aerospace Research and Development, North Atlantic Treaty Organization, AGARD-AG-243.

Duque, P. N., van Dam, C. P. and Hughes, S. C. (1999) Navier–Stokes simulations of the NREL Combined Experiment rotor, AIAA Paper 99-0037, *Proc. 37th AIAA Aerospace Sciences Meeting and Exhibit, Reno,* NV.

Ebert, P. R. and Wood, D. H. (1994) Three dimensional measurements in the wake of a wind turbine, *Proc. of the 1994 European Wind Energy Conference, Thessalonika*, pp. 460–464.

Eggleston, D. M. and Stoddard, F. S. (1987) *Wind Turbine Engineering Design*. Van Nostrand Reinhold, New York.

Eppler, R. and Somers, K. M. (1980) *A Computer Program for the Design and Analysis of Low-Speed Airfoils*, NASA TM-80210, NASA Langley Research Center. Hampton, VA.

Flettner, A. (1926) *The Story of the Rotor*. F. O. Wilhofft, New York.

Glauert, H. (1935) Airplane Propellers, in *Aerodynamic Theory* (Ed. W. F. Durand), Div. L. Chapter XI, Springer Verlag, Berlin (reprinted by Peter Smith (1976) Gloucester, MA).

Glauert, H. (1948) *The Elements of Aerofoil and Airscrew Theory*. Cambridge University Press, Cambridge, UK.

Goankar, G. H. and Peters, D. A. (1986) Effectiveness of current dynamic-inflow models in hover and forward flight. *Journal of the American Helicopter Society*, **31**(2), 47–57.

Gormont, R. E. (1973) *A Mathematical Model of Unsteady Aerodynamics and Radial Flow for Application to Helicopter Rotors*. US Army Air Mobility Research and Development Laboratory, Technical Report, 76–67.

Hansen, A. C. (1992) *Yaw Dynamics of Horizontal Axis Wind Turbines: Final Report*. SERI Report, Subcontract No. XL-6-05078-2.

Hansen, A. C. and Butterfield, C. P. (1993) Aerodynamics of horizontal axis wind turbines. *Annual Review of Fluid Mechanics*, **25**, 115–149.

Islam, M. Q. and Islam, A. K. M. S. (1994) The aerodynamic performance of a horizontal axis wind turbine calculated by strip theory and cascade theory. *JSME International Journal Series B*, **37** 871–877.

Lysen, E. H. (1982) *Introduction to Wind Energy*. Steering Committee Wind Energy Developing Countries. Amersfoort, NL.

Manwell, J. F. (1990) A simplified method for predicting the performance of a horizontal axis wind turbine rotor. *Proc. of the 1990 American Wind Energy Association Conference.* Washington, DC.

Miley, S. J. (1982) *A Catalog of Low Reynolds Number Airfoil Data for Wind Turbine Applications*. Rockwell Int., Rocky Flats Plant RFP-3387, NTIS.

Paraschivoiu, I. (2002) *Wind Turbine Design with Emphasis on Darrieus Concept*, Ecole Polytechnique de Montreal.

Pitt, D. M. and Peters, D. A. (1981) Theoretical predictions of dynamic inflow derivatives. *Vertica*, **5**(1), 21–34.

Selig, M. S. and Tangler, L. T. (1995) Development and application of a multipoint inverse design method for horizontal axis wind turbines. *Wind Engineering*, **19**(2).

Sengupta, A. and Verma, M. P. (1992) An analytical expression for the power coefficient of an ideal horizontal-axis wind turbine. *Inernational. Journal of Energy Research*, **16**, 453–456.

Simms, D., Schreck, S., Hand, M., Fingersh, L.J. (2001) *NREL Unsteady Aerodynamics Experiment in the NASA-Ames Wind Tunnel: A Comparison of Predictions to Measurements*. NREL/TP-500-29494. National Renewable Energy Laboratory, Golden, CO.

Snel, H. (2002) Technology state of the art, from wind inflow to drive train rotation. *Proc. 2002 Global Windpower Conference and Exhibition,* Paris.

Snel, H. and Schepers, J. G. (1991) Engineering models for dynamic inflow phenomena. *Proc. 1991 European Wind Energy Conference, Amsterdam*, pp. 390–396.

Snel, H. and Schepers, J. G. (1993) Investigation and modelling of dynamic inflow effects. *Proc. 1993 European Wind Energy Conference, Lübeck*, pp. 371–375.

Sorensen, J. N. and Shen, W. Z. (1999) Computation of wind turbine wakes using combined Navier–Stokes actuator-line methodology. *Proc. 1999 European Wind Energy Conference, Nice*, pp. 156–159.

Sorensen, N. N., Michelsen, J. A. and Schrenk, S. (2002) Navier–Stokes predictions of the NREL Phase VI rotor in the NASA Ames 80-by-120 wind tunnel. *Collection of Technical Papers, AIAA-2002-31*. 2002 ASME Wind Energy Symposium, AIAA Aerospace Sciences Meeting and Exhibit, Reno, Nevada.

Spera, D. A. (Ed.) (1994) *Wind Turbine Technology*. American Society of Mechanical Engineers, New York.

Tangler, J. L. (1987) *Status of Special Purpose Airfoil Families.* SERI/TP-217-3264, National Renewable Energy Laboratory, Golden, CO.

Tangler, J. (2000) The evolution of rotor and blade design. *Proc. 2000 American Wind Energy Conference.* Palm Springs, CA.

Tangler, J., Smith, B., Jager, D. and Olsen, T. (1990) Atmospheric performance of the status of the special-purpose SERI thin-airfoil family: final results. *Proc. 1990 European Wind Energy Conference,* Madrid.

Timmer, W. A. and van Rooij, R. P. J. O. M. (2003) Summary of Delft University wind turbine dedicated airfoils. *Journal of Solar Energy Engineering*, **125**, 488–496.

Viterna, L. A. and Corrigan, R. D. (1981) Fixed pitch rotor performance of large horizontal axis wind turbines. *Proc. Workshop on Large Horizontal Axis Wind Turbines*, NASA CP-2230, DOE Publication CONF-810752, 69–85, NASA Lewis Research Center, Cleveland, OH.

Voutsinas, S. G., Rados K. G. and Zervos, A. (1993) Wake effects in wind parks: a new modelling approach. *Proc. 1993 European Community Wind Energy Conference,* Lübeck, pp. 444–447.

Wilson, R. E. and Lissaman, P. B. S. (1974) *Applied Aerodynamics of Wind Power Machine*. Oregon State University.

Wilson, R. E., Lissaman, P. B. S. and Walker, S. N. (1976) *Aerodynamic Performance of Wind Turbines*. Energy Research and Development Administration, ERDA/NSF/04014-76/1.

Wilson, R. E., Walker, S. N. and Heh, P. (1999) *Technical and User's Manual for the FAST_AD Advanced Dynamics Code. OSU/NREL Report 99-01*, Oregon State University, Corvallis OR.

4

Mechanics and Dynamics

4.1 Background

The interplay of the forces from the external environment, primarily due to the wind, and the motions of the various components of the wind turbine, result not only in the desired energy production from the turbine, but also in stresses in the constituent materials. For the turbine designer, these stresses are of primary concern, because they directly affect the strength of the turbine and how long it will last.

To put it succinctly, in order to be a viable contender for providing energy, a wind turbine must:

- produce energy;
- survive;
- be cost effective.

That means that the turbine design must not only be functional in terms of extracting energy. It must also be structurally sound so that it can withstand the loads it experiences, and the costs to make it structurally sound must be commensurate with the value of the energy it produces.

The purpose of this chapter is to discuss the mechanical framework within which the turbine must be designed if it is to meet these three requirements. The chapter consists of four sections, beyond this background. Section 4.2 provides an overview of wind turbine loads. Section 4.3 gives a summary of the fundamental principles of mechanics relevant to wind turbines. Section 4.4 deals more directly with wind turbine motions, forces, and stresses. Section 4.5 describes some of the more detailed methods used to analyze wind turbine structural response.

Section 4.3 includes a very brief overview of the basics: statics, dynamics, and strength of materials. This overview is brief because it is assumed that the reader already has some familiarity with the concepts involved. A slightly longer discussion, however, is devoted to a few concepts of particular relevance. This section includes a more detailed discussion of one

other topic: vibrations. This topic is discussed in more detail because it is presumed that it may be less familiar to many readers. The topic of vibrations is important not only because the concepts are relevant to actual structural vibrations, but also because the concepts can be used to describe many aspects of the behavior of the wind turbine rotor. Fatigue is another important and related topic because it affects how turbine components are expected to withstand a lifetime of continuously varying loads. Fatigue is closely connected to the design details of turbine components and to the types of materials that may be used and so is discussed in Chapter 6.

Section 4.4 examines the response of the wind turbine to aerodynamic forces, using progressively more detailed approaches. The first approach uses a simple steady state approach that follows directly from the discussions of the ideal rotor in Chapter 3. The second approach includes the effects of the rotation of the wind turbine rotor. In addition, the operating environment is not assumed to be uniform, so the effects of vertical wind shear, yaw motion, and turbine orientation are all accounted for. This approach uses a number of simplifications to make the problem solvable, resulting in solutions that are more representative than precise.

Finally, some of the more detailed approaches to investigating wind turbine dynamics are discussed in Section 4.5. These are, in general, more comprehensive or specialized, but are also more complex and less intuitive. For that reason, they are only discussed briefly and the reader is referred to other sources for more details.

Although the fundamentals apply to all types of wind turbine design, the focus of this next section is exclusively on horizontal axis turbines.

4.2 Wind Turbine Loads

This section provides an overview of wind turbine loads: the types of loads, their sources, and their effects.

4.2.1 Types of Loads

In this chapter, the term 'load' refers to forces or moments that may act upon the turbine. The loads that a turbine may experience are of primary concern in assessing the turbine's structural requirements. These loadings may be divided into five types:

- steady (static and rotating);
- cyclic;
- transient (including impulsive);
- stochastic;
- resonance-induced loads.

The key characteristics of these loads and some examples for wind turbines are summarized below.

4.2.1.1 Steady Loads

Steady loads are ones that do not vary over a relatively long time period. They can be either static or rotating. Static loads, as used in this text, refer to non-time-varying loads that impinge

on a non-moving structure. For example, a steady wind blowing on a stationary wind turbine would induce static loads on the various parts of the machine. In the case of steady rotating loads the structure may be in motion. For example, a steady wind blowing on a rotating wind turbine rotor while it is generating power would induce steady loads on the blades and other parts of the machine. The calculation of these particular loads has been detailed in Chapter 3.

4.2.1.2 Cyclic Loads

Cyclic loads are those which vary in a regular or periodic manner. The term applies particularly to loads which arise due to the rotation of the rotor. Cyclic loads arise as a result of such factors as the weight of the blades, wind shear, and yaw motion. Cyclic loads may also be associated with the vibration of the turbine structure or some of its components.

As noted in Chapter 3, a load which varies an integral number of times in relation to a complete revolution of the rotor is known as a 'Per rev' load, and given the symbol P. For example, a blade rotating in wind with wind shear will experience a cyclic $1P$ load. If the turbine has three blades, the main shaft will experience a cyclic $3P$ load.

4.2.1.3 Transient Loads

Transient loads are time-varying loads which arise in response to some temporary external event. There may be some oscillations associated with the transient response, but they eventually decay. Examples of transient loads include those in the drive train resulting from the application of a brake.

Impulsive loads are transient time-varying loads of relatively short duration, but of perhaps significant peak magnitude. One example of an impulsive load is that experienced by a blade of a downwind rotor when it passes behind the tower (through the 'tower shadow'). Two-bladed rotors are often 'teetered' or pinned at the low-speed shaft. This allows the rotor to rock back and forth, reducing bending loads on the shaft, but necessitating the use of teeter dampers. The force on a teeter damper when the normal range of teeter is exceeded is another example of an impulsive load.

4.2.1.4 Stochastic Loads

Stochastic loads are time varying, as are cyclic, transient, and impulsive loads. In this case, the loading varies in a more apparently random manner. In many cases the mean value may be relatively constant, but there may be significant fluctuations from that mean. Examples of stochastic loads are those which arise due to turbulence in the wind.

4.2.1.5 Resonance-Induced Loads

Resonance-induced loads are cyclic loads that result from the dynamic response of some part of the wind turbine being excited at one of its natural frequencies. They may reach high magnitudes. Resonance-induced loads are to be avoided whenever possible, but may occur under unusual operating circumstances or due to poor design. While these loads are not truly

a different type of load, they are mentioned separately because of their possibly serious consequences.

4.2.2 Sources of Loads

There are four primary sources of loads to consider in wind turbine design:

- aerodynamics;
- gravity;
- dynamic interactions;
- mechanical control.

The following briefly describes each of these sources.

4.2.2.1 Aerodynamics

The first source of wind turbine loads that one would typically consider is aerodynamics. Aerodynamics, particularly as related to power production, was described in Chapter 3. The loadings of particular concern in the structural design are those which could arise in very high winds, or those which generate fatigue damage. When a wind turbine is stationary in high winds, drag forces are the primary consideration. When the turbine is operating, it is lift forces which create the aerodynamic loadings of concern.

4.2.2.2 Gravity

Gravity is an important source of loads on the blades of large turbines, although it is less so on smaller machines. In any case, tower top weight is significant to the tower design and to the installation of the machine.

4.2.2.3 Dynamic Interactions

Motion induced by aerodynamic and gravitational forces in turn induces loads in other parts of the machine. For example, virtually all horizontal axis wind turbines allow some motion about a yaw axis. When yaw motion occurs while the rotor is turning there will be induced gyroscopic forces. These forces can be substantial when the yaw rate is high.

4.2.2.4 Mechanical Control

Control of the wind turbine may sometimes be a source of significant loads. For example, starting a turbine which uses an induction generator or stopping the turbine by applying a brake can generate substantial loads throughout the structure.

4.2.3 Effects of Loads

The loadings experienced by a wind turbine are important in two primary areas: (1) ultimate strength and (2) fatigue. Wind turbines may occasionally experience very high loads, and they

must be able to withstand those loads. Normal operation is accompanied by widely varying loads, due to starting and stopping, yawing, and the passage of blades through continuously changing winds. These varying loads can cause fatigue damage in machine components, such that a given component may eventually fail at much lower loads than it would have when new. More details on fatigue are given in Chapter 6. Accounting for the effect of loads in the design process is discussed in Chapter 7.

4.3 General Principles of Mechanics

This section presents an overview of some of the principles of basic mechanics and dynamics which are of particular concern in wind turbine design. The fundamentals of the mechanics of wind turbines are essentially the same as those of other similar structures. For that reason, the topics taught in engineering courses in statics, strength of materials, and dynamics are equally applicable here. Topics of particular relevance include Newton's Second Law, especially when applied in polar coordinates; moments of inertia; bending moments; and stresses and strains. These topics are well discussed in many physics and engineering texts, such as Pytel and Singer (1987), Meriam and Kraige (2008), Beer *et al.* (2008), and Den Hartog (1961) and will not be pursued here in any detail, except where a particular example is especially relevant.

4.3.1 Selected Topics from Basic Mechanics

There are a few topics from basic engineering mechanics which are worth singling out, because they have a particular relevance to wind energy and may not be familiar to all readers. These are summarized briefly below.

4.3.1.1 Inertia Forces

In most current teaching of dynamics, the forces that are considered are exclusively real forces. It is sometimes convenient, however, to describe certain accelerations in terms of fictitious 'inertia forces'. This is often done in the case of rotating systems, including in the analysis of wind turbine rotor dynamics. For example, the effect of the centripetal acceleration associated with the rotation of the rotor is accounted for by the inertial centrifugal force. The effect of the inertia force, as reflected in the 'Principle of D'Alembert,' is that the sum of all forces acting on a particle, including the inertia force, is zero. The method is most useful when dealing with larger rigid bodies, which can be considered to be made up of a large number of particles rigidly connected together. Specifically, the Principle of D'Alembert states that the internal forces in a rigid body having accelerated motion can be calculated by the methods of statics on that body under the influence of the external and inertia forces. Furthermore, a rigid body of any size will behave as a particle if the resultant of its external forces passes through its center of gravity.

4.3.1.2 Bending of Cantilevered Beams

The bending of beams is an important topic in strength of materials. A wind turbine blade is basically a cantilevered beam, so the topic is of particular relevance. A simple but interesting

example of a cantilevered beam is one that is uniformly loaded. For this case, the bending moment diagram, $M(x)$, is described by an inverted partial parabola:

$$M(x) = \frac{w}{2}(L-x)^2 \tag{4.1}$$

The maximum bending moment, M_{max}, is at the side of attachment and is given by:

$$M_{max} = \frac{wL^2}{2} = \frac{WL}{2} \tag{4.2}$$

where L is the length of the beam, x is the distance from the fixed end of the beam, w is the loading (force/unit length), and W is the total load.

The maximum stress in the beam is also at the point of attachment and, in addition, is at the maximum distance, c, from the neutral axis. For a wind turbine blade in bending, the neutral axis would be nearly the same as the chord line and c would be approximately half the airfoil thickness.

In equation form, the maximum stress, σ_{max}, in a beam with area moment of inertia I would be:

$$\sigma_{max} = \frac{M_{max}c}{I} \tag{4.3}$$

4.3.1.3 Rigid Body Planar Rotation

Two-Dimensional Rotation
When a body, such as a wind turbine rotor, is rotating, it acquires angular momentum. Angular momentum, H, is characterized by a vector whose magnitude is the product of the rotational speed Ω and the polar mass moment of inertia, J. The direction of the vector is determined by the right-hand rule (whereby if the fingers of the right hand are curled in the direction of rotation, the thumb points in the appropriate direction). In equation form:

$$\boldsymbol{H} = J\boldsymbol{\Omega} \tag{4.4}$$

From basic principles, the sum of the applied moments, M, about the mass center is equal to the time rate of change of the angular momentum about the mass center. That is:

$$\sum M = \dot{\boldsymbol{H}} \tag{4.5}$$

In most situations of interest in wind turbine dynamics the moment of inertia can be considered constant. Therefore the magnitude of the sum of the moments is:

$$\left|\sum M\right| = J\dot{\Omega} = J\alpha \tag{4.6}$$

where α is the angular acceleration of the inertial mass.

In the context of this text, a continuous moment applied to a rotating body is referred to as torque, and denoted by 'Q.' The relation between applied torques and angular acceleration, α, is analogous to that between force and linear acceleration:

$$\sum Q = J\alpha \tag{4.7}$$

When rotating at a constant speed, there is no angular acceleration or deceleration. Thus the sum of any applied torques must be zero. For example, if a wind turbine rotor is turning at a constant speed in a steady wind, the driving torque from the rotor must be equal to the generator torque plus the loss torques in the drive train.

Rotational Power/Energy

A rotating body contains kinetic energy, E, given by:

$$E = \frac{1}{2}J\Omega^2 \tag{4.8}$$

The power P consumed or generated by a rotating body is given by the product of the torque and the rotational speed:

$$P = Q\,\Omega \tag{4.9}$$

4.3.1.4 Gears and Gear Ratios

Gears are frequently used to transfer power from one shaft to another, while maintaining a fixed ratio between the speeds of the shafts. While the input power in an ideal gear train remains equal to the output power, the torques and speed vary in inverse proportion to each other. In going from a smaller gear (1) to a larger one (2), the rotational speed drops, but the torque increases. In general:

$$Q_1\Omega_1 = Q_2\Omega_2 \tag{4.10}$$

The ratio between the speeds of two gears, Ω_1/Ω_2, is inversely proportional to the ratio of the number of teeth on each gear, N_1/N_2. The latter is proportional to the gear diameter. Thus:

$$\Omega_1/\Omega_2 = N_2/N_1 \tag{4.11}$$

When dealing with geared systems, consisting of shafts, inertias, and gears, as shown in Figure 4.1, it is possible to refer shaft stiffnesses (Ks) and inertias (Js) to equivalent values on a single shaft. (Note that in the following it is assumed that the shafts themselves have no inertia.) This is done by multiplying all stiffnesses and inertias of the geared shaft by n^2 where n is the speed ratio between the two shafts. The equivalent system is shown in Figure 4.2.
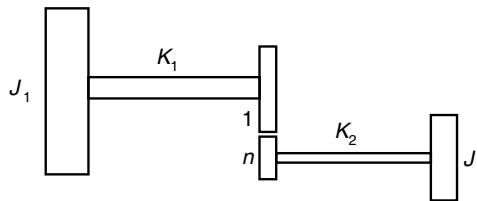
Figure 4.1 Geared system; J, inertia; K, stiffness; n, speed ratio between the shafts; subscripts 1 and 2, gear 1 and 2
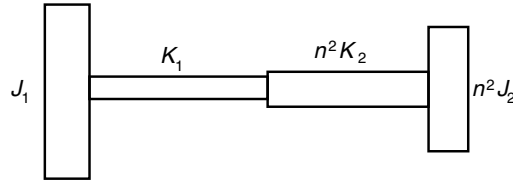
Figure 4.2   System equivalent to geared system; J, inertia; K, stiffness; n, speed ratio between the shafts; subscripts 1 and 2, gear 1 and 2

These relations can be derived by applying principles of kinetic energy (for inertias) and potential energy (for stiffnesses), as described in Thomson and Dahleh (1997). More information on gears and gear trains is provided in Chapter 6.

4.3.1.5 Gyroscopic Motion

Gyroscopic motion is of particular concern in the design of wind turbines, because yawing of the turbine while the rotor is spinning may result in significant gyroscopic loads. The effects of gyroscopic motion are illustrated in the Principal Theorem of the Gyroscope, which is summarized below.

In this example, it is assumed that a rigid body, with a constant polar mass moment of inertia of J, is rotating with angular momentum $J\Omega$. The Principal Theorem of the Gyroscope states that if a gyroscope of angular momentum $J\Omega$ rotates with speed ω about an axis perpendicular to Ω ('precesses'), then a moment, $J\Omega\omega$, acts on the gyroscope about an axis perpendicular to both the gyroscopic axis, Ω, and the precession axis, ω. Conversely, an applied moment that is not parallel to Ω can induce precession.

Gyroscopic motion may be considered with the help of Figure 4.3. A bicycle wheel of weight W is shown rotating in the counter-clockwise direction, supported at the end of one axle by a string. The wheel would fall down if it were not rotating. In fact, it is rotating, and rather than falling, it precesses in a horizontal plane (counter-clockwise when seen from above).

The moment acting on the wheel is Wa, so

$$Wa = J\Omega\omega \tag{4.12}$$

Thus, the rate of precession is

$$\omega = \frac{Wa}{J\Omega} \tag{4.13}$$

The relative directions of rotation are related to each other by cross products and the right-hand rule as follows:

$$\sum \boldsymbol{M} = Wa = \boldsymbol{\omega} \times J\boldsymbol{\Omega} \tag{4.14}$$

where, $\boldsymbol{M}$, $\boldsymbol{\omega}$, and $\boldsymbol{\Omega}$ are the moment, rate of precession, and angular velocity vectors, respectively.
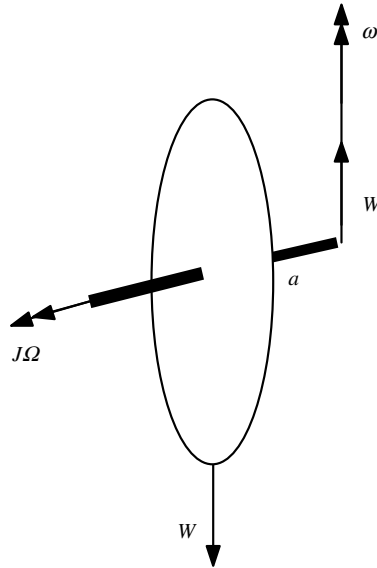
Figure 4.3 Gyroscopic motion; a, distance to weight; J, inertia; W, weight; ω, rate of precession; Ω, angular velocity

4.3.2 Vibrations

The term 'vibration' refers to the limited reciprocating motion of a particle or an object in an elastic system. The motion goes to either side of an equilibrium position. Vibration is important in wind turbines because they are partially elastic structures and they operate in an unsteady environment that tends to result in a vibrating response. The presence of vibrations can result in deflections that must be accounted for in turbine design and can also result in the premature failure due to fatigue of the materials which comprise the turbine. In addition, much of wind turbine operation can be best understood in the context of vibratory motion. The following section provides an overview of those aspects of vibrations most important to wind turbine applications.

4.3.2.1 Single Degree of Freedom Systems

Undamped Vibrations
The simplest vibrating system is mass m attached to a massless spring with spring constant k, as shown in Figure 4.4. When displaced a distance x and allowed to freely move, the mass will vibrate back and forth.

Applying Newton's Second Law, the governing equation is:

$$m\ddot{x} = -kx \tag{4.15}$$

When $t = 0$ at $x = x_0$ the solution is:

$$x = x_0 \cos(\omega_n t) \tag{4.16}$$
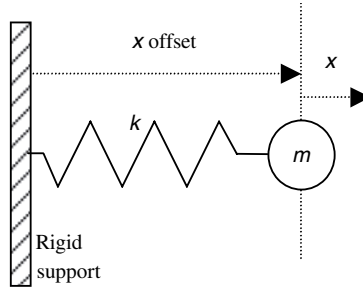
Figure 4.4   Undamped vibrating system; k, spring constant; m, mass; x, displacement

where $\omega_n = \sqrt{k/m}$ is the natural frequency of the motion. In general, when the mass is not at rest at $t = 0$, the solution contains two sinusoids:

$$x = x_0 \cos(\omega_n t) + \frac{\dot{x}_0}{\omega_n} \sin(\omega_n t) \tag{4.17}$$

where $\dot{x}_0$ is the velocity at $t = 0$.

The solution can also be written in terms of a single sinusoid of amplitude C and phase angle ϕ. That is:

$$x = C \sin(\omega_n t + \phi) \tag{4.18}$$

The amplitude and phase angle can be expressed in terms of the other parameters as:

$$C = \sqrt{x_0^2 + \left(\frac{\dot{x}_0}{\omega_n}\right)^2} \tag{4.19}$$

$$\phi = \tan^{-1}\left[\frac{x_0 \omega_n}{\dot{x}_0}\right] \tag{4.20}$$

Damped Vibrations

Vibrations as described above will continue indefinitely. In all real vibrations, the motions will eventually die out. This effect can be modeled by including a viscous damping term. Damping involves a force, usually assumed to be proportional to the velocity, which opposes the motion. Then, the equation of motion becomes:

$$m\ddot{x} = -c\dot{x} - kx \tag{4.21}$$

where c is the damping constant and k is the spring constant. Depending on the ratio of the damping and spring constant, the solution may be oscillatory ('underdamped') or non-oscillatory ('overdamped'). The limiting case between the two is 'critically damped,' in which case:

$$c = c_c = 2\sqrt{km} = 2m\omega_n \tag{4.22}$$

For convenience, a non-dimensional damping ratio $\xi = c/c_c$ is used to characterize the motion. For $\xi < 1$ the motion is underdamped; for $\xi > 1$ the motion is overdamped.

The solution for underdamped oscillation is:

$$x = Ce^{-\xi\omega_n t}\sin(\omega_d t + \phi) \tag{4.23}$$

where $\omega_d = \omega_n\sqrt{1-\xi^2}$ is the natural frequency for damped oscillation. Note that the frequency of damped oscillation is slightly different from that of undamped vibration. The amplitude, C, and phase angle, ϕ, are determined from initial conditions.

Forced Harmonic Vibrations

Consider the mass, spring, and damper discussed above. Suppose that it is driven by a sinusoidal force of magnitude F_0 and frequency ω (which is not necessarily equal to ω_n or ω_d). The equation of motion is then:

$$m\ddot{x} + c\dot{x} + kx = F_0\sin(\omega t) \tag{4.24}$$

It may be shown that the steady state solution to this equation is:

$$x(t) = \frac{F_0}{k}\frac{\sin(\omega t - \phi)}{\sqrt{[1-(\omega/\omega_n)^2]^2 + [2\xi(\omega/\omega_n)^2]}} \tag{4.25}$$

The phase angle in this case is:

$$\phi = \tan^{-1}\left[\frac{2\xi(\omega/\omega_n)}{1-(\omega/\omega_n)^2}\right] \tag{4.26}$$

It is of particular interest to consider the non-dimensional response amplitude (see Figure 4.5) which is given by:

$$\frac{xk}{F_0} = \frac{1}{\sqrt{[1-(\omega/\omega_n)^2]^2 + [2\xi(\omega/\omega_n)^2]}} \tag{4.27}$$
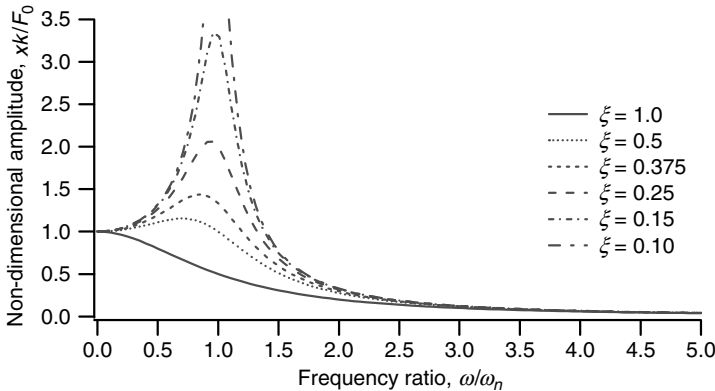
Figure 4.5 System responses to forced vibrations; ξ, non-dimensional damping ratio
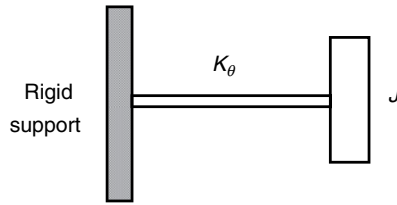
Figure 4.6 Rotational vibrating system; J, polar mass moment of inertia; k_θ, rotational stiffness of spring

As the excitation (forcing) frequency gets closer to the natural frequency, the amplitude of the response gets larger. Increasing the damping reduces the peak value and also shifts it slightly. Furthermore, although the peak is highest when the excitation frequency equals the natural frequency (ignoring the effect of damping), there may still be a significant increase in amplitude when the excitation is close to the natural frequency, as shown in Figure 4.5.

Rotational Vibration
If a body with polar mass moment of inertia J is attached to a rigid support via a rotational spring with rotational stiffness k_θ, as shown in Figure 4.6, its equation of motion is given by:

$$J\ddot{\theta} = -k_\theta \theta \qquad (4.28)$$

Solutions for rotational vibration are analogous to those for linear vibrations discussed previously. Rotational vibration is of particular importance in wind turbine design for shaft systems and drive train dynamics. It is also used in the linearized hinge–spring rotor model, which is described in Section 4.4.2.

4.3.2.2 Vibration of Cantilevered Beams

It is of interest to consider in some detail the vibration of a cantilevered beam, since many aspects of wind turbines have similarities to cantilevered beams. These include, in particular, the tower which supports the turbine and the blades.

Modes and Mode Shapes
Recall that a single vibrating mass on a massless spring oscillates with a single characteristic natural frequency. There is also only one path that the mass will take during its motion. For multiple masses the number of natural frequencies and possible paths will increase. For continuous objects there are actually an infinite number of natural frequencies. To each natural frequency there corresponds a characteristic mode shape of vibration. In practice, however, only the lowest few natural frequencies of a beam are usually important.

Vibration of Uniform Cantilevered Beams
Vibration of an ideal, uniform beam of constant cross-section and material properties can be modeled by an analytic equation known as the Euler equation for beams. This equation is particularly useful because it allows first order approximations of natural frequencies to be made very easily for many beams. The reader is referred to other sources (e.g. Thomson and

Dahleh, 1997) for the details of the development of the Euler beam equation. This section will confine itself to presenting the equation for a cantilevered beam in enough detail for it to be applied.

The form of the Euler equation for the deflection, y_i, of a uniform cantilevered beam of length L and mode shape i is:

$$y_i = A\left\{\cosh\left(\frac{(\beta L)_i}{L}x\right) - \cos(\beta x) - \frac{\sinh(\beta L)_i - \sin(\beta L)_i}{\cosh(\beta L)_i + \cos(\beta L)_i}\left[\sinh\left(\frac{(\beta L)_i}{L}x\right) - \sin\left(\frac{(\beta L)_i}{L}x\right)\right]\right\}$$

(4.29)

The dimensionless parameter $(\beta L)_i$ is related to the natural frequencies, ω_i, density per unit length, $\tilde{\rho}$, area moment of inertia, I, and modulus of elasticity, E, of the beam by the following equation:

$$(\beta L)_i^4 = \tilde{\rho}\omega_i^2 / (EIL^4)$$

(4.30)

From Equation (4.30), the natural frequencies (radians/second) are:

$$\omega_i = \frac{(\beta L)_i^2}{L^2}\sqrt{\frac{EI}{\tilde{\rho}}}$$

(4.31)

for values of $(\beta L)_i$ that solve:

$$\cosh(\beta L)_i\cos(\beta L)_i + 1 = 0$$

(4.32)

Equation (4.29) enables us to determine the mode shapes of the vibration. Note that since A is not known, it may be determined by assuming a deflection of $y_i = 1$ at the free end of the beam.

The products $(\beta L)_i^2$ are dimensionless constants, and for the case of a uniform cantilevered beam the numerical values for the first three modes are 3.52, 22.4, and 61.7. Figure 4.7 illustrates the shape of the first three vibration modes of a uniform cantilevered beam, based on Equations (4.29) and (4.32).
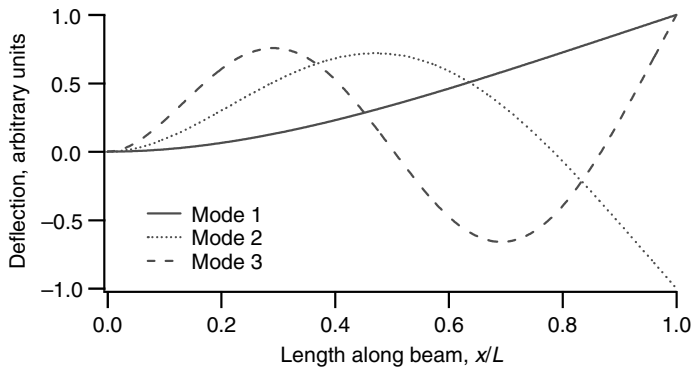
Figure 4.7 Vibration modes of uniform cantilevered beam
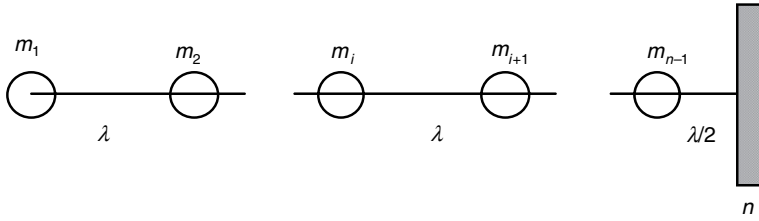
Figure 4.8 Model of cantilevered beam; m_i, mass; λ, distance between masses; n, number of stations

Vibration of General Beams

The previous discussion dealt with a uniform beam. This section concerns a more general case. It summarizes the use of the Myklestad method, which involves modeling the beam with a number of lumped masses connected by massless beam elements. The Myklestad method is quite versatile and can be applied to nearly any beam but, as before, the discussion will be confined to the cantilevered beam. More details may be found in Thomson and Dahleh (1997).

The method is illustrated in Figure 4.8. The beam is divided into $n - 1$ sections with the same number of masses, m_i. An additional station is at the point of attachment. All of the distances λ_i between masses are the same (and here equal to λ). In the figure it is assumed that the masses are located at the center of equal-sized sections, so the distance from the mass closest to the attachment is 1/2 of the others. The flexible connections have moments of inertia I_i and modulus of elasticity E_i. The beam in this example may be rotating with a speed Ω about an axis perpendicular to the beam and passing through station 'n'.

The Myklestad method involves solving a set of sequence equations. The sequence equations can be developed by considering the forces and moments acting on each of the masses and the point of attachment. Figure 4.9 illustrates the free body diagram of one section of a rotating beam. The diagram shows shear forces, S_i, inertial (centrifugal) forces, F_i, bending moments, M_i, deflections, y_i, and angular deflections, θ_i.

The complete equations for a rotating beam follow. The centrifugal forces at distance x_j from the attachment are:

$$F_i = \Omega^2 \sum_{j=1}^{i-1} m_j x_j \tag{4.33a}$$
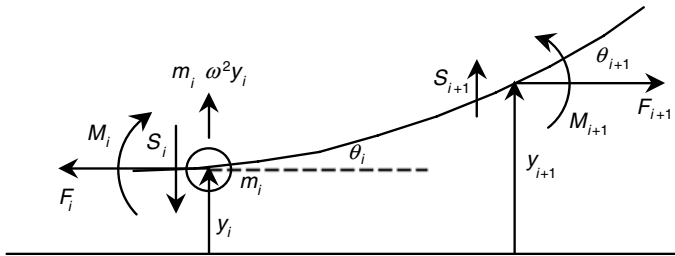
Figure 4.9 Free body diagram of beam section. For definition of variables, see text

It follows that:

$$F_{i+1} = F_i + \Omega^2 m_i x_i \tag{4.33b}$$

Using small-angle approximations, the shear forces are:

$$S_{i+1} = S_i - m_i \omega^2 y_i - F_{i+1} \theta_i \tag{4.34}$$

The moments are:

$$M_{i+1} = \left[M_i - S_{i+1} \left(\lambda_i - F_{i+1} \frac{\lambda_i^3}{3E_i I_i} \right) + \theta_i \lambda_i F_{i+1} \right] / \left(1 - F_{i+1} \frac{\lambda_i^2}{2E_i I_i} \right) \tag{4.35}$$

The angles of the beam sections from horizontal are:

$$\theta_{i+1} = \theta_i + M_{i+1} \left(\frac{\lambda_i}{E_i I_i} \right) + S_{i+1} \left(\frac{\lambda_i^2}{2E_i I_i} \right) \tag{4.36}$$

Finally, the deflections from a horizontal line passing through the fixed end are:

$$y_{i+1} = y_i + \theta_i \lambda_i + M_{i+1} \left(\frac{\lambda_i^2}{2E_i I_i} \right) + S_{i+1} \left(\frac{\lambda_i^3}{3E_i I_i} \right) \tag{4.37}$$

The series of equations is solved by iteratively finding natural frequencies which result in a calculated deflection of zero at the point of attachment. The process – normally done with a computer – begins by assuming a natural frequency ω and performing a series of calculations. The calculations are repeated with a new assumption for the natural frequency until a deflection sufficiently close to zero is found. Two sets of calculations are undertaken. They start at the free end of the beam first with $y_{1,1} = 1$ and $\theta_{1,1} = 0$ and then with $y_{1,2} = 0$ and $\theta_{1,2} = 1$, where the second subscript refers to the sets of calculations. Calculations are performed sequentially for each section until section n is reached. The calculations yield $y_{n,1}$, $y_{n,2}$, $\theta_{n,1}$ and $\theta_{n,2}$. The desired deflection (which should approach zero) is:

$$y_n = y_{n,1} - y_{n,2}(\theta_{n,1}/\theta_{n,2}) \tag{4.38}$$

The entire process can be repeated to find additional natural frequencies. There should be as many natural frequencies as there are masses. Because inertial forces on the rotating beam effectively stiffen the beam, natural frequencies of a rotating beam will be higher than those of the same non-rotating beam.

4.3.2.3 Torsional Systems

Many wind turbine components, particularly those in the drive train, can be modeled by a series of discs connected by shafts. In these models, the discs are assumed to have inertia, but are completely rigid, whereas the shafts have stiffness, but no inertia. The natural frequencies for such systems can be determined by Holzer's method. As with the Myklestad method, sequence equations can be used to determine each angle and torque along the shaft. The details of this method are beyond the scope of this book. The reader is referred to Thomson and Dahleh (1997) or similar texts for more information.

4.4 Wind Turbine Rotor Dynamics

Imposed loads and dynamic interactions produce forces and motions in wind turbines which need to be understood during the design process. The effects of all of the various types of loads (static, steady, cyclic, transient, impulsive, and stochastic) need to be determined. In this section, two approaches for analyzing the forces and motions of a wind turbine are considered. The first approach uses a very simple ideal rigid rotor model to illustrate basic concepts about steady turbine loads. The second approach includes the development of a highly linearized dynamic model of a horizontal axis wind turbine. The simplified model can be used to illustrate the nature of the turbine response to steady and cyclic loads. A few of the more detailed dynamic models are discussed in Chapter 7. These can more accurately predict turbine response to stochastic or transient loads, but tend to be quite complex.

4.4.1 Loads in an Ideal Rotor

The most important rotor loads on a wind turbine are those associated with thrust on the blades and torque to drive the rotor. Modeling the rotor as a simple rigid, aerodynamically ideal rotor is useful to get a feeling for the steady loads on a wind turbine. As discussed in Chapter 3, the principal aerodynamic loads on an ideal rotor satisfying the Betz limit can be found fairly easily.

4.4.1.1 Thrust

As shown in Chapter 3, the thrust, T, may be found from the following equation.

$$T = C_T \frac{1}{2} \rho \pi R^2 U^2 \tag{4.39}$$

where C_T is the thrust coefficient, ρ is the density of air, R is the radius of rotor and U is the free stream velocity.

For the ideal case, $C_T = 8/9$. In terms of this simple model, then, total thrust on a given rotor varies only with the square of the wind speed.

4.4.1.2 Bending Moments and Stresses

Blade bending moments are usually designated as either flapwise or edgewise. Flapwise bending moments cause the blades to bend upwind or downwind. Edgewise moments are parallel to the rotor axis and give rise to the power-producing torque. They are sometimes referred to as 'lead–lag.'

Axial Forces and Moments
The flapwise bending moment at the root of an ideal blade of a turbine with multiple blades is given by the product of the thrust force per blade and 2/3 of the radius. This can be seen as follows.

Consider the rotor as being made up of a series of concentric annuli of width dr. The root flapwise bending moment on a single blade, M_β, for a turbine with B blades is:

$$M_\beta = \frac{1}{B} \int_0^R r \left(\frac{1}{2} \rho \pi \frac{8}{9} U^2 2r\,\mathrm{d}r \right) \tag{4.40}$$

Upon integrating and gathering terms, the result is:

$$M_\beta = \frac{T}{B} \frac{2}{3} R \tag{4.41}$$

The maximum flapwise stress, $\sigma_{\beta,max}$, due to bending at the root is given by Equation (4.3) (repeated here as Equation (4.42)):

$$\sigma_{\beta,max} = M_\beta c / I_b \tag{4.42}$$

where c is the distance from the flapwise neutral axis and I_b is the area moment of inertia of blade cross-section at the root.

It is worth noting that the term in brackets in Equation (4.40) is the same as the incremental normal force used in Chapter 3. The subscript, β, the angle of the blade deflection in the flap direction, is used to emphasize continuity with terms in the hinge–spring dynamic model discussed in the next section.

The shear force, S_β, in the root of the blade is simply the thrust divided by the number of blades:

$$S_\beta = T / B \tag{4.43}$$

In summary, for a given ideal rotor, bending forces and stresses vary with the square of the wind speed and are independent of blade angular position (azimuth). Furthermore, blades on rotors designed for higher tip speed ratio operation have smaller chords and cross-sectional area moment of inertia, so they experience higher flapwise stresses.

Edgewise Forces and Moments

As mentioned above, the edgewise moments give rise to the power-producing torque. In terms of blade strength, aerodynamic edgewise moments are generally of less significance than their flapwise counterparts. (It should be noted, however, that edgewise moments due to blade self-weight can be quite significant in larger turbines.) The mean torque Q is the power divided by the rotational speed. For the ideal rotor, as shown in Chapter 3, torque is given by:

$$Q = \frac{P}{\Omega} = \frac{1}{\Omega} \frac{16}{27} \frac{1}{2} \rho \pi R^2 U^3 = \frac{8}{27} \rho \pi R^2 \frac{U^3}{\Omega} \tag{4.44}$$

In the more general case, torque can then be expressed in terms of a torque coefficient, $C_Q = C_P / \lambda$ (the power coefficient divided by the tip speed ratio), where:

$$Q = C_Q \frac{1}{2} \rho \pi R^2 U^2 \tag{4.45}$$

For an ideal rotor, the rotational speed varies with the wind speed, so torque varies as the square of the wind speed. Furthermore, rotors designed for higher tip speed ratio operation have

lower torque coefficients, so they experience lower torques (but not necessarily lower stresses). Again, according to this simple model there is no variation in torque with blade azimuth.

Edgewise (Lead–Lag) Moment

The bending moment in the edgewise direction (designated by ζ) at the root of single blade, M_ζ, is simply the torque divided by the number of blades:

$$M_\zeta = Q/B \tag{4.46}$$

There is no correspondingly simple relation for edgewise shear force S_ζ, but it can be found from integrating the tangential force, which is discussed in Chapter 3:

$$S_\zeta = \int_0^R dF_T \tag{4.47}$$

4.4.2 Linearized Hinge–Spring Blade Rotor Model

Actual wind turbine dynamics can get quite complicated. Loads can be variable, and the structure itself may move in ways that affect the loads. To analyze all of these interacting effects, very detailed mathematical models must be used. Nonetheless great insight can be gained by considering a simplified model of the rotor and examining its response to simplified loads. The method described below is based on that of Eggleston and Stoddard (1987). This model provides insight not only into turbine responses to steady loads, but also to cyclic loads.

The simplified model is known as the 'linearized hinge–spring blade rotor model' or 'hinge–spring model' for short. The essence of the model is that it incorporates enough detail to be useful, but it is sufficiently simplified that analytic solutions are possible. By examining the solutions, it is possible to discern some of the most significant causes and effects of wind turbine motion. The hinge–spring model consists of four basic parts: (1) a model of each blade as a rigid body attached to a rigid hub by means of hinges and springs, (2) a linearized steady state, uniform flow aerodynamic model, (3) consideration of non-uniform flow as 'perturbations', and (4) an assumed sinusoidal form for the solutions.

4.4.2.1 Types of Blade Motion

The hinge–spring model allows for three directions of blade motion and incorporates hinges and springs for all of them. The three directions of motion allowed by the hinges are: (1) flapwise, (2) lead–lag, (3) torsion. The springs return the blade to its 'normal' position on the hub.

As mentioned above, flapping refers to motion parallel to the axis of rotation of the rotor. For a rotor aligned with the wind, flapping would be in the direction of the wind, or opposite to it. Thrust forces in the flapping direction are of particular importance, since the largest stresses on the blades are normally due to flapwise bending.

Lead–lag motion lies in the plane of rotation. It refers to motion relative to the blade's rotational motion. In leading motion the blade will be moving faster than the overall rotational speed, and in lagging motion it will be moving slower. Lead–lag motions and forces are associated with fluctuations in torque in the main shaft and with fluctuations in power from the generator.

Torsional motion refers to motion about the pitch axis. For a fixed pitch wind turbine, torsional motion is generally not of great significance. In a variable pitch wind turbine, torsional motion can cause fluctuating loads in the pitch control mechanism.

In the following development, the focus will mainly be on flapping motion. The details of lead–lag and torsional motion can be found in Eggleston and Stoddard (1987).

4.4.2.2 Sources of Loads

The hinge–spring model as developed below includes an analysis of how the rotor responds to six sources of loads:

- rotor rotation;
- gravity;
- steady yaw rate;
- steady wind;
- yaw error;
- linear wind shear.

These loads may be applied independently or in combination with the others. The analysis will provide a general solution for the rotor response which is a function of blade azimuth, the angular position of blade rotation. The solution will be seen to contain three terms: the first independent of azimuthal position, the second a function of the sine of azimuthal position, and the third a function of the cosine of azimuthal position. The development is broken into two parts: (1) 'free' motion, and (2) forced motion. The free motion includes the effects of gravity and rotation. The forced motion case includes steady wind and steady yaw. Deviations from steady wind (yaw error and wind shear) are considered to be perturbations on the steady wind.

4.4.2.3 Coordinate Systems for the Model

The following sections describe the coordinate systems to be used in all of the model analysis, develop the hinge–spring blade model, and derive the equations of motion for the hinge–spring blade for the case of flapwise motion. This section focuses on the coordinate systems used in the model.

The development is for horizontal axis wind turbines. Figure 4.10 illustrates a typical wind turbine for which the model may be applied. In the figure, and in the development which follows, the turbine is assumed to have a three-bladed, downwind rotor. In this view, the observer is looking upwind. Note, however, that the model is equally applicable to an upwind turbine and to a two-bladed turbine.

Factors affecting the free motion that are considered here include: (1) geometry, (2) rotational speed, and (3) blade weight. The effects of external forces on blade motion are discussed subsequently.

The model, as developed below, embodies a number of assumptions regarding each blade. They include:

- the blade has a uniform cross-section;
- the blade is rigid;
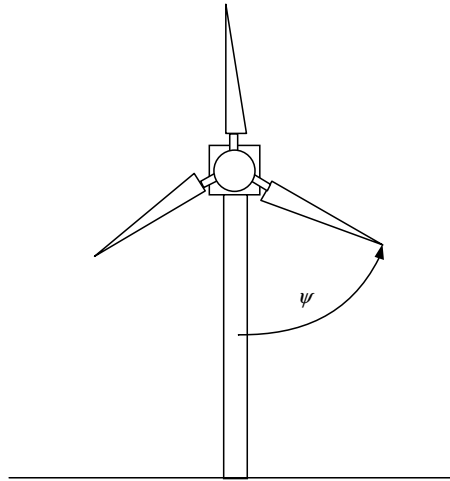
Figure 4.10   Typical turbine appropriate for hinge–spring model

- the blade hinge may be offset from the axis of rotation;
- when rotating, the rotational speed is constant.

The development of the appropriate hinge–spring stiffness and offset for the model are discussed later in this section.

Figure 4.11 illustrates the coordinate system for the model, focusing on one blade. As shown, the X', Y', Z' coordinate system is defined by the turbine itself whereas X, Y, Z are fixed to the earth. The X' axis is along the tower, the Z' axis is the axis of rotor rotation, and the Y' axis is perpendicular to both of them. The X'', Y'', Z'' axes rotate with the rotor. For the case of the blade shown, X'' is aligned with the blade, but in the plane of rotation. The blade is at an azimuth angle ψ with respect to the X' axis. The blade itself is turned out of the plane of rotation by the flapping angle β. The figure also reflects the assumption that the direction of rotation of the rotor, as well as yaw, is consistent with the right-hand rule with respect to the positive sense of the X, Y, and Z axes. Specifically, when looking in the downwind direction, the rotor rotates clockwise.

Figure 4.12 shows a top view of a blade which has rotated past its highest point (azimuth of π radians) and is now descending. Specifically, the view is looking down the Y'' axis.

4.4.2.4 Development of Flapping Blade Model

This dynamic model uses the hinged and offset blade to represent a real blade. The hinge offset and spring stiffness are chosen such that the rotating hinge and spring blade has the same natural frequency and flapping inertia as the real blade. Before the details of the hinge–spring offset blade model are provided, the dynamics of a simplified hinged blade are examined. As mentioned above, the focus is on the flapping motion in order to illustrate the approach taken in the model.
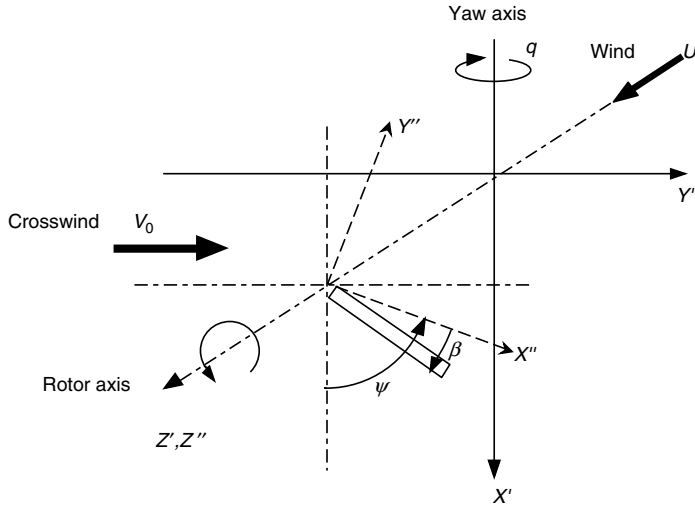
Figure 4.11 Coordinate system for hinge–spring model (Eggleston and Stoddard, 1987). Reproduced by permission of Kluwer Academic/Plenum Publisher

In general, the blade-flapping characteristics will be described by a differential equation with constant coefficients of the form:

$$\ddot{\beta} + [f(\text{Restoring moments})]\beta = g(\text{Forcing moments})$$

The restoring moments are due to gravity, rotor rotation, and the hinge spring. The forcing moments are due to yaw motion and aerodynamic forces.

The development of the linearized hinge–spring rotor model starts with the development of the equations of motion for a few simplified blade models, assuming no forcing functions. These equations of free motion all have the form:
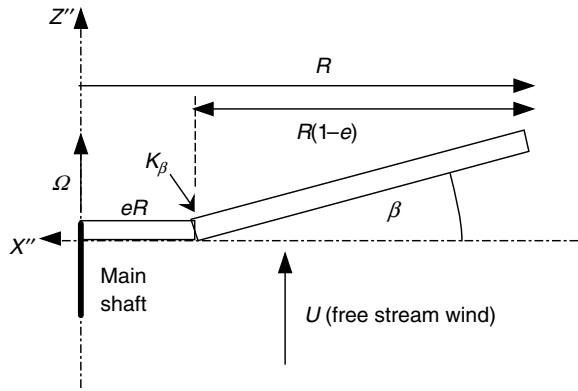
Figure 4.12 Hinge–spring model definitions

$$\ddot{\beta} + [f(\text{Restoring moments})]\beta = 0$$

The solutions to these equations are used to illustrate characteristic dynamic responses of rotor blades. The equation of free motion for the full hinge–spring blade model is then described and derived.

The development of the full equation of motion that includes the forcing moments requires linearized models for the forcing moments due to the wind, yaw motion, yaw error, and wind shear. Once these terms have been derived, the complete equation of motion can be assembled. This equation is then converted into a slightly simpler form for solution. The final form uses the derivative of the flap angle as a function of azimuth angle rather than time.

Dynamics of a Simplified Flapping Blade Model

The development of the hinge–spring model is best understood by considering first the dynamics of a flapping blade with no offset. Here, the effects of the spring and then of rotation of the blade with and without a spring are considered.

(i) Spring, No Rotation, No Offset

The first case to consider is the natural frequency (flapwise) of a non-rotating blade–hinge–spring system. Analogously to mass–spring vibration (see Equation (4.15)), the non-rotating natural frequency for vibration about the flapping hinge, ω_{NR}, is found from:

$$\ddot{\beta} = -(K_\beta/I_b)\beta \tag{4.48}$$

where I_b is the blade mass moment of inertia about the flapping axis and K_β is the flapping hinge spring constant.

The natural flapping frequency of the non-rotating blade, ω_{NR}, is immediately apparent:

$$\omega_{NR} = \sqrt{K_\beta/I_b} \tag{4.49}$$

Since one of the assumptions is that the blade has a uniform cross-section, the mass moment of inertia of a blade of mass m_B (with no offset) is:

$$I_b = \int_0^R r^2 \mathrm{d}m = \int_0^R r^2 (m_B/R)\mathrm{d}r \tag{4.50}$$

Thus:

$$I_b = m_B R^2/3 \tag{4.51}$$

(ii) Rotation, No Spring, No Offset

When the blade is rotating with a hinge at the axis of rotation and has no spring, the flapwise natural frequency is the same as the speed of rotation. This can be seen as follows. The only restoring force is the centrifugal inertial force F_c. Its magnitude is proportional to the square of the speed and to the cosine of the flapping angle. The restoring component is determined by the sine of the flapping angle. Thus:

$$I_b\ddot{\beta} = \int_0^R [-r\sin(\beta)]\mathrm{d}F_c = \int_0^R [r\cos(\beta)\Omega^2][-r\sin(\beta)]\rho_{blade}\mathrm{d}r \tag{4.52}$$

Assuming small angles such that $\cos(\beta) \approx 1$ and $\sin(\beta) \approx \beta$:

$$\ddot{\beta} = -(\Omega^2/I_b)\beta \int_0^R r^2\,\mathrm{d}m = -\Omega^2\beta \tag{4.53}$$

The solution to the above equation, again by analogy to Equation (4.15), is:

$$\omega = \Omega \tag{4.54}$$

(iii) Rotation, Spring, No Offset

When a blade with no offset is hinged and also includes a spring, the natural frequency is determined by a sum of the spring solution and the rotational solution. The appropriate equation is then:

$$\ddot{\beta} + (K_\beta/I_b + \Omega^2)\beta = 0 \tag{4.55}$$

The solution to this is immediately apparent from the above discussion:

$$\omega_R^2 = K_\beta/I_b + \Omega^2 = \omega_{NR}^2 + \Omega^2 \tag{4.56}$$

where ω_R is the rotating natural frequency and ω_{NR} is the non-rotating natural frequency.

As can be seen, the rotating natural frequency is now higher than it was with the spring alone. Thus, it is said that the rotation 'stiffens' the blade.

Dynamics of Flapping Blade with Offset

The flapping blade model can be extended by including the blade offset and gravity, as shown next.

(i) Rotation, Spring, Offset

In general a real blade does not behave as if it had a hinge–spring right at the axis of rotation. Thus, in general:

$$\omega_R^2 \neq \omega_{NR}^2 + \Omega^2 \tag{4.57}$$

To correctly model blade motions, the blade dynamics, represented by ω_R and ω_{NR}, need to be properly represented. This can be accomplished by including the non-dimensional hinge offset, e. This can be thought of as the fractional distance from the axis of rotation to the location of the blade hinge. Then all the constants of the hinge–spring model can be estimated if the natural frequencies of the rotating and non-rotating real blade are known. Following the method described in Eggleston and Stoddard (1987), it may be shown that the offset is given by:

$$e = 2(Z-1)/[3+2(Z-1)] \tag{4.58}$$

where $Z = (\omega_R^2 - \omega_{NR}^2)/\Omega^2$.

The addition of the offset can be accounted for by adjusting the moment of inertia. The mass moment of inertia of the hinged blade is approximated by:

$$I_b = m_B(R^2/3)(1-e)^3 \tag{4.59}$$

The flapping spring constant is:

$$K_\beta = \omega_{NR}^2 I_b \qquad (4.60)$$

Note that the rotating and non-rotating natural frequencies may be calculated by the Myklestad method as described previously or from experimental data, if they are available.

Thus, the flapping characteristics of the blade are modeled by a uniform blade with an offset hinge and spring that has one degree of freedom and that responds in the same manner to forces as the first vibration mode of the real blade. Similar constants can be determined for the lead–lag motion of the real blade. Torsion does not require an offset hinge model, but it does require a stiffness constant. With all of the constants, the blade model allows for three degrees of freedom, flapping, lead–lag, and torsion.

Equation of Motion of Full Flapping Blade Model (Free Motion)

When gravity and an offset are included, the full flapping equation of free (*unforced*) motion for a single blade becomes:

$$\ddot{\beta} + [\Omega^2(1 + \varepsilon) + G\cos(\psi) + K_\beta/I_b]\beta = 0 \qquad (4.61)$$

where G is the gravity term, given by $G = m_B r_g/I_b$, r_g is the radial distance to the center of mass, ε is the offset term, given by $\varepsilon = 3e/[2(1 - e)]$ and ψ is the azimuth angle. The derivation of this flapping equation is given in the next section.

4.4.2.5 Derivation of Flapping Equation of Motion (Free)

A flapping blade, shown in Figure 4.13, is viewed from the downwind direction (as in Figure 4.11). The blade is turned out of the plane of rotation, towards the viewer, by the flapping angle, β. The blade's long axis is also inclined at an azimuth angle ψ. Recall that zero azimuth corresponds to the blade tip pointing down. The azimuth angle increases in the direction of rotation. The flapping angle is positive in the downwind direction. Note that in the following
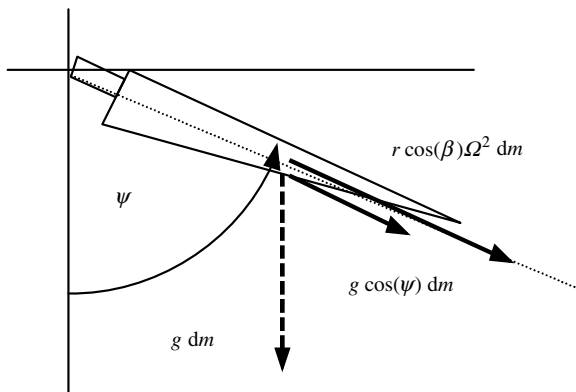
Figure 4.13   Flapping blade viewed from downwind direction; g, gravitational force; m, mass; r, radial distance from axis of rotation; β, flapping angle; Ω, rotational speed; ψ, azimuth angle
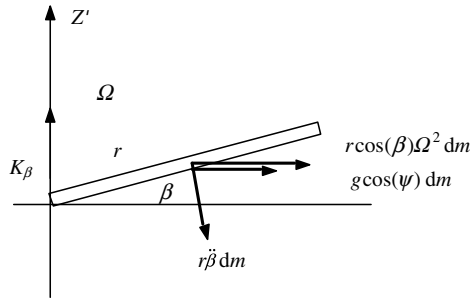
Figure 4.14 Flapping blade viewed from above (Eggleston and Stoddard, 1987). Reproduced by permission of Kluwer Academic/Plenum Publisher

discussion many of the inputs vary as the sine or the cosine of the azimuth angle. They are commonly referred to as 'cyclics', more specifically as sine cyclics or cosine cyclics. It will later be shown that these cyclical inputs can be related to cyclic turbine responses.

In Figure 4.13, two forces act along the axis of the blade on an element of the blade with mass dm. The centrifugal force depends on the square of the rotational speed and the distance to the axis of rotation. The gravity component, due to the weight of the blade, depends on the azimuth.

The equation of motion of a flapping blade without an offset, subject to restoring forces due to rotation (centrifugal force), gravity, the hinge–spring and inertial forces (due to acceleration), will be developed here. The modified equation of motion for a blade with an offset is then described. The full development of the equation with the offset included is left to the reader, but it will be seen that the two equations are very similar.

Figure 4.14 illustrates the blade as seen from above, looking down the Y'' axis. This figure also includes the flapping spring constant and the flapping acceleration.

The following summarizes the effects of the various forces. As mentioned above, initially the effect of the blade hinge offset is ignored.

Centrifugal Force
The centrifugal force serves to bring the flapping blade back into the plane of rotation. As stated above, its magnitude depends on the square of the speed of rotation and is independent of blade azimuth. Centrifugal force acts on the center of mass of the blade, perpendicular to the rotor's axis of rotation.

As shown in Figure 4.14, the magnitude of the centrifugal force F_c is:

$$F_c = r\cos(\beta)\Omega^2\,\mathrm{d}m \tag{4.62}$$

The moment about the flapping hinge axis due to the centrifugal force is:

$$M_c = r\sin(\beta)[r\cos(\beta)\Omega^2\,\mathrm{d}m] \tag{4.63}$$

Gravitational Force
Gravity acts downward on the center of mass of the blade. When the blade is up, gravity tends to increase the flapping angle; when down it tends to decrease it. The gravitational force is independent of rotational speed.

The magnitude of the gravitational force, F_g, is:

$$F_g = g \cos(\psi) \, dm \tag{4.64}$$

Since the gravitational force varies with the cosine of the azimuth, it can be said to be a 'cosine cyclic' input.

The restoring moment due to the gravitational force depends on the sine of the flapping angle. Its magnitude is:

$$M_g = r \sin(\beta)[g \cos(\psi) \, dm] \tag{4.65}$$

Hinge–Spring Force

The hinge–spring creates a moment, M_s, at the hinge. Its magnitude is proportional to the flapping angle. The spring tends to bring the blade back into the plane of the hinge, which in this case is the plane of rotation.

The magnitude of the hinge–spring moment is:

$$M_s = K_\beta \beta \tag{4.66}$$

Acceleration

The flapping acceleration inertial force caused by mass dm is given by the angular acceleration in the flapping direction, $\ddot{\beta}$, multiplied by its distance from the flapping axis. The moment due to this force M_f is the product of that inertia force and, again, the distance. In other words:

$$M_f = r^2 \ddot{\beta} \, dm \tag{4.67}$$

The Effect of All the Forces

The acceleration of mass dm is the result of the sum of the moments resulting from the forces. In the absence of external forces, that sum is zero:

$$\sum M = M_f + M_c + M_g + M_s = 0 \tag{4.68}$$

Integrating over the entire blade gives:

$$\int_0^R (M_f + M_c + M_g) + M_s = 0 \tag{4.69}$$

Expanding the terms gives:

$$\int_0^R [r^2 \ddot{\beta} + r \cos(\beta) r \sin(\beta) \Omega^2 + rg \cos(\psi) \sin(\beta)] \, dm + K_\beta \beta = 0 \tag{4.70}$$

Recall that the blade mass moment of inertia is $I_b = \int_0^R r^2 dm$. The mass and distance to the center of mass, r_g, are related by:

$$\int_0^R r \, dm = m_B r_g \tag{4.71}$$

Therefore, we have:

$$I_b\ddot{\beta} + I_b\cos(\beta)\Omega^2\sin(\beta) + g\cos(\psi)\sin(\beta)m_Br_g + K_\beta\beta = 0 \qquad (4.72)$$

Using the small-angle approximation for β, defining a 'gravity term', $G = gm_Br_g/I_b$, and rearranging we obtain:

$$\ddot{\beta} + [\Omega^2 + G\cos(\psi) + K_\beta/I_b]\beta = 0 \qquad (4.73)$$

Note the similarity to what has been discussed previously (Equation (4.61)).

Recalling that the blade model assumes a uniform cross-section, we can add the offset, e, and define an offset term, ε:

$$\varepsilon = m_Ber_gR/I_b = 3e/[2(1-e)] \qquad (4.74)$$

When the offset is included in the analysis, the final flapping equation of motion becomes:

$$\ddot{\beta} + [\Omega^2(1+\varepsilon) + G\cos(\psi) + K_\beta/I_b]\beta = 0 \qquad (4.75)$$

which was to be shown.

4.4.2.6 Equations of Motion (Forced)

This section expands the development of the blade equation of motion by considering the effect of forcing functions: yaw motion and wind speed.

Yaw Motion

Yaw motion results in gyroscopic moments acting upon the blade. By applying an analysis similar to the one given in Section 4.2.1.5, one may show that the gyroscopic moment in the flapping direction due to steady yaw motion of rate q is:

$$M_{yaw} = -2q\Omega\cos(\psi)I_b \qquad (4.76)$$

Effects of Wind: The Linearized Aerodynamics Model

The effect of wind on blade motion is incorporated via a linearized aerodynamics model. The model is similar to that developed in the aerodynamics section of this text, but it also includes some simplifying assumptions. The aerodynamic model that was developed in Chapter 3 is appropriate for performance estimates, but it is too complex to be useful in this simplified dynamic analysis. Conversely, the previous analysis only considered steady, axial flowing wind, whereas in its linearized form, vertical wind shear, crosswind, and yaw error can more easily be included. Finally, in the linearized aerodynamics model, drag is ignored altogether. This is a reasonable approach for the purpose of this model since drag forces are small in comparison to lift forces during normal operation. It should also be noted that in a truly comprehensive dynamic model, the aerodynamics model would be quite detailed.

The linearized aerodynamics model consists of a linearized description of the lift force on the blade and a linearized characterization of the axial and tangential components of the wind at the rotor (U_P and U_T, respectively). The lift force is a function of these two components of the wind. U_P and U_T, in turn, are functions of the mean wind speed, blade flapping speed, yaw rate,

crosswind, and wind shear. The equation for the flapping moment that arises from the lift force will be developed after the full aerodynamics model is explained.

The following equation is used for lift per unit length, $\tilde{L}$, on the airfoil. The derivation of this equation is developed subsequently, starting from principles presented in Chapter 3:

$$\tilde{L} \approx \frac{1}{2}\rho c C_{l\alpha}(U_P U_T - \theta_p U_T^2) \tag{4.77}$$

where c is the chord length, $C_{l\alpha}$ is the slope of lift curve, U_P is the wind velocity perpendicular (normal) to the rotor plane, U_T is the wind velocity tangential to the blade element, and θ_p is the pitch angle.

The equations for the wind velocity components, which take into account axial flow, flap rate, yaw rate, yaw error, and wind shear, follow. The equations for these components will also be developed subsequently. The velocity components are:

$$U_P = U(1 - a) - r\dot{\beta} - (V_0\beta + qr)\sin(\psi) - U(r/R)K_{vs}\cos(\psi) \tag{4.78}$$

$$U_T = \Omega r - (V_0 + qd_{yaw})\cos(\psi) \tag{4.79}$$

where U is the free stream wind velocity, a is the axial induction factor, V_0 is the crosswind velocity (due to yaw error), K_{vs} is the wind shear coefficient, and d_{yaw} is the distance from rotor plane to yaw axis.

Development of Linearized Aerodynamics Model

This section develops the aerodynamics model presented above. Initially, the model is developed for a steady, axial flowing wind. Deviations from the steady wind (due to yaw error, yaw motion, and wind shear) are subsequently considered as perturbations on that wind.

The development of the linearized aerodynamics model begins by reference to Figure 4.15. In addition to the variables defined previously, the following nomenclature is used:

$\phi =$ relative wind angle $= \tan^{-1}(U_P/U_T)$
$\alpha =$ angle of attack
$U_R =$ relative wind $= \sqrt{U_P^2 + U_T^2}$
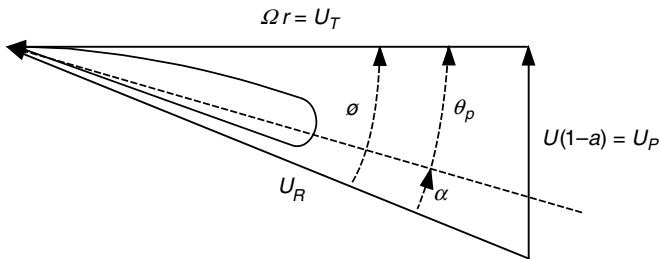
Figure 4.15   Nomenclature for linearized aerodynamics model; a, axial induction factor; r, radial distance from axis of rotation; U_R, relative wind velocity; U_P and U_T perpendicular and tangential components of the wind velocity respectively; Ω, angular velocity

The development is based on the following assumptions:

- The rotational speed is high relative to the wind speed; thus $U_T \gg U_P$.
- The lift curve is linear and passes through zero; thus $C_l = C_{l\alpha}\alpha$, where $C_{l\alpha}$ is the slope of the lift curve.
- The angle of attack is small.
- Small-angle assumptions may be used as appropriate.
- There is no wake rotation.
- The blade has a constant chord and no twist (although the model could be expanded to include a non-constant chord and blade twist).

Axial Flow

Taking into account the assumption about the lift curve, and using the relations from Chapter 3, the lift per unit length on the airfoil is:

$$\tilde{L} = \frac{1}{2}\rho c C_l U_R^2 \approx \frac{1}{2}\rho c C_{l\alpha} U_R^2 \alpha \tag{4.80}$$

Using the small-angle approximation, $\tan^{-1}(\text{angle}) \approx \text{angle}$

$$\alpha = \phi - \theta_p = \tan^{-1}(U_P/U_T) - \theta_p \approx U_P/U_T - \theta_p \tag{4.81}$$

Therefore

$$\tilde{L} = \frac{1}{2}\rho c C_{l\alpha} U_R^2 [U_P/U_T - \theta_p] \tag{4.82}$$

Recalling that $U_R^2 = U_P^2 + U_T^2 \approx U_T^2$, one gets:

$$\tilde{L} = \frac{1}{2}\rho c C_{l\alpha} U_T^2 (U_P/U_T - \theta_p) = \frac{1}{2}\rho c C_{l\alpha}(U_P U_T - \theta_p U_T^2) \tag{4.83}$$

which was to be proved.

For the flapping blade, the tangential velocity is, as usual, the radial position multiplied by the angular speed. It is actually reduced by the cosine of the flapping angle, but because of the small-angle approximation, that effect is ignored:

$$U_T = \Omega r \tag{4.84}$$

The perpendicular component of velocity is, as usual, the free stream wind speed less the induced axial wind speed, Ua. The flapping velocity $r\dot{\beta}$ also reduces the speed. Therefore:

$$U_P = U(1 - a) - r\dot{\beta} \tag{4.85}$$

Various factors such as yaw error, crosswind, vertical wind, wind shear, etc. will affect the wind actually experienced by the blade. These are accounted for as perturbations on the main flow. These perturbations are assumed to be small compared to the axial wind speed. They are referred to as 'deltas' in the following discussion.

Crosswind and Yaw Error

A crosswind, V_0, is perpendicular to the axis of the rotor and parallel to the ground. It arises due to yaw error (misalignment of the rotor axis and the wind) or a sudden change in wind direction. It serves to increase the tangential velocity at the advancing blade and decrease it at the retreating blade. As shown in Figure 4.11, the crosswind is defined as going from left to right. Since the blade is turning counter-clockwise (looking upwind), the crosswind decreases the tangential wind speed when the blade is below the hub axis and increases it when above. Thus, the change in the tangential component of the wind due to crosswind, $\Delta U_{T,crs}$ is:

$$\Delta U_{T,crs} = -V_0 \cos(\psi) \tag{4.86}$$

When the blade is out of the plane of rotation by the flapping angle, β, there will be a component that decreases the perpendicular wind speed at the blade, $\Delta U_{P,crs}$:

$$\Delta U_{P,crs} = -V_0 \sin(\beta)\sin(\psi) \approx -V_0\beta \sin(\psi) \tag{4.87}$$

Note that yaw error is predominantly a cosine cyclic disturbance, affecting the tangential velocity.

Yaw Motion

Yaw motion also affects blade velocities, besides inducing gyroscopic moments. Consider the blade straight up and a yaw rate of q. The blade will experience a velocity due to the yaw rotation of qd_{yaw} (where d_{yaw} is the distance from the axis of the tower to the center of the rotor). If the blade is inclined away (downwind) from the plane of rotation by the flapping angle, β, this will increase the effect by $rq \sin(\beta)$. The effect is greatest when the blade is up or down and nonexistent when the blade is horizontal.

Taking the small-angle approximation as before and recognizing that $d_{yaw}\beta + r \approx r$ and $r\beta + d_{yaw} \approx d_{yaw}$, the yaw rate deltas are:

$$\Delta U_{T,yaw} = -qd_{yaw} \cos(\psi) \tag{4.88}$$

$$\Delta U_{P,yaw} = -qr \sin(\psi) \tag{4.89}$$

Note that yaw terms are similar in form to the crosswind terms, with the tangential term varying as $\cos(\psi)$ and the perpendicular varying as $\sin(\psi)$.

Vertical Wind Shear

In Chapter 2 of this text, vertical wind shear was modeled by the equation:

$$U_1/U_2 = (h_1/h_2)^\alpha \tag{4.90}$$

where $\alpha = $ power law exponent and the subscripts correspond to different heights.

In the simplified aerodynamic model it is assumed that vertical wind shear is linear across the rotor. Consequently, the 'free stream' wind at height h is given by:

$$U_h = U[1 - (r/R)K_{vs} \cos(\psi)] \tag{4.91}$$

where $h = H - R$ when the blade tip is down, $h = H + R$ when the blade tip is up, $H = $ hub height, K_{vs} is the linear wind shear constant, and the subscript 'vs' indicates vertical shear.

Thus, at the center of the rotor and on the horizontal, $U_h = U$. At the top, with zero flapping, $U_h = U(1 + K_{vs})$ and at the bottom $U_h = U(1 - K_{vs})$.

Table 4.1 Wind speed perturbations

Case	ΔU_P	ΔU_T
Axial flow	$U(1-a) - r\dot{\beta}$	Ωr
Crosswind	$-V_0\beta\sin(\psi)$	$-V_0\cos(\psi)$
Yaw rate	$-qr\sin(\psi)$	$-qd_{yaw}\cos(\psi)$
Vertical wind shear	$-U(r/R)K_{vs}\cos(\psi)$	0

The incremental effect of vertical shear is predominantly on the perpendicular component of wind, so the tangential wind shear delta can be assumed to equal zero:

$$\Delta U_{T,vs} = 0 \tag{4.92}$$

The perpendicular wind shear delta is found directly from Equation (4.91):

$$\Delta U_{P,vs} = -U(r/R)K_{vs}\cos(\psi) \tag{4.93}$$

Horizontal wind shear can be modeled analogously, but will not be discussed here.

In summary, with all angles approximated as small angles, the contributions of the various deviations from the steady wind are as shown in Table 4.1.

Note that vertical wind shear is exclusively a cosine perturbation. Crosswind is primarily a cosine perturbation (to the tangential velocity component). Analogously, a vertical component of the wind (upslope) should be a sine perturbation.

The total velocities in both the perpendicular and tangential directions are found by adding the deltas to the contributions of the axial flow (Equations (4.84) and (4.85)):

$$U_T = \Omega r - (V_0 + qd_{yaw})\cos(\psi) \tag{4.94}$$

$$U_P = U(1-a) - r\dot{\beta} - (V_0\beta + qr)\sin(\psi) - U(r/R)K_{vs}\cos(\psi) \tag{4.95}$$

Aerodynamic Forces and Moments
The terms developed above can all be used to express the aerodynamic moments on the blade. It can be shown, as discussed below, that the flapping moment due to aerodynamic forces is:

$$M_\beta = \frac{1}{2}\gamma I_b \Omega^2 \left\{ \frac{\varLambda}{3} - \frac{\beta'}{4} - \frac{\theta_p}{4} - \cos(\psi)\left[\bar{V}\left(\frac{\varLambda}{2} - \frac{\beta'}{3} - \frac{2\theta_p}{3} \right) + \frac{K_{vs}\bar{U}}{4} \right] - \sin(\psi)\left[\frac{\bar{V}_0\beta}{3} + \frac{\bar{q}}{4} \right] \right\} \tag{4.96}$$

where

$$\varLambda = \text{Non-dimensional inflow, } \varLambda = U(1-a)/\Omega R$$
$$\bar{V}_0 = \text{Non-dimensional cross flow, } \bar{V}_0 = V_0/\Omega R$$
$$\bar{V} = \text{Non-dimensional total cross flow, } \bar{V} = (V_0 + qd_{yaw})/\Omega R$$
$$\beta' = \text{Azimuthal derivative of flap angle, } \beta' = \dot{\beta}/\Omega$$
$$\gamma = \text{Lock number, } \gamma = \rho C_{l\alpha}cR^4/I_b$$
$$\bar{q} = \text{Non-dimensional yaw rate term, } \bar{q} = q/\Omega$$
$$\bar{U} = \text{Non-dimensional wind velocity, } \bar{U} = U/\Omega R = 1/\lambda$$

Development of Aerodynamic Force and Moment Equation

For the linear model, the components of the blade forces in the tangential (torque) and normal directions are calculated as discussed in Chapter 3, except that: (1) the flapping angle is accounted for and (2) drag is assumed to be zero. The normal force per unit length, $\tilde{F}_N$, is:

$$\tilde{F}_N = \tilde{L}\cos(\phi)\cos(\beta) \tag{4.97}$$

The tangential force per unit length, $\tilde{F}_T$, is

$$\tilde{F}_T = \tilde{L}\sin(\phi) \tag{4.98}$$

The various forces must be summed (integrated) over the blade to give the shear forces, or multiplied by the distances first and then summed (integrated) to give moments. As before, simplifications are made so that $\sin(\phi) = U_P/U_T$, $\cos(\phi) = 1$ and $\cos(\beta) = 1$.

The flapwise shear force at the root of the blade is the integral of the normal force per unit length over the length of the blade:

$$S_\beta = \int_0^R \tilde{F}_N \, dr = \int_0^R \tilde{L}\cos(\phi)\cos(\beta) dr = \int_0^1 \tilde{L}R d\eta \tag{4.99}$$

where $\eta = r/R$.

This flapwise bending moment at the root of the blade is the integral of the normal force per unit length multiplied by the distance at which the force acts, over the length of the blade:

$$M_\beta = \int_0^R \tilde{F}_N r dr = \int_0^R \tilde{L}\cos(\phi)\cos(\beta) r dr = \int_0^1 \tilde{L}R^2 \eta d\eta \tag{4.100}$$

The flapping moment equation can be expanded, using Equation (4.77) to yield:

$$M_\beta = \int_0^1 \tilde{L}R^2 \eta d\eta = \int_0^1 \left[\frac{1}{2}\rho c C_{l\alpha}\left(U_P U_T - \theta_p U_T^2\right)\right]R^2 \eta d\eta \tag{4.101}$$

By making appropriate substitutions and performing the algebra one may derive Equation (4.96) above.

Complete Equations of Motion

The complete flapping equation of motion is found by including the moments due to aerodynamics and yaw rate (gyroscopic effects) and performing the appropriate algebraic manipulations. It is:

$$\beta'' + \left[1 + \varepsilon + \frac{G}{\Omega^2}\cos(\psi) + \frac{K_\beta}{\Omega^2 I_b}\right]\beta = \frac{M_\beta}{\Omega^2 I_b} - 2\bar{q}\cos(\psi) \tag{4.102}$$

where $\beta'' = \ddot{\beta}/\Omega^2 = $ the azimuthal second derivative of β and where the aerodynamic forcing moment, M_β, is from Equation (4.96). Note that the equations are now expressed in terms of the azimuthal derivative, which is discussed in more detail later in this chapter. This is convenient for solving the equation.

Development of Complete Flapping Equation of Motion

In this section the complete flapping equation of motion, which was presented above in Equation (4.102), is developed.

The original flapping equation of free motion, when the aerodynamic and gyroscopic moments are included, becomes:

$$\ddot{\beta} + \left[\Omega^2(1+\varepsilon) + G\cos(\psi) + \frac{K_\beta}{I_b} \right]\beta = \frac{M_\beta}{I_b} - 2q\Omega\cos(\psi) \tag{4.103}$$

Dividing by Ω^2 yields

$$\frac{\ddot{\beta}}{\Omega^2} + \left[1 + \varepsilon + \frac{G}{\Omega^2}\cos(\psi) + \frac{K_\beta}{\Omega^2 I_b} \right]\beta = \frac{M_\beta}{\Omega^2 I_b} - 2\bar{q}\cos(\psi) \tag{4.104}$$

The flapping equation above is in the time domain. Because the rotational speed is assumed to be constant, it is more interesting to express the equation as a function of angular (azimuthal) position.

The chain rule can be used to yield:

$$\dot{\beta} = \frac{d\beta}{dt} = \left(\frac{d\beta}{d\psi}\right)\left(\frac{d\psi}{dt}\right) = \Omega\left(\frac{d\beta}{d\psi}\right) = \Omega\beta' \tag{4.105}$$

Similarly $\ddot{\beta} = \Omega^2 \beta''$

Note that the 'dot' over the variable signifies a derivative with respect to time, whereas the prime signifies a derivative with respect to azimuth.

The flapping equation can now be rewritten as given above in Equation (4.102).

Arrangement of Flapping Equation of Motion for Solution

Upon substituting the complete expression for the aerodynamic moment (Equation (4.96)) and collecting terms, one gets:

$$\beta'' + \left[\frac{\gamma}{8}\left(1 - \frac{4}{3}\bar{V}\cos(\psi) \right) \right]\beta' + \left[1 + \varepsilon + \frac{G}{\Omega^2}\cos(\psi) + \left(\frac{\gamma\bar{V}_o}{6} \right)\sin(\psi) + \frac{K_\beta}{\Omega^2 I_b} \right]\beta$$

$$= -2\bar{q}\cos(\psi) + \frac{\gamma}{2}\left(\frac{\Lambda}{3} - \frac{\theta_P}{4} \right) - \frac{\gamma}{8}\bar{q}\sin(\psi) - \cos(\psi)\left\{ \frac{\gamma}{2}\left[\bar{V}\left(\frac{\Lambda}{2} + \frac{2\theta_P}{3} \right) + \frac{K_{vs}\bar{U}}{4} \right] \right\} \tag{4.106}$$

The complete flapping equation of motion can then be written in a slightly simpler form for solution:

$$\beta'' + \frac{\gamma}{8}\left[1 - \frac{4}{3}\cos(\psi)\left(\bar{V}_o + \bar{q}\bar{d} \right) \right]\beta' + \left[K + 2B\cos(\psi) + \frac{\gamma}{6}\bar{V}_o\sin(\psi) \right]\beta$$

$$= \frac{\gamma A}{2} - \frac{\gamma\bar{q}}{8}\sin(\psi) - \left\{ 2\bar{q} + \frac{\gamma}{2}\left[A_3\left(\bar{V}_o + \bar{q}\bar{d} \right) + \left(\frac{K_{vs}\bar{U}}{4} \right) \right] \right\}\cos(\psi) \tag{4.107}$$

where:

$K=$ Flapping inertial natural frequency (includes rotation, offset, hinge–spring),
$\quad K = 1 + \varepsilon + K_\beta/I_b\Omega^2$
$A =$ First axisymmetric flow term $= (\Lambda/3) - (\theta_p/4)$
$A_3 =$ Second axisymmetric flow term $= (\Lambda/2) - (2\theta_P/3)$
$B =$ Gravity term $= G/2\,\Omega^2$
$\bar{d} =$ Normalized yaw moment arm $= d_{yaw}/R$

This final equation includes all of the restoring forces and all of the forcing moments mentioned above and can now be used to determine the rotor behavior under a variety of wind and dynamic conditions.

Discussion of Flapping Equation

A few important aspects of wind turbine dynamics are evident in the complete flapping equations of motion.

The final equation includes a damping term. The term multiplying β' depends on the Lock number, which equals 0 when aerodynamics are not involved. This means that the only damping in this model is due to aerodynamics. The Lock number, which may be thought of as the ratio of aerodynamic forces to inertial forces, is:

$$\gamma = \rho c C_{l\alpha} R^4 / I_b \qquad (4.108)$$

If the lift curve slope is zero or negative, as in stall, the Lock number will also be zero or negative, and there will be no damping. This could be a problem for a teetered rotor with its larger range of flapping motion. It may also be a problem in rigid rotors with dynamic coupling between lead–lag and edgewise motions. In such cases negatively damped flap motions may cause edgewise vibrations. Note that, strictly speaking, the linear model we have used does not include stall. However, it could be modified slightly to allow general trends to be considered, such as the effect of a negative Lock number. With no crosswind or yawing the damping ratio (see Section 4.3) is:

$$\xi = \frac{\gamma}{16} \frac{1}{\omega_\beta / \Omega} \qquad (4.109)$$

where $\omega_\beta =$ the flapping frequency. For teetered or articulated blades, $\omega_\beta = \Omega$, so the flapping damping ratio is approximately $\gamma/16$. For rigid blades ω_β is on the order of 2 to 3 times higher than Ω, and the flapping damping ratio is correspondingly smaller. So, with Lock numbers ranging from 5 to 10, the damping ratio is on the order of 0.5–0.16. This amount of damping is enough to damp the flapping mode vibrations. While the details of lead–lag motions are not being pursued here, it should be noted that a full development of the lead–lag equation of motion would show no aerodynamic damping. The lack of damping in lead–lag can lead to blade instabilities.

Note that there is a constant term on the right-hand side of the complete flapping equation of motion ($\gamma A / 2$). This describes the blade coning, which is a constant deflection of the blades away from the plane of rotation due to the steady force of the wind. This coning will be in addition to any preconing. Preconing is sometimes incorporated in the rotor design for a number of reasons: (1) it keeps the tips away from the tower, (2) it helps to reduce root flap bending moments on a downwind, rigid rotor, and (3) it contributes to yaw stability.

4.4.2.7 Solutions to Flapping Equation of Motion

The flapping equation of motion has been written in terms of constants and sines and cosines of the azimuth angle. A full solution could be written as a Fourier series, that is to say a sum of sines and cosines of the azimuth with progressively higher frequencies. This can be seen by
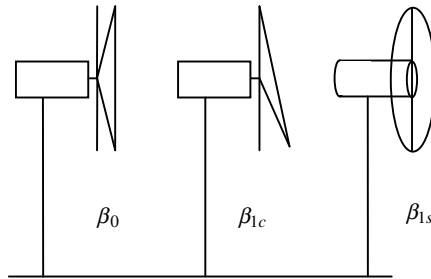
Figure 4.16   Effect of various terms in solution; β_0 collective response coefficient; β_{1c} cosine cyclic response coefficient; β_{1s} sine cyclic response coefficient (Eggleston and Stoddard, 1987). Reproduced by permission of Kluwer Academic/Plenum Publisher

noting that the azimuth ψ is actually equal to the rotational frequency Ω multiplied by the time. That is, $\psi = \Omega\, t$. The frequencies in the Fourier series would begin with sinusoids of the azimuth, and increase by integer multiples.

To a good approximation, however, the solution can also be assumed to be a sum of constants and sines and cosines of the azimuth angle. Using these assumptions, the solution to the flapping equation of motion can be expressed in terms of three constants, β_0, β_{1c}, β_{1s}, and the flapping angle will be:

$$\beta \approx \beta_0 + \beta_{1c}\cos(\psi) + \beta_{1s}\sin(\psi) \qquad (4.110)$$

where β_0 is the coning or 'collective' response constant, β_{1c} is the cosine cyclic response constant, and β_{1s} is the sine cyclic response constant.

It is important to note the directional effects of the different terms in the solution equation. These are illustrated in Figure 4.16. The coning term is positive. This indicates that the blade bends away from the free stream wind, as expected. Referring to Figure 4.16, a positive cosine constant indicates that when the blade is pointing straight down, it is pushed further downwind. When pointing upwards, the blade tends to bend upwind. In either horizontal position, the cosine of the azimuth equals zero. Thus, a plane determined by a path of the blade tip would tilt about a horizontal axis, upwind at the top, downwind at the bottom. The positive sine constant means that the blade which is rising tends to be bent downwind when horizontal. When descending, the blade goes upwind. Overall, the plane described by the tip would tilt to the left (in the direction of positive yaw) in the figure.

In summary:

- The constant term, β_0, indicates that the blade bends downwind by a constant amount as it rotates (as in coning).
- The cosine term, β_{1c}, indicates that the plane of rotation tilts downwind when the blade is pointing down, upwind when pointing up.
- The sine term, β_{1s}, indicates that the plane of rotation tilts downwind when the blade is rising, upwind when descending.

The constants above are functions of the various parameters in the model. The coning term is related primarily to axial flow, blade weight, and the spring constant. The sine and cosine terms depend on yaw rate, wind shear, and crosswind (yaw error) as well as the same terms that affect coning.

By applying the assumption that the flapping angle can be expressed as given in Equation (4.110), it is possible to solve the flapping equation in closed form. This is done by taking derivatives of Equation (4.110), substituting the results into Equation (4.107), and collecting terms to match coefficients of the functions of azimuth. The result can be conveniently expressed in the following matrix equation.

$$
\begin{bmatrix}
K & B & -\dfrac{\gamma \bar{q} \bar{d}}{12} \\[2ex]
2B & K-1 & \dfrac{\gamma}{8} \\[2ex]
\dfrac{\gamma \bar{U}_0}{6} & -\dfrac{\gamma}{8} & K-1
\end{bmatrix}
\begin{bmatrix}
\beta_0 \\[2ex]
\beta_{1c} \\[2ex]
\beta_{1s}
\end{bmatrix}
=
\begin{bmatrix}
\dfrac{\gamma}{2}A \\[2ex]
-2\bar{q} - \dfrac{\gamma}{2}\left[(\bar{V}_0 + \bar{q}\bar{d})A_3 + \left(\dfrac{K_{vs}\bar{U}}{4}\right)\right] \\[2ex]
-\dfrac{\gamma}{8}\bar{q}
\end{bmatrix}
\qquad (4.111)
$$

Simple Solutions of the Flapping Equation

In general the useful form of the solution to the equations of motion can be found by applying Cramer's Rule to Equation (4.111). That approach will, in fact, be taken in the next section. In the meantime, it is of more interest to look at some special cases and to gain some insight into blade response to isolated inputs. It will be seen that the dynamic response of a turbine to fairly simple inputs can be complex blade motions, even without considering the effects of turbulence and nonlinear aerodynamics.

(i) Rotation Only

First consider the simplest case with rotation but where:

gravity $= 0$
crosswind $= 0$
yaw rate $= 0$
offset $= 0$
hinge–spring $= 0$

The only non-zero terms in Equation (4.111) are aerodynamic and centrifugal forces:

$$
\begin{bmatrix}
1 & 0 & 0 \\[2ex]
0 & 0 & \dfrac{\gamma}{8} \\[2ex]
0 & -\dfrac{\gamma}{8} & 0
\end{bmatrix}
\begin{bmatrix}
\beta_0 \\[2ex]
\beta_{1c} \\[2ex]
\beta_{1s}
\end{bmatrix}
=
\begin{bmatrix}
\dfrac{\gamma}{2}A \\[2ex]
0 \\[2ex]
0
\end{bmatrix}
\qquad (4.112)
$$

The solution to this is immediately apparent:

$$
\beta_0 = \frac{\gamma}{2}A \qquad (4.113)
$$

Thus, there is only coning in this case. There is a balance between aerodynamic thrust and centrifugal force which determines the flapping angle. There is no dependence on azimuth.

(ii) Rotation + Hinge–Spring + Offset

Adding the spring and offset terms gives the same form for the solution. The flapping angle is reduced, however. The solution equation is now:

$$
\begin{bmatrix} K & 0 & 0 \\ 0 & K-1 & \dfrac{\gamma}{8} \\ 0 & -\dfrac{\gamma}{8} & K-1 \end{bmatrix}
\begin{bmatrix} \beta_0 \\ \beta_{1c} \\ \beta_{1s} \end{bmatrix} =
\begin{bmatrix} \dfrac{\gamma}{2}A \\ 0 \\ 0 \end{bmatrix}
\tag{4.114}
$$

The solution is $\beta_0 = \gamma A/2K$. The coning angle now results from a balance between the aerodynamic moments on the one hand and the centrifugal force and hinge–spring moments opposing them. As to be expected, the stiffer the spring, the smaller the coning angle.

(iii) Rotation + Hinge–Spring + Offset + Gravity

The addition of gravity complicates the solution. As in the previous cases, there is assumed to be no yaw, no crosswind, and no wind shear. The solution matrix to the flapping equation above becomes:

$$
\begin{bmatrix} K & B & 0 \\ 2B & K-1 & \dfrac{\gamma}{8} \\ 0 & -\dfrac{\gamma}{8} & K-1 \end{bmatrix}
\begin{bmatrix} \beta_0 \\ \beta_{1c} \\ \beta_{1s} \end{bmatrix} =
\begin{bmatrix} \dfrac{\gamma}{2}A \\ 0 \\ 0 \end{bmatrix}
\tag{4.115}
$$

To solve this we can use Cramer's Rule. For that we need the determinant, D, of the coefficient matrix in Equation (4.115). This is given in the usual way by:

$$
D = K \begin{vmatrix} K-1 & \dfrac{\gamma}{8} \\ -\dfrac{\gamma}{8} & K-1 \end{vmatrix} - B \begin{vmatrix} 2B & \dfrac{\gamma}{8} \\ 0 & K-1 \end{vmatrix} = K\left[(K-1)^2 + \left(\dfrac{\gamma}{8}\right)^2\right] - 2B^2(K-1) \tag{4.116}
$$

According to Cramer's Rule, one finds the desired values by substituting the right-hand side vector into the corresponding column of the matrix, finding the determinant of the new matrix and dividing by the original determinant.

The solution, for the first time, has sines and cosines of the azimuth angle. Note the gravity term B multiplying both of the sine and cosine terms:

$$
\beta_0 = \dfrac{\gamma A}{2D}\left[(K-1)^2 + \left(\dfrac{\gamma}{8}\right)^2\right] \tag{4.117}
$$

$$\beta_{1c} = -B\frac{A}{D}\gamma(K-1) \tag{4.118}$$

$$\beta_{1s} = -B\frac{A}{D}\left(\frac{\gamma^2}{8}\right) \tag{4.119}$$

Because the cosine and sine terms are negative, the rotor disc is tilted downwind and to the left.

The magnitude of the sine and cosine terms can be related by a 'cyclic sharing' term:

$$\beta_{1s} = \frac{\gamma}{8(K-1)}\beta_{1c} \tag{4.120}$$

The cyclic sharing term indicates the relative amount of moment backwards compared to sideways. For a rotor with independent freely hinged blades (K approaching 1) there will be mostly yawing. For a stiff-bladed machine, there will be mostly tilting. This can also be considered in terms of phase lag. Recall that gravity is a cosine input for flapping. For a stiff blade the response is mostly a cosine response, so there will be little phase lag. For a teetered rotor, the response to a cosine input is only a function of the sine of the azimuth angle. That means that the response has a $\pi/2$ (90 degree) phase lag from the disturbance.

(iv) Wind Shear + Hinge–Spring

This example ignores the gravity, yaw, and crossflow terms, but includes wind shear. The equation to be solved takes the form:

$$\begin{bmatrix} K & 0 & 0 \\ 0 & K-1 & \frac{\gamma}{8} \\ 0 & -\frac{\gamma}{8} & K-1 \end{bmatrix}\begin{bmatrix} \beta_0 \\ \beta_{1c} \\ \beta_{1s} \end{bmatrix} = \begin{bmatrix} \frac{\gamma}{2}A \\ -\frac{\gamma}{8}K_{vs}\bar{U} \\ 0 \end{bmatrix} \tag{4.121}$$

The determinant of the coefficient matrix is simply:

$$D = K\left[(K-1)^2 + \left(\frac{\gamma^2}{8}\right)\right] \tag{4.122}$$

Applying Cramer's Rule again, one has:

$$\beta_0 = \frac{\gamma}{2}\frac{A}{K} \tag{4.123}$$

$$\beta_{1c} = -\frac{1}{D}\left[\frac{\gamma}{8}K_{vs}\bar{U}K(K-1)\right] \tag{4.124}$$

$$\beta_{1s} = -\frac{1}{D}\left[\frac{\gamma^2}{8}K_{vs}\bar{U}K\right] \tag{4.125}$$

Recall that wind shear is a cosine input. In response, a stiff rotor will have both cosine and sine responses. A teetered rotor with $K = 1$ will only have a sine response. The turbine response to other inputs, as described below, exhibits similar combinations of sine and cosine cyclic responses.

General Solution to Flapping Equation of Motion

The general solution to the flapping motion can, in principle, be found simply by applying Cramer's Rule to Equation (4.111). The resulting algebraic expressions, however, are not particularly illuminating. One approach that helps to add some clarity is to express the terms in the flapping angle as the sum of other constants, which represent the contributions of the various forcing effects:

$$\beta_{1c} = \beta_{1c,ahg} + \beta_{1c,cr} + \beta_{1c,yr} + \beta_{1c,vs} \tag{4.126a}$$

$$\beta_{1s} = \beta_{1s,ahg} + \beta_{1s,cr} + \beta_{1s,yr} + \beta_{1s,vs} \tag{4.126b}$$

where the subscripts are *ahg* for axial flow, hinge–spring, and gravity (blade weight), *cr* for crosswind, *vs* for vertical wind shear, and *yr* for yaw rate.

Each of these constants is also a function of the parameters in the equations of motion. Rather than expand the matrix solution by itself, we will present below the various subscripted terms which could be obtained from such a solution.

The dominant constant coning term, which includes axial flow, hinge–spring, and gravity, is:

$$\beta_0 = \frac{1}{D}\frac{\gamma A}{2}\left[(K-1)^2 + \left(\frac{\gamma}{8}\right)^2\right] \tag{4.127}$$

The cosine and sine terms are summarized in Table 4.2.

Table 4.2 Contributions to flapping responses

*	Cosine, $\beta_{1c,*}$	Sine, $\beta_{1s,*}$
ahg	$-\frac{1}{D}\gamma BA(K-1)$	$-\frac{1}{D}\frac{\gamma}{8}BA$
cr	$\frac{\bar{V}_0}{D}\left[\left(\frac{\gamma}{8}\right)^2\left(\frac{\gamma}{2}\right)\frac{4}{3}A - \frac{\gamma A_3}{2}K(K-1)\right]$	$-\frac{4\bar{V}_0}{D}\left(\frac{\gamma}{8}\right)^2\left[\frac{4}{3}A(K-1)+A_3K\right]$
vs	$-\frac{K_{sh}\bar{U}}{D}\frac{\gamma}{8}K(K-1)$	$-\frac{K_{sh}\bar{U}}{D}\left(\frac{\gamma}{8}\right)^2K$
yr	$\frac{K\bar{q}}{D}\left[\left(\frac{\gamma}{8}\right)^2 - 2(K-1) - \frac{\gamma A_3}{2}(K-1)\bar{d}_{yaw}\right]$	$-\frac{K\bar{q}}{D}\left(\frac{\gamma}{8}\right)\left[\frac{\gamma}{2}A_3\bar{d}_{yaw}+K+1\right]$

The important point to note about the various subscripted constants is that they can help to illustrate the amount of the response that is due to a particular input. For example, in a particular situation, if the wind shear sine cyclic response were close in magnitude to the total sine cyclic response constant, then it would be immediately apparent that other factors were of little significance.

4.4.2.8 Blade and Hub Loads

The blade flapping motions, determined using Equation (4.111), can be used to determine blade root loads. Moments and forces on the hub and tower can then be determined from those blade forces.

For a rigid rotor turbine (with cantilevered and not teetered blades), both flapping and lead–lag moments are transmitted to the hub. Flapping is usually the predominant aerodynamic load, and in the following discussion the focus will be on the effect of loads of that type. In a teetered rotor, on the other hand, no flapping moments are transmitted to the hub (unless the teeter stops are hit). Only in-plane forces (in the direction of the torque) are transferred to the hub. A detailed discussion of teetered rotor response, however, is beyond the scope of this text.

Figure 4.17 illustrates the coordinate system for the forces and moments transmitted to the hub of a typical rotor.

Recall that the blade flapping angle is approximated by the sum:

$$\beta \approx \beta_0 + \beta_{1c}\cos(\psi) + \beta_{1s}\sin(\psi) \tag{4.128}$$

The corresponding blade root bending moment for each blade is:

$$M_\beta = K_\beta \beta \tag{4.129}$$
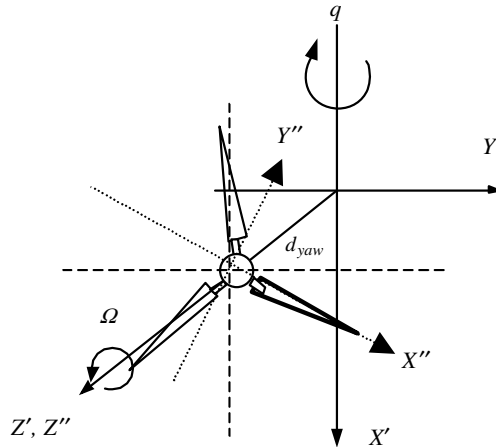
Figure 4.17 Coordinate system for hub moments and forces; d_{yaw} yaw moment arm; q, yaw rate; Ω, angular velocity

Table 4.3 Hub reactions for teetered and cantilevered blades

Hub reaction	Teetered rotor	Cantilevered
Flapping moment	None	Full flap moment
Flapping shear	Total thrust on hinge	Thrust of each blade
Lead–lag moment	Power torque	Power torque
Lead–lag shear	Force producing torque	Force producing torque
Blade tension	Centrifugal force, weight	Centrifugal force, weight
Blade torsion	Pitching moment	1 blade pitching moment

In a manner similar to the development of the flap equations, one could develop lead–lag and torsion equations and use the full set of responses to get hub loads. The terms summarized in Section 4.4.1.2 are sufficient for such an expansion of the model.

In order to find the hub loads from multiple blades, the forces and moments from all of them are determined and the effects are summed. Note that in each case the proper azimuth must be used. For example, in a rotor with three blades, azimuths should be 120 degrees apart for each of them. It should be noted that, with this simplified model, if the blades are spaced symmetrically around the rotor, the cumulative effect on rotor torques is that they are constant throughout the rotation. Table 4.3 summarizes the key hub reactions for both teetered and cantilevered blades.

4.4.2.9 Tower Loads

Tower loads result from aerodynamic loads on the tower, the weight of the turbine and tower, and from all of the forces on the machine itself, whether steady, cyclic, impulsive, etc.

Aerodynamic Tower Loads
Aerodynamic tower loads include the rotor thrust during normal operation, the moment from the rotor torque, and extreme wind loads. Extreme wind loads are those that could occur as a result of an exceptional gust when the turbine is running at rated power or due to an unusually high wind when the turbine is not operating. More details on conditions giving rise to tower loads are given in Chapter 7.

Tower Vibration
Tower natural frequencies (for cantilevered towers) can be calculated by methods described in Section 4.2.2, including the tower top weight. Guyed towers involve methods beyond the scope of this text. The most important consideration in tower design is to avoid natural frequencies near rotor frequencies ($1P$, $2P$, or $3P$). A 'soft' tower is one whose fundamental natural frequency is below the blade-passing frequency whereas a stiff tower has its dominant natural frequency above that frequency. Further discussion of tower vibration can be found in Chapter 6.

Dynamic Tower Loads
Dynamic tower loads are loads on the tower resulting from the dynamic response of the wind turbine itself. For a rigid rotor, blade moments are the main source of dynamic tower loads. The

three moments for each blade (flapwise, lead–lag, and torsion) are transferred to the tower coordinates as:

$$M_{X'} = M_\beta \sin(\psi) \tag{4.130}$$

$$M_{Y'} = -M_\beta \cos(\psi) \tag{4.131}$$

$$M_{Z'} = M_\zeta \tag{4.132}$$

where X' refers to yawing, Y' to pitching backwards, and Z' to rolling of the nacelle.

For multiple blades the contribution from each blade is summed up, adjusted by the relative azimuth angle.

For a teetered rotor the flapping moment is not transferred to the hub (or the tower) unless the teeter stops are hit, and so contributes little to dynamic tower loads under normal operation.

4.4.2.10 Yaw Stability

Yaw stability is an issue for free-yaw turbines. It is a complicated problem, and the simplified dynamic model is of limited utility in its analysis. Nonetheless it does provide insights into some of the basic physics. The key point is that various inputs contribute to cyclic responses. Any net sine response would result in a net torque about the yaw axis. (The cosine cyclic term would tend to rock the turbine up and down on its yaw bearing, but would not affect yaw motion.) Conversely, for the rotor to be stable under any given conditions, the sine cyclic response term must be equal to zero. The sine cyclic response is affected by gyroscopic motion, yaw error, wind shear, and gravity. Referring back to the solution of the flapping equations of motion, it was pointed out that the sine cyclic term could be subdivided into the terms due to different effects (Equation (4.126b)). The dominant contributions to the 'sine cyclic' motion are given in Table 4.2.

The first thing to note is that both vertical wind shear and the gravitational force on the bent blades tend to turn the rotor out of the wind in the same direction (in the negative yaw direction in Figure 4.17). That means that the rotor tends to experience a crosswind from the negative direction. The crosswind, due to yaw error, will tend to turn the rotor back in the other direction. For yaw stability then, if gravity, steady wind, and wind shear are the only effects considered, there will be a yaw angle such that:

$$\beta_{1s,cr} = \beta_{1s,ahg} + \beta_{1s,vs} \tag{4.133}$$

Using this equation, but ignoring wind shear, and assuming small-angle approximations, it can be shown that the steady state yaw error, Θ, would be approximately:

$$\Theta \approx \frac{\Omega R}{V}\left(\frac{3B}{2(2K-1)}\right) \tag{4.134}$$

The steady state yaw error, then, in the absence of vertical wind shear, is greater at faster rotor speeds and for softer rotors (smaller K). Vertical wind shear would increase the steady state yaw error even more. Finally, a thorough analysis of the various terms in the solution shows that a rotor with preconing tends to be more stable than one without.

The linearized hinge–spring dynamic model provides insight into yaw stability, but the subject is more complicated than a first-order model indicates. Changing angles of attack, stall, turbulence, and unsteady aerodynamic effects all influence the yaw stability of real turbines. Additional analysis of the ability of a relatively simplified dynamic model to provide insights into yaw stability can be found in Eggleston and Stoddard (1987). Experience has shown, however, that in the matter of yaw motion in particular, a more comprehensive method of analysis is required.

4.4.2.11 Applicability and Limitations of the Linearized Hinge–Spring Dynamic Model

The linearized dynamic model developed above can be very useful in providing insight into wind turbine dynamics. On the other hand, there are some important aspects of rotor behavior that do not appear in the model. Actual data often exhibit oscillations which are not predicted. For example, Figure 4.18 illustrates a 5-second time trace of the bending moment in the flapwise (axial) direction at the blade root of a typical three-bladed wind turbine, using arbitrary units. The rotor in this case turns at just a little more than once per second. As can be seen, the largest oscillations do occur at approximately that frequency, but smaller ones occur considerably more often.

The significance of this can be illustrated even more graphically in a power spectral density (psd), which is also known as a power spectrum. As may be recalled, the psd was introduced in Chapter 2 in relation to turbulent wind speed fluctuations. The psd is also described in more detail in Appendix C. Figure 4.19 shows a power spectrum (in arbitrary units) obtained from the data used in Figure 4.18.

As would be expected, the $1P$ spike in the measured data (at 72 rpm or 1.2 Hz) is very strong. In addition, spikes appear at approximately $2P$ and $4P$. The other spikes are presumably due to turbulence in the wind and some natural frequencies of the blade. The important thing to note is
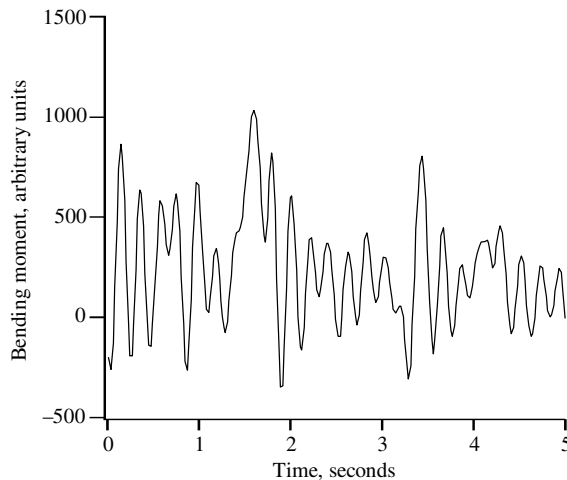
Figure 4.18   Sample root flap bending moment
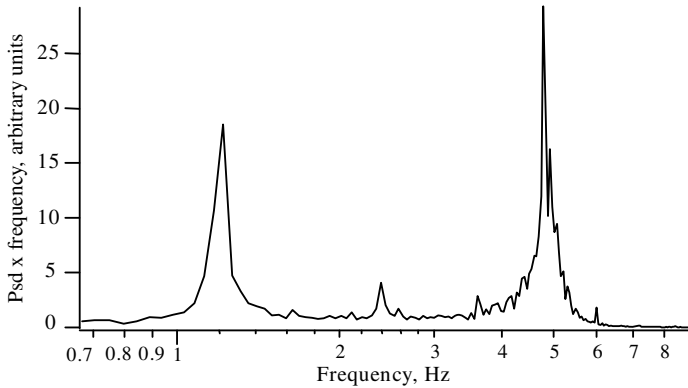
Figure 4.19   Power spectrum of root flap bending moment; psd, power spectral density

that the linearized hinge–spring model can only reproduce (to some extent) the 1P response. None of the higher frequency responses are predicted and, as can be seen from the figure, there is a significant amount of energy associated with those higher frequencies.

4.5 Methods for Modeling Wind Turbine Structural Response

As should already be clear, wind turbines are complex structures. It is frequently necessary to determine various aspects of their response, such as stresses within the structure, deflections, natural frequencies, etc. This is typically done using mathematical models. These are sets of mathematical relations that are to describe the behavior of the real system. Models can differ greatly in their complexity, and so different types of models are used for different applications. The general rule is that the model should be as complex as it needs to be, but no more so.

Typical applications for mechanical models in wind turbine design are the following:

- simple model for control;
- model sufficient for illustration;
- detailed model for investigating fatigue, deflection, and extreme response;
- model for determining natural frequency of component or complete system.

The linearized hinge–spring dynamic model discussed in Section 4.4, for example, can be useful for elucidating the first-order response of a wind turbine rotor to a range of input conditions. It is less useful, however, in those situations where important aspects of the response would not become apparent using such a simplified approach. In order to overcome this limitation, it has been necessary to develop more detailed and sometimes more specialized models. Typically, these models require numerical solutions and are implemented in digital computer code. Specialized nonlinear models can be used to investigate the dynamics of turbine subsystems such as tip flaps, blades, pitch linkages, gear trains, etc. No single model has so far been able to deal with all of these situations, but an understanding of approaches to modeling provides the tools for more detailed analyses. Some examples of these computer

models will be described in Chapter 7. This section discusses some of the methods that are used in those models.

The most common methods used in the structural analysis of wind turbines are:

- finite element method;
- lumped parameter method;
- modal analysis;
- multibody analysis.

4.5.1 Finite Element Method

The finite element method (FEM) is a technique used for analyzing behavior in a variety of situations, including structures. The technique is based on dividing the structure into a large number of relatively small elements. Each element includes a number of 'nodes.' Some of these nodes may be interior to the element; others are on the boundary. Elements only interact through the nodes at the boundary. Each element is characterized by a number of parameters, such as thickness, density, stiffness, shear modulus, etc. Also associated with each node are displacements or degrees of freedom. These may include translations, rotation, axial motion, etc. The finite element method is most often used to study in detail individual components within a larger system. For more complex systems consisting of various components moving differently with respect to each other, other approaches such as multibody dynamics (see below) are used. A finite element model may then be used subsequently, for example, to study variations in stresses within a component. See Figure 4.20 for an illustration of blade stresses calculated on a blade using FEM. More details on the finite element method are given in Rao (1999) and Chopra (2007) as well as various other textbooks on the subject.
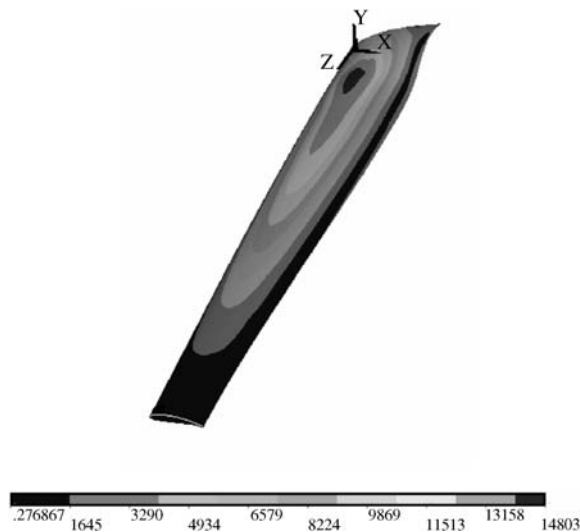
Figure 4.20 Stress distribution on a blade, based on FEM; shades indicate stress level, units arbitrary

4.5.2 Lumped Parameter Method

A lumped parameter model is one in which a non-uniform body is considered to be made up of a relatively small number of bodies which can be simply characterized. This characterization may consist of as little as the mass of the body, or it may include other parameters as well, such as stiffnesses. For example, the drive train of a wind turbine in reality consists of a number of rotating components, such as the rotor itself, shafts, gears, and the generator rotor. In modeling a drive train it is common to characterize it as a few lumped inertias and stiffnesses. See Chopra (2007) for a discussion of the use of lumped masses. The Myklestad method (Section 4.3) is actually an example of the lumped parameter method.

4.5.3 Modal Analysis Method

Modal analysis is a method used to solve the equations of motion in multiple degree of freedom vibrating systems. The modal analysis approach allows coupled equations of motion to be transformed into uncoupled 'modal' equations which can each be solved separately. The results from each of the modal equations are then added ('superposition') to give the complete result. Modal analysis is most useful for linear systems with classical damping. (Classical damping refers to situations in which the same damping mechanism applies throughout a structure). More details on modal analysis may be found in Fertis (1995) or Chopra (2007). Modal analysis requires that the structure of interest be first conceptually divided into analyzable sections. These sections are then pre-analyzed to determine a number of the natural frequencies and mode shapes. These natural frequencies and mode shapes may be found by applying basic techniques such as the Euler or Myklestad method (see Section 4.3) or more detailed techniques which use the finite element method.

4.5.4 Multibody Analysis

Multibody analysis refers to the modeling of the motion of a mechanical system comprising more than one component or 'body.' Bodies are distinguishable subdivisions of the larger structure, which are relatively uniform within themselves. Wind turbine examples include tapered or twisted beams (such as the blades or tower), various other tapered parts, couplings, generators, gears, etc. The bodies may move in a variety of ways with respect to each other. The bodies may be rigid or flexible. Bodies are joined together by 'links' which may incorporate certain constraints. Note that the description of the bodies in multibody systems is significantly more detailed than those of lumped parameter models. The multibody method involves the creation of dynamical equations involving the various bodies and their constraints. The equations are then solved by suitable numerical techniques. Multibody analysis grew out of classical mechanics as an extended application of Newton's Second Law, but it has become progressively more complex and inclusive with time. More details may be found in a variety of texts, such as Shabana (2005).

References

Beer, F. P., Johnston, E. R., Jr., DeWolf, J. and Mazurek, D. (2008) *Mechanics for Engineers*, 5th edition. McGraw Hill Book Co., New York.

Chopra, A. K. (2007) *Dynamics of Structures: Theory and Application to Earthquake Engineering*, 3rd edition. Pearson Prentice Hall, Upper Saddle River, NJ.

Den Hartog, J. P. (1961) *Mechanics*. Dover Publications, New York.

Eggleston, D. M. and Stoddard, F. S. (1987) *Wind Turbine Engineering Design*. Van Nostrand Reinhold, New York.

Fertis, D. G. (1995) *Mechanical and Structural Vibrations*. John Wiley & Sons, Inc., New York.

Meriam, J. L. and Kraige, L. G. (2008) *Engineering Mechanics: Vol. 1, Statics. Engineering Mechanics: Vol. 2, Dynamics*. John Wiley & Sons, Inc., New York.

Pytel, A. and Singer, F. L. (1987) *Strength of Materials*, 4th edition. Harper and Row, New York.

Rao, S. S. (1999) *The Finite Element Method in Engineering*, 3rd edition. Butterworth-Heinemann, Boston.

Shabana, A. A. (2005) *Dynamics of Multibody Systems*, 3rd edition. Cambridge University Press. Cambridge.

Thomson, W. T. and Dahleh, M. D. (1997) *Theory of Vibrations with Applications*, 5th edition. Prentice-Hall, Englewood Cliffs, NJ.

5

Electrical Aspects of Wind Turbines

5.1 Overview

Electricity is associated with many aspects of modern wind turbines. Most obviously, the primary function of the majority of wind turbines is the generation of electricity. A large number of topics in power systems engineering are thus directly relevant to issues associated with wind turbines. These include generation at the turbine itself as well as power transfer at the generator voltage, transforming to higher voltage, interconnection with power lines, distribution, transmission, and eventual use by the consumer. Electricity is used in the operation, monitoring, and control of most wind turbines. It is also used in site assessment and data collection and analysis. For isolated or weak grids, or systems with a large amount of wind generation, storage of electricity is an issue. Finally, lightning is a naturally occurring electrical phenomenon that may be quite significant to the design, installation, and operation of wind turbines.

The principal areas in which electricity is significant to the design, installation, or operation of wind turbines are summarized in Table 5.1.

This chapter includes two main parts. First, it includes an overview of the fundamentals. Second, it presents a description of those issues related to the turbine itself, particularly generators and power converters. The interconnection of the generator to the electrical grid and issues related to the system as a whole are described in Chapter 9.

The fundamentals overview focuses on alternating current (AC). Alternating current issues include phasor notation, real and reactive power, three-phase power, fundamentals of electromagnetism, and transformers. Wind turbine related issues include the common types of generators, generator starting and synchronization, power converters, and ancillary electrical equipment.

Table 5.1   Examples of electrical issues significant to wind energy

Power generation	Generators Power electronic converters	Storage	Batteries Rectifiers Inverters
Interconnection and distribution	Power cables Switch gear Circuit breakers Transformers Power quality	**Lightning protection**	Grounding Lightning rods Safe paths
Control	Sensors Controller Yaw or pitch motors Solenoids	**End loads**	Lighting Heating Motors
Site monitoring	Data measurement & recording Data analysis		

5.2 Basic Concepts of Electrical Power

5.2.1 Fundamentals of Electricity

In this chapter it is assumed that the reader has an understanding of the basic principles of electricity, including direct current (DC) circuits. For that reason these topics will not be discussed in detail here. The reader is referred to other sources, such as Nahvi and Edminster (2003), for more information. Specific topics with which the reader is assumed to be familiar include:

- voltage;
- current;
- resistance;
- resistivity;
- conductors;
- insulators;
- DC circuits;
- Ohm's Law;
- electrical power and energy;
- Kirchhoff's laws for loops and nodes;
- capacitors;
- inductors;
- time constants of RC and RL circuits;
- series/parallel combinations of resistors.

5.2.2 Alternating Current

The form of electricity most commonly used in power systems is known as alternating current (AC). In this text it is assumed that the reader has some familiarity with AC circuits, so only the

key points will be summarized. In AC circuits (at steady state) all voltages and currents vary in a sinusoidal manner. There is a complete sinusoidal cycle each period. The frequency, f, of the sine wave is the number of cycles per second. It is the reciprocal of the period. In the United States and much of the Western Hemisphere, the standard frequency for AC is 60 cycles per second (known as 'Hertz', and abbreviated to Hz). In much of the rest of the world, the standard frequency for AC is 50 Hz.

The instantaneous voltage, v, in an AC circuit may be described by the following equation:

$$v = V_{max} \sin(2\pi ft + \phi) \tag{5.1}$$

where V_{max} is the maximum value of the voltage, t is time, and ϕ is the phase angle.

The phase angle indicates the angular displacement of the sinusoid from a reference sine wave with a phase angle of zero. Phase angle is important because currents and voltages, although sinusoidal, are not necessarily in phase with each other. In analysis of AC circuits it is often useful to start by assuming that one of the sinusoids has zero phase, and then find the phase angles of the other sinusoids with respect to that reference.

An important summary measure of the voltage is its root mean square (rms) value V_{rms}:

$$V_{rms} = \sqrt{\int_{cycle} v^2 \mathrm{d}t} = V_{max} \sqrt{\int_{cycle} \sin^2(2\pi ft) \mathrm{d}t} = V_{max} \frac{\sqrt{2}}{2} \tag{5.2}$$

Note that the rms value of the voltage is $\sqrt{2}/2$, or about 70% of the maximum voltage for a pure sine wave. The rms voltage is often referred to as the magnitude of the voltage, so $|V| = V_{rms}$.

5.2.2.1 Capacitors in AC Circuits

The current through a capacitor is proportional to the derivative of the voltage across it. Thus, if the voltage across a capacitor is $v = V_{max} \sin(2\pi ft)$ then the instantaneous current, i, is:

$$i = C \frac{\mathrm{d}v}{\mathrm{d}t} = 2\pi f \, V_{max} C \sin(2\pi ft + \pi/2) \tag{5.3}$$

where C is the capacitance. Equation (5.3) can be rewritten as:

$$i = I_{max} \sin(2\pi ft + \pi/2) \tag{5.4}$$

where $I_{max} = V_{max}/X_C$ and $X_C = 1/(2\pi fC)$. The term X_C is known as capacitive reactance. Reactance is somewhat analogous to resistance in DC circuits. Note that as the current varies in time, the sinusoid will be displaced by $\pi/2$ radians ahead of the voltage sinusoid. For that reason the current in a capacitive circuit is said to lead the voltage.

5.2.2.2 Inductors in AC Circuits

The current in an inductor is proportional to the integral of the voltage. The relation between the voltage and current in an inductor can be found from:

$$i = \frac{1}{L} \int v \, \mathrm{d}t = \frac{V_{max}}{2\pi fL} \sin(2\pi ft - \pi/2) \tag{5.5}$$

where L is the inductance. Analogously to the equation for capacitors, Equation (5.5) can be rewritten as:

$$i = \frac{V_{max}}{X_L} \sin(2\pi ft - \pi/2) \tag{5.6}$$

where $X_L =$ inductive reactance ($X_L = 2\pi fL$). Note that in an inductive circuit the current lags the voltage.

5.2.2.3 Phasor Notation

Manipulations of sines and cosines with various phase relationships can become quite complicated. Fortunately, the process can be greatly simplified, as long as frequency is constant. This is the normal case with most AC power systems. (Note that transient behavior requires a more complicated analysis method.) The procedure uses phasor notation, which is summarized below.

The use of phasors involves representing sinusoids by complex numbers. For example, the voltage in Equation (5.1), can be represented by a phasor:

$$\hat{\mathbf{V}} = V_{rms}e^{j\phi} = a + jb = V_{rms}\angle\phi \tag{5.7}$$

The bold and circumflex are used to indicate a phasor. Here $j = \sqrt{-1}$, $\angle$ indicates the angle between phasor and real axis, ϕ is the phase angle and

$$a = V_{rms}\cos(\phi) \tag{5.8}$$

$$b = V_{rms}\sin(\phi) \tag{5.9}$$

Figure 5.1 illustrates a phasor. Note that it can be equivalently described in rectangular or polar coordinates.

In this method of representation the frequency is implicit. To recover the time series waveform one can use the following relation:

$$V(t) = \sqrt{2}\text{Re}\{V_{rms}\ e^{j\phi}e^{j2\pi ft}\} \tag{5.10}$$

where $\text{Re}\{\ \}$ signifies that only the real part is to be used and, as before, $e^{j\phi} = \cos(\phi) + j\sin(\phi)$.
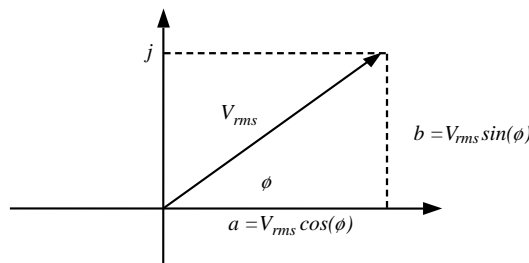
Figure 5.1   Phasor

In an analogous manner, current can be expressed as a phasor, $\hat{I}$, defined by I_{rms} and the phase of the current.

A few rules can be applied when using phasors. These are summarized below. Note that sometimes it is more convenient to use rectangular form; other times the polar form. Begin by defining two phasors $\hat{A}$ and $\hat{C}$.

$$\hat{A} = a + jb = A_m e^{j\phi_a} = A_m \angle \phi_a \tag{5.11}$$

$$\hat{C} = c + jd = C_m e^{j\phi_c} = C_m \angle \phi_c \tag{5.12}$$

where

$$\phi_a = \tan^{-1}(b/a) \tag{5.13}$$

$$\phi_c = \tan^{-1}(d/c) \tag{5.14}$$

$$A_m = \sqrt{a^2 + b^2} \tag{5.15}$$

$$C_m = \sqrt{c^2 + d^2} \tag{5.16}$$

The rules for phasor addition, multiplication, and division are:

Phasor addition

$$\hat{A} + \hat{C} = (a + c) + j(b + d) \tag{5.17}$$

Phasor multiplication

$$\hat{A}\hat{C} = A_m \angle \phi_a C_m \angle \phi_c = A_m C_m \angle (\phi_a + \phi_c) \tag{5.18}$$

Phasor division

$$\hat{A}\,\hat{C} = \frac{A_m \angle \phi_a}{C_m \angle \phi_c} = \frac{A_m}{C_m} \angle (\phi_a - \phi_c) \tag{5.19}$$

More details on phasors can be found in most texts on AC circuits, as well as in Brown and Hamilton (1984) There are also a number of Internet sites that provide useful information on phasors and other aspects of electrical circuitry. One of these is http://www.ece.ualberta.ca/~knight/ee332/fundamentals/f_ac.html.

5.2.2.4 Complex Impedance

The AC equivalent of resistance is complex impedance, $\hat{Z}$, which takes into account both resistance and reactance. Impedance can be used with the phasor voltage to determine phasor current and vice versa. Impedance consists of a real part (resistance) and an imaginary part (inductive or capacitive reactance.) Resistive impedance is given by $\hat{Z}_R = R$, where R is the resistance. Inductive and capacitive impedances are given by, respectively, $\hat{Z}_L = j2\pi fL$ and $\hat{Z}_C = -j/(2\pi fC)$, where f is the AC frequency in Hertz. Note that for a circuit which is completely resistive, the impedance is equal to the resistance. For a circuit which is completely

inductive or capacitive, the impedance is equal to the reactance. Note, also, that inductive and capacitive impedances are a function of the frequency of voltage fluctuations of the AC system.

The rules relating voltage, current, and impedance in AC circuits are analogous to those of DC circuits.

Ohm's Law

$$\hat{V} = \hat{I}\,\hat{Z} \tag{5.20}$$

Impedances in series

$$\hat{Z}_S = \sum_{i=1}^{N} \hat{Z}_i \tag{5.21}$$

Impedances in parallel

$$\hat{Z}_P = 1 \left/ \sum_{i=1}^{N} 1\hat{Z}_i \right. \tag{5.22}$$

where $\hat{Z}_S$ is the effective impedance of N impedances ($\hat{Z}_i$) in series and $\hat{Z}_P$ is the effective impedance of N parallel impedances. Kirchhoff's laws also apply to phasor currents and voltages in circuits with complex impedances.

5.2.2.5 Power in AC Circuits

By measuring the rms voltage, V_{rms}, and rms current, I_{rms}, in an AC circuit, and multiplying them together, as would be done in a DC circuit, one can obtain the apparent power, S. That is:

$$S = V_{rms}\,I_{rms} \tag{5.23}$$

Apparent power, which is measured in units of volt-amperes (VA), however, can be somewhat misleading. In particular, it may not correspond to the real power either consumed (in the case of a load) or produced (in the case of a generator).

Real power, P, is obtained by multiplying the apparent power by the cosine of the phase angle between the voltage and the current. It is thus given by:

$$P = V_{rms}\,I_{rms}\,\cos(\phi) \tag{5.24}$$

Real electrical power is measured in units of Watts.

Current that is flowing in the inductive or capacitive reactances does not result in real power, but does result in reactive power, Q. It is given by:

$$Q = V_{rms}\,I_{rms}\,\sin(\phi) \tag{5.25}$$

Reactive power, which is measured in units of 'volt-amperes reactive' (VAR) is significant because it must be produced somewhere on the system. For example, currents creating the magnetic field in a generator correspond to a requirement for reactive power. Reactive current can also result in higher line losses in distribution or transmission lines, because of the resistance in the lines.

The 'power factor' of a circuit or device describes the fraction of the apparent power that is real power. Thus, the power factor is simply the ratio of real to apparent power. For example, a power factor of 1 indicates that all of the power is real power. The power factor is often defined as the cosine of the phase angle between the voltage and the current, $\cos(\phi)$. This quantity is correctly called the displacement power factor. In circuits with sinusoidal currents and voltages, the two types of power factor are equivalent. In circuits with non-sinusoidal currents and voltages, the displacement power factor is not applicable.

The phase angle between current and voltage is called the power factor angle, since it is the basis for determining the power factor. It is important to note that the power factor angle may be either positive or negative, corresponding to whether the current sine wave is leading the voltage sine wave or vice versa, as discussed earlier. Accordingly, if the power factor angle is positive, the power factor is said to be leading; if it is negative, the power factor is lagging.

An example of the waveforms relating voltage, current, and apparent power is shown in Figure 5.2 for a circuit with a resistor and capacitor. For this example, the current and voltage are out of phase by 45 degrees, so the power factor is 0.707. The current sine wave precedes the voltage wave, so the power factor is leading.

A simple example of the use of phasors for calculations in an AC circuit is the following. Consider a simple circuit with an AC voltage source, a resistor, an inductor, and a capacitor, all connected in series in a single loop. The resistance of the resistor is 4Ω, the reactances of the inductor and capacitor are $j3\,\Omega$ and $-j6\,\Omega$, respectively. The rms voltage is $100\angle0$. The problem is to find the current and the power dissipated in the resistor.

Solution: the total impedance, $\hat{\boldsymbol{Z}}$, is $\hat{\boldsymbol{Z}} = \hat{\boldsymbol{Z}}_R + \hat{\boldsymbol{Z}}_L + \hat{\boldsymbol{Z}}_C = 4 + j3 - j6 = 4 - j3 = 5\angle - 36.9°$. The current is then $\hat{\boldsymbol{I}} = \hat{\boldsymbol{V}}/\hat{\boldsymbol{Z}} = 20\angle36.9$. The power can be found from either $P = \left|\hat{\boldsymbol{I}}\right|^2 R = 20^2 4 = 1600\,\text{W}$ or $P = |\hat{\boldsymbol{I}}||\hat{\boldsymbol{V}}|\cos(36.9) = 1600\,\text{W}$. Note the use of the absolute value for the equivalent rms.

5.2.2.6 Three-phase AC Power

Power generation and large electrical loads commonly operate on a three-phase power system. A three-phase power system is one in which the voltages supplying the loads all have a fixed phase difference from each other of 120 degrees ($2\pi/3$ radians). Individual three-phase
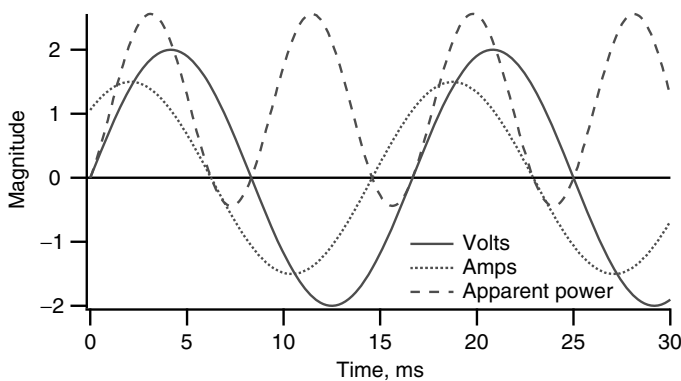
Figure 5.2 AC voltage, v, current, i, and apparent power, vi, in a circuit with a resistor and capacitor
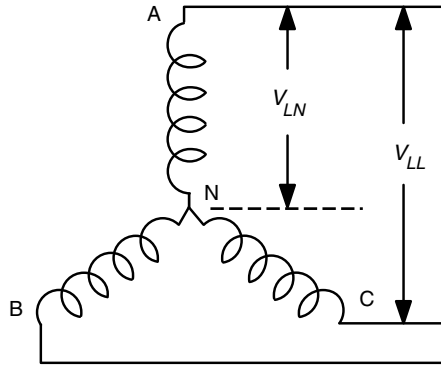
Figure 5.3   Y-connected coils; V_{LN} and V_{LL}, line-to-neutral and line-to-line voltage, respectively

transformers, generators, or motors all have their windings arranged in one of two ways. These are: (1) Y (or wye) and (2) Δ (delta), as illustrated in Figures 5.3 and 5.4. The appearance of the windings is responsible for the names. Note that the Y system has four wires (one of which is the neutral), whereas the Δ system has three wires.

Loads in a three-phase system are, ideally, balanced. That means the impedances are all equal in each phase. If that is the case, and assuming that the voltages are of equal magnitude, then the currents are equal to each other but are out of phase from one another by 120 degrees, as are the voltages. Voltages in three-phase systems may be line-to-neutral, V_{LN}, or line-to-line voltages, V_{LL}. They may also be described as line voltages (V_{LL}) or phase voltages (voltages across loads or coils). Currents in each conductor, outside the terminals of a load, are referred to as line currents. Currents through a load are referred to as load or phase currents. In general, in a balanced Y-connected load, the line currents and phase currents are equal, the neutral current is zero, and the line-to-line voltage, V_{LL}, is $\sqrt{3}$ multiplied by the line-to-neutral voltage, V_{LN}. In a balanced delta-connected load, the line voltages and phase voltages are equal, whereas the line current is $\sqrt{3}$ multiplied by the phase current. Figure 5.5 illustrates Y-connected three-phase loads, assumed to be balanced and all of impedance $\hat{Z}$.

If a three-phase system is known to be balanced, it may be characterized by a single phase equivalent circuit. The method assumes a Y-connected load, in which each impedance is equal to $\hat{Z}$. (A delta-connected load could be used by applying an appropriate $Y-\Delta$ transformation to the impedances, giving $\hat{Z}_Y = \hat{Z}_\Delta/3$.) The one-line equivalent circuit is one phase of a four-wire,
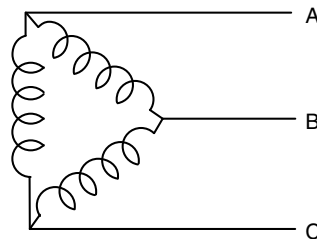
Figure 5.4   Delta-connected coils
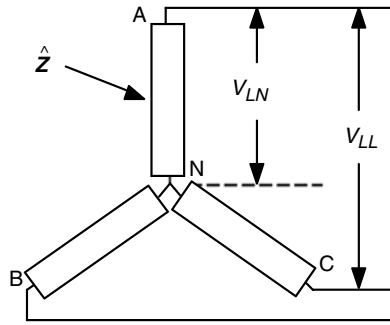
Figure 5.5 Y-connected loads; V_{LN} and V_{LL}, line-to-neutral and line-to-line voltage, respectively; $\hat{Z}$, impedance

three-phase Y-connected circuit, except that the voltage used is the line-to-neutral voltage, with an assumed initial phase angle of zero. The one-line equivalent circuit is illustrated in Figure 5.6.

More details on three-phase circuits can be found in most texts on electrical power engineering, including Brown and Hamilton (1984) and Chapman (2001).

Power in Three-Phase Loads

It is most convenient to be able to determine power in a three-phase system in terms of easily measurable quantities. These would normally be the line-to-line voltage difference and the line currents. In a balanced delta-connected load, the power in each phase is one-third of the total power. The real power in one phase, P_1, using line-to-line voltage and phase current, I_P, would be:

$$P_1 = V_{LL}I_P \cos(\phi) \tag{5.26}$$
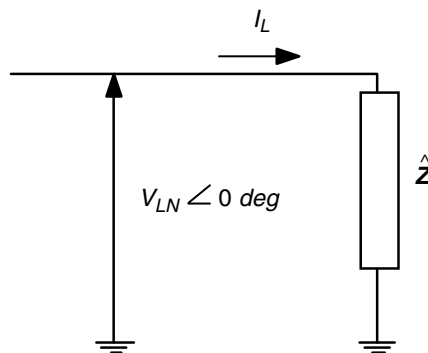
Figure 5.6 One-line equivalent circuit; I_L, line current in three-phase system; V_{LN}, line-to-neutral voltage; $\hat{Z}$, impedance

Since the line current is given by $I_L = \sqrt{3}I_P$, and there are three phases, the total real power is:

$$P = \sqrt{3}V_{LL}\,I_L\,\cos(\phi) \tag{5.27}$$

Similarly, the total three-phase apparent power and reactive power are:

$$S = \sqrt{3}V_{LL}I_L \tag{5.28}$$

$$Q = \sqrt{3}V_{LL}\,I_L\,\sin(\phi) \tag{5.29}$$

The above relations for three-phase power also hold for balanced Y-connected loads. Calculation of power in unbalanced loads is beyond the scope of this text. The interested reader should refer to any book on power system engineering for more information.

5.2.2.7 Voltage Levels

One of the major advantages of AC power is that the voltage level may be readily changed by the use of power transformers. Power may be used conveniently and safely at relatively low voltage, but be transformed to a much higher level for transmission or distribution. To a close approximation, power is conserved during transforming, so that when the voltage is raised, currents are lowered. This serves to reduce losses in transmission or distribution lines, allowing much smaller and less expensive conductors.

Wind turbines typically produce power at 480 V (in the United States) or 690 V (in Europe). Wind turbines are often connected to distribution lines with voltages in the range of 10 kV to 69 kV. See Chapter 9 for more information on electrical grids and interconnection to the grid.

5.2.3 Fundamentals of Electromagnetism

The fundamental principles governing transformers and electrical machinery, in addition to those of electricity, which were summarized above, are those of the physics of electromagnetism. As with electricity, it is assumed that the reader is familiar with the basic concepts of electromagnetism. These principles are summarized below. More details can be found in most physics or electrical machinery texts. By way of a quick overview, it may be noted that the magnetic field intensity in an electromagnet is a function of the current. The forces due to magnetic fields are a function of the magnetic flux density. This depends on the materials within the magnetic field as well as the intensity of the magnetic field.

5.2.3.1 Ampere's Law

Current flowing in a conductor induces a magnetic field of intensity $\boldsymbol{H}$ in the vicinity of the conductor. This is described by Ampere's Law:

$$\oint \boldsymbol{H} \cdot \mathrm{d}\ell = I \tag{5.30}$$

which relates the current in the conductor, I, to the line integral of the magnetic field intensity along a path, ℓ, around the conductor.

5.2.3.2 Flux Density and Magnetic Flux

The magnetic flux density, $\boldsymbol{B}$ (Wb/m^2), is related to the magnetic field intensity by the permeability, μ, of the material in which the field is occurring:

$$\boldsymbol{B} = \mu\boldsymbol{H} \tag{5.31}$$

where $\mu = \mu_0\mu_r$ is the permeability (Wb/A-m) which can be expressed as the product of two terms: μ_0, the permeability of free space, $4\pi \times 10^{-7}$ Wb/A-m, and μ_r, the dimensionless relative permeability of the material.

The permeability of non-magnetic materials is close to that of free space and thus the relative permeability, μ_r, is close to 1.0. The relative permeability of ferromagnetic materials is very high, in the range of 10^3 to 10^5. Consequently, ferromagnetic materials are used in the cores of windings in transformers and electrical machinery in order to create strong magnetic fields.

These laws can be used to analyze the magnetic field in a coil of wire. Current flowing in a wire coil will create a magnetic field whose strength is proportional to the current and the number of turns, N, in the coil. The simplest case is a solenoid, which is a long wire wound in a close packed helix. The direction of the field is parallel to the axis of the solenoid. Using Ampere's Law, the magnitude of the flux density inside a solenoid of length L can be determined:

$$B = \mu I \frac{N}{L} \tag{5.32}$$

The flux density is relatively constant across the cross-section of the interior of the coil.

Magnetic flux Φ(Wb) is the integral of the product of the magnetic field flux density and the cross-sectional area A through which it is directed:

$$\Phi = \int \boldsymbol{B} \cdot \mathrm{d}\boldsymbol{A} \tag{5.33}$$

Note that the integral takes into account, via the dot product, the directions of the area through which the flux density is directed as well as that of the flux density itself. For example, magnetic flux inside a coil is proportional to the magnetic field strength and the cross-sectional area, A, of the coil:

$$\Phi = BA \tag{5.34}$$

5.2.3.3 Faraday's Law

A changing magnetic field will induce an electromotive force (EMF, or voltage) E in a conductor within the field. This is described by Faraday's Law of Induction:

$$E = -\frac{\mathrm{d}\Phi}{\mathrm{d}t} \tag{5.35}$$

Note the minus sign in the above equation. This reflects the observation that the induced current flows in a direction such that it opposes the change that produced it (Lenz's Law). Note also that, in this text, the symbol E is used to indicate induced voltages, while V is used for voltages at the terminals of a device.

As a result of Faraday's Law, a coil in a changing magnetic field will have an EMF induced in it that is proportional to the number of turns:

$$E = -\frac{d(N\varPhi)}{dt} \tag{5.36}$$

The term $\lambda = N\varPhi$ is often referred to as the flux linkages in the device.

5.2.3.4 Induced Force

A current flowing in a conductor in the presence of a magnetic field will result in an induced force acting on the conductor. This is the fundamental property of motors. Correspondingly, a conductor which is forced to move through a magnetic field will have a current induced in it. This is the fundamental property of generators. In either case the force $d\boldsymbol{F}$ in a conductor of incremental length $d\ell$ (a vector), the current and the magnetic field $d\boldsymbol{B}$ are related by the following vector equation:

$$d\boldsymbol{F} = I d\ell \times d\boldsymbol{B} \tag{5.37}$$

Note the cross product ($\times$) in Equation (5.37). This indicates that the conductor is at right angles to the field when the force is greatest. The force is also in a direction perpendicular to both the field and the conductor.

5.2.3.5 Reluctance

A concept that can be useful in understanding some electrical conversion devices such as transformers and rotating machinery is that of 'reluctance.' First of all, in electromagnetic circuits in such devices, the quantity that drives the flux is the product of the number of turns in a coil, N, and the current, i. This product, Ni, is sometimes referred to as the magnetomotive force (MMF). The reluctance is the ratio of MMF to flux and can be thought of as resistance to the generation of magnetic flux by the MMF. In general, the reluctance is proportional to the distance through which the flux travels and inversely proportional to the relative permeability of the material. The relative permeability of magnetic materials is often about 10^4 times greater than that of air. In electrical machines, magnetic flux flows across air gaps from stationary to rotating parts of the system. Normally, it is important to keep these gaps as narrow as possible. In some cases, the geometry of a rotor causes the reluctance to vary during rotation. This variation in reluctance can be taken advantage of in certain types of generator (see Section 5.4.7).

5.2.3.6 Additional Considerations

In practical electromagnetic devices, additional considerations affect machine performance, including leakage and eddy current losses, and the nonlinear effects of saturation and hysteresis.

Magnetic fields can never be restricted to exactly the regions where they can do useful work. Because of this there are invariably losses. These include leakage losses in transformers and electrical machinery. The effect of the leakage losses is to decrease the magnetic field from what would be expected from the current in the ideal case, or conversely to require additional
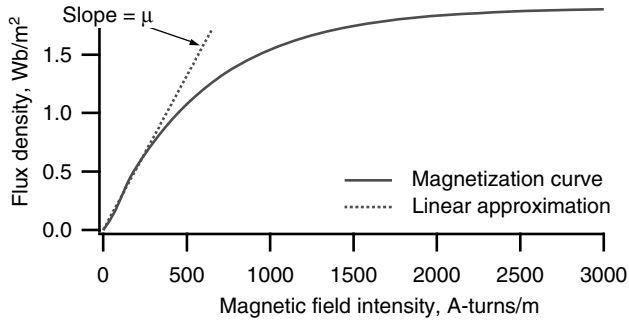
Figure 5.7 Sample magnetization curve; μ, permeability

current to obtain a given magnetic field. Eddy currents are secondary and, generally undesired, currents induced in parts of a circuit experiencing an alternating flux. These contribute to energy losses.

Ferromagnetic materials, such as are used in electrical machinery, often have nonlinear properties. For example, the magnetic flux density, B, is not always proportional to field intensity, H, especially at higher intensities. At some point B ceases to increase even though H is increasing. This is called saturation. The properties of magnetic materials are typically shown in magnetization curves. An example of such a curve is shown in Figure 5.7.

Another nonlinear phenomenon that affects electrical machine design is known as hysteresis. This describes a common situation in which the material becomes partially magnetized, so B does not vary with H when H is decreasing in the same way that it does when H is increasing.

5.3 Power Transformers

Power transformers are important components in any AC power system. Most wind turbine installations include at least one transformer for converting the generated power to the voltage of the local electrical network to which the turbine is connected. In addition, other transformers may be used to obtain voltages of the appropriate level for various ancillary pieces of equipment at the site (lights, monitoring and control systems, tools, compressors, etc.) Transformers are rated in terms of their apparent power (kVA). Distribution transformers are typically in the 5–50 kVA range, and may well be larger, depending on the application. Substation transformers are typically between 1000 kVA and 60 000 kVA.

A transformer is a device which has two or more coils, coupled by a mutual magnetic flux. Transformers are usually comprised of multiple turns of wire, wrapped around a laminated metal core. In the most common situation the transformer has two windings, one known as the primary, the other as the secondary. The wire is normally of copper, and is sized so there will be minimal resistance. The core consists of laminated sheets of metal, separated by insulation so that there will be a minimum of eddy currents circulating in the core.

The operating principles of transformers are based on Faraday's Law of Induction (Section 5.2.3.3). An ideal transformer is one which has: (1) no losses in the windings, (2) no losses in the core, and (3) no flux leakage. An electrical circuit diagram of an ideal transformer is illustrated in Figure 5.8.
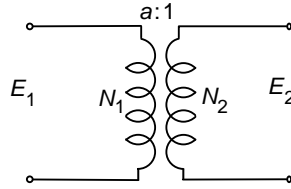
Figure 5.8 Ideal transformer; a, turns ratio; E, induced voltage; N, number of turns; subscripts 1 and 2 refer to the primary and secondary windings, respectively

Assume that E_1 is applied to the primary of an ideal transformer with N_1 coils on the primary and N_2 coils on the secondary. The ratio between the voltages across the primary and the secondary is equal to the ratio of the number of turns:

$$E_1/E_2 = N_1/N_2 = a \qquad (5.38)$$

The parameter a is known as the 'turns ratio' of the transformer.

The primary and secondary currents are inversely proportional to the number of turns (as they must be to keep the power or the product IV constant):

$$I_2/I_1 = N_1/N_2 = a \qquad (5.39)$$

Real, or non-ideal, transformers do have losses in the core and windings, as well as leakage of flux. A non-ideal transformer can be represented by an equivalent circuit as shown in Figure 5.9.

In Figure 5.9, R refers to resistances, X to reactances, 1 and 2 to the primary and secondary coils, respectively. R_1 and R_2 represent the resistance of the primary and secondary windings. X_1 and X_2 represent the leakage inductances of the two windings. The subscript M refers to magnetizing inductance and the subscript c to core resistance. V refers to terminal voltages and E_1 and E_2 are the induced voltages at the primary and secondary whose ratio is the turns ratio.

Parameters on either side of the coils may be referred to (or viewed from) one side. Figure 5.10 illustrates the equivalent circuit of the transformer when referred to the primary side.

A transformer will draw current whether or not there is a load on it. There will be losses associated with the current, and the power factor will invariably be lagging. The magnitude of the losses and the power factor can be estimated if the resistances and reactances in Figure 5.10
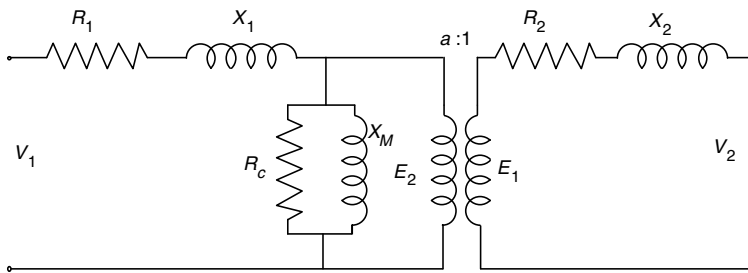
Figure 5.9 Non-ideal transformer; for the notation, see the text
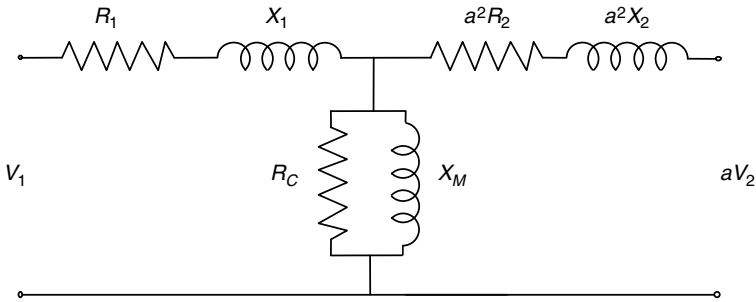
Figure 5.10   Non-ideal transformer, referred to primary winding; for notation, see text

are known. These parameters can be calculated by the use of two tests: (1) measurement of the voltage, current, and power at no load (open circuit on one of the coils) and (2) measurement of voltage, current, and power with one of the coils short circuited. The latter test will be at reduced voltage to prevent burning out the transformer. Most texts on electrical machinery describe these tests in more detail. For example, see Nasar and Unnewehr (1979).

It is worth noting here that the equivalent circuit of the transformer is similar in many ways to that of induction machines, which are discussed in Section 5.4.4 and which are used as generators in many wind turbines.

5.4 Electrical Machines

Generators convert mechanical power to electrical power; motors convert electrical power to mechanical power. Both generators and motors are frequently referred to as electrical machines, because they can usually be run as one or the other. The electrical machines most commonly encountered in wind turbines are those acting as generators. The two most common types are induction generators and synchronous generators. In addition, some smaller turbines use DC generators. The following section discusses the principles of electrical machines in general and then focuses on induction and synchronous generators.

5.4.1 Simple Electrical Machines

Many of the important characteristics of most electrical machines are evident in the operation of the simplest electrical machine, such as is shown in Figure 5.11.
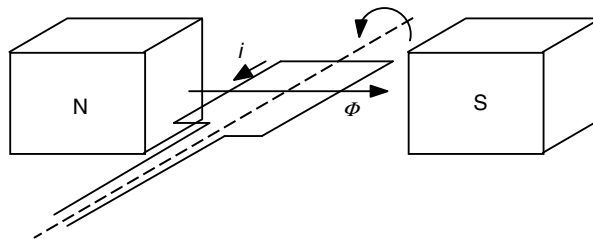
Figure 5.11   Simple electrical machine; i, current; Φ, magnetic flux; N, North magnetic pole; S, South magnetic pole

In this simple electrical machine, the two magnetic poles (or pair of poles) create a field. The loop of wire is the armature. The armature can rotate, and it is assumed that there are brushes and slip rings or a commutator present to allow current to pass from a stationary frame of reference to the rotating one. (A commutator is a device which can change the direction of an electrical current. Commutators are used in DC generators to change what would otherwise be AC to DC.) If a current is flowing in the armature, a force acts on the wire. The force on the left side is down, and on the right side is up. The forces then create a torque, causing the machine to act as a motor. In this machine the torque will be a maximum when the armature loop is horizontal, and a minimum (of zero) when the loop is vertical.

Conversely, if there is initially no current in the wire, but if the armature loop is rotated through the field, a voltage will be generated in accordance with Faraday's Law. If the loop is part of a complete circuit, a current will then flow. In this case the machine is acting as a generator. In general the directions of current or voltage, velocity, field direction, and force are specified by cross-product relations.

When slip rings are used there are two metal rings mounted to the shaft of the armature with one ring connected to one end of the armature coil and the other ring connected to the other coil. Brushes on the slip rings allow the current to be directed to a load. As the armature rotates, the direction of the voltage will depend on the position of the wire in the magnetic field. In fact, the voltage will vary sinusoidally if the armature rotates at fixed speed. In this mode, this simple machine acts as an AC generator. Similarly in the motoring mode, the force (and thus torque) reverses itself sinusoidally during a revolution.

A simple commutator for this machine would have two segments, each spanning 180 degrees on the armature. Brushes would contact one segment at a time, but segment–brush pairing would reverse itself once during each revolution. The induced voltage would then consist of a sequence of half sine waves, all of the same sign. In the motoring mode the torque would always be in the same direction. The commutator principle is the basis of conventional DC motors and generators.

Real electrical machines are similar in many ways to this simple one, but there are also some major differences:

- Except in machines with fields supplied by permanent magnets, the fields are normally produced electrically.
- The fields are most often on the rotating part of the machine (the rotor), while the armature is on the stationary part (the stator).
- There is also a magnetic field produced by the armature which interacts with the rotor's field. The resultant magnetic field is often of primary concern in analyzing the performance of an electrical machine.

5.4.2 Rotating Magnetic Fields

By suitable arrangement of windings in an electrical machine it is possible to establish a rotating magnetic field, even if the windings are stationary. This property forms an important basis of the design of most AC electrical machines. In particular, it is the interaction of the stator's rotating magnetic field with the rotor's magnetic field which determines the operating characteristics of the machine.

The principle of rotating fields can be developed in a number of ways, but the key points to note are that: (1) the coils in the stator are 120 degrees ($2\pi/3$ radians) apart, (2) the magnitude of each field varies sinusoidally, with the current in each phase differing from the others by 120 degrees, and (3) the windings are such that the distribution of each field is sinusoidal. The resultant magnetic field, $\boldsymbol{H}$, expressed in phasor form in terms of the three individual magnetic fields $\boldsymbol{H}_i$ is:

$$\boldsymbol{H} = \boldsymbol{H}_1 \angle 0 + \boldsymbol{H}_2 \angle 2\pi/3 + \boldsymbol{H}_3 \angle 4\pi/3 \qquad (5.40)$$

Substituting in sinusoids for the currents, and introducing an arbitrary constant C to signify that the field results from the currents, we have:

$$\boldsymbol{H} = C[\cos(2\pi ft)\angle 0 + \cos(2\pi ft + 2\pi/3)\angle 2\pi/3 + \cos(2\pi ft + 4\pi/3)\angle 4\pi/3] \qquad (5.41)$$

After performing the algebra, we obtain the interesting result that the magnitude of $\boldsymbol{H}$ is constant, and its angular position is $2\pi ft$ radians. The latter result implies immediately that the field is rotating at a constant speed of f revolutions per second, which is the same as the electrical system frequency. A graphical illustration of this result has been prepared as an animated applet. The applet is available at many sites on the Internet. One of these sites is: http://www.uno.it/utenti/tetractys/askapplets/RotatingField1.htm.

The above discussion implicitly involved a pair of magnetic poles per phase. It is quite possible to arrange windings so as to develop an arbitrary number of pole pairs per phase. By increasing the number of poles, the resultant rotating magnetic field will rotate more slowly. At no load, the rotor of an electrical machine will rotate at the same speed as the rotating magnetic field, called the synchronous speed. In general, the synchronous speed is:

$$n = \frac{60f}{P/2} \qquad (5.42)$$

where n is the synchronous speed in rpm, f is the frequency of the AC electrical supply in Hz, and P is the number of poles.

The above equation implies, for example, that any two-pole AC machine connected to a 60 Hz electrical network would turn with no load at 3600 rpm, a four-pole machine would turn at 1800 rpm, a six-pole machine at 1200 rpm, etc. It is worth noting here that most wind turbine generators are four-pole machines, thus having a synchronous speed of 1800 rpm when connected to a 60 Hz power system. In a 50 Hz system, such generators would turn at 1500 rpm.

5.4.3 Synchronous Machines

5.4.3.1 Overview of Synchronous Machines

Synchronous machines are used as generators in large central station power plants. In wind turbine applications they are used occasionally on large grid-connected turbines, or in conjunction with power electronic converters in variable-speed wind turbines (see Section 5.6). A type of synchronous machine using permanent magnets is also used in some stand-alone wind turbines (see Section 5.4.6). In this case the output is often rectified to DC before the power is delivered to the end load. Finally, synchronous machines may be used as a means of voltage control and a source of reactive power in autonomous AC networks. In this case they are known as synchronous condensers.

In its most common form the synchronous machine consists of: (1) a magnetic field on the rotor that rotates with the rotor and (2) a stationary armature containing multiple windings. The field on the rotor is created electromagnetically by a DC current (referred to as excitation) in the field windings. The DC field current is normally provided by a small DC generator mounted on the rotor shaft of the synchronous machine. This small generator is known as the 'exciter', since it provides excitation to the field. The exciter has its field stationary and its output is on the synchronous machine's rotor. The output of the exciter is rectified to DC right on the rotor and fed directly into the synchronous machine's field windings. Alternatively, the field current may be conveyed to the synchronous machine's rotor via slip rings and brushes. In either case the synchronous machine's rotor field current is controlled externally.

A simple view of a synchronous machine can give some insight into how it works. Assume, as in Section 5.4.2, that a rotating magnetic field has been set up in the stationary windings. Assume also that there is a second field on the rotor. These two fields generate a resultant field that is the sum of the two fields. If the rotor is rotating at synchronous speed, then there is no relative motion between any of these rotating fields. If the fields are aligned, then there is no force acting upon them that could change the alignment. Next, suppose that the rotor's field is displaced somewhat from that of the stator, causing a force, and hence an electrical torque, which tends to align the fields. If an external torque is continually applied to the rotor, it could balance the electrical torque. There would then be a constant angle between the fields of the stator and the rotor. There would also be a constant angle between the rotor field and the resultant field, which is known as the power angle, and it is given the symbol delta (δ). It can be thought of as a spring, since, other things being equal, the power angle increases with torque. It is important to note that as long as $\delta > 0$ the machine is a generator. If input torque drops, the power angle may become negative and the machine will act as a motor. Detailed discussion of these relations is outside the scope of this text, however, and is not needed to understand the operation of a synchronous machine for the purposes of interest here. A full development is given in most electrical machinery texts. See, for example, Brown and Hamilton (1984) or Nasar and Unnewehr (1979).

5.4.3.2 Theory of Synchronous Machine Operation

The following presents an overview of the operation of synchronous machines, based on an equivalent circuit which can be derived for it and two electrical angles. The latter are the power factor angle, ϕ, and the power angle, δ.

The current in the synchronous machine's field windings, I_f, induces a magnetic flux. The flux, Φ, depends on the material and the number of turns in the winding, as explained in Section 5.2.3, but, to a first approximation, the flux is proportional to the current.

$$\Phi = k_1 I_f \tag{5.43}$$

where $k_1 =$ constant of proportionality. The voltage produced in the stationary armature, E, is proportional to: (1) the magnetic flux and (2) the speed of rotation, n:

$$E = k_2 n \Phi \tag{5.44}$$

where k_2 is another constant of proportionality. This voltage causes currents to flow in the armature windings.
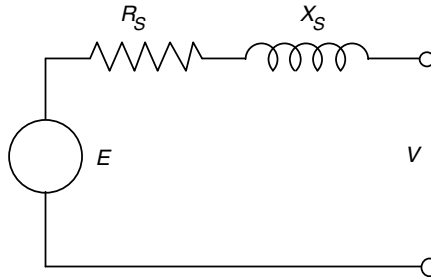
Figure 5.12 Equivalent circuit of a synchronous machine; E, voltage produced in stationary armature; R_s, resistance; V, terminal voltage; X_s, synchronous reactance

The generator armature winding is an inductor, which can be represented by a reactance, called the synchronous reactance, X_s, and a small resistance, R_s. The reactance has a constant value when the rotational speed (and hence grid frequency) is constant. Recall that $X_s = 2\pi f L$ where $L =$ inductance. The synchronous impedance is:

$$\hat{Z}_s = R_s + jX_s \tag{5.45}$$

The resistance is usually small compared to the reactance, so the impedance is often approximated by considering only the reactance.

An equivalent circuit may be developed which can be used to facilitate analysis of the machine's operation. The equivalent circuit for a synchronous machine is shown in Figure 5.12. For completeness, the resistance, R_s, is included, even though it is often ignored in analyses.

The equivalent circuit can be used to develop phasor relations, such as are shown in Figures 5.13 and 5.14. These figures illustrate the phasor relations between the field induced voltage (E), the terminal voltage (V), and the armature current I_a for a synchronous machine with a lagging or leading power factor. The figures may be derived by first assuming a terminal voltage, with reference angle of zero. With a known apparent power and power factor (lagging or leading), the magnitude and angle of the current may be found. Using the equivalent circuit, the magnitude and angle of the field voltage may then be determined. The equation corresponding to the equivalent circuit, ignoring the resistance, is:

$$\hat{E} = \hat{V} + jX_s \, \hat{I}a \tag{5.46}$$

The power angle, δ, shown in Figures 5.13 and 5.14 is, by definition, the angle between the field voltage and the terminal voltage. As described above, it is also the angle between the rotor and the resultant fields.

The things to note are: (1) the armature current in Figure 5.13 is lagging the terminal voltage, indicating a lagging power factor; (2) the armature current in Figure 5.14 is leading the terminal voltage, indicating a leading power factor; and (3) the field-induced voltage leads the terminal voltage, giving a positive power angle, as it should with the machine in a generating mode.
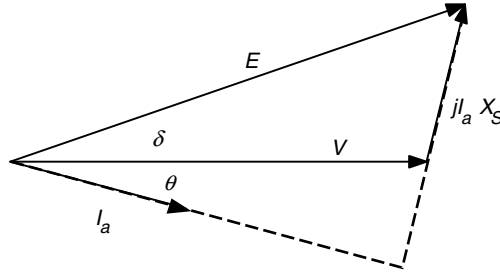
Figure 5.13 Phasor diagram for synchronous generator, lagging power factor; E, field-induced voltage; I_a, armature current; j, $\sqrt{-1}$; V, terminal voltage; X_s, synchronous reactance; δ, power angle; θ, power factor angle

By performing the phasor multiplication with reference to Figure 5.13 or 5.14, as explained in Section 5.2.3, one can find that the real power, P, is:

$$P = \frac{\left|\hat{E}\right|\left|\hat{V}\right|}{X_S}\sin(\delta) \tag{5.47}$$

Similarly, the reactive power, Q, out of the generator is:

$$Q = \frac{\left|\hat{E}\right|\left|\hat{V}\right|\cos(\delta) - \left|\hat{V}\right|^2}{X_S} \tag{5.48}$$

It is worth emphasizing that, in a grid-connected application with a constant terminal voltage (controlled by other generators), a synchronous machine may serve as a source of reactive power, which may be required by loads on the system. Changing the field current will change the field-induced voltage, E, while the power stays constant. For any given power level, a plot of armature current vs. field current will have a minimum at unity power factor. An example of this is shown in Figure 5.15. This example is for a generator with a line-to-neutral terminal voltage of 2.4 kV. In the generator mode, higher field current (and therefore higher field voltage) will result in a lagging power factor; lower field current (lower field voltage) will result in a leading
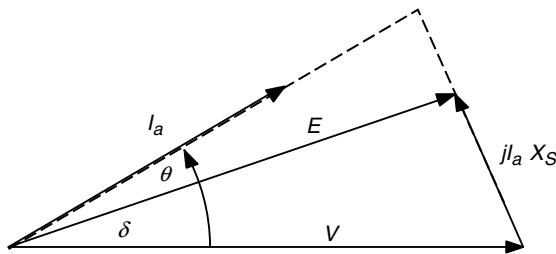
Figure 5.14 Phasor diagram for synchronous generator, leading power factor; E, field-induced voltage; I_a, armature current; j, $\sqrt{-1}$; V, terminal voltage; X_s, synchronous reactance; δ, power angle; θ, power factor angle
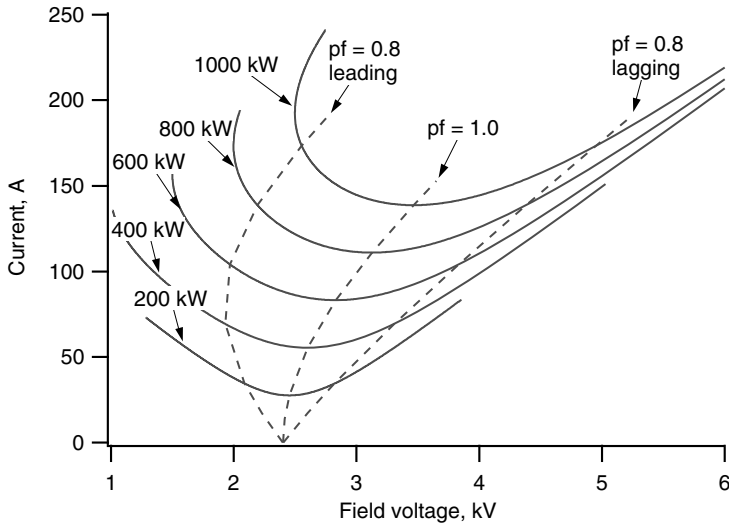
Figure 5.15 Synchronous machine armature current vs. field current in generator mode

power factor. In practice, the field current is generally used to regulate the generator's terminal voltage. A voltage regulator connected to the synchronous generator automatically adjusts the field current so as to keep the terminal voltage constant.

An additional consideration relates to the details of the synchronous machine's windings. Most synchronous generators have salient poles, though there are some with round rotors. The terms direct-axis and quadrature-axis are associated with salient pole machines. These terms are discussed in detail in electrical machinery texts such as Brown and Hamilton (1984) or Chapman (2001).

5.4.3.3 Starting Synchronous Machines

Synchronous machines are not intrinsically self-starting. In some applications the machine is brought up to speed by an external prime mover and then synchronized to the electrical network. For other applications, a self-starting capability is required. In this case the rotor is built with 'damper bars' embedded in it. These bars allow the machine to start like an induction machine does (as described in the next section.) During operation the damper bars also help to damp oscillations in the machine's rotor.

Regardless of how a synchronous machine is brought up to operating speed, particular attention must be given to synchronizing the generator with the network to which it is to be connected. A very precise match is required between the angular position of the rotor and the electrical angle of the AC power at the instant of connection. Historically, synchronization was done manually with the help of flashing lights, but it is now done with electronic controls.

Wind turbines with synchronous generators are normally started by the wind (unlike many turbines with induction generators, which can be motored up to speed). When the turbine is to be connected to an AC network which is already energized, active speed control of the turbine may be needed as part of the synchronizing process. In some isolated electrical grids, the AC

power is supplied by a synchronous generator on either a diesel generator or a wind turbine, but not both. This obviates the need for a synchronizer.

5.4.4 Induction Machines

5.4.4.1 Overview of Induction Machines

Induction machines (also known as asynchronous machines) are commonly used for motors in most industrial and commercial applications. It has long been known that induction machines may be used as generators, but they were seldom employed that way until the advent of distributed generation in the mid 1970s. Induction machines are now the most common type of generator on wind turbines, and they are used for other distributed generation (hydroelectric, engine-driven) as well.

Induction machines are popular because (1) they have a simple, rugged construction, (2) they are relatively inexpensive, and (3) they may be connected and disconnected from the grid relatively simply.

The stator on an induction machine consists of multiple windings, similar to that of a synchronous machine. The rotor in the most common type of induction machine has no windings. Rather it has conducting bars, embedded in a solid, laminated core. The bars make the rotor resemble a squirrel cage. For this reason, machines of this type are commonly called squirrel cage machines. Throughout this book, however, induction generators with squirrel cage rotors are often referred to simply as 'induction generators.'

Some induction machines do have windings on the rotor. These are known as wound rotor machines. These machines are sometimes used in variable-speed wind turbines (see Section 5.6.3). They are more expensive and less rugged than those with squirrel cage rotors. Depending on how wound rotor machines are used, they may also be referred to as doubly fed. This is because power may be sent to or taken from the rotor, as well as from the stator.

Induction machines require an external source of reactive power. They also require an external constant frequency source to control the speed of rotation. For these reasons, they are most commonly connected to a larger electrical network. In these networks synchronous generators connected to prime movers with speed governors ultimately set the grid frequency and supply the required reactive power.

When operated as a generator, the induction machine can be connected to the network and brought up to operating speed as a motor, or it can be accelerated by the prime mover, and then connected to the network. There are issues to be considered in either case. Some of these are discussed later in this section.

Induction machines often operate with a poor power factor. To improve the power factor, capacitors are frequently connected to the machine at or near the point of connection to the electrical network. Care must be taken in sizing the capacitors when the machine is operated as a generator. In particular it must not be possible for the generator to be 'self-excited' if connection to the grid is lost due to a fault.

Induction machines can be used as generators in small electrical networks or even in isolated applications. In these cases, special measures must sometimes be taken for them to operate properly. The measures involve reactive power supply, maintaining frequency stability, and bringing a stationary machine up to operating speed. Some of these measures are described in Chapter 9.

5.4.4.2 Theory of Induction Machine Operation

The theory of operation of a squirrel cage induction machine can be summarized as follows:

- The stator has windings arranged such that the phase-displaced currents produce a rotating magnetic field in the stator (as explained in Section 5.4.2).
- The rotating field rotates at exactly synchronous speed (e.g. 1800 rpm for a four-pole generator in a 60 Hz electrical network).
- The rotor turns at a speed slightly different from synchronous speed (so that there is relative motion between the rotor and the field on the stator).
- The rotating magnetic field induces currents and hence a magnetic field in the rotor due to the difference in speed of the rotor and the magnetic field.
- The interaction of the rotor's induced field and the stator's field causes elevated voltage at the terminals (in the generator mode) and current to flow from the machine.

One parameter of particular importance in characterizing induction machines is the slip, s. Slip is the ratio of the difference between synchronous speed n_s and rotor operating speed n, and synchronous speed:

$$s = \frac{n_s - n}{n_s} \tag{5.49}$$

When slip is positive, the machine is a motor; when negative it is a generator. Slip is often expressed as a percentage. Typical values of slip at rated conditions are on the order of 2%.

Most characteristics of interest can be described in terms of the equivalent circuit shown in Figure 5.16. The equivalent circuit and the relations used with it are derived in most electrical machinery texts. They will be presented, but will not be derived here.

Here V is the terminal voltage, I is the stator current, I_M is the magnetizing current, I_R is the rotor current, X_{LS} is the stator leakage inductive reactance, R_S is the stator resistance, X'_{LR} is the rotor leakage inductive reactance (referred to the stator), R'_R is the rotor resistance (referred to the stator), X_M is the magnetizing reactance, and R_M is the resistance in parallel with the mutual inductance. Note that primes (''') are used with the rotor parameters to indicate that they are referred to the stator, by taking into account the turns ratio between the stator and the rotor.
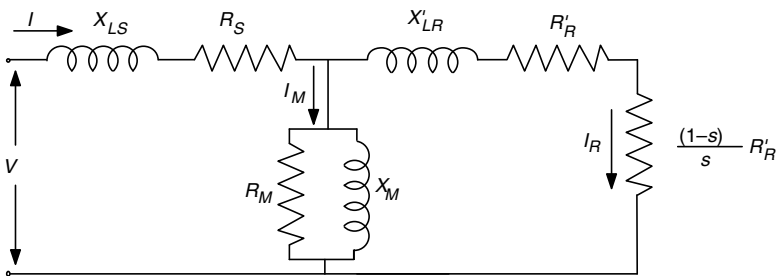
Figure 5.16   Induction machine equivalent circuit; for notation, see text

A few items of particular note are:

- X_M is always much larger than X_{LS} and X'_{LR}.
- The term $\frac{1-s}{s}R'_R$ is essentially a variable resistance. For a motor it is positive; for a generator it is negative.
- R_M is a large resistance and is often ignored.

The values of the various resistances and reactances can be derived from tests. These tests are:

- stator resistance measurement (with an ohmmeter capable of measuring small resistances);
- locked rotor test (current, voltage, and power measured at approximately rated current and reduced voltage);
- no load current and voltage test (current, voltage, and power measured at no load);
- mechanical tests to quantify windage losses and friction losses (described below).

Measurements of induction machine parameters are described in many books on electrical machinery. In the no-load test, the slip is very close to zero, so the resistance R_r/s in the right-hand loop of the circuit shown in Figure 5.16 is very large, and currents in that loop can be ignored. From measurements of voltage current and power factor, it is straightforward to determine X_M (assumed to be much larger than X_{LS}), and R_M. In the locked rotor test, the rotor is held fast; the slip is therefore equal to 1 so the resistance in the rotor circuit is just R'_R. A reduced voltage is applied to the stator terminals so that rated current will flow into the machine. Most of this current will flow through the right-hand side of the circuit in Figure 5.16, with little going through the mutual inductance. Once the voltage, current, and power factor are measured, the values of $R_S + R'_R$ and $X_{LS} + X'_{LR}$ may be determined. R'_R may be found by subtracting the previously measured value of R_S. The stator and rotor leakage reactances are often assumed to be the same.

Not all of the power converted in an induction machine is useful power. There are some losses. The primary losses are (1) mechanical losses due to windage and friction, (2) resistive and magnetic losses in the rotor, and (3) resistive and magnetic losses in the stator. Windage losses are those associated with drag on the rotor from air friction. Friction losses are primarily in the bearings. More information on losses may be found in most texts on electrical machinery (see, for example, Brown and Hamilton (1984)).

In the generator mode, mechanical power input to the machine, P_{in}, that is available to produce electricity is reduced by mechanical losses, $P_{mechloss}$. The mechanical power available to be converted at the generator's rotor, P_m, is:

$$P_m = -(P_{in} - P_{mechloss}) \tag{5.50}$$

(Note: the minus sign is consistent with the convention of generated power as negative). In electrical terms this converted power is:

$$P_m = I_R^2 \quad R'_R \frac{1-s}{s} \tag{5.51}$$

Recall that slip is negative for generation.

Electrical and magnetic losses in the rotor reduce the power that may be transferred from the rotor across the air gap to the stator. The power that is transferred, P_g, is:

$$P_g = I_R^2 R'_R \frac{1-s}{s} + I_R^2 R'_R \tag{5.52}$$

(Note: $I_R^2 R'_R$ is the electrical power loss in the rotor, making P_g less negative than P_m)

Thus:

$$P_g = \frac{P_m}{1-s} \tag{5.53}$$

The power lost in the stator is:

$$P_{loss} = I_s^2 R_S \tag{5.54}$$

The power delivered (negative) at the terminals of the generator, P_{out}, is:

$$P_{out} = P_g + P_{loss} \tag{5.55}$$

The overall efficiency (in the generator mode), η_{gen}, is:

$$\eta_{gen} = -\frac{P_{out}}{P_{in}} \tag{5.56}$$

The power factor, PF, (which is always lagging in an induction machine) is the ratio of the real power to apparent power:

$$PF = \frac{-P_{out}}{VI} \tag{5.57}$$

The previous equations show the relations between real power, reactive power, and currents, but still do not allow complete calculations in terms of machine parameters. This can be done most conveniently by first simplifying the equivalent circuit in Figure 5.16, as shown in Figure 5.17.

If the parameters in the detailed equivalent circuit are known, then the resistance R and reactance X in this simplified model can be found as follows. From Figure 5.16, ignoring R_M,
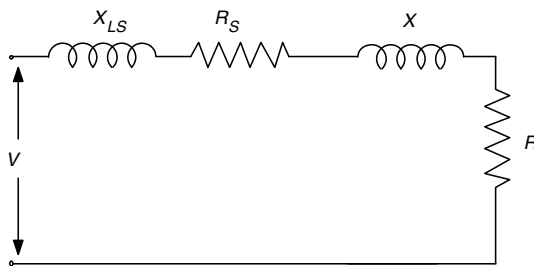
Figure 5.17 Induction machine equivalent circuit; R, resistance; X_{LS}, stator leakage inductive reactance; R_S, stator resistance; X, reactance; V, terminal voltage

and using Equations (5.21) and (5.22) for series and parallel impedances, we have:

$$R + jX = jX_M \left(jX'_{LR} + \frac{R'_R}{s} \right) \bigg/ \left[\frac{R'_R}{s} + j(X_M + X'_{LR}) \right] \qquad (5.58)$$

This gives for the resistance, R:

$$R = X_M^2 \frac{R'_R}{s} \bigg/ \left[(R'_R/s)^2 + (X'_{LR} + X_M)^2 \right] \qquad (5.59)$$

The reactance, X, is then:

$$X = X_M \left[(R'_R/s)^2 + X'_{LR}(X'_{LR} + X_M) \right] \bigg/ \left[(R'_R/s)^2 + (X'_{LR} + X_M)^2 \right] \qquad (5.60)$$

The power converted in R will be $I_S^2 R$ where $\hat{I}_S$ is the current (a phasor) in the loop. The total impedance is:

$$\hat{Z} = (R + R_s) + j(X + X_{LS}) \qquad (5.61)$$

The phasor current is:

$$\hat{I}_S = \hat{V} / \hat{Z} \qquad (5.62)$$

The mechanical power converted per phase is then:

$$P_m = (1 - s)I_S^2 R \qquad (5.63)$$

The real power generated per phase is:

$$P_{out} = I_S^2 (R'_R + R) \qquad (5.64)$$

The reactive power per phase is:

$$Q = I_S^2 (X_{LS} + X) \qquad (5.65)$$

The total mechanical torque, Q_m, applied to a three-phase induction machine (as a generator) is the total input power divided by the rotational speed:

$$Q_m = 3P_{in}/n \qquad (5.66)$$

Note that in this chapter Q without a subscript refers to reactive power. Q with a subscript is used for torque to maintain consistency with other chapters and conventional engineering nomenclature. The mechanical torque is, to a very good approximation, linearly related to slip over the range of slips that are generally encountered in practice.

Figures 5.18 and 5.19 illustrate the results of applying the equivalent circuit to find properties of a three-phase induction machine. Figure 5.18 shows power, current, and torque for operating speeds ranging from 0 to twice synchronous speed. Between standstill and 1800 rpm, the machine is motoring; above that it is generating. As a generator in a wind turbine, the machine
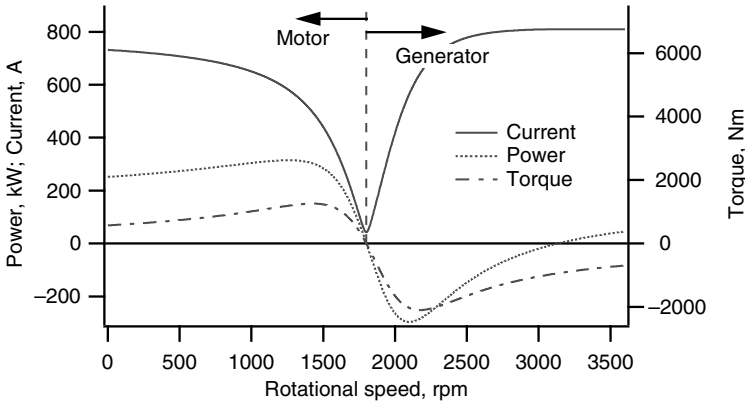
Figure 5.18   Power, current, and torque of an induction machine

would never operate above approximately 3% above synchronous speed, but it would operate at speeds under 1800 while starting. Note that the peak current during startup is over 730 A, more than five times the rated value of 140 A. Peak torque is about two and half times rated (504 Nm). The zero speed starting torque is approximately equal to the rated value at standstill. Peak terminal power is approximately three times rated value (100 kW).

Figure 5.19 shows efficiency and power factor from startup to 2000 rpm. The machine has roughly the same efficiency and power factor when motoring during normal operation as when generating, but both decrease to zero at no load.

Matrix Form of Induction Machine Equations

It is often convenient to express the relations between currents, voltages, and machine parameters in matrix form. The result is a compact equation which can be conveniently solved using matrix methods. These methods are available, for example, in MatLab® or can be
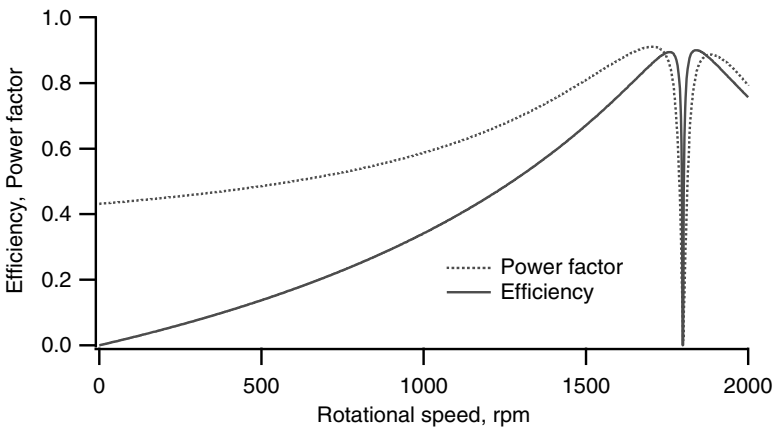
Figure 5.19   Efficiency and power factor of an induction machine

programmed from procedures in Press *et al.* (1992). It can be shown that the matrix equation described the circuit in Figure 5.16 (assuming R_M can be ignored) is:

$$\begin{bmatrix} R_S + j(X_{LS} + X_M) & -(0 + jX_M) \\ (0 - jX_M) & (R'_R/s + j(X'_{LR} + X_M)) \end{bmatrix} \begin{bmatrix} I_{S,r} + jI_{S,i} \\ I_{R,r} + jI_{R,i} \end{bmatrix} = \begin{bmatrix} V \\ 0 \end{bmatrix} \qquad (5.67)$$

Note that the subscripts r and i refer to the real and imaginary components of the current. The matrix form of the equation will also be useful in describing more complex circuits such as those involving wound rotor induction generators (see Section 5.6.3). It is assumed here that the stator voltage, V, has a phase angle of zero.

5.4.4.3 Starting Wind Turbines with Induction Generators

There are two basic methods of starting a wind turbine with an induction generator:

- Using the wind turbine rotor to bring the generator rotor up to operating speed, and then connecting the generator to the grid.
- Connecting the generator to the grid and using it as a motor to bring the wind turbine rotor up to speed.

When the first method is used, the wind turbine rotor must obviously be self-starting. This method is common with pitch-controlled wind turbines, which are normally self-starting. Monitoring of the generator speed is required so that it may be connected when the speed is as close to synchronous speed as possible.

The second method is commonly used with stall-controlled wind turbines. In this case, the control system must monitor the wind speed and decide when the wind is in the appropriate range for running the turbine. The generator may then be connected directly 'across the line' to the electrical grid, and it will start as a motor. In practice, however, across the line is not a desirable method of starting. It is preferable to use some method of voltage reduction or current limiting during starting. Options for doing this are discussed in Section 5.6.3. As the speed of the wind turbine rotor increases, the aerodynamics become more favorable. Wind-induced torque will impel the generator rotor to run at a speed slightly greater than synchronous, as determined by the torque–slip relation described in Section 5.4.4.2.

5.4.4.4 Induction Machine Dynamic Analysis

When a constant torque is applied to the rotor of an induction machine it will operate at a fixed slip. If the applied torque is varying, then the speed of the rotor will vary as well. The relationship can be described by:

$$J \frac{d\omega_r}{dt} = Q_e - Q_r \qquad (5.68)$$

where J is the moment of inertia of the generator rotor, ω_r is the angular speed of the generator rotor (rad/s), Q_e is the electrical torque and Q_r is the torque applied to the generator rotor.

When the applied torque varies slowly relative to the electrical grid frequency, a quasi steady state approach may be taken for the analysis. That is, the electrical torque may be assumed to be

a function of slip as described in Equation (5.66) and preceding equations. The quasi steady state approach may normally be used in assessing wind turbine dynamics. This is because the frequency of fluctuations in the wind-induced torque and those of mechanical oscillations are generally much less than the grid frequency. The induction generator equation used in this way was applied, for example, in the dynamic wind turbine drive train model, *DrvTrnVB*. This is described in Manwell *et al.* (1996).

It is worth noting that induction machines are somewhat 'softer' in their dynamic response to changing conditions than are synchronous machines. This is because induction machines undergo a small, but significant, speed change (slip) as the torque in or out changes. Synchronous machines, as indicated previously, operate at constant speed, with only the power angle changing as the torque varies. Synchronous machines thus have a very 'stiff' response to fluctuating conditions.

5.4.4.5 Off-design Operation of Induction Machines

Induction machines are designed for operation at a particular operating point. This operating point is normally the rated power at a particular frequency and voltage. In wind turbine applications, there are a number of situations when the machine may run at off-design conditions. Four of these situations are:

- starting (mentioned above);
- operation below rated power;
- variable-speed operation;
- operation in the presence of harmonics.

Operation below rated power, but at rated frequency and voltage, is a very common occurrence. It generally presents few problems. The efficiency and power factor are normally both lower under such conditions, however. Operating behavior below rated power may be examined through application of the induction machine equivalent circuit and the associated equations.

There are a number of presumed benefits of running a wind turbine rotor at variable speed. A wind turbine with an induction generator can be run at variable speed if an electronic power converter of appropriate design is included in the system between the generator and the rest of the electrical network. Such converters work by varying the frequency of the AC supply at the terminals of the generator. These converters must also vary the applied voltage. This is because an induction machine performs best when the ratio between the frequency and voltage ('Volts to Hertz ratio') of the supply is constant (or nearly so.) When that ratio deviates from the design value, a number of problems can occur. Currents may be higher, for example, resulting in higher losses and possible damage to the generator windings. Figure 5.20, for example, compares currents for an induction machine operated at its rated frequency and half that value, but both at the same voltage. The machine in this case is the same one used in the previous example (Figure 5.18).

Operation in the presence of harmonics can occur if there is a power electronic converter of significant size on the system to which the machine is connected. This would be the case for a variable-speed wind turbine, and could also be the case in isolated electrical networks (see Chapter 9). Harmonics are AC voltages or currents whose frequency is an integer multiple of
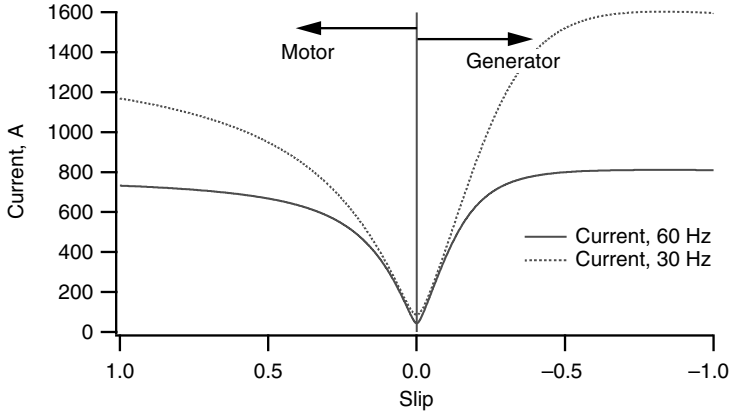
Figure 5.20   Current at different frequencies

the fundamental grid frequency. The source of harmonics is discussed in Section 5.5.4. Harmonics may cause bearing and electrical insulation damage and may interfere with electrical control and data signals as well.

5.4.5 DC Generators

An historically important type of electrical machine for wind turbine applications is the shunt wound DC generator. These were once used commonly in smaller, battery-charging wind turbines. In these generators the field is on the stator and the armature is on the rotor. The electric field is created by currents passing through the field winding which is in parallel ('shunt') with the armature windings. A commutator on the rotor in effect rectifies the generated power to DC. The full generated current must be passed out through the commutator and brushes.

In these generators, the field current, and hence magnetic field (up to a point), increases with operating speed. The armature voltage and electrical torque also increase with speed. The actual speed of the turbine is determined by a balance between the torque from the turbine rotor and the electrical torque.

DC generators of this type are seldom used today because of high costs and maintenance requirements. The latter are associated particularly with the brushes. More details on generators of this type may be found in Johnson (1985).

5.4.6 Permanent Magnet Generators

A type of electrical machine that is being used more frequently in wind turbine applications is the permanent magnet generator. This is now the generator of choice in most small wind turbine generators, up to at least 10 kW, and they can be used in larger wind turbines as well. In these generators, permanent magnets provide the magnetic field, so there is no need for field windings or supply of current to the field. In one example, the magnets are integrated directly into a cylindrical cast aluminum rotor. The power is taken from a stationary armature, so there is

no need for commutator, slip rings, or brushes. Because the construction of the machine is so simple, the permanent magnet generator is quite rugged.

The operating principles of permanent magnet generators are similar to those of synchronous machines. In fact, they are frequently referred to as permanent magnet synchronous generators, with the acronym PMSG. The main difference is that the field is provided by permanent magnets instead of electromagnets. In addition, these machines are usually run asynchronously. That is, they are not generally connected directly to the AC network. The power produced by the generator is initially variable voltage and frequency AC. This AC is often rectified immediately to DC. The DC power is then either directed to DC loads or battery storage, or else it is inverted to AC with a fixed frequency and voltage. In the latter case, they are an option for variable-speed wind turbines, as discussed in Section 5.6. See Section 5.5 for a discussion of power electronic converters. Development of a permanent magnet generator specifically for wind turbine applications is described by Fuchs *et al.* (1992).

5.4.7 Other Electrical Machines

There are at least two other types of generators that may be considered for wind turbine applications: (1) direct drive generators and (2) switched reluctance generators.

Direct drive generators are essentially synchronous machines of special design. The main difference from standard machines is that they are built with a sufficient number of poles to enable the generator rotor to turn at the same speed as the wind turbine rotor. This eliminates the need for a gearbox. Because of the large number of poles, the diameter of the generator is relatively large. Direct drive generators on wind turbines are frequently used in conjunction with power electronic converters. This provides some leeway in the voltage and frequency requirements of the generator itself. Their use in variable-speed wind turbines is described in Section 5.6.1.

Switched reluctance generators employ a rotor with salient poles (without windings). As the rotor turns, the reluctance of the magnetic circuit linking the stator and rotor changes. The changing reluctance varies the resultant magnetic field and induces currents in the armature. A switched reluctance generator thus does not require field excitation. The switched reluctance generators currently being developed are intended for use with power electronic converters. Switched reluctance generators need little maintenance due to their simple construction. There are no switched reluctance generators currently being used in commercial wind turbines, but research towards that end is underway. See Hansen *et al.* (2001) for more information on switched reluctance generators.

5.4.8 Generator Mechanical Design

There are a number of issues to consider regarding the mechanical design of a generator. The rotor shaft and main bearings are designed according to the basic principles to be discussed in Chapters 6 and 7. The stator housing of the generator is normally of steel. Commercial generator housings come in standard frame sizes. Windings of the armature (and field when applicable) are of copper wire, laid into slots. The wire is not only insulated, but additional insulation is added to protect the windings from the environment and to stabilize them. Different types of insulation may be specified depending on the application.
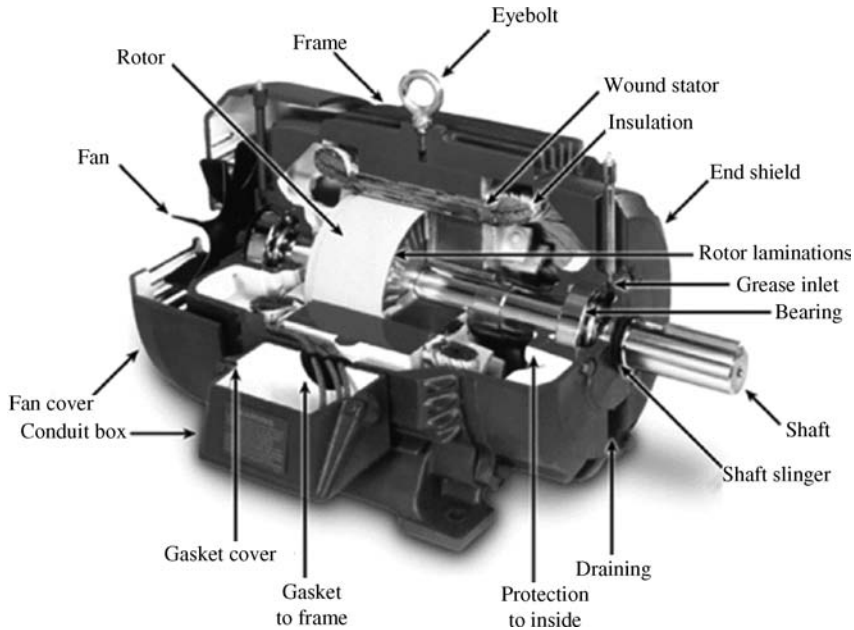
Figure 5.21   Construction of typical three-phase induction machine (Rockwell International Corp.)

The exterior of the generator is intended to protect the interior from condensation, rain, dust, blowing sand, etc. Two designs are commonly used: (1) open drip-proof and (2) totally enclosed, fan-cooled (TEFC). The open drip-proof design has been used on many wind turbines, because it is less expensive than other options, and it has been assumed that the nacelle is sufficient to protect the generator from the environment. In many situations, however, it appears that the additional protection provided by a TEFC design may be worth the cost.

A schematic of a typical induction machine (squirrel cage) is illustrated in Figure 5.21.

5.4.9 Generator Specification

Wind turbine designers are not, in general, generator designers. They either select commercially available electrical machines, with perhaps some minor modifications, or they specify the general requirements of the machine to be specially designed. The basic characteristics of the important generator types have been discussed previously. The following is a summary list of the key considerations from the point of view of the wind turbine designer:

- operating speed;
- efficiency at full load and part load;
- power factor and source of reactive power (induction machines);
- voltage regulation (synchronous machines);
- method of starting;
- starting current (induction machines);
- synchronizing (synchronous machines);

- frame size and generator weight;
- type of insulation;
- protection from environment;
- ability to withstand fluctuating torques;
- heat removal;
- feasibility of using multiple generators;
- operation with high electrical noise on conductors.

5.5 Power Converters

5.5.1 Overview of Power Converters

Power converters are devices used to change electrical power from one form to another, as in AC to DC, DC to AC, one voltage to another, or one frequency to another. Power converters have many applications in wind energy systems. They are being used more often as the technology develops and as costs drop. For example, power converters are used in generator starters, variable-speed wind turbines, and in isolated networks. This section provides an overview of many of the types of power converters that are used in wind energy applications. For more details, see Baroudi *et al.* (2007), Bhadra *et al.* (2005), Ackerman (2005), or Thorborg (1988).

Modern converters are power electronic devices. Basically, these consist of an electronic control system turning on and off electronic switches, often called 'valves.' Some of the key circuit elements used in the inverters include diodes, silicon-controlled rectifiers (SCRs, also known as thyristors), gate turn off thyristors (GTOs), and power transistors. Diodes behave as one-way valves. SCRs are essentially diodes which can be turned on by an external pulse (at the 'gate'), but are turned off only by the voltage across them reversing. GTOs are SCRs which may be turned off as well as on. Transistors require the gate signal to be continuously applied to stay on. The overall function of power transistors is similar to GTOs, but the firing circuitry is simpler. The term 'power transistor,' as used here, includes Darlingtons, power MOSFETS, and insulated gate bipolar transistors (IGBTs). The present trend is towards increasing use of IGBTs. Figure 5.22 shows the symbols used in this chapter for the most important power converter circuit elements.

5.5.2 Rectifiers

Rectifiers are devices which convert AC into DC. They may be used in: (1) battery-charging wind systems or (2) as part of a variable-speed wind power system.
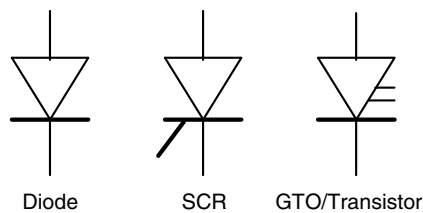
Figure 5.22 Converter circuit elements; SCR, silicon-controlled rectifier; GTO, gate turn off thyristor
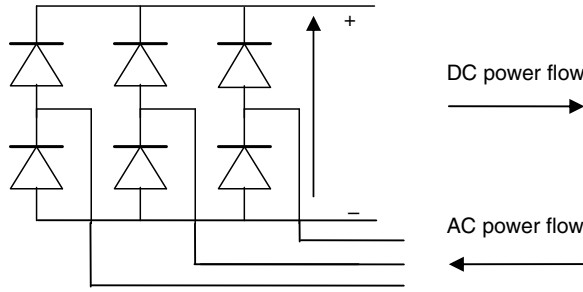
Figure 5.23   Diode bridge rectifier using three-phase supply

The simplest type of rectifier utilizes a diode bridge circuit to convert the AC to fluctuating DC. An example of such a rectifier is shown in Figure 5.23. In this rectifier, the input is three-phase AC power; the output is DC.

Figure 5.24 illustrates the DC voltage that would be produced from a three-phase, 480 V supply using the type of rectifier shown in Figure 5.23. Some filtering may be done (as with the inductors shown in the figure) to remove some of the fluctuations. See Section 5.5.4 for a discussion of filtering. The average DC voltage, V_{DC}, resulting from rectifying a three-phase voltage of RMS V_{rms} is:

$$V_{DC} = \frac{3\sqrt{2}}{\pi} V_{LL} \tag{5.69}$$

5.5.2.1 Controlled Rectifiers

In some cases it is useful to be able to vary the output voltage of a rectifier. This may be done by using a controlled rectifier. In this case the primary elements in the bridge circuit are SCRs rather than diodes, as illustrated in Figure 5.25. The SCRs remain off until a certain fraction
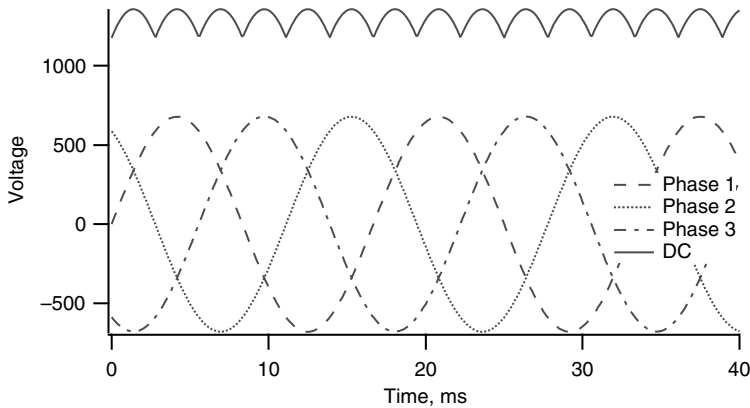
Figure 5.24   DC voltage from three-phase rectifier
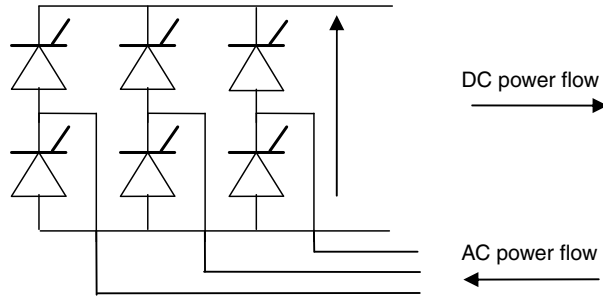
Figure 5.25   Controlled bridge rectifier using three-phase supply

through the cycle, corresponding to the firing delay angle, α, and then they are turned on. The average voltage out of the SCR then is reduced by the cosine of the firing delay angle, as shown in Equation (5.70). A typical rectified waveform (with a firing delay angle of 60°) is illustrated in Figure 5.26. The upper line there is the DC voltage; the others are the phase voltages.

$$V_{DC} = \frac{3\sqrt{2}}{\pi} V_{LL} \cos(\alpha) \qquad (5.70)$$

5.5.3 Inverters

5.5.3.1 Overview of Inverters

In order to convert DC to AC, as from a battery or from rectified AC in a variable-speed wind turbine, an inverter is used. Historically, motor generator sets have been used to convert DC into AC. These are AC generators driven by DC motors. This method is very reliable, but is also expensive and inefficient. Because of their reliability, however, they are still used in some demanding situations.
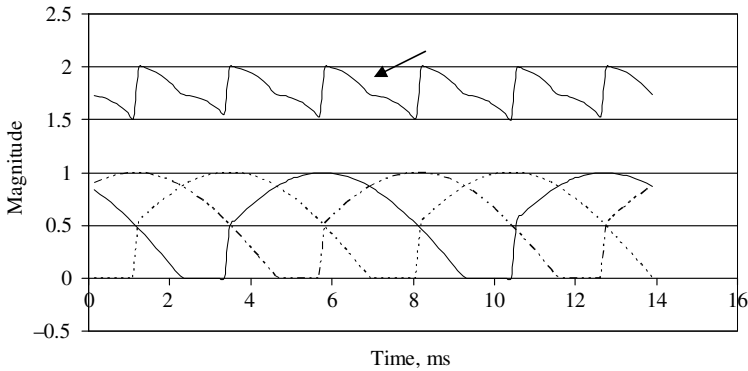
Figure 5.26   DC voltage from phase-controlled rectifier
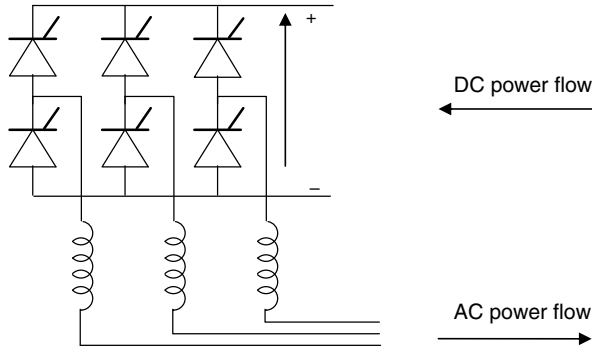
Figure 5.27   Line-commutated silicon-controlled rectifier (SCR) inverter

At the present time most inverters are of the electronic type. An electronic inverter typically consists of circuit elements that switch high currents and control circuitry that coordinates the switching of those elements. The control circuitry determines many aspects of the successful operation of the inverter. There are two basic types of electronic inverter: line-commutated and self-commutated inverters. The term commutation refers to the switching of current flow from one part of a circuit to another.

Inverters that are connected to an AC grid and that take their switching signal from the grid are known by the rather generic name of line-commutated inverters. Figure 5.27 illustrates an SCR bridge circuit, such as is used in a simple three-phase line-commutated inverter. The circuit is similar to the three-phase bridge rectifier shown above, but in this case the timing of the switching of the circuit elements is externally controlled and the current flows from the DC supply to the three-phase AC lines.

Self-commutated inverters do not need to be connected to an AC grid. Thus, they can be used for autonomous applications. They tend to be more expensive than line-commutated inverters.

The actual circuitry of inverters may be of a variety of designs, but inverters fall into one of two main categories: (1) voltage source inverters and (2) current source inverters. In current source inverters, the current from the DC source is held constant regardless of the load. They are typically used to supply high power factor loads where the impedance is constant or decreasing at harmonic frequencies. Overall efficiencies are good (around 96%), but the control circuitry is relatively complex. Voltage source inverters operate from a constant voltage DC power source. They are the type most commonly used to date in wind energy applications. (Note that most of the devices described here can operate as rectifiers or inverters, so the term converter is also appropriate.)

5.5.3.2 Voltage Source Inverters

Within the voltage source inverter category are two main types of interest: (1) six-pulse inverters and (2) pulse width modulation (PWM) inverters.

The simplest self-commutated voltage source inverter, referred to here as the 'six-pulse' inverter, involves the switching on and off of a DC source through different elements at specific time intervals. The switched elements are normally GTOs or power transistors, but SCRs with turn-off circuitry could be used as well. The circuit combines the resulting pulse into a
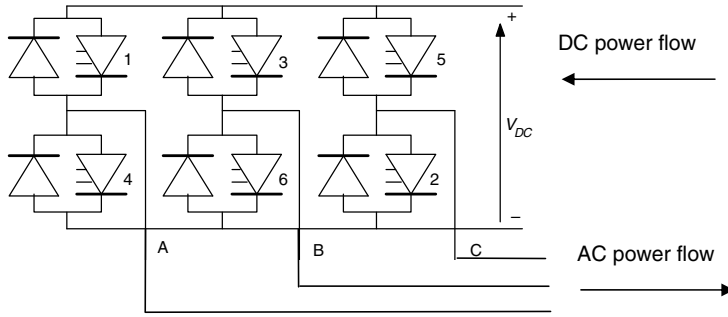
Figure 5.28 Voltage source inverter circuit

staircase-like signal, which approximates a sinusoid. Figure 5.28 illustrates the main elements in such an inverter. Once again, the circuit has six sets of switching elements, a common feature of three-phase inverter and rectifier circuits, but in this case both switching on and off of the switches can be externally controlled.

If the valves are switched on one sixth of a cycle apart, in sequence according to the numbers shown on the figure, and if they are allowed to remain on for one-third of a cycle, an output voltage of a step-like form will appear between any two phases of the three-phase terminals, A, B, and C. A few cycles of such a waveform (with a 60 Hz fundamental frequency) are illustrated in Figure 5.29.

It is apparent that the voltage is periodic, but that it also differs significantly from a pure sine wave. The difference can be described by the presence of harmonic frequencies resulting from the switching scheme. These harmonics arise because of the nature of the switching. Some type of filtering is normally needed to reduce the effect of these harmonics. Harmonics and filtering are discussed in more detail in Section 5.5.4.

In pulse width modulation (PWM), an AC signal is synthesized by the high-frequency switching on and off of the supply voltage to create pulses of a fixed height. The duration ('width') of the pulse may vary. Many pulses will be used in each half wave of the desired output. Switching frequencies on the order of 8 to 20 kHz may be used. The rate of switching is
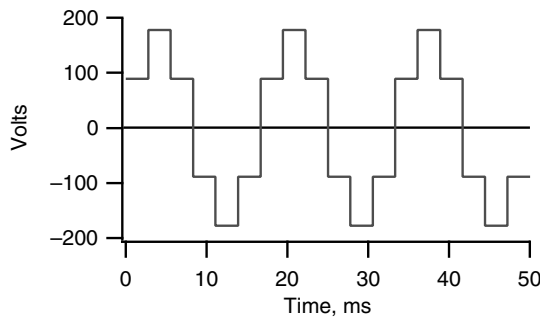
Figure 5.29 Self-commutated inverter voltage waveform
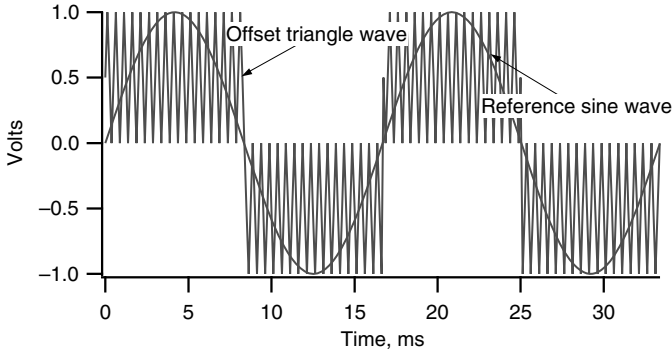
Figure 5.30 Pulse width modulation (PWM) control waves

limited by the losses that occur during the switching process. Even with such losses, inverter efficiencies can be 94%. PWM inverters normally use power transistors (IGBTs) or GTOs as the switching elements.

Figure 5.30 illustrates the principle behind one method of obtaining pulses of the appropriate width. In this method a reference sine wave of the desired frequency is compared with a high-frequency offset triangle wave. Whenever the triangle wave becomes less than the sine wave, the transistor is turned on. When the triangle next becomes greater than the sine wave, the transistor is turned off. An equivalent approach is taken during the second half of the cycle. Figure 5.30 includes two complete reference sine waves, but note that the triangle wave is of a much lower frequency than would be used in a real application. The pulse train corresponding to Figure 5.30 is shown in Figure 5.31. It is apparent that the pulses (in the absolute sense) are widest near the peaks, so the average magnitudes of the voltages are greatest there, as they should be. The voltage wave is still not a pure sine wave, but it does contain a few low-frequency harmonics, so filtering is easier. Other methods are also used for generating pulses of the appropriate width. Some of these are discussed in Thorborg (1988) and Bradley (1987).
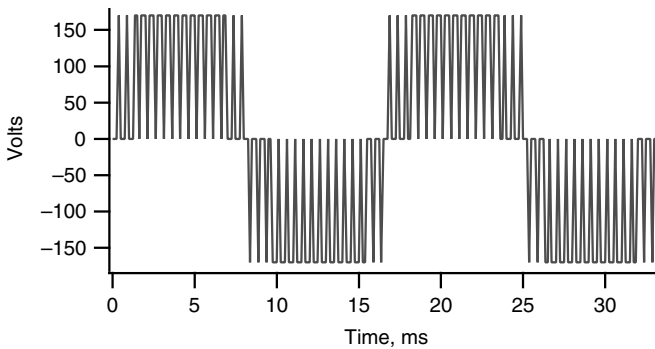
Figure 5.31 Pulse width modulation (PWM) voltage pulse train

5.5.4 Harmonics

Harmonics are AC voltages or currents whose frequency is an integer multiple of the fundamental grid frequency. Harmonic distortion refers to the effect on the fundamental waveform of non-sinusoidal or higher frequency voltage or current waveforms resulting from the operation of electrical equipment using solid state switches. Harmonic distortion is caused primarily by inverters, industrial motor drives, electronic appliances, light dimmers, fluorescent light ballasts, and personal computers. It can cause overheating of transformers and motor windings, resulting in premature failure of the winding insulation. The heating caused by resistance in the windings and eddy currents in the magnetic cores is a function of the square of the current. Thus, small increases in current can have a large effect on the operating temperature of a motor or transformer. A typical example of harmonic distortion of a current waveform is illustrated in Figure 5.32.

Harmonic distortion is often characterized by a measure called total harmonic distortion (THD), which is the ratio of the total energy in the waveform at all of the harmonic frequencies to the energy in the waveform at the basic system frequency. The higher the THD, the worse the waveform. More on calculating THD and on standards for THD can be found in Chapter 9.

Any periodic waveform $v(t)$ can be expressed as a Fourier series of sines and cosines:

$$v(t) = \frac{a_0}{2} + \sum_{n=1}^{\infty} \left\{ a_n \cos\left(\frac{n\pi t}{L}\right) + b_n \sin\left(\frac{n\pi t}{L}\right) \right\} \tag{5.71}$$

where n is the harmonic number, L is half the period of the fundamental frequency, and

$$a_n = \frac{1}{L} \int_0^{2L} v(t)\cos\left(\frac{n\pi t}{L}\right) dt \tag{5.72}$$

$$b_n = \frac{1}{L} \int_0^{2L} v(t)\sin\left(\frac{n\pi t}{L}\right) dt \tag{5.73}$$

The fundamental frequency corresponds to $n = 1$. Higher order harmonic frequencies are those for which $n > 1$. For normal AC voltages and currents there is no DC component, so in general $a_0 = 0$.
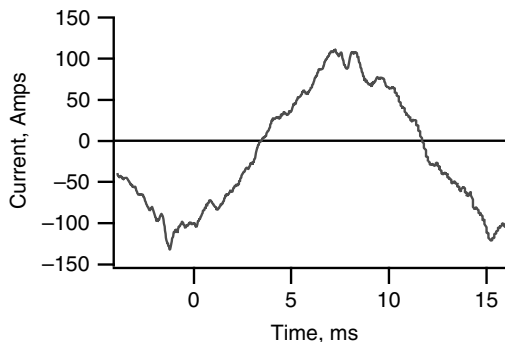
Figure 5.32 Example of harmonic distortion
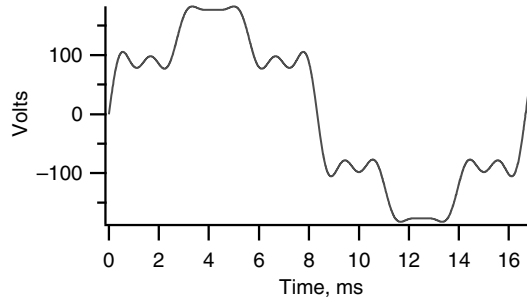
Figure 5.33   Fourier series of voltage; fifteen terms

Figure 5.33 shows an approximation to the converter voltage output shown originally in Figure 5.27. The approximation is done with 15 frequencies in the Fourier series. Note that if more terms were added, the mathematical approximation would be more accurate and the ripples would decrease. Since the voltage as shown is an odd function, that is $f(-x) = -f(x)$, only sine terms are non-zero.

The relative magnitudes of the coefficients of the various harmonic voltages are shown in Figure 5.34. (It can be shown, in general, for this particular wave that all higher harmonics are zero except those for which $n = 6\,k \pm 1$ where $k = 0$, 1, 2, 3, etc. and $n > 0$.)

5.5.4.1 Harmonic Filters

Since the voltage and current waveforms from power electronic converters are never pure sine waves, electrical filters are frequently used. These improve the waveform and reduce the adverse effects of harmonics. Harmonic filters of a variety of types may be employed, depending on the situation. The general form of an AC voltage filter includes a series impedance and a parallel impedance, as illustrated in Figure 5.35.

In Figure 5.35 the input voltage is V_1 and the output V_2. The ideal voltage filter results in a low reduction in the fundamental voltage and a high reduction in all the harmonics.
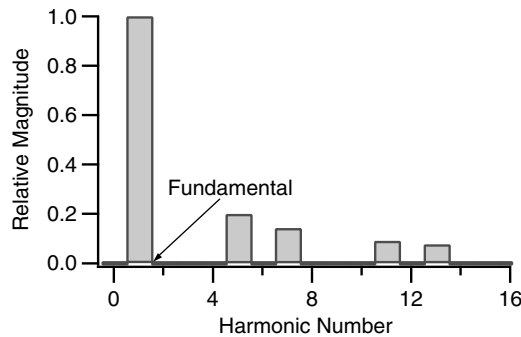
Figure 5.34   Relative harmonic content of voltage
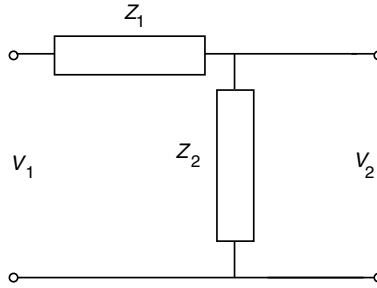
Figure 5.35 AC voltage filter; V_1. AC voltage at filter input; V_2. AC voltage at filter output; Z_1 resonant filter series impedance; Z_2 resonant filter parallel impedance

An example of an AC voltage filter is the series–parallel resonance filter. It consists of one inductor and capacitor in series with the input voltage and another inductor and capacitor in parallel, as shown in Figure 5.36.

As discussed in most basic electrical engineering texts, a resonance condition exists when inductors and capacitors have a particular relation to each other. The effect of resonance in a capacitor and inductor in series is, for example, to greatly increase the voltage across the capacitor relative to the total voltage across the two. Resonance in a filter helps to make the higher-order harmonics small relative to the fundamental. The resonance condition requires, for the capacitor and inductor in series, that:

$$L_1 2\pi f = \frac{1}{C_1 2\pi f}(= X') \tag{5.74}$$

where X' is the reactance of either the capacitor or the inductor and f is the frequency of the fundamental. For the capacitor and inductor in parallel, resonance implies that:

$$C_2 2\pi f = \frac{1}{L_2 2\pi f}(= Y'') \tag{5.75}$$

where $Y'' =$ the reciprocal of the reactance ('admittance') of either the capacitor or the inductor.
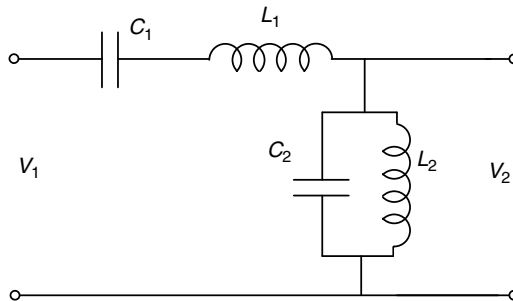
Figure 5.36 Series–parallel resonance filter; C_1 and L_1 series capacitance and inductance, respectively; C_2 and L_2 parallel capacitance and inductance, respectively; V_1 and V_2 input and output voltages, respectively

For this particular filter, the output voltage harmonics will be reduced relative to the input by the following scale factor:

$$f(n) = \left| \frac{V_n}{V_1} \right| = \left| \frac{1}{1 - [n - (1/n)]^2 X' Y''} \right| \qquad (5.76)$$

From Equation (5.76), $f(1) = 1$ and $f(n)$ approaches $1/n^2$ for high values of n. For certain values of n, the denominator of Equation (5.76) goes to zero, indicating a resonant frequency. For example, there is a resonant frequency for a value of $n > 1$ at:

$$n = \tfrac{1}{2} \left[\sqrt{\frac{1}{X'Y''}} + \sqrt{\left(\frac{1}{X'Y''} + 4 \right)} \right] \qquad (5.77)$$

Near this resonant frequency, input harmonics are amplified. Thus, this resonant frequency should be chosen lower than the lowest occurring input harmonic voltage.

Further discussion of filters is outside the scope of this text. It is important to realize, however, that sizing of the inductors and capacitors in a filter is related to the harmonics to be filtered. Higher frequency harmonics can be filtered with smaller components. As far as filtering is concerned, then, the higher the switching rate in a PWM inverter, for example, the better. This is because higher switching rates can reduce the lower frequency harmonics, but increase higher ones. More information on filters is given in Thorborg (1988).

5.6 Electrical Aspects of Variable-Speed Wind Turbines

Variable-speed operation of wind turbines is often desirable for two reasons: (1) below rated wind speed, the wind turbine rotor can extract the most energy if the tip speed ratio can be kept constant, requiring that the rotor speed vary with the wind speed, and (2) variable-speed operation of the turbine's rotor can result in reduced fluctuating stresses, and hence reduced fatigue, of the components of the drive train. While variable-speed operation of the turbine rotor may be desirable, however, such operation complicates the generation of AC electricity at a constant frequency.

There are, at least in principle, a variety of ways to allow variable-speed operation of the turbine rotor, while keeping the generating frequency constant. These may be either mechanical or electrical, as described by Manwell *et al.* (1991). Nearly all of the approaches to variable-speed operation of wind turbines in use today, however, are electrical. Variable-speed operation is possible with the following types of generators:

- synchronous generators;
- induction generators (squirrel cage);
- wound rotor induction generators;
- switched reluctance generators.

The following discusses the first three of the above, which are the most common. As already noted, discussion of switched reluctance generators can be found in Hansen *et al.* (2001).
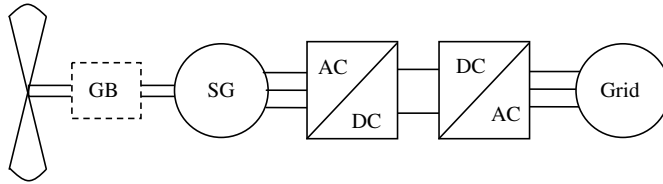
Figure 5.37   Variable-speed wind turbine with synchronous generator

5.6.1 Variable-speed Operation of Synchronous Generators

As explained previously, there are basically two types of synchronous generator: (1) those whose fields are separately excited, and (2) those whose fields are provided by permanent magnets. In either case the output frequency is a direct function of the speed of the generator and the number of poles that it has. This was quantified in Equation (5.42). For a synchronous generator to be used in a variable-speed wind turbine, the output of the generator must first be rectified to DC and then converted back to AC. An arrangement that would allow this to take place is shown in Figure 5.37. In this figure the wind turbine's rotor is shown on the left-hand side. Moving progressively towards the right are the main shaft, gearbox (GB), generator (SG), rectifier (AC/DC), DC link, inverter (DC/AC), and grid. The inverter may be either a diode rectifier or a controlled rectifier, depending on the situation. The inverter may either be an SCR inverter or a PWM inverter. In the case of a separately excited synchronous generator, there may be voltage control on the generator itself. If it is a permanent magnet synchronous generator, voltage control must take place somewhere in the converter circuit. Some wind turbines use a multiple pole synchronous generator with a sufficient number of poles that the generator may be directly connected to the main shaft, with no need for a gearbox. In this case, it is referred to as a direct drive generator. Accordingly, the gearbox in Figure 5.37 is shown with a dotted line, indicating that it may or may not be included. It should be noted that direct drive, multipole generators are physically much larger than are generators commonly used with gearboxes.

5.6.2 Variable-speed Operation of Squirrel Cage Induction Generators

Conventional, squirrel cage induction generators (SQIG) may be used in variable-speed wind turbines, although the method of doing so is not as conceptually straightforward as that of synchronous generators. In particular, induction generators require a source of reactive power, which must be supplied by a power electronic converter. These converters are expensive and they also introduce additional losses into the system. The losses are often of the same order of magnitude as the gains in aerodynamic efficiency, so the net gain in energy production may be relatively small. In this case, the main benefit of variable-speed operation could be in the reduction of fatigue damage to the rest of the turbine.

A typical variable-speed squirrel cage induction generator configuration is illustrated in Figure 5.38. This figure shows the wind turbine rotor, gearbox, induction generator, two PWM power converters, a DC link between them, and the electrical grid. In this configuration the generator side converter (PWM 1) provides reactive power to the generator rotor as well as accepting real power from it. It controls the frequency to the generator rotor, and hence its
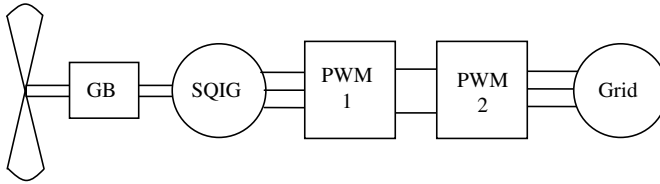
Figure 5.38   Variable-speed wind turbine with squirrel cage induction generator

speed. PWM 1 also converts the rotor power to DC. The grid side power converter (PWM 2) converts the DC power to AC at the appropriate voltage and frequency. Note that there may be other components in the circuit, including capacitors, inductors, or transformers.

5.6.3 Variable-speed Operation with Wound Rotor Induction Generators

Another approach to variable-speed turbine operation is through the use of a wound rotor induction generator (WRIG). Wound rotor induction generators are similar in many ways to squirrel cage induction generators, except in the design of their rotors. The rotor in the WRIG, as the name implies, has windings of copper wire rather than metal bars. The stator has windings just as in the SQIG. The ends of the rotor windings are accessible, normally via brushes and slip rings. Power can either be extracted or injected into the rotor via these brushes and slip rings. WRIGs have many of the features of squirrel cage induction generators, in that they are compact and fairly rugged (except for the brushes and slip rings). They are also less expensive than synchronous generators, although they are more expensive than SQIGs. The main advantage of the WRIG is that it is possible to have variable-speed operation of the wind turbine while using power converters of approximately 1/3 of the capacity that would be required if all the power were to go through the converters. The converters will not only be smaller but they will also be less expensive than those that would be used with either SGs or SQIGs of the same rating.

Wound rotor induction generators can be used in a variety of ways to facilitate variable-speed operation. These include: (1) high slip operation, (2) slip power recovery) and (3) true variable-speed operation. The following section steps through some of the possibilities. Table 5.2 summarizes the key features of these topologies.

Table 5.2   Topology options for variable-speed wind turbine using wound rotor induction generators

Topology	Rotor side converter	Line side converter	Speed range
High slip	Adjustable resistor	N/A	Limited super-synchronous
Slip power recovery	Rectifier	Inverter	Super-synchronous only
	Phase-controlled rectifier		Super-synchronous; limited subsynchronous
True variable speed	PWM converter	PWM converter	Super or subsynchronous
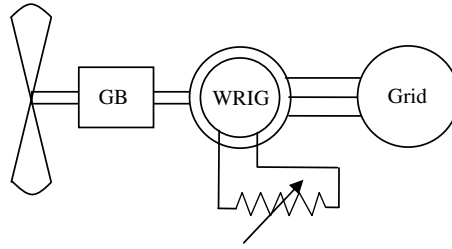
Figure 5.39   Wind turbine with WRIG and external rotor resistance

The first thing to note is that the slip for a given power output of a conventional induction generator can be increased by increasing the resistance of the rotor. This will increase the range of possible operating speeds. Accordingly, one could, in principle, create a variable-speed induction generator by simply increasing the rotor resistance. On the other hand, the losses in the rotor also increase with the resistance, and so the overall efficiency decreases.

5.6.3.1 High Slip Operation

When a wound rotor is used rather than a squirrel cage rotor, there are more options available. For example, since the rotor windings are accessible, they could just be short circuited. In this case the rotor would function just like a squirrel cage rotor. With access to the rotor circuit from the outside, it is also possible to introduce resistance into the circuit at certain times, and remove it at other times. Furthermore, the resistance may be changed depending on the situation. A schematic of this arrangement is shown in Figure 5.39. In this figure the outer circle in the WRIG element corresponds to the stator, the inner circle to the rotor. The external resistor is shown to be variable. The key observation is that when the rotor circuit resistance is made higher by whatever means, the operating speed range is increased. As with a high-resistance rotor, however, this comes at the cost of greater losses, unless the rotor power (known as 'slip power') can be recovered.

The equivalent circuit for one phase of this configuration is illustrated in Figure 5.40. Note that this circuit is very similar to Figure 5.16. The main differences are: (1) the mutual
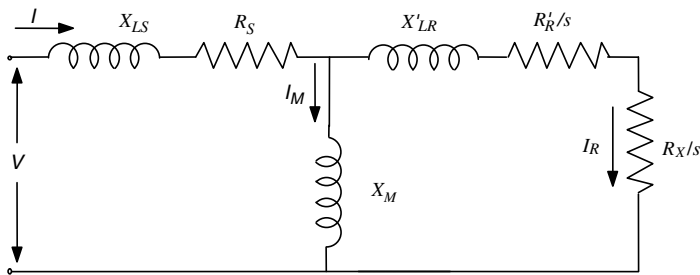
Figure 5.40   Equivalent circuit for WRIG with external rotor resistance

resistance R_M is assumed to be very large, and hence is ignored, (2) an external resistance, R_x. has been added, and (3) use has been made of the following: $R'_R + (1 - s)R'_R/s = R'_R/s$

For many calculations, Equations (5.58)–(5.64) can be used directly, except that $R'_R + R_X$ must be used instead of R'_R. The matrix form of the equation corresponding to the equivalent circuit in Figure 5.40 is Equation (5.78). Note the similarity to Equation (5.67), the only difference being that R'_R has been replaced by $R'_R + R_X$

$$\begin{bmatrix} R_S + j(X_{LS} + X_M) & -(0 + jX_M) \\ (0 - jX_M) & ((R'_R + R_X)/s + j(X'_{LR} + X_M)) \end{bmatrix} \begin{bmatrix} I_{S,r} + jI_{S,i} \\ I_{R,r} + jI_{R,i} \end{bmatrix} = \begin{bmatrix} V \\ 0 \end{bmatrix} \qquad (5.78)$$

The capability of adjusting the external resistance in the rotor circuit can be put to good use, for example by allowing the rotor to accelerate briefly in a gust. In order to do this safely, however, the stator current must be kept at or below its rated level. This can be done by varying the external rotor resistance, R_x, according to the following relation:

$$(R'_R + R_X)/s = \text{constant} \qquad (5.79)$$

When the resistance is varied according to Equation (5.79), it is possible to allow the speed of the rotor to vary when desired, but to keep losses low under other conditions. The most straightforward way to vary the external rotor resistance is to have no resistance when the generator output is less than rated, but then to gradually increase the rotor resistance at higher input powers.

By varying the external rotor circuit resistance in accordance with Equation (5.79), as higher winds result in greater shaft input power, stator power can be held constant (with currents kept at rated). The excess shaft power can be dissipated in the external resistance. This provides a convenient way to quickly shed power, for example from a sudden gust of wind. Otherwise, this excess power would have to be accommodated by changing the blade pitch (which might be too slow) or allowing it to overload the generator. This type of control has been applied by Vestas® Wind Systems A/S under the name of Opti-Slip®. This latter implementation is also of particular interest, in that the external resistors remain on the rotor, so no slip rings or brushes are required. Communication is done with fiber optics.

5.6.3.2 Slip Power Recovery

In the method of using a WRIG described above, all of the rotor power, also known as 'slip power' is dissipated immediately and serves no useful purpose. There are, however, a number of ways to recover the slip power. A few of these are described below. First of all, it must be noted that the power coming off the rotor is AC, but its frequency is that of the slip multiplied by the line frequency. Accordingly, the slip power cannot be used directly by conventional AC devices, nor can it just be fed directly into the grid. The slip power can be made useful ('recovered'), however, by first rectifying it to DC and then inverting the DC to grid frequency AC power.

The conceptually simplest arrangement for doing this is illustrated in Figure 5.41. This method changes the effective resistance of the rotor but captures the power otherwise lost in the resistance and allows for a wider range of slips. In this arrangement the power can flow in only one direction, that is to say, out of the rotor. This takes place when the rotor is driven above its synchronous speed. The converter options are the same as those described previously.
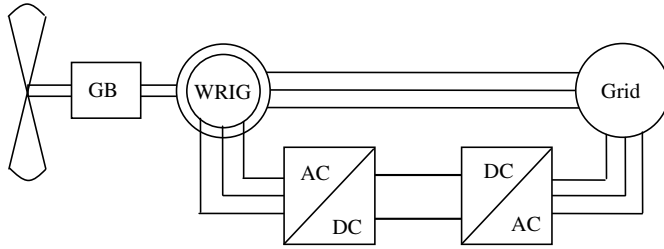
Figure 5.41   Variable-speed wind turbine with WRIG and slip power recovery

The matrix form of the equation for the circuit corresponding to the topology shown in Figure 5.41 is:

$$
\begin{bmatrix} R_S + j(X_{LS} + X_M) & -(0 + jX_M) \\ (0 - jX_M) & \left(\dfrac{R'_R}{s} + j(X'_{LR} + X_M)\right) \end{bmatrix} \begin{bmatrix} I_{S,r} + jI_{S,i} \\ I_{R,r} + jI_{R,i} \end{bmatrix} = \begin{bmatrix} V \\ \dfrac{V_{R,r}}{s} + j\dfrac{V_{R,i}}{s} \end{bmatrix}
\tag{5.80}
$$

where $V_{R,r}$ is the real component of the rotor voltage and $V_{R,i}$ is the imaginary component (both referred to the stator). Note that the difference between Equation (5.80) and (5.78) is that the effect of the voltage at the rotor terminals is now being considered rather than an external resistance in the rotor circuit.

The question arises as to what the voltage across the rotor is. One of the prime requirements is that the stator currents be kept below the current for which the machine is rated. That condition can be maintained as long as $(R_r + R_x)/s \geq$ constant. The rectifier/inverter is not really a resistor. Nonetheless, it could be viewed as a resistive load in which $R_x = V_R/I_R$, where V_R = rotor voltage and I_R = rotor current. The limiting condition for the rotor voltage can be derived from Equation (5.79) above.

We may assume that the rotor current is also limited at some rated value, $I_{R, rated}$. The value of the constant can be determined from the rated conditions, which we assume to occur when the rotor circuit is short circuited:

$$
\text{constant} = R'_{r,rated}/s_{rated}
\tag{5.81}
$$

Accordingly, for any given slip the magnitude of the voltage is:

$$
V_R = I_{R,rated}((R'_{r,rated}/s_{rated})s - R'_r)
\tag{5.82}
$$

The rotor side rectifier can be of the phase-controlled type. In this case, its output is adjustable downwards to zero from some maximum, which is a function of the line voltage and the turns ratio between the rotor and the stator. The actual voltage is then a function of the phase angle of the rectifier. It should also be noted that the rotor voltage and current are out of phase by 180° (indicating that the power is going out of the rotor) in this arrangement.

The control of the rectifier and inverter in the rotor circuit is of great interest, of course, but it is beyond the scope of this text. More details may be found in Petersson (2005) or Bhadra *et al.* (2005).
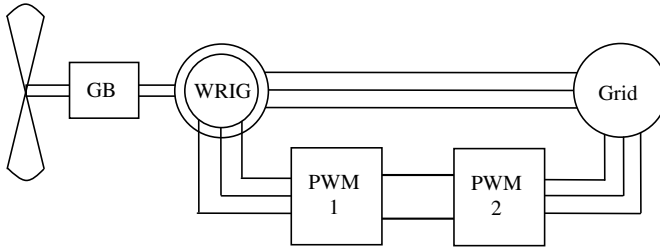
Figure 5.42   Variable-speed operation with turbine with doubly fed WRIG

5.6.3.3 True Variable-speed Operation

In the various types of slip power recovery discussed above, speed during generation would vary from synchronous speed to above synchronous (super-synchronous). This type of operation was always accompanied by conversion of power coming out of the rotor. It is also possible, however, to feed power into the rotor. This arrangement allows operation at subsynchronous speeds, which is a feature of what we call true variable-speed operation. There are various ways that this can be accomplished, but the essential characteristic of these arrangements is that there is a rotor-side converter which is capable of interacting directly with the AC of the rotor. The most common arrangement in wind turbine applications is illustrated in Figure 5.42.

In this arrangement there are two power PWM power converters, separated by a DC link. These power converters are both bidirectional. In super-synchronous operation, converter PWM 1 operates as a rectifier and PWM 2 operates as an inverter; power flows out of the rotor as well as out of the stator. In subsynchronous operation, rotor power goes the other way; PWM 1 operates as an inverter and PWM 2 operates as a rectifier. The complete WRIG generator/ converter system often goes under the name of 'doubly fed induction generator (DFIG).' The term emphasizes the ability of this arrangement to transfer power into or out of the rotor, as well as out of the stator.

In the simplest view of the DFIG, power transfer into or out of the rotor takes place with both the voltage and the current in phase. Thus, the rotor load looks like either a resistor or a 'negative resistor.' In reality, however, the PWM converters have the capability of providing current and voltage at different phase angles. This capability has many advantages. In particular, it allows the power factor of the DFIG to be adjusted at will, and even to supply reactive power to the network if so required. The presence of PWM converters in the circuit allows a wide range of control options. These are discussed in various sources, including Petersson (2005), but they are outside the scope of this text.

The DFIG arrangement allows a range of operating speed of the induction generator, from approximately 50% below synchronous speed to 50% above.

Worked Example

Consider a wound rotor induction machine with the following parameters: $R_s = 0.005\,\Omega$, $X_s = 0.01\,\Omega$, $R'_R = 0.004\,\Omega$, $X'_R = 0.008\,\Omega$, $X_m = 0.46\,\Omega$. The line-line voltage is 480 V. The machine is rated as a generator with a nominal power of 2.0 MW at a slip of −0.036. Find:

(a) the rated stator and rotor currents, the actual delivered power, and the input shaft power when the rotor is short circuited. Suppose that an external resistor is added to the rotor circuit to dissipate excess power. The rated current ratings cannot be exceeded. Find (b) the resistance when the slip is −0.4 and (c) the power dissipated in the resistor.

Solution: We can use Equations (5.58)–(5.64) to find that $I_S = 2631$ A, $I_R = 2516$ A, and $P_{out} = -2.006$ MW. The shaft power is −2.186 MW. Using Equation (5.81), together with the rated rotor current of 2516 A and the slip of −0.4, we find the external resistance R_X to be 0.04044 Ω. Using $R'_R + R_X$ in place of R'_R in Equation (5.51), we find the shaft input power to be −2.954 MW. The power dissipated in the external resistor is the new shaft power minus the original shaft power. This is 0.768 MW. Note that if this power were recovered and supplied to the grid, the effective rating of the generator would now be 2.774 MW.

5.7 Ancillary Electrical Equipment

There is a variety of ancillary electrical equipment associated with a wind turbine installation. It normally includes both high-voltage (generator voltage) and low-voltage items. Figure 5.43 illustrates the main high-voltage components for a typical installation. Dotted lines indicate items that are often not included. These items are discussed briefly below.

5.7.1 Power Cables

Power must be transferred from the generator down the tower to electrical switch gear at the base. This is done via power cables. Three-phase generators have four conductors, including
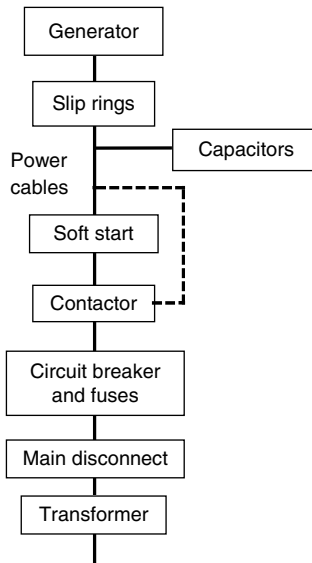
Figure 5.43   Wind turbine high-voltage equipment

the ground or neutral. Conductors are normally made of copper, and they are sized to minimize voltage drop and power losses.

In most larger wind turbines, the conductors are continuous from the generator down the tower to the main contactor. In order that the cables not be wrapped up and damaged as the turbine yaws, a substantial amount of slack is left in them so that they 'droop' as they hang down the tower. The power cables are thus often referred to as droop cables. The slack is taken up as the turbine yaws and then released as it yaws back the other way. With sufficient slack, the cables seldom or never wrap up tight in most sites. When they do wrap up too far, however, they must be unwrapped. This may be done manually, after first disconnecting them, or by using a yaw drive.

5.7.2 Slip Rings

Some turbines, particularly smaller ones, use discontinuous cables. One set of cables is connected to the generator. Another set goes down the tower. Slip rings and brushes are used to transfer power from one set to the other. In a typical application the slip rings are mounted on a cylinder attached to the bottom of the main frame of the turbine. The axis of the cylinder lies on the yaw axis, so the cylinder rotates as the turbine yaws. The brushes are mounted on the tower in such a way that they contact the slip rings regardless of the orientation of the turbine.

Slip rings are not commonly used on larger wind turbines to carry power down the tower, since they become quite expensive as the current-carrying capacity increases. In addition, maintenance is required as the brushes wear. As previously noted, however, slip rings and brushes may be used to carry the slip power out of the rotor of a wound rotor induction generator into the stationary electrical system of the nacelle.

5.7.3 Soft Start

As indicated in Section 5.4.4, induction generators will draw much more current while starting across the line than they produce when running. Starting in this way has numerous disadvantages. High currents can result in early failure of the generator windings, and can result in voltage drops for loads nearby on the electrical network. Rapid acceleration of the entire wind turbine drive train can result in fatigue damage. In isolated grids with a limited supply of reactive power, it may not be possible to start a large induction machine at all.

Due to the high currents that accompany across the line starting of induction machines, most wind turbines employ some form of soft start device. These can take a variety of forms. In general, they are a type of power electronic converter that, at the very least, provides a reduced current to the generator.

5.7.4 Contactors

The main contactor is a switch that connects the generator cables to the rest of the electrical network. When a soft start is employed, the main contactor may be integrated with the soft start or it may be a separate item. In the latter case power may be directed through the main contactor only after the generator has been brought up to operating speed. At this point the soft start is simultaneously switched out of the circuit.

5.7.5 Circuit Breakers and Fuses

Somewhere in the circuit between the generator and the electrical grid are circuit breakers or fuses. These are intended to open the circuit if the current gets too high, presumably as a result of a fault or short circuit. Circuit breakers can be reset after the fault is corrected. Fuses need to be replaced.

5.7.6 Main Disconnect

A main disconnect switch is usually provided between the electrical grid and the entire wind turbine electrical system. This switch is normally left closed, but can be opened if any work is being done on the electrical equipment of the turbine. The main disconnect would need to be open if any work were to be done on the main contactor and would, in any case, provide an additional measure of safety during any electrical servicing.

5.7.7 Power Factor Correction Capacitors

Power factor correction capacitors are frequently employed to improve the power factor of the generator when viewed from the utility. These are connected as close to the generator as is convenient, but typically at the base of the tower or in a nearby control house.

5.7.8 Turbine Electrical Loads

There may be a number of electrical loads associated with the operation of wind turbines. These could include actuators, hydraulic motors, pitch motors, yaw drives, air compressors, control computers, etc. Such loads typically require 120 V or 240 V. Since the generator voltage is normally higher than that, a low-voltage supply needs to be provided by the utility, or step-down transformers need to be obtained.

References

Ackerman, T. (2005) *Wind Power in Power Systems.* John Wiley & Sons, Ltd, Chichester.

Baroudi, J. A, Dinavahi, V. and Knight, A. M. (2007) A review of power converter topologies for wind generators. *Renewable Energy*, **32**(14), 2369–2385.

Bhadra, S. N., Kastha, D. and Banerjee, S. (2005) *Wind Electrical Systems.* Oxford University Press, Delhi.

Bradley, D. A. (1987) *Power Electronics.* Van Nostrand Reinhold, Wokingam, UK.

Brown, D. R. and Hamilton, E. P. (1984) *Electromechanical Energy Conversion.* Macmillan Publishing, New York.

Chapman, S. J. (2001) *Electric Machinery and Power System Fundamentals.* McGraw-Hill Companies, Columbus.

Fuchs, E. F., Erickson, R. W. and Fardou, A. A. (1992) Permanent magnet machines for operation with large speed variations. *Proc. 1992 American Wind Energy Association Conference,* Washington.

Hansen, L. H., Helle, L., Blaabjerg, F., Ritchie, E., Munk-Nielsen, S., Bindner, H., Sørensen, P. and Bak-Jensen, B. (2001) *Conceptual Survey of Generators and Power Electronics for Wind Turbines*, Risø-R-1205 (EN). Risø National Laboratory, Roskilde, DK.

Johnson, G. L. (1985) *Wind Energy Systems.* Prentice-Hall, Inc., Englewood Cliffs, NJ. (Available from http://eece.ksu.edu/~gjohnson/).

Manwell, J. F., McGowan, J. G. and Bailey, B. (1991) Electrical/mechanical options for variable speed wind turbines. *Solar Energy*, **41**(1), 41–51.

Manwell, J. F., McGowan, J. G., Adulwahid, U., Rogers, A. L. and McNiff, B. P. (1996) A graphical interface based model for wind turbine drive train dynamics. *Proc. 1996 American Wind Energy Association Conference,* Washington.

Nahvi, M. and Edminster, J. A. (2003) *Electric Circuits*, 4th edition, Schaum's Outline Series in Engineering, McGraw Hill Book Co., New York.

Nasar, S. A. and Unnewehr, L. E. (1979) *Electromechanics and Electric Machines*. John Wiley & Sons, Inc., New York.

Petersson, A. (2005) *Analysis, Modeling and Control of Doubly-Fed Induction Generators for Wind Turbines*, PhD Dissertation, Chalmers University of Technology, Göteborg.

Press, W. H., Flannery, B. P., Teukolsky, S. A. and Vetterling, W. T. (1992) *Numerical Recipes in FORTRAN: The Art of Scientific Computing*. Cambridge University Press, Port Chester.

Thorborg, K. (1988) *Power Electronics*. Prentice-Hall, Englewood Cliffs, NJ.

6

Wind Turbine Materials
and Components

6.1 Overview

This chapter considers the materials and components that are commonly used in wind turbines. Since fatigue is so significant to wind turbines, this topic is discussed at some length early in the chapter (Section 6.2). The focus is then on materials that are of particular concern in wind turbines, particularly composites. This is the subject of Section 6.3. Components are discrete items that are used to make up a larger structure. Some components that are widely available from a variety of sources and are common to a wide range of machinery are often called elements. Some of the machine elements most commonly used in wind turbines are discussed in Section 6.4. The various larger components in wind turbines are covered in Section 6.5. How these components are then combined to form a complete turbine is the subject of Chapter 7.

6.2 Material Fatigue

It is well known that many materials which can withstand a load when applied once, will not survive if that load is applied, removed, and then applied again ('cycled') a number of times. This increasing inability to withstand loads applied multiple times is called fatigue damage. The underlying causes of fatigue damage are complex, but they can be most simply conceived of as deriving from the growth of tiny cracks. With each cycle, the cracks grow a little, until the material fails. This simple view is also consistent with another observation about fatigue: the lower the magnitude of the load cycle, the greater the number of cycles that the material can withstand.

6.2.1 Fatigue in Wind Turbines

Wind turbines, by their very nature, are subject to a great number of cyclic loads. The lower bound on the number of many of the fatigue-producing stress cycles in turbine components is

proportional to the number of blade revolutions over the turbine's lifetime. The total cycles, n_L, over a turbine's lifetime would be:

$$n_L = 60\,k\,n_{rotor}H_{op}Y \tag{6.1}$$

where k is the number of cyclic events per revolution, n_{rotor}, is the rotational speed of rotor (rpm), H_{op}, is the operating hours per year and Y is the years of operation.

For blade root stress cycles, k would be at least equal to 1 while, for the drive train or tower, k would be at least equal to the number of blades. A turbine with an rpm of approximately 30 operating 4000 hours per year would experience more than 10^8 cycles over a 20-year lifetime. This may be compared to many other manufactured items, which would be unlikely to experience more than 10^6 cycles over their lifetime.

In fact, the number of cyclic events on a blade can be much more than once per revolution of the rotor. This can be seen, for example, in Figure 4.18. In that case the rotor frequency was just above 1 Hz, but there were a substantial number of cycles in the range of 5 Hz. These would result in fluctuating stresses which would contribute to fatigue damage and would need to be considered in wind turbine design.

6.2.2 Assessment of Fatigue

Procedures have been developed to estimate fatigue damage. Many of these techniques were developed for analysis of metal fatigue, but they have been extended to other materials, such as composites, as well. The following sections summarize fatigue analysis methods most commonly used in wind turbine design. More detail on fatigue in general may be found in Shigley *et al.* (2003), Spotts *et al.* (2003), and Ansell (1987). Information on fatigue in wind turbines is given in Garrad and Hassan (1986), Sutherland *et al.* (1995), and Sutherland (1999). Many relevant reports on material fatigue in wind turbines may be found at http://www.sandia. gov/wind/topical.htm.

The estimation of the fatigue life of a wind turbine component requires three things: (1) appropriate fatigue life properties of the material in question, (2) a model or theory that can be used to determine material damage and component lifetime from the loading and material properties, and (3) a method to characterize the loading incurred by the component during the turbine lifetime. Each of these topics is described below.

6.2.2.1 Fatigue Life Characterization

Fatigue resistance of materials is traditionally tested by subjecting successive samples to a sinusoidally applied load until failure. One type of test is a rotating beam test. A sample is mounted on a test machine and loaded to a given stress with a side load. The sample is then rotated in the machine so that the stress reverses every cycle. The test is continued until the sample fails. The first load is somewhat less than the ultimate load (the maximum load that the sample will withstand). The number of cycles and the load are recorded. The load is then reduced on another sample and the process is repeated. The data is summarized in a fatigue life, or '*S–N*', curve, where *S* refers to the stress (in spite of the customary use of σ to indicate stress) and *N* refers to the number of cycles to failure. Figure 6.1 illustrates a typical *S–N* curve. With tests of this type it is important to note that (1) the mean stress is zero and (2) the stresses are fully reversing.
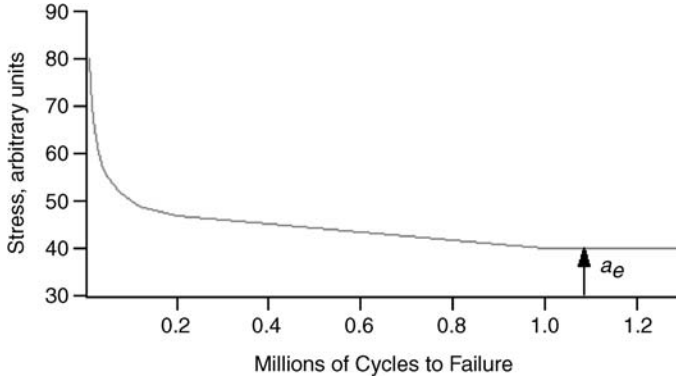
Figure 6.1 Typical *S–N* curve

Most manufactured items of commercial interest, with the exception of wind turbines, do not experience more than 10 million cycles in their lifetimes. Thus, if a sample does not fail after 10^7 cycles at a particular stress (as the loads are progressively reduced), the stress is referred to as the endurance limit, σ_{el}. Endurance limits typically reported are in the range of 20%–50% of the ultimate stress, σ_u, for many materials. (Recall that the ultimate stress is the maximum stress that a material can withstand.) In reality, the material may not actually have a true endurance limit, and it may be inappropriate to use that assumption in wind turbine design.

Alternating Stresses with Non-zero Mean

Alternating stresses typically do not have a zero mean. In this case they are characterized by the mean stress, σ_m, the maximum stress, σ_{max}, and the minimum stress σ_{min}, as shown in Figure 6.2.

The stress range, $\Delta\sigma$, is defined as the difference between the maximum and the minimum.

$$\Delta\sigma = \sigma_{max} - \sigma_{min} \tag{6.2}$$

The stress amplitude, σ_a, is half the range:

$$\sigma_a = (\sigma_{max} - \sigma_{min})/2 \tag{6.3}$$
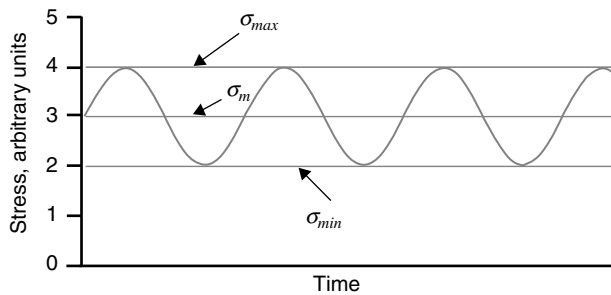
Figure 6.2 Alternating stresses with non-zero mean

The stress ratio, R, is the ratio between the maximum and the minimum. That is:

$$R = \sigma_{\min}/\sigma_{\max} = (\sigma_m - \sigma_a)/(\sigma_m + \sigma_a) \tag{6.4}$$

For alternating stress with zero mean ('completely reversing'), $R = -1$.

An example of alternating stress with a non-zero mean is shown in Figure 6.3.

Goodman Diagram

Material fatigue tests may also be performed at a variety of mean stress levels and amplitudes (or R values). The resulting data may be presented in an *S-N* diagram with multiple curves for the various test conditions or in a Goodman diagram. A Goodman diagram depicts constant-life curves on a plot of stress amplitude versus mean stress. Often, the stress amplitude and mean stress are normalized by the ultimate strength of the material. An example is shown in Figure 6.4.

In Goodman diagrams all points with a constant R value are on a straight line with its origin at zero mean and zero amplitude. Fully reversed bending with a zero mean stress level ($R = -1$) is on the vertical axis. The ultimate compressive strength bounds the fatigue life data on the compressive (left) side of the diagram and the ultimate tensile strength bounds the curves on the tensile (right) side of the diagram. Constant-life curves are shown for 10^5, 10^6, and 10^7 cycles. This example is of a symmetric material for which the left and right sides of the diagram are mirror images of each other.

Goodman diagrams for fiberglass materials are typically not symmetric. For example a Goodman diagram (based on strain rather than stress) for one sample fiberglass composite is shown in Figure 6.5.

As mentioned above, the fatigue life for a given alternating stress depends on R (i.e., the mean). In fact, the allowed alternating stress for a given fatigue life will decrease as the mean increases. This relationship is often approximated by Goodman's Rule:

$$\sigma_{al} = \sigma_e(1 - \sigma_m/\sigma_u)^c \tag{6.5}$$
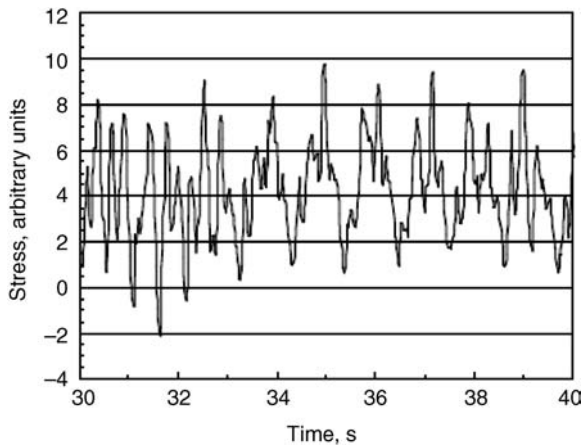
Figure 6.3   Alternating stress with non-zero mean (Sutherland, 2001)
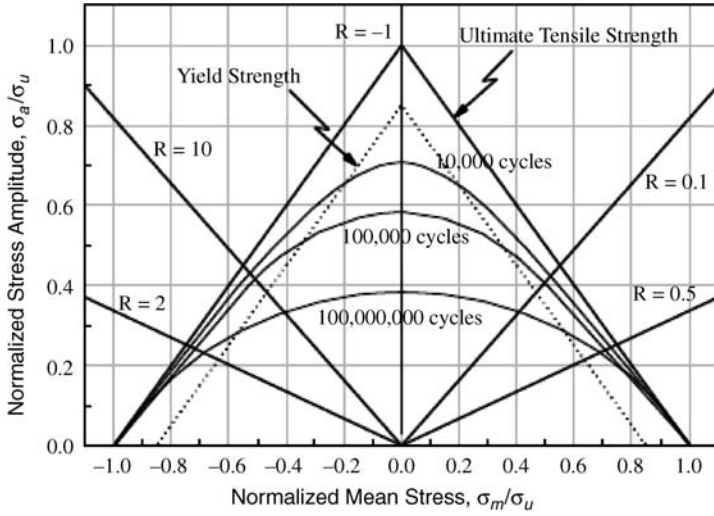
Figure 6.4 Sample Goodman diagram (Sutherland, 1999)

where σ_{al} is the allowable stress amplitude for a given fatigue life, and the mean stress, σ_e is the zero mean ($R = -1$) alternating stress for the desired fatigue life, σ_u is the ultimate stress, and c is an exponent that depends on the material but which is often assumed to be equal to one.

Goodman's Rule can be inverted and used with non-zero mean alternating stress data to find the equivalent zero mean alternating stress (assuming $c = 1$) (see, for example, Ansell (1987)):

$$\sigma_e = \sigma_{al}/(1 - \sigma_m/\sigma_u) \tag{6.6}$$
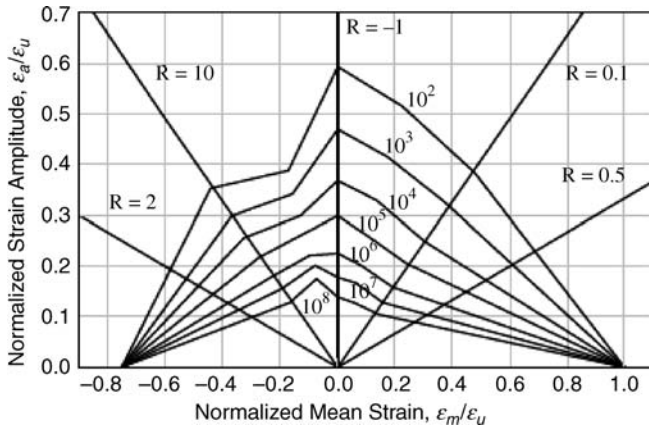
Figure 6.5 Goodman diagram for a sample fiberglass composite (Sutherland, 1999)

6.2.2.2 Fatigue Damage Model

If a component undergoes fewer load cycles than would cause it to fail, it will still suffer damage. The component might fail at a later time, after additional load cycles are applied. To quantify this, a damage term, d, is defined. It is the ratio of the number of cycles applied, n, to the number of cycles to failure, N, at the given amplitude.

$$d = n/N \tag{6.7}$$

This damage model assumes that equivalent amounts of damage occur with each cycle, as opposed to, for example, most of the damage occurring at the end of the life of a component.

Cumulative Damage and Miner's Rule

A component may experience multiple load cycles of different amplitudes, as illustrated in Figure 6.6.

In this case, the cumulative damage, D, is defined by Miner's Rule to be the sum of the damages due to each of the cycles at each amplitude. The component is deemed to have failed when the total damage is equal to 1.0. In the general case of load cycles of M different amplitudes, the cumulative damage would be given by:

$$D = \sum_{i=1}^{M} n_i/N_i \leq 1 \tag{6.8}$$

where n_i is the number of cycles at the ith amplitude and N_i is the number of cycles to failure at the ith amplitude.

To illustrate this, suppose that a material undergoes four cycles each of magnitude 1, 2, and 3 stress units and that the life at those stress units is 20, 16, and 10 cycles respectively. The cumulative damage due to the 12 cycles would be:

$$D = (4/20) + (4/16) + (4/10) = 0.85$$

Randomly Applied Load Cycles

When loads are not applied in blocks (as was the case in Figure 6.6) but rather occur more randomly, it is difficult to identify individual load cycles. Figure 6.7 illustrates such a situation.
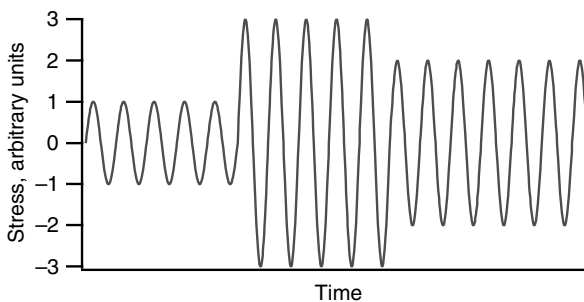
Figure 6.6   Load cycles of different amplitude
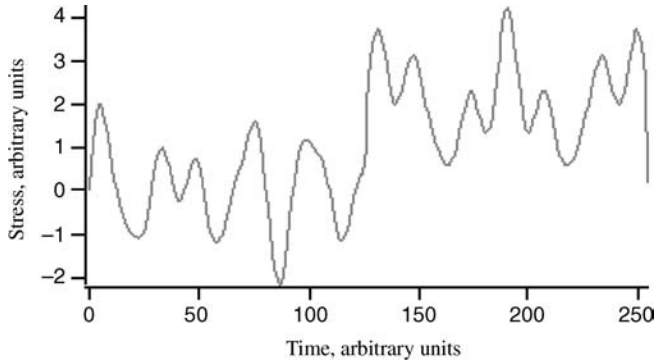
Figure 6.7   Random load cycles

A technique known as rainflow cycle counting (Downing and Socie, 1982) has been developed to identify alternating stress cycles and mean stresses from time series of randomly applied loads. Once the mean and alternating stress data have been found, they can be converted to zero mean alternating stresses and the total damage estimated using Miner's Rule, as discussed above.

The rainflow counting method is most appropriately applied to strain data, rather than stress data, and can deal with inelastic as well as elastic regions of the material. For most wind turbine applications, the material is in the elastic region, so either stress or strain data can be used. When strain is used, results are ultimately converted to stresses.

The essence of the rainflow counting technique is summarized next, and an algorithm for performing the counting is given in Appendix C. Local highs and lows in the data are identified as 'peaks' or 'valleys'. The range between every peak and valley and between every valley and every peak are all considered to be 'half cycles'. The algorithm then pairs the half cycles to find complete cycles, and associates them with a mean.

The term 'rainflow' derives from an aspect of the method, in which the completion of a cycle resembles rain water dripping from a roof (a peak) and meeting water flowing along another roof (from a valley below). In this view of the method, the peak–valley history is imagined to be oriented vertically so that the 'rain' descends with increasing time. An example of a complete cycle is shown in Figure 6.8, which is derived from Figure 6.7. Here rain (indicated by heavy arrows) running down roof C–D encounters rain running down roof E–F. The cycle C–D–E is then eliminated from further consideration, but peak C is retained for use in identifying
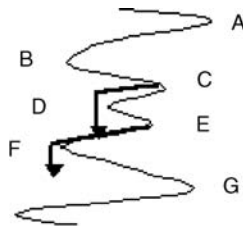
Figure 6.8   Rainflow cycle counting

subsequent cycles. In this particular case, point F is slightly to the left of point B, so the next complete cycle is B–C–F.

Effect of Operating Conditions

The loads that contribute to fatigue of a wind turbine originate from a variety of sources, which are closely connected to the operating conditions. The loads include steady loads from high winds; periodic loads from wind shear, yaw error, yaw motion, and gravity; stochastic loads from turbulence; transient loads from such events as gusts, starts, and stops, etc.; and resonance-induced loads from vibration of the structure. The magnitude of the contribution from each of these load sources to component fatigue will depend on the operational state of the wind turbine. Thus, the task of characterizing the loading on a component, during its lifetime, requires the cumulative counting of damage over all operating states and all stress levels that are encountered during its lifetime. The damage to a component over the course of a year, D_y, can be expressed as:

$$D_y = \sum_{All\ conditions}\ \sum_{All\ stress\ levels} \frac{\#\ of\ stress\ cycles}{\#\ cycles\ to\ failure} \tag{6.9}$$

The conditions that need to be considered include:

1. Normal power production where the fatigue is assumed to be a function of wind speed (between cut-in and cut-out wind speeds).
2. Non-operating states when the turbine is being buffeted by the wind (typically at wind speeds greater than the cut-out wind speed).
3. Normal or emergency start/stop operations or other operations that cause transient loading.

Typically the stress levels are determined using measurements on turbine prototypes or computational models that include a detailed description of the turbulent inflow to the turbine and the structural dynamics of the turbine. The measurements or model outputs describe the strains or moments at specific points in the turbine structure. These must be converted to stress levels in specific components using stress concentration factors, based on the location of the measurements and the geometry of the turbine, and partial safety factors (see Chapter 7). Data are typically collected for multiple ten-minute periods at discrete operating states in order to characterize the stress spectrum (the number of cycles of various ranges) at each operating state. A total of five hours of data at each operating state may be needed to ensure a representative data set. Equations for the damage that occurs during each of the three types of operating states, described above, follow. See Sutherland (1999) for more details.

The cumulative damage from normal operation over the course of a year, $D_{y,O}$, is a function of the stress levels at each wind speed and the frequency of occurrence of each wind speed:

$$D_{y,o} = C \sum_{i=U_{in}}^{U_{out}} \sum_j \sum_k F_{U_i} \frac{n(\sigma_{m,j}, \sigma_{a,k}, U_i, \Delta t)_O}{N(\sigma_{m,j}, \sigma_{a,k})} \tag{6.10}$$

where:

C = constant for adjusting time to appropriate units, total number of time intervals per year
i = index for wind speeds (incremented from cut-in to cut-out wind speed)
j = index for mean stress level (covering the range of all mean stress levels encountered)
k = index for stress amplitude (covering the range of all stress amplitudes encountered)
Δt = the length of the time interval during which fatigue cycles are evaluated
U_i = the free stream wind speed
$\sigma_{m,j}$ = mean stress
$\sigma_{a,k}$ = stress amplitude
$n(\sigma_{m,j}, \sigma_{a,k}, U_i, \Delta t)_x$ = the number of cycles of mean stress j and stress amplitude k at wind speed i during interval of length Δt; $x = O$ for normal operation, $x = P$ for parked, $x = T$ for transient (see below)
$N(\sigma_{m,j}, \sigma_{a,k})$ = the number of cycles to failure at mean stress j and stress amplitude k
F_{U_i} = the fraction of time that the wind speed, U, is between U_{i-1} and U_i:

$$F_{U_i} = \int_{U_{i-1}}^{U_i} p(U) \mathrm{d}U \tag{6.11}$$

where $p(U)$ = the wind speed probability density function.

The cumulative damage from buffeting above operational wind speeds when the turbine is parked (stopped), $D_{y,P}$, is also a function of the stress levels at each wind speed and the frequency of occurrence of each wind speed:

$$D_{y,P} = C \sum_{i=U_{out}}^{U_{max}} \sum_j \sum_k F_{U_i} \frac{n(\sigma_{m,j}, \sigma_{a,k}, U_i, \Delta t)_P}{N(\sigma_{m,j}, \sigma_{a,k})} \tag{6.12}$$

In this case, i, the index for wind speeds, is incremented from the cut-out wind speed, U_{out}, to the maximum wind speed, U_{max}, that might occur. Note that the subscript P is used here rather than O to distinguish fatigue resulting when the turbine is parked rather than operating.

The cumulative damage from transient conditions is also a function of the stress levels at each transient condition and the frequency of occurrence of each condition:

$$D_{y,T} = \sum_h \sum_j \sum_k M_h \frac{n(\sigma_{m,j}, \sigma_{a,k}, m_h)_T}{N(\sigma_{m,j}, \sigma_{a,k})} \tag{6.13}$$

In this case, h is the index for each type of discrete transient event, m_h is the number of occurrences of the discrete event h during which n cycles occurred, and M_h is the average number of times per year that discrete event h occurs.

The total cumulative damage from all conditions is expressed as:

$$D_y = D_{y,O} + D_{y,P} + D_{y,T} \tag{6.14}$$

Finally, note that the reciprocal of the annual damage is the expected lifetime of the component.

Table 6.1   Materials used in wind turbines

Subsystems or components	Material category	Material subcategory
Blades	Composites	Glass fibers, carbon fibers, wood laminates, polyester resins, epoxies
Hub	Steel	
Gearbox	Steel	Various alloys, lubricants
Generator	Steel, copper	Rare earth based permanent magnets
Mechanical equipment	Steel	
Nacelle cover	Composites	Fiberglass
Tower	Steel	
Foundation	Steel, concrete	
Electrical and control system	Copper, silicon	

6.3 Wind Turbine Materials

Many types of materials are used in wind turbines, as summarized in Table 6.1. Two of the most important of these are steel and composites. The composites typically comprise fiberglass, carbon fibers, or wood together with a matrix of polyester or epoxy. Other common materials include copper and concrete. The following provides an overview of some of the aspects of materials most relevant to wind turbine applications.

6.3.1 Review of Basic Mechanical Properties of Materials

In this text it is assumed that the reader has a familiarity with the fundamental concepts of material properties, as well as with the most common materials themselves. The following is a list of some of the essential concepts, (for more details, see a text on mechanical design, such as Spotts *et al.*, 2003):

- Hooke's Law;
- modulus of elasticity;
- yield strength, breaking strength;
- ductility and brittleness;
- hardness and machinability;
- failure by yielding or fracture.

Fatigue was discussed in the previous section. It should be noted, however, that fatigue properties differ significantly from one material to another.

6.3.2 Steel

Steel is one of the most widely used materials in wind turbine fabrication. Steel is used for many structural components including the tower, hub, main frame, shafts, gears and gear cases, fasteners as well as the reinforcing in concrete. Information on steel properties can be found in Spotts *et al.* (2003), Baumeister (1978), and data sheets from steel suppliers.

6.3.3 Composites

Composites are described in more detail in this text than are most other materials, because it is assumed that they may be less familiar to many readers than are more traditional materials. They are also the primary material used in blade construction. Composites are materials comprising at least two dissimilar materials, most commonly fibers held in place by a binder matrix. Judicious choice of the fibers and binder allows tailoring of the composite properties to fit the application. Composites used in wind turbine applications include those based on fiberglass, carbon fiber, and wood. Binders include polyester, epoxy, and vinyl ester. The most common composite is fiberglass reinforced plastic, known as GRP. In wind turbines, composites are most prominently used in blade manufacture, but they are also used in other parts of the machine, such as the nacelle cover. The main advantages of composites are: (1) ease of fabrication into the desired aerodynamic shape, (2) high strength, and (3) high stiffness to weight ratio. They are also corrosion resistant, are electrical insulators, are resistant to environmental degradation, and lend themselves to a variety of fabrication methods.

6.3.3.1 Glass Fibers

Glass fibers are formed by spinning glass into long threads. The most common glass fiber is known as E-glass, a calcium aluminosilicate glass. It is a low-cost material, with reasonably good tensile strength. Another common fiber is S-glass, a calcium-free aluminosilicate glass. It has approximately 25–30% higher tensile strength than E-glass but it is significantly more expensive (more than twice as much). There is also a glass fiber, HiPER-tex, from Owens-Corning, which claims the strength of S-glass with a cost near E-glass.

Fibers are sometimes used directly, but are most commonly first combined into other forms (known as 'preforms'). Fibers may be woven or knitted into cloth, formed into continuous strand or chopped strand mat, or prepared as chopped fibers. Where high strength is required, unidirectional bundles of fibers known as 'tows' are used. Some fiberglass preforms are illustrated in Figure 6.9. More information is presented in Chou *et al.* (1986) and McGowan *et al.* (2007).
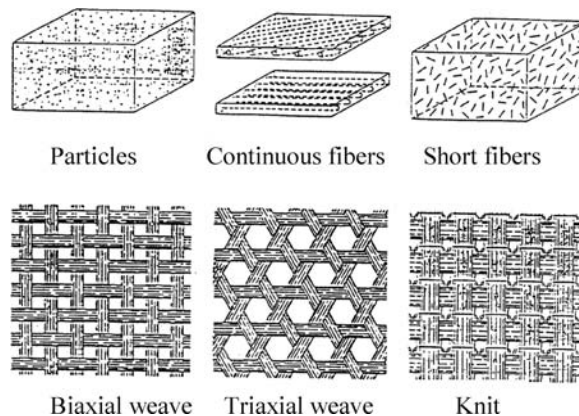
Figure 6.9 Fiberglass preforms (National Research Council, 1991)

6.3.3.2 Matrix (Binder)

There are three types of resins commonly used in matrices of composites. They are:
(1) unsaturated polyesters, (2) epoxies, and (3) vinyl esters. These resins all have the general
property that they are used in the liquid form during the lay up of the composite, but when they
are cured they are solid. As solids, all of the resins tend to be somewhat brittle. The choice of
resin affects the overall properties of the composite.

Polyesters have been used most frequently in the wind industry because they have a short
cure time and low cost. Cure time is from a few hours to overnight at room temperature, but with
the addition of an initiator, curing can be done at elevated temperatures in a few minutes.
Shrinkage upon curing is relatively high, however. The present cost (2009) is in the range of
$2.20/kg ($1/lb.)

Epoxies are stronger, have better chemical resistance, good adhesion, and low shrinkage
upon curing, but they are also more expensive (approximately 50% more expensive than
polyesters) and have a longer cure time than polyesters.

Vinyl esters are epoxy-based resins which have become more widely used over recent years.
These resins have similar properties to epoxies, but are somewhat lower in cost and have a
shorter cure time. They have good environmental stability and are widely used in marine
applications.

6.3.3.3 Carbon Fiber Reinforcing

Carbon fibers are more expensive than are glass fibers (by approximately a factor of 8), but they
are stronger and stiffer. One way to take advantage of carbon fibers' advantages, without paying
the full cost, is to use some carbon fibers along with glass in the overall composite.

6.3.3.4 Wood–Epoxy Laminates

Wood is used instead of synthetic fibers in some composites. In this case the wood is preformed
into laminates (sheets) rather than fibers, or fiber-based cloth. The most common wood for wind
turbine laminates is Douglas Fir. Properties of wood vary significantly with respect to the
direction of the wood's grain. In general, though, wood has good strength to weight ratio, and is
also good in fatigue. One important characteristic of wood is its strong anisotropy in tensile
strength. This means that laminates have to be built up with grain going in different directions if
the final composite is to be strong enough in all directions. More information on the properties
of wood may be found in Hoadley (2000).

The use of wood together with an epoxy binder was developed for wind turbine applications
based on previous experience from the high-performance boat-building industry. A technique
known as the wood–epoxy saturation technique (WEST) is used in this process. Wood–epoxy
laminates have good fatigue characteristics: according to one source (National Research
Council, 1991), no wood–epoxy blade has ever failed in service due to fatigue.

6.3.3.5 Fatigue Damage in Composites

Fatigue damage occurs in composites as it does in many other materials, but it does not
necessarily occur by the same mechanism. The following sequence of events is typical. First,

the matrix cracks, then cracks begin to combine and there is debonding between the matrix and the fibers. Then there is debonding and separation (delamination) over a wider area. This is followed by breaking of the individual fibers, and finally by complete fracture.

The same type of analysis techniques that are used for other materials (explained in Section 6.2) are also used for predicting fatigue in composites. That is, rainflow cycle counting is used to determine the range and mean of stress cycles, and Miner's Rule is used to calculate the damage from the cycles and the composite's S–N curve. S–N curves for composites are modeled by an equation that has a somewhat different shape than that used in metals, however:

$$\sigma = \sigma_u (1 - B \log N). \tag{6.15}$$

where σ is the cyclic stress amplitude, σ_u is the ultimate strength, B is a constant, and N is the number of cycles.

The parameter B is approximately equal to 0.1 for a wide range of E-glass composites when the reversing stress ratio $R = 0.1$. This is tension–tension fatigue. Life is reduced under fully reversed tension–compression fatigue ($R = -1$) and compression–compression fatigue.

Fatigue strength of glass fibers is only moderate. The ratio of maximum stress to static strength is 0.3 at 10 million cycles. Carbon fibers are much more fatigue resistant than are glass fibers: the ratio of maximum stress to static strength is 0.75 at 10 million cycles, two and half times that of glass. Fatigue life characteristics of E-glass, carbon fiber, and some other common fibers are illustrated in Figure 6.10.

Owing to the complexity of the failure method of composites and the lack of complete test data on all composites of interest, it is, in practice, still difficult to predict fatigue life accurately. Summary information on the degradation of composites used in wind turbines may be found in McGowan *et al.* (2007). More details on the fatigue life of composites in wind turbine blades may be found in Nijssen (2007).
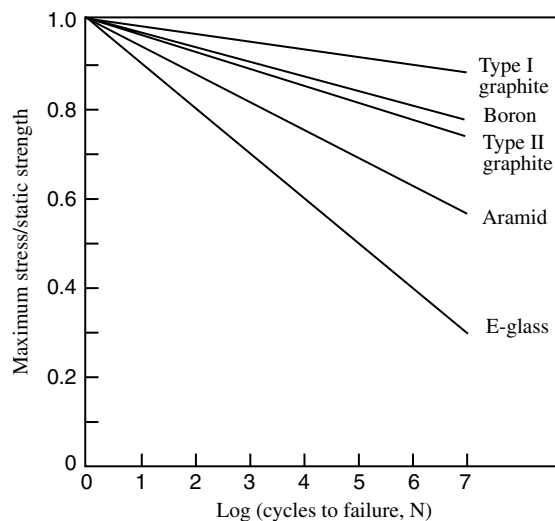
Figure 6.10   Fatigue life of some composite fibers (National Research Council, 1991)

6.3.4 Copper

Copper has excellent electrical conductivity and for that reason it is used in nearly all electrical equipment on a wind turbine, including the power conductors. The mechanical properties of copper are, in general, of much less interest than the conductivity. The weight, however, can be significant. A substantial part of the weight of the electrical generator is due to the copper windings, and the weight of the main power conductors may also be of importance. Information on copper relative to its use in electrical applications can be found in many sources, including Baumeister (1978).

6.3.5 Concrete

Reinforced concrete is frequently used for the foundations of wind turbines. It has sometimes been used for the construction of towers as well. Discussion of reinforced concrete, however, is outside the scope of this text.

6.4 Machine Elements

Many of the principal components of a wind turbine are composed, at least partially, of machine elements. These are manufactured items which typically have a much wider applicability, and with which there has been a great deal of experience. Many of these elements are commercially available and are fabricated according to recognized standards. This section presents a brief overview of some machine elements that are often found in wind turbine applications. Specifically, those discussed here include shafts, couplings, bearings, gears, and dampers. Some other commonly used machine elements include clutches, brakes, springs, screws, and wire rope. For details on any of these, the reader should consult a text on machine design, such as Spotts *et al.* (2003) or Shigley *et al.* (2003).

6.4.1 Shafts

Shafts are cylindrical elements designed to rotate. Their primary function is normally to transmit torque, and so they carry or are attached to gears, pulleys, or couplings. In wind turbines shafts are typically found in gearboxes and generators, and in linkages.

   In addition to being loaded in torsion, shafts are often subjected to bending. The combined loading is often time-varying, so fatigue is an important consideration. Shafts also have resonant natural frequencies at 'critical speeds'. Operation near such speeds is to be avoided, or large vibrations can occur.

   Materials used for shafting depend on the application. For the least severe conditions, hot-rolled plain carbon steel is used. For greater strength applications, somewhat higher carbon content steel may be used. After machining, shafts are often heat treated to improve their yield strength and hardness. Under the most severe conditions, alloy steels are used for shafts.

6.4.2 Couplings

Couplings are elements used for connecting two shafts together for the purpose of transmitting torque between them. A typical use of couplings in wind turbines is the connection between the generator and the high-speed shaft of the gearbox.
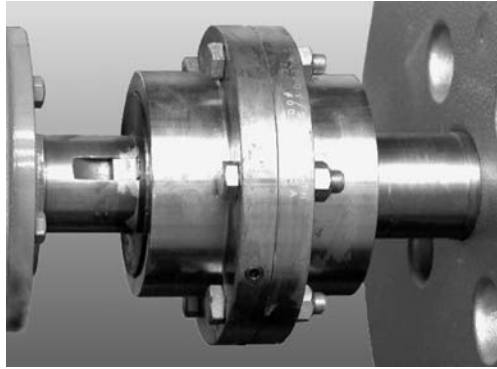
Figure 6.11 Typical solid coupling

Couplings consist of two major pieces, one of which is attached to each shaft. They are often kept from rotating relative to the shaft by a key. The two pieces are, in turn, connected to each other by bolts. In a solid coupling, the two halves are bolted together directly. In a typical flexible coupling, teeth are provided to carry the torque and rubber bumpers are included between the teeth to minimize effects of impact. Shafts to be connected should ideally be collinear, but flexible couplings are designed to allow some slight misalignment. An example of a solid coupling is shown in Figure 6.11.

6.4.3 Bearings

Bearings are used to reduce frictional resistance between two surfaces undergoing relative motion. In the most common situations, the motion in question is rotational. There are many bearing applications in wind turbines. They are found in main shaft mountings, gearboxes, generators, yaw systems, blade pitch systems, and teetering mechanisms to name just a few.

Bearings come in a variety of forms, and they are made from a variety of materials. For many high-speed applications, ball bearings, roller bearings, or tapered roller bearings may be used. These bearings are typically made from steel. In other situations bushings made from plastics or composites may be used.

Ball bearings are widely used in wind turbine components. They consist of four types of parts: an inner ring, an outer ring, the balls, and the cage. The balls run in curvilinear grooves in the rings. The cage holds the balls in place and keeps them from touching each other. Ball bearings are made in a range of types. They may be designed to take radial loads or axial thrust loads. Radial ball bearings can also withstand some axial thrust.

Roller bearings are similar in many respects to ball bearings, except that cylindrical rollers are used instead of balls. They are commonly used in wind turbines in applications such as gearboxes. A typical roller bearing is shown in Figure 6.12.

Other types of bearings also have applications in wind turbine design. Two examples are the sleeve bearings and thrust bearings used in the teetering mechanism of some two-bladed wind turbines.

Figure 6.12   Cutaway view of typical roller bearing (Torrington Co., http://howstuffworks. lycos.com/ bearing.htm, 2000)

Generally speaking, the most important considerations in the design of a bearing are the load it experiences and the number of revolutions it is expected to survive. Detailed information on all types of bearings may be found in manufacturers' data sheets. Bearings used in wind turbine gearboxes are discussed in IEC (2008).

6.4.4 Gears

Gears are elements used in transferring torque from one shaft to another. Gears are described in somewhat more detail in this section than are other elements because they are widely used in wind turbines. The conditions under which they operate differ in significant ways from many other applications, and it has been necessary to investigate in some detail these conditions and the gears' response so that they perform as desired.

There are numerous applications for gears in wind turbines. The most prominent of these is probably the drive train gearbox. Other examples include yaw drives, pitch linkages, and erection winches. Common types of gears include spur gears, helical gears, worm gears, and internal gears. All gears have teeth. Spur gears have teeth whose axes are parallel to the rotational axis of the gear. The teeth in helical gears are inclined at an angle relative to the gear's rotational axis. Worm gears have helical teeth, which facilitate transfer of torque between shafts at right angles to each other. An internal gear is one which has teeth on the inside of an annulus. Some common types of gears are illustrated in Figure 6.13.

Gears may be made from a wide variety of materials, but the most common material in wind turbine gears is steel. High strength and surface hardness in steel gear teeth is often obtained by carburizing or other forms of heat treating.

Gears may be grouped together in gear trains. Typical gear trains used in wind turbine applications are discussed in Section 6.5.
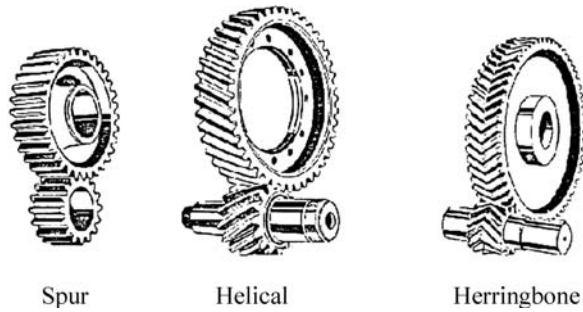
Figure 6.13 Common gear types

6.4.4.1 Gear Terminology

The most basic, and most common, gear is the spur gear. Figure 6.14 illustrates the most important characteristics. The pitch circle is the circumference of a hypothetical smooth gear (or one with infinitesimally small teeth). Two smooth gears would roll around each other with no sliding motion at the point of contact. The diameter of the pitch circle is known as the pitch diameter, d. With teeth of finite size, some of each tooth will extend beyond the pitch circle, some of it below the pitch circle. The face of the tooth is the location that meets the corresponding face of the mating gear tooth. The width of the face, b, is the dimension parallel to the gear's axis of rotation. The circular pitch, p, of the gear is the distance from one face on one tooth to the face on the same side of the next tooth around the pitch circle. Thus, $p = \pi d/N$ where N is the number of teeth.

Ideally, the thickness of a tooth, measured on the pitch circle, is exactly one half of the circular pitch (i.e. the width of the teeth and the space between them are the same on the pitch circle). In practice, the teeth are cut a little smaller. Thus, when the teeth mesh, there is some free space between them. This is known as backlash. Excessive backlash can contribute to accelerated wear, so it is kept to a minimum. Backlash is illustrated in Figure 6.15.
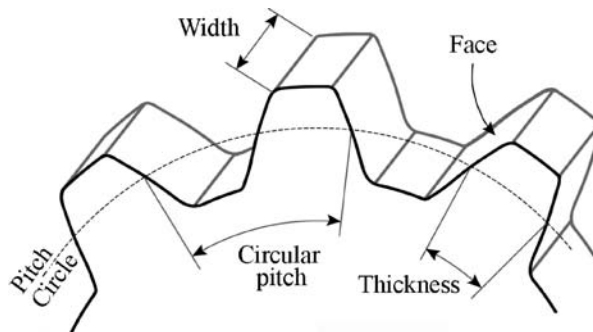
Figure 6.14 Principal parts of a gear
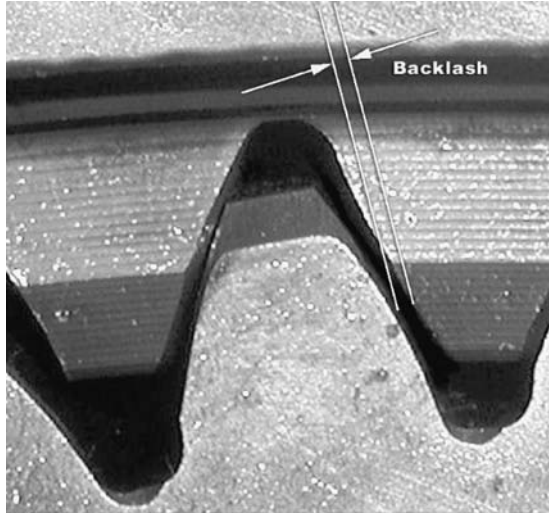
Figure 6.15   Backlash between gears

6.4.4.2 Gear Speed Relations

When two meshing gears, 1 and 2, are of different diameter, they will turn at different speeds. The relation between their rotational speeds n_1 and n_2 is inversely proportional to their pitch diameters d_1 and d_2 (or number of teeth). That is:

$$n_1/n_2 = d_2/d_1 \tag{6.16}$$

6.4.4.3 Gear Loading

Loading on a gear tooth is determined by the power being transmitted and the speed of the tooth. In terms of power, P, and pitch circle velocity, $V_{pitch} = \pi\,dn$, the tangential force, F_t, on a tooth is:

$$F_t = P/V_{pitch} \tag{6.17}$$

As the gear turns, individual teeth will be subjected to loading and unloading. At least one pair of teeth is always in contact, but, at any given time, more than one pair is likely to be in contact. For example, one pair may be unloading while another is taking a greater fraction of the load.

The bending stress, σ_b, on a gear tooth of width b and height h is calculated by application of the bending equation for a cantilevered beam:

$$\sigma_b = \frac{6M}{bh^2} \tag{6.18}$$

The moment, M, is based on a load F_b (which is closely related to F_t) applied at a distance L to the weakest point on the tooth. The result is:

$$\sigma_b = \frac{F_b}{b}\frac{6L}{h^2} \tag{6.19}$$

The factor $h^2/6L$ is a property of the size and shape of the gear and is frequently expressed in terms of the pitch diameter as the form factor (or Lewis factor), $y = h^2/6pL$. In this case, Equation (6.19) can be expressed as:

$$\sigma_b = \frac{F_b}{y\,p\,b}$$

(6.20)

The form factor is available in tables for commonly encountered numbers of teeth and pressure angles. Typical values for spur gears range from 0.056 for 10 teeth/gear to 0.170 for 300 teeth/gear.

6.4.4.4 Gear Dynamic Loading

Dynamic loading can induce stresses that are also significant to the design of a gear. Dynamic effects occur because of imperfections in the cutting of gears. The mass and spring constant of the contacting teeth and the loading and unloading of the teeth as the gear rotates are also contributing factors. Dynamic effects can result in increased bending stresses and can exacerbate deterioration and wear of the tooth surfaces.

The effective spring constant, k_g, of two meshing gear teeth can be important in the dynamic response (natural frequency) of a wind turbine drive train. The following equation gives an approximation to that spring constant. This equation accounts for gears (1 and 2) of different materials. Assuming moduli of elasticity E_1 and E_2, k_g is given by:

$$k_g = \frac{b}{9}\frac{E_1 E_2}{E_1 + E_2}$$

(6.21)

Dynamic effects and wear are very significant to the design of gears for wind turbine gearboxes. More discussion, however, is beyond the scope of this book. Information on gear tooth wear in general can be found in Spotts *et al.* (2003) and Shigley *et al.* (2003). Gears in wind turbine gearboxes in particular are discussed in McNiff *et al.* (1990) and IEC (2008).

6.4.5 Dampers

Wind turbines are subject to dynamic events, with potentially adverse effects. These effects may be decreased by the use of appropriate dampers. There are at least three types of device that act as dampers and that have been used on wind turbines: (1) fluid couplings, (2) hydraulic pumping circuits, and (3) linear viscous fluid dampers.

Fluid couplings are sometimes used between a gearbox and generator to reduce torque fluctuations. They are used most commonly in conjunction with synchronous generators, which are inherently stiff. Hydraulic pumping circuits consist of a hydraulic pump and a closed hydraulic loop with a controllable orifice. Such circuits may be used for damping yaw motion. Linear viscous fluid dampers are essentially hydraulic cylinders with internal orifices. They may be used as teeter dampers on one- or two-bladed rotors.

Detailed discussion of dampers is beyond the scope of this book. More information on the general topic of hydraulics, on which many damper designs are based, can be found in the Hydraulic Handbook (Hydraulic Pneumatic Power Editors, 1967).

6.4.6 Fastening and Joining

Fastening and joining is an important concern in wind turbine design. The most important fasteners are bolts and screws. Their function is to hold parts together, but in a way which can be undone if necessary. Bolts and screws are tightened so as to exert a clamping force on the parts of interest. This is often accomplished by tightening the bolt to a specified torque level. There is a direct relation between the torque on a bolt and its elongation. Thus, a tightened bolt acts like a spring as it clamps. Fatigue can be an important factor in specifying bolts. The effects of fatigue can often be reduced by prestressing the bolts.

Bolts and screws on wind turbines are frequently subjected to vibration, and sometimes to shock. These tend to loosen them. To prevent loosening, a number of methods are used. These include washers, locknuts, lock wire, and chemical locking agents.

There is also a variety of other fasteners, and the use of ancillary items, such as washers and retainers, may be critical in many situations. Joining by means which are not readily disassemblable, such as welding, riveting, soldering, or bonding with adhesives, is also frequently applied in wind turbine design. More details on fastening and joining may be found in Parmley (1997).

6.5 Principal Wind Turbine Components

The principal component groups in a wind turbine are the rotor, the drive train, the main frame, the yaw system, and the tower. The rotor includes the blades, hub, and aerodynamic control surfaces. The drive train includes the gearbox (if any), the generator, mechanical brake, and shafts and couplings connecting them. The yaw system components depend on whether the turbine uses free yaw or driven yaw. The type of yaw system is usually determined by the orientation of the rotor (upwind or downwind of the tower). Yaw system components include at least a yaw bearing and may include a yaw drive (gear motor and yaw bull gear), yaw brake, and yaw damper. The main frame provides support for mounting the other components and a means for protecting them from the elements (the nacelle cover). The tower group includes the tower itself, its foundation, and may include the means for self-erection of the machine.

The following sections discuss each of the component groups. Unless specifically noted, it is assumed that the turbine has a horizontal axis.

6.5.1 Rotor

The rotor is unique among the component groups. Other types of machinery have drive trains, brakes, and towers, but only wind turbines have rotors designed for the purpose of extracting significant power from the wind and converting it to rotary motion. As discussed elsewhere, wind turbine rotors are also nearly unique in that they must operate under conditions that include steady as well as periodically and stochastically varying loads. These varying loads occur over a very large number of cycles, so fatigue is a major consideration. The designer must strive to keep the cyclic stresses as low as possible, and to use material that can withstand those stresses as long as possible. The rotor is also a generator of cyclic loadings for the rest of the turbine, in particular the drive train.

The next three sections focus on the topics of primary interest in the rotor: (1) blades, (2) aerodynamic control surfaces, and (3) hub.

6.5.1.1 Blades

The most fundamental components of the rotor are the blades. They are the devices that convert the force of the wind into the torque needed to generate useful power.

Design Considerations
There are many things to consider in designing blades, but most of them fall into one of two categories: (1) aerodynamic performance and (2) structural strength. Underlying all of these, of course, is the need to minimize life cycle cost of energy, which means that not only should the cost of the turbine itself be kept low, but that the operation and maintenance costs should be kept low as well. There are other important design considerations as well; they are all summarized in the following list.

- aerodynamic performance;
- structural strength;
- blade materials;
- recyclability;
- blade manufacturing;
- worker health and safety;
- noise reduction;
- condition/health monitoring;
- blade roots and hub attachment;
- passive control or smart blade options;
- costs.

The first nine of these considerations are discussed immediately below. Passive control options are discussed in Section 6.5.1.2 (Aerodynamic control options). Cost is related to all the topics here, but is outside the scope of this chapter. See Chapter 11, however, for more information on wind turbine costs.

There are a number of sources of information on wind turbine blades. See, for example, Veers *et al.* (2003) and the presentations given at Sandia blade workshops in 2004, 2006, and 2008 (See http://www.sandia.gov/wind.)

Blade Shape Overview
The basic shape and dimensions of the blades are determined primarily by the overall topology of the turbine (see Chapter 7) and aerodynamic considerations, which were discussed in Chapter 3. Details in the shape, particularly near the root, are also influenced by structural considerations. For example, the planform of most real wind turbines differs significantly from the optimum shape, because the expense of blade manufacture would otherwise be too high. Figure 6.16 illustrates some typical planform options. Material characteristics and available methods of fabrication are also particularly important in deciding upon the exact shape of the blades.

Aerodynamic Performance
The primary aerodynamic factors affecting blade design are:

- design rated power and rated wind speed;
- design tip speed ratio;
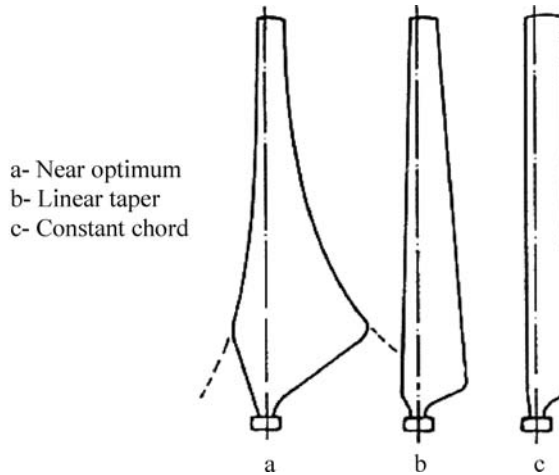
Figure 6.16 Blade planform options (Gasch, 1996). Reproduced by permission of B. G. Teubner GmbH

- solidity;
- airfoil;
- number of blades;
- rotor power control (stall or variable pitch);
- rotor orientation (upwind or downwind of the tower).

The overall size of the rotor swept area, and hence the length of the blades, is directly related to design rated power and rated wind speed. Other things being equal, it is usually advantageous to have a high design tip speed ratio. A high tip speed ratio results in a low solidity, which in turn results in less total blade area. This, in turn, should result in lighter, less expensive blades. The accompanying higher rotational speed is also of benefit to the rest of the drive train. On the other hand, high tip speed ratios result in more aerodynamic noise from the turbine. Because the blades are thinner, the flapwise stresses tend to be higher. Thinner blades are also more flexible. This can sometimes be an advantage, but thinner blades may also experience vibration problems, and extreme deflections can result in blade–tower impacts. The tip speed ratio also has a direct effect on the chord and twist distribution of the blade.

As design tip speed ratios increase, selection of the proper airfoil becomes progressively more important. In particular it is necessary to keep the lift-to-drag ratio high if the rotor is to have a high power coefficient. It is also of note that the lift coefficient will have an effect on the rotor solidity and hence the blade's chord: the higher the lift coefficient, the smaller the chord. In addition, the choice of airfoil is, to a significant extent, affected by the method of aerodynamic control used on the rotor. For example, an airfoil suitable for a pitch-regulated rotor may not be appropriate for a stall-controlled turbine. One concern is fouling: certain airfoils, particularly on stall-regulated turbines, are quite susceptible to fouling (due, for example, to a build up of insects on the leading edge). This can result in a substantial decrease in power production. Selection of an airfoil can be done with the help of databases such as those developed by Selig (2008).
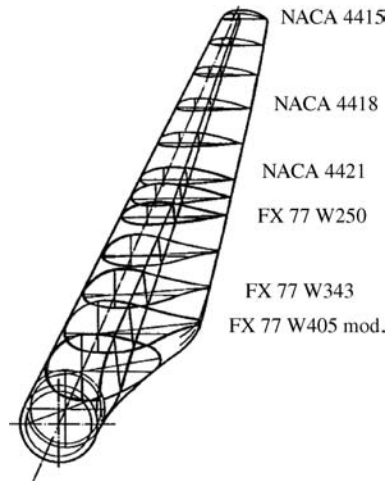
Figure 6.17 Airfoil cross-sections with radius (from Gasch, 1996). Reproduced by permission of B. G. Teubner GmbH

Wind turbine blades frequently do not have just one airfoil shape along the entire length. See, for example, Figure 6.17. More commonly (but not always), the airfoils are all of the same family, but the relative thickness varies. Thicker airfoils near the root provide greater strength, and can do so without seriously degrading the overall performance of the blade.

With present manufacturing techniques it is generally advantageous to have as few blades as possible. This is primarily because of the fixed costs in fabricating the blades. In addition, when there are more blades (for a given solidity) they will be less stiff and may have higher stresses at the roots. At the present time all commercial wind turbines have either two or three blades, and that will be assumed to be the case here as well. Two-bladed wind turbines have historically had a lower solidity than three-bladed machines. This keeps the blade cost low, which is one of the presumed advantages of two blades over three blades.

The method of power control (stall or variable pitch) has a significant effect on the design of the blades, particularly in regard to the choice of the airfoil. A stall-controlled turbine depends on the loss of lift which accompanies stall to reduce the power output in high winds. It is highly desirable that the blades have good stall characteristics. They should stall gradually as the wind speed increases, and they should be relatively free of transient effects, such as are caused by dynamic stall. In pitch-controlled turbines, stall characteristics are generally much less important. On the other hand, it is important to know that the blades perform acceptably when being pitched in high winds. It is also worth noting that blades can be pitched towards either feather (decreasing angle of attack) or stall (increasing angle of attack).

The rotor orientation with respect to the tower has some effect on the geometry of the blades, but mostly in a secondary manner related to the preconing of the blades. This preconing is a tilting of the blades away from a plane of rotation as defined by the blade roots. Most downwind turbines have historically operated with free yaw. The blades then must be coned away from the plane of rotation to enable the rotors to track the wind and maintain some yaw stability. Some upwind rotors also have preconed blades. In this case, the preconing is in the upwind direction and the purpose is to keep the blades from hitting the tower.

Blade design often involves a number of iterations to properly account for both aerodynamic and structural requirements. In each iteration a tentative design is developed and then analyzed. One approach to expedite this process, known as an inverse design method, has been developed by Selig and Tangler (1995). It involves the use of a computer code (PROPID) to propose designs which will meet certain requirements. For example, it is possible to specify overall dimensions, an airfoil series, a peak power and blade lift coefficient along the span, and then use the code to determine the chord and twist distribution of the blade.

Structural Strength

The exterior shape of wind turbine blades is based on aerodynamics, but the interior architecture is determined primarily by considerations of strength. The blade structure must be sufficiently strong both to withstand extreme loads and to survive many fatigue cycles. The blade must also not deflect more than a specified amount when under load. Figure 6.18 illustrates the cross-section of a typical blade. As shown in the figure, an interior spar provides the interior strength, primarily via forward and aft shear webs. Spar caps transfer loads from the outer skin to the shear webs.

In order to provide sufficient strength, particularly near the root of the blade, inboard sections are relatively thick. As blades have become larger and larger, chords near the root have become larger as well. This has caused some problems, including in transportation. One solution has been to develop 'flatback' airfoils, such as the one illustrated in Figure 6.19.

Blade Materials

Historically, wind turbine blades were made from wood, sometimes covered with cloth. Until the middle of the 20th century, blades for larger wind turbines were made from steel. Examples include both the Smith–Putnam 1250 kW turbine (1940s) and the Gedser 200 kW turbine (1950s).

Since the 1970s, most blades for horizontal axis wind turbines have been made from composites. The most common composites consist of fiberglass in a polyester resin, but vinyl ester and wood–epoxy laminates have also been used. More recently, carbon fibers have become widely used in blade construction, not necessarily as a replacement for fiberglass, but to augment it. Typical composites used for wind turbine blades were described in more detail in Section 6.3.
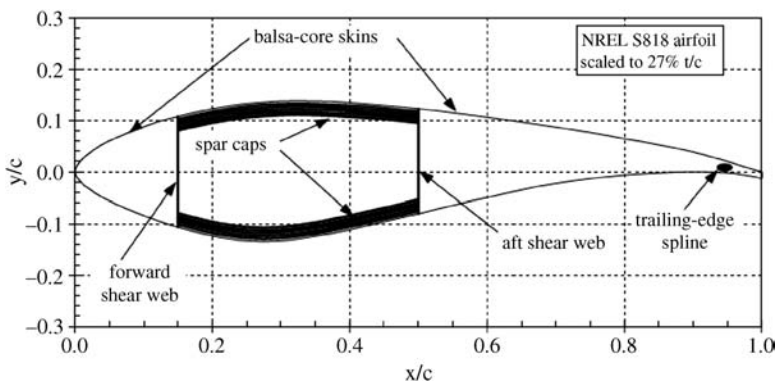
Figure 6.18 Typical wind turbine blade structural architecture (Veers *et al.*, 2003)

FB-51-110
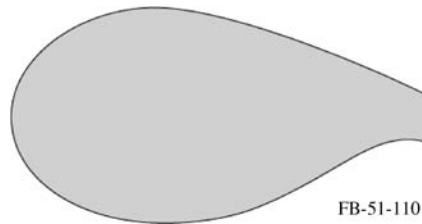
Figure 6.19   Example of a flatback airfoil (Veers *et al.*, 2003)

Some wind turbines have used aluminum for blade construction. Aluminum has been a popular choice for vertical axis wind turbines. VAWT blades normally have a constant chord with no twist, so lend themselves to formation by aluminum pultrusion (see blade manufacturing discussion below.) A few horizontal axis wind turbines have used aluminum blades, but aluminum is not commonly used for HAWTs at this time.

Recyclability

An important concern, especially for the future, is blade recyclability. As more and more turbines are built, and as older turbines are replaced by newer ones, the issue of blade disposal and securing raw materials for new blades will become more significant. One way to deal with both issues, at least partly, is by making the blades of recyclable materials. This is a relatively new topic of study, but is expected to become more significant over time.

Blade Manufacturing

There are a number of options for manufacturing composite wind turbine blades. The most important of these are summarized below.

(i) Wet Lay-up

Wet lay-up of fiberglass involves placing multiple layers (plies) of fiberglass cloth into a mold. Each layer is soaked in a binder (polyester or epoxy resin plus a hardener). The lay-up is typically done by hand, with the resin being forced into the glass with rollers or squeegees. In this method there are two parts to mold, one for the upper surface and one for the lower surface. When the two halves of the blade are completed, they are removed from the molds. They are then bonded together, with the spar (separately fabricated) in between. An example of part of the process is shown in Figure 6.20. Hand lay-up is very labor intensive and it is hard to ensure consistency and avoid defects in the product. Another difficulty with this approach is that fumes are released into the air, making the process hazardous to the workers (Cairns and Skramstad, 2000).

(ii) Pre-preg

In the pre-preg method, the fiberglass cloth has been previously impregnated with a resin which remains firm at room temperature. After all the cloth has been placed in the mold, the entire mold is heated so that the resin will flow and then harden permanently. The heating is done in a low temperature oven or an autoclave. This method has the advantage that the resin to glass ratio is consistent and it is easier to achieve good results. On the other hand, the material cost is higher, and it is both difficult and expensive to provide heating for large blades.

Figure 6.20   Laying fiberglass cloth into blade molds. Reproduced by permission of LM Glasfibre

(iii) Resin Infusion

In resin infusion, dry fiberglass cloth is laid into the mold and then resin is impelled by some means to flow into the glass. One method is known as vacuum-assisted resin transfer molding (VARTM). In this method, air can be removed from one side of the mold via a vacuum pump. A vacuum bag is placed over the cloth and arranged in such a way that resin from an external reservoir will be pushed through the cloth by atmospheric pressure into the space evacuated by the vacuum pump. This method avoids many of the quality issues associated with wet lay-up. An additional advantage is that toxic byproducts are not released into the air. A variant of the VARTM method is the SCRIMP™ method, which has been developed by TPI, Inc. This process is illustrated in Figure 6.21.
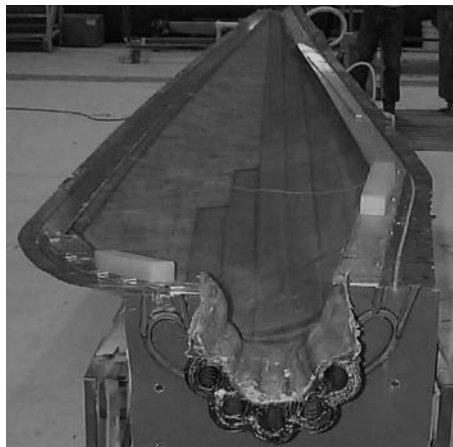
Figure 6.21   VARTM mold. Reproduced by permission of TPI, Inc.

(iv) Compression Molding

In compression molding, the fiberglass and resin are placed in a two-part mold which is then closed. Heat and pressure are applied until the product is ready. This method has a number of advantages, but so far has not proven to be adaptable to large blades. It may be useful for smaller blades, however.

(v) Pultrusion

Pultrusion is a fabrication method in which material is pulled through a die to form an object of specific cross-sectional shape but indefinite length. The object is cut to the desired length afterwards. The material can be either metal or a composite. If a composite is used, provision is also made for adding resin and heating the mold to assist in curing. Pultrusion is well suited to making blades of constant cross-section such as blades for vertical axis wind turbines. So far, however, pultrusion has not proven attractive for twisted and tapered blades of horizontal axis turbines.

(vi) Wood–Epoxy Saturation Technique (WEST)

Sometimes wind turbine blades are made of wood–epoxy laminates. The procedure is similar to that of wet lay-up fiberglass. Typically a process known as WEST (see Section 6.3.3.4), developed originally by Gougeon Brothers for boat building, is used. The main difference is that wood plies are used in the laminate rather than fiberglass cloth. In addition, the thickness of the skin relative to the blade thickness is usually greater than in a fiberglass blade, and rather than a box beam spar, a plywood strip is used to provide stiffness.

(vii) Filament Winding

This is another technique for making fiberglass blades, but the process is quite different from that of the mold method described previously. In the filament winding method, glass fibers are wound about a mandrel, while resin is applied simultaneously. This method, developed originally in the aerospace industry, can be automated and results in a consistent product. It is difficult to use with concave shapes, however. It is also hard to align blade fibers lengthwise, something which is often desirable.

Worker Health and Safety

As noted previously, some methods of blade fabrication, particularly wet lay-up, can result in toxic gases being released into the air. These gases can be hazardous for the workers who are building the blades. It may therefore be expected that there will be a continuing trend to replace wet lay-up with other fabrication methods, such as VARTM.

Noise Reduction

A wind turbine's rotor can be a source of unwanted sound (i.e. noise), as will be discussed in Chapter 12. One way to reduce the noise is through the selection of suitable airfoils. Another way is to design the rotor to operate best at a relatively low tip speed ratio.

Condition/Health Monitoring

Wind turbine blades can suffer various types of damage over time. Ideally, they are inspected periodically. In practice, however, it is difficult to do a thorough inspection, especially of the blades' interior. One way to deal with this issue is via condition or health monitoring. In this technique, sensors are embedded in the blades during manufacture. The sensors are afterwards

integrated into a monitoring system, which can be used to alert operators that repairs are necessary. See Hyers *et al.* (2006) for more information on this topic.

Blade Roots and Hub Attachment

Blades are attached to the hub via the blade root, which is the end of the blade nearest the hub. The root experiences the highest loads, and is also the location that must provide for the connection to the hub. In order to reduce stresses, the root is generally made as thick as is practical in the flapwise direction. Connection between the root and the hub has often proven to be difficult. This is largely due to dissimilarities in material properties and stiffnesses between the blades, the hub, and the fasteners. Highly variable loads also contribute to the problem.

One type of root is known as the Hütter design, named after its inventor, the German wind energy pioneer Ulrich Hütter. In this method long fiberglass strands are bonded into the lower part of the blade. Circular metal flanges are provided at the base of the blade, and attached to these flanges are circular hollow spacers. The fiberglass strands are wrapped around the spacers and brought back into the rest of the blade. Resin keeps all the strands and the flanges in place. The blades are eventually attached to the hub via bolts through the flanges and spacers. As described here, this root design is most applicable to fixed-pitch rotors. The method can be modified, however, for variable-pitch rotors as well. This root is illustrated in Figure 6.22.

Details of a variant of the Hütter root design, which was widely used in the 1970s and 1980s, are shown in Figure 6.23. In this figure, which illustrates part of a cross-section of the root, the lower surface of the base plate is closest to the hub. The base plate and a steel pressure ring form a 'sandwich', inside of which are glass fiber roving bundles (twisted strands of fibers). The roving bundles originate in the fiberglass of the rest of the blade, and wrap around steel bushings. Bolts pass through the pressure plate, bushing, and base plate to complete the connection to the hub.

The modified Hütter root has some limitations. The problem is that it is subject to fatigue. Cyclic stresses during operation have tended to loosen the matrix resin, allowing relative motion of the fiberglass. Movement of the glass then exacerbates the problem. Voids in the matrix and other manufacturing details appear to be the ultimate source of the problem. Careful quality control reduces the frequency of occurrence.
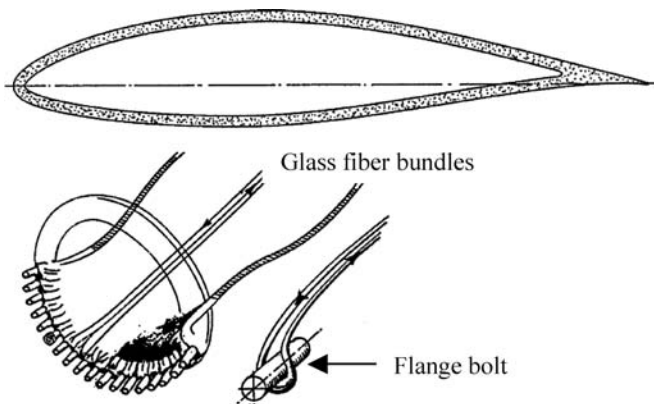
Figure 6.22   Hütter root (Hau, 1996). Reproduced by permission of Springer Verlag GmbH
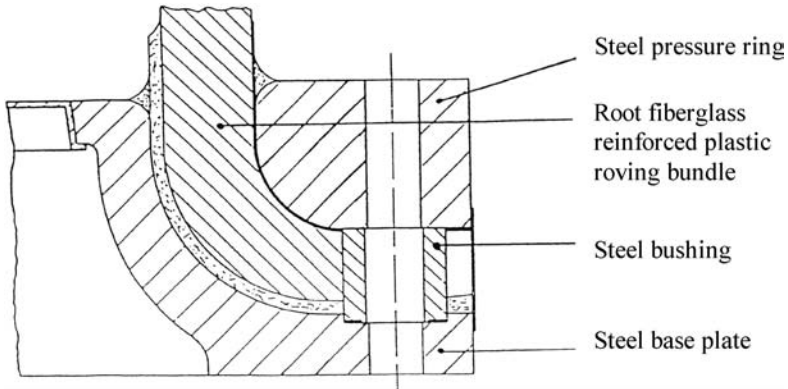
Figure 6.23   Modified Hütter root (National Research Council, 1991)

Another method of attachment is the use of studs or threaded inserts bonded directly into the blades. The use of studs was originally developed in conjunction with wood–epoxy blades, but it has proven applicable to fiberglass blades as well. Threaded inserts are illustrated in Figure 6.24.

Fixed-pitch wind turbine blades normally are fastened to the hub with bolts or studs which are aligned radially, and perpendicular to the bottom of the blade root. These fasteners must withstand all the loads arising from the blades.

The construction of a variable-pitch blade root is rather different from that of a fixed-pitch blade. In particular, the root–hub connection must incorporate bearings so that the blade can be rotated. These bearings must be able to withstand the bending moments and shear forces imposed by the rest of the blade. In addition, these, or other, bearings must take the centrifugal load resulting from the rotor's rotation.

The blade attachment methods discussed above are most common on medium size or larger turbines. Blades on small turbines normally employ different attachment techniques. In one
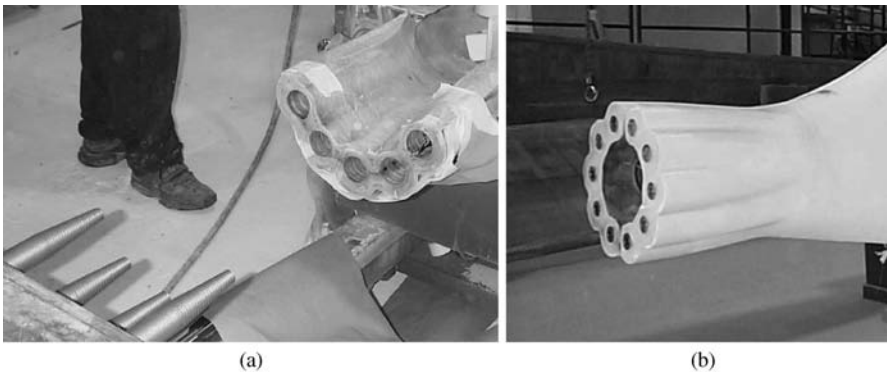
Figure 6.24   (a) Threaded inserts being installed; (b) bladed root with threaded inserts. Reproduced by permission of TPI, Inc.

method the root is thickened, and bolts are placed through the root and a matching part on the hub. The bolts are perpendicular to both the long axis and chord of the blade.

Blade Properties
Properties of the overall blade, such as total weight, stiffness, and mass distributions, and moments of inertia are needed in the structural analysis of the rotor. Important concerns are the blade's strength, its tendency to deflect under load, its natural vibration frequencies, and its resistance to fatigue. These were all discussed previously. Some of the blade properties can be difficult to obtain due to the complex geometry of the blade, which varies from root to tip. The normal method used is to divide the blade into sections, in a manner similar to that for aerodynamic analysis. Properties for each section are found, based on the dimensions and material distribution, and then combined to find values for the entire blade.

6.5.1.2 Aerodynamic Control Options

There are a number of ways to modify the aerodynamic performance of a blade. These include pitch control, control surfaces, and passive control. These are discussed below. More details on wind turbine control in general are provided in Chapter 8.

Control Surfaces
An aerodynamic control surface is a device which can be moved to change the aerodynamic characteristics of a rotor. A variety of types of aerodynamic control surfaces can be incorporated in wind turbine blades. They must be designed in conjunction with the rest of the rotor, especially the blades. The selection of aerodynamic control surfaces is strongly related to the overall control philosophy. Stall-regulated wind turbines usually incorporate some type of aerodynamic brake. These can be tip brakes, flaps, or spoilers. An example of a tip flap is illustrated in Figure 6.25.

Turbines which are not stall-controlled usually have much more extensive aerodynamic control. In conventional pitch-controlled turbines the entire blade can rotate about its long axis.
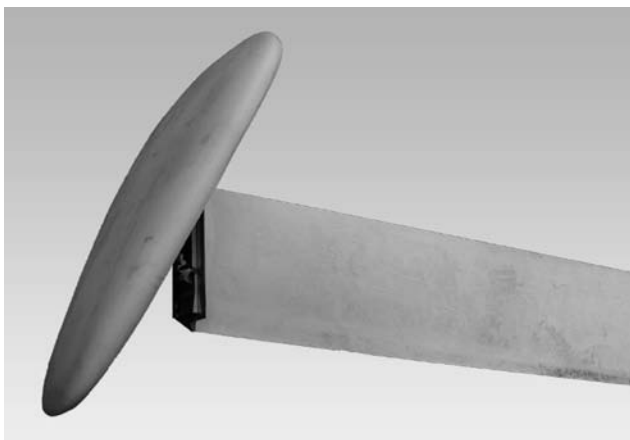
Figure 6.25   Example of a tip flap aerodynamic brake

Thus, the entire blade forms a control surface. Some turbine designs use partial span pitch control. In this case the inner part of the blade is fixed relative to the hub. The outer part is mounted on bearings and can be rotated about the radial axis of the blade. The advantage of partial span pitch control is that the pitching mechanism need not be as massive as it must be for full span pitch control.

Another type of aerodynamic control surface is the aileron. This is a movable flap, located at the trailing edge of the blade. The aileron may be approximately 1/3 as long as the entire blade, and extend approximately 1/4 of the way towards the leading edge.

Any control surface is used in conjunction with a mechanism that allows or causes it to move as required. This mechanism may include bearings, hinges, springs, and linkages. Aerodynamic brakes often include electromagnets to hold the surface in place during normal operation, but to release the surface when required. Mechanisms for active pitch or aileron control include motors for operating them.

Passive Control

One way to passively limit the loads on a wind turbine blade is via pitch-twist coupling. In this concept, thrust forces create a moment about the pitch axis of the blade, causing it to twist. The twisting changes the pitch angle along the blade, decreasing the lift force and thus limiting the load. Blades that employ pitch-twist coupling typically incorporate carbon fibers, laid in asymmetrically with respect to the glass. They sometimes have a swept planform, such as the one shown in Figure 6.26.

Another means of passive control utilizing the blade architecture is pre-bending. In this concept the blade is fabricated with a built in bend. The bend is such that the unloaded tip will project upwind from the plane of rotation when the blade is affixed to the hub (on an upwind rotor). Under load, the tip will bend back into the plane of rotation, rather than bending downwind of the rotor plane and possibly into the tower. The disadvantage with this concept is that the molds themselves must be larger than they otherwise would be so as to incorporate the bend. Shipping large bent blades can also be problematic.

Smart Blades

The term 'smart blades' refers to the aerodynamic control of wind turbine blades via distributed and embedded intelligence and actuators. Smart blades may incorporate flaps, micro-tabs, boundary layer suction or blowing, piezo-electric elements, and shape memory alloys. See IEA (2008) for a discussion of this topic.

6.5.1.3 Hub

Function

The hub of the wind turbine is the component that connects the blades to the main shaft and ultimately to the rest of the drive train. The hub transmits and must withstand all the loads

Figure 6.26 Swept blade. Reproduced by permission of Knight & Carver

generated by the blades. Hubs are generally made of steel, either welded or cast. Details of hubs differ considerably depending on the overall design philosophy of the turbine.

Types

There are three basic types of hub design that have been applied in modern horizontal axis wind turbines: (1) rigid hubs, (2) teetering hubs, and (3) hubs for hinged blades. Rigid hubs, as the name implies, have all major parts fixed relative to the main shaft. They are the most common design, and are nearly universal for machines with three (or more) blades. Teetering hubs allow relative motion between the part that connects to the blades and that which connects to the main shaft. Like a child's teeter-totter (seesaw), when one blade moves one way, the other blade moves the other way. Teetering hubs are commonly used for two- and one-bladed wind turbines. Hubs for hinged blades allow independent flapping motion relative to the plane of rotation. Such hubs are not presently used on any commercial wind turbines but they have been employed on some historically important turbines (Smith–Putnam) and are presently receiving renewed attention. Some of the common types of hubs are illustrated in Figure 6.27.

(i) Rigid Hub

As indicated above, a rigid hub is designed to keep all major parts in a fixed position relative to the main shaft. The term rigid hub does, however, include those hubs in which the blade pitch can be varied, but in which no other blade motion is allowed.

   The main body of a rigid hub is a casting or weldment to which the blades are attached, and which can be fastened to the main shaft. If the blades are to be preconed relative to the main shaft, provision for that is made in the hub geometry. A rigid hub must be strong enough to withstand all the loads that can arise from any aerodynamic loads on the blades, as well as dynamically induced loads, such as those due to rotation and yawing. These loads are discussed in Chapters 4 and 7. A typical rigid hub is shown in Figure 6.28.

   A hub on a pitch-controlled turbine must provide for bearings at the blade roots, a means for securing the blades against all motion except pitching, and a pitching mechanism. Pitching mechanisms may use a pitch rod passing through the main shaft, together with a linkage on the
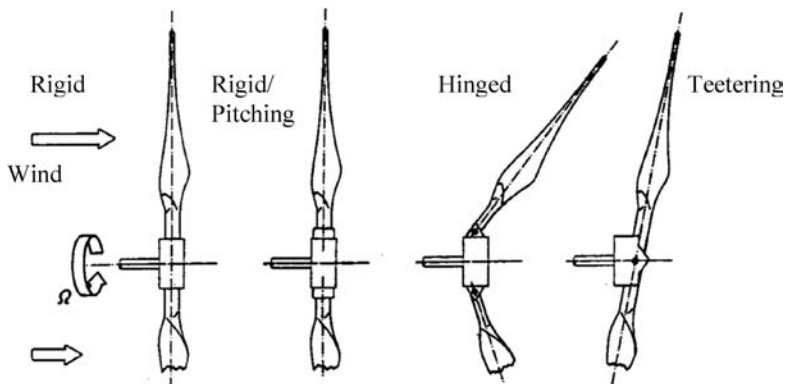
Figure 6.27   Hub options (Gasch, 1996). Reproduced by permission of B. G. Teubner GmbH

Figure 6.28 Typical rigid wind turbine hub. Photo by Paul Anderson. Reproduced under Creative Commons License

hub. This linkage is, in turn, connected to the roots of the blades. The pitch rod is driven by a motor mounted on the main (non-rotating) part of the turbine. An alternative method is to mount electric gear motors on the hub and have them pitch the blades directly. In this case, power still needs to be provided to the motors. This can be done via slip rings or a rotary transformer. Regardless of the design philosophy of the pitching mechanism, it should be fail-safe. In the event of a power outage, for example, the blades should pitch themselves into a no-power position. An example of a blade pitching mechanism is illustrated in Figure 6.29.

The hub must be attached to the main shaft in such a way that it will not slip or spin on the shaft. Smaller turbines frequently employ keys, with keyways on the shaft and the hub. The shaft is also threaded and the mating surfaces are machined (and perhaps tapered) for a tight fit.
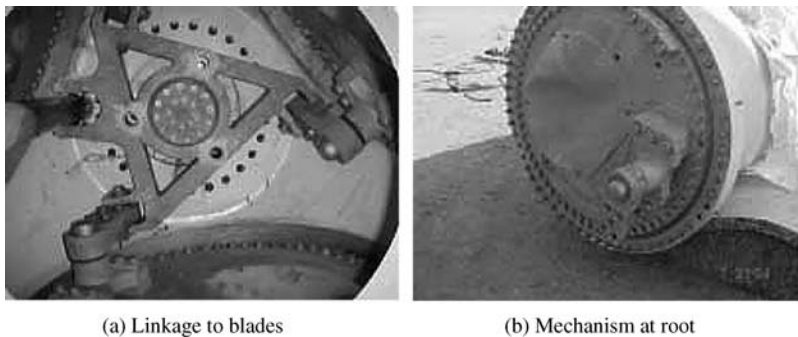
(a) Linkage to blades   (b) Mechanism at root

Figure 6.29 Blade pitching mechanism. Reproduced by permission of Vestas Wind Systems A/S
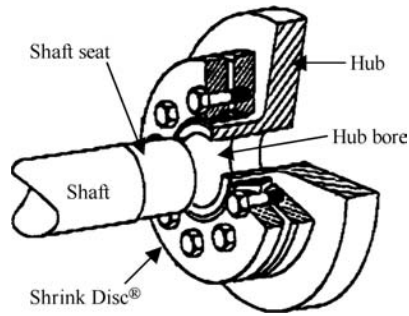
Figure 6.30   Ringfeder® hub attachment. Reproduced by permission of Ringfeder Corp.

The hub can then be held on with a nut. Such a method of attachment is less desirable on a larger machine, however. First of all, a keyway weakens the shaft. Machining threads on a large shaft can also be inconvenient. One method used to attach hubs to wind turbine shafts is the Ringfeder® Shrink Disc®, which is illustrated in Figure 6.30. In the arrangement shown, a projection on the hub slides over the end of the main shaft. The diameter of the hole in the hub projection is just slightly larger than the end of the main shaft. The Shrink Disc® consists of a ring and two discs. The inner surface of the ring slides over the outside of the hub projection. The outside of the ring is tapered in both axial directions. The two discs are placed on either side of the taper, and then pulled together with bolts. As they approach each other, the ring is compressed and this, in turn, compresses the hub projection. The compression of the hub projection clamps it to the hub.

Another method of hub attachment involves the use of a permanent flange on the end of the shaft. The flange may be either integral to the shaft or added later. The hub is attached to the flange by bolts.

(ii) Teetering Hub

Teetering hubs are used on nearly all two-bladed wind turbines. This is because a teetering hub can reduce loads due to aerodynamic imbalances or loads due to dynamic effects from rotation of the rotor or yawing of the turbine. Teetering hubs are considerably more complex than are rigid hubs. They consist of at least two main parts (the main hub body and a pair of trunnion pins) as well as bearings and dampers. A typical teetering hub is illustrated in Figure 6.31. The main hub body is a steel weldment. At either end are the attachment points for the blades. This hub has blades that are preconed downwind from the plane of rotation, so the planes of attachment are not perpendicular to the long axis of the hub. On either side of the hub body are teeter bearings. They are held in place by removable bearing blocks. The arrangement is such that the bearings lie on an axis perpendicular to the main shaft, and equidistant from the blade tips. The teeter bearings carry all of the loads passing between the hub body and the trunnion pin. The trunnion pin is connected rigidly to the main shaft.

In the hub shown in Figure 6.31 a line through the axis of the trunnion pins and in the plane of the rotor is collinear with a line perpendicular to the long axis of the hub and also in the plane of the rotor. In general, however, these lines need not be collinear. The angle between the two is known as the delta-3 angle (δ_3, a term borrowed from the helicopter industry). When the lines
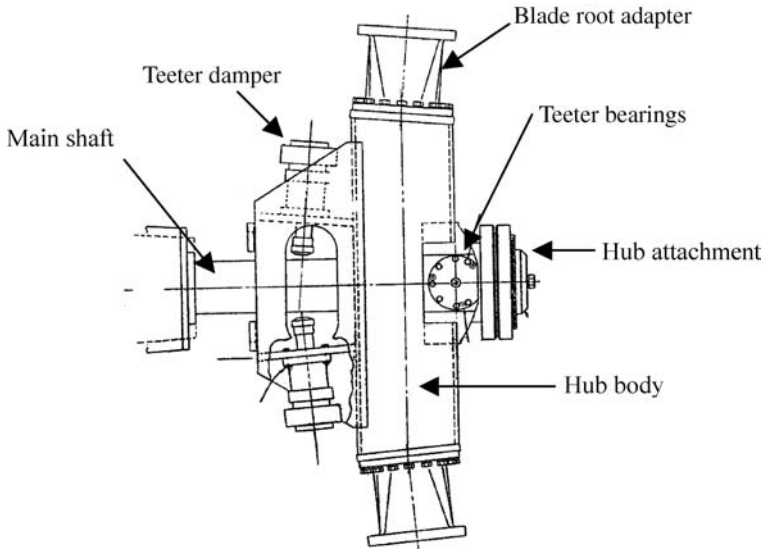
Figure 6.31   Teetering hub (ESI-80)

are collinear ($\delta_3 = 0$) all blade motion is in the flapping direction during teetering. When $\delta_3 \neq 0$ then there is a pitching component as well. There may be some benefit to having a non-zero delta-3 angle, but there is no consensus in the wind energy industry as to if and when it should be employed, and how big the angle should be. A hub with a non-zero delta-3 angle is illustrated in Figure 6.32.

Most teetering hubs have been built for fixed-pitch turbines, but they can be used on variable-pitch turbines as well. Design of the pitching system is more complex since the pitching mechanism is on the part of the hub which moves relative to the main shaft. A pitching teetering hub is described in more detail by Van Bibber and Kelly (1985).

Teetering hubs require two types of bearing. One type is a cylindrical, radially loaded bearing; the other is a thrust bearing. There is one bearing of each type on each pin. The cylindrical bearings carry the full load when the pin axis is horizontal. When the pin axis is not horizontal, there is an axial component due primarily to the weight of the rotor. One of the thrust bearings will carry that part of the load. Teeter bearings are typically made of special purpose composites.

During normal operation a teetering hub will move only a few degrees forwards and backwards. During high winds, starts and stops, or high yaw rates, greater teeter excursions can occur. To prevent impact damage under these conditions, teeter dampers and compliant stops are provided. In the hub shown in Figure 6.31 (which has a maximum allowed range of ± 7.0 degrees) the dampers are on the side of the hub opposite the bearings.

The options for attaching a teetering hub to the main shaft are the same as for rigid hubs.

(i) Hinged Hub

A hinged hub is, in some ways, a cross between a rigid hub and a teetering hub. It is basically a rigid hub with 'hinges' for the blades. The hinge assembly adds some complexity, however.
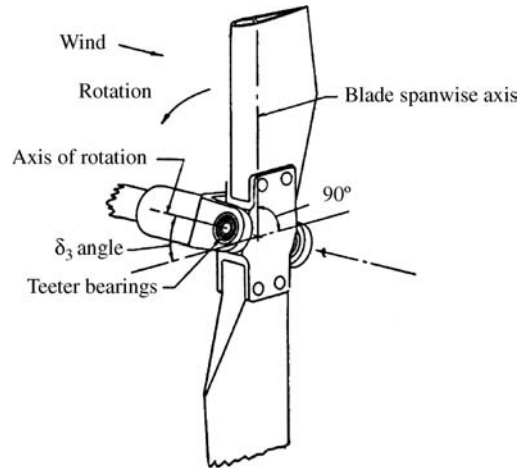
Figure 6.32   Teetering hub with non-zero delta-3 (δ_3) angle (Perkins and Jones, 1981)

As with a teetering hub, there must be bearings at the hinges. Teetering hubs have the advantage that the two blades tend to balance each other, so lack of centrifugal stiffening during low rpm operation is not a major problem. There is no such counterbalancing on a hinged blade, however, so some mechanism must be provided to keep the blades from flopping over during low rotational speed. This could include springs. It would almost certainly include dampers as well.

6.5.2 Drive Train

A complete wind turbine drive train consists of all the rotating components: rotor, main shaft, couplings, gearbox, brakes, and generator. With the exception of the rotor components, which were considered above, all of these are discussed in the following sections. Figure 6.33 illustrates a typical drive train.

6.5.2.1 Main Shaft

Every wind turbine has a main shaft, sometimes referred to as the low-speed or rotor shaft. The main shaft is the principal rotating element, providing for the transfer of torque from the rotor to the rest of the drive train. It also supports the weight of the rotor. The main shaft is supported, in turn, by bearings, which transfer reaction loads to the main frame of the turbine. Depending on the design of the gearbox, the shaft and/or the bearings may be integrated into the gearbox or they may be completely separate from it, connected only by a coupling. The main shaft is sized in accordance with methods described in Chapter 7, taking into account the combined loads of torque and bending. Main shafts are normally made of steel. Methods of connecting the main shaft to the rotor were discussed in Section 6.5.1. Figure 6.34 illustrates some options for the main shaft.
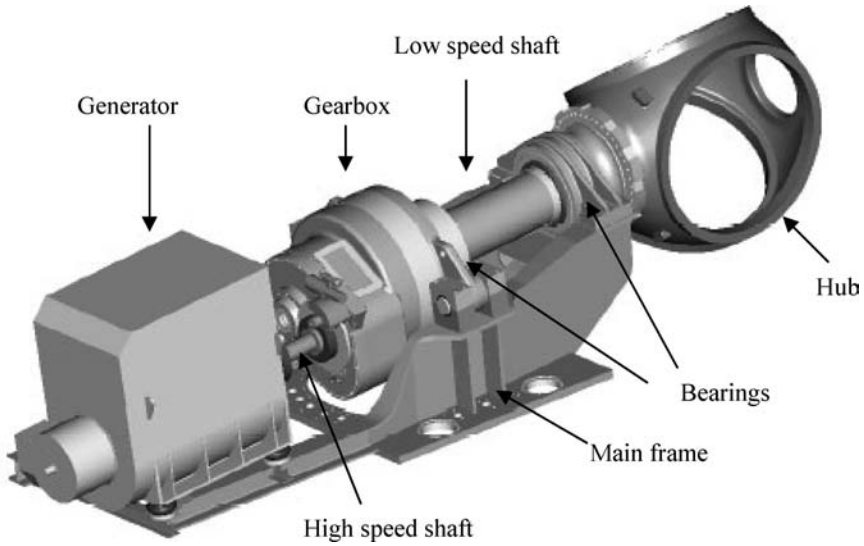
Figure 6.33   Typical drive train and associated components (Poore and Liettenmaier, 2003)

6.5.2.2 Couplings

Function
Couplings, as discussed in Section 6.4.2, are used to connect shafts together. There are two locations in particular where large couplings are likely to be used in wind turbines: (1) between the main shaft and the gearbox and (2) between the gearbox output shaft and the generator.
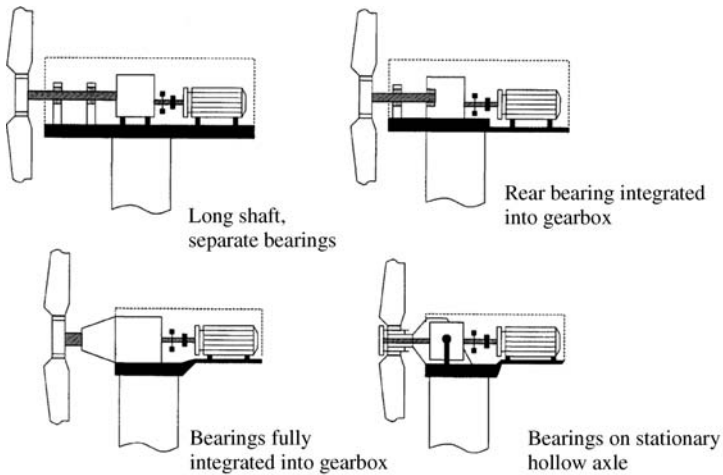
Figure 6.34   Main shaft options (Harrison *et al.*, 2000)

The primary function of the coupling is to transmit torque between two shafts, but it may have another function as well. Sometimes it is advantageous to dampen torque fluctuations in the main shaft before the power is converted to electricity. A coupling of appropriate design can serve this role. A fluid coupling may be used for this purpose. Since couplings were described in Section 6.4.2, more detail will not be provided here.

6.5.2.3 Gearbox

Function
Most wind turbine drive trains include a gearbox to increase the speed of the input shaft to the generator. An increase in speed is needed because wind turbine rotors, and hence main shafts, turn at a much lower speed than is required by most electrical generators. Small wind turbine rotors turn at speeds on the order of a few hundred rpm. Larger wind turbines turn more slowly. Most conventional generators turn at 1800 rpm (60 Hz) or 1500 rpm (50 Hz).

Some gearboxes also perform functions other than increasing speed, such as supporting the main shaft bearings. These are secondary to the basic purpose of the gearbox, however.

The gearbox is one of the heaviest and most expensive components in a wind turbine. Gearboxes are normally designed and supplied by a different manufacturer to the one actually constructing the wind turbine. Since the operating conditions experienced by a wind turbine gearbox are significantly different than those in most other applications, it is imperative that the turbine designer understand gearboxes, and that the gearbox designer understand wind turbines. Experience has shown that underdesigned gearboxes are a major source of wind turbine operational problems.

Types
All gearboxes have some similarities: they consist of torque transmitting parts, such as shafts and gears, machine elements such as bearings and seals, and structural components, such as the case. In most cases there is a single input shaft and a single output shaft, but in at least one case (Clipper Windpower's Liberty) there are multiple output shafts connected to multiple generators. Beyond that there are two basic types of gearbox used in wind turbine applications: (1) parallel-shaft gearboxes and (2) planetary gearboxes.

In parallel-shaft gearboxes, gears are carried on two or more parallel shafts. These shafts are supported by bearings mounted in the case. In a single-stage gearbox there are two shafts: a low-speed shaft and a high-speed shaft. Both of these shafts pass out through the case. One of them is connected to the main shaft or rotor and the other to the generator. There are also two gears, one on each shaft. The two gears are of different size, with the one on the low-speed shaft being the larger of the two. The ratio of the pitch diameter of the gears is inversely proportional to the ratio of the rotational speeds (as described in Section 6.4).

There is a practical limit to the size ratio of the two gears that can be used in a single-stage parallel-shaft gearbox. For this reason, gearboxes with large speed-up ratios use multiple shafts and gears. These gears then constitute a gear train. A two-stage gearbox, for example, would have three shafts: an input (low-speed) shaft, an output (high-speed) shaft, and an intermediate shaft. There would be gears on the intermediate shaft, the smaller driven by the low-speed shaft. The larger of these gears would drive the gear on the high-speed shaft. A typical parallel-shaft gearbox is illustrated in Figure 6.35.
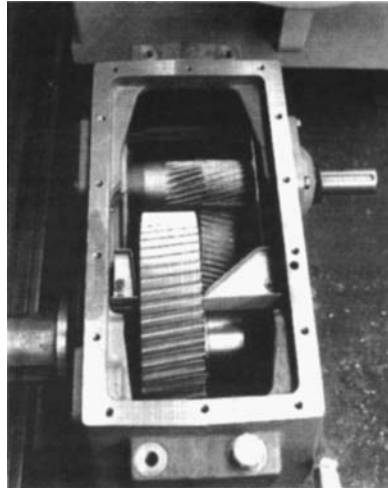
Figure 6.35   Parallel-shaft gearbox (Hau, 1996). Reproduced by permission of Springer Verlag GmbH

Planetary gearboxes have a number of significant differences from parallel-shaft gearboxes. Most notably, the input and output shafts are coaxial. In addition, there are multiple pairs of gear teeth meshing at any time, so the loads on each gear are reduced. This makes planetary gearboxes relatively light and compact. A typical planetary gearbox is illustrated in Figure 6.36.

In planetary gearboxes, a low-speed shaft, supported by bearings in the case, is rigidly connected to a planet carrier. The carrier holds three identical small gears, known as planets. These gears are mounted on short shafts and bearings and are free to turn. These planets mesh with a large-diameter internal or ring gear and a small-diameter sun gear. When the low-speed shaft and carrier rotate, meshing of the planets in the ring gear forces the planets to rotate, and to do so at a speed higher than the speed of the carrier. The meshing of the planets with the sun gear causes it to rotate as well. The sun gear then drives the high-speed shaft, to which it is
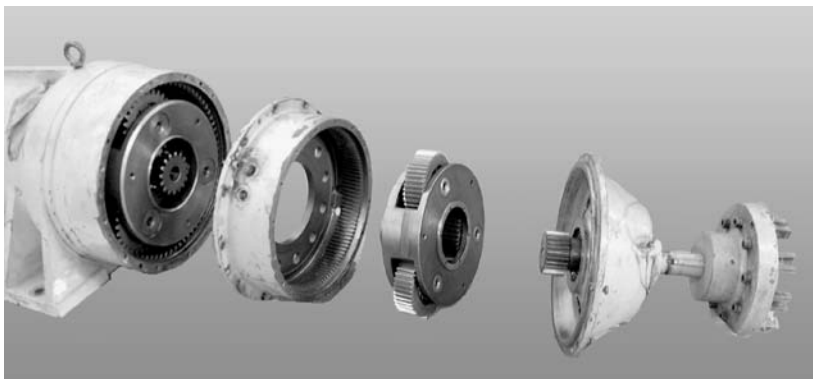
Figure 6.36   Exploded view of two-stage planetary gearbox
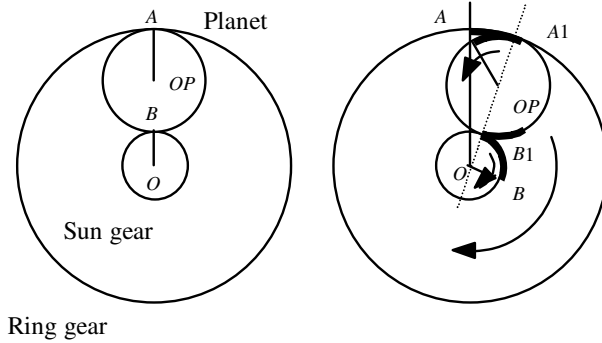
Figure 6.37 Relations between gears in a planetary gearbox

rigidly connected. The high-speed shaft is supported by bearings mounted in the case. Figure 6.37 illustrates the relation between the gears and the angles made during a small angle of rotation. Note that before the rotation the sun and planet gear mesh at point B, while the planet and ring gear mesh at point A. After the rotation the corresponding meshing points are $B1$ and $A1$. The centers of the sun and the planet are at O and OP respectively.

The speed-up ratio for the configuration shown in Figure 6.37 (with the ring gear stationary) is:

$$\frac{n_{HSS}}{n_{LSS}} = 1 + \frac{D_{Ring}}{D_{Sun}} \tag{6.22}$$

where n_{HSS} is the speed of the high-speed shaft, n_{LSS} is the speed of the low-speed shaft, D_{Ring} is the diameter of the ring gear, and D_{Sun} is the diameter of the sun gear.

As with the parallel-shaft gearbox, there is a limit to the speed-up ratio that can be achieved by a single-stage planetary gear set. Generally, any one stage will not provide a speed-up of more than 6:1. To achieve a higher speed-up ratio, multiple stages are placed in series. When there are multiple stages in series, the overall speed-up is the product of the speed-up of the individual stages. For example, one could gain a speed-up of 30:1 by having two stages of 5:1 and 6:1 in series.

Gears in many wind turbine gearboxes are of the spur type, but helical gears are found as well. Bearings are ball bearings, roller bearings, or tapered roller bearings, depending on the loads. Gears and bearings were discussed in more detail in Section 6.4.

Design Considerations
There are a great many issues to consider in the design and selection of a gearbox. These include:

- basic type (parallel-shaft or planetary), as discussed above;
- separate gearbox and main shaft bearings, or an integrated gearbox;
- speed-up ratio;
- number of stages;
- gearbox weight and cost;
- gearbox loads;

- lubrication;
- effects of intermittent operation;
- noise;
- reliability.

Wind turbine gearboxes are either separate components, or they are combined with other components. In the latter case they are known as integrated or partially integrated gearboxes. For example, in a number of turbines with a partially integrated gearbox, the main shaft and main shaft bearings are integrated into the rest of the gearbox. A fully integrated gearbox is one in which the gearbox case is really the main frame of the wind turbine. The rotor is attached to its low-speed shaft. The generator is coupled to the high-speed shaft and is also bolted directly to the case. Part of the yaw system is integrated into the bottom of the case. Figure 6.38 illustrates a partially integrated planetary gearbox.

The speed-up ratio of a gearbox is directly related to the desired rotational speed of the rotor and the speed of the generator. As previously indicated, the rotor speed is determined primarily by aerodynamic considerations. Generator speed is often 1800 rpm in 60 Hz grids or 1500 rpm in 50 Hz grids, although other fixed speeds or a range of speeds are also possible (as was discussed in Chapter 5). For example, a wind turbine with a rotor designed to operate at 60 rpm and an 1800 rpm generator would need a gearbox with a 30 : 1 speed-up ratio.

The number of stages in a gearbox is generally of secondary concern to the wind turbine designer. It is important primarily because it affects the complexity, size, weight, and cost of the gearbox. The more stages there are, the more internal components, such as gears, bearings, and shafts, that there are.

The weight of a gearbox increases dramatically with increasing power rating of the turbine. In fact, the gearbox weight will scale approximately with the cube of the radius, as does the weight of the rotor. Since planetary gearboxes are lighter than parallel-shaft boxes, there is a weight advantage to be gained by using them. On the other hand, due to their greater complexity, they also cost more than would be indicated by their reduced weight.

The loads that the gearbox must withstand are due primarily to those imposed by the rotor. These will include at least the main shaft torque, and may include the weight of the rotor and
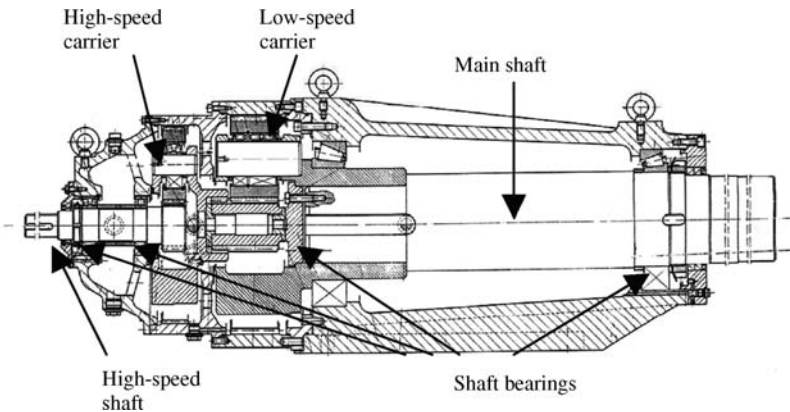
Figure 6.38 Partially integrated, two-stage planetary gearbox

various dynamic loads, depending on the degree of integration of the gearbox with the main shaft and bearings. Loads are also imposed by the generator, both during normal operation and while starting, and by any mechanical brake located on the high-speed side of the gearbox. Over an extended period of time, the gearbox, like the rotor, will experience some loads that are relatively steady, other loads that vary periodically or randomly, and still others that are transient. All of these contribute to fatigue damage and wear on the gear teeth, bearings, and seals.

Lubrication is a significant issue in gearbox operation. Oils must be selected to minimize wear on the gear teeth and bearings, and to function properly under the external environmental conditions in which the turbine will operate. In some cases, it may be necessary to provide filtering or active cooling of the oil. In any event, periodic oil samples should be taken to assess the state of the oil, as well as to check for signs of internal wear.

Intermittent operation, a common situation with wind turbines, can have a significant impact on the life of a gearbox. When the turbine is not running, oil may drain away from the gears and bearings, resulting in insufficient lubrication when the turbine starts.

In cold weather the oil may have too high a viscosity until the gearbox has warmed up. Turbines in such environments may benefit by having gearbox oil heaters. Condensation of moisture may accelerate corrosion. When the rotor is parked (depending on the nature and location of a shaft brake) the gear teeth may move slightly back and forth. The movement is limited by the backlash, but it may be enough to result in some impact damage and tooth wear.

Gearboxes may be a source of noise. The amount of noise is a function of, among other things, the type of gearbox, the materials from which the gears are made and how they are cut. Designing gearboxes for a minimum of noise production is presently an area of significant interest.

Reliability is a key consideration in the design of a gearbox. A detailed and carefully planned process is required to ensure that the design is sufficiently reliable. It requires close coordination between the turbine designer and the gearbox designer. Similar to the turbine as a whole, the gearbox design requires the following steps:

- specification of design load cases (see IEC, 2005);
- calculation of design loads at pertinent locations;
- preliminary detailed design;
- fabrication of a prototype;
- workshop testing of the prototype;
- installation of prototype gearbox in a wind turbine;
- field testing of the gearbox;
- final design of gearbox.

More details on wind turbine gearboxes, relating particularly to design, are given in design guidelines from AGMA (1997) and IEC (2008).

6.5.2.4 Generator

The generator converts the mechanical power from the rotor into electrical power. Generator options were described in detail in Chapter 5 and will not be discussed here. One of the important things to recall is that, until recently, most grid-connected generators have turned at

constant or nearly constant speed. This resulted in the rotors also turning at constant or nearly constant speed. At present, however, most large wind turbines operate at variable speed, such that both the rotor and the generator speeds vary by roughly a factor of two during normal operation.

6.5.2.5 Brakes

Function
Nearly all wind turbines employ a mechanical brake somewhere on the drive train. Such a brake is normally included in addition to an aerodynamic brake. In fact, some design standards (Germanischer Lloyd, 1993) require two independent braking systems, one of which is usually aerodynamic and the other of which is on the drive train. In most cases, the mechanical brake is capable of stopping the turbine. In other cases, the mechanical brake is used only for parking. That is, it keeps the rotor from turning when the turbine is not operating. Brakes that can be used only for parking are becoming less common, because of the influence of design standards. Generally, such lightweight brakes would only be used on a turbine with a fail-safe, pitch-controlled rotor.

Types
There are two types of mechanical brake in common usage on wind turbines: disc brakes and clutch brakes. The disc brake operates in a manner similar to that on an automobile. A steel disc is rigidly affixed to the shaft to be braked. During braking a hydraulically actuated caliper pushes brake pads against the disc. The resulting force creates a torque opposing the motion of the disc, thus slowing the rotor. An example of a disc brake is shown in Figure 6.39.

Clutch-type brakes consist of at least one pressure plate and at least one friction disc. See, for example, http://www.icpltd.co.uk/index1.html. Actuation of clutch brakes is normally via springs, so they are fail-safe by design. These brakes are released by compressed air or hydraulic fluid.
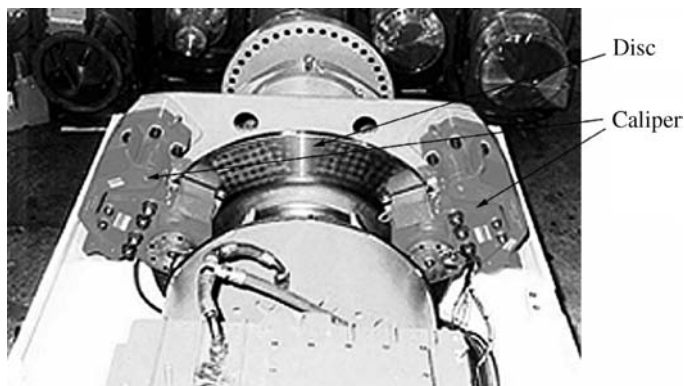
Figure 6.39   Disc brake. Reproduced by permission of Svendborg Brakes A/S

Another, less common, type of brake is electrically based and is known as a 'dynamic brake'. The basic principle is to feed power to a resistor bank after disconnecting the wind turbine's generator from the electrical grid. This puts a load on the generator, and hence a torque on the rotor, thereby decelerating it. More details on dynamic brakes are presented in Childs *et al.* (1993).

Location

Mechanical brakes can be located at any of a variety of locations on the drive train. For example, they may be on either the low-speed or high-speed side of the gearbox. If on the high-speed side, they may be on either side of the generator.

It is important to note that a brake on the low-speed side of the gearbox must be able to exert a much higher torque than would be the case with one on the high-speed side. It will thus be relatively massive. On the other hand, if the brake is on the high-speed side, it will necessarily act through the gearbox, possibly increasing the gearbox wear. Furthermore, in the event of an internal failure in the gearbox, a brake on the high-speed side might be unable to slow the rotor.

Activation

Brake activation depends on the type of brake used. Disc brakes require hydraulic pressure. This is normally supplied by a hydraulic pump, sometimes in conjunction with an accumulator. There are also designs in which springs apply brake pressure, and the hydraulic system is used to release the brakes.

Clutch-type brakes are normally spring-applied. Either a pneumatic system or hydraulic system is used to release the brake. In the case of pneumatics, an air compressor and storage tank must be provided, as well as appropriate plumbing and controls.

Performance

Three important considerations in the selection of a brake include:

- maximum torque;
- length of time required to apply;
- energy absorption.

A brake intended to stop a wind turbine must be able to exert a torque in excess of what could plausibly be expected to originate from the rotor. Recommended standards indicate that a brake design torque should be equal to the maximum design torque of the wind turbine (Germanischer Lloyd, 1993).

A brake intended to stop a turbine should begin to apply almost immediately, and should ramp up to full torque within a few seconds. The ramp-up time selected is a balance between instantaneous (which would apply a very high transient load to the drive train) and so slow that acceleration of the rotor and heating of the brake during deceleration could be concerns. Normally the entire braking event, from initiation until the rotor is stopped, is less than five seconds.

Energy absorption capability of the brake is an important consideration. First of all, the brake must absorb all the kinetic energy in the rotor when turning at its maximum possible speed. It must also be able to absorb any additional energy that the rotor could acquire during the stopping period.

6.5.3 Yaw System

6.5.3.1 Function

With very few exceptions, all horizontal axis wind turbines must be able to yaw so as to orient themselves in line with the wind direction. Some turbines also use active yaw as a means of power regulation. In any case, a mechanism must be provided to enable the yawing to take place, and to do so at a slow enough rate that large gyroscopic forces are avoided.

6.5.3.2 Types

There are two basic types of yaw system: active yaw and free yaw. Turbines with active yaw are normally upwind machines. They employ a motor to actively align the turbine. Turbines with free yaw are normally downwind machines. They rely on the aerodynamics of the rotor to align the turbine. As turbines get larger, however, active yaw will likely be considered for downwind turbines as well.

6.5.3.3 Description

Regardless of the type of yaw system, all horizontal axis wind turbines have some type of yaw bearing. This bearing must carry the weight of the main part of the turbine, as well as transmitting thrust loads to the tower.

In a turbine with active yaw, the yaw bearing includes gear teeth around its circumference, making it, in effect, a bull gear. A pinion gear on the yaw drive engages with these teeth, so that it can be driven in either direction.

The yaw drive normally consists of an electric motor, speed reduction gears, and a pinion gear. The speed must be reduced so that the yaw rate is slow, and so that adequate torque can be supplied from a small motor. Historically, some yaw drives have used small wind-driven rotors mounted at right angles to the main rotor. This has the advantage of not requiring a separate power source or controls. On the other hand, it lacks the flexibility of those with motors, and is not now commonly used.

One problem encountered with active yaw has been rapid wear or breaking of the yaw drive due to continuous small yaw movements of the turbine. This is possible because of backlash between the yaw drive pinion and the bull gear. The motion results in many shock load cycles between those gears. In order to reduce these cycles, a yaw brake is frequently used now in active yaw systems. This brake is engaged whenever the turbine is not yawing. It is released just before yawing begins. A typical yaw drive with a brake is illustrated in Figure 6.40.

The yaw motion in an active yaw system is controlled using yaw error as an input. Yaw error is monitored by means of a wind vane mounted on the turbine. When the yaw error is outside the allowed range for some period of time, the drive system is activated and the turbine is moved in the appropriate direction.

In turbines with free yaw, the yaw system is normally simpler. Often there is nothing more than the yaw bearing. Some turbines, however, include a yaw damper. Yaw dampers are used to slow the yaw rate, helping to reduce gyroscopic loads. They are most useful for machines which have a relatively small polar moment of inertia about the yaw axis.
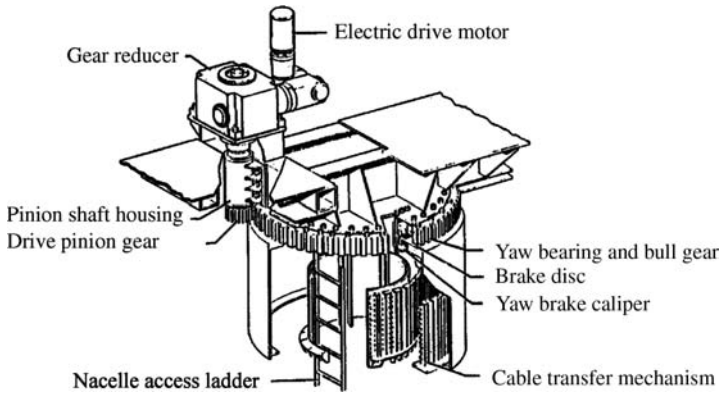
Figure 6.40   Typical yaw drive with brake (Van Bibber and Kelly, 1985)

6.5.4 Main Frame and Nacelle

The nacelle is the housing for the principal components of the wind turbine (with the exception of the rotor). It includes the main frame and the nacelle cover.

6.5.4.1 Main Frame

Function
The main frame is the structural component to which the gearbox, generator, and brake are attached. It provides a rigid structure to maintain the proper alignment among those other components. It also provides a point of attachment for the yaw bearing, which in turn is bolted to the top of the tower.

Types
There are basically two types of main frame. The main frame is either a separate component, or it is part of an integrated gearbox.

Description
When the main frame is a separate component, it is normally a rigid steel casting or weldment. Threaded holes or other attachment points are provided in appropriate locations for bolting on the other components.
   When the main frame is part of an integrated gearbox, the case is made thick enough that it can carry the requisite loads. As with the separate main frame, attachment points are provided for securing the other items.

Loads
The main frame must transmit all the loads from the rotor and reaction loads from the generator and brake to the tower. It must also be rigid enough that it allows no relative movement between the rotor support bearings, gearbox, generator, and brake.

6.5.4.2 Nacelle Housing

The nacelle housing provides weather protection for the wind turbine components which are located in the nacelle. These include, in particular, electrical and mechanical components that could be affected by sunlight, rain, ice, or snow.

Nacelle housings are normally made from a lightweight material, such as fiberglass. On larger machines the nacelle housing is of sufficient size that it can be entered by personnel for inspecting or maintaining the internal components. On small and medium-size turbines, a separate nacelle housing is normally attached to the main frame in such a way that it can be readily opened for access to items inside. The exterior and interior of the nacelle of a 5 MW turbine are shown in Figure 6.41. A component which some turbines have, and which is closely related to the nacelle cover, is the spinner or nose cone. This is the cover for the hub. One of these can also be seen in Figure 6.41.

6.5.5 Tower

Towers are supports to raise the main part of the turbine up in the air. A tower is normally at least as high as the diameter of the rotor. For smaller turbines the tower may be much higher than that. Generally, tower height should not be less than 24 m because the wind speed is lower and more turbulent so close to the ground.

6.5.5.1 General Tower Issues

There are three types of tower in common use for horizontal axis wind turbines:

- free-standing lattice (truss);
- cantilevered pipe (tubular tower);
- guyed lattice or pole.

Historically, free-standing lattice towers were used more commonly until the mid-1980s. For example, the Smith–Putnam, US Department of Energy MOD-0, and early US Windpower

Figure 6.41 Exterior and interior of the nacelle of a 5 MW wind turbine
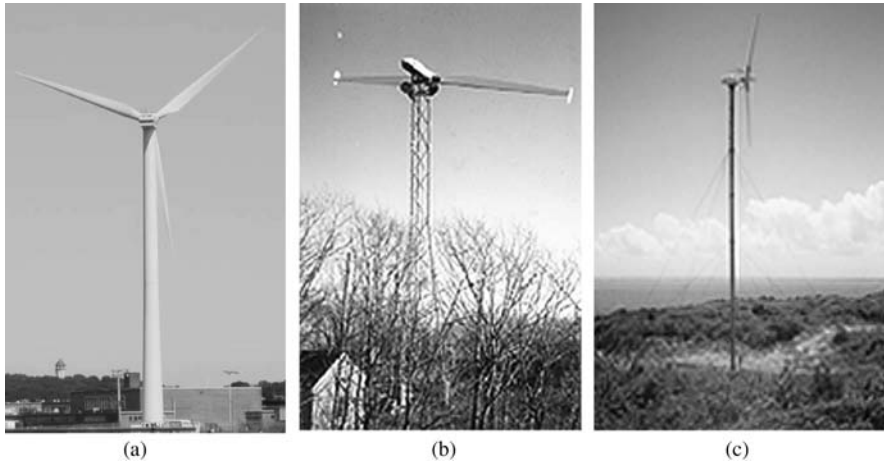
Figure 6.42   Tower options, (a) tubular tower; (b) truss tower; (c) guyed tower.   Reproduced by permission of Vergnet SA

turbines all used towers of this type. Since that time tubular towers have been used more frequently. With a few notable exceptions (such as the Carter and Wind Eagle turbines), guyed towers have never been very common for machines of medium size or larger. Some tower options are illustrated in Figure 6.42.

Tubular towers have a number of advantages. Unlike lattice towers, they do not rely on many bolted connections which need to be torqued and checked periodically. They provide a protected area for climbing to access the machine. Aesthetically, they provide a shape which is considered by some to be visually more pleasing than an open truss.

Materials
Wind turbine towers are usually made of steel, although sometimes reinforced concrete is used. When the material is steel, it is normally galvanized or painted to protect it from corrosion. Sometimes Cor-Ten® steel, which is inherently corrosion resistant, is used.

Loads
The tower can experience two major types of load: (1) steady and (2) dynamic. Steady tower loads arise primarily from aerodynamically produced thrust and torque. These were discussed in detail in Chapter 4. The weight of the machine itself is also a significant load. The loading on the tower is evaluated for at least two conditions: (1) operating at rated power and (2) stationary at survival wind speed. In the latter case, IEC standards recommend that the 50-year extreme wind speed be used (see Chapter 7). The effects of loading must be considered especially on bending and buckling.

Dynamic effects can be a significant source of loads, especially on soft or soft–soft towers. Recall that a stiff tower is one whose fundamental natural frequency is above the blade-passing frequency, a soft tower is one whose natural frequency is between the blade-passing frequency and the rotor frequency, and a soft–soft tower is one whose natural frequency is below both the rotor frequency and the blade-passing frequency. For either a soft or soft–soft tower, the tower can be excited during start-up or shutdown of the turbine.

Determination of the tower natural frequency may be done by methods discussed in Chapter 4. For the simple case, when the turbine/tower can be approximated by a uniform cantilever with a point mass on the top, the following equation (Baumeister, (1978)) may be used.

$$f_n = \frac{1}{2\pi} \sqrt{\frac{3\,E\,I}{(0.23\,m_{Tower} + m_{Turbine})\,L^3}} \tag{6.23}$$

where f_n is the fundamental natural frequency (Hz), E is the modulus of elasticity, I is the moment of inertia of the tower cross-section, m_{Tower} is the mass of the tower, $m_{Turbine}$ is the mass of the turbine, and L is the height of the tower.

For non-uniform or guyed towers, the Rayleigh method may be quite useful. The method is described in general by Thomson (1981) and by Wright *et al.* (1981) for wind turbines. Comprehensive analysis of towers, including natural frequency estimation, may be done with finite element methods. An example of this is given in El Chazly (1993).

A tower should be designed so that its natural frequency does not coincide with the turbine's excitation frequencies (the rotor frequency or the blade-passing frequency). In addition, the excitation frequencies should generally not be within 5% of tower natural frequency during prolonged operation. When operation is intended in a region where the excitation frequencies are between 30% and 140% of tower natural frequency, a dynamic magnification factor, D, should be used to multiply the design loads in evaluating the structure. The magnification factor is determined by the damping properties of the tower and the relation between the excitation frequencies. It is equivalent to the non-dimensional amplitude which was developed in Chapter 4 (Equation (4.27)):

$$D = \frac{1}{\sqrt{\left[1 - (f_e/f_n)^2\right]^2 + \left[2\,\xi\,(f_e/f_n)^2\right]}} \tag{6.24}$$

where f_e = excitation frequency, f_n = natural frequency, ξ = damping ratio.

The damping ratio is found from the 'logarithmic damping decrement', δ, by the relation:

$$\xi = \frac{\delta}{2\,\pi} \tag{6.25}$$

Damping of tower vibrations is due to both aerodynamic and structural factors. The damping decrement suggested by Germanischer Lloyd (1993) is 0.1 for reinforced concrete and between 0.05 and 0.15 for steel.

A comparative assessment of wind turbine tower options is given in Babcock and Connover (1994).

6.5.5.2 Tower Climbing Safety

Nearly all wind turbines must be climbed occasionally for inspection or maintenance. Provision must be made in the tower design for safe climbing. This typically includes a ladder or climbing pegs and an anti-fall system. Figure 6.43 illustrates tower climbing safety equipment.

Figure 6.43   Tower climbing safety equipment. Reproduced by permission of Vestas Wind Systems A/S

6.5.5.3 Tower Top

The tower top provides the interface for attaching the main frame of the wind turbine to the tower. The stationary part of the yaw bearing is attached to the tower top. The shape of the tower top depends strongly on the type of tower. It is usually made from cast steel.

6.5.5.4 Tower Foundation

The foundation of a wind turbine must be sufficient to keep the turbine upright and stable under the most extreme design conditions. At most sites, the foundation is constructed as a reinforced concrete pad. The weight of the concrete is chosen to provide resistance to overturning under all conditions. Sometimes turbines are installed on rock. In this case the foundation may consist of rods grouted into holes drilled deep into the rock. A concrete pad may be used to provide a level surface, but any tensile loads are taken ultimately by the rods. Some of the possibilities that may be encountered in wind turbine foundations are illustrated in Figure 6.44.

6.5.5.5 Tower Erection

The intended method of tower erection will have a direct impact on the design of the tower. Larger turbines are most commonly erected with cranes. Small and medium-size turbines are often self-erecting. The most common method of self erection is to use a gin pole or 'A-frame' at a right angle to the tower. The A-frame is connected to the top of the tower by a cable. A winch is then used, in conjunction with sheaves, to raise the tower. With such a method of erection, the tower base must include hinges as well as a way of securing the tower in place once it is vertical. The turbine itself is connected to the tower before it is raised. Some of the methods for erecting towers are shown in Figure 6.45.
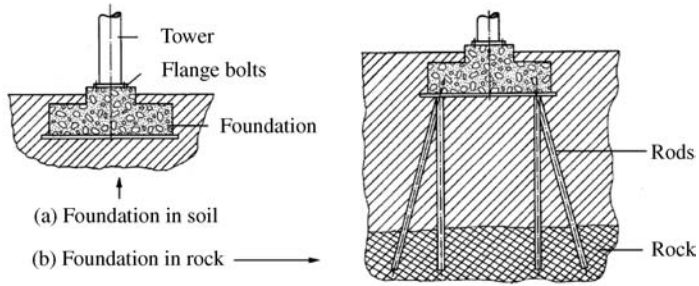
Figure 6.44 Wind turbine foundations (adapted from Hau, 1996). Reproduced by permission of Springer Verlag GmbH

Figure 6.45 Tower erection methods (a) crane erection of tubular tower (reproduced by permission of Vestas Wind Systems A/S); (b) tilt up with gin pole (reproduced by permission of Vergnet SA)

Regardless of the method of erection, an important consideration in the design of the tower is the load that it will experience during the installation.

References

AGMA (1997) *Recommended Practices for Design and Specification of Gearboxes for Wind Turbine Generator Systems.* AGMA Information Sheet. AGMA/AWEA 921-A97.

Ansell, M. P. (1987) Layman's guide to fatigue: the Geoff Pontin Memorial Lecture. *Proc. of the 9th British Wind Energy Association Conference.* Mechanical Engineering Publications, London.

Babcock, B. A. and Connover, K. E. (1994) Design of cost effective towers for an advanced wind turbine. *Proc. of the 15th ASME Wind Energy Symposium.* American Society of Mechanical Engineers, New York.

Baumeister, T. (Ed.) (1978) *Marks' Standard Handbook for Mechanical Engineers*, 8th edition. McGraw Hill, New York.

Cairns, D. and Skramstad, J. (2000) *Resin Transfer Molding and Wind Turbine Blade Construction, SAND99-3047.* Sandia National Laboratory, Albuquerque, NM.

Childs, S., Hughes, P. and Saeed, A. (1993) Development of a dynamic brake model. *Proc. 1993 American Wind Energy Association Conference,* Washington.

Chou, T. W., McCulloch, R. L. and Pipes, R. B. (1986) Composites. *Scientific American*, **255**(4), 192–203.

Downing, S. D. and Socie, D. F. (1982) Simple rainflow counting algorithms. *International Journal of Fatigue* **4**(1), 31–40.

El Chazly, N. (1993) Wind turbine tower structural and dynamic analysis using the finite element method. *Proc. 15th British Wind Energy Association Conference.* Mechanical Engineering Publications, London.

Garrad, A. D. and Hassan, U. (1986) The dynamic response of a wind turbine for fatigue life and extreme load prediction. *Proc. 1996 European Wind Energy Association Conference.* A. Ragguzi, Bookshop for Scientific Publications, Rome.

Gasch, R. (Ed.) (1996) *Windkraftanlagen* (Windpower Plants). B. G. Teubner, Stuttgart.

Germanischer Lloyd (1993) *Regulation of the Certification of Wind Energy Conversion Systems.* Germanischer Lloyd, Hamburg.

Harrison, R. Hau, E. and Snel, H. (2000) *Large Wind Turbines: Design and Economics.* John Wiley & Sons, Ltd, Chichester.

Hau, E. (1996) *Windkraftanlagen* (Windpower Plants). Springer, Berlin.

Hoadley, R. B. (2000) *Understanding Wood: A Craftsman's Guide to Wood Technology*. The Taunton Press, Newtown, CT.

Hydraulic Pneumatic Power Editors (1967) *Hydraulic Handbook.* Trade and Technical Press, Ltd., Morden, Surrey, UK.

Hyers, R. W. McGowan, J. G. Sullivan, J.F. and Syret, B. C. (2006) Condition monitoring and prognosis of utility scale wind turbines. *Energy Materials*, **1**(3), 187–203.

IEA (2008) *Introductory Note: IEA Topical Expert Meeting #56 on the Application of Smart Structures for Large Wind Turbine Rotor Blades*, International Energy Agency, available at: http://www.ieawind.org/Task_11/ComingEvents/Smart/Invitation_Smart_Struct.pdf

IEC (2005) *Wind Turbines Part 1: Design Requirements*, 61400-1, 3rd edition. International Electrotechnical Commission, Geneva.

IEC (2008) *Design Requirements for Wind Turbine Gearboxes*, 61400-4 WD3 2008-06. International Electrotechnical Commission, Geneva.

McGowan, J. G. Hyers, R. W. Sullivan, K. L. Manwell1, J. F. Nair, S. V. McNiff, B. and Syrett, B. C. (2007) A review of materials degradation in utility scale wind turbines. *Energy Materials*, **2**(1), 41–64.

McNiff, B. P. Musial, W. D. and Erichello, R. (1990) Variations in gear fatigue life for different braking strategies. *Proc. 1990 American Wind Energy Association Conference,* Washington, DC.

National Research Council (1991) *Assessment of Research Needs for Wind Turbine Rotor Materials Technology*. National Academy Press, Washington, DC.

Nijssen, R. P. L. (2007) *Fatigue Life Prediction and Strength Degradation of Wind Turbine Rotor Blade Composites*, SAND2006-7810P. Sandia National Laboratories, Albuquerque, NM.

Parmley, R. D. (1997) *Standard Handbook of Fastening and Joining*, 3rd edition. McGraw Hill, New York.

Perkins, F. and Jones, R. W. (1981) The effect of delta 3 on a yawing HAWT blade and on yaw dynamics. *Proc. Wind Turbine Dynamics Workshop, Cleveland, OH*, pp. 295–301.

Poore, R. and Liettenmaier, T. (2003) *Alternative Design Study Report: WindPact: Advanced Wind Turbine Drive Train Designs Study*, NREL/SR-500-33196, National Renewable Energy Laboratory, Golden, CO.

Selig, M. (2008) UIUC *Airfoil Coordinates Data Base*, UIUC Airfoil Data Site, available at: http://amber.aae.uiucc.edu/~m-selig/ads.html.

Selig, M. and Tangler, J. L. (1995) Development of a multipoint inverse design method for horizontal axis wind turbines. *Wind Engineering*, **19**(2), 91–105.

Shigley, R. G. Mischke, C. R. and Budynas, R. (2003) *Mechanical Engineering Design*, 7th edition. McGraw Hill, New York.

Spotts, M. F. Shoup, T. E. and Hornberger, L. E. (2003) *Design of Machine Elements*, 8th edition. Prentice Hall, Englewood Cliffs, NJ.

Sutherland, H. J. (1999) *On the Fatigue Analysis of Wind Turbines*, SAND99-0089, Sandia National Laboratories, Albuquerque, NM.

Sutherland, H. J. (2001) Preliminary analysis of the structural and inflow data from the LIST turbine. *Proc. of the 2001 ASME/AIAA Wind Energy Symposium AIAA-2001-0041*.

Sutherland, H. J. Veers, P. S. and Ashwill, T. D. (1995) *Fatigue Life Prediction for Wind Turbines: A Case Study on Loading Spectra and Parameter Sensitivity*. Standard Technical Publication 1250, American Society for Testing and Materials, Philadelphia, PA.

Thomson, W. T. (1981) *Theory of Vibrations with Applications*, 2nd edition. Prentice-Hall, Englewood Cliffs, NJ.

Van Bibber, L. E. and Kelly, J. L. (1985) Westinghouse 600 kW wind turbine design. *Proc. of Windpower 1985,* American Wind Energy Association, Washington, DC.

Veers, P. Ashwill, T. D. Sutherland, H. J. Laird, D. L. Lobitz, D. W. Griffin, D. A. Mandell, J. F. Musial, W. D. Jackson, K. Zuteck, M. Miravete, A. Tsai, S. W. and Richmond, J. L. (2003) Trends in the design, manufacture and evaluation of wind turbine blades. *Wind Energy*, **6**(3), 245–259.

Wright, A. D. Sexton, J. H. and Butterfield, C. P. (1981) SWECS tower dynamics analysis methods and results. *Proc. of the Wind Turbine Dynamics Workshop,* Cleveland, OH, pp. 127–147.

7

Wind Turbine Design and Testing

7.1 Overview

7.1.1 Overview of Design Chapter

The design process includes conceptual design, detailed design of components to withstand the loads they will be expected to experience, and then testing of full wind turbines and components to ensure that they have indeed met those design goals. This chapter covers all of these aspects of the design process. The substance of the chapter begins in Section 7.2 with an overview of the design process and then continues with a more in-depth examination of the various steps involved. This is then followed in Section 7.3 by a review of the basic wind turbine topologies. Section 7.4 gives an overview of international standards related to wind turbines. Section 7.5 then examines the types of loads that a wind turbine experiences, particularly with reference to the key international design standard IEC 61400-1. After that, Section 7.6 provides an overview of scaling relationships for loads and natural frequencies. These can be used for the initial starting point of a new wind turbine design. Section 7.7 discusses how a wind turbine power curve may be predicted, once the basic aspects of the design have been chosen. This is followed in Section 7.8 by an overview of some of the analysis tools that are available to assist in the development of a new design. Once a new design has been developed, it must be evaluated. This is the topic of Section 7.9. The chapter ends in Section 7.10 with a review of wind turbine testing methods and issues and aspects of component and certification testing.

7.1.2 Overview of Design Issues

The process of designing a wind turbine involves the conceptual assembling of a large number of mechanical and electrical components into a machine which can convert the fluctuating power in the wind into a useful form. This process is subject to a number of constraints, but the fundamental ones involve the potential economic viability of the design. Ideally, the wind turbine should be able to produce power at a cost lower than its competitors,

which are typically petroleum-derived fuels, natural gas, nuclear power, or other renewables. At the present state of the technology, this is often a difficult requirement, so sometimes incentives are provided by governments to make up the difference. Even in this case, it is a fundamental design goal to keep the cost of energy lower than it would be from a turbine of a different design.

The cost of energy from a wind turbine is a function of many factors, but the primary ones are the cost of the turbine itself and its annual energy productivity. In addition to the first cost of the turbine, other costs (as will be discussed in more detail in Chapter 11) include installation, operation, and maintenance. These will be influenced by the turbine design and must be considered during the design process. The productivity of the turbine is a function both of the turbine's design and the wind resource. The designer cannot control the resource, but must consider how best to utilize it. Other factors that affect the cost of energy, such as loan interest rates, discount rates, etc. tend to be of secondary importance and are largely outside the purview of the designer.

The constraint of minimizing the cost of energy has far-reaching implications. It impels the designer to minimize the cost of the individual components, which in turn pushes him or her to consider the use of inexpensive materials. There is also an impetus to keep the weight of the components as low as possible to minimize component cost and the cost of the supporting structure. On the other hand, the turbine design must be strong enough to survive any likely extreme events, and to operate reliably and with a minimum of repairs over a long period of time. Finally, wind turbine components, because they are kept small, tend to experience relatively high stresses. By the nature of the turbine's operation, the stresses also tend to be highly variable. Varying stresses result in fatigue damage. This eventually leads to either failure of the component or the need for replacement.

The need to balance the initial cost of the wind turbine with the requirement that the turbine have a long, fatigue-resistant life should be the fundamental concern of the designer.

7.2 Design Procedure

There are a number of approaches that can be taken towards wind turbine design, and there are many issues that must be considered. This section outlines the steps in one approach. The following sections provide more details on those steps.

The key design steps include the following:

 1. Determine application.
 2. Review previous experience.
 3. Select topology.
 4. Estimate preliminary loads.
 5. Develop tentative design.
 6. Predict performance.
 7. Evaluate design.
 8. Estimate costs and cost of energy.
 9. Refine design.
10. Build prototype.
11. Test prototype.
12. Design production machine.

Steps 1 through 7 and 11 are the subjects of this chapter. Turbine cost and cost of energy estimates (Step 8) can be made using methods discussed in Chapter 11. Steps 9, 10, and 12 are beyond the scope of this text, but they are based on the principles outlined here.

7.2.1 Determine Application

The first step in designing a wind turbine is to determine the application. Wind turbines for producing bulk power for supply to large utility networks, for example, will have a different design than will turbines intended for operation in remote communities.

The application will be a major factor in choosing the size of the turbine, the type of generator it has, the method of control, and how it is to be installed and operated. For example, wind turbines for utility power will tend to be as large as practical. At the present time, such turbines typically have power ratings in the range of 500 kW to 3.0 MW with rotor diameters in the range of 38 m to 90 m. (Such machines are often installed in clusters or wind farms, and may be able to utilize fairly developed infrastructure for installation, operation, and maintenance.

Turbines for use by utility customers, or for use in remote communities, tend to be smaller, typically in the 10 to 500 kW range. Ease of installation and maintenance and simplicity in construction are important design considerations for these turbines.

7.2.2 Review Previous Experience

The next step in the design process should be a review of previous experience. This review should consider, in particular, wind turbines built for similar applications. A wide variety of wind turbines has been conceptualized. Many have been built and tested, at least to some degree. Lessons learned from those experiences should help guide the designer and narrow the options.

A general lesson that has been learned from every successful project is that the turbine must be designed in such a way that operation, maintenance, and servicing can be done in a safe and straightforward way.

7.2.3 Select Topology

There are a wide variety of possible overall layouts or 'topologies' for a wind turbine. Most of these relate to the rotor. The most important choices are listed below. These choices are discussed in more detail in Section 7.3.

- rotor axis orientation: horizontal or vertical;
- power control: stall, variable pitch, controllable aerodynamic surfaces, or yaw control;
- rotor position: upwind of tower or downwind of tower;
- yaw control: driven yaw, free yaw, or fixed yaw;
- rotor speed: constant or variable;
- design tip speed ratio and solidity;
- type of hub: rigid, teetering, hinged blades, or gimballed;
- number of blades;
- generator speed: synchronous speed, multiple synchronous speeds, or variable speed;
- tower structure.

7.2.4 Estimate Preliminary Loads

Early in the design process it is necessary to make a preliminary estimate of the loads that the turbine must be able to withstand. These loads will serve as inputs to the design of the individual components. Estimation of loads at this stage may involve the use of scaling of loads from turbines of similar design, 'rules of thumb', or simple computer analysis tools. These estimates are improved throughout the design phase as the details of the design are specified. At this stage it is important to keep in mind all the loads that the final turbine will need to be able to withstand. This process can be facilitated by referring to recommended design standards. It is normal in this stage to prepare a 'design basis ' for the turbine. This is the set of conditions that must be considered in the design. These will include external environmental conditions, such as the maximum expected wind speed, and functional requirements. These conditions are used in the preliminary loads estimate as well as in more detailed estimates later in the process.

7.2.5 Develop Tentative Design

Once the overall layout has been chosen and the loads approximated, a preliminary design will be developed. The design may be considered to consist of a number of subsystems. These subsystems, together with some of their principal components, are listed below. Each of these subsystems was discussed in more detail in Chapter 6.

- rotor (blades, hub, aerodynamic control surfaces);
- drive train (shafts, couplings, gearbox, mechanical brakes, generator);
- nacelle and main frame;
- yaw system;
- tower (foundation and erection).

There are also a number of general considerations, which may apply to the entire turbine. Some of these include:

- fabrication methods;
- ease of maintenance;
- aesthetics;
- noise;
- other environmental conditions.

7.2.6 Predict Performance

Early in the design process it is also necessary to predict the performance (power curve) of the turbine. This will be primarily a function of the rotor design, but it will also be affected by the type of generator, efficiency of the drive train, the method of operation (constant speed or variable speed), and choices made in the control system design. Power curve prediction is discussed in Section 7.7.

7.2.7 Evaluate Design

The preliminary design must be evaluated for its ability to withstand the loading the turbine may reasonably be expected to encounter. It goes almost without saying that the wind turbine

must be able to easily withstand any loads likely to be encountered during normal operation. In addition, the turbine must be able to withstand extreme loads that may only occur infrequently, as well as holding up to cumulative, fatigue-induced damage. Fatigue damage arises from fluctuating stress levels, which may occur in a periodic manner at frequencies proportional to rotor speed, in a stochastic ('random') manner, or as a result of transient loads.

The categories of loads the wind turbine must withstand, as described in Chapter 4, include:

- steady loads:
  o time-invariant loads not associated with rotation
  o time-invariant loads associated with rotation, such as centrifugal force;
- cyclic loads (due to wind shear, blade weight, yaw motion);
- transient or impulsive loads:
  o loads due to starting and stopping
  o short-duration loads, such as blades passing through tower shadow;
- stochastic loads (due to turbulence);
- resonance-induced loads (due to excitations near the natural frequency of the structure).

The turbine must be able to withstand these loads under all plausible conditions, including during both normal operation and extreme events. These conditions will be discussed in more detail in Section 7.5.

The loads of primary concern are those in the rotor, especially at the blade roots, but any loads at the rotor also propagate through the rest of the structure. Therefore, the loading at each component must also be carefully assessed.

Analysis of wind turbine loads and their effects is typically carried out with the use of computer-based analysis codes. In doing so, reference is normally made to accepted practices or design standards. The principles underlying the analysis of wind turbine loads were discussed in detail in Chapter 4. A more in-depth discussion of wind turbine loads as related to design is given in Section 7.5.

7.2.8 Estimate Costs and Cost of Energy

An important part of the design process is the estimation of the cost of energy from the wind turbine. The key factors in the cost of energy are the cost of the turbine itself and its productivity. It is therefore necessary to be able to predict the cost of the machine, both in the prototype stage and, most importantly, in production. Wind turbine components are typically a mix of commercially available items and specially designed and fabricated items. The commercially available items will typically have prices that will be lowered only slightly when bought in volume for mass production. Special items will often be quite expensive in the prototype level, because of the design work and the effort involved in building just one or a few of the items. In mass production, however, the price for the component should drop so as to be close to that of commercial items of similar material, complexity, and size.

Wind turbine costs and cost of energy calculations are discussed in more detail in Chapter 11.

7.2.9 Refine Design

When the preliminary design has been analyzed for its ability to withstand loads, its performance capability has been predicted, and the eventual cost of energy has been estimated,

it is normal that some areas for refinement will have been identified. At this point another iteration of the design is made. The revised design is analyzed in a similar manner to the process summarized above. This design, or perhaps a subsequent one if there are more iterations, will be used in the construction of a prototype.

7.2.10 Build Prototype

Once the prototype design has been completed, a prototype should be constructed. The prototype may be used to verify the assumptions in the design, test any new concepts, and ensure that the turbine can be fabricated, installed, and operated as expected. Normally, the turbine will be very similar to the expected production version, although there may be provision for testing and instrumentation options which the production machine will not need.

7.2.11 Test Prototype

After the prototype has been built and installed, it is subjected to a wide range of field tests. Power is measured and a power curve developed to verify the performance predictions. Strain gauges are applied to critical components. Actual loads are measured and compared to the predicted values.

7.2.12 Design Production Machine

The final step is the design of the production machine. The design of this machine should be very close to the prototype. It may have some differences, however. Some of these may be improvements, the need for which was identified during testing of the prototype. Others may have to do with lowering the cost for mass production. For example, a weldment may be appropriate in the prototype stage, but a casting may be a better choice for mass production.

7.3 Wind Turbine Topologies

This section provides a summary of some of the key issues relating to the most commonly encountered choices in the overall topology of modern wind turbines. The purpose of this section is not to advocate a particular design philosophy, but to provide an overview of what must be considered. It should be noted that there are, in the wind energy community, strong proponents of particular aspects of design, such as rotor orientation, number of blades, etc. A good overview of some issues of design philosophy is given by Dörner (2008) on his Internet site.

One of the general topics of great interest at the present time is how light a turbine can be and still survive for the desired amount of time. Some of the issues in this regard are discussed by Geraets *et al.* (1997).

7.3.1 Rotor Axis Orientation: Horizontal or Vertical

The most fundamental decision in the design of a wind turbine is probably the orientation of the rotor axis. In most modern wind turbines the rotor axis is horizontal (parallel to the ground),

or nearly so. The turbine is then referred to as a 'horizontal axis wind turbine' (HAWT), as discussed in Chapter 1. There are a number of reasons for that trend; some are more obvious than others. Two of the main advantages of horizontal axis rotors are the following:

1. The rotor solidity of an HAWT (and hence total blade mass relative to swept area) is lower when the rotor axis is horizontal (at a given design tip speed ratio). This tends to keep costs lower on a per kW basis.
2. The average height of the rotor swept area can be higher above the ground. This tends to increase productivity on a per kW basis.

Vertical axis wind turbines (VAWTs) were discussed in Chapter 3. As noted there, the major advantage of VAWTs is that there is no need for a yaw system. That is, the rotor can accept wind from any direction. Another advantage is that in most vertical axis wind turbines, the blades can have a constant chord and no twist. These characteristics should enable the blades to be manufactured relatively simply (e.g. by aluminum pultrusion) and thus cheaply. A third advantage is that much of the drive train (gearbox, generator, brake) can be located on a stationary tower, relatively close to the ground.

In spite of some promising advantages of the vertical axis rotor, the design has not met with widespread acceptance. Many machines that were built in the 1970s and 1980s suffered fatigue damage of the blades, especially at connection points to the rest of the rotor. This was an outcome of the cyclic aerodynamic stresses on the blades as they rotate and the fatigue properties of the aluminum from which the blades were commonly fabricated.

Incompatibilities between structure and control have also caused problems. From a structural viewpoint, the Darrieus troposkein ('skipping rope') shape has appeared most desirable (in comparison with the straight-bladed design). This is because the blade is not subject to any radial bending moments, but only tension. On the other hand, it is very difficult to incorporate aerodynamic control, such as variable pitch or aerodynamic brakes, on a blade of this type. For this reason, stall control is the primary means of limiting power in high winds. Owing to the aerodynamics of the stall-controlled vertical axis rotor, the rated wind speed tends to be relatively high. This results in the need for drive train components to be larger than they might otherwise be, and for overall capacity factors of the wind turbine to be relatively low.

In summary, a horizontal axis is probably preferable. There are enough advantages, however, to the vertical axis rotor that it may be worth considering for some applications. In this case, however, the designer should have a clear understanding of what the limitations are, and should also have some plausible options in mind for addressing those limitations.

Because of the predominance of horizontal axis wind turbines presently in use or under development, the remainder of this chapter, unless otherwise specified, applies primarily to wind turbines of that type.

7.3.2 Rotor Power Control: Stall, Pitch, Yaw, or Aerodynamic Surfaces

There are a number of options for controlling power aerodynamically. The selection of which of these is used will influence the overall design in a variety of ways. The following presents a brief summary of the options, focusing on those aspects that affect the overall design of the turbine. Details on control issues are discussed in Chapter 8.

Stall control takes advantage of reduced aerodynamic lift at high angles of attack to reduce torque at high wind speeds. For stall to function, the rotor speed must be separately controlled, most commonly by an induction generator (see Chapter 5) connected directly to the electrical grid. Blades in stall-controlled machines are fastened rigidly to the rest of the hub, resulting in a simple connection. The nature of stall control, however, is such that maximum power is reached at a relatively high wind speed. The drive train must be designed to accommodate the torques encountered under those conditions, even though such winds may be relatively infrequent. Stall-controlled machines invariably incorporate separate braking systems to ensure that the turbine can be shut down under all eventualities.

Variable-pitch machines have blades which can be rotated about their long axis, changing the blade's pitch angle. Changing pitch also changes the angle of attack of the relative wind and the amount of torque produced. Variable pitch provides more control options than does stall control. On the other hand, the hub is more complicated because pitch bearings need to be incorporated, and some form of pitch actuation system must also be included. In some wind turbines, only the outer part of the blades may be pitched. This is known as partial span pitch control.

Some wind turbines utilize aerodynamic surfaces on the blades to control or modify power. These surfaces can take a variety of forms, but in any case the blades must be designed to hold them, and means must be provided to operate them. In most cases aerodynamic surfaces are used for braking the turbine. In some cases, specifically when ailerons are used (see Chapter 6), the surfaces may also provide a fine-tuning effect.

Another option for controlling power is yaw control. In this arrangement, the rotor is turned away from the wind, reducing power. This method of control requires a robust yaw system. The hub must be able to withstand gyroscopic loads due to yawing motion, but can otherwise be relatively simple.

7.3.3 Rotor Position: Upwind of Tower or Downwind of Tower

The rotor in a horizontal axis turbine may be either upwind or downwind of the tower. A downwind rotor in principle allows the turbine to have free yaw, which is simpler to implement than active yaw. In reality, free yaw is not necessarily desirable, however (see Section 7.3.4). Another advantage of the downwind configuration is that it is easier to take advantage of centrifugal forces to reduce the blade root flap bending moments. This is because the blades are normally coned downwind, so centrifugal moments tend to counteract moments due to thrust. On the other hand, the tower produces a wake in the downwind direction, and the blades must pass through that wake every revolution. This wake is a source of periodic loads, which may result in fatigue damage to the blades and may impose a ripple on the electrical power produced. Blade passage through the wake is also a source of noise. The effects of the wake (known as 'tower shadow') may, to some extent, be reduced by utilizing a tower design which provides minimal obstruction to the flow.

7.3.4 Yaw Control: Free or Active

All horizontal axis wind turbines must provide some means to orient the machine as the wind direction changes. In downwind machines yaw motion has historically been free. The turbine follows the wind like a weather vane. For free yaw to work effectively, the blades are typically

coned a few degrees in the downwind direction. Free yaw machines sometimes incorporate yaw dampers to limit the yaw rate and thus gyroscopic loads in the blades.

Upwind turbines invariably have some type of active yaw control. This usually includes a yaw motor, gears, and a brake to keep the turbine stationary in yaw when it is properly aligned (see Chapter 6). Towers supporting turbines with active yaw must be capable of resisting the torsional loads that will result from use of the yaw system.

7.3.5 Rotor Speed: Constant or Variable

Historically, most rotors on grid-connected wind turbines have operated at a nearly constant rotational speed, determined by the electrical generator and the gearbox. In many turbines today, however, the rotor speed is allowed to vary. Variable-speed rotors can be operated at the optimum tip speed ratio to maximize power conversion in low wind and at lower tip speed ratios in high winds to reduce loads in the drive train. On the other hand, variable-speed rotors may require more complicated and expensive power conversion equipment in the drive train or electrical components of the wind turbine. See Chapter 5 for discussion of the electrical aspects of variable-speed wind turbines.

7.3.6 Design Tip Speed Ratio and Solidity

The design tip speed ratio of a rotor is that tip speed ratio where the power coefficient is a maximum. Selection of this value will have a major impact on the design of the entire turbine. First of all, there is a direct relation between the design tip speed ratio and the rotor's solidity (the area of the blades relative to the swept area of the rotor), as was discussed in Chapter 3. A high tip speed ratio rotor will have less blade area than the rotor of a slower machine of the same diameter. For a constant number of blades, the chord and thickness will decrease as the solidity decreases. Owing to structural limitations, there is a lower limit to how thin the blades may be. Thus, as the solidity decreases, the number of blades usually decreases as well.

There are a number of incentives for using higher tip speed ratios. First of all, reducing the number of blades or their weight reduces the cost. Second, higher rotational speeds imply lower torques for a given power level. This should allow the balance of the drive train to be relatively light. On the other hand, there are some drawbacks to high tip ratios as well. For one thing, high tip speed rotors tend to be noisier than slower ones (see Chapter 12).

7.3.7 Hub: Rigid, Teetering, Hinged Blades, Gimballed

The hub design of a horizontal axis wind turbine is an important constituent of the overall layout. The main options are rigid, teetering, or hinged. Most wind turbines employ rigid rotors. This means that the blades cannot move in the flapwise and edgewise directions. The term 'rigid rotor' does include those with variable-pitch blades, however.

The rotors in two-bladed turbines are usually teetering. That means that a portion of the hub is mounted on bearings and can teeter back and forth, in and out of the plane of rotation. The blades in turn are rigidly connected to the teetering portion of the hub, so during teetering one blade moves in the upwind direction, while the other moves downwind. See Chapter 6 for more discussion of teetering. An advantage of teetering rotors is that the bending moments in the blades can be very low during normal operation.

Some two-bladed wind turbines use hinges on the hub. The hinges allow the blades to move into and out of the plane of rotation independently of each other. Since the blade weights do not balance each other, however, other provisions must be made to keep them in the proper position when the turbine is not running, or is being stopped or started.

One design variant is known as a 'gimballed turbine'. It uses a rigid hub, but the entire rotor nacelle assembly is mounted on horizontal bearings so that the machine can tilt up or down from horizontal. This motion can help to relieve imbalances in aerodynamic forces.

7.3.8 Rigidity: Flexible or Stiff

Turbines with lower design tip speed ratios and higher solidities tend to be relatively stiff. Lighter, faster turbines are more flexible. Larger turbines are also more flexible than smaller turbines of a similar design. Flexibility may have some advantages in relieving stresses, but blade motions may also be more unpredictable. Most obviously, a flexible blade in an upwind turbine may be far from the tower when unloaded, but could conceivably hit it in high winds. Flexible components such as blades or towers may have natural frequencies near the operating speed of the turbine. This is something to be avoided. Flexible blades may also experience 'flutter' motion, which is a form of unstable and undesirable operation.

7.3.9 Number of Blades

Most modern wind turbines used for generating electricity have three blades, although some have two or even one. Three blades have the particular advantage that the polar moment of inertia with respect to yawing is constant, and is independent of the azimuthal position of the rotor. This characteristic contributes to relatively smooth operation even while yawing. A two-bladed rotor, however, has a lower moment of inertia when the blades are vertical than when they are horizontal. This 'imbalance' is one of the reasons that most two-bladed wind turbines use a teetering rotor. Using more than three blades could also result in a rotor with a moment of inertia independent of position, but more than three blades are seldom used. This is primarily because of the higher costs that would be associated with the additional blades.

A key consideration in selecting the number of blades is that the stress in the blade root increases with the number of blades for a turbine of a given solidity. Thus, all other things being equal, increasing the design tip speed ratio entails decreasing the number of blades.

A few single-bladed turbines have been built in the last thirty years. The presumed advantage is that the turbine can run at a relatively high tip speed ratio, and that the cost should be lower because of the need for only one blade. On the other hand, a counterweight must be provided to balance the weight of the single blade. The aesthetic factor of the appearance of imbalance is another consideration.

7.3.10 Generator Speed

Generator speed choices include having one synchronous speed, multiple synchronous speeds, or a range of continuously variable speeds. Typical squirrel cage induction and synchronous generators, as a function of their design, have one synchronous speed. Other options are a generator with two sets of windings, resulting in a generator with two operational speeds, depending on which winding is energized. The variable-speed options include small ranges

of variable-speed operation provided by high-slip induction generators, or larger ranges of variable-speed operation which are accomplished with wound rotor induction generators, permanent magnet generators, or standard generators with full-load power conversion. More details on variable-speed generation were provided in Chapter 5.

The choice of generator speed has a significant effect on the design and weight of other components such as the gearbox and power electronics. The choice of generator speed will determine the need for power electronics. The choices of rotor and generator characteristics (fixed or variable speed) will also determine various aspects of the drive train design. Fixed rotor and generator speeds, or rotor and generator speeds that vary but track each other, will generally use a parallel-shaft or planetary gearbox or a hybrid of the two. If the rotor speed and generator speed are to be the same, no gearbox is needed. If, on the other hand, the rotor speed and generator speed are to vary and not be the same, then something like a torque converter will be needed in the drive train (see Chapter 8 for an example of a wind turbine with a torque converter).

7.3.11 Tower Structure

The tower of a wind turbine serves to elevate the rotor nacelle assembly up into the air. For a horizontal axis machine the tower must be at least high enough to keep the blade tips from touching the ground as they rotate. In practice, towers are usually much higher than that. Winds are nearly always much stronger as elevation above ground increases, and they are less turbulent. All other things being equal, the tower should be as high as practical. Choice of tower height is based on an economic trade-off of increased energy capture versus increased cost. Towers were discussed in more detail in Chapter 6.

7.3.12 Design Constraints

There are inevitably a number of other factors that will influence the general design of a wind turbine. These include climatic factors, site-specific factors, and environmental factors, as summarized below.

7.3.12.1 Climatic Factors Affecting Design

Turbines designed for more energetic or turbulent sites need to be stronger than those in more conventional sites. Expected conditions at such sites must be considered if the turbines are to meet international standards. This topic is discussed in more detail in Section 7.4.

General climate can affect turbine design in a number of ways. For example, turbines for use in hot climates may need provisions for extra cooling, whereas turbines for cold climates may require heaters, special lubricants, or even different structural materials. Turbines intended for use in marine climates need protection from salt, and should be built of corrosion-resistant materials wherever possible.

7.3.12.2 Site-specific Factors Affecting Design

Turbines which are intended for relatively inaccessible sites have their designs constrained in a number of ways. For example, they might need to be self-erecting. Difficulty in transport could also limit the size or weight of any one component.

Limited availability of expertise and equipment for installation and operation would be of particular importance for machines intended to operate singly or in small groups. This would be particularly important for applications in remote areas or developing countries. In this case it would be especially important to keep the machine simple, modular, and designed to require only commonly available mechanical skills, tools, and equipment.

Offshore turbines, even if close to shore, may be inaccessible in high seas for both personnel and especially for the barges that would be needed for a crane. These and other site-specific constraints on the design of offshore wind turbines are discussed in Chapter 10.

7.3.12.3 Environmental Factors Affecting Design

Wind turbine proponents inevitably extol the environmental benefits that accrue to society through the use of wind-generated electricity. On the other hand, there will always be some impacts on the immediate environment where the turbine may be installed, and not all of these may be appreciated by the neighbors. Careful design, however, can minimize many of the adverse effects. Four of the most commonly noted environmental impacts of wind turbines are noise, visual appearance, effects on birds, and electromagnetic interference. Some of the key issues affecting overall wind turbine design are summarized below. More details are provided in Chapter 12.

There will always be some sound generated by wind turbines when they are operating, but noise can be can minimized through careful design. In general, upwind machines are quieter than downwind machines, and lower tip speed ratio rotors are quieter than those with higher tip speed ratios. Selection of airfoils, fabrication details of the blades, and design of tip brakes (if any) will also affect noise. Gearbox noise can be reduced by including sound proofing in the nacelle or eliminated by using a direct drive generator. Variable-speed turbines tend to make less noise at lower wind speeds, since the rotor speed is reduced under those conditions.

In general, it appears that turbines with lower tip speeds and towers with few perching opportunities are the least likely to adversely affect birds.

Visual appearance is very subjective, but there are reports that people prefer the sight of three blades to two, slow rotors to faster ones, and solid towers to lattice ones. A neutral color is often preferred as well.

Electromagnetic interference created by wind turbines has been the source of considerable concern. Concerns about electromagnetic interference include interference with television signals, the creation of false images or masking of flying objects in military and aviation radar systems, and blocking of microwave transmissions.

7.4 Wind Turbine Standards, Technical Specifications, and Certification

A variety of standards relevant to the design, testing, and operation of wind turbines has been prepared or are in the process of being prepared. This section provides a summary of wind turbine-related standards and how they are applied through the certification process. Section 7.5 then provides some detail on the application of the key design standard (IEC 61400-1) and later sections of this chapter provide more description of some other standards where appropriate. Closely related to standards are technical specifications. These are similar to standards, but are considered to be more recommendations than requirements.

Table 7.1 Wind turbine-related IEC standards

Source/Number	Title
IEC WT01	IEC System for Conformity Testing and Certification of Wind Turbines Rules and Procedures
IEC 61400-1	Wind Turbines – Part 1: Design Requirements, edition 2
IEC 61400-2	Wind Turbines – Part 2: Safety Requirements for Small Wind Turbines
IEC 61400-3	Wind Turbines – Part 3: Design Requirements for Offshore Wind Turbines
ISO/IEC 81400-4	Wind Turbines – Part 4: Gearboxes for Turbines from 40 kW to 2 MW
IEC 61400-11 TS	Wind Turbines – Part 11: Acoustic Emission Measurement Techniques
IEC 61400-12	Wind Turbines – Part 12: Power Performance Measurements of Electricity Producing Wind Turbines
IEC 61400-13 TS	Wind Turbines – Part 13: Measurement of Mechanical Loads
IEC 61400-14	Wind Turbines – Part 14: Declaration of Apparent Sound Power Levels and Tonality Value of Wind Turbines
IEC 61400-21	Wind Turbines – Part 21: Power Quality Measurements
IEC 61400-22 TS	Wind Turbines – Part 22: Conformity Testing and Certification of Wind Turbines
IEC 61400-23 TS	Wind Turbines – Part 23: Full-scale Structural Testing of Rotor Blades
IEC 61400-24 TR	Wind Turbines – Part 24: Lightning Protection
IEC 61400-25	Wind Turbines – Part 25: Communications for Monitoring and Control of Wind Turbines

7.4.1 Wind Turbine Standards and Technical Specifications

Until recently, standards and technical specifications were developed country by country, or by such entities as Germanischer Lloyd (GL) or Det Norske Veritas (DNV). The lead in wind turbine standards is now being taken by the International Electrotechnical Commission (IEC). The most important standards that are in use or being developed are listed in Table 7.1. Note that some of these are not yet official international (IEC) standards. If they are not, but are in the process of becoming so, their status is generally indicated by the following abbreviations: CD = committee draft, CDV = committee draft for voting, FDIS = final draft international standard. Technical specifications are denoted by 'TS.' Some other useful, but non-IEC, standards and guidelines are listed in Table 7.2.

All of the standards referred to in Tables 7.1 and 7.2 have some relevance to wind turbine design, although some are more directly relevant than others. It should be noted that the

Table 7.2 Other wind turbine-related standards

Source/Number	Title
Germanischer Lloyd	Regulations for the Certification of Wind Energy Conversion Systems
Danish Energy Agency DS-472	Code of Practice for Loads and Safety of Wind Turbine Construction
DNV	Guidelines for the Design of Wind Turbines, 2nd edition
DNV-OS-J101	Design of Offshore Wind Turbine Structures
DNV-OS-J102	Design and Manufacture of Wind Turbine Blades

majority of the IEC standards are still in draft form (CD, CDV, or FDIS) and others are in a continuous process of revision and updating. The most important IEC standard is IEC 61400-1 (IEC, 2005a). It deals explicitly with design requirements. It applies particularly to larger, land-based turbines, but it is relevant to smaller turbines and offshore turbines as well. IEC 61400-1 will be discussed in more detail in the next section. IEC 61400-2 (IEC, 2005b) is, as its name implies, concerned with small turbines. IEC 61400-3 (IEC, 2008b) applies to offshore wind turbines. It is consistent with IEC 61400-1 and focuses particularly on those design issues of relevance (such as waves, ocean currents, etc.) not considered in IEC 61400-1. ISO/IEC 81400-4 (ISO, 2004) is concerned specifically with the design of wind turbine gearboxes. IEC 61400-11 TS (IEC, 2006a) deals with acoustic emissions from wind turbines. This technical specification is indirectly relevant to design, since it would be used in evaluating, for example, the noise emission of a prototype. After the evaluation, it is possible that the design would be modified in a subsequent iteration to reduce noise emissions. IEC 61400-12 (IEC, 2005c) is concerned with power performance measurements. IEC 61400-13 TS (IEC, 2001a) concerns the measurement of mechanical loads. As with IEC 61400-11, design modifications could be made after the performance testing of a prototype in accordance with IEC 61400-12 and IEC 61400-13 TS. It may be presumed that the testing undertaken in this process would help identify areas where structural design changes might be made. IEC 61400-14 (IEC, 2004) is concerned with the sound emitted from a wind turbine. It would be used in conjunction with IEC 61400-11 TS. IEC 61400-21 (IEC, 2008a) is concerned with power quality measurements. This standard has most relevance for the electrical and electronic components of a wind turbine. IEC 61400-22 TS (IEC, 2008c) is a technical specification for certification (see Section 7.4.2). IEC 61400-23 TS (IEC, 2001b) concerns testing of wind turbine blades. Blades could be tested before the complete prototype is built. Results from blade tests could result in modifications to the blades' structural design. IEC 61400-24 TR (IEC, 2002) is a technical report concerned with lightning protection. It is relevant to certain details of the wind turbine's design, specifically those that are particularly likely to be adversely affected by lightning. Finally, IEC 61400-25 (IEC, 2006b) is concerned with monitoring and control of wind turbines, and is relevant to the associated aspects of the design.

The first two documents included in Table 7.2 (GL, 2003; DEA, 1992) are particularly concerned with the certification of wind turbines (see next section), but have indirect implications for the turbine design. The third document (DNV, 2006) is directly relevant to the design process. The fourth document listed, DNV-OS-J101 (DNV, 2007), is a preliminary offshore turbine design standard, and may be superseded once IEC 61400-3 is finalized. The fifth document listed, DNV-OS-J102 (DNV, 2006), is concerned with the design of wind turbine blades.

It may be noted that there are many other standards that are relevant to the design of wind turbines. These standards are typically referred to where applicable. For example, IEC 61400-1 includes references to a number of other IEC standards that are of broader scope than wind turbines, as well as International Standard Organization (ISO) standards. One example of another IEC standard is IEC 60204-1: 1997: Safety of Machinery – Electrical Equipment of Machines – Part 1: General requirements. Similarly, an example of an ISO standard is ISO 4354: 1997: Wind Actions on Structures. Development of the wind turbine gearbox standard (ISO, 2004) is a joint ISO/IEC activity.

7.4.2 Certification

Certification is a process used to ensure that the wind turbines are actually built and installed in accordance with the standards. Certification in general is the confirmation of compliance of a product or a service with defined requirements (e.g. guidelines, codes, and standards). The certification of activities associated with wind turbines is undertaken by an approved, independent entity such as a national laboratory. Certification typically involves application of computer models and tests, undertaken in accordance with design standards, to verify that the design is consistent with the standard. Certification may apply to the following: (1) a specific design or type, (2) turbines, their support structures, and associated equipment or activities within a project, (3) components, or (4) prototypes. More details on the certification process for wind turbines are given in the technical specification IEC TS 61400-22 (IEC, 2008c).

7.5 Wind Turbine Design Loads

7.5.1 Overview

Once the basic layout of the turbine is selected, the next step in the design process is to consider in detail the loads that the turbine must be able to withstand. As is commonly used in mechanics, the loads are the externally applied forces or moments to the entire turbine or to any of the components considered separately.

Wind turbine components are designed for two types of load: (1) ultimate loads and (2) fatigue loads. Ultimate loads refer to likely maximum loads, multiplied by a safety factor. Fatigue loads refer to the component's ability to withstand an expected number of cycles of possibly varying magnitude. As discussed in Chapter 4, wind turbine loads can be considered to fall into five categories: (1) steady (here including static loads), (2) cyclic, (3) stochastic, (4) transient (here including impulsive loads), and (5) resonance-induced loads. These loads and their origins are illustrated in Figure 7.1.

Steady loads, which were discussed in detail in Chapter 4, include those due to the mean wind speed, centrifugal forces in the blades due to rotation, weight of the machine on the tower, etc.

Cyclic loads, which were also discussed in Chapter 4, are those which arise due to the rotation of the rotor. The most basic periodic load is that experienced at the blade roots (of an HAWT) due to gravity. Other periodic loads arise from wind shear, crosswind (yaw error), vertical wind, yaw velocity, and tower shadow. Mass imbalances or pitch imbalances can also give rise to periodic loads.

Stochastic loads are due to the turbulence in the wind. Short-term variations in the wind speed, both in time and space across the rotor, cause rapidly varying aerodynamic forces on the blades. The variations appear random, but they can be described in statistical terms. In addition, the nature of the turbulence on the rotor is affected by the rotation itself. This effect is described under the term 'rotational sampling'. Rotational sampling is discussed in detail by Connell (1988).

Transient loads are those which occur only occasionally and are due to events of limited duration. The most common transient loads are associated with starting and stopping. Other transient loads arise from sudden wind gusts, changes in wind direction, blade-pitching
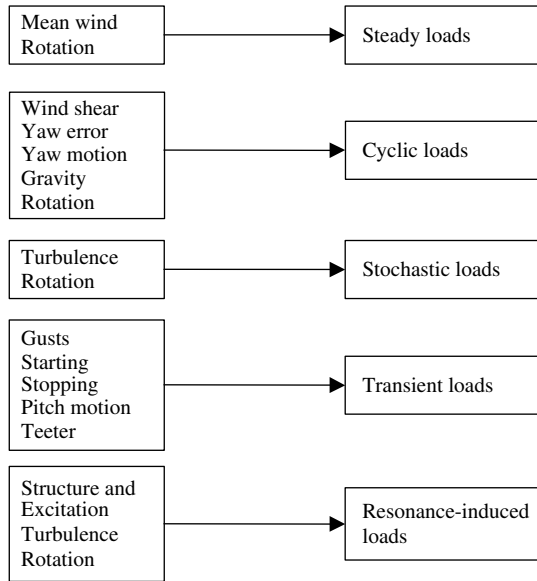
Figure 7.1   Sources of wind turbine loads

motions, or teetering. Gusts are discussed in Section 7.5. Loads due to starting and stopping can be quite significant, as illustrated in Figure 7.2. A detailed description of transient loads is outside the scope of this text, but some discussion of such loads on the drive train can be found in Manwell *et al.* (1996).
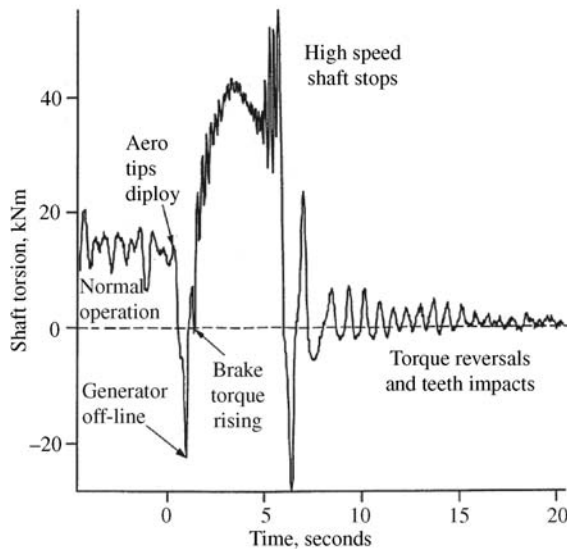
Figure 7.2   Example of drive train loads during stopping (Manwell *et al.*, 1996)

Resonance-induced loads arise as a result of some part of the structure being excited at one of its natural frequencies. The designer tries to avoid the possibility of that happening, but response to turbulence often inevitably excites some resonant response.

Vibrations and natural frequencies of wind turbine components were discussed in Chapter 4. It was also noted there that operation of the turbine in such a way as to excite those natural frequencies should be avoided. One way to identify points of correspondence between natural frequencies and excitation from the rotor is to use a Campbell diagram. A Campbell diagram illustrates the most important natural frequencies of the turbine as a function of rotor speed. Superimposed on those are lines corresponding to excitation frequency as a function of rotor speed, specifically the rotor rotation frequency ($1P$) and the blade-passing frequency (BP), where B is the number of blades and P is an abbreviation for 'per revolution.' Points of intersection indicate operating speeds that are to be avoided. A Campbell diagram for a three-bladed turbine is shown in Figure 7.3.

As can be seen in Figure 7.3, there may be a number of different frequencies to consider, and they correspond to a variety of types of motion. For example, the figure includes frequencies of combined rotor and nacelle motion; tower bending, both fore and aft and laterally; and blade bending, among others.

Sometimes operation at or near a natural frequency cannot be completely avoided. This may occur during start-up or shutdown, or at some rotor speeds of a variable-speed wind turbine. Effects of operation under such conditions must be considered. Wind turbine design standards developed by Germanischer Lloyd (GL, 2003) offer some guidance in this area.

7.5.2 Wind Turbine Design Loads and Design Standards

Many manufactured items are designed with reference to a particular 'design point'. This corresponds to an operating condition such that, if the item can meet that condition, it will perform at least adequately at any other realistic set of conditions.
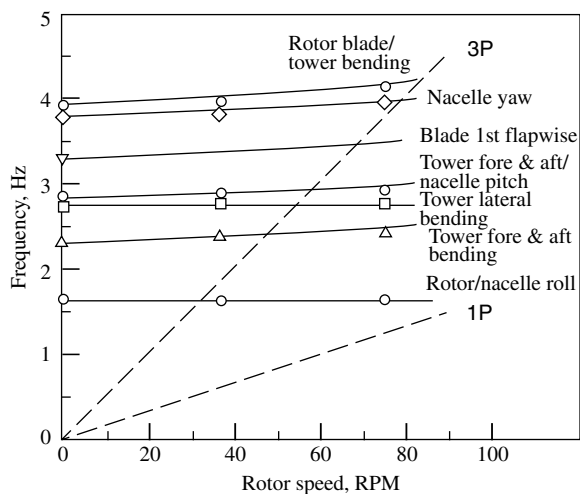
Figure 7.3 Example of a Campbell diagram for a wind turbine; P, per revolution (Eggleston and Stoddard, 1987). Reproduced by permission of Kluwer Academic Publishers

A single design point is not adequate for wind turbine design. Rather, the wind turbine must be designed for a range of conditions. Some of these will correspond to normal operation, where most of the energy will be produced. Others are extreme or unusual conditions which the turbine must be able to withstand with no significant damage. The most important considerations are: (1) expected events during normal operation, (2) extreme events, and (3) fatigue.

Enough experience has been gained with wind turbines that it has been possible to define a set of design conditions under which a turbine should be able to perform. These have been codified in IEC 61400-1 (IEC, 2005a), which was introduced in Section 7.4. The designer should be aware of this standard, since a turbine's ability to meet these conditions must be demonstrated if it is intended for use in any country which enforces those standards.

7.5.2.1 The IEC 61400-1 Design Standard

The following sections provide a summary of the IEC 61400-1 design standard as it applies to the design process. It should be noted that a complete assessment of a turbine's ability to meet these requirements is not possible until a full design has been completed and analyzed. Information in this standard, however, provides a target for the design, so it should be considered early in the design process.

As previously mentioned, IEC 61400-1 may be considered to be the fundamental wind turbine design standard. Its purpose is to specify 'design requirements to ensure the engineering integrity of wind turbine [and] . . . to provide an appropriate level of protection against damage from all hazards during the planned lifetime.' As such, it does not contain all the information that is needed to design a wind turbine and there are issues to consider that are outside the scope of the standard.

In accordance with IEC 61400-1, the process of incorporating loads into the design process consists of the following:

- determine a range of design wind conditions;
- specify design load cases of interest, including operating and extreme wind conditions;
- calculate the loads for the load cases;
- verify that the stresses due to the loads are acceptable.

Design Wind Conditions
The design wind conditions comprise the most important part of the design basis. The IEC 61400-1 standard defines three classes of wind conditions – I, II, and III – ranging from the most windy (50 m/s reference wind speed) to the least windy (37.5 m/s reference wind speed), under which a wind turbine might reasonably be expected to operate. Within those classes, three ranges of turbulence are defined. They are denoted A, B, and C, corresponding to high, medium, and low turbulence. These classes are summarized in Table 7.3. The important thing to note is that each class is characterized by a reference speed and a turbulence intensity. Other conditions of interest are referenced to the basic characterizations. To cover special cases, a fourth class, S, is also provided where the specific parameters are specified by the designer.

(i) Normal Wind Conditions
Under normal wind conditions the frequency of occurrences of wind speeds are assumed to be described by the Rayleigh distribution (see Chapter 2).

Table 7.3 IEC wind classes

Wind turbine class		I	II	III	S
Reference wind speed, U_{ref} (m/s)		50	42.5	37.5	Values to be specified by designer
A	$I_{ref}(-)$		0.16		
B	$I_{ref}(-)$		0.14		
C	$I_{ref}(-)$		0.12		

Normal Wind Profile (NWP)

The wind profile, $U(z)$, is the variation in wind speed with the height, z, above the ground. For the purposes of the IEC requirements, the variation in wind speed with height is assumed to follow a power law model (see Chapter 2), with an exponent of 0.2. It is then known as the normal wind profile (NWP).

Normal Turbulence Model (NTM)

The standard deviation of the turbulence in the longitudinal direction (direction of the mean wind), σ_x, is assumed to be given by:

$$\sigma_x = I_{ref}(0.75U_{hub} + 5.6) \tag{7.1}$$

where I_{ref} = turbulence intensity at 15 m/s and U_{hub} = wind speed at hub height.

The power spectral density of the turbulence can be modeled with the Mann spectrum (a variant of the von Karman) or the Kaimal spectrum (see Chapter 2 and Fordham, 1985).

(ii) Extreme Wind Conditions

There are five extreme wind conditions to be used in determining extreme loads under the IEC standards: (1) extreme wind speed (EWM), (2) extreme operating gust (EOG), (3) extreme coherent gust (ECG), (4) extreme coherent gust with change in direction (ECD), and (5) extreme wind shear (EWS).

Extreme Wind Speed (EWM)

Extreme wind speeds are very high, sustained winds which will probably occur, but only rarely. Two extreme wind speeds are defined by the frequency with which they are expected to recur: the 50-year extreme wind (U_{e50}) and the 1-year extreme wind (U_{e1}). They are based on the reference wind (See Table 7.3). The 50-year wind is approximately 40% higher than the reference wind, while the 1-year wind is 30% higher than the reference wind.

Extreme Operating Gust (EOG)

An extreme operating gust is a sharp increase and then decrease in wind speed which occurs over a short period of time while the turbine is operating. The magnitude of the 50-year extreme operating gust (U_{gust50}) is related to the turbulence intensity, the scale of the turbulence, and the rotor diameter of the turbine. The gust is also assumed to rise and fall over a period of 10.5 seconds. An illustration of an extreme operating gust is shown in Figure 7.4. More details can be found in IEC 61400-1.

Extreme Direction Change (EDC)

Extreme direction changes are defined in an analogous manner to extreme gusts. In a typical example, the wind direction may change by 64 degrees over six seconds.
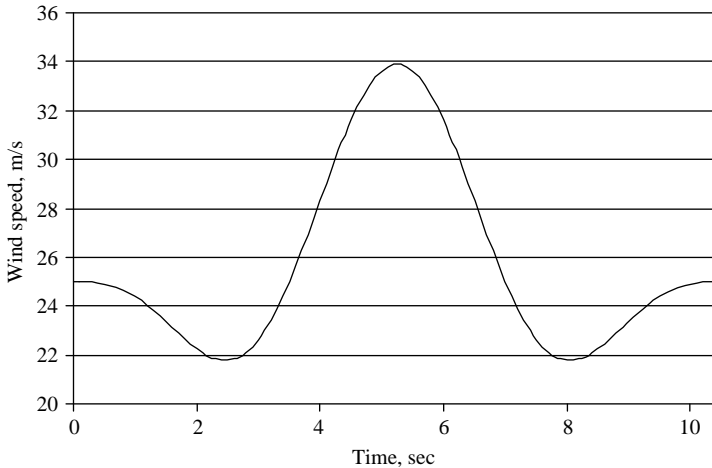
Figure 7.4   Sample extreme operating gust

Extreme Coherent Gust (ECG)
A coherent gust is a rapid rise in wind speed across the rotor. The IEC extreme coherent gust is assumed to have an amplitude of 15 m/s and to be superimposed on the mean wind. The wind rises sinusoidally to a new level over a period of ten seconds.

Extreme Coherent Gust with Change in Direction (ECD)
In the extreme coherent gust with change in direction, a rise in wind speed is assumed to occur simultaneously with a direction change. Details are provided in the IEC standard.

Extreme Wind Shear (EWS)
Two transient wind shear conditions are also defined, one for horizontal shear and the other for vertical wind shear. Transient wind shears will be much larger than the normal conditions described above.

(iii) Rotationally Sampled Turbulence

Rotationally sampled wind speed is normally synthesized by first applying an inverse Fourier transform to the power spectral density, via the Shinozuka technique (Shinozuka and Jan, 1972) to generate a stochastic time series. Then, a model of the cross-spectral density is used to estimate the wind that a blade would experience as it rotated through the turbulence. This process is described in Appendix C. A somewhat simpler approach is given in Stiesdal (1990).

In many situations, however, a simple deterministic model may be used for simulating the rotationally sampled turbulent input. In particular, this method can be used where the wind turbines are relatively stiff, such that vibrations are unlikely to be excited by the turbulence. A sample of data produced by such a model, illustrating the basic characteristics of rotational sampling, is shown in Figure 7.5. For this case, a mean of 15 m/s, a turbulence intensity of 0.18, a turbulence length scale of 10 m, and a diameter of 25 m were used. The rotational speed was 0.25 rotations per second.
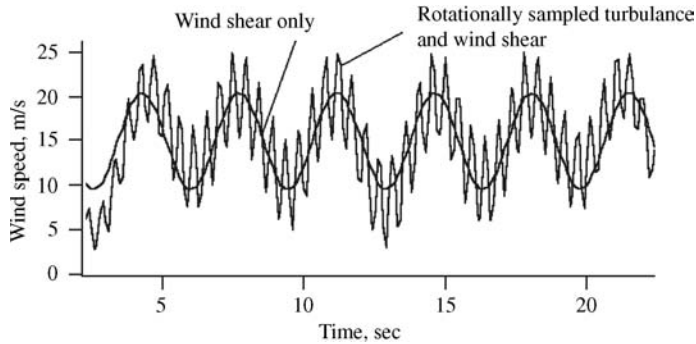
Figure 7.5   Sample deterministic turbulence

Design Load Cases

The next step is defining the load cases. The load cases are based on the turbine's various operating states, as they are affected by the wind conditions and possible electrical or control system faults. Load cases are defined for eight situations:

1. Power production.
2. Power production plus fault.
3. Start-up.
4. Normal shutdown.
5. Emergency shutdown.
6. Parked.
7. Parked plus fault.
8. Transport, assembly, maintenance, and repair.

Many of the situations have more than one load case. Most of the cases deal primarily with ultimate loads, but also include one fatigue load case.

(i) Power Production

'Power production' has five load cases which cover the full range of design wind conditions.

(ii) Power Production Plus Fault

This has three load cases which assume normal wind conditions and one with an extreme operating gust. Each of the load cases considers some type of fault, either with the turbine or the electrical network.

(iii) Start-up

'Start up' load cases include a 1-year extreme operating gust and a 1-year extreme wind direction change for ultimate loading, as well as normal wind conditions (resulting in multiple starts) for fatigue.

(iv) Shutdown

'Shutdown' includes a 1-year extreme operating gust for ultimate loading and normal wind conditions (resulting in multiple stops) for fatigue.

(v) Emergency Shutdown

'Emergency shutdown' includes one case in which normal winds are assumed. More extreme wind conditions are not considered here since the emergency shutdown event is the focus of the loading being evaluated.

(vi) Parked

The 'parked' case considers extreme wind speed together with a loss of electrical connection (to make sure that the machine will not start up) and normal turbulence for fatigue. Note that 'parked' can refer to either standstill or idling

(vii) Parked Plus Fault

'Parked plus fault' considers extreme wind speed, together with a possible fault (other than loss of electrical connection).

(viii) Transport, Assembly, Maintenance, and Repair

The eighth category, as the name implies, considers transport, assembly, maintenance, and repair. These cases are to be specified by the manufacturer.

Application of Design Load Cases

The design load cases are used to guide the analysis of critical components to ensure that they are adequate. Four types of analyses are undertaken:

1. Analysis of maximum strength.
2. Analysis of fatigue failure.
3. Stability analysis (e.g. buckling).
4. Deflection analysis (e.g. preventing blades from striking tower).

Fundamentally, the analyses first involve calculation of the expected loads for the various operating wind conditions. From the loads and the dimensions of the components, the maximum stresses (or deflections) are then found. Those stresses (or deflections) are then compared with the design stresses (or allowed deflections) of the material from which the component is constructed to make sure that they are low enough.

Calculation of the loads can be a very complex process. The principles that affect the loads are discussed in Chapter 4. Precise predictions of loads involve the use of detailed computer simulations, but such analysis is best applied once a preliminary design has been completed. The simplified methods of Chapter 4 can be used to predict trends, but they are too general to allow accurate load estimates. They can, however, be used in the early stages of design for rough sizing of the components. The estimates from simple methods can also be improved if there are some data available from similar machines with which to 'calibrate' the predictions. When such data are available, scaling methods, discussed in Section 7.6, can help to facilitate the calibrations.

Method of Partial Safety Factors

There are usually uncertainties in both the load estimates and the actual characteristics of the material. For this reason, the method of partial safety factors is used in specifying materials and in sizing the various components. The method consists of two parts:

1. Determining design properties for materials by de-rating their characteristic (or published) properties.

2. Selecting safety factors, which in effect increase estimates of the loads.

The general requirement for ultimate loading is that the expected 'load function', $S(F_d)$, multiplied by a 'consequence of failure' safety factor, γ_n, must be equal to or less than the 'resistance function', $R(f_d)$. In the most basic case, the load function is the highest value of the expected stress, and the resistance function is the maximum allowable design value. The requirement can be expressed as:

$$\gamma_n S(F_d) \leq R(f_d) \tag{7.2}$$

where F_d = design values for loads and f_d = design values for materials.

The design values for loads are found from the expected or 'characteristic' values of the loads, F_k, by applying a partial safety factor for loads, γ_f:

$$F_d = \gamma_f F_k \tag{7.3}$$

The design values for the materials are found from the characteristic values of the materials, f_k, by applying a partial safety factor for materials, γ_m:

$$f_d = (1/\gamma_m)f_k \tag{7.4}$$

Partial safety factors are typically greater than 1.0. Normally, partial safety factors for loads range from 1.0 to 1.5. Partial safety factors for materials are at least 1.1, and partial safety factors for consequence of failure are equal to at least 1.0. More discussion can be found in IEC (2005a). Partial safety factors for materials can also be found in many sources.

7.6 Load Scaling Relations

Sometimes design information is available about one turbine, and one wishes to design another turbine which is similar, but of a different size. In this case, one can take advantage of some scaling relations for the rotor in laying out the preliminary design.

7.6.1 Scaling Relations

Scaling relations for wind turbines start with the following assumptions:

- the tip speed ratio remains constant;
- the number of blades, airfoil, and blade material are the same;
- geometric similarity is maintained to the extent possible.

The scaling relations for a number of important turbine characteristics are described below; first when the radius is doubled and then for the general case. They are also summarized in Table 7.4.

7.6.2 Power

Power, as discussed previously, is proportional to the swept area of the rotor, so doubling the radius will quadruple the power. In general, power is proportional to the square of the radius.

Table 7.4 Summary of scaling relations

Quantity	Symbol	Relation	Scale dependence
Power, forces, and moments			
Power	P	$P_1/P_2 = (R_1/R_2)^2$	$\sim R^2$
Torque	Q	$Q_1/Q_2 = (R_1/R_2)^3$	$\sim R^3$
Thrust	T	$T_1/T_2 = (R_1/R_2)^2$	$\sim R^2$
Rotational speed	Ω	$\Omega_1/\Omega_2 = (R_1/R_2)^1$	$\sim R^{-1}$
Weight	W	$W_1/W_2 = (R_1/R_2)^3$	$\sim R^3$
Aerodynamic moments	M_A	$M_{A,1}/M_{A,2} = (R_1/R_2)^3$	$\sim R^3$
Centrifugal forces	F_c	$F_{c,1}/F_{c,2} = (R_1/R_2)^2$	$\sim R^2$
Stresses			
Gravitational	σ_g	$\sigma_{g,1}/\sigma_{g,2} = (R_1/R_2)^1$	$\sim R^1$
Aerodynamic	σ_A	$\sigma_{A,1}/\sigma_{A,2} = (R_1/R_2)^0 = 1$	$\sim R^0$
Centrifugal	σ_c	$\sigma_{c,1}/\sigma_{c,2} = (R_1/R_2)^0 = 1$	$\sim R^0$
Resonances			
Natural frequency	ω	$\omega_{n,1}/\omega_{n,2} = (R_1/R_2)^1$	$\sim R^{-1}$
Excitation	Ω/ω	$(\Omega_1/\omega_{n,1})/(\Omega_2/\omega_{n,2}) = (R_1/R_2)^0 = 1$	$\sim R^0$

Note: R, radius

7.6.3 Rotor Speed

With the tip speed ratio held constant, the rotor speed will be halved when the radius is doubled. In general, rotor speed will be inversely proportional to the radius.

7.6.4 Torque

As noted above, when the radius is doubled, the power is quadrupled. Since the rotor speed will drop by half, the torque will be increased by a factor of 8. In general, the rotor torque will be proportional to the cube of the radius.

7.6.5 Aerodynamic Moments

The forces in the blades go up as the square of the radius, and the moments are given by the forces multiplied by the distances along the blade. When the radius is doubled, the aerodynamic moments will increase by a factor of 8. In general, aerodynamic moments will be proportional to the cube of the radius.

7.6.6 Rotor Weight

By the assumption of geometric similarity, as the turbine size gets larger, all dimensions will increase. Therefore, if the radius doubles, the volume of each blade goes up by a factor of 8. Since the material remains the same, the weight must also increase by a factor of 8. In general,

rotor weight will be proportional to the cube of the radius. Note that the fact that the weight goes up as the cube of the dimension whereas the power output goes up as its square gives rise to the famous 'square–cube law' of wind turbine design. It is this 'law' which may eventually limit the ultimate size that turbines may reach.

7.6.7 Maximum Stresses

Maximum bending stresses, σ_b, in the blade root due to flapwise moments applied to the blade, M, are related to the thickness of the root, t, and its area moment of inertia, I, by $\sigma_b = M(t/2)/I = M/(2I/t)$, as should be clear from discussions in Chapter 4.

   To determine how bending stresses change with rotor size, scaling laws for the area moment of inertia need to be determined. For simplicity, consider the blade root to be approximated by a rectangular cross-section of width c (corresponding to the chord) and thickness t. The moment of inertia about the flapping axis is $I = ct^3/12$. If the radius is doubled, then the moment of inertia goes up by a factor of 16, and the thickness by a factor of 2. The ratio $2I/t$ which is given by $2I/t = ct^2/6$, is then increased by a factor of 8, just like the aerodynamic moments. In general, the blade root area moment of inertia scales as R^3.

   Maximum stresses due to aerodynamic moments, blade weight, and centrifugal force are a function of the area moment of inertia and the applied moments. They are discussed in more detail below.

7.6.7.1 Stresses Due to Aerodynamic Moments

Aerodynamically induced stresses, σ_A, are unchanged with scaling. This is true for both the flapwise and lead–lag directions, as should be apparent from the discussion above. The proof of this for flapwise bending is the subject of one of the problems for this chapter.

7.6.7.2 Stresses Due to Blade Weight

Stresses due to blade weight, unlike most other stresses in the rotor, are not independent of size. In fact, they increase in proportion to the radius. Allowance for that difference must be made during the design process.

   Consider a horizontal blade of weight, W, and center of gravity distance, r_{cg}, from the hub. The maximum moment due to gravity, M_g, is:

$$M_g = Wr_{cg} \tag{7.5}$$

   The maximum stress due to gravity, σ_g, in the edgewise direction for a rectangular blade root (here with $I = tc^3/12$)) is therefore:

$$\sigma_g = (Wr_{cg})(c/2)/I = Wr_{cg}/(tc^2/6) \tag{7.6}$$

   Since weight scales as R^3 and the other dimensions scale as R, the stress due to weight also scales as R. The general relation is then:

$$\sigma_{g,1}/\sigma_{g,2} = (R_1/R_2)^1 \tag{7.7}$$

7.6.7.3 Stresses Due to Centrifugal Force

Stresses due to centrifugal force are unchanged by scaling. This can be illustrated as follows. The tensile stress, σ_c, due to centrifugal force, F_c, applied across area A_c is given by:

$$\sigma_c = F_c/A_c \tag{7.8}$$

Centrifugal force itself is found from:

$$F_c = \frac{W}{g} r_{cg} \Omega^2 \tag{7.9}$$

where Ω is the rotor rotational speed. Blade weight scales as R^3, rcg scales as R and Ω scales as R^1. Thus $F_c \sim R^2$. It is also the case that $A_c \sim R^2$, so σ_c is independent of R. In general

$$\sigma_{c,1}/\sigma_{c,2} = (R_1/R_2)^0 = 1 \tag{7.10}$$

7.6.8 Blade Natural Frequencies

Blade natural frequencies decrease in proportion to the radius. This can be seen by modeling a blade as a rectangular cantilevered beam of dimensions c wide, t thick, and R long. As shown in Chapter 4, the natural frequencies of a cantilevered beam are given by:

$$\omega_n = \frac{(\beta R)_i^2}{R^2} \sqrt{EI\tilde{\rho}} \tag{7.11}$$

where E is the modulus of elasticity, I is the area moment of inertia, $\tilde{\rho}$ is the mass per unit length, and $(\beta R)_i^2$ is a series of constants such that $(\beta R)_i^2 = (3.52, 22.4, 61.7, \ldots)$.

For the example, $I = ct^3/12$ and $\tilde{\rho} = \rho_b c\, t$ (where $\rho_b =$ mass density of blade). In this case:

$$\omega_n = \frac{(\beta R)_i^2}{R^2} \sqrt{\frac{Ect^3}{12\rho_b ct}} = \frac{(\beta R)_i^2}{R^2} t \sqrt{\frac{E}{12\rho_b}} \tag{7.12}$$

Blade thickness is proportional to the radius. Therefore, it is apparent that $\omega_n \sim R^1$. In general, the relation of natural frequencies between two blades (1 and 2) is:

$$\omega_{n,1}/\omega_{n,2} = (R_1/R_2)^{-1} \tag{7.13}$$

Since rotor rotational speed also decreases with radius, the propensity of the rotor to excite a particular resonance condition is independent of radius.

It should be emphasized that scaling relations are only useful guidelines and cannot be used to make exact predictions. Other factors, such as technology development, can also alter the implications. For example, recent developments of larger machines indicate an increase of mass at a rate of somewhat less than the 'square–cube law' (power and mass vs. radius) predicts. More discussion on this topic is provided in Jamieson (1997).

7.7 Power Curve Prediction

Prediction of a wind turbine's power curve is an important step in the design process. It involves consideration of the rotor, gearbox, generator, and control system. The process is slightly

different with a fixed-speed than a variable-speed wind turbine. The process will be illustrated first with a fixed-speed, fixed-pitch machine, followed by a discussion of variable-speed and variable-pitch wind turbines.

The method used in predicting the power curve for a fixed-speed, fixed-pitch wind turbine is to match the power output from the rotor as a function of wind speed and rotational speed to the power produced by the generator, also as a function of rotational speed. The effects of component efficiencies are also considered where appropriate. In this discussion it is assumed that all drive train efficiencies are accounted for by adjusting the rotor power. The process may be done either graphically or in a more automated fashion. The graphical method best illustrates the concept and will be described here.

Rotor power as a function of rotational speed is predicted for a series of wind speeds by applying estimates for the power coefficient, C_p. The power coefficient as a function of tip speed ratio, and hence rpm, may be obtained as described in Chapter 3. The rotor power, P_{rotor}, is then:

$$P_{rotor} = C_p \eta \frac{1}{2} \rho \pi R^2 U^3 \tag{7.14}$$

where η = drive train efficiency, ρ = air density, R = rotor radius, and U = wind speed.

The rotor speed, n_{rotor}, in rpm is found from the tip speed ratio, λ:

$$n_{rotor} = \frac{30}{\pi} \lambda \frac{U}{R} \tag{7.15}$$

A power vs. rpm relation is found for the generator and referred to the low-speed side of the gearbox by dividing the generator speed by the gearbox speed-up ratio. This relation is superimposed on a series of plots (for a range of wind speeds) for rotor power vs. rotor rpm. Every point where a generator line crosses a rotor line defines a pair of power and wind speed points on the power curve. These points also define the operating speed of the rotor.

As was explained in Chapter 5, generators which are directly connected to the grid are usually either of the synchronous or induction (squirrel cage) type. Synchronous generators turn at a fixed speed, determined by the number of magnetic poles and the grid frequency. Induction generators turn at a nearly fixed speed, determined primarily by the number of poles and grid frequency but also by the power level. For normal operation, power varies directly with 'slip', as explained in Chapter 5. The relation may also be expressed as:

$$P_{generator} = \frac{g n_{rotor} - n_{sync}}{n_{rated} - n_{sync}} P_{rated} \tag{7.16}$$

where $P_{generator}$ is the generator power, g is the gearbox ratio, P_{rated} is the rated generator power, n_{sync} is the synchronous speed of the generator, and n_{rated} is the speed of the generator at rated power.

Variable-speed wind turbines, as discussed in Chapter 5, are connected to the grid indirectly. They typically have either a synchronous generator or a wound rotor induction generator, together with power electronic converters, as also explained in Chapter 5. The generator power vs. speed curve is different in those cases, but the principle in determining the overall wind turbine power curve is the same.
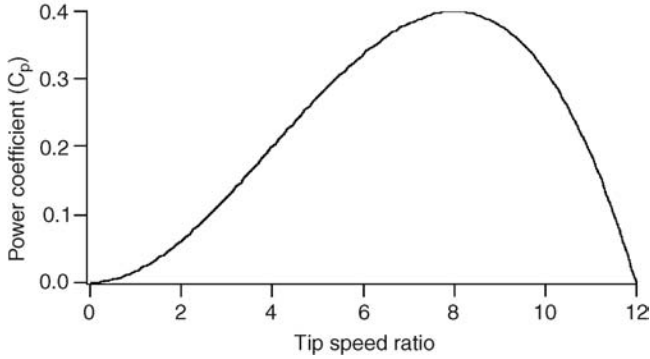
Figure 7.6   Rotor power coefficient vs. tip speed ratio

7.7.1 Example

The following example illustrates the process of estimating the power curve for a hypothetical wind turbine. The turbine has a rotor of 20 m diameter with a power coefficient vs. tip speed ratio relation illustrated in Figure 7.6.

The overall mechanical and electrical efficiency is assumed to be 0.9. Two possible pairs of gear ratios and generator ratings are considered. Six wind speeds are used, ranging from 6 m/s to 16 m/s. It is assumed that power will be regulated at above rated wind speed (16 m/s), so only the part of the power curve at or below 16 m/s is shown. Gearbox 1 has a speed-up ratio of 36:1, whereas gearbox 2 has a speed-up ratio of 24 : 1. The rated power of generator 1 is 150 kW and that of generator 2 is 225 kW. Both generators are of the squirrel cage induction type. They have a synchronous speed of 1800 rpm and a speed of 1854 rpm at rated power. Figure 7.7 illustrates the power vs. rotational speed curves for the six wind speeds and two generator/gearbox combinations.
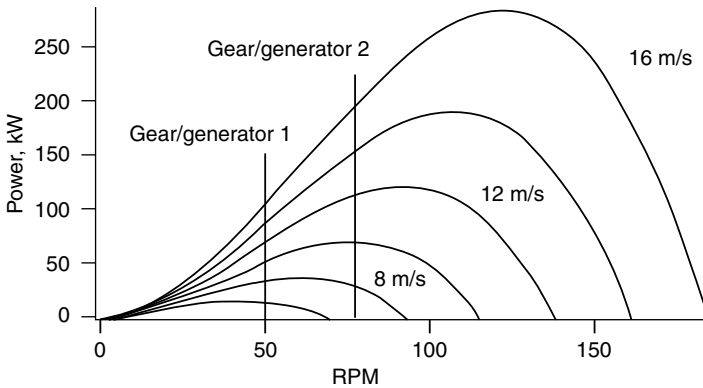
Figure 7.7   Rotor and generator power vs. rotor speed
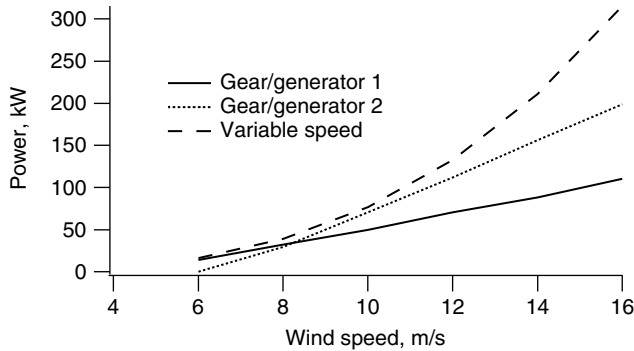
Figure 7.8 Power curves

The power curves that can be derived from Figure 7.7 are shown in Figure 7.8. For comparison, an ideal variable-speed power curve is shown for the same wind speed range. The ideal curve was obtained by assuming a constant power coefficient of 0.4 over all wind speeds. As can be seen from the figure, gearbox/generator combination 1 would produce more power than combination 2 at winds less than about 8.5 m/s, but less than combination 2 at higher winds.

Curves of the type developed above can be useful in selecting the generator size and gearbox ratio. By combining the power curves with characterizations of prospective wind regimes (as described in Chapter 2), the effect on annual energy production can be estimated. Generally speaking, as illustrated in this example, a smaller generator and slower rotor speed (larger gearbox ratio) will be beneficial when the wind speeds are lower. Conversely, a larger generator and faster rotor speed are more effective in higher winds.

Variable-speed wind turbines, as discussed in Chapter 5, are connected to the grid indirectly. They typically have either a synchronous generator or a wound rotor induction generator, together with power electronic converters, as also explained in Chapter 5. The generator power vs. speed curve is different in those cases, but the approach to determining the overall wind turbine power curve is the same. Various aspects of the generator power vs. speed curve may be determined by the control system. In this case, the decision of how to control the generator and over what load or wind speed ranges will need to be decided. Figure 7.9 illustrates the case of a variable-speed, variable-pitch wind turbine with operational characteristics displayed as a function of rotor torque and rotational speed. The wind turbine is to operate at variable speed, tracking the optimum tip speed ratio to ensure that the turbine operates at its maximum C_P. As wind speeds increase, once the rotor speed is reached, the generator is to be operated at fixed speed. In this example, the rotor reaches rated speed before rated wind speed is reached and the turbine operates with fixed pitch and fixed speed until the wind speed reaches rated speed. Above rated wind speed, the blades pitch to maintain power and torque at their rated values. Figure 7.9 shows the rotor torque-speed curves for a variety of wind speeds between cut-in and rated power and for operation with blade pitch set for optimum aerodynamic efficiency. The figure also shows two torque-speed curves for operation above rated wind speeds at pitch angles that ensure that the rotor torque remains at its rated value. Finally, the figure includes the loci of constant C_P operation, rated power operation and rated rotor speed, and the turbine operating curve. At point A the turbine starts to generate power and, as the wind speeds increase,
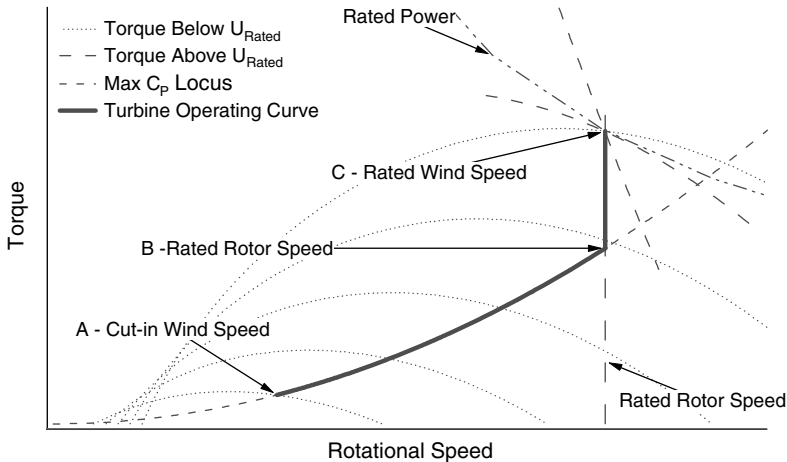
Figure 7.9   Variable-speed operation locus for power curve determination

operation follows the locus of maximum C_P operation. At point B, rated rotor speed is reached and the control system maintains generator and rotor speed constant. At point C, rated torque is reached. At this point, the torque is maintained by pitching the blades. In the torque-speed plane shown in the figure, operation remains at point C. In a manner similar to the fixed-speed example above, once the rotor characteristics as a function of tip speed and pitch angle have been determined and the generator characteristics as a function of rotor speed have been defined, as in Figure 7.9, the power curve for the desired modes of operation can be determined.

7.8 Computer Codes for Wind Turbine Design

7.8.1 Overview of the Use of Computer Codes in the Wind Industry

Computer codes play a very large role in the overall design process. They are used to specify and evaluate the design of subcomponents and of the complete wind turbine itself. Testing of components and prototype wind turbines provide a significant database for the evaluation of a design, but no testing program can duplicate all of the operating conditions that a wind turbine might experience in its lifetime without prohibitively long and costly testing. Computer codes may be used to model many of those operating conditions and to provide assurances that the wind turbine will operate as desired and last as long as desired. These computer codes may be developed by private companies or may be publicly available codes developed by government research laboratories.

Testing of a wind turbine design requires models for (1) the turbulent inflow and other atmospheric conditions that might be important, (2) the generation of aerodynamic torques and forces at the surfaces of the blades and the structure, (3) the dynamics of the drive train and structure (including the foundation), and (4) the conversion of the loads into stresses, fatigue, and any other variables that are of interest. It is important to ensure that the models that are used are designed to simulate those aspects of the system operation that are of most importance to the end-user. Modeling results should also be compared with test results to validate the models.

Computer Codes Used in Turbine design
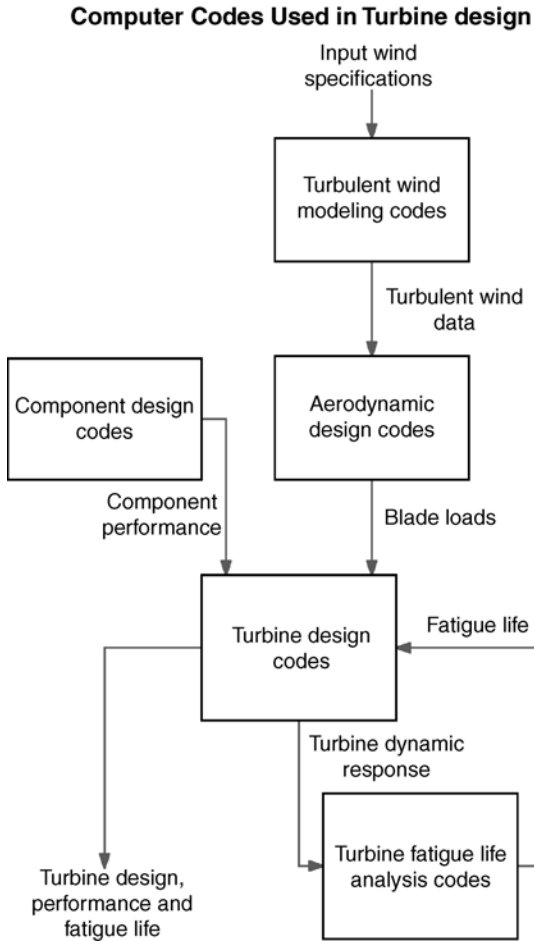
Figure 7.10 Overview of design codes

7.8.2 Categories of Models Used in the Wind Industry

Figure 7.10 categorizes the codes used in wind turbine design into five groups. The turbulent wind modeling codes take input parameters such as turbulence intensity, shear, mean hub height, wind speed, and various statistical parameters that describe the turbulent flow field (turbulent length scale, characterization of the frequency spectrum of the turbulence, etc.) and generate wind speeds across the rotor that represent a turbulent wind field (see Appendix C for more information on the synthesis of wind data). Many different wind speed cases are often generated, including special cases of extreme conditions specified in the IEC 61400-1 design standards. The component design codes shown in Figure 7.10 might be used by suppliers of turbine components to simulate the performance of their products. The aerodynamic design codes are those codes that take the input aerodynamic conditions and the current rotor configuration and motions to determine the aerodynamic loading on the blade surface.

Table 7.5 Some computer codes used in wind turbine design

Code	Source	Purpose
TurbSim	NREL	Wind simulator; preprocessor
IECWind	NREL	Wind simulator; preprocessor
AirfoilPrep	Windward Engineering/NREL	Generates airfoil data; aerodynamics preprocessor
WT_Perf	OSU and NREL	Rotor performance code
PROPID	Univ. of Illinois	Rotor design code
PreComp	NREL	Computes coupled section properties of composite blades; structural response preprocessor
BModes	NREL	Computes mode shapes and frequencies of blades and towers; structural response preprocessor
AeroDyn	Windward Engineering/NREL	Generates aerodynamic forces; input to structural models
YawDyn	Windward Engineering/NREL	Simplified structural dynamics model
FAST	OSU and NREL	Moderately detailed structural dynamics model
ADAMS2AD	NREL	Detailed structural dynamics model
NuMAD	Sandia	Preprocessor for finite element model, ANSYS
GH Bladed	Garrad Hassan	Detailed structural dynamics model

These are closely coupled with the turbine design codes which model the rest of the wind turbine structural dynamics and control system to generate a description of the loads in the system. Those loads are used to determine the fatigue life of the various components of the wind turbine. All of the load and fatigue life information is then used to evaluate and improve the wind turbine design until the performance and cost are acceptable. The final design specifications are then used to evaluate the performance of the turbines at the intended installation. The codes may be separate and free-standing, or multiple capabilities may be included in a single code.

7.8.3 Examples of Computer Codes Used in Wind Turbine Design

Over the past twenty years, a number of computer codes for wind turbine design have been developed and refined. Some of them are listed in Table 7.5 and then described in more detail below.

7.8.3.1 TurbSim

TurbSim is used to synthesize time series of turbulent wind data, including coherent structures, for input to design codes such as YawDyn and FAST. It is based on techniques such as are described in Appendix C and Veers (1988). See http://wind.nrel.gov/designcodes/preprocessors/turbsim/ for details.

7.8.3.2 IECWind

IECWind may be used to synthesize wind data for input to design codes. The synthesized data is of the form required by the IEC 61400-1 standard. See Section 7.5 and http://wind.nrel.gov/designcodes/preprocessors/iecwind/.

7.8.3.3 AirfoilPrep

AirfoilPrep generates airfoil data for use by other codes. It was developed by Windward Engineering and NREL. It adjusts two-dimensional data to account for rotational effects, using methods from Selig for stall delay and Eggers for drag. It extrapolates to high angles of attack using the Viterna method or flat plate theory. It also computes dynamic stall characteristics. See http://wind.nrel.gov/designcodes/preprocessors/airfoilprep/ for details.

7.8.3.4 WT_Perf

WT_Perf calculates rotor performance using blade element/momentum theory. It was developed by NREL from a model known as PROP, which was originally written in the 1970s by Oregon State University. This is a steady state model. It computes power, torque, thrust, and blade root bending moment from rotor geometry and airfoil data. See http://wind.nrel.gov/designcodes/simulators/wtperf/ for details.

7.8.3.5 PropID

PropID was developed to facilitate the design of wind turbine blades, considering aerodynamics, structure, cost, and noise. It can also be used to analyze a given rotor, similar to WT_Perf. See http://www.ae.uiuc.edu/m-selig/propid/.

7.8.3.6 PreComp

This code is a preprocessor which calculates section properties of composite blades. It finds section properties such as inertias and stiffnesses. Inputs are external blade shape and internal lay-up of composite layers. See http://wind.nrel.gov/designcodes/preprocessors/precomp/ for details.

7.8.3.7 BModes

This code is a preprocessor which calculates mode shapes and frequencies of cantilevered beams, particularly blades and towers. The beam is divided into a number of finite elements. Each element has three internal and two boundary nodes and is characterized by 15 degrees of freedom. Inputs for a blade include geometric and structural properties, rotational speed, and pitch angle. More details may be found at http://wind.nrel.gov/designcodes/preprocessors/bmodes/.

7.8.3.8 Aerodyn

Aerodyn is a code which calculates aerodynamic loads. It is typically used in conjunction with a structural model such as YawDyn, FAST, or ADAMS (q.v.). Like WT_Perf, AeroDyn

is based on blade element/momentum theory, but it is more detailed in many ways. It includes the following features, most of which are not in the simplified model: skewed wake (Generalized Dynamic Wake model), dynamic stall (Beddoes–Leishman approach), tower shadow, vertical wind shear, horizontal wind shear, vertical wind, tower shadow, and unsteady inflow (turbulence). More details may be found at http://wind.nrel.gov/designcodes/simulators/aerodyn/.

7.8.3.9 YawDyn

YawDyn was developed to model the basic dynamics of two- or three-bladed wind turbines. It consists of an aerodynamic model, now maintained separately as AeroDyn (q.v.), and a simplified dynamic model. The dynamic model of the turbine is very similar to that of the linearized hinge–spring model (Chapter 4). Blades are assumed to be rigid beams, connected to the hub by a hinge and spring. In addition, unsteady yaw motion of the entire turbine about the yaw axis is allowed and yaw drive stiffness is accounted for. Another feature is that turbines with teetered rotors may be modeled. More details may be found in Hansen (1992; 1996) and at http://wind.nrel.gov/designcodes/simulators/yawdyn/.

7.8.3.10 FAST

FAST is a medium-complexity code for aerodynamic and dynamic analysis of horizontal axis wind turbines with two or three blades and a teetering or rigid hub. The code was developed by Oregon State University, NREL, and Windward Engineering. The code models the wind turbine as a combination of rigid and flexible bodies, and so uses a combination of lumped parameter and modal analysis. In its current form, FAST incorporates AeroDyn to calculate the aerodynamic forces on the blades. The dynamic analysis allows for 14 degrees of freedom including multiple tower bending modes, three blade-bending modes, yaw, teeter, and drive train torsion. The code is intended to allow more degrees of freedom than YawDyn, but provide faster results than ADAMS (q.v.). FAST has been approved for calculation of onshore wind turbine loads for design and certification. See http://wind.nrel.gov/designcodes/simulators/fast/ for more details.

7.8.3.11 ADAMS2AD

ADAMS is a commercial motion simulation solution software package for analyzing the complex behavior of mechanical assemblies using the multibody method. ADAMS2AD is a separate code whose purpose is to interface AeroDyn to ADAMS. This allows ADAMS to model in detail the dynamics of a wind turbine tower, nacelle, drive train, hub, and blades. The degree of detail in each of the subsystem models is up to the user. For example, the blades and tower can be modeled as a uniform beam or a series of lumped masses with connections of different area moments of inertia and stiffnesses. The ADAMS/AeroDyn combination has been approved for calculation of onshore wind turbine loads for design and certification. See http://wind.nrel.gov/designcodes/simulators/adams2ad/ for more details.

7.8.3.12 NuMAD

NuMAD is a preprocessor and post-processor for ANSYS, which is commercial finite element analysis software. It is intended for use in analyzing wind turbine blade structures. This code is available from Sandia National Laboratory. See Laird (2001) for more details.

7.8.3.13 GH Bladed

GH Bladed is a commercial software package for wind turbine performance and load calculations. It is used for preliminary or design and wind turbine certification. It includes aerodynamics, rotor, support structure, drive train, generator, and control system. It is based on the modal analysis approach. Details may be found in Bossanyi (2006).

7.8.3.14 Other Computer Codes

Other computer codes used in wind turbine design include DUWECS (TU Delft, Netherlands), PHATAS (Energy Center of the Netherlands, ECN), TURBU (Energy Center of the Netherlands, ECN), FLEX5 (TU Denmark), HAWC2 (Risø National Laboratory, Denmark), and DHAT (Germanischer Lloyd, Germany).

7.8.4 Verification and Validation of Computer Codes

The computer codes described above have all been verified or validated to some degree. Verification typically refers to making comparisons to other codes or analytical results whereas validation is generally assumed to involve comparison to test data. These distinctions are not always made consistently, however, so the reader must pay close attention to situation. Some examples of code verifications are presented in Buhl and Manjock (2006) and Jonkman and Buhl (2007). An example of model comparison to test data is given in Schepers *et al.* (2002).

7.9 Design Evaluation

Once a detailed design for the wind turbine has been developed, its ability to meet basic design requirements, such as those discussed in Section 7.6, must be assessed. This design evaluation should use the appropriate analytical tools. Where possible, validated computer codes, such as those described in Section 7.8, should be used. When necessary, models specific to the application may need to be developed.

There are five steps that need to be taken in performing a detailed design evaluation:

1. Prepare the wind input.
2. Model the turbine.
3. Perform a simulation to obtain loads.
4. Convert predicted loads to stresses.
5. Assess damage.

Each of these steps is summarized below. An extensive discussion of detailed design evaluations for a number of turbine types is given in Laino (1997).

7.9.1 Wind Input

Wind input data that will correspond to the design input conditions need to be generated. For extreme winds and discrete gusts, specifying the wind input is relatively straightforward, given the guidelines summarized in Section 7.4. Converting that wind input to time series inputs can also be done fairly simply. Rotationally sampled synthetic turbulent wind can be produced by using public domain computer codes such as TurbSim, which was described in Section 7.8.

7.9.2 Model of Turbine

The next step is developing a detailed model of the wind turbine. This should include both aerodynamics and dynamics. This can be done from basics, using the methods discussed in Chapters 3 and 4, but, when possible, it is preferable to use models that are already available. Some of the presently available models that may be appropriate include YawDyn, FAST, ADAMS, and GH Bladed. These codes and others were discussed in more detail in Section 7.8.

Once the model has been selected or developed, inputs describing the specific turbine need to be assembled. These generally include weight and stiffness distributions, dimensions, aerodynamic properties, etc.

7.9.3 Simulation

The simulation is the actual running of the computer model to generate predictions. Multiple runs may have to be made to study the full range of design conditions.

7.9.4 Converting Simulation Outputs to Stresses

Outputs from simulation codes are frequently in the form of time series loads; that is, forces, bending moments, and torques. In that case they must be converted to stresses. This can be done with the help of simple programs, which use the loads together with geometric properties of the components of interest. Laino (1997) describes one approach to this task.

7.9.5 Damage Assessment

As discussed above, there are two basic aspects of design evaluation: (1) ultimate loads and (2) fatigue loads. If the maximum stresses are low enough during the extreme load design cases, then the turbine passes the ultimate loads test.

The fatigue case is more complicated. For one thing, the total amount of damage that is generated over an extended period of time will depend on the damage arising as a result of particular wind conditions and the fraction of time that those various conditions occur. Thus, the distribution of the wind speed is an important factor which needs to be taken into account. In order to expedite fatigue damage estimates it is advantageous to use such codes as LIFE2 (Sutherland and Schluter, 1989) to carry out the assessment. See also Chapter 6, Section 6.2.

7.10 Wind Turbine and Component Testing

Testing of complete wind turbines and of wind turbine components is an integral part of the design process. It is critical to ensuring a safely operating turbine, to confirming design

calculations, and to identifying improvements that may be needed in the design process or future test procedures. Testing occurs during research in order to refine our understanding of scientific issues, during the design process as part of the development of novel designs, in prototype testing to ensure that the intended design will meet the design criteria, and, finally, as part of the turbine certification process. Each of these tests is performed according to quality control standards appropriate to the goal of the testing. Testing may also be done as part of the certification process, as discussed in Section 7.4.

7.10.1 A Wind Turbine Test Program

7.10.1.1 Overview

The successful testing of a wind turbine or wind turbine components requires:

- **Testing goals.** This goal of testing might be testing the validity of the results of a computer model of a wind turbine, testing the hypothesis that a newly designed component will withstand certain forces, or testing the hypothesis that the failure of a part is due to fatigue failure due to resonance. The test goal will determine what is measured and under what conditions and against what measure the results will be evaluated.
- **A test plan.** The test plan should clearly lay out the purposes of the tests, the important characteristics of the sensors and data acquisition systems to be used, the method for producing or identifying the presence of the desired test conditions, the duration of the tests, how the results are to be interpreted, and what documentation is required.
- **Testing facilities.** Testing facilities need to be able to safely reproduce the desired test conditions with accommodation for staff and the data acquisition equipment. If the tests are for certification, the test facilities will need to be an accredited testing laboratory. Safety concerns and quality control are very important.
- **Appropriate data acquisition systems.** The data acquisition systems will need to include appropriate sensors, signal conditioning, and measurement and recording systems. The sensors should be able to respond with acceptable accuracy and with adequate response time and should survive the environmental conditions. The signal conditioning filters the signals and may transform them for measurement. Finally, the data measurement and recording system needs to have adequate data storage space and needs to have adequate data acquisition rates.
- **Procedures for testing, data analysis, and reporting.** The details of the test set-up, instrument calibration, the progress of the tests, and the analysis of the test results all need to be well documented to ensure that the results are accurate and useful. The results of the analysis need to be presented in a complete and detailed report.

7.10.2 Full-scale Wind Turbine Testing

Tests of full-scale wind turbines may have many different purposes:

- prototype testing to support the design and development of a new wind turbine design;
- testing according to international standards for the purpose of obtaining design certification;

- testing to identify the source of problems or to test a solution for problems which have been identified during operation;
- testing for research purposes to advance the state of the art.

These tests might focus on any aspect of wind turbine operation, including power production, component loads, system dynamics, operation of any one of a number of components, control system performance, power quality, sound emissions, aerodynamic performance, etc. Such full-scale tests generally require a fairly large set of sensors to ensure that the inflow and operating conditions can be correlated with whatever output variable is being measured.

7.10.2.1 Sensors for Wind Turbine Testing

The sensors that might be needed for full-scale testing of a wind turbine include, or might include, sensors to measure:

- **Inflow.** These include wind speed and direction, temperature (overall or differential temperatures across various heights of the boundary layer), and atmospheric pressure. Wind speed and direction sensors that may be used include cup anemometers, sonic anemometers, direction vanes, and possibly SODAR or LIDAR.
- **Strain.** The strain of components is used to determine stresses and loads in the system. Strain is most usually measured with strain gauges. Strain gauges are often employed at various locations on the blades, tower, shafts, and bed plate. Networks of strain gauges can be set up to measure either linear strain or torsion. More recently, fiber-optic Bragg grating (FBG) strain gauges have been used. FBG strain gauges use an optical grating that consists of a series of changes in refractive index in a glass fiber. As the length of the glass fiber changes, the frequency of the light reflected by the grating changes. FBG strain gauges are currently being tested in fiber-optic cables embedded in wind turbine blades.
- **Forces and torques.** Forces and torques may also be measured directly with load cells. A variety of technologies may be used to measure forces or torques, but many rely on the strain of the instrument and use strain gauges of some sort.
- **Position or motions.** The positions or speeds and accelerations of the blade pitch angle, yaw angle, rotor azimuth, and shafts are all important for evaluating the turbine operation and to control the operation of the turbine. Position and motion may be measured with linear variable differential transformers (LVDTs), inductive, magnetic, or optical proximity sensors or encoders.
- **Pressures.** Pressures in hydraulic or pneumatic systems are measured with a variety of possible technologies that usually provide an output voltage or current directly proportional to pressure.
- **Voltages, currents, power, or power factor.** Voltages, currents, power, and power factor measurements are generally derived from a sensor that measures voltage or a voltage that is proportional to current. Signal conditioning units then convert the instantaneous voltage and current measurements into measures of real and reactive power, power factor, etc.
- **Sound.** Wind turbine sound emissions are measured with calibrated microphones. Care must be taken to account for background noise. Sound measurements may also be used to measure the emissions of individual components like a gearbox to help identify changes in operation. This type of measurement might be done with a small piezoelectric microphone.

- **Vibration.** There are many components in a wind turbine that vibrate, and the technology for measuring those vibrations will depend on the nature of the vibrations to be measured. Vibrations are typically measured with an accelerometer, but may be measured with strain gauges or other motion sensors or derived from sound measurements.

7.10.2.2 Modal Testing

Modal testing refers to a technique for determining the modal frequencies and mode shapes of a structure. There are a number of methods of carrying out modal testing on wind turbines, but fundamentally they involve exciting the wind turbine's response and then measuring the response and analyzing the data acquired. More details may be found in Lauffer *et al.* (1988). One of these methods, known as the Natural Excitation Technique (NExT), is especially applicable to an operating wind turbine (James *et al.*, 1993).

7.10.2.3 Example of Full-scale Wind Turbine Testing

An example of the data that can be gleaned from full-scale testing is illustrated in Figure 7.11. This figure shows data obtained from the Long-term Inflow and Structural Test turbine (LIST) (Sutherland, 2002). The LIST turbine is located in Bushland, TX. It is a 115 kW, three-bladed, upwind, stall-regulated wind turbine. The turbine is part of a long-term research study of factors contributing to fatigue. An array of sensors measures the inflow to the wind turbine. Figure 7.11(a) illustrates the differences in the wind speeds at the bottom and the top of the rotor for
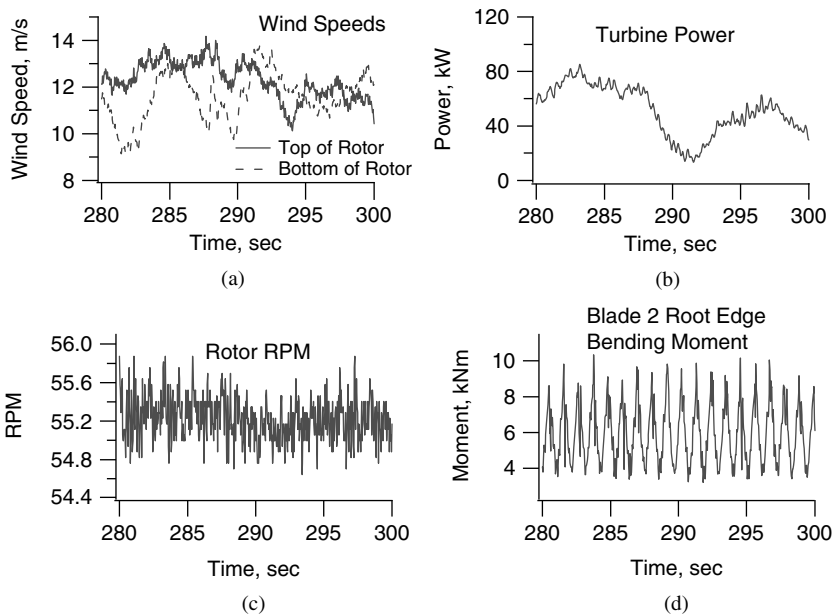
Figure 7.11 Sample test results from the LIST turbine (a) wind speeds at the turbine rotor; (b) electrical power; (c) rotor RPM; (d) blade root edge bending moment

a 20-second period. Figure 7.11(b) shows the fluctuations in electrical power. Figure 7.11(c) shows the changing rotor RPM as the slip of this squirrel cage induction generator changes with power level. Finally, Figure 7.11(d) shows the edgewise bending moment at the root of one of the blades.

7.10.3 Component Testing

7.10.3.1 Material Tests

The properties of all of the materials that comprise a wind turbine need to be understood in order to design the system. Typically, these are determined by testing material coupons (smaller samples of materials) in tension, compression, and torsion, either with constant loads or fluctuating loads to determine fatigue properties.

The testing of composite materials has presented a particular challenge. Composite structures come in many different combinations of matrices, fibers, layout patterns, geometries, and manufacturing methods. Each of these affects the strength of the structure. Testing of entire composite structures or important substructures is important for confirming the endurance limits of the item, but may involve significant expense and effort (see Section 7.10.3.3). Nevertheless, the many possible structural failure modes in composites can be reduced to tests on coupons for determining material properties. The test results can then be used to evaluate the strength of a full structure. Coupon tests of composite materials need to be carefully designed to avoid issues with geometry-dependent failure modes, test results influenced by the type of connection between the coupon and the test stand or the anisotropy of the material, or by failure due to heating of the coupon as the shear energy is dissipated in the material.

7.10.3.2 Testing of Drive Train Components

One of the more problem-prone components in wind turbines has been the drive train, including the gearbox, shafts, and generator. Gearbox and generator manufacturers test their products, in consultation with the wind turbine manufacturers, prior to shipping them to the manufacturers. In addition to this, manufacturers may test the drive train as a unit. For example, the National Renewable Energy Laboratory (NREL) in the US maintains a wind turbine dynamometer test bed for this specific purpose (Musial and McNiff, 2000).

The NREL dynamometer is designed specifically to test wind turbine drive trains. Wind turbine drive trains are unique in that they have very high input torques at very low shaft speeds. They are also subject to shaft bending and thrust loads that vary significantly over time.

The NREL dynamometer is driven by a 4169 V motor coupled to a three-stage epicyclic gearbox. The system can deliver 2.5 MW to the drive train to be tested. The whole motor/gearbox assembly that provides the torque to the test drive train can be raised as much as 2.4 m and tilted up to 6 degrees to accommodate drive trains with a shaft tilt. The motor is driven by a variable-speed drive whose output can be controlled to provide either a user-defined torque profile or a user-defined speed. In addition, the control system of the variable-speed drive can be programmed to mimic the inertial characteristics of the rotor that would be connected to the drive train of an actual wind turbine. The dynamometer is pictured in Figure 7.12.

Shaft bending loads can be reproduced using a hydraulic actuator system that provides a side load of up to 489 kN. The side loading can be controlled and can be synchronized with the
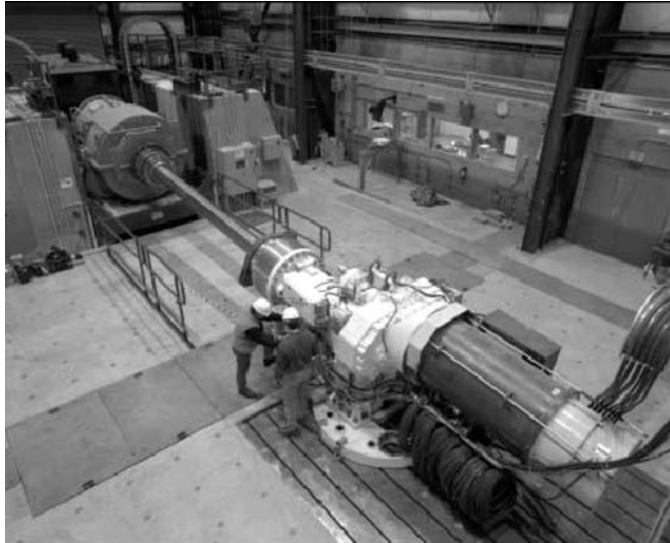
Figure 7.12 NREL's 2.5 MW wind turbine drive train dynamometer test bed (Musial and McNiff, 2000)

rotation of the low-speed shaft to provide the periodic per-rev shaft loading that would be seen in actual turbine operation.

The tests that can be performed include:

- **Drive train endurance testing.** Drive train endurance testing involves prolonged operation at high loads combined with the additional application of side loads, and also transient load cases, to reflect the operating conditions that would be experienced in the field. Loads as much as 1.7 times the rated capacity of the drive train are used to generate, in three to six months of testing, the expected wear experienced by a drive train over its lifetime.
- **Turbulent wind conditions.** Turbulent wind testing is used to demonstrate the proper operation of the drive train and control system under normal operating conditions and a variety of conditions near the operational limits of the system.
- **Load event testing.** Load event testing can be used to test the operation of the full drive train and control system under extreme operating conditions. In this manner, the brake system and the control system response to generator failures and grid faults can be tested.
- **Component testing.** These tests focus on the operation of individual components within the system, such as the gearbox, the generator, or, more specifically, gears, shafts, housing, bearings, isolated control systems, or power electronics, with or without the full drive train assembly.

7.10.3.3 Full-scale Testing of Blades

Full-scale testing of wind turbine blades is done to confirm the ultimate and fatigue strength of the blades. Full-scale blade structural testing is covered by IEC standard IEC 61400-23. The goal of tests is to load the blade or a section of the blade in a manner that will

approximate ultimate or fatigue design loads and to demonstrate that the blade will, indeed, survive these loads. The standard defines three types of tests (static testing, fatigue testing, and selected load cases), the partial safety factors to use for the tests, methods with which to document that the desired load or the desired fatigue damage cycle has indeed been achieved, what constitutes structural failure, and, finally, reporting requirements. Full-scale blade tests provide confidence that the blade design and production have no large errors that would lead to unsafe operation. They may also provide direct measurements of blade strength and information with which to evaluate and improve design computations. Thus, they provide critical feedback in the design process but do not replace the detailed design calculations required to evaluate the strength, stiffness, fatigue life, and resistance to multiple modes of failure.

The static tests are used to ensure that the blade successfully survives the ultimate design loads. Tests might apply loads in a variety of directions or with a variety of load distributions to represent different extreme load cases. These are not tests to failure but tests to ensure that the blade will survive the extreme case design loads. Additionally, tests to failure may be conducted to determine the static strength design margin. Failure is generally indicated by a reduction in stiffness at some point along the blade.

The fatigue tests cyclically load the blade in one or more directions to confirm estimates of the blade fatigue life and to identify the mode and location of initial fatigue failure. Again, failure is defined by a reduction in stiffness at some point along the blade. Fatigue tests generally use higher loads than the wind turbine is expected to experience to reduce the length of the tests (Freebury and Musial, 2000). In the fatigue tests, it may be difficult to duplicate the exact distribution of loading expected along the blade and the load history expected over the life of the blade. In addition, time and cost usually limit the number of samples that can be tested. Nevertheless, full-blade testing provides a test of many aspects of the design analysis, including basic blade properties, fatigue life, and the nature and location of the most likely point of failure.

Fatigue Test Blade Loading

Ideally, full-scale fatigue tests of blades would subject the blade to the full range of blade loading that it would experience in operation, in terms of magnitudes, directions, load distribution, and time histories. Wind turbine blades are typically subjected to on the order of 10^9 loading cycles during their lifetime. These loads include axial, in-plane, out-of-plane, and torsional loads. Typically the out-of-plane loads have a non-zero mean and, depending on operating conditions, may reverse direction. For smaller blades, the out-of-plane loading is the primary direction of loading and fatigue damage. As wind turbine blades have increased in size, the in-plane bending loads, due to the increased blade weight, have become an important factor. In-plane loading tends to have a negative R value (see Chapter 6) with reversing loading as the rotor rotates (White, 2004). Typically, loading is performed in only one direction at a time and with higher than expected loads to approximate the total fatigue damage that a blade would experience in a reasonable amount of time. On the other hand, two-axis loading may become standard for large blades. With two-axis loading, the location of the greatest stresses in the blade is a function of the vector sum of the two loads, or equivalently, of the phase angle between the two. Analysis has shown that, in the field, the phase angle between these two components varies quite a bit over time, but that the mean phase angle is linearly related to the wind speed (White and Musial, 2004).

Figure 7.13   NREL's dual-axis forced displacement test set-up (White, 2004)

Blade Fatigue Testing Approaches

There are only a few laboratories in the world which can do full-scale blade testing. They generally use variations on two approaches to apply the loads for the fatigue tests: (1) forced displacement and (2) resonant excitation.

The forced displacement method uses hydraulic actuators to load the blade in one or two different directions simultaneously. Figure 7.13 shows a two-axis forced displacement testing system. When performing two-axis testing, the primary advantage of the system is that loading in two axes with a desired phase angle can be achieved, thus duplicating with more fidelity the loading that the blade experiences. The disadvantages of the method are the size and power requirements of the equipment required and the resulting costs and the duration of fatigue testing with the equipment. Cycling rates are typically below the natural frequencies of the blades, resulting in very long tests to failure.

The resonance method excites the blade using an eccentric mass on a rotating shaft or a reciprocating mass driven by hydraulic actuators to excite the blade at its natural frequency. The force amplification near resonance results in much lower power requirements than with the forced displacement method. Weights can be added to the blade to get the desired load distribution and, finally, the resonant frequency is typically much higher than the excitation frequency of the forced displacement systems, resulting in shorter testing periods. On the other hand, these systems can only test the blade in one axis at a time. For dual-axis testing, a hybrid approach has been developed by the US National Renewable Energy Laboratory (NREL) (White *et al.*, 2004). It uses the resonance method to excite vibrations in one axis while using a hydraulic actuator to load the blade in the perpendicular direction. Figure 7.14 shows a two-axis forced displacement testing system. The equipment requirements for the forced displacements in the edgewise direction are lower than in the flap direction, so the actuator can excite the edgewise motions at the same frequency as the resonance in the flap direction. The result is a system that can provide two-axis tests with the shorter durations of the resonance method.
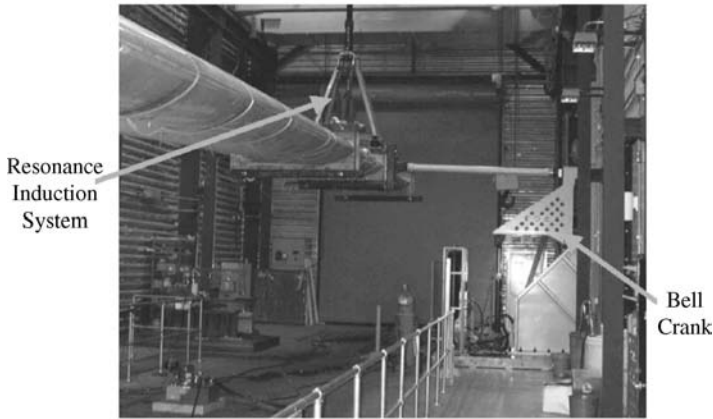
Figure 7.14   NREL's hybrid resonance/forced displacement blade test system (White *et al.*, 2004)

Non-destructive Blade Testing

In many of the cases discussed above, the component or sample is tested to failure or until some damage occurs, and then the damage is assessed by cutting up the item prior to its examination. In many situations it is desirable to undertake a test without affecting the item. This is known as non-destructive testing. There are numerous approaches that can be undertaken. Three of them are briefly described below.

In one technique, an infrared camera is used to measure dynamic temperature distribution (due to thermoelastic effects) on the surface of the sample which is being stressed. The temperature distribution gives a measure of the sum of the principal stresses at each point on the surface, and can be used to determine mode shapes and also to find cracks. See Beattie and Rumsey (1998).

Another means of non-destructive testing is acoustic emissions testing. In general, a sample which is being stressed will emit low energy sound. In acoustic emissions testing, this sound is monitored and then analyzed to determine fatigue damage. See Beattie (1997).

A third method of non-destructive testing is the acousto-ultrasonic technique (Gieske and Rumsey, 1997). In one variant of this technique, which has been successfully applied to a wind turbine blade joint, an ultrasonic pulse is sent through a sample. The pulse is then monitored on the other side of the sample and the data analyzed. The results of the analysis can be used to identify any material damage inside the blade.

7.10.4 Turbine Testing for Certification

Once a wind turbine has been designed and prototyped, testing for certification requires numerous types of test programs, some of which can be pursued in parallel. A number of these testing programs are described below and the requirements for each are described in the relevant IEC standard (see Section 7.4).

7.10.4.1 Load Measurements

One aspect of the certification process is a description of the design loads and the presentation of evidence that that turbine will survive IEC design load cases. In order to demonstrate that the calculated loads are indeed correctly calculated, the manufacturer needs to either (1) demonstrate that the codes used to calculate the loads provide correct values at various measured load conditions or (2) measure the loads under a variety of design load conditions. The IEC standard for the measurement of mechanical loads, IEC 61400-13 TS, provides guidance for the measurement of mechanical loads in the wind turbine.

7.10.4.2 Power Performance Testing

The most critical measure of performance of a wind turbine is the power curve. The IEC 61400-12 specifies the testing requirements for measuring power curves of grid-connected wind turbines. These tests require anemometer measurements upwind of the turbine and electrical power measurements. The standard specifies the location of the met tower, the calibration procedures, specifications for the anemometers and other sensors used in the test, and the data analysis procedures. The location of the wind speed measurement, uneven flow effects at the site, and issues with anemometer measurement uncertainties play an important role in the standard. To ensure that the data are representative, there is also a requirement that each 0.5 m/s wind speed bin have a minimum of 30 minutes of data.

7.10.4.3 Sound Emission Tests

Wind turbine sound emission levels are very important when communities are considering new wind turbine projects. IEC 61400-11 TS and IEC 61400-14 specify just how the sound emission levels are to be determined (for more details on wind turbine sound emissions, see Chapter 12). Because sounds are emitted from the machinery in the nacelle, from the blade surfaces and tips, and may also be radiated by the tower, it is impractical to measure and track the sound emissions from all locations on a wind turbine. Thus, sound emissions are measured a distance away from the wind turbine and at multiple locations around the wind turbine, and the effective wind turbine sound emission levels are calculated from these data. Simultaneous wind speed measurements are also made, as the sound emission levels will depend on the wind speed and the operation of the wind turbine, which will be a function of wind speed. The calculations use additional background sound measurements (without the turbine operating) at all of the wind speeds at which turbine measurements are done to correct for the additional noise generated at the test site from wind or other activities. As with other standards, the IEC standards specify the location and specifications of the wind speed and sound measuring equipment and the procedures for analyzing the data. Typically, sound levels averaged over ten minutes are used to characterize the wind turbine operation.

References

Beattie. A. G. (1997) Acoustic emission monitoring of a wind turbine blade during a fatigue test. *Proc. of the 1997 AIAA Aerospace Sciences Meeting*, pp. 239–248.
Beattie, A. G. and Rumsey, M. (1998) *Non-Destructive Evaluation of Wind Turbine Blades Using an Infrared Camera*, SAND98-2824C, Sandia National Laboratory, Albuquerque, NM.

Bossanyi, E. A. (2006) *GH Bladed Theory Manual 282/BR/009* Garrad-Hassan, Brighton, UK.

Buhl, M. and Manjock, A. (2006) A comparison of wind turbine aeroelastic codes used for certification. *Proc. of the AIAA Aerospace Sciences Meeting,* Reno.

Connell, J. (1988) A primer of turbulence at the wind turbine rotor. *Solar Energy*, **41**(3), 281–293.

DEA (1992) *Dansk Ingeniørforenings norm for last og sikkerhed for vindmøllekonstruktioner (Code of Practice for Loads and Safety of Wind Turbine Construction)*, DS472, Danish Energy Agency.

DNV (2006) *Design and Manufacture of Wind Turbine Blades, Offshore and Onshore Wind Turbines*, DNV-JS-102. Det Norske Veritas, Oslo.

DNV (2007) *Design of Offshore Wind Turbine Structures*, DNV-JS-101. Det Norske Veritas, Oslo.

Dörner, H. (2008) *Philosophy of the wind power plant designer a posteriori*. Available at: http://www.ifb.uni-stuttgart. de/~doerner/edesignphil.html.

Eggleston, D. M. and Stoddard, F. S. (1987) *Wind Turbine Engineering Design*. Van Nostrand Reinhold, New York.

Fordham, E. J. (1985) Spatial structure of turbulence in the atmosphere. *Wind Engineering*, **9**, 95–135.

Freebury, G. and Musial, W. (2000) *Determining Equivalent Damage Loading for Full-Scale Wind Turbine Blade Fatigue Tests*. NREL/CP-500-27510. National Renewable Energy Laboratory, Golden, CO.

Geraets, P. H., Haines, R. S. and Wastling, M. A. (1997) Light can be tough. *Proc. of the 19th British Wind Energy Association Annual Conference.* Mechanical Engineering Publications, London.

Gieske, J. H. and Rumsey, M. A. (1997) Non-destructive evaluation (NDE) of composite/metal bond interface of a wind turbine blade using an acousto-ultrasonic technique. *Proc. of the 1997 AIAA Aerospace Sciences Meeting*, pp. 249–254.

GL (2003) *Regulation of the Certification of Wind Energy Conversion Systems, Rules and Regulations IV: Non Marine Technology Part 1, Wind Energy*. Germanischer Lloyd, Hamburg.

Hansen, A. C. (1992) *Yaw Dynamics of Horizontal Axis Wind Turbines: Final Report*, TP 442-4822. National Renewable Energy Laboratory, Golden, CO.

Hansen, A. C. (1996) *User's Guide to the Wind Turbine Dynamics Computer Programs YawDyn and AeroDyn for ADAMS®, Version 9.6*. University of Utah, Salt Lake City.

IEC (2001a) *Wind Turbines – Part 13: Measurement of Mechanical Loads*, IEC 61400-13 TS, 1st edition. International Electrotechnical Commission, Geneva.

IEC (2001b) *Wind Turbines – Part 23: Full-scale Structural Testing of Rotor Blades. IEC 61400-23 TS*, 1st edition. International Electrotechnical Commission, Geneva.

IEC (2002) *Wind Turbines – Part 24: Lightning Protection, IEC 61400-24 TR*, 1st edition. International Electro-technical Commission, Geneva.

IEC (2004) *Wind Turbines – Part 14: Declaration of Apparent Sound Power Level and Tonality Values of Wind Turbines, IEC 61400-14*, 1st edition. (FDIS) International Electrotechnical Commission, Geneva.

IEC (2005a) *Wind Turbines – Part 1: Design Requirements, IEC 61400-1*, 3rd edition. International Electrotechnical Commission, Geneva.

IEC (2005b) *Wind Turbines – Part 2: Design Requirement for Small Wind Turbines, 61400-2*, 1st edition. (FDIS) International Electrotechnical Commission, Geneva.

IEC (2005c) *Wind Turbines – Part 12: Power Performance Measurements of Grid Connected Wind Turbines, IEC 61400-12*, 1st edition. International Electrotechnical Commission, Geneva.

IEC (2006a) *Wind Turbines – Part 11: Acoustic Noise Measurement Techniques, IEC 61400-11 TS* 2nd edition. International Electrotechnical Commission, Geneva.

IEC (2006b) *Wind Turbines – Part 25: Communications for Monitoring and Control of Wind Power Plants, 61400-25* (in 4 documents). International Electrotechnical Commission, Geneva.

IEC (2008a) *Wind Turbines – Part 21: Measurement and Assessment of Power Quality Characteristics of Grid Connected Wind Turbines IEC 61400-21*. International Electrotechnical Commission, Geneva.

IEC (2008b) *Wind Turbines – Part 3: Design of Offshore Wind Turbines IEC 61400-3 (FDIS)*. International Electrotechnical Commission, Geneva.

IEC (2008c) *Wind Turbines – Part 22: Conformity Testing and Certification of Wind Turbines, IEC 61400-22 TS (DTS)*. International Electrotechnical Commission, Geneva.

ISO (2004) *Wind Turbines – Part 4: Gearboxes for Turbines from 40 kW to 2 MW and Larger, ISO/IEC 81400-4*, 1st edition. International Organization for Standardization, Geneva.

James, G. H. III, Carrie, T. J. and Lauffer, J. P. (1993) *The Natural Excitation Technique (NExT) for Modal Parameter Extraction From Operating Wind Turbines*, SAND92–1666 UC-261. Sandia National Laboratory, Albuquerque, NM.

Jamieson, P. (1997) Common fallacies in wind turbine design. *Proc. of the 19th British Wind Energy Association Annual Conference.* Mechanical Engineering Publications, London.

Jonkman, B. J. and Buhl, M. L. (2007) Development and verification of a fully coupled simulator for offshore wind turbines. *Proc. of the 45th AIAA Aerospace Sciences Meeting and Exhibit, Wind Energy Symposium,* Reno, NV.

Laino, D. J. (1997) *Evaluating Sources of Wind Turbine Fatigue Damage.* PhD dissertation, University of Utah, Salt Lake City.

Laird, D. L. (2001) *NuMAD User's Manual.* SAND2001-2375. Sandia National Laboratory, Albuquerque, NM.

Lauffer, J. P., Carrie, T. G. and Ashwill, T. D. (1988) *Modal Testing in the Design Evaluation of Wind Turbines.* SAND87–2461 UC–60. Sandia National Laboratory, Albuquerque, NM.

Manwell, J. F., McGowan, J. G., Adulwahid, U., Rogers, A. and McNiff, B. P. (1996) A graphical interface based model for wind turbine drive train dynamics. *Proc. of the 1996 American Wind Energy Association Conference.* American Wind Energy Association, Washington DC.

Musial, W. and McNiff, B. (2000) Wind turbine testing in the NREL dynamometer test bed. *Proc. 2000 American Wind Energy Association Conference.* American Wind Energy Association, Washington, DC.

Schepers, J. G., Heijdra, J., Foussseкis, D., Ralinson-Smith, R., Belessis, M., Thomsen, K., Larsen, T., Kraan, I., Ganander, H. and Drost, L. (2002) *Verification of European Wind Turbine Design Codes, VEWTDC.* Final Report, ECN-C-01-055, ECN, Petten.

Shinozuka, M. and Jan, C. M. (1972) Digital simulation of random processes and its application *Journal of Sound and Vibration*, **25**(1), 111–128.

Stiesdal, H. (1990) The 'Turbine' dynamic load calculation program. *Proc. of the 1990 American Wind Energy Association Conference. American Wind Energy Association,* Washington, DC.

Sutherland, H. J. (2002) Analysis of the structural and inflow data from the LIST turbine. *ASME Journal of Solar Energy Engineering*, **124**(44), 432–445.

Sutherland, H. J. and Schluter, L. L. (1989) The LIFE2 computer code, numerical formulation and input parameters. *Proc. of the 1989 American Wind Energy Association Conference.* American Wind Energy Association, Washington, DC.

Veers, P. S. (1988) *Three-dimensional Wind Simulation*, SAND88-0152 UV-261. Sandia National Laboratory, Albuquerque, NM.

White, D. (2004) *New Method for Dual-Axis Fatigue Testing of Large Wind Turbine Blades Using Resonance Excitation and Spectral Loading*, NREL/TP-500-35268. National Renewable Energy Laboratory, Golden, CO.

White, D. and Musial, W. (2004) The effect of load phase angle on wind turbine blade fatigue damage. *Proc. of the 42nd AIAA Aerospace Sciences Meeting and Exhibit,* Reno, NV.

White, D., Musial, W. and Engberg, S. (2004) *Evaluation of the New B-REX Fatigue Testing System for Multi-Megawatt Wind Turbine Blades*, NREL/CP-500-37075. National Renewable Energy Laboratory, Golden, CO.

8

Wind Turbine Control

8.1 Introduction

The previous chapters have discussed the numerous components of wind turbines and their operation. To successfully generate power from these various components, wind turbines need a control system that ties the operation of all the subsystems together. For example, a control system might sequence wind speed measurements, check the health of system components, release the parking brake, implement blade pitch settings, and close contactors to connect a wind turbine to the grid. Control systems may dynamically adjust blade pitch settings and generator torque to control power in high winds on variable-speed wind turbines. Without some form of control system, a wind turbine cannot successfully and safely produce power.

Two levels of control system operation are covered in this chapter: supervisory and dynamic control. Supervisory control manages and monitors turbine operation and sequences control actions (e.g. brake release and contactor closing). Dynamic control manages those aspects of machine operation in which the machine dynamics affect the outcome of control actions (e.g. changing blade pitch in response to turbulent winds). The operation and design of all these aspects of turbine control systems is reviewed in this chapter.

The information here is intended to provide the reader with an overview of the important aspects of control systems that are specifically relevant to wind turbine control. Section 8.1 starts with a description of the levels of wind turbine control and examples of control systems in commercial wind turbines. The section includes information on the various subsystems, actuators, and measurement sensors that comprise the turbine control system. In Section 8.2 a basic wind turbine model is developed that is used to explain control system components in general, and the specifics of control system components in wind turbines. This is followed, in Section 8.3, by the important aspects of common turbine operating strategies that are found in modern turbines, and then, in Section 8.4, by the details of the supervisory control systems that are used to implement these strategies. Finally, Section 8.5 presents an overview of dynamic control system design approaches and dynamic control issues that are specifically important in wind turbines.

Control system design for wind turbines is a very large topic area. The material presented here provides an overview of the more relevant issues. Introductory information on the implementation of control systems in wind turbines can be found in Grimble *et al.* (1990). Discussion of various aspects of wind turbine control systems can also be found in Gasch (1996), Gasch and Twele (2002), Heier (1996), Hau (2006), Freris (1990), Bianchi *et al.* (2007), and Munteanu *et al.* (2008).

8.1.1 Types of Control Systems in Wind Turbines

The purpose of the control system of a wind turbine is to manage the safe, automatic operation of the turbine. This reduces operating costs, provides consistent dynamic response and improved product quality, and helps to ensure safety. This operation is usually designed to maximize annual energy capture from the wind while minimizing turbine loads.

Wind turbine control systems are typically divided, functionally if not physically, into three separate parts: (1) a controller that controls numerous wind turbines in a wind farm, (2) a supervisory controller for each individual turbine, and (3) separate dynamic controllers for the various turbine subsystems in each turbine. These three levels of control operate hierarchically with interlocking control loops (see Figure 8.1).

The wind farm controller, often called a supervisory control and data acquisition (SCADA) system, can initiate and shut down turbine operation and coordinate the operation of numerous
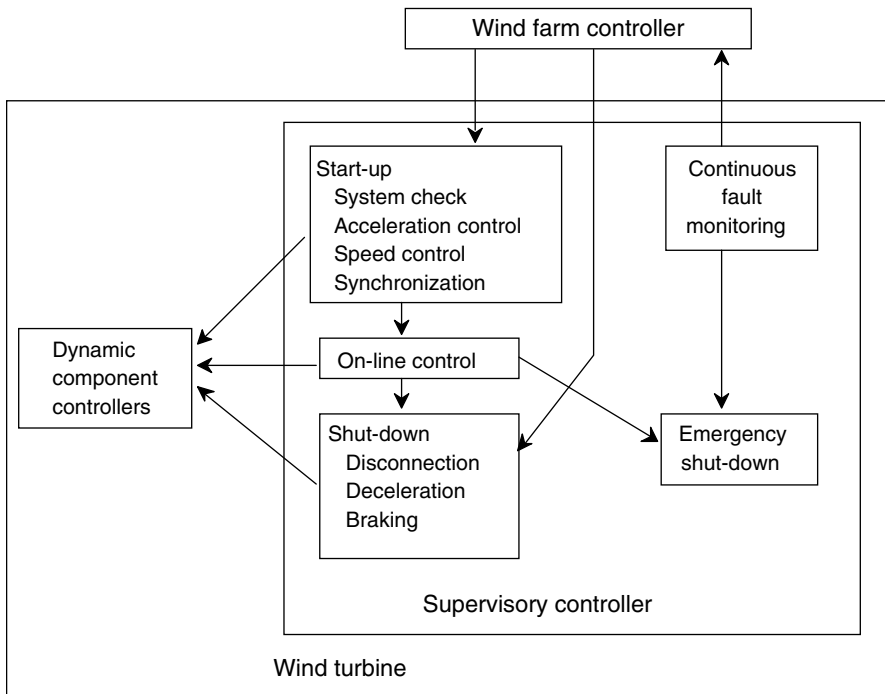

Figure 8.1   Control system components

wind turbines. These SCADA systems communicate with the supervisory controllers for each wind turbine. More information on SCADA systems is included in Chapter 9.

The functions delegated to the supervisory controllers in the individual turbines are characterized by reactions to medium- and long-term changes in environmental and operating conditions. Thus, there may be a relatively long time between supervisory controller actions. Typically, the supervisory controller switches between turbine operating states (power production, low wind shutdown, etc.), monitors the wind and fault conditions such as high loads and limit conditions, starts and stops the turbine in an orderly fashion, and provides control inputs to the turbine dynamic controllers, for example the desired tip speed ratio or rpm.

In contrast, dynamic controllers make continuous high-speed adjustments to turbine actuators and components as they react to high-speed changes in operating conditions. Dynamic control is used for control systems in which the larger system dynamics affect the outcome of control actions. Typically, a dynamic controller will manage only one specific subsystem of the turbine, leaving control of other subsystems to other dynamic controllers and coordination of the various dynamic controllers and other operations to the supervisory control system. Dynamic control systems are used to adjust blade pitch to reduce drive train torques, to control the power flow in a power electronic converter, or to control the position of an actuator. Each of these controllers operates actuators or switches which affect some aspect of a turbine subsystem and thereby the overall operation of the wind turbine. The effect of controller actions is often measured and used as an input to the dynamic control system.

8.1.2 Examples of Wind Turbine Control Systems

Wind turbine control systems vary significantly from turbine to turbine. The choice of control system components and configurations depends significantly on the specific wind turbine design. Before examining control systems in general, a few highlights of some aspects of wind turbine control systems illustrate the variety of possibilities.

8.1.2.1 10 kW Bergey Excel

The Bergey Windpower Company's 10 kW Excel wind turbine has a 7 m diameter variable-speed rotor with a direct drive permanent magnetic alternator providing variable-frequency, three-phase power (see Figure 8.2). Depending on the application, that power is used directly for water pumping, rectified to regulated DC power for battery charging, or converted, through an inverter, to 240 V AC power for grid connection. The turbine has two hardware control systems plus an electronic controller that controls the power for the specific application (Bergey Wind Power, Inc., 2009).

The two hardware control systems keep the turbine oriented into the wind and protect against rotor over-speed in extreme winds. The first control system orients the turbine into the wind with a tail vane. The downwind vane keeps the upwind rotor facing into the wind by means of aerodynamic forces on the vane surface. The rotor is protected against over-speed in high winds by another hardware-based control system. Above wind speeds of about 15 m/s the rotor is turned partially out of the wind through the action of aerodynamic and gravitational forces, without the use of springs.

An additional electronic controller manages the interface between the turbine generator and the intended application. For battery charging, a dedicated controller monitors battery voltage

Figure 8.2   Bergey Excel. Reproduced by permission of Bergey Windpower Co

and controls current to ensure that the battery is not overcharged. Water pumping motors are usually driven directly by the alternator output, with the pump controller turning the pump on when sufficient voltage of enough frequency is being produced to power the pump without damage. For grid connection, a controller in the inverter manages the power flow to the grid and includes diagnostics to ensure safe operation of the inverter.

8.1.2.2 Siemens SWT-2.3-82

The Siemens SWT-2.3-82 wind turbine is a utility-scale 2.3 MW wind turbine. The design has a rotor that can operate at two different nearly constant speeds. It also has active stall regulation. The induction generator, with a squirrel cage rotor and two separate stator windings, is connected directly to the grid. Use of the six-pole winding results in operation at a generator speed of 1000 rpm and a rotor speed of about 11 rpm in a 50 Hz system. This winding is used for power levels up to 400 kW. Once the wind speed exceeds about 7 m/s, the generator switches to the main four-pole winding, which can handle the full rated power of the rotor and results in a rotor speed of 17 rpm and a generator speed of 1500 rpm. The pitch mechanism is used to actively control the power above rated wind speed by pitching to stall and provides aerodynamic braking in the event of an emergency stop. An additional power factor correction system can be used to control some of the characteristics of the power supplied to the grid and to provide ride-through of normal grid faults (see Chapter 9).

8.1.2.3 Vestas V90

The Vestas V90 comes in a 1.8 MW and a 2.0 MW version. The V90 includes active pitch control and some range of variable-speed operation due to the design of the induction generator (Vestas, 2007). The rotor is connected to the generator through the gearbox and the generator is directly connected to the grid. The rated slip of the generator can be changed by electronically changing the rotor resistance. This allows the generator speed (and the corresponding rotor speed) to vary by up to 30% above the synchronous speed of the generator. The blade pitch system is used to control the mean power output from the turbine in high winds. Power fluctuations about the mean are reduced by allowing the rotor speed to vary from 9.0 to 14.9 rpm. All of these functions are under the control of microprocessors. Braking is accomplished by pitching the blades to feather, each of which is independently hydraulically actuated, or by using the mechanical brake.

8.1.2.4 Ecotécnia 80 2.0 MW Wind Turbine

In contrast to the Siemens SWT-2.3-82 and the Vestas V90, which are based on constant speed induction generator technology, the Ecotécnia 80 2.0 MW wind turbine has true variable-speed operation. As with the two other turbines, the rotor is connected to the generator through a gearbox. The Ecotécnia 80 2.0 MW turbine uses a doubly fed induction generator with an inverter on the rotor of the generator to smoothly vary the rotor speed to any desired value within its range of operation (Ecotécnia, 2007). This allows the rotor speed to be varied from 9.7 to 19.9 rpm as the generator speed varies from 1000 to 1800 rpm. The digital signal processor controlling the converter can also control the voltage and assure that the grid-side power factor is between 0.95 leading and 0.95 lagging. Similar to many variable-speed wind turbines based on doubly fed induction generators, the blade pitch system is used to control the average power supplied to the grid, once the turbine reaches rated power and is used for aerodynamic braking. In addition, the Ecotécnia 80 2.0 MW wind turbine utilizes the capabilities of the independently controlled electrical blade pitch systems to adjust the pitch of individual blades to compensate for poor blade performance due to soiling and to reduce loads in the drive train. The blade controllers use nacelle accelerometer measurements to adjust the blade pitch to limit drive train vibrations.

8.1.2.5 DeWind D8.2 2000 kW Wind Turbine

The DeWind D8.2 2000 kW wind turbine is also a variable-speed wind turbine. In this case, the constant speed synchronous generator is directly connected to the grid but it is driven by a torque converter that provides a variable ratio transmission system that links the constant speed generator with the variable-speed drive train (Composite Technology Corp., 2009). A two-stage planetary gearbox between the rotor and the torque converter increases the shaft speed of the drive train before it enters the torque converter. The torque converter helps to minimize drive train vibrations and problems that might result from shaft misalignment. The rotor rotational speed varies from 11.1 to 20.7 rpm. The pitch mechanism adjusts the rotor torque to control the mean power delivered to the grid, as in other variable-speed designs. The grid voltage and power factor are controlled using the generator excitation. Meanwhile, the

torque converter speed ratio is set based on the rotor speed and the power that needs to be transferred to the grid. Similarly, the blade pitch is controlled depending on the rotor speed and wind speed.

8.2 Overview of Wind Turbine Control Systems

While the details of the control systems on different turbines vary, all the turbines considered here have a common purpose: the conversion of wind energy into electrical energy. This common purpose defines common elements that need to be considered in any control system design. This section starts with a simple turbine model that can be used to illustrate these turbine components and then reviews the basic functional elements common to all control systems and the forms those elements take in wind turbines.

8.2.1 Basic Turbine Model

A simplified horizontal axis wind turbine model is useful for understanding the integration of control systems into a modern wind turbine. A typical wind turbine can be modeled as a drive shaft with a large rotor inertia at one end and the drive train (including the generator) inertia at the other end (see Figure 8.3). An aerodynamic torque acts on the rotor and an electrical torque acts on the generator. Somewhere on the shaft is a brake.

The aerodynamic torque affects all turbine operations and provides the power that is delivered to the load. As discussed in Chapters 3 and 4, the aerodynamic torque is the net torque from the wind, consisting of contributions related to the rotor tip speed ratio, blade geometry, wind speed, yaw error, and any added rotor drag. Each of these inputs to the aerodynamic torque, except wind speed, may be able to be changed by a control system. Variable-speed turbines can operate at different speeds (and different tip speed ratios); pitch-regulated turbines can change the rotor or blade geometry; turbines with yaw drives or yaw orientation systems can control yaw error; and turbines with auxiliary drag devices can modify rotor drag. Below rated wind speed, control systems might attempt to maximize aerodynamic torque (or power); above rated wind speed, a control system would attempt to limit aerodynamic torque.
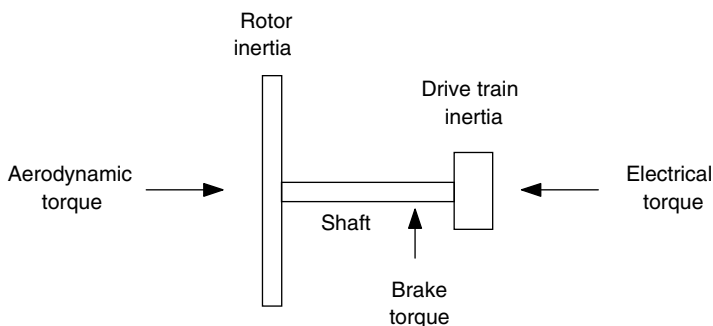
Figure 8.3   Simple wind turbine model

In a turbine designed to operate at nearly constant speed, the generator torque is a function of the fluctuating aerodynamic torque and drive train and generator dynamics. That is:

Constant speed generator torque $= f$(aerodynamic torque, system dynamics)   (8.1)

The drive train and generator dynamics are determined by the design of the various components and are not controllable. Thus, the only method for controlling generator torque in a constant-speed wind turbine is by affecting the aerodynamic torque.

In a variable-speed, pitch-regulated turbine, the generator torque can be varied independently of the aerodynamic torque and other system variables. That is:

Variable-speed generator torque $= f$(generator torque control system)   (8.2)

In such a system the aerodynamic and generator torques can be independently controlled. The speed can be altered by changing either the aerodynamic or generator torque, resulting in either an acceleration or deceleration of the rotor.

8.2.2 Control System Components

Control of mechanical and electrical processes requires five main functional components (see Figure 8.4):

1. A process that has a point or points that allow the process to be changed or influenced.
2. Sensors or indicators to communicate the state of the process to the control system.
3. A controller, consisting of hardware or software logic, to determine what control actions should be taken. Controllers may consist of computers, electrical circuits, or mechanical systems.
4. Power amplifiers to provide power for the control action. Typically, power amplifiers are controlled by a low-power input that is used to control power from an external high-power source.
5. Actuators or components for intervening in the process to change the operation of the system.

Examples of each of these functional components are provided in the following sections.

8.2.2.1 Controllable Processes in Wind Turbines

Controllable wind turbine processes include, but are not limited to:

- The development of aerodynamic torque (see Chapters 3 and 4).
- The development of generator torque (see Chapter 5).

Figure 8.4   Control system components

- The conversion of electrical current and fluid flow into motion. Yaw drives and pitch mechanisms often use the control of electrical current or the flow of hydraulic fluid to control valves and the direction and speed of mechanical motion.
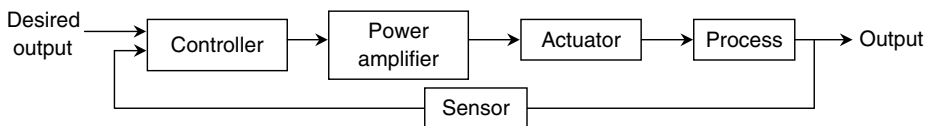- The conversion of electrical power from one form into another. Using power electronic converters (see Chapter 5), the voltage and power factor of the power from the turbine can be determined separately from that of the power from the generator.
- Overall conversion of wind energy into electrical power. The successful conversion of the kinetic energy in the wind into useful electrical energy requires the monitoring and sequencing of a number of subprocesses. These larger aspects of turbine operation are also subject to control system actions. These might include connecting the generator to the grid, turning on compressors and pumps, or opening valves.

8.2.2.2 Wind Turbine Sensors

On a large modern wind turbine, many sensors are used to communicate important aspects of turbine operation to the control system. These measured variables might include:

- speeds (generator speed, rotor speed, wind speed, yaw rate, direction of rotation);
- temperatures (gearbox oil, hydraulic oil, gearbox bearing, generator bearing, generator winding, ambient air, electronic temperatures);
- position (blade pitch, teeter angle, aileron position, blade azimuth, yaw position, yaw error, tilt angle, wind direction);
- electrical characteristics (grid power, current, power factor, voltage, grid frequency, ground faults, converter operation);
- fluid flow parameters (hydraulic or pneumatic pressures, hydraulic oil level, hydraulic oil flow);
- motion, stresses, and strain (tower top acceleration, tower strain, shaft torque, gearbox vibration, blade root bending moment);
- environmental conditions (turbine or sensor icing, humidity, lightning).

Sensors may also be composed of machine elements that act as part of the control system. For example, in the Bergey Excel turbine, the rotor thrust is used as a sensor to control the rotor speed of the turbine.

8.2.2.3 Wind Turbine Controllers

Controllers provide the connection between the measurement of an aspect of turbine operation and actions to affect that turbine operation. Typical controllers in a wind turbine include:

- **Mechanical mechanisms.** Mechanical mechanisms, including tail rotors, linkages, springs, fly ball governors, etc., can be used to control blade pitch, yaw position, and rotor speed.
- **Electrical circuits.** Electrical circuits may provide a direct link from the output of a sensor to the desired control action. For example, sensor signals can be used to energize coils in relays or switches. Electrical circuits can also be designed to include a dynamic response to input signals from sensors in order to shape the total system dynamic operation.

- **Computers.** Computers are often used for controllers. Computers can be configured to handle digital and analog inputs and outputs, and can be programmed to perform complicated logic and to provide dynamic responses to inputs. The ease with which control code, and thus control operation, can be changed by reprogramming the computer is a major advantage of computer control systems.

More detail on the different types of controllers is presented in Sections 8.4.4 and 8.5.4.

8.2.2.4 Power Amplifiers in Wind Turbines

When the control signal from the controller is not powerful enough power to power the actuator, then an amplifier is needed between the controller and the actuator. Typical power amplifiers in a wind turbine include:

- **Switches.** There are a variety of switches which can be controlled with a small amount of current or a small force, but which act as amplifiers in that they can switch high currents or high forces. These include relays, contactors, power electronic switches such as transistors and silicon-controlled rectifiers (SCRs), and hydraulic valves.
- **Electrical amplifiers.** Electrical amplifiers that directly amplify a control voltage or current to a level that can drive an actuator are often used as power amplifiers in a control system.
- **Hydraulic pumps.** Hydraulic pumps provide high-pressure fluid that can be controlled with valves that require very little power.

Note that power amplifiers are not always needed. In the Bergey Excel, for example, the thrust of the blades, driven by aerodynamic forces, develops enough power to change the blade orientation, without amplification, to limit the rotor speed.

8.2.2.5 Wind Turbine Actuators

Actuators in a wind turbine may include:

- **Electromechanical devices.** Electromechanical devices include DC motors, stepper motors, AC motors with solid state controllers, linear actuators, magnets, and solid state switching components.
- **Hydraulic pistons.** Hydraulic pistons are often used in positioning systems that need high power and speed.
- **Resistance heaters and fans.** Resistance heaters and fans are used to control temperature.

Actuator systems may include gears, linkages, and other machine elements that modify the actuating force or direction.

8.2.3 Control of Turbine Processes

Wind turbine processes such as the development of aerodynamic and generator torque and the conversion of current into motion can be affected by controller action. The details of some of the typical approaches to affecting these processes in wind turbines are described in this section.

8.2.3.1 Aerodynamic Torque Control

As mentioned above, aerodynamic torque consists of contributions related to the rotor tip speed ratio and C_P (determined by blade design, wind speed, and rotor speed), rotor geometry (blade pitch and aileron settings), wind speed, yaw error, and any added rotor drag. All of these, except wind speed, can be used to control aerodynamic torque.

Tip speed ratio variations can be used to change the rotor efficiency and thereby the rotor torque. In stall-regulated, fixed-speed wind turbines, low tip speed ratios (and accompanying low C_P) are used to regulate the aerodynamic torque in high winds. In variable-speed wind turbines, the rotor speed can be changed to either maintain a favorable tip speed ratio or to change the tip speed ratio to reduce the power coefficient.

Changing the rotor geometry changes the lift and drag forces on the blade, affecting the aerodynamic torque. Aerodynamic torque control through rotor geometry adjustments can be accomplished with full span pitch control or by changing the geometry of only a part of the blade, as described below.

Full span pitch control requires rotating the blade about its long axis. Full span pitch control can be used to regulate aerodynamic torque by either pitching the blade to feather (reducing the angle of attack) or toward stall (increasing the angle of attack) to reduce loads. Blades for pitch-regulated wind turbines are usually designed for optimum power production, with no provision for gradually increasing stall as the wind increases. These blades are usually operated at the most efficient point with relatively high angles of attack. From this position, rotating the blade toward stall can often be accomplished faster than rotations to feather. Rotations to feather result in quieter operation and, in principle, more exact control because each angle of attack is associated with one operating condition. In practice, gusts requiring pitching actions may occur much faster than the blade can be pitched, resulting in large load fluctuations. In contrast, inducing stall increases thrust forces on the turbine and increasing noise, but the thrust and torque loads are less sensitive to changes in wind speed and pitch angle and so fatigue loads may be reduced compared to pitching to feather (Bossanyi, 2003). Full span pitch control may be implemented as collective pitch control, in which all blades are moved to the same pitch angle, cyclic pitch control, in which the pitch of each blade is the same as the others at the same rotor azimuth angle, or individual pitch control, in which the pitch of each individual blade is determined separately (for more information on individual pitch control, see Section 8.5.3.6).

Ailerons can be used to affect rotor geometry by changing the blade geometry over part of the blade. They are used to reduce the lift coefficient and increase the drag coefficient over the length of the blade with the aileron. Ailerons do not require the use of as powerful an actuator as full span pitch control does, but at least some of the actuating mechanism must be installed in the blade. The necessity of separating the blade into articulated pieces and providing actuation inside the blade significantly affects the blade design.

More recent approaches to modifying the aerodynamic torque of the rotor include research into methods of tailoring the aerodynamics along the blade in response to local flow changes. These include the use of jets of air to improve the attachment of the flow to the blade surface, deformable trailing edges or microtabs which modify the flow over the blade, effectively changing the blade camber, and plasma actuators which create an auxiliary flow near the surface of the blade, modifying the boundary layer profile and postponing separation, among others devices (see Johnson *et al.*, 2008). These devices are sometimes described as 'smart'
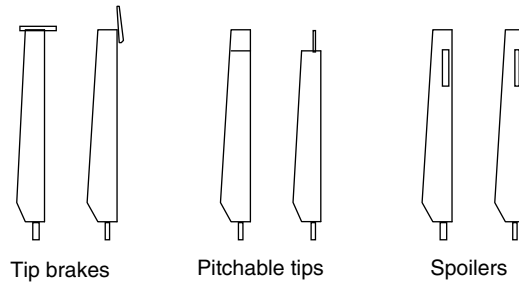
Tip brakes   Pitchable tips   Spoilers

Figure 8.5   Aerodynamic drag devices (Gasch, 1996). Reproduced by permission of B. G. Teubner GmbH

blade technologies: distributed actuators and sensors which, with microprocessors, actively control the localized flow. For example, deformable trailing edges are similar to ailerons but have no sudden change in the surface configuration or openings in the blade surface to disturb the flow over the blade or to generate noise. The degree of deformation can also vary along the blade. It is anticipated that the last 10% of the chord could be bent 5 degrees up or down with an actuator in the blade of only moderate power consumption. Microtabs (see, for example, Mayadi *et al.*, 2005) are small tabs on the under side of the blade that, when unused, are retracted into the trailing edge of the blade, but when deployed are about as high as the boundary layer on the pressure side of the blade. In general, these active flow control devices may increase or decrease lift or delay stall and are being considered to minimize instantaneous peak loads and fatigue loads over the life of the turbine. For more information on load control, see Section 8.5.3.6. Johnson *et al.* (2008) provide an excellent summary of the current state of the art of smart blade technologies.

Auxiliary rotor devices such as tip brakes or spoilers can also be used to modify the rotor torque (see Figure 8.5). Tip flaps and pitchable tips add a negative torque to the rotor and spoilers disrupt the flow around the blade, decreasing lift and increasing drag.

Increasing the yaw error (turning the rotor out of the wind) and tilting the rotor and/or drive train can also be used to decrease or regulate the aerodynamic torque.

8.2.3.2 Generator Torque Control

Generator torque may be regulated by the design characteristics of the grid-connected generator or independently controlled with the use of power electronic converters.

Grid-connected generators operate over a very small or no speed range and provide whatever torque is required to maintain operation at or near synchronous speed (see Chapter 5). Grid-connected synchronous generators have no speed variations and, thus, any imposed torque results in an almost instantaneous compensating torque. This can result in high torque and power spikes under some conditions. Grid-connected induction generators change speed by as much as a few percent of the synchronous speed. This results in a softer response and lower torque spikes than with a synchronous generator.

Alternatively, the generator can be connected to the grid through a power electronic converter. This allows the generator torque to be very rapidly set to almost any desired value.

The converter determines the frequency, phase, and voltage of the current flowing from the generator, thus controlling generator torque.

8.2.3.3 Brake Torque Control

Parking a wind turbine and stopping a stall-regulated wind turbine are often accomplished with a brake system on either the high-speed or the low-speed shaft (more on brakes can be found in Chapter 6). Brakes are typically pneumatically, hydraulically, or spring applied. Thus, control of brakes usually requires the activation of solenoid valves or, possibly, controllable valves to actively control the braking torque. Additional braking methods include (1) braking the rotor using the generator torque on machines controlled by power converters and (2) dynamic brakes, which are auxiliary electrical components that provide an electrical braking torque to the generator.

8.2.3.4 Yaw Orientation Control

A number of different designs have been used for controlling wind turbine power by changing the direction of the wind entering the rotor. This approach is typically used in small wind turbines and may involve either yawing the rotor out of the wind or rotating the nacelle upwards to limit power output. Gyroscopic loads need to be considered in the design of a yaw power regulation system. If gyroscopic loads are a concern, yaw rate can be limited, but limiting yaw rate may affect the ability to regulate power output.

8.3 Typical Grid-connected Turbine Operation

Each of the processes mentioned above (aerodynamic torque control, generator torque control, brake torque control, and yaw orientation control), as well as others, can be used in a variety of combinations to enable a wind turbine to successfully convert the kinetic energy in the wind into electrical energy. The overall operating strategy determines how the various components will be controlled. For example, as part of an overall control strategy, the control of rotor torque can be used to maximize energy production, minimize shaft or blade fatigue, or simply to limit peak power. Blade pitch changes can be used to start the rotor, control energy production, or to stop the rotor.

In general, the goals of wind turbine control strategies are (1) maximizing energy production while keeping operation within the speed and load constraints of the turbine components, (2) preventing extreme loads, including excessive transient and resonance-induced loads, and minimizing fatigue damage, (3) providing acceptable power quality at the point of connection to the grid, and (4) ensuring safe turbine operation. The control scheme used for operating a turbine depends on the turbine design. Within the limits of the design, the best overall strategy to meet these goals is chosen. Typical wind turbine operating strategies are explained in Section 8.3.1.

The exact approach to wind turbine control and the immediate goals for the control strategy depend on the operating regime of the turbine. Below rated wind speed, one generally attempts to maximize energy production. Above rated wind speed, power limitation is the goal. Typical wind turbine control strategies for pitch- and stall-regulated machines, illustrated in Figure 8.6,
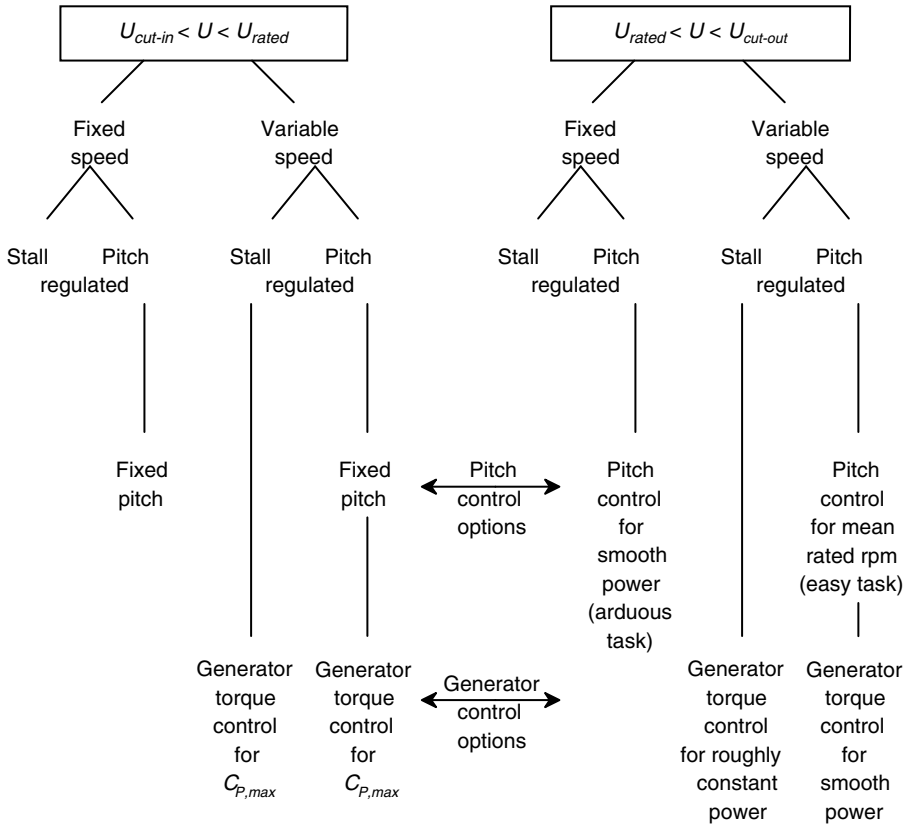
$U_{cut\text{-}in} < U < U_{rated}$

$U_{rated} < U < U_{cut\text{-}out}$

Fixed speed   Variable speed   Fixed speed   Variable speed

Stall   Pitch regulated   Stall   Pitch regulated   Stall   Pitch regulated   Stall   Pitch regulated

Fixed pitch

Fixed pitch   ← Pitch control options →   Pitch control for smooth power (arduous task)   Pitch control for mean rated rpm (easy task)

Generator torque control for $C_{P,max}$ Generator torque control for $C_{P,max}$ ← Generator control options →   Generator torque control for roughly constant power   Generator torque control for smooth power

Figure 8.6 Overview of typical control strategies; U, mean wind velocity; U_{cut-in}, $U_{cut-out}$, U_{rated}, cut-in, cut-out, and rated wind speed, respectively

are a function of wind speed and the options for control input. Fixed-speed, stall-regulated wind turbines usually have no options for control input other than the use of a shaft brake and connecting or disconnecting the generator from the grid. Fixed-speed, pitch-regulated wind turbines typically use the pitch regulation for start-up and, after start-up, only to control power above rated wind speed. Variable-speed wind turbines typically use pitch control, if it is available, only above rated wind speed, but use generator torque control over the whole operating range of the turbine. It should be remembered that there are other approaches to turbine control that are used or are possible, but that are less frequently found in commercial designs, including, for example, yaw control to limit output power.

The details of typical turbine control operating strategies are summarized in the next section, with constant-speed turbine and variable-speed turbine descriptions described separately.

Turbine start-up strategy is also a function of available control options. Fixed-speed, pitch-regulated wind turbines usually adjust the blade pitch to accelerate the rotor to operating speed, at which point the generator is connected. Many fixed-speed, stall-regulated wind turbines cannot count on aerodynamics to accelerate the rotor. These turbines start by connecting the generator to the grid and motoring to operating speed. Variable-speed wind turbines can use the

same start-up strategies as fixed-speed wind turbines, but usually with the generator connected to the grid through a power converter.

8.3.1 Typical Constant-speed Operating Schemes

Among constant-speed wind turbines, a few different standard designs have emerged, each with their typical operating strategy. These are described below. The description also includes one two-speed design that operates at two distinct speeds. This design is included with the constant-speed designs because it is not a true variable-speed design, but a turbine that operates as a constant-speed machine at one of two selectable speeds. The descriptions of these typical turbine designs (and the variable-speed designs) include the most frequently occurring designs and their control strategies. Again, it should be kept in mind that any given wind turbine design has its unique aspects, and that other turbine designs and control strategies exist and are possible.

8.3.1.1 Stall-regulated Turbines

Constant-speed, stall-regulated wind turbines have blade designs that passively regulate the power produced by the turbine. The fixed-pitch blades are designed to operate near the optimal tip speed ratio at low wind speeds. As the wind speed increases, so, too, does the angle of attack and an increasingly large part of the blade, starting at the blade root, enters the stall region. This reduces rotor efficiency and limits output power. The most common stall-regulated design has been a rigid-hub, three-bladed wind turbine with an induction generator. The rotors of these turbines tend to be heavy welded or cast structures designed to withstand the blade-bending loads inherent in the stall-regulated design. There are also some lighter, two-bladed, stall-regulated wind turbines with teetering hubs.

Typically, control of stall-regulated wind turbines requires only starting and stopping of the wind turbine based on wind speed and/or power criteria. Once the brake is disengaged, the turbine may be allowed to freewheel up to operating speed before the generator is connected to the grid or the turbine may be motored up to operating speed. Thus, this design only requires control of the generator or soft-start contactor (see Chapter 5) and brake operation.

8.3.1.2 Two-speed, Stall-regulated Turbines

A variation of the stall-regulated concept involves operating the wind turbine at two distinct, constant operating speeds. In low winds, the slower operating speed is chosen to improve the rotor efficiency and reduce noise. The higher rotor speed is chosen for moderate and high winds. One way to do this is to use a generator with switchable poles and therefore a switchable synchronous operating speed. Another approach is the use of two generators of different sizes. The operating speeds are determined by choosing the number of generator poles and/or the gear ratio for connecting these generators to the rotor. The smaller generator is used in low winds and the larger in high winds. Both generators operate close to maximum efficiency. Two-speed wind turbines require more complicated equipment for transferring power between generators and for avoiding transient power and current spikes when switching generators or generator poles.

8.3.1.3 Active Pitch-regulated Turbines

Rotors with adjustable pitch have been used in constant-speed machines to provide better control of turbine power. Blade pitch can be changed to provide power smoothing in high winds. Because pitchable blades are often designed for optimum power production, with no provision for stall regulation, the aerodynamic torque can be sensitive to gusts. One solution is to use fairly fast pitch mechanisms. The faster the pitch mechanism responds to gusts, the smoother the power in high winds will be. However, blade rotation velocities are limited by the strength of the pitching mechanism and blade inertia. In practice, power is only controlled in the average and some power fluctuations still exist. Below rated power the blade pitch is usually, though not always, held constant in these machines to limit pitch mechanism wear. This reduces energy capture but may improve the overall system economics and reliability.

8.3.2 Typical Variable-speed Operating Schemes

Variable-speed, grid-connected wind turbine operation has been made possible primarily by improvements in power electronics. The cost of power electronics for grid connection tends to limit variable-speed operation to larger wind turbines. However, small variable-speed wind turbines with dedicated loads have successfully operated for generations. The descriptions below of typical variable-speed turbine operation are limited to grid-connected machines.

8.3.2.1 Stall-regulated Turbines

Variable-speed operation of stall-regulated wind turbines has been a topic of research in Europe and the United States, but no commercially viable designs have been produced. Variable-speed, stall-regulated wind turbines are controlled by using power electronics to regulate the generator torque. By using the generator torque to regulate the rotor speed, the turbine can be operated at any desired tip speed ratio within the limits of the generator and rotor design constraints. By decreasing generator torque below the aerodynamic torque, the rotor is allowed to accelerate. The rotor decelerates when the generator torque is set higher than the aerodynamic torque.

Variable-speed, stall-regulated wind turbines operate in one of three modes (see Figure 8.7). At low wind speeds the turbine operates with variable speed to maintain an optimum power coefficient. Once the maximum design rotor speed is reached, the turbine is operated in a constant-speed mode similar to normal stall-regulated operation. As the wind speed increases, the power will increase and the blade will be increasingly stalled. Above rated power the turbine is operated in a constant-power mode in which the rotor speed is regulated to limit rotor power. This involves reducing the rotor speed in high winds to increase stall and reduce the rotor efficiency.

Control of variable-speed, stall-regulated turbines includes the same connection and disconnection logic required for constant-speed, stall-regulated operation. Once it is grid-connected, the power from a constant-speed, grid-connected machine is regulated by the rotor aerodynamics and the generator design. In a variable-speed machine, grid-connected power is managed by a dynamic controller that regulates the generator torque with the goal of either constant tip speed ratio, constant speed, or constant power, depending on the wind speed.
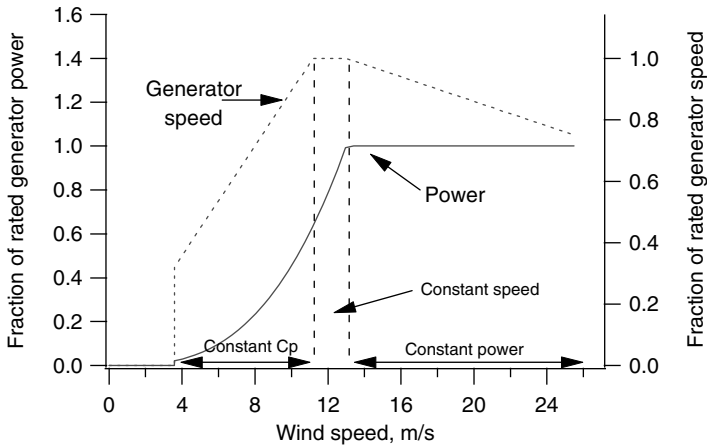
Figure 8.7   Variable-speed, stall-regulated operation

8.3.2.2 Active Pitch-regulated Turbines

Variable-speed, pitch-regulated wind turbines have two methods for affecting turbine operation: speed changes and blade pitch changes. In part load operation, these wind turbines operate at fixed pitch with a variable rotor speed to maintain an optimal tip speed ratio. Once rated power is reached, the generator torque is used to control the electrical power output, while the pitch control is used to maintain the rotor speed within acceptable limits. During gusts, the generator power can be maintained at a constant level while the rotor speed increases. The increased energy in the wind is stored in the kinetic energy of the rotor. If the wind speed drops, the reduced aerodynamic torque results in a deceleration of the rotor while the generator power is kept constant. If the wind speed remains high, the blade pitch can be changed to reduce the aerodynamic efficiency (and aerodynamic torque), once again reducing the rotor speed. In this manner the power can be very closely controlled and the pitch mechanism can be much slower than the pitch mechanism used in a constant-speed machine.

8.3.2.3 Small-range Variable-speed Turbines

One approach to approximating some of the advantages of full variable speed without all of the costs is the use of a variable slip induction generator. For example, the Vestas V90 has a wound rotor induction generator with a control system to control the rated slip of the generator (see Section 5.4.4) by changing the rotor resistance. At part load, the generator operates as a regular induction generator. Once full load is reached, the rotor resistance is changed to increase the slip to allow the rotor to absorb the energy in gusts. The pitch mechanism is used to modulate the power fluctuations. See Chapter 5 for more details on the electrical aspects of this configuration.

8.4 Supervisory Control Overview and Implementation

This section provides details of the operation of supervisory control systems for wind turbines. The supervisory control system manages the various operating states of the turbine (ready for

operation, power production, shutdown, etc.), switching between operating states, and reporting to turbine operators. An overview of supervisory control functions and the details of typically used operating states are described in this section, as well as the various forms for implementing supervisory control systems.

8.4.1 Supervisory Control System Overview

The supervisory control system manages safe, automatic operation of the turbine, identifying problems and activating safety systems. Automatic turbine operation is typically managed by switching relays to change from one predefined operating state, such as grid-connected power production, to another, perhaps freewheeling in low winds without grid connection. At the same time, operating conditions are continuously checked against preset limits. If any input exceeds a safe value, appropriate action is taken. These tasks may be managed by hardware relay logic, electrical circuits, or, most often nowadays, by an industrial computer. A separate part of a supervisory control system is the fail-safe backup system needed to safely shut the turbine down if the main supervisory system should fail.

The tasks performed by the supervisory control system may include:

- **Monitoring for safe operation.** This includes (1) monitoring sensors to ensure that no turbine components have failed, (2) monitoring to make sure that operating conditions are within expected limits, (3) monitoring the grid condition, and (4) looking for troublesome environmental conditions.
- **Information gathering and reporting.** This includes gathering information on operation, notification of the necessity for repairs and maintenance, and communication via phone, the Internet, radio, or satellite, etc. with operators.
- **Monitoring for operation.** This includes monitoring the wind speed and direction and grid condition to determine the appropriate operating condition.
- **Managing turbine operation.** This involves choosing operating states and managing the transition between operating states, sequencing and timing of tasks within operating states, and providing limits and set points for dynamic control subsystems.
- **Actuating safety and emergency systems.** This includes disconnecting from the grid, and activating aerodynamic and regular braking systems in emergencies.

8.4.2 Operating States

Experience has shown that a number of distinct operating states are appropriate for the operation of most wind turbines (see Figure 8.8). These include the system check, ready for operation, start, grid connection, power production, grid disconnection, freewheeling, shutdown, and emergency shutdown operating states. Each of these is described below. Depending on the turbine design, some of these states may be absent, some may be subdivided into multiple separate states, or some may be combined onto one state. The turbine may remain in some operating states for long periods of time, depending on the wind and operating conditions. These states are designated as stationary states. Other operating states may only be entered during changes from one stationary operating state to another. The nature of the operating state (whether transitional or stationary) is indicated in Figure 8.8.
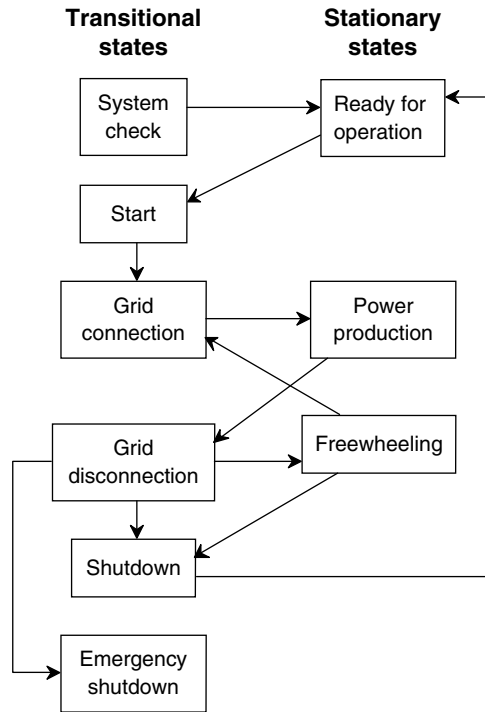
Transitional   **Stationary**
states   **states**

```
   ┌──────────┐          ┌──────────┐
   │  System  │─────────▶│ Ready for│◀───────┐
   │  check   │          │ operation│        │
   └──────────┘          └──────────┘        │
                              │               │
                              ▼               │
         ┌──────────┐                         │
         │  Start   │                         │
         └──────────┘                         │
              │                               │
              ▼                               │
   ┌──────────┐          ┌──────────┐         │
   │   Grid   │─────────▶│  Power   │         │
   │connection│          │production│         │
   └──────────┘          └──────────┘         │
         ▲     ╲        ╱    │                │
          ╲     ╲      ╱     │                │
   ┌──────────┐ ╳     ┌──────────┐            │
   │   Grid   │────▶  │Freewheel │            │
   │disconnect│       │   ing    │            │
   └──────────┘       └──────────┘            │
     │    │                 │                 │
     │    ▼                 │                 │
     │ ┌──────────┐         │                 │
     │ │ Shutdown │◀────────┘                 │
     │ └──────────┘──────────────────────────┘
     │
     ▼
   ┌──────────┐
   │Emergency │
   │ shutdown │
   └──────────┘
```

Figure 8.8   Typical turbine operating states

8.4.2.1 System Check and Initialization (Transitional)

The system check state is entered when the control system is initialized for operation. This transitional state includes any initial tasks that need to be performed to make sure that the system is ready to operate or to get it ready to operate. When the system is first put into operation, faults may need to be cleared, the rotor and yaw position may need to be determined, variables need to be initialized, and sensor inputs need to be checked to make sure that the turbine systems are operating correctly. In this effort, actuators may be exercised and the results measured to determine that they are ready for operation.

8.4.2.2 Ready for Operation (Stationary)

The ready for operation state is characterized by a stationary rotor and engaged parking brake. Once put online, the supervisory controller must: (1) maintain the readiness of the turbine for operation by monitoring turbine and grid conditions for problems, maintaining pressures in hydraulic and pneumatic reservoirs, and correcting the yaw error, if necessary, and (2) identify appropriate conditions for operation by monitoring the wind speed and direction. When appropriate operating conditions are identified and system checks find no fault that would preclude operation, the start state is entered. Owing to the fluctuating nature of the wind, averages and statistical measures must be used to determine if there is enough wind to start the

turbine with the expectation that it will continue to run for a while and not be shut down in the next lull. Typically, the supervisory controller will determine that the turbine is ready to start when the wind speed, averaged over some time period, is above a predetermined set point and/or if the wind is over some limiting value for a certain time. This is a stationary state in which the turbine may remain for long periods of time.

8.4.2.3 Start and Brake Release (Transitional)

Once conditions are appropriate, the start state is entered and the brake is released. Many turbines, especially pitch-regulated turbines, will accelerate up to operating speed without other intervention, but the pitch mechanism set point may need to be updated in order to position the blades to accelerate the rotor. The starting procedure for variable-speed turbines may require initiating the operation of dynamic controllers and providing speed set points. Meanwhile, system operation and the grid condition are monitored to identify problems that might require a shutdown.

8.4.2.4 Grid Connection (Transitional)

Some turbines, generally stall-regulated turbines, may need to be motored up to operating speed by connecting the generator to the grid subsequent to disengaging the brake. For those turbines not requiring motoring, when the rotor speed approaches operating speed, the generator or converter contactor is closed. Power production commences with the completion of grid connection and the achievement of the correct operating speed. During grid connection, system and grid faults continue to be checked and the turbine continues to be oriented into the wind.

8.4.2.5 Power Production (Stationary)

During power production current flows into the electrical grid. Controller tasks during power production will depend on the turbine design and whether the turbine is operating at part or full load. In constant-speed, stall-regulated wind turbines, power production may require only monitoring turbine operation and component health. In pitch-regulated turbines, blade pitch may be varied continuously at part load or only at full load. In variable-speed turbines, different control goals may be required for different load or wind speed ranges. The supervisory controller performs a number of tasks during power production including system fault detection, turbine yaw orientation, and continuous monitoring of power and rotor speed to identify operating problems and to determine set points for speed and power controllers. In high wind gusts, power production may be allowed to exceed the turbine's rated power for short periods of time to limit the duty cycle of the pitch actuator and to allow short-period gusts to pass without increasing start–stop cycles.

8.4.2.6 Grid Disconnection (Transitional)

The tasks of this state may include disconnecting the generator–grid connection, disengaging various control systems, or providing new control goals and set points. This state may be a transition state to either a shutdown or freewheeling mode.

8.4.2.7 Freewheeling (Stationary)

In low winds the rotor may be allowed to rotate freely, 'freewheeling,' until the winds drop even further or pick up and power production can resume. During freewheeling the generator is not connected to the grid and the controller monitors conditions for connecting to the grid or shutting down the turbine. System checks are performed. In a controlled-yaw turbine, the rotor is oriented into the wind during freewheeling. In a free-yaw turbine, the yaw error is monitored during freewheeling. Rotor speed is closely monitored and the blade pitch may be used, where applicable, to maintain the rotor speed within a specific range.

8.4.2.8 Shutdown (Transitional)

This state is entered when winds or power are above specified upper levels, when winds drop below specified lower levels, or when system monitoring indicates that the turbine should not be operated. Stopping the turbine may require slowing the rotor with aerodynamic drag devices or by pitching the blades for shutdown, engaging the parking brake, and checking that the rotor has indeed ceased motion. Shutdown may also include parking the blades in a specific orientation and engaging the yaw brake. Upon completely shutting down, unless for a component problem, the turbine is ready for another operating cycle.

8.4.2.9 Emergency Shutdown (Transitional)

The emergency shutdown state is entered when critical operating or limit conditions are exceeded, when the normal shutdown procedure is deemed too slow to protect the turbine, or when the normal shutdown procedure is deemed ineffective because of a component failure. Typically, emergency shutdown results in a rapid deployment of all brakes, and a shutdown of numerous systems for safety or protection of equipment. Further operation of the turbine is not allowed without operator intervention.

8.4.3 Fault Diagnosis

The continuous fault diagnosis capabilities of the supervisory controller must include monitoring for component failures, including sensor failures, operation beyond safe operating limits, grid failure or grid problems, and other undesirable operating conditions.

Component failures may be detected directly or indirectly. For example, the failure of a coupling between the generator and the gearbox could be directly detected if the generator and rotor speeds are known and do not correspond to each other. Such a failure could also be detected by noting that the rotor speed is accelerating or is too high, or by the detection of the deployment of a tip drag device designed to release in an over-speed condition. Monitoring safe operating limits of a variety of components will ensure that most component failures will be detected, but critical failure modes may need to be monitored specifically to ensure that they are detected before operation is adversely affected. Thus, successful failure mode detection requires a full analysis of possible failure modes and the consequences of those failure modes, and an evaluation of the necessary sensors to detect those consequences.

While the most robust and accurate sensors that can be afforded should be chosen for a wind turbine, sensor failures can also occur. Sensor problems can be protected against if the system is designed such that any problem condition would trigger two different sensors. Sensors may need to be selected to withstand cold, wet, or dry weather, vibration, high electrical and magnetic fields, condensation, ice deposits, oil or dirt deposits, high wind, or salt spray.

8.4.4 Supervisory Control System Implementation

Supervisory controllers can be implemented using hardware logic, electronic circuits, or computers. The choice of which approach to take will typically depend on the size and complexity of the wind turbine. Smaller wind turbines may utilize hardware or electronic controllers, but all large wind turbines are equipped with sophisticated computer controllers.

8.4.4.1 Hardware Logic Control Systems

Hardware logic control systems are most easily implemented for simpler control strategies. These systems often use hardware logic called 'ladder logic.' Ladder logic systems may use a variety of components:

- industrial relays that may have multiple relay outputs;
- sensors with relay outputs triggered by user-selectable set points;
- industrial timers with relay contacts that close only after a preset time period has elapsed;
- a common power system for all actuators and relays.

Ladder logic uses a cascading series of relays to control turbine operation. A simple ladder logic design example is illustrated in Figure 8.9. In this example, a small stall-regulated wind turbine is assumed to have the following equipment:

- an induction generator that connects to the grid with a contactor;
- a brake that is released by introducing pressurized air from a reservoir tank through a solenoid and a brake pressure switch that indicates if the pressure in the brake is above a preset level;
- a compressor that supplies air to the reservoir tank for brake operation (the compressor is switched on when the low tank pressure switch indicates that the air pressure in the tank is low);
- a vibration switch that opens and remains open if the turbine vibrates too much;
- a wind speed sensor that closes relay contacts when the wind speed is between cut-in and cut-out.

As shown in Figure 8.9, operator actuation of the start button energizes the coil of the start relay, a relay with multiple sets of contacts (rung 1). Once the start relay is energized, the compressor of the brake will be powered up if the low tank pressure relay on the reservoir tank is closed (rung 2). If there is adequate pressure in the tank, the compressor remains off. If at any time the pressure drops, the compressor comes on. If the start relay has been energized *and* the vibration sensor indicates that no excess vibration has occurred *and* the wind speed is within
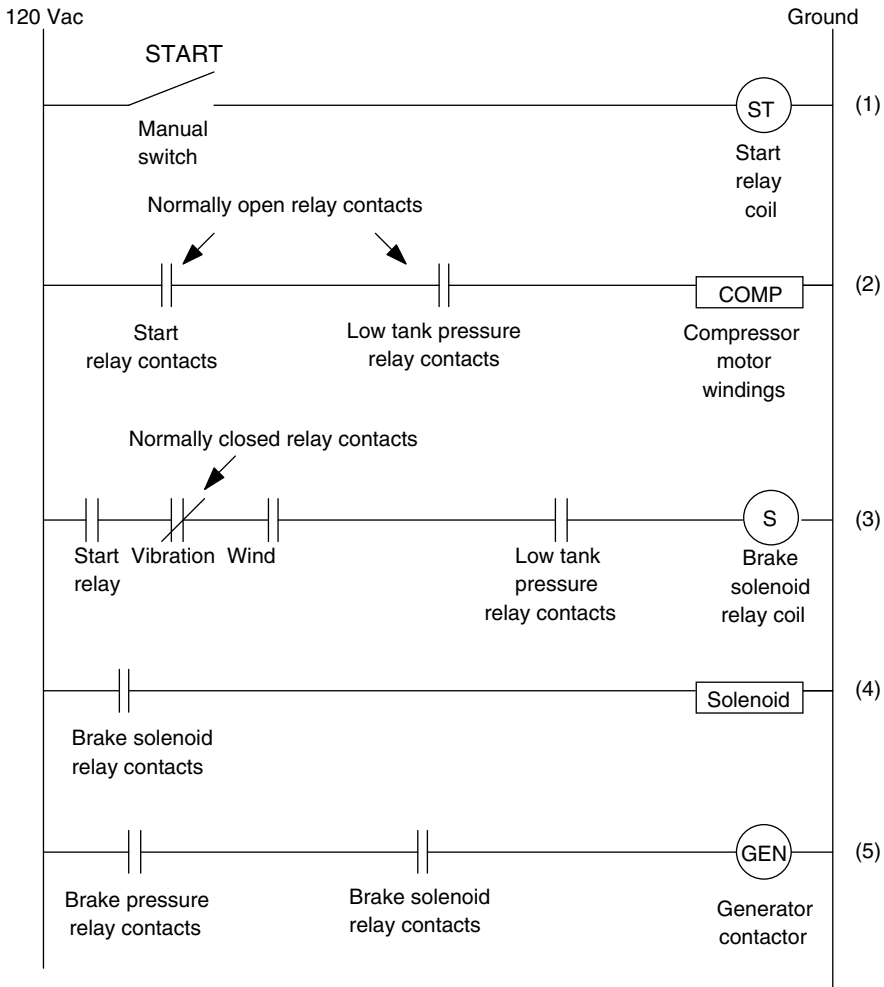
Figure 8.9   Ladder logic example

operating range *and* the tank pressure is high enough, then the brake solenoid relay is energized (rung 3). Contacts on this relay open the solenoid to put air into the brake to release the brake (rung 4). Other contacts on this same relay allow the generator contactor to be energized if there is enough air in the brake piston (rung 5). At this point, the turbine accelerates to operating speed and generates power. If the wind drops, the brake solenoid will be closed, releasing air from the brake (rungs 3 and 4). As a consequence of the solenoid closing, the generator contactor will be disconnected from the grid (rung 5). The brake will stop the wind turbine and the turbine will be ready for operation once the wind is within range and no vibration or low air pressure problems arise.

   Some aspects of hardware logic controls can also be used as a backup system to ensure that the turbine shuts down, for example, in emergency situations if the main computer has failed.

8.4.4.2 Electrical Logic Control Circuits

Supervisory controllers can also be partially or completely composed of electronic circuits. These might include:

- switches such as transistors and silicon-controlled rectifiers (SCRs) for switching circuits with high current and power;
- logic chips such as AND and OR gates and 'flip-flops' to implement controller logic;
- circuits to limit currents during start-up (soft-start circuits) or circuits to detect coincident AC waveforms to control contactors when synchronizing a synchronous generator with the power supply.

Electronic circuits might range from electronic implementations of ladder logic circuits to much more complicated measuring and timing circuits.

8.4.4.3 Computer Control Systems

Most wind turbines use computer control systems for supervisory control. These controllers use industrial computers that are designed for dirty environments and with capabilities to interact with other industrial equipment through digital input and output (I/O) ports, analog-to-digital (A/D) and digital-to-analog (D/A) converters, and communication ports. Industrial computers may be similar to desktop computers with slots for user-selected interface boards or they may be designed for dedicated logic control and may come equipped with digital I/O ports and relay contacts ready to switch industrial equipment. Computer control systems may use one central processing unit (CPU) to manage all of the logic and control functions of the controller or may have CPUs distributed around the turbine, with each CPU communicating with a master controller.

8.4.5 Fail-safe Backup Systems

Wind turbine control systems rely on: (1) power, (2) control logic, and (3) sensors and actuators. The control system must include fail-safe backup systems in case any of these elements fail. These fail-safe systems must safely shut down the turbine in cases of grid loss, rotor over-speed, excessive vibration, and other emergency situations.

Fail-safe backup systems should include the following components or functions:

- **Orderly shutdown on grid loss.** If the power grid supplies the power for the actuators on the turbine, the loss of grid power removes the ability of the controller to shut the turbine down with these actuators. If contactors are designed to fail open and brakes are designed to fail closed when power is removed, then a grid loss results in a safe turbine shutdown. Power for shutdown may come from springs, hydraulic accumulators, or backup power supplies.
- **Backup controller power.** Should the grid fail, backup power for the controller allows the supervisory controller to set relays in a safe position to ensure that the turbine will not restart when power is restored and to continue to monitor the turbine state and store data for later use.

- **Independent emergency shutdown.** If sensors fail, the supervisory controller may not be aware of a problem situation. Simple fail-safe backup systems could shut down the turbine in case of rotor over-speed and excessive vibration.
- **Independent hardware shutdown for supervisory controller failure.** A software hang-up could leave the turbine in an ambiguous operational state or operating with no supervision. Should the supervisory controller hardware or software fail, or should the control computer lose power, the system needs to be designed so that the turbine stops safely.

8.5 Dynamic Control Theory and Implementation

This section includes an overview of dynamic control systems, the dynamic control system design process, and examples of dynamic control system design issues specific to wind turbine applications. Background information on dynamic control system design can be found in textbooks such as Nise (2004).

8.5.1 Purpose of Dynamic Control

Dynamic control systems are used to control those aspects of machine operation in which machine dynamics have an effect on the outcome of the control action. Typically, control systems can be designed to improve the accuracy and dynamics of machine response, to improve the machine response to unwanted outside disturbances imposed on the system, and to reduce machine sensitivity to variations in machine components or machine operation under different circumstances. To achieve this, control systems use feedback: a measure of the outcome of the control action that is then included as an input to the control system. The control system uses this measure of the machine output in determining the next control action to help ensure that the machine works properly.

This can be illustrated with the example of a pitch control mechanism. A simple pitch control mechanism might use an electric motor to rotate the blade about its pitch axis. To rotate the blade, a specific amount of current might be applied to the motor for a predetermined amount of time. Whether the blade pitch changes by the desired amount is a function of many factors:

- changes in pitch system operation over time, such as changes in motor operation due to temperature, pitch axis bearing friction or wear of components;
- variability among the components installed in different wind turbines (different winding resistance, bearing friction, blade mass and distribution);
- external disturbances such as pitching moments, due to aerodynamic and dynamic forces, or changes in blade inertia due to icing.

Thus, it can be seen that such a control system may not always work as desired. As an alternative, a 'closed-loop' control system might be designed which uses a measure of the position of the blade root as an input to the control system. If, for any reason, the blade did not move the desired amount, corrections could be made, making machine operation less sensitive to variations and disturbances. Closed-loop control can also be used to improve system dynamics. In the example above, the blade would always move about the same distance in about the same amount of time. A properly designed control system might quickly increase the motor

current in order to accelerate the blade and then decelerate the blade as it reached its goal, improving the response time of the system.

Wind turbine operation imposes its own unique constraints on control system design. Some of these are related to the turbine dynamics such as the use of long cantilevered blades and tall towers that vibrate, and the use of metal shafts with little inherent damping. Other constraints come from control goals changing with power level. A variable-speed turbine might attempt to maintain a constant tip speed ratio (constant maximum C_P) over some range of wind speeds. The control system must then try to track variations in the wind speed, changing the generator torque in order to change the rotor speed. In this case the wind speed determines the goal of the control system. Above the rated wind speed, the aim of the control system might be completely different. Above rated wind speed, the generator torque and blade pitch of a pitch-controlled variable-speed machine are adjusted to reduce loads and to maintain constant rated power or torque. The purpose of the control system is, then, just the opposite of constant C_P operation: the maintenance of constant power in the face of wind speed changes which are now disturbances to the system operation.

The next section provides an overview of the dynamic control system design process. Section 8.5.3 discusses specific issues in the design of dynamic controllers for wind turbines. Examples illustrate both general dynamic control concepts (open- versus closed-loop control) and some specifics of wind turbine control problems. The final section in the chapter provides examples of the implementation of dynamic control systems.

8.5.2 Dynamic Control System Design

8.5.2.1 Classic Control System Design Methodology

The classic control system design process, as described in Grimble *et al.* (1990) and De LaSalle *et al.* (1990), includes the following steps (see Figure 8.10):

- **Problem analysis.** The problem analysis must include consideration of the desired machine operation, the available control effort, appropriate sensors and actuators, and any other design constraints. This analysis may indicate the need for an updated machine design with improved control characteristics.
- **Formulation of specifications.** Preliminary design specifications include measures such as system response time, the overshoot in the response of the controlled system to a step input, and controlled system stability. There may be hardware tradeoffs to consider. Faster system response requires greater actuator power, increases component loads, and decreases component fatigue life.
- **Model development.** Control system design requires an understanding of system dynamics, usually through the use of mathematical models. Depending on the system, these may be linear or nonlinear models. Each of the subsystem models needs to correctly reflect the system dynamics in the frequency range of interest.
- **Model linearization.** For initial control system design, these models are often linearized. This allows the use of numerous straightforward approaches to linear system design.
- **Control design.** During the design process, the engineer attempts to design the dynamics of the controller such that the overall controlled machine dynamics meet the design specifications. In the 'classical' design approach, the dynamic response of the controlled system is designed to
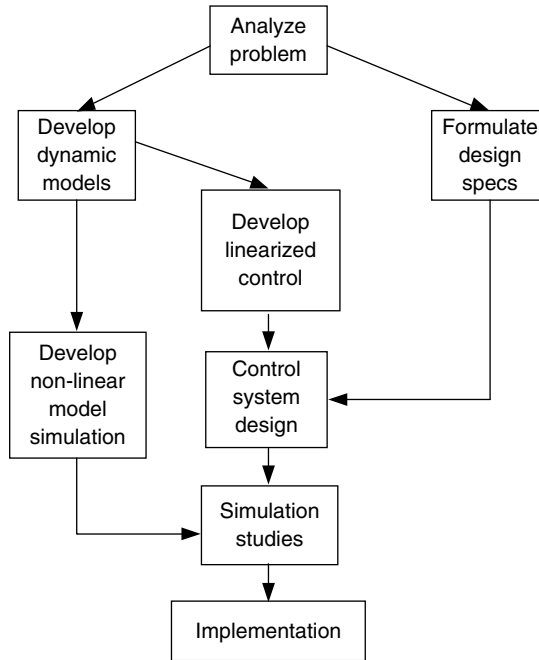
Figure 8.10 Control system design methodology (Grimble *et al.*, 1990). Reproduced by permission of the Institution of Mechanical Engineers

conform to certain criteria over three different frequency ranges of interest. Low-frequency system behavior is designed to track the desired control commands. At mid-frequency ranges, the system response is designed to ensure stability and adequate system response time. Higher frequency dynamics must ensure that unmodeled dynamics and sensor measurement noise do not affect system behavior. Other design approaches are described below.

- **Simulation development.** In order to test the operation of a controller design, computer codes for nonlinear simulations are developed, based on nonlinear system models. If possible, these models should be validated against real data.
- **Simulation studies.** Once a tentative controller has been designed for the linearized system, the nonlinear simulation model is used to investigate behavior of the more realistic nonlinear system including the new controller design.
- **Implementation.** Once an adequate design has been achieved, the controller is implemented on a wind turbine and tested in the field.

This process is highly iterative and at any point one might return to a previous step to redefine control objectives, refine models, or redesign the controller.

8.5.2.2 Other Control Design Approaches

Other control design approaches that build on or deviate from classical linear system design include adaptive control, optimal control, search algorithms, and quantitative feedback robust

design (see De LaSalle *et al.*, 1990; Di Steffano *et al.*, 1967; Horowitz, 1993; Munteanu *et al.*, 2008), among others. Each of these approaches may have advantages over classic linear control design methods, especially in the control of nonlinear systems.

Adaptive Control

The dynamic behavior of a wind turbine is highly dependent on wind speed due to the nonlinear relationship between wind speed, turbine torque, and pitch angle. System parameter variations can be accommodated by designing a controller for minimum sensitivity to changes in these parameters. These adaptive control schemes are also useful in systems in which system parameters change, especially if they change rapidly or over a wide range. Adaptive control schemes continuously measure the value of system parameters and then change the control system dynamics in order to make sure that the desired performance criteria are always met.

Optimal Control

Optimal design is a time domain approach in which variances in the system output (for example, loads) are balanced against variances in the input signal (for example, pitch action). Optimal design approaches are inherently multivariable, making them suitable for variable-speed wind turbine control design. Optimal control theory formulates the control problem in terms of a performance index. The performance index is often a function of the error between the commanded and actual system responses. Sophisticated mathematical techniques are then used to determine values of design parameters to maximize or minimize the value of the performance index. Optimal control algorithms often need a measurement of the various system state variables or a 'state estimator,' an algorithm to estimate unmeasured variables based on a machine model.

Search Algorithms

Search algorithms can also be used to control wind turbines. These algorithms might constantly change the rotor speed in an attempt to maximize measured rotor power. If a speed reduction resulted in decreased power then the controller would slightly increase the speed. In this manner the rotor speed could be kept near the maximum power coefficient as the wind speed changed. The controller would not need to use a machine model and would, thus, be immune to changes in operation due to dirty blades, local air flow effects, or incorrectly pitched blades.

Quantitative Feedback Robust Control

Quantitative Feedback Theory (Horowitz, 1993) is a frequency domain approach for designing robust controllers for systems with uncertain dynamics. It provides methods for designing a closed-loop system with specific performance and stability criteria for systems within a defined range of operating parameters. It can ensure that one controller design will perform well for a system with a range of dynamic properties.

8.5.2.3 Gain Scheduling

Wind turbines are highly nonlinear systems with different control goals over different wind speed ranges. Meanwhile, many of the controller design approaches above are based on time-invariant linear models that are only applicable within certain operational ranges. The variation of control goal is usually addressed with a strategy for a smooth transition between control goals that avoids unwanted load transients. The variation of dynamic behavior across the range

of operating conditions is addressed by the design of a controller that is robust enough to perform reasonably well under a variety of conditions or by using some variation of 'gain scheduling.' Given the wide range of dynamic behavior of a wind turbine, the robust controller may provide better performance under some conditions but only barely acceptable performance under others. The approach that is most often used to address changes in system dynamics is gain scheduling, which, in this case, refers to the adjustment of the controller operation as a function of the scheduling variable (wind speed or power level), as described above (see Bianchi *et al.*, 2007 for more details).

The design of a controller with gain scheduling involves:

- the definition of the operating points for which a unique linear controller is to be designed;
- the design of a linear controller that meets the desired performance and stability design criteria;
- the definition of an approach to modifying the controller function as the scheduling variable changes.

The method for changing the controller function may be fairly simple. For example, if each individual controller is a second order controller with two parameters, then the applicable control parameter for any operating point might be defined by interpolation between operating points. More complicated approaches are also possible.

The primary concern of these approaches is that stability of the system may not be guaranteed between the operating points for which the controllers were designed. Bianchi *et al.* (2007) describe the application of linear parameter varying (LPV) approaches to wind turbines. LPV methods use the tools of optimal control design, including the gain scheduling function, to design a controller and gain scheduling with guaranteed performance and stability over the whole range of operation.

8.5.2.4 Wind Turbine System Models

System models used for control system design are often mathematical models based on the principles of physics. When such models cannot be developed, an experimental approach termed 'system identification' can be used.

Models Based on Physical Principles
Dynamic models are used to understand, analyze, and characterize system dynamics for control system design. The models consist of one or more differential equations describing system operation. These differential equations are usually written in one of two forms: the transfer function representation or a state space representation. Both of these descriptions assume a linear system. The transfer function representation involves the use of Laplace transforms and characterizes the system in the frequency domain, while the state space representation characterizes the system in the time domain. These system representations is interchangeable and the choice of approach depends on the degree of complexity of the system and the analytical tools available to the system designer.

It should be remembered that the results of control system design are only as good as the model used to describe the system. A control system based on a model that ignores critical dynamics of any part of the machine can result in catastrophic failure. However, an excessively

detailed model adds complexity and cost to the analysis and may require machine input parameters that are unknown. Engineering judgment is required in developing the system model. Simple, yet appropriate, models often describe a system as a set of lumped masses or ideal machine elements, ignoring less important machine details. These models are useful if the masses or stiffness of the idealized elements are chosen so that the model truly represents system behavior. Often, data from machine operation are used to determine these parameters. In this way the simple model is 'fit' so that it best represents true operation of the machine. As long as the chosen machine model represents the system dynamics of interest, then a successful control system can be developed. When a nonlinear system has been linearized for control system design, simulations of system behavior over a wide range of nonlinear operation should be used to check operation of the full controlled system.

The important wind turbine subsystems that need to be modeled are:

- wind structure;
- drive train dynamics;
- aerodynamics;
- generator dynamics;
- converter dynamics;
- actuator dynamics;
- structural dynamics;
- measurement dynamics;
- controller dynamics.

The interactions of these subsystems in a constant-speed, pitch-controlled wind turbine are illustrated in Figure 8.11. Some sample mathematical models of wind turbine subsystems can be found in Novak *et al.* (1995).
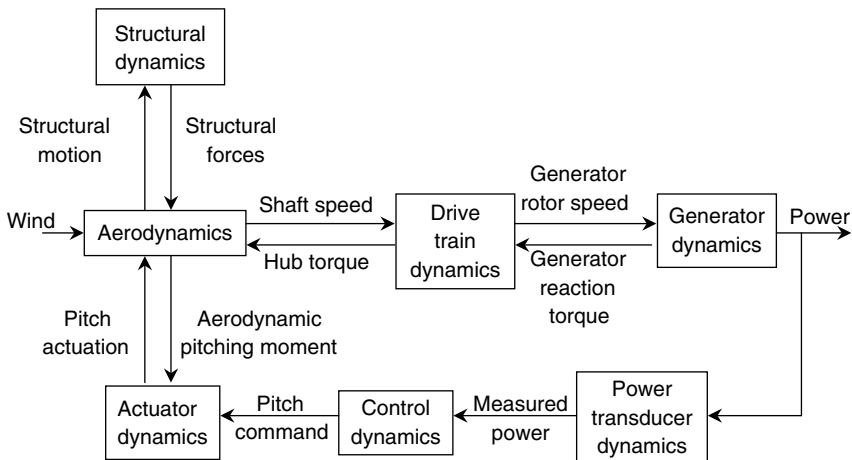

Figure 8.11   Wind turbine dynamics (Grimble *et al.*, 1990). Reproduced by permission of the Institution of Mechanical Engineers

System Identification

In cases where models for disturbances or for complicated systems cannot easily be determined from physical principles, the experimental approach of system identification can be used (see Ljung, 1999). The system identification approach involves four main steps:

1. Planning the experiments.
2. Selecting a model structure.
3. Estimating model parameters.
4. Validating the model.

System identification involves measuring the system output, given a controlled input signal or measurements of the system inputs. Simpler approaches to system identification require sinusoidal or impulsive inputs. Other approaches can use any input, but may require increased computational capability to determine the system model. In order to correctly identify the dynamics of a system, the input signal should be designed to excite all the modes of the system sufficiently to provide measurable outputs.

The data from experiments are used to fit parameters for a model of the system. That system model may be based on a priori knowledge of the system and disturbances. If the system is known to behave in a linear manner over a particular operating range, then general representations of linear systems called 'black box models' may be used. In these cases, the parameters as well as the order of the models are to be identified. It may be possible to reduce the number of unknown parameters by using models developed from physical principles.

Parameter estimation is usually formulated as an optimization problem using some criteria for the best fit to the data. There are many different possible approaches to the system identification calculations and the optimization criteria. Online methods provide parameter estimation while measurements are being obtained. These methods are useful for time-varying systems or for use in adaptive controllers. Offline methods usually have more reliability and precision. They most often use an optimization criterion in some variation of a least squares approach.

Once the model parameters have been determined, it is important to test and validate the model. The model is often tested by checking the step and impulse responses, and determining model and prediction errors. A sensitivity analysis reveals the sensitivity of the model to parameter variations. Depending on the results of these steps, the process may be iterated in order to develop a more adequate model. This might require further development of the model and more experiments.

8.5.3 Control Issues in Wind Turbine Design

8.5.3.1 Control Issues Specific to Wind Turbines

Wind turbines present a number of unique challenges for a control system designer (see De LaSalle *et al.*, 1990; Bianchi *et al.*, 2007; Munteanu *et al.*, 2008). Conventional power generation plants have an easily controllable source of energy and are subject to only small disturbances from the grid. In contrast, the energy source for a wind turbine is subject to large rapid fluctuations, resulting in large transient loads in the system. The consequences of these

large fluctuations and other aspects of wind turbines introduce unique issues in control system design for wind turbines:

- The penalty for a poorly regulated wind turbine is high structural and component loads. These result in heavier components, a heavier structure, and increased turbine costs.
- A wind turbine system consists of numerous lightly damped structures (in order to avoid energy dissipation in the system) that are excited by forcing functions at the frequency of the rotor rotation and its harmonics and by wind turbulence. The component, including rotor, drive train, tower, and control system, may all have significant dynamic responses in the frequency range of the rotor rotation. Any resonance conditions would impose severe constraints on system operation. Resonances between the controllers, the natural frequencies of the system (blades, drive train, tower), and system forcing functions (harmonics of the blade rotation frequency and possibly frequencies of fluctuations in the wind field) must be avoided.
- The aerodynamics are highly nonlinear. This results in significantly different dynamic descriptions of turbine behavior at different operating conditions. These differences may require the use of nonlinear controllers or different control laws for different wind regimes.
- Transitions under dynamic operation from one control law or algorithm to another require careful design.
- The control goal is not only the reduction of transient loads, but also of fatigue loads, caused by the load fluctuations about the mean load.
- Control measurement and actuator hardware cost and weight must be minimized.
- Reliable torque measurements for feedback are often difficult to obtain.
- Adequate system models are often difficult to determine. System models need to be compared with measurements to confirm that the model parameters represent the true machine operation. The control system designer attempts to make a system model that represents the dynamics of the system without being overly complex. Complexity increases design time and also results in models with numerous parameters that may be difficult to determine. Simple models may represent the system well, but not with the expected parameters. A drive train includes gearbox dynamics (backlash, flexing of gear teeth), shafts with low and difficult to quantify damping ratios, and a non-rigid rotor subject to nonlinear aerodynamics. These can result in behavior that deviates from that of a simple model (see Novak *et al.*, 1995).
- Extensive research has been required and is still ongoing into the exact loads that a wind turbine experiences.

Some examples of these issues are presented below. First, the advantages of closed-loop over open-loop control systems are illustrated using a simple pitch control system. The system response to outside disturbances is analyzed. Then, issues of natural frequencies and resonance are illustrated using the same closed-loop pitch control system. In the following two subsections, issues related to variable-speed turbine operation are considered, including control for constant optimum tip speed ratio in low winds and issues related to transitioning to other operating modes at higher wind speeds. Finally, some of the details of modeling disturbances in a pitch control system are provided.
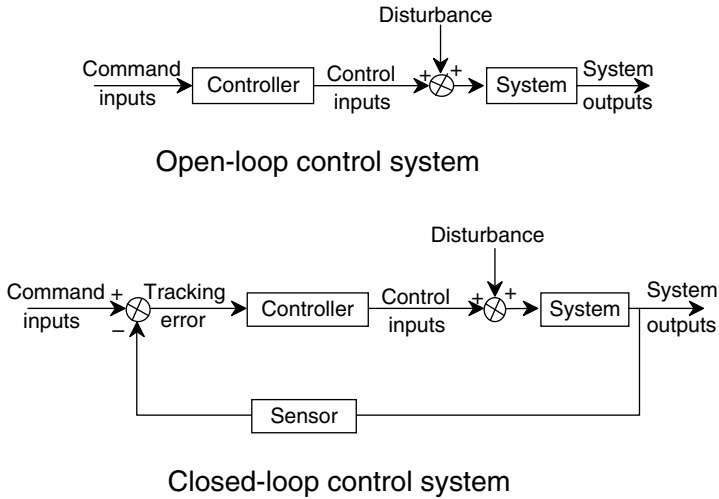
Figure 8.12   Comparison of open-loop and closed-loop control systems

8.5.3.2 Open-loop and Closed-loop Response to Disturbances

The basic differences between open- and closed-loop control systems are illustrated in Figure 8.12. In an open-loop system, the controller actions are based on the desired system state, with no reference to the actual state of the process. In closed-loop feedback systems, the controller is designed to use the difference between the desired and the actual system output to determine its actions.

Some aspects of control systems can be illustrated with a simple pitch mechanism driven by an AC servo motor with a spring return and subject to external pitching moments (disturbances to the system). The blade and pitch mechanism model includes moments from the spring and viscous friction. The torque from an AC servo motor can be modeled as a linear combination of terms that are a function of motor speed and of applied voltage (see Kuo and Golnaraghi, 2002). In the model presented here, the motor torque and speed are referred to the blade side of the pitch mechanism. The differential equation for this system has the system dynamics terms on the left and the external torques from the motor and disturbance on the right:

$$J\ddot{\theta}_p + B\dot{\theta}_p + K\theta_p = kv(t) + m\dot{\theta}_p + Q_p \qquad (8.3)$$

where θ_p is the angular position of the motor (the pitch angle), J is the total inertia of the blade and motor, B is the pitch system coefficient of viscous friction, K is the pitch system spring constant, k is the slope of the torque–voltage curve for motor/pitch mechanism combination, $v(t)$ is the voltage applied to the motor terminals, m is the slope of the torque–speed curve for motor/pitch mechanism combination, and Q_p is a pitching moment due to dynamic and aerodynamic forces that acts as a disturbance in the system.

If the system is at steady state, then the derivatives of the pitch angle are zero and $v(t)$, the voltage to the motor, is a constant value, v. In this case the differential equation becomes:

$$\theta_p = \frac{k}{K}v + \frac{Q_p}{K} \tag{8.4}$$

From this it can be seen that the steady state pitch angle will be a function of the voltage applied to the motor, the spring constant, and any pitching moment on the blade. The greater the pitching moment (or the weaker the spring), the greater the error in the pitch angle will be.

Assuming that the airfoil designer has tried to minimize any pitching moment, one could design a control system that applied a specific voltage to the motor for a desired 'reference' pitch angle, $\theta_{p,ref}$:

$$v = \frac{K}{k}\theta_{p,ref} \tag{8.5}$$

In this case, the differential equation for the open-loop system is:

$$J\ddot{\theta}_p + (B-m)\dot{\theta}_p + K\theta_p = K\theta_{p,ref} + Q_p \tag{8.6}$$

Here, the pitch angle is the output and the system has two inputs, the voltage to the pitch motor and a disturbance torque from the aerodynamic and dynamic pitching moments on the blade. If one assumes that all derivatives and the pitching disturbance torque are zero, it can be seen that the steady state response of the system to a desired pitch angle command is, indeed, that desired pitch angle.

The relationships between the various dynamic elements in a controlled system are often illustrated with the use of block diagrams. A block diagram for this system is shown in Figure 8.13.

Laplace transforms can be used to solve Equation (8.6). In addition, the Laplace transform of the system response about steady state operation to an impulse input is referred to in classical control theory as the system transfer function. It is often used in control system design to characterize system dynamics (for more background information, see Kuo and Golnaraghi, 2002 or Nise, 2004). The system transfer function can be found by taking the Laplace transform of the open-loop differential equation, solving for the pitch angle, and assuming that initial conditions are all zero. The transfer function of this system would be:

$$\Theta_p(s) = \frac{K\Theta_{p,ref}(s)}{Js^2 + (B-m)s + K} + \frac{Q_p(s)}{Js^2 + (B-m)s + K} \tag{8.7}$$
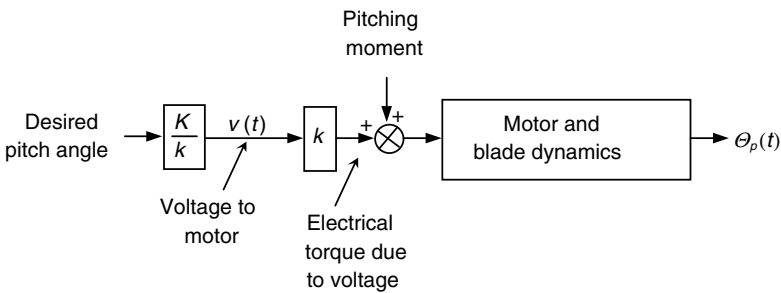

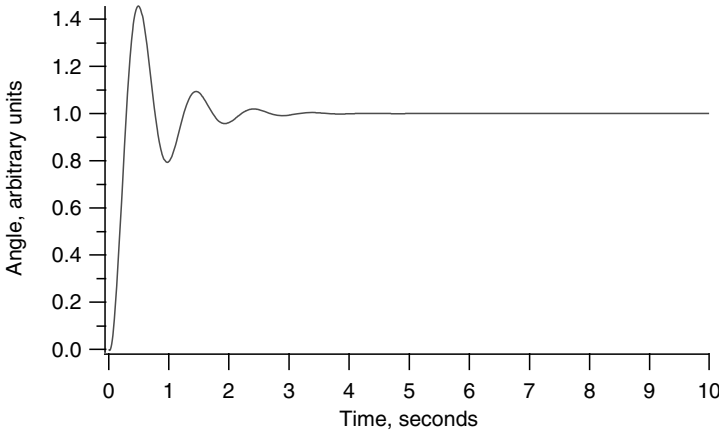**Figure 8.13** Open-loop pitch control mechanism; for notation, see text

Figure 8.14   Sample pitch system step response

where $\Theta_p(s)$, $\Theta_{p,ref}(s)$, and $Q_p(s)$ are the Laplace transforms of θ_p, $\theta_{p,ref}$, and $Q_p(t)$. The first term in Equation (8.7) is the transfer function from the voltage input to the pitch angle output. The second term is the transfer function from the disturbance (the pitching moment) to the pitch angle.

The dynamic response of the open-loop system to a unit step disturbance can be found from the inverse Laplace transform of the transfer function that relates the disturbance to the pitch angle:

$$\Theta_p(s) = \frac{Q_p(s)}{Js^2 + (B-m)s + K} \tag{8.8}$$

where $Q_p(s)$ would be $1/s$ for a step input. If, for example, the motor and blade dynamics are:

$$\Theta_p(s) = \frac{1}{(s^2/16) + (s/4) + 1} \tag{8.9}$$

where $J = 1/16$, $(B-m) = 1/4$ and K, Q_p, and k are all equal to 1, the response to a step disturbance is shown in Figure 8.14.

In Figure 8.14, the deviation from ideal operation should be zero, but the pitch disturbance results in a steady pitch angle error. From Equation (8.4), the steady state positioning error due to the pitching moment is:

$$\theta_p - \theta_{p,ref} = \frac{Q_p}{K} \tag{8.10}$$

In practice, open-loop control systems often have failings that significantly affect system operation. Manufacturing variability, wear, changes in operation with temperature and time, and outside disturbances can affect open-loop system performance. In this example, changes in the wind speed, rotor speed, blade icing, or anything else that might affect the pitching moment would change the pitch. If the effects of these changes in operation become a problem, closed-loop control systems could be used to improve system performance without significantly complicating the control system.
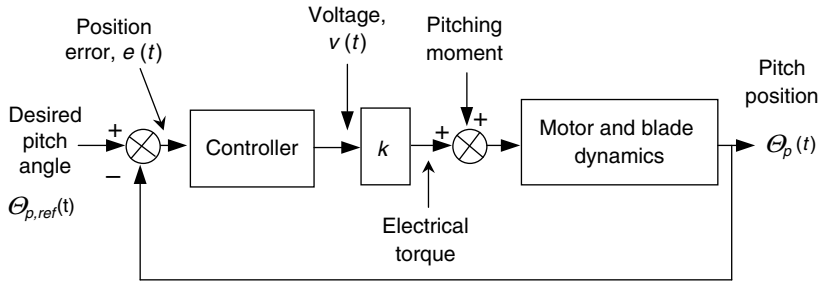
Figure 8.15   Closed-loop pitch mechanism example; for notation, see text

In a closed-loop control system, a measurement of the pitch angle can be incorporated into the input to the pitch control system, and corrections can be made for errors in the position of the blade. Typically, the controller provides a control output that is a function of the 'tracking error', the difference between the desired system output and the measured output. The block diagram of such a closed-loop system is shown in Figure 8.15. The controller would include appropriate dynamics and a power amplifier to adjust the voltage to the motor.

The controller can be designed with any dynamic properties that might help the system achieve the desired operation. There are, however, some standard approaches to control systems that are often implemented and are used as references in considering control system design. Some of these standard approaches include *proportional*, *derivative*, and *integral* control. Often these approaches are combined to yield a proportional–integral (PI) controller or a proportional–integral–derivative (PID) controller.

The differential equation of a PID controller for the pitch system would be:

$$v(t) = K_P e(t) + K_I \int e(t)\mathrm{d}t + K_D \dot{e}(t) \tag{8.11}$$

where the constants of proportionality are K_P, K_I, and K_D and where $e(t) = \theta_{p,ref}(t) - \theta_p(t)$ is the error, the difference between the desired and the measured pitch angle.

If the closed-loop controller were designed with just the proportional and integral terms (a PI controller), then the differential equation for the complete system could be found by substituting the definition of the controller, Equation (8.10) without the derivative term, into Equation (8.3). One could use the definition of $e(t)$ from above, differentiate the complete equation and rearrange, to get Equation (8.11). The resulting controlled system is now a third order system with two controller constants, K_P and K_I:

$$J\dddot{\theta}_p + (B - m)\ddot{\theta}_p + (K + kK_P)\dot{\theta}_p + kK_I\theta_p = kK_P\dot{\theta}_{p,ref} + kK_I\theta_{p,ref} + \dot{Q}_p \tag{8.12}$$

Once again, the dynamic response of the closed-loop system to a unit step disturbance can be found from using inverse Laplace transforms. For example, if it is assumed that the motor and blade dynamics remain the same, and that $K_P = K_I = 2$ then the response to a step disturbance is shown in Figure 8.16. The figure includes the open-loop response for comparison. The disturbance clearly affects the closed-loop system less than the open-loop system.

While further improvements might be made to improve dynamic response of the system, the PI controller would correctly position the blade under a variety of wind and operating
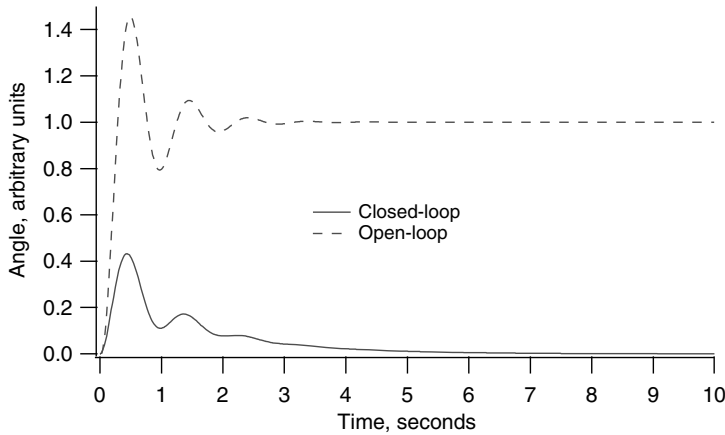
Figure 8.16 Sample closed-loop and open-loop pitch system response to a step disturbance

conditions. Thus, without adding too much complexity, the blade can be positioned at any desired position in high or low winds, under icing conditions, and with a sticking bearing on the pitch mechanism. This is a significant improvement over the open-loop controller.

8.5.3.3 Resonances

Wind turbines consist of long lightly damped members that vibrate and operate in an environment in which gusts, wind shear, tower shadow, and dynamic effects from other turbine components can excite vibrations. Control systems need to be designed to ensure that the wind turbine avoids excitation at certain frequencies and the controller does not excite the turbine at those frequencies as a result of its own operation. The control system also needs to be designed to avoid being one of the turbine components that are excited by the numerous possible forcing functions. This can occur in otherwise acceptable control system designs.

The pitch controller of the previous example provides reasonable disturbance rejection of a step input. This indicates that step changes and less severe changes in operating conditions can be compensated for by the pitch control system. Analysis of the differential equation for the closed-loop system (Equation 8.10) or of the system transfer function shows that the closed-loop system has a natural frequency of 6.76 radians/second (1.08 Hz), and a damping ratio of 0.24 (see Chapter 4 for information on natural frequencies and damping ratios). If this pitch control system experienced a sinusoidal disturbance, as it might with wind shear, with a frequency near the natural frequency of the closed-loop system, then the system response might be significantly magnified over that due to other disturbances. For example, the response to a sinusoidal disturbance with a magnitude of 1 and a frequency of 1.04 Hz is shown in Figure 8.17.

The closed-loop system clearly does a much poorer job of managing disturbances near the system response frequency than it does managing step disturbances. The response magnitude depends on the frequency of the disturbance and the damping in the system. Not only could the pitch fluctuations induced by the disturbance wear out the pitch mechanism, but oscillating shaft torque from the aerodynamics caused by the oscillating blade pitch could
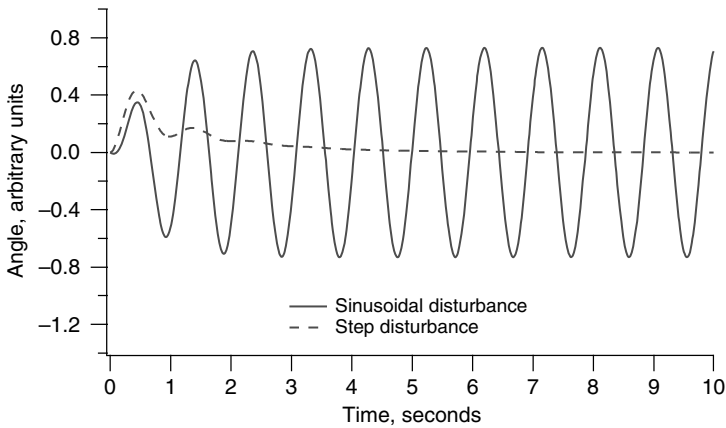
Figure 8.17 Closed-loop pitch system response to unit sinusoidal and step disturbances

introduce resonances in other feedback paths. This sample control system was designed specifically to illustrate these issues. A well-designed control system would avoid exciting system natural frequencies and might even be able to provide additional damping at those frequencies.

8.5.3.4 Optimum Tip Speed Ratio Control Issues

As previously discussed, wind turbines are sometimes operated at variable speed to reduce loads and to maximize energy capture at low winds. Maximizing energy capture in low winds requires operating the rotor at its most efficient tip speed ratio (see Chapter 3). A number of approaches to this control problem are described in Munteanu *et al.*, 2008. To maximize energy capture in low winds, the rotor speed must vary with the wind speed. A number of issues arise with such optimum tip speed ratio operation:

- **Design tradeoffs.** The efficiency of the turbine over time depends on the controller's success in changing rotor speed as the wind speed changes. For maximum efficiency, rotor speed changes should occur rapidly, but this has the disadvantage of increasing torque fluctuations in the drive train. The flatter the $C_p - \lambda$ curve, the less tight the tracking of the wind needs to be.
- **Determining rotor tip speed ratio.** Tip speed ratio is the ratio of the rotor tip speed to the wind speed. It is difficult to determine accurately. Turbulent winds vary in time and location over the rotor area. Wind speed measurements on the hub do not measure the undisturbed free stream wind speed and, in any case, they only measure the wind speed at one point on the rotor. Wind speed measurements on a measuring tower sample the wind only at one location in the wind field and at a distance from the turbine. Tip speed can also be inferred from rotor speed, torque, or power measurements, and machine models. Efforts to determine tip speed from rotor operation may be difficult because of noise on torque sensors and inaccurate rotor models.

- **Rotor energy.** Energy stored in the rotor rotation causes power spikes during rotor decelerations that can confuse measurements of rotor power or torque and that have the potential to cause an over-power situation if the rotor is decelerated too rapidly. The contribution to rotor shaft power, P_r, that is due to changes in stored energy in the rotor is a function of rotor inertia, J_r, and changes in rotor speed, Ω, as described by Equation (8.12). The more rapid the rotor speed changes, the greater the power fluctuations:

$$P_r = \frac{\mathrm{d}}{\mathrm{d}t}\left(\tfrac{1}{2}\,J_r\Omega^2\right) = J_r\dot{\Omega} \qquad (8.13)$$

- **Nonlinear aerodynamics.** The change in rotor aerodynamic torque or rotor aerodynamic power as a function of speed is highly nonlinear, often requiring a nonlinear controller for control in both low and high winds.

Tracking the optimum tip speed ratio is usually accomplished with a rotor model, in spite of the possibility that the model may be a poor representation of rotor operation. Another approach that is sometimes considered is a search algorithm that seeks to find the rotor speed for maximum power at each moment. Such an approach, if successful, will maximize rotor energy capture in spite of poorly understood rotor performance, icing, mispitched blades, etc.

One common approach (see Novak *et al.*, 1995) which does not directly attempt to determine the tip speed uses a rotor model to specify the desired rotor torque, Q_{ref}, as a function of rotor speed:

$$Q_{ref} = \frac{\rho\pi R^5 C_{p,\max}}{2(\lambda_{opt})^3}\,\Omega^2 \qquad (8.14)$$

where Q_{ref} is the desired rotor torque, ρ is the air density, R is the rotor radius, and $C_{p,\max}$ is the rotor power coefficient at the rotor's optimum tip speed ratio, λ_{opt}.

The rotor speed is measured and the generator torque is continually set to the rotor torque that corresponds to the present rotor speed. If the rotor speed is low for the existing wind speed, the torque is set to a low value, allowing the rotor speed to increase. If the rotor speed is high for the wind speed, the rotor torque is set to a high value, slowing the rotor to make it more efficient. The torque command is filtered to avoid high-speed rotor changes.

This approach works fairly well, but the filtering to avoid rapid power or torque fluctuations may need to change for different wind regimes. The change in rotor power with changes in rotor speed varies significantly over the operating range of a turbine and may need to be considered to control power and torque fluctuations. This requires knowing the tip speed ratio.

Linders and Thiringer (1993) have proposed a method of determining the rotor tip speed ratio from a turbine model and measurements of turbine power. Once the operating tip speed ratio is determined, the rate of change of power due to a change in rotor speed can be determined from a rotor model. The difficulty in using power or torque measurements to determine the tip speed ratio is that there are two tip speed ratios that correspond to any C_p. Linders and Thiringer define a monotonic function from which the tip speed ratio can be determined unambiguously:

$$\frac{C_p(\lambda)}{\lambda^3} = \frac{P_r}{\frac{1}{2}\rho A\Omega^3 R^3} = \frac{P_{el}}{\eta\frac{1}{2}\rho A\Omega^3 R^3} \qquad (8.15)$$

where P_r is the rotor power, P_{el} is the electrical power, R is the radius, η is the drive train efficiency, ρ is the air density, A is the rotor area, and $C_p(\lambda)$ is the rotor power coefficient at a tip speed ratio of λ.

The derivative of the power with respect to the generator speed is then:

$$\frac{\mathrm{d}P_{el}}{\mathrm{d}\Omega_{el}} = \left(\frac{\mathrm{d}C_p(\lambda)}{\mathrm{d}\lambda}\right)\frac{\eta\frac{1}{2}\rho AV^2 R}{np} \tag{8.16}$$

where Ω_{el} is the generator speed, p is the number of generator poles, and n is the gearbox gear ratio.

The machine control can then be improved by modeling power flows in and out of the rotor as the rotor speed changes and by subtracting these from the measured power.

8.5.3.5 Transitions Between Variable-speed Operating Modes

Numerous other issues arise in the design of variable-speed wind turbines. In general, variable-speed wind turbines may have three different control goals, depending on the wind speed. In low to moderate wind speeds, the control goal is maintaining a constant optimum tip speed for maximum aerodynamic efficiency. This is achieved by varying the rotor speed as the wind speed changes. In moderate winds, if the rotor reaches its rated speed before the rated power is reached, the rotor speed must be limited while the power fluctuates. The control goal is then the maintenance of approximately constant rotor speed. In moderate to high winds, the control goal is the maintenance of constant rated power output. This is required as the available power in the wind increases above the power conversion capabilities of the wind turbine. Transitions between these operating strategies must be managed smoothly by any successful control system design.

These same general control goals apply to both stall-regulated and pitch-regulated variable-speed wind turbines. With pitch-regulated wind turbines, two control inputs, pitch angle and generator torque, can be varied instead of just generator torque. The blade pitch is typically held fixed during constant tip speed ratio and constant speed operation, but during constant power operation, the blade pitch can be used to control rotor speed while the generator torque can be used to control output power. During constant speed operation, there may be large fluctuations in generator torque and thus output power, as the wind speed and rotor torque change. During constant power operation, generator power and torque fluctuations are minimized because the control goal is the maintenance of rated power. The pitch controller does most of the work of maintaining average rated rotor speed.

The turbulence in the wind makes successfully designing a controller to transition between these control goals difficult. In low winds with constant tip speed operation, the change in output power, P, as a function of changes in rotor speed, Ω, $\mathrm{d}P/\mathrm{d}\Omega$, is relatively small. In moderate winds with approximately constant speed operation, $\mathrm{d}P/\mathrm{d}\Omega$ can be quite large. In high winds, $\mathrm{d}P/\mathrm{d}\Omega$ should be close to zero. With two control inputs in moderate and high winds (pitch angle and generator torque) and only one in low winds, and significantly different controller behavior at different wind speeds, fluctuating wind speeds can result in rapid actuator actions and large power excursions in a poorly designed control system.

An example of such difficulties is presented below. The example uses a turbine with the common controller configuration illustrated in Figure 8.18. In this design, the desired, or
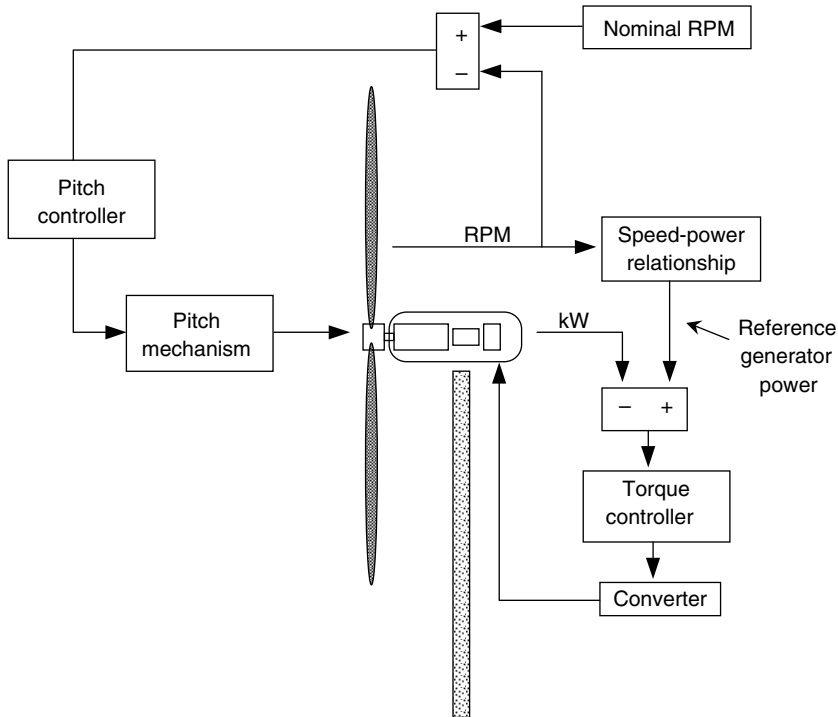
Figure 8.18   Variable-speed closed-loop control system

'reference,' generator power is set to be a function of rotor speed, based on a desired power versus generator speed curve.

This desired power vs. generator speed relationship for the sample wind turbine is shown in Figure 8.19 (see Hansen *et al.*, 1999). The variable-speed operation in the lower part of the curve is based on the aerodynamic performance of the rotor and is intended to maintain a constant tip speed ratio. Once the generator speed approaches the nominal rated speed, 1000 rpm, the slope of the desired power vs. speed curve is very steep. Finally, once the turbine power reaches 225 kW, the control goal is constant power with some small variation of the rotor speed. Only during constant power operation is the pitch control loop trying to control the rotor speed to near the rated rotor speed.

Difficulties have arisen with this control approach when fluctuating winds cause the generator speed to decrease from over to under nominal rated generator speed. Because of the sharp change in slope ($dP/d\Omega$), even small changes in generator speed cause large changes in the commanded power from the generator. This has caused sudden, sharp reductions in power of as much as 150 kW. Improvements to the control strategy have been made by limiting the allowed rate of change of the desired generator power. This has the effect of significantly limiting power fluctuations near rated power, but it also increases rotor speed fluctuations. The net effects of decreasing generator torque fluctuations and allowing the rotor speed to vary over a wider range are lower power fluctuations, which might affect the grid, and decreased drive train loads.
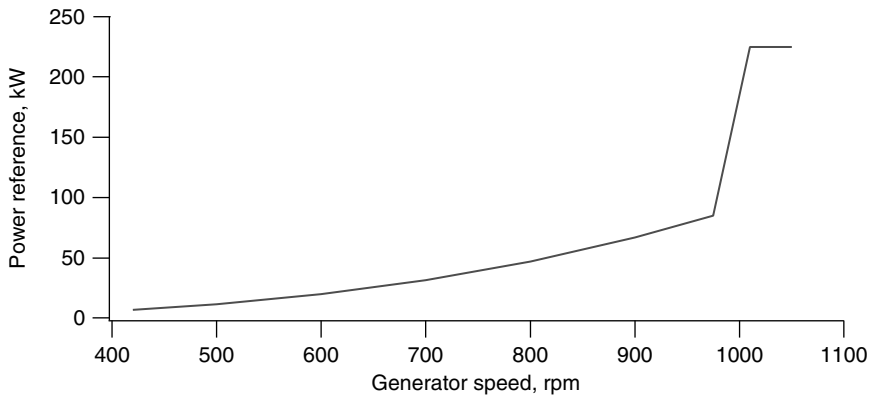
Figure 8.19 Example of grid power–generator speed control relationship (Hansen *et al.*, 1999). Reproduced by permission of James & James (Science Publishers) Ltd. and A. D. Hansen, H. Bindner and A. Rebsdorf

8.5.3.6 Wind Turbine Loads and Disturbances

The design of wind turbine controllers requires information on the magnitude and frequency characteristics of disturbances that affect the components being designed. This information affects both actuator design and the design of the control algorithm itself. More information on the types and origins of the loads in wind turbines can be found in Chapters 4 and 7.

For example, the design of pitch mechanisms and controllers for pitch mechanisms requires knowledge of the magnitude and kinds of loads and disturbances that the mechanisms will experience. Knowledge of which loads are or are not significant in control system design ensures an acceptable control system with as little complexity as possible.

The loads and disturbances on pitch systems include:

- **Gravity loads.** Gravity loads include the effect of gravity on the distributed mass of the blade that cause moments that act about the pitch axis.
- **Centrifugal loads.** Centrifugal loads include the effect of inertial forces on the distributed mass of the blade that causes moments that act about the pitch axis.
- **Pitch bearing friction.** Pitch bearing friction is a function of the axial loads and edgewise and flapwise moments on the pitch bearings as well as the bearing design.
- **Actuator torque.** Actuator torques must be transferred through linkages or gears from hydraulic or electrical systems.
- **Aerodynamic pitching moment.** The aerodynamic pitching moment is a function of integrated effects of the aerodynamics over the length of the blade. It includes the effects of blade design, blade vibration and bending, turbulence, wind shear, off-axis winds, and blade rotation.
- **Loads due to other turbine motions.** The effects of other turbine motions such as changes in rotor speed, yaw motions, and tower vibrations can be transferred to the blades and can cause additional moments about the pitch axis.

In normal operation of a given turbine, some of these moments may be of little significance to control system design. Nevertheless, during emergency pitching events or under unusual operating conditions, the contribution of each of these moments needs to be considered to ensure that the control design works in all situations.

The pitch system response to these loads depends on the compliance and backlash in the pitch actuator system (including any linkages), the stiffness of the blades, the compliance and backlash in the pitch bearing, the inertia of the actuator system, the moment of inertia of the blade, and the pitch control system dynamics.

Research has shown (see Bossanyi and Jamieson, 1999) that pitch bearing friction and blade bending can significantly affect overall pitching disturbance moments. Generally, roller bearing-type pitch bearings have a very low coefficient of friction, but net friction forces are also a function of the load on the bearing. The high preload required to minimize bearing wear and the large overturning moments on the bearing from the blade can cause unexpectedly high pitching moment disturbances. Blade deflections can result in significant translations of the locus of the aerodynamic forces and of the center of gravity of blade sections from the pitch axis of the blade. Translations of the blade section center of mass can significantly affect the contribution of gravity to the pitching moment. Blade motions also affect the polar moment of inertia of the blade and the aerodynamics at each blade section. The combination of these effects has been shown to result in significantly higher pitching moment disturbances with the use of flexible blades than would be found with the stiffer blades.

8.5.3.7 Load Reduction as a Control Goal

Often, load reduction is included as a control goal in variable-speed wind turbines. For example, in addition to controlling the rotor speed and generator torque above rated wind speed, the wind turbine control system may also be designed to damp resonances in the drive train and in the tower.

Controlling Drive Train Torsional Vibrations
In constant-speed wind turbines with induction generators, the generator slip provides a significant amount of damping of drive train oscillations. In variable-speed wind turbines, when the torque of the generator is fixed, there is very little damping in the drive train, which acts like two large masses (the generator and the rotor) on a flexible shaft. The first collective rotor torsional vibration mode may act like an additional inertial mass connected to the hub by a torsional spring. Finally, if the second side-to-side tower vibration mode is excited (which causes angular displacements at the top of the tower), this can add additional rotational oscillations to the system. If left undamped, these can lead to large torque oscillations in the gearbox (Bossanyi, 2003). One approach to controlling drive train torsional vibrations is the use of bandpass filters that effectively add small torque ripples to the drive train of a magnitude and phase that cancel out the vibrations excited by the other turbine dynamics.

Controlling Fore and Aft Tower Vibrations
Changes in blade pitch are intended primarily to control the aerodynamic torque at wind speeds above rated. They also have a significant effect on the rotor thrust, which excites tower

vibrations. Tower vibrations (and therefore translations of the rotor back and forth) affect the relative wind speed seen by the blades and, thereby, the rotor torque. Thus, the effects of control actions feed back into the pitch control system. This feedback path is strong enough that careful controller design is needed to avoid exacerbating tower vibrations or making a pitch control system that is completely unstable (Bossanyi, 2003). One approach to solving this is similar to that mentioned above for solving torsional vibrations, namely the use of a filter tuned to the tower vibration frequency that shifts the phase of any control actions at that frequency and effectively damps the tower vibrations. Another approach uses the signal from a tower accelerometer as an input to the control system and to the tower damping algorithm. Such approaches have been shown to be very effective at damping the excitation of the first tower vibration mode. When implementing this approach, care must be taken to ensure that the two control goals of the pitch control system, control of aerodynamic torque and reduction of loads, do not conflict, thereby degrading the efforts to achieve both goals.

Individual Blade Pitch Control
The control systems described so far assume that the blades are pitched similarly, either collectively or cyclically (as a function of azimuth angle). Control of the pitch of each blade individually allows the turbine to respond to asymmetric loads caused by turbulence across the rotor or soiling of a blade, etc. (for example, see Geyler and Caselitz, 2007; Bossanyi, 2003). It offers additional possibilities for load reduction, but requires more complicated control algorithms, faster processors, and some measure of asymmetrical rotor loads. Loads that might be useful as control inputs are blade root bending moments, shaft bending moments, or yaw bearing moments, but typical strain gauges have not been robust enough for this type of application. Recent advances in optical and solid state strain gauges make individual pitch control more feasible. Some of the most effective approaches to individual pitch control transform the asymmetric loading into a mean load and loads in two orthogonal directions. Fairly simple control algorithms can then be used to determine control actions in this new coordinate system. These are then transformed back into control commands for each of the blade pitch actuators. This approach has been shown to provide significant additional load reduction over collective pitch control.

As wind turbines increase in size, the changes in wind speed and direction across the rotor increase proportionally. Additionally, large wind turbines operate within regions of the upper atmospheric boundary layer where organized, coherent turbulent structures and low-level jets may occur. These conditions may increase fatigue damage significantly (Hand *et al.*, 2006). An example of the use of individual blade pitch actuation for load mitigation due to large, coherent vortices in the atmosphere is described in Hand and Balas (2007). The authors showed that, with adequate sensors and models for the structure of atmospheric vortices, blade root bending moments could be reduced by 30%.

8.5.4 Dynamic Control System Implementation

Dynamic control can be implemented as mechanical systems, as analog electrical circuits, in digital electronic form, or in combinations of these. Mechanical control systems are commonly used only in relatively small wind turbines. Most wind turbines use some combination of analog and digital circuits or only digital circuits. Examples of some of these and related issues are presented below.

8.5.4.1 Mechanical Control Systems

Hardware dynamic control systems use linkages, springs, and weights to actuate system outputs in response to some input. Two examples of hardware control systems are tail vanes to orient wind turbines into the wind and pitch mechanisms that vary blade pitch on the basis of aerodynamic forces or rotor speed. The pitch system that is used on the Bergey Excel is an example of a mechanical control system.

8.5.4.2 Analog Electrical Circuit Control Systems

Analog electrical circuits have also been used and are still used in control system implementation. They are often used as distributed controllers in a larger control network. Once a control algorithm has been developed and tested it can be hardwired into circuit boards that are robust and easy to manufacture. The controllers may operate independently of the supervisory controller, making the supervisory control scheme simpler. One disadvantage of using analog circuits is that changes in the control algorithm can only be made by changing the hardware.

Electrical circuits with the appropriate power amplifiers and actuators can be used to control all controllable parts of a wind turbine. Linear dynamic controllers can be easily implemented with electronic components. For example, the operational amplifier circuit in Figure 8.20 is the hardware realization of a PID controller with a differential equation given in Equation (8.16) (see Nise, 1992):

$$g(t) = -[K_P e(t) + K_D \dot{e}(t) + K_I \int e(t) \mathrm{d}t]$$
$$= -\left[\left(\frac{R_2}{R_1} + \frac{C_1}{C_2} \right) e(t) + (R_2 C_1) \dot{e}(t) + \frac{1}{R_1 C_2} \int e(t) \mathrm{d}t \right] \tag{8.17}$$

where $g(t)$ is the controller output, R and C are the resistances and capacitances of the respective circuit elements, and $e(t)$ is the error signal that is input to the controller.

8.5.4.3 Digital Control Systems

The systems described so far have been analog control systems. Analog control systems respond in a continuous manner to continuous inputs such as forces or voltages. Many modern dynamic control systems are implemented in digital controllers. Digital control systems respond periodically to data that are sampled periodically. They are implemented in digital
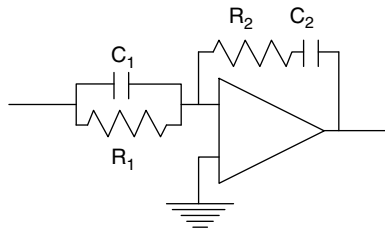

Figure 8.20 Example of proportional–integral–derivative (PID) controller; C, capacitance; R, resistance; 1, 2, circuit elements
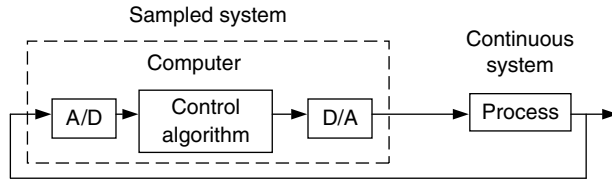
Figure 8.21 Schematic of computer-controlled system; A/D, analog-to-digital converter; D/A, digital-to-analog converter

computers. These digital control systems may include controllers that are distributed around the turbine and that communicate with the supervisory controller in a master–slave configuration or there may only be one central controller that handles many supervisory and dynamic control tasks. Digital control algorithms are relatively easy to upgrade, and systems with centralized processing result in significantly less control hardware and cost than hardwired systems. Digital control systems also allow for easy implementation of nonlinear control approaches. This can result in improved system behavior compared with the same system with a linear controller.

Digital control systems, as illustrated in Figure 8.21, must communicate with analog sensors, actuators, and other digital systems (see Astrom and Wittenmark, (1996)). Thus, the central processing units (CPUs) may need analog-to-digital (A/D) converters to convert analog sensor inputs into digital form or digital-to-analog (D/A) converters to convert digital control commands to analog voltages for amplification for actuators. Depending on the distances that any digital information is being transmitted and the noise immunity desired, different communication standards might be needed.

Digital control systems are not continuous, but rather are sampled. Sampling and the dynamics of the A/D converters give rise to a number of issues specific to digital control systems. The sampling rate, controlled by the system clock, affects (1) the frequency content of processed information, (2) the design of control system components, and (3) system stability.

The effect that sampling has on the frequency content of the processed information can be illustrated by considering a sinusoidal signal, $\sin(\omega t)$ where ω is the frequency of the sinusoid and t is the time. If this signal is sampled at a frequency of ω, then the ith sample is sampled at time

$$t_i = i\frac{2\pi}{\omega} + t_0 \qquad (8.18)$$

for some starting time t_0 and for integer, i. The value of each sample, s_i, is then:

$$s_i = \sin\left[\omega\left(i\frac{2\pi}{\omega} + t_0\right)\right] = \sin(2\pi i + \omega\,t_0) = \sin(\omega\,t_0) \qquad (8.19)$$

But $\sin(\omega t_0)$ is a constant. Thus, sampling the signal at the frequency of the signal yields no information at all about fluctuations at that frequency. In fact, in a system that samples information at a frequency ω, there will be no useful information at frequencies above $\omega_n = \omega/2$, referred to as the Nyquist frequency (see Appendix C). Furthermore, unless the input signal is filtered with a cut-off frequency below ω_n, then the high-frequency information in the signal will distort the desired lower frequency information.

Sampling rate also affects the design of the control system. Digital control system dynamics are a function of the sampling rate. Thus, the sampling rate affects the subsequent control system design and operation, including the determination of the values of constants in the controller and the final system damping ratio, system natural frequency, etc. Because of this, changes in sampling rate can also turn a stable system into an unstable one. Stability can be a complicated issue, but, in general, a closed-loop digital control system will become unstable if the sampling rate is slowed down too much.

Digital control may be implemented in small stand-alone single-board computers or in larger industrial computers. Single-board computers include a central processing unit and often include analog and digital inputs and outputs. They are small enough to be easily housed with other hardware for distributed control systems or as controllers for smaller wind turbines. Larger industrial computers have power supplies and slots for numerous additional communication and processing boards, filters and fans to ensure a clean environment, memory and data storage, and a housing to protect the electronics from environmental damage.

References

Astrom, K. J. and Wittenmark, B. (1996) *Computer Controlled Systems*, 3rd edition. Prentice-Hall, Englewood Cliffs, NJ.

Bergey Wind Power, Inc. (2009) BWC Excel-R Description, http://www.bergey.com/, accessed 4/19/09.

Bianchi, F. D. de Battista, H. and Mantz, R. J. (2007) *Wind Turbine Control Systems*, Springer-Verlag London Limited, London.

Bossanyi, E. A. (2003) Wind Turbine Control for Load Reduction, *Wind Energy*, **6**(3), 229–244.

Bossanyi, E. A. and Jamieson, P. (1999) Blade pitch system modeling for wind turbines. *Proc. of the 1999 European Wind Energy Conference, Nice*, pp. 893–896.

Composite Technology Corp. (2009) *DeWind D8.2 Technical Brochure*. http://www.compositetechcorp.com/DeWind/Dewind_D8-2_A4_small.pdf. Accessed 4/20/09.

De LaSalle, S. A. Reardon, D. Leithead, W. E. and Grimble, M. J. (1990) Review of wind turbine control. *International Journal of Control*, **52**(6), 1295–1310.

Di Steffano, J. J. Stubberud, A. R. and Williams, I. J. (1967) *Theory and Problems of Feedback and Control Systems*. McGraw-Hill, New York.

Ecotécnia, (2007) *Ecotécnia 80 2.0 Características técnicas, 2007, Dossier_80_20_ES.pdf*. Ecotécnia, s.coop.c.l. Barcelona, Spain.

Freris, L. L. (Ed.) (1990) *Wind Energy Conversion Systems*. Prentice Hall International, Hertfordshire, UK.

Gasch, R. (Ed.) (1996) *Windkraftanlagen*. B. G. Teubner, Stuttgart.

Gasch, R. and Twele, J. (2002) *Wind Power Plants*. James and James, London.

Geyler, M. and Caselitz, P. (2007) Individual blade pitch control design for load reduction on large wind turbines, *Scientific Proceedings, 2007 European Wind Energy Conference*, Milan, pp. 82–86.

Grimble, M. J. De LaSalle, S.A. Reardon, D. and Leithead, W. E. (1990) A lay guide to control systems and their application to wind turbines. *Proc. of the 12th British Wind Energy Association Conference*, pp. 69–76, Mechanical Engineering Publications, London.

Hand, M. M. and Balas, M. J. (2007) Blade load mitigation control design for a wind turbine operating in the path of vortices. *Wind Energy*, **10**(4), 339–355.

Hand, M. M. Robinson, M. C. and Balas, M. J. (2006) Wind turbine response to parameter variation of analytic inflow vortices. *Wind Energy*, **9**(3), 267–280.

Hansen, A. D. Bindner, H. and Rebsdorf, A. (1999) Improving transition between power optimization and power limitation of variable speed/variable pitch wind turbines. *Proc. of the 1999 European Wind Energy Conference*, Nice, pp. 889–892.

Hau, E. (2006) *Wind Turbines: Fundamentals, Technologies, Application, Economics*. Springer-Verlag, Berlin.

Heier, S. (Ed.) (1996) *Windkraftanlagen im Netzbetrieb*. B. G. Teubner, Stuttgart.

Horowitz, I. M. (1993) *Quantitative Feedback Design Theory*, Vol. 1. QFT Publications, Boulder, CO.

Johnson, J. J., van Dam, C. P. and Berg, D. E. (2008) *Active Load Control Techniques for Wind Turbines*, Sandia Report SAND2008-4809. Sandia National Laboratories, Albuquerque, NM.

Kuo, B. C. and Golnaraghi, F. (2002) *Automatic Control Systems*, 8th edition. John Wiley & Sons, Inc., New York.

Linders, J. and Thiringer, T. (1993) Control by variable rotor speed of a fixed-pitch wind turbine operating in a wide speed range. *IEEE Transactions on Energy Conversion*, **8**(3), 520–526.

Ljung, L. (1999) *System Identification – Theory for the User*. Prentice-Hall, Upper Saddle River, NJ.

Mayadi, E. A. van Dam, C. P. and Yen-Nakafuji, D. (2005) Computational investigation of finite width microtabs for aerodynamic load control, *Proc. AIAA Conference Wind Energy Symposium,* Reno, NV. AIAA Paper 2005-1185.

Munteanu, I. Bratcu, A. I. Cutululis, N. and Changa, E. (2008) *Optimal Control of Wind Energy Systems*. Springer-Verlag London Limited, London.

Nise, N. S. (1992) *Control System Engineering*. The Benjamin/Cummings Publishing Company, Inc., Redwood City, California.

Nise, N. S. (2004) *Control System Engineering*, 4th edition. John Wiley & Sons, Inc., New York.

Novak, P. Ekelund, T. Jovik, I. and Schmidtbauer, B. (1995) Modeling and control of variable-speed wind-turbine drive-system dynamics. *IEEE Control Systems*, **15**(4), 28–38.

Vestas (2007) *V90-1.8 MW & 2.0 MW, Built on Experience*, ProductbrochureV9018UK.pdf. Vestas Wind Systems A/S, Denmark.

9

Wind Turbine Siting, System Design, and Integration

9.1 General Overview

Wind turbines operate as part of power-producing and consuming systems such as large electrical networks, isolated diesel-powered grid systems, or as stand-alone power for a specific load. The process of integrating wind power into such systems includes decisions about where to install the wind turbines, connection to the power-consuming systems, and turbine operation. Meanwhile, turbine design and operation need to take into consideration the numerous kinds of interactions between turbines and connected systems. This chapter reviews the issues that need to be considered for the completion of a successful project with a special focus on the integration of land-based wind turbines into large grid systems. Issues unique to the integration of offshore turbines and related to integration into isolated grid systems and systems with dedicated loads are covered in Chapter 10.

Wind turbines may be installed as single units or in large arrays known as 'wind farms' or 'wind parks.' The installation of individual wind turbines and wind farms requires a significant amount of planning, coordination, and design work. Mistakes can be very costly. Before wind turbines can be installed and connected to an electrical system, the exact locations for the future turbines need to be determined. A primary consideration is maximizing energy capture, but numerous constraints may limit where turbines can be situated. The material in Section 9.2 focuses on siting issues for wind turbines and wind farms that are to be connected to large electrical grids.

Once locations for the turbines are chosen, the installation and integration of wind turbines into large power grids requires obtaining permits, preparing the site, erecting the turbines, and getting them operational. These topics are covered in Section 9.3.

Significant interactions can occur between wind turbines and with the systems to which they are connected. When multiple wind turbines are located together in close proximity to each

other, the fatigue life and operation of those wind turbines located downwind of other turbines may be affected. These issues are all considered in Section 9.4.

Finally, wind turbines connected to large electrical grids may have both local effects on the grid and, as the fraction of wind-generated energy becomes large, effects on the overall operation and control of the grid. Local and large-scale effects of the integration of wind power into modern grid systems are covered in Section 9.5.

9.2 Wind Turbine Siting

9.2.1 Overview of Wind Turbine Siting Issues

Before wind turbines can be installed, the most appropriate location or locations for them needs to be determined. The major objective of the siting process is to locate a wind turbine (or turbines) such that net revenue is maximized while minimizing such things as noise, environmental and visual impacts, and overall cost of energy. The scope of this process can have a very wide range, which could include everything from wind prospecting for suitable turbine sites over a wide geographical area to considering the placement of a single wind turbine on a site or of multiple wind turbines in a wind farm (this is generally called micrositing). The decision of which areas to consider for siting wind farms and where to place wind turbines within a project is only one aspect of the development process which includes acquiring land rights, applying for permits, obtaining power purchase agreements, financing and public support, procuring turbines, and installation of the wind turbine or wind farm (note, installation and operation is addressed in Section 9.3).

The siting of a single turbine or a large-scale wind system for utility interconnection can be broken down into five major stages (see Hiester and Pennell, 1981; Pennell, 1982; AWEA, 2008a):

1. **Identification of geographic areas needing further study.** Areas with high average wind speeds within the region of interest are identified using a wind resource atlas and any other available wind data. The characteristics of turbine types or designs under consideration are used to establish the minimum useful wind speed for each type.
2. **Selection of candidate sites.** Potential windy sites within the region are identified where the installation of one or more wind turbines appears to be practical from engineering and public acceptance standpoints. If the nature of the terrain in the candidate region is such that there is significant variation within it, then a detailed analysis is required to identify the best areas. At this stage, topographical considerations, ecological observations, and computer modeling may be used to evaluate the wind resource. Geologic, social, and cultural issues are also considered.
3. **Preliminary evaluation of candidate sites.** In this phase, each potential candidate site is ranked according to its economic potential, and the most viable sites are examined for any environmental impact, public acceptance, safety, and operational problems that would adversely affect their suitability as a wind turbine site. Once the best candidate sites are selected, a preliminary measurement program may be required.
4. **Final site evaluation.** For the best remaining candidate sites, a more comprehensive wind resource measurement may be required. At this point, the measurements should include wind shear and turbulence in addition to wind speed and prevailing wind directions.

5. **Micrositing.** Once a site is chosen, or possibly as part of the final site evaluation, the exact locations of the turbines and their energy production need to be determined. This may be able to be done with computer programs that can model the wind field and the various aerodynamic interactions between turbines that affect energy capture (see Section 9.4.2). The more complex the terrain, and the less the available data from nearby sites, the less accurate these models are. A site in complex terrain may require detailed measurements at numerous locations to determine the local wind field for micrositing decisions.

The evaluation of problems that might adversely affect a site's suitability should include:

- **Economic issues** such as cost of access rights, energy production, wake losses, local taxes, substation costs.
- **Topographical issues** such as road access and the slope of the terrain at potential turbine sites.
- **Legal issues** such as ownership of the land, zoning issues and rights of adjacent land owners (for example, to the wind resource), and existing environmental contamination at the site.
- **Permitting issues** such as the number of permits needed, previous rulings of permitting agencies, permitting restrictions, and time frames for completion of permitting procedures.
- **Geological issues** related to the foundation design, ground resistance for lightning protection, and the potential for erosion.
- **Environmental issues** such as the presence of environmentally sensitive areas, bird flyways, and the presence of endangered species.
- **Public acceptance issues** such as visual and noise impacts, distance from residences, public safety, the presence of culturally, historically, or archaeologically important areas, competing land uses, and interference with microwave links and other communication.
- **Safety issues** related to proximity to populated areas or hiking trails.
- **Interconnection issues** such as the proximity of power lines and the voltage and current handling capacities of those power lines.

9.2.2 Estimating the Wind Resource

An estimation of the wind resource at potential project sites is at the heart of the siting process. As the siting process proceeds, knowledge of the wind resource in finer and finer detail is required. Initially, windy areas will need to be identified. For micrositing and the final evaluation of the economics of a project, as much detail as possible of the spatial variability of the wind resource across the site and the temporal variation over longer time scales is desired.

There are a number of possible approaches to determining the wind resource at candidate sites. Each of these has advantages and disadvantages and, thus, might be used at different stages of the siting process, depending on the information needed. These methods include (1) ecological methods, (2) the use of wind atlas data, (3) computer modeling, (4) mesoscale weather modeling, (5) statistical methods, and (6) long-term site-specific data collection. These methods build on the material presented in Chapter 2, which described the meteorological effects that create surface level winds and methods for estimating the exploitable wind resource in a region. Some of the methods presented here can also be used for more general estimates of wind resource.

9.2.2.1 Ecological Methods

Vegetation deformed by high average winds can be used both to estimate the average annual wind speed and to compare candidate sites, even when no wind data are available. These methods are most useful during initial site selection and in geographic areas with very little available wind data. This technique works best in three regions (Wegley *et al.*, 1980): coastal regions, in river valleys and gorges exhibiting strong channeling of the wind, and in mountainous terrain.

Ecological indicators are especially useful in remote mountainous terrain, not only because there is usually little wind data there, but also because the winds are highly variable over small areas and are difficult to characterize. Among the many effects of wind on plant growth, the effects of wind on trees are the most useful for the wind-prospecting phases of siting (Hiester and Pennell, 1981). Trees have two advantages: height and a long lifetime over which to gather evidence. Research work has produced numerous indices relating tree deformation to long-term average wind speeds. Three of the more common ones are the Griggs–Putnam index for conifers, which is explained below, the Barsch index for hardwoods, and the deformation ratio, which applies to both hardwoods and conifers (see Hiester and Pennell, 1981, for more information on these indices).

The Griggs–Putnam index, for example (Putnam, 1948; Wade and Hewson, 1980), applies to conifers and defines eight classes of tree deformation (see Figure 9.1) ranging from no effect
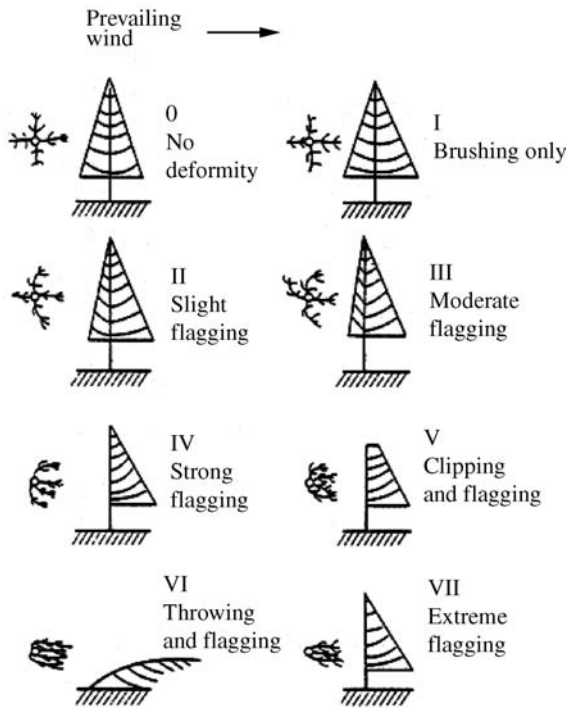
Figure 9.1   The Griggs–Putnam index of wind deformation (Wegley *et al.*, 1980)

Table 9.1 Quantification of the Griggs–Putnam index

Deformation type (Griggs–Putnam index)	Description	Tree height m	Velocity range at tree height, m/s
Brushing (I)	Balsam not flagged	12.2	3.1–4.1
Flagging (II)	Hemlock, white pine and balsam minimally flagged	12.2	3.8–5.2
Flagging (III)	Balsam moderately flagged	9.1	4.7–6.3
Flagging (IV)	Balsam strongly flagged	9.1	5.4–7.4
Clipping (V)	Balsam, spruce and fir held to 1.3 m	1.2	6.3–8.5
Throwing (VI)	Balsam thrown	7.6	7.2–9.7
Carpeting (VIII)	Balsam, spruce and fir held to 0.3 m	0.3	>7.9

(class 0) to the predominance of lateral growth in which the tree takes the form of a shrub (class VII). The Griggs–Putnam index for different types of trees can be related to mean wind speed at the tree top, as shown in Table 9.1.

9.2.2.2 Using Wind Atlas Data

As mentioned in Chapter 2, wind atlas data (or other archived data) may be able to be used to determine local long-term wind conditions. Some of the available atlases are described here.

The *European Wind Atlas* (Troen and Petersen, 1989 and Petersen and Troen, 1986), for example, includes data from 220 sites spread over Europe, including information on the terrain at each site, wind direction distributions, and Weibull parameters for each wind direction. The effects of surface roughness, topography, and nearby obstacles have been removed from the data in order to have data that represent the basic surface flow patterns. The database in the *European Wind Atlas* is often used in conjunction with the WA^{S}P (Wind Atlas Analysis and Application Program) computer program to determine the wind resource at a candidate site. WA^{S}P was developed, as part of the international effort that produced the *European Wind Atlas*, to provide a tool to use the data in the atlas (see Petersen *et al.*, 1988). More details of the WA^{S}P program are provided below.

The methodology for using local data sets to create local or regional wind atlases using the WA^{S}P program has been applied to numerous countries around the world (see http://www.windatlas.dk/index.htm).

Numerous wind atlases have been created using historical upper-level wind data as an input to an atmospheric model to estimate the wind resource near the ground. The model results are adjusted using data from met towers or airports when they are available to ensure that the estimates are as accurate as possible. The results consist of estimates of mean long-term wind speeds at a few heights above the ground. The estimates may also include wind roses and Weibull parameters of the wind speed distribution. The spatial resolution of the data typically varies from 5 km down to 200 m. The accuracy of the estimates depends on the terrain, the map resolution, and the modeling approach but is often on the order of 0.5 m/s. Wind atlas estimates can vary significantly from actual conditions when the elevation, exposure, or surface roughness are substantially different from those assumed in the modeling, such as in areas of
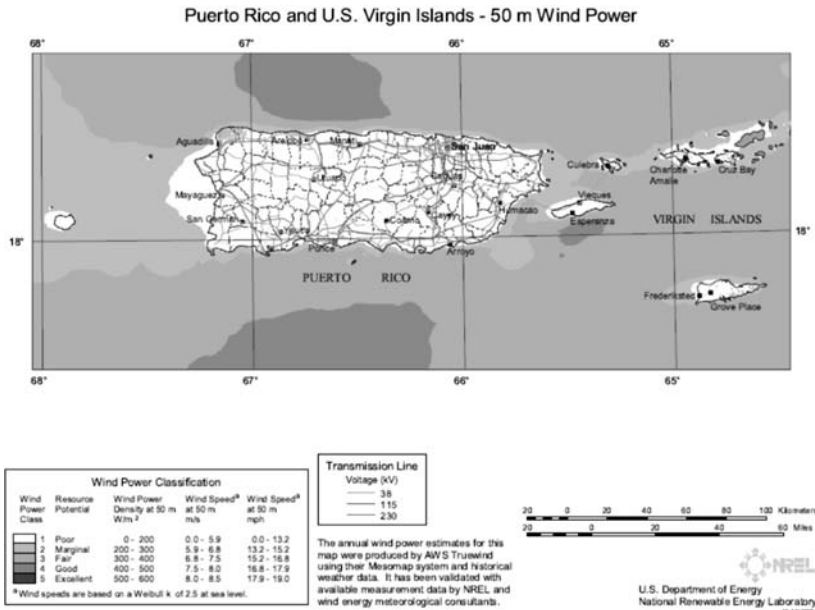
Figure 9.2   Wind map of Puerto Rico (NREL, 2007)

complex terrain. These atlases are usually available in digital form appropriate for geographic information systems (GIS). An example of a map from a wind atlas for mean wind speeds at 50 m for Puerto Rico is shown in Figure 9.2.

9.2.2.3 Computer Modeling Based on Local Data

Computer models may also be used to estimate the local wind field and to optimize turbine layout in a wind farm if local wind data are available. These programs use topographical and surface roughness information in conjunction with nearby wind data. The more nearby data that are available and the smoother the terrain is, the more accurate these predictions are. A number of such programs are commercially available, each with advantages and disadvantages. Computer models using local data provide spatial estimates of wind speeds but are only valid for the time period of the input data sets. It is thus important to make sure that the input data are as representative as possible of the conditions at the site.

   One family of models uses linearized fluid flow equations to estimate wind speeds across a project site or a region given the available tower measurements. One such model is WA^{S}P. WA^{S}P includes the effects of the atmospheric stability, surface roughness, obstacles, and topography at the candidate site in the determination of the site-specific wind conditions. The linearized fluid flow model includes mass and momentum conservation to determine the flow field at the candidate site, based on the nearby reference sites. One advantage of WA^{S}P is that it determines the local wind field using a polar coordinate grid centered on the candidate site. This provides a high resolution around the candidate site, allowing the wind field for a complete wind farm to be predicted. It also can use data from a wind atlas as an input and

works at any height and location. Disadvantages are that the method may give inexact results in complex terrain and that it does not include thermally driven effects such as sea breezes.

Another family of models uses more complex nonlinear computational fluid dynamics models. These models have the potential to capture many more of the features of the flow field in complex terrain but require significantly more computational power and take longer to run. Examples of such programs include WindSim and Meteodyn WT. Calculations are performed in a 3-D grid of cells that spans a region greater than the area of interest and high enough into the atmosphere that the effects of topographic features are captured. To reduce calculation time, calculations are often performed within a coarse grid and the results of those calculations are then used as the starting point for calculations within a finer, smaller grid that is located over the proposed project site. These more complicated models have a variety of parameters that may be adjusted, and experience setting these parameters tends to improve the accuracy of the results.

9.2.2.4 Mesoscale Weather Model Results

Mesoscale weather model results are also available from atmospheric modeling companies. The estimates are similar to those generated for the wind atlases mentioned above but the resolution may be able to be improved with respect to available wind atlases and the developer's local data can be used to remove any bias in the model results. These models use archived upper-level atmospheric data which are extrapolated to ground level to estimate wind speeds at any desired height above the ground. One advantage of these methods is that the archived upper level data may span numerous decades so the results represent estimates of the true long-term wind speeds across a site. Mesoscale atmospheric motions are those with time scales from minutes to days and spatial scales from one to 100 km. While these scales include the passage of weather fronts, land and sea breezes, and even thunderstorms and tornadoes (Lutgens and Tarbuck, 1998), typical model resolutions do not include all of these details. Indeed, as with all fluid flow models, the resolution and accuracy of the topographic data, surface roughness information, and the upper-level input data, the resolution at which the model is run and the resolution for which the equations of fluid flow are appropriate must all be considered when evaluating the accuracy of the results.

9.2.2.5 Statistical Methods

When data from a candidate site and long-term data from a nearby site are available, statistical methods can be used to directly estimate the long-term wind conditions at the measurement site. These methods are generally referred to as Measure–Correlate–Predict (MCP) methods. Many MCP methods are used in the wind industry or have been proposed for this purpose. Some determine a relationship between the concurrent data sets, which is then used with the long-term reference site data to estimate the long-term characteristics at the candidate site. Others determine the relationship between the period of concurrent reference site data and long-term reference site data and apply that to the shorter-term candidate site data in order to obtain, for example, a year of data that is representative of the long-term conditions. MCP methods may be used to estimate wind direction as well as wind speed characteristics. Finally, the data may be analyzed separately by month or by wind direction sector to improve the estimates of long-term wind characteristics.

Data sets used as long-term references include data from airports, weather balloon data, archived upper-level atmospheric data (reanalysis data), and data from meteorological towers. These towers have often been installed by government agencies to support the wind industry. When using these data sets, the quality of the data needs to be carefully evaluated.

The main difference between the various MCP methods is the form of the functional relationship that is used to relate the wind speeds and directions of the long-term data set to those of the short-term data set. This relationship may be a simple ratio, a linear relationship, or a more complicated nonlinear or probabilistic relationship. Linear wind speed relationships that have been used include linear regression (see Derrick, 1993; Landberg and Mortensen, 1993; Joensen *et al.*, 1999) and the 'variance' method (Rogers *et al.*, 2005). Probabilistic algorithms have been proposed by Mortimer 1994 and García-Rojo (2004). These references also mention additional approaches. Two of these approaches will be highlighted here.

The variance method determines a linear relationship between hourly (or ten-minute) wind speed averages of the reference site and candidate site data sets. This relationship is used to estimate the wind speeds at the candidate site, $\hat{u}_c$ (the caret indicates an estimated value), when the wind speed at the reference site is u_r:

$$\hat{u}_c = au_r + b \tag{9.1}$$

In this relationship the slope, b, is the ratio of the standard deviations of the hourly averages at the candidate site, σ_c, and reference site, σ_r, during the concurrent data period:

$$b = \left(\frac{\sigma_c}{\sigma_r}\right) \tag{9.2}$$

The offset, a, is a function of the mean wind speeds at the concurrent reference site, μ_r, and the candidate site, μ_c, as well as of the standard deviations:

$$a = \left(\mu_c - \left(\frac{\sigma_c}{\sigma_r}\right)\mu_r\right) \tag{9.3}$$

Equation (9.1) is then used with all of the hourly averages of the reference site data set to estimate the long-term wind speeds at the candidate site. These estimated wind speeds are then used to determine the statistics of the long-term wind speeds at the candidate site.

The slope and offset in this model have been chosen to ensure that the mean and the variance of the estimated long-term wind speeds during the period of concurrent data are the same as those of the measured values. This ensures that not only the mean wind speed but also the wind speed distribution is correctly modeled. The variance method has been shown to correctly predict the statistics of long-term wind speeds at a variety of sites (see Rogers *et al.*, 2005).

Joint probability distributions can also be used to map the relationship between the reference site wind speeds and directions and the candidate site values. For example, the probability that the wind speed, u_c, and direction, θ_c, at the candidate site have specific values, $P(u_c, \theta_c)$, when the wind speed and direction at the reference site have values u_r and θ_r is $P(u_c, \theta_c | u_r, \theta_r)$. $P(u_c, \theta_c | u_r, \theta_r)$ can be determined from the concurrent data at each site. Then, the long-term probability distribution of the wind speeds and directions at the candidate site, $\hat{P}(u_c, \theta_c)$, can be estimated by summing up all of the probabilities of occurrences of u_c, θ_c for all occurrences of u_r, θ_r in the long-term reference site data set. The advantage of this method is that it directly

provides estimates of both long-term wind speed and long-term direction distributions at the candidate site. On the other hand, it does not provide estimates of the temporal characteristics of the winds at the site. These may be needed, for example, for studies of time-of-day pricing of the electricity generated by wind turbines at the candidate site.

The accuracy of an MCP method depends on a variety of factors. First, it assumes that the long-term reference data and candidate data are accurate. Errors in these data sets will obviously result in erroneous predictions. Second, the longer the data set at the candidate site, the more accurately the results will represent long-term trends. In any case, the data collection at the candidate site should include representative data from all wind speeds and directions. Third, the reference site data should be representative of the climate at the candidate site. The relationship between the two data sets may be affected by diurnal effects, time delays between weather patterns arriving at the two sites, unique weather patterns, the distance between the two sites, and stability differences or topographic effects that create unique flow patterns at one site or the other. Finally, unknown stochastic or systematic changes in the relationship between the two sites at time scales greater than the period of concurrent data may introduce additional uncertainty into the final result. In any case, the results are also only good for the height of the measurements and for the specific mast location at the candidate site. More detailed modeling may still be necessary to define the specific flow patterns at candidate sites if the terrain is such that the predictions cannot be applied to nearby proposed turbine locations.

9.2.2.6 Site-specific Data Collection

The best way to determine the long-term wind resource at a site is by measuring the winds at the exact location(s) of interest. These measurements should include wind speed and direction, wind shear, turbulence intensity, and temperature (for determining air density and the potential for icing). Long-term site-specific measurements are the ideal approach to determining the wind resource, but the most costly and time consuming. See Chapter 2 for more information on resource measurement.

9.2.3 Micrositing

Micrositing is the use of resource assessment tools to determine the exact position of one or more wind turbines on a parcel of land to maximize net revenues. There are numerous computer codes available for micrositing of wind turbines. Wind farm design and analysis codes used for micrositing use wind data for the potential site, turbine data, and information on the site constraints to determine an optimum layout for the wind turbines on the site. Site constraints include turbine exclusion areas (for example, due to geological or environmental concerns), noise limits at points adjacent to the wind farm, etc. Site information is usually provided using digital contour maps. The outputs of these programs include turbine locations, noise contours and contours of energy capture predictions, energy yield estimates for individual turbines and the overall site, and related economic calculations. Some wind farm optimization codes also determine the visibility of the wind farm from nearby locations and can optimize the wind farm layout to minimize visual impact in addition to maximizing energy capture and minimizing noise.

9.3 Installation and Operation Issues

The installation of a wind power project is a complex process involving a number of steps and legal and technical issues. The process starts with securing legal rights and permit approvals. Once permits are obtained, the site needs to be prepared and the turbine transported to the site and erected. Only after the turbine is connected to the grid and commissioned does regular operation commence. At this point the owner is responsible for oversight of the turbine, safe operation, and maintenance. The project owner might be an individual or company, a utility, a local government, or a developer.

9.3.1 Predevelopment Work and Permitting

The first steps in the development process include securing legal rights to land (if the land is not already owned by the project owner) and access to power lines, starting to line up power purchase agreements (if the power is not to be used on-site), and obtaining permits. It may also include finding investors. Most of these legal and financial aspects of the development process are beyond the scope of this text, but the permitting process involves significant engineering issues and is addressed here.

The permitting process varies greatly from country to country, state to state, and even from town to town. It is intended to ensure that land is used appropriately, and that operation of the installed wind turbine or wind farm will be safe and environmentally benign. Generally, permits that must be obtained may include those related to: building construction, noise emission, land use, grid connection, environmental issues (birds, soil erosion, water quality, waste disposal, and wetland issues), public safety, occupational safety, and/or valuable cultural or archaeological sites. More information on environmental issues is included in Chapter 12. In the permit approval process the technical certification of the turbine may also be important. Wind power professionals in many countries have published information on issues to be considered in the permitting process. For example, more information on the permitting process in the United States can be found in *Permitting of Wind Energy Facilities, A Handbook* (NWCC, 2002) and in *Wind Energy Siting Handbook* (AWEA, 2008a).

9.3.2 Site Preparation

Once permits have been obtained, the site needs to be prepared for turbine installation and operation. Roads may need to be built; the site needs to be cleared for delivery, assembly, and erection of turbines; power lines need to be installed and foundations need to be built. The extent and difficulty of the site preparation will depend on the site location, proximity to power lines, and the turbine design and site terrain. Turbine foundation design (see Chapter 6) needs to be site and turbine specific. Expected turbine loading, tower design, and soil properties (sand, bedrock, etc.) will affect the type and size of foundation needed. Road design will also depend heavily on the size and weight of the loads to be transported, the terrain, local weather conditions, soil properties, and any environmental restrictions. Obviously, rugged terrain can make all aspects of site preparation difficult and costly.

9.3.3 Turbine Transportation

The next significant hurdle may be transportation of the wind turbines to the site. Smaller turbines can often be packed in containers for easy transport over roads. Larger turbines must be transported in subsections and assembled at the site. In remote locations, difficult access may limit the feasible turbine size or design or may require expensive transportation methods such as helicopters or special purpose vehicles.

9.3.4 Turbine Assembly and Erection

Once at the site, the turbine must be assembled and erected. Issues related to assembly and erection need to be considered during the design phase (see Chapter 7) to minimize installation costs. Ease of erection depends on the turbine size and weight, the availability of an appropriately sized crane, the turbine design, and site access. Small to medium-sized turbines can usually be assembled on site with a crane. Some can even be assembled on the ground and the whole tower and turbine placed on the foundation with a crane. Where site access is difficult or cranes are not available, such as in developing countries, it may be advantageous to use a turbine with a tilt-up tower. The complete turbine and tower are assembled on the ground and hydraulic pistons or winches are used to raise the tower about a hinge. This erection method can make maintenance easy, as the turbine can be lowered to the ground for easy access. The erection of large wind turbines can present a significant technical challenge. The tower sections, blades, and the nacelle can each be very heavy and large. For example, the tower, nacelle, and blade weights of one 3 MW turbine are 156, 88, and 6.6 metric tonnes respectively. Very large cranes are often needed. Turbines have also been designed with telescoping towers for easier tower erection, or with lifting devices integral to the tower. The tower then acts not only as the support for the turbine, but also as the crane for placement of the tower top on the tower.

9.3.5 Grid Connection

The turbine–grid connection consists of electrical conductors, transformers, and switchgear to enable connection and disconnection. All of this equipment must be thermally rated to handle the expected current and the electrical conductors must be sized large enough to minimize voltage drops between the turbine and the point of connection (POC) to the electrical grid (see Figure 9.3). The POC is a commonly used term to denote the grid connection at the wind turbine owner's property boundary. Another frequently used term is the point of common coupling, PCC. The PCC is the closest point in the grid system at which other users are connected to the grid. Details of the turbine–grid connection are presented in Section 9.5. Once the turbine is installed and connected to the grid, it is ready for operation.

9.3.6 Commissioning

Wind turbines need to be 'commissioned' before the turbine owner takes control of the turbine operation. Commissioning consists of (1) appropriate tests to ensure correct turbine operation and (2) maintenance and operation training for the turbine owner or operator. The extent of the
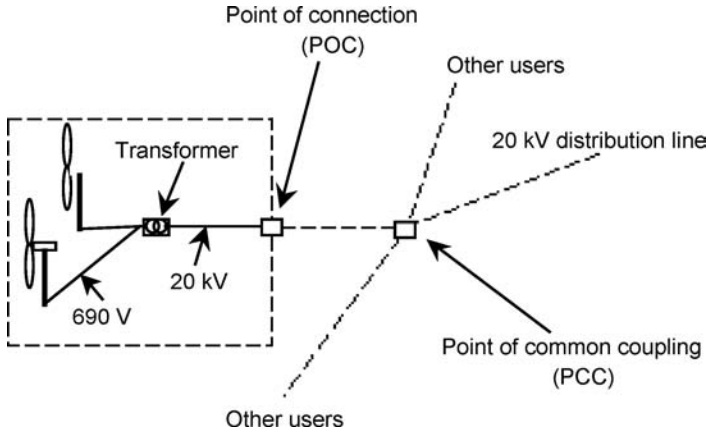
Figure 9.3   Schematic of typical grid connection (with voltages used in Europe)

commissioning process depends on the technical complexity of the turbine and the degree to which the design has been proven in previous installations. For mature turbine designs, commissioning consists of tests of the lubrication, electrical, and braking systems, operator training, confirmation of the power curve, and tests of turbine operation and control in a variety of wind speeds. Commissioning of (one-of-a-kind) research or prototype turbines includes numerous tests of the various subsystems while the turbine is standing still (lubrication and electrical systems, pitch mechanisms, yaw drives, brakes, etc.) before any tests with the operating turbine are performed.

9.3.7 Turbine Operation

Successful operation of a turbine or wind farm requires (1) information systems to monitor turbine performance, (2) understanding of factors that reduce turbine performance, and (3) measures to maximize turbine productivity.

Automatic turbine operation requires a system for oversight in order to provide operating information to the turbine owner and maintenance personnel. Many individual turbines and turbines in wind farms have the capability to communicate with remote oversight systems via phone connections. Remote oversight (SCADA) systems (as explained in Chapter 8) receive data from individual turbines and display it on computer screens for system operators. These data can be used to evaluate turbine energy capture and availability (the percentage of time that a wind turbine is available for power production).

The availability of wind turbines with mature designs is typically between 94% and 97% but may be below 90% (Johnson, 2008). Reduced availability is caused by scheduled and unscheduled maintenance and repair periods, power system outages, and control system faults. For example, the inability of control systems to properly follow rapid changes in wind conditions, imbalance due to blade icing, or momentary high component temperatures can cause the controller to stop the turbine. The controller usually clears these fault conditions and operation is resumed. Repeated tripping usually causes the controller to take the turbine offline

until a technician can determine the cause of anomalous sensor readings. This results in decreased turbine availability.

Wind turbine manufacturers provide power curves representing turbine power output as a function of wind speed (see Chapters 1 and 7). A number of factors may reduce the energy capture of a turbine or wind farm from that expected, based on the published power curve and the wind resource at the site. These include (Baker, 1999) reduced availability, poor aerodynamic performance due to soiled blades and blade ice, lower power due to yaw error, control actions in response to wind conditions, and interactions between turbines in wind farms (see Section 9.4). Soiled blades have been observed to degrade aerodynamic performance by as much as 10–15%. Airfoils that are sensitive to dirt accumulation require either frequent cleaning or replacement with airfoils whose performance is less susceptible to degradation by the accumulation of dirt and insects. Blade ice accumulation can, similarly, degrade aerodynamic performance. Energy capture is also reduced when the wind direction changes. Controllers on some upwind turbine designs might wait until the magnitude of the average yaw error is above a predetermined value before adjusting the turbine orientation, resulting in periods of operation at high yaw errors. This results in lower energy capture. Turbulent winds can also cause a number of types of trips. For example, in turbulent winds, sudden high yaw errors might cause the system to shut down and restart, also reducing energy capture. In high winds, gusts can cause the turbine to shut down for protection when the mean wind speed is still well within the turbine operating range. These problems may reduce energy capture by as much as 15% of projected values. Operators should not only be prepared to minimize these problems, but should also anticipate them in their financing and planning evaluations.

9.3.8 Maintenance and Repair

Wind turbine components require regular maintenance and inspection to make sure that lubrication oil is clean, seals are functioning, and that components subject to normal wear processes are replaced. Problem conditions identified by oversight systems may require that the turbine be taken out of operation for repairs.

9.3.9 Safety Issues

Finally, the installed wind turbine needs to provide a safe work environment for operating and maintenance personnel. The turbine also needs to be designed and operated in a manner that it is not a hazard for neighbors. Safety issues include such things as protection against contact with high voltage electricity, protection against lightning damage to personnel or the turbine, protection from the effects of ice build-up on the turbine or the shedding of ice, the provision of safe tower-climbing equipment, and lights to warn local night time air traffic of the existence of the wind turbine. Maintenance and repairs may be performed by on-site personnel or turbine maintenance contractors.

9.4 Wind Farms

Wind farms or wind parks, as they are sometimes called, are locally concentrated groups of wind turbines that are electrically and commercially tied together. There are many advantages

to this electrical and commercial structure. Profitable wind resources are limited to distinct geographical areas. The introduction of multiple turbines into these areas increases the total wind energy produced. From an economic point of view, the concentration of repair and maintenance equipment and spare parts reduces costs. In wind farms of more than about 10 or 20 turbines, dedicated maintenance personnel can be hired, resulting in reduced labor costs per turbine and financial savings to wind turbine owners.

Wind farms were developed first in the United States in the late 1970 s and then in Europe. Recently, wind farms have been developed in many other places around the world, most notably in India, but also in China, Japan, and South and Central America.

The oldest existing concentration of wind farms in the United States is in California. The California wind farms, discussed in Chapter 1, originated as a result of a number of economic factors, including tax incentives and the high cost of new conventional generation. These factors spurred a significant boom in wind turbine installation activity in California. The boom started in the late 1970 s and then leveled off after 1984 when economic forces changed. The result has been the development of three main areas of California: (1) Altamont Pass, east of San Francisco, (2) the Tehachapi mountains, and (3) San Gorgonio Pass in southern California (see Figure 9.4). Many of these first wind turbines suffered from reliability problems, but in recent years older turbines have been replaced with larger, more reliable, turbines in what is known as 'repowering' of the wind farms. In the 1990 s, wind farms were also developed in the Midwest region of the United States. Since about 2000, development has continued at an exponential pace in the United States, with significant installations in the upper Midwest, Texas, and the state of Washington. As of the end of 2008, the United States had over 21 GW of installed wind power capacity, almost all of it in wind farms (AWEA, 2008b).

Figure 9.4 A wind farm in San Gorgonio Pass, Palm Springs, California (Reproduced by permission of Henry Dupont)

Wind farms in Europe started in the late 1980 s in Denmark. In recent years, the number of wind turbines installed in Europe has increased tremendously as individual wind turbines and wind farms have been developed, primarily in Denmark, Germany, Spain, the Netherlands, and Great Britain. Many of these wind turbines are in coastal areas. As available land for wind power development has become more limited in Europe, smaller installations have been built on inland mountains and in offshore wind parks, primarily in the North Sea. As of the end of 2007, Europe had over 57 GW of installed wind power capacity, most of it in wind farms (EWEA, 2008).

Wind farms are also being installed around the world. The growth of wind farms in India and China has been especially rapid. As of 2008, India had over 9 GW and China had over 12 GW of installed wind power, primarily in wind farms (WWEA, 2008).

9.4.1 Wind Farm Infrastructure

In addition to the individual wind turbines and their switchgear, wind farms have their own electrical distribution system, roads, data collection systems, and support personnel.

9.4.1.1 Electrical Collection System

The electrical collection systems in wind farms typically operate at higher voltages than the turbine generator voltage in order to decrease resistive losses on the way to the substation at the grid connection. They also have switchgear for the whole wind farm at the connection to the grid. The voltage levels of the wind farm collection system depend on the distances between turbines and transformer and cable costs. Many modern wind turbines come with a transformer installed in the tower base, but groups of lower voltage wind turbines in close proximity could share one transformer for cost reduction. Cost is also an issue when decisions are made as to whether the wind farm collection system should be overhead or underground. Underground lines, used in Europe and often in the United States, are more expensive, especially in rough terrain. Overhead lines are often used in India.

9.4.1.2 Roads

Access roads between wind turbines and maintenance and connecting roads to main highways may represent a significant cost, especially in environmentally sensitive areas with rough terrain. Roads need to be constructed in a manner that disturbs the landscape as little as possible, and that does not result in erosion. Grades and curves should be gentle enough that heavy equipment can reach the turbine sites. The lengths of the blades or tower sections are important considerations in this regard.

9.4.1.3 Control, Monitoring, and Data Collection Systems

Modern wind farms include systems for controlling individual turbines and displaying and reporting information on wind farm operation. These systems, introduced in Chapter 8, are called SCADA (supervisory control and data acquisition) systems. SCADA systems display operating information on computer screens. Information about the whole wind farm, sets of

turbines, or one individual turbine can be displayed. The information typically includes turbine operating states, power level, total energy production, wind speed and direction, and maintenance and repair notes. SCADA systems also display power curves or graphs of other information and allow system operators to shut down and reset turbines. Newer SCADA systems connected to modern turbines may also display oil temperatures, rotor speed, pitch angle, etc. SCADA systems also provide reports on turbine and wind farm operation to system operators, including information on operation and revenue from each turbine based on turbine energy production and utility rate schedules.

9.4.1.4 Support Personnel

Once a certain number of turbines are placed in a wind farm, it becomes economical to provide dedicated operating and maintenance staff, sometimes called 'windsmiths.' The staff needs to be appropriately trained and provided with suitable facilities.

9.4.2 Wind Farm Technical Issues

Numerous technical issues arise with the close spacing of multiple wind turbines. The most important are related to the question of where to locate and how closely to space the wind turbines (common terms for referring to wind turbine array spacing are illustrated in Figure 9.5). As mentioned in Section 9.2, the wind resource may vary across a wind farm as a result of terrain effects. In addition, the extraction of energy by those wind turbines that are upwind of other turbines results in lower wind speeds at the downwind turbines and increased turbulence. As described in this section, these wake effects can decrease energy production and increase wake-induced fatigue in turbines downwind of other machines. Wind turbine spacing also affects fluctuations in the output power of a wind farm. As described in Section 9.5, the fluctuating power from a wind farm may affect the local electrical grid to which it is attached. This section describes the relationship between wind farm output power fluctuations and the spacing of the turbines in a wind farm.
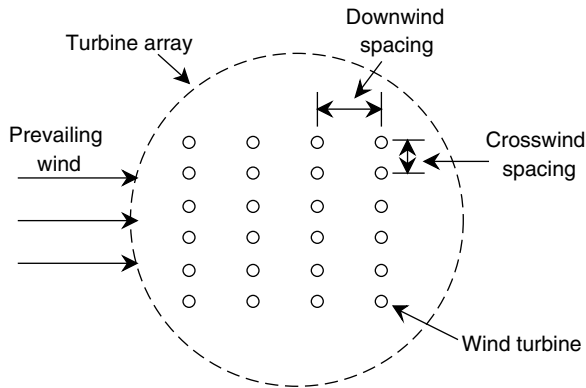
Figure 9.5   Wind farm array schematic

9.4.2.1 Array Losses

Wind energy comes from the conversion of kinetic energy in the wind. This results in lower wind speeds behind a wind turbine and less energy capture by the downstream turbines in an array. Thus, a wind farm will not produce 100% of the energy that a similar number of isolated turbines would produce in the same prevailing wind. The energy loss is termed 'array loss.' Array losses are mainly functions of:

- wind turbine spacing (both downwind and crosswind);
- wind turbine operating characteristics;
- the number of turbines and size of the wind farm;
- turbulence intensity;
- frequency distribution of the wind direction (the wind rose).

The extraction of energy from the wind results in an energy and velocity deficit, compared with the prevailing wind, in the wake of a wind turbine. The energy loss in the turbine wake will be replenished over a certain distance by exchange of kinetic energy with the surrounding wind field. The extent of the wake in terms of its length as well as its width depends primarily on the rotor size and power production.

Array losses can be reduced by optimizing the geometry of the wind farm. Different distributions of turbine sizes, the overall shape and size of the wind farm turbine distribution, and turbine spacing within the wind farm all affect the degree to which wake effects reduce energy capture.

The momentum and energy exchange between the turbine wake and the prevailing wind is accelerated when there is higher turbulence in the wind field. This reduces the velocity deficits downstream, and so reduces array losses. Typical turbulence intensities are between 10% and 15%, but may be a low as 5% over water or as high as 50% in rough terrain. Turbulence intensity also increases through the wind farm due to the interaction of the wind with the turning rotors.

Finally, array losses are also a function of the annual wind direction frequency distribution. The crosswind and downwind distances between wind turbines will vary depending on the geometry of the wind turbine locations and the direction of the wind. Thus, array losses need to be calculated based on representative annual wind direction data in addition to wind speed and turbulence data.

The geometry of turbine placement and ambient turbulence intensity have been shown to be the most important parameters affecting array losses. Studies have shown that, for turbines that are spaced 8 to 10 rotor diameters, D, apart in the prevailing downwind direction and five rotor diameters apart in the crosswind direction, array losses are typically less than 10% (Lissaman *et al.*, 1982). Figure 9.6 illustrates array losses for a hypothetical 6 x 6 array of turbines with a downwind spacing of ten rotor diameters. The graph presents array losses as a function of crosswind spacing and turbulence intensity. Results are shown for conditions when the wind is only parallel to turbine rows (turbines directly in the wake of other turbines) and when wind is evenly distributed from all directions.

Array losses may also be expressed as array efficiencies where:

$$\text{Array efficiency} = \frac{\text{Annual energy of whole array}}{(\text{Annual energy of one isolated turbine})(\text{total no. of turbines})} \quad (9.4)$$
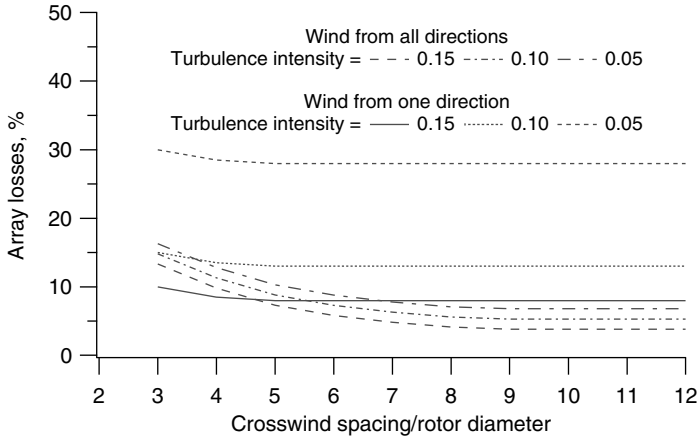
Figure 9.6 Wind farm array losses (after Lissaman *et al.*, 1982). Reproduced by permission of BHR Group Limited

It can be seen that array efficiency is just 100% minus the array losses in percent.

The design of a wind farm requires careful consideration of these effects in order to maximize energy capture. Closer spacing of wind turbines may allow more wind turbines on the site, but will reduce the average energy capture from each turbine in the wind farm.

9.4.2.2 The Calculation of Array Losses – Wake Models

The calculation of array losses requires knowledge of the location and characteristics of the turbines in the wind farm, knowledge of the wind regime, and appropriate models of turbine wakes to determine the effect of upstream turbines on downstream ones. A number of turbine wake models have been proposed. These fall into the following categories:

- surface roughness models;
- semi-empirical models;
- eddy viscosity models;
- full Navier–Stokes solutions.

The surface roughness models are based on data from wind tunnel tests. The first models to attempt to characterize array losses were of this type. A review by Bossanyi *et al.* (1980) describes a number of these models and compares their results. These models assume a logarithmic wind velocity profile upstream of the wind farm. They characterize the effect of the wind farm as a change in surface roughness that results in a modified velocity profile within the wind farm. This modified velocity profile, when used to calculate turbine output, results in appropriately lower power output for the total wind farm. These models are usually based on regular arrays of turbines in flat terrain.

The semi-empirical models provide descriptions of the energy loss in the wake of individual turbines. Examples include models by Lissaman (Lissaman and Bates, 1977), Vermeulen

(Vermeulen, 1980), and Katić (Katić *et al.*, 1986). These models are based on simplified assumptions about turbine wakes (based on observations) and on conservation of momentum. They may include empirical constants derived from either wind tunnel model data or from field tests of wind turbines. They are useful for describing the important aspects of the energy loss in turbine wakes, and, therefore, for modeling wind farm array losses.

Eddy viscosity models are based on solutions to simplified Navier–Stokes equations. The Navier–Stokes equations are the defining equations for the conservation of momentum of a fluid with constant viscosity and density. They are a set of differential equations in three dimensions. The use of the Navier–Stokes equations to describe time-averaged turbulent flow results in terms that characterize the turbulent shear stresses. These stresses can be related to flow conditions using the concept of eddy viscosity. Eddy viscosity models use simplifying assumptions such as axial symmetry and analytical models to determine the appropriate eddy viscosity. These models provide fairly accurate descriptions of the velocity profiles in turbine wakes without a significant computational effort and are also used in array loss calculations. Examples include the model of Ainslie (1985 and 1986) and that of Smith and Taylor (1991).

Figures 9.7 and 9.8 illustrate measured wind speed data behind wind turbines. The graphs also include the results of one of these eddy viscosity wake models. Figure 9.7 shows non-dimensionalized vertical velocity profiles at various distances (measured in rotor diameters) behind a wind turbine. The velocity deficit and its dissipation downwind of the turbine are clearly illustrated. Figure 9.8 illustrates the hub height velocity profiles as a function of distance from the rotor axis for the same conditions. The Gaussian shape of the hub height velocity deficit in the far wake can clearly be seen.
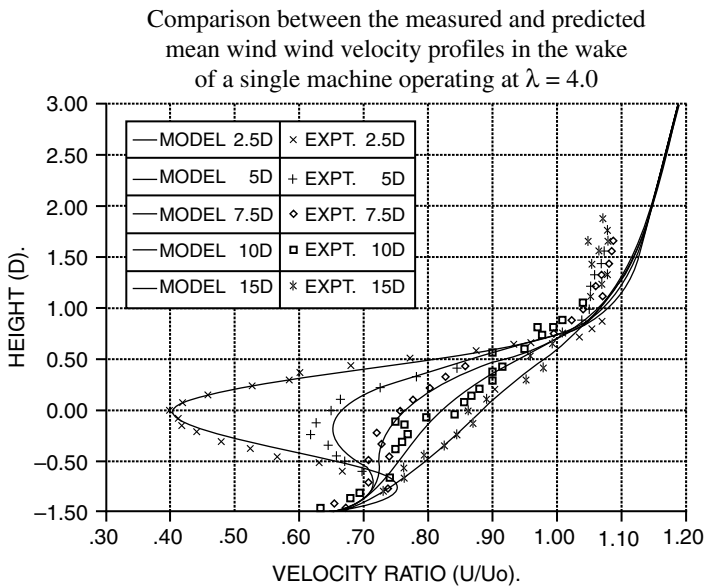
Figure 9.7 Vertical velocity profiles downwind of a wind turbine (Smith and Taylor, 1991); λ, tip speed ratio, U_0, free stream wind speed, D, height with respect to turbine rotor centerline. Reproduced by permission of Professional Engineering Publishing
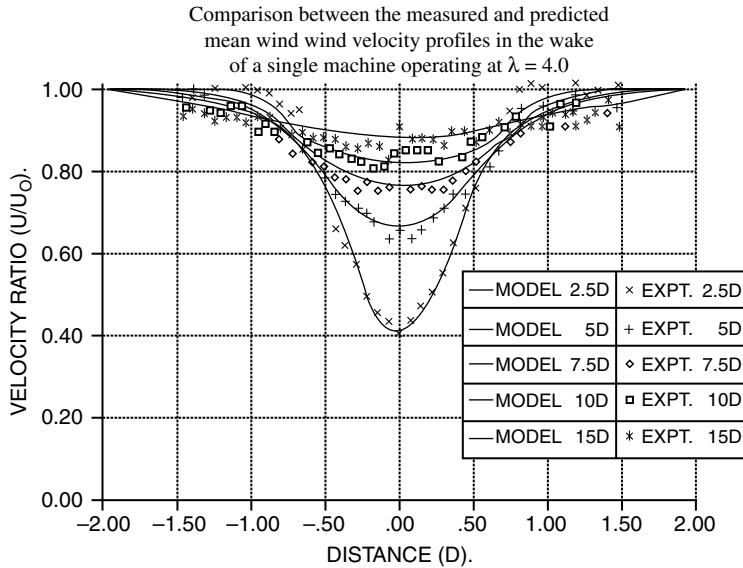
Figure 9.8 Hub height velocity profiles downwind of a wind turbine (Smith and Taylor, 1991); λ, tip speed ratio. Reproduced by permission of Professional Engineering Publishing

Finally, a variety of approaches exist to solving the complete set of Navier–Stokes equations. These models require a significant computational effort and may use additional models to describe the transport and dissipation of turbulent kinetic energy (the k–ε model) to converge to a solution. These models are best suited for research, for detailed descriptions of wake behavior, and to guide the development of simpler models. Examples include models by Crespo *et al.* (Crespo *et al.*, 1985; Crespo and Herandez, 1986; Crespo *et al.*, 1990; Crespo and Herandez, 1993), Voutsinas *et al.* (1993), and Sørensen and Shen (1999).

A number of factors affect the accuracy of the results of applying these models to specific wind farms. When used to calculate wind farm power production, decisions must be made about how to handle the superposition of multiple wakes and the effects of complex terrain on both wake decay and ambient wind speed. A number of the models mentioned above address some of these issues. Typically, multiple wakes are combined based on the combination of the energy in the wakes, although some models assume linear superposition of velocities. The effects of complex terrain may be significant (see Smith and Taylor, 1991) but are more difficult to address and are often ignored.

The use of these models can be illustrated by considering one of the semi-empirical models (Katić *et al.*, 1986) that is often used for micrositing and wind farm output predictions. The model attempts to characterize the energy content in the flow field and ignores the details of the exact nature of the flow field. As seen in Figure 9.9, the flow field is assumed to consist of an expanding wake with a uniform velocity deficit that decreases with distance downstream. The initial free stream velocity is U_0 and the turbine diameter is D. The velocity in the wake at a distance X downstream of the rotor is U_X with a diameter of D_X. The wake decay constant, k, determines the rate at which the wake diameter increases in the downstream direction.
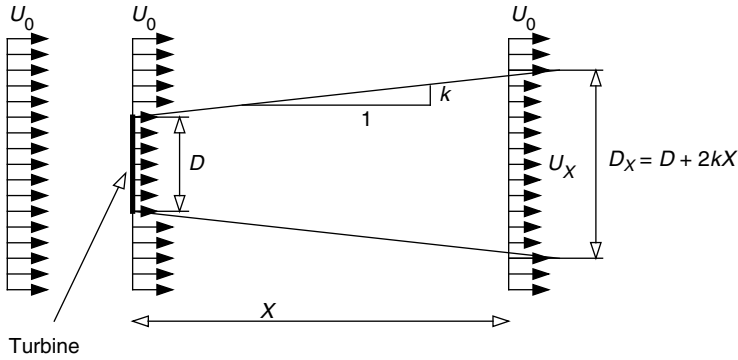
Figure 9.9 Schematic view of wake description (after Katić *et al.*, 1986); U_0, initial free stream velocity; D, turbine diameter; U_X, velocity at a distance X; D_X, wake diameter at a distance X; k, wake decay constant

In this and many other semi-empirical models, the initial non-dimensional velocity deficit (the axial induction factor), a, is assumed to be a function of the turbine thrust coefficient:

$$a = \tfrac{1}{2}(1 - \sqrt{1 - C_T}) \tag{9.5}$$

where C_T is the turbine thrust coefficient. Equation (9.5) can be derived from Equations (3.16) and (3.17) for the ideal Betz model. Assuming conservation of momentum, one can derive the following expression for the velocity deficit at a distance X downstream:

$$1 - \frac{U_X}{U_0} = \frac{(1 - \sqrt{1 - C_T})}{\left(1 + 2k\frac{X}{D}\right)^2} \tag{9.6}$$

The model assumes that the kinetic energy deficit of interacting wakes is equal to the sum of the energy deficits of the individual wakes (indicated by subscripts 1 and 2). Thus, the velocity deficit at the intersection of two wakes is:

$$\left(1 - \frac{U_X}{U_0}\right)^2 = \left(1 - \frac{U_{X,1}}{U_0}\right)^2 + \left(1 - \frac{U_{X,2}}{U_0}\right)^2 \tag{9.7}$$

The only empirical constant in the model is the wake decay constant, k, which is a function of numerous factors, including the ambient turbulence intensity, turbine-induced turbulence, and atmospheric stability. Katić notes that in a case in which one turbine was upstream of another, $k = 0.075$ adequately modeled the upstream turbine, but $k = 0.11$ was needed for the downstream turbine, which was experiencing more turbulence. He notes also that the results for a complete wind farm with wind coming from multiple directions are relatively insensitive to minor changes in the value of k. A small constant gives a large power reduction in a narrow zone, while a large value gives a smaller reduction in a wider zone. The net effect of varying this parameter, when analyzing wind farm performance at many wind speeds from a variety of directions, is small.

The following steps are used to determine the output of a wind farm using the model:

1. The wind turbine radius, hub heights, power, and thrust characteristics are determined.
2. The wind turbine locations are determined such that the coordinate system can be rotated for analysis of different wind directions.
3. The site wind data are binned by wind direction with, for example, 45 degree wide bins. Weibull parameters are determined for each bin together with the frequency of the wind occurring from each sector.
4. The annual average wind power is calculated by stepping through all wind speeds and directions. Thrust coefficients are determined from the operating conditions at each turbine.

9.4.2.3 Wake Turbulence

The turbines in wind farms that are downwind of other machines experience increased turbulence due to power production upwind. Turbine wakes consist not only of regions of lower average velocity, but of swirling vortices caused by (1) interaction of the wind over the rotor with the rotor surfaces and (2) differential flow patterns over the upper and lower blade surfaces at the rotor tips. In general, the turbulence intensities in the wake are increased over ambient levels, with an annular area in the far wake of higher relative turbulence (caused by the tip vortices) surrounding the turbulent core of the wake. Figure 9.10 shows measured and predicted turbulence intensities at a variety of rotor distances downstream of a turbine rotor in a wind field with an ambient turbulent intensity of 0.08. The resulting turbulence increases material fatigue, reducing turbine life, in the turbines in a wind farm that are downwind of other
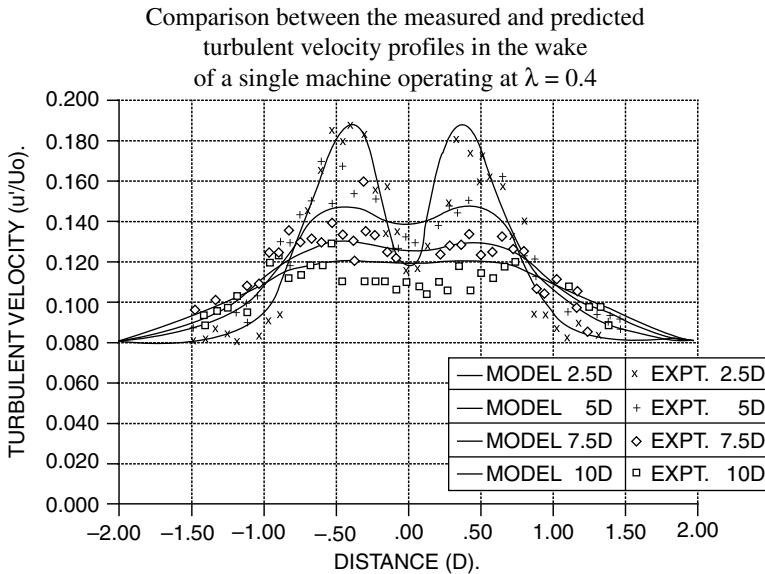
Figure 9.10   Turbulence intensity downwind of a wind turbine (Smith and Taylor, 1991); λ, tip speed ratio. Reproduced by permission of Professional Engineering Publishing

machines (for more details, see Hassan *et al.*, 1988). The increased turbulence in the downwind areas of wind farms has also been observed to reduce the energy capture of the turbines in those locations. High turbulence means higher velocity gusts and more extreme wind speed changes over short periods. Control actions to limit loads in gusts cause turbines to shut down more frequently, decreasing overall energy capture (Baker, 1999).

9.4.2.4 Direction Sector Management

As a consequence of wake turbulence and its effect on the fatigue life of wind turbines, in special situations wind turbines may be stopped to limit fatigue damage when winds are from certain directions. This practice is referred to as direction sector management. For example, at a wind farm with almost unidirectional winds, the turbines may be closely spaced perpendicular to the prevailing wind. On those rare occasions when the wind is along the closely spaced rows, every second wind turbine might be shut down to limit the turbulence that the wind turbines experience.

9.4.2.5 Wind Farm Power Curves

The result of array losses and wake turbulence is a modification of the operation of the individual turbines with respect to the overall prevailing wind speed. As the wind approaching an array of wind turbines increases from zero, the first row of turbines will start to produce power. That power production will reduce the wind speed behind the first row and no other turbines will operate. As the wind increases, more and more rows of turbines will produce power until all of the turbines are producing power, with the front row producing the most power per turbine. Once the wind reaches rated wind speed, only the first row of turbines will produce rated power. Each turbine will be producing rated power only after the winds are somewhat higher than rated for the turbines in the wind farm. Thus, not only is the total wind farm energy production lower than that of multiple isolated turbines, but the energy production as a function of wind speed has a different shape for the whole wind farm than for an individual turbine (see Figure 9.11).The example in the figure assumes that all wind turbines
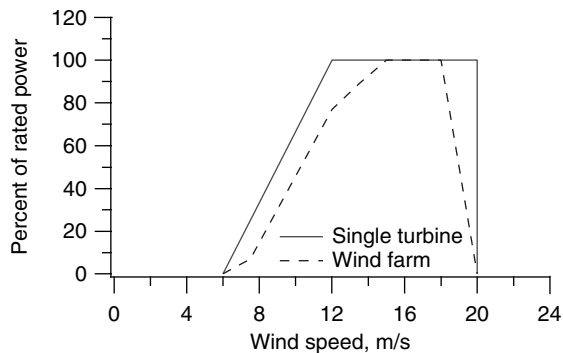
Figure 9.11   Comparison of single turbine and wind farm power curves

are operating correctly. If some turbines are out of service, the effective wind farm power will be shifted down.

9.4.2.6 Power Smoothing

The total output power of a wind farm is the sum of the power produced by the individual turbines in a wind farm. Turbulent wind fluctuations result in fluctuating power from each of the wind turbines and, thus, from the wind farm. Turbulent wind conditions result in different winds at widely spaced turbines. This means that the power from one turbine may be rising as the power from another turbine is falling. This results in some reduction in wind farm power fluctuations compared with the power that would be expected from turbines all experiencing the same wind.

For example, assume that one wind turbine produces an average power P_1 over some time interval with a standard deviation of $\sigma_{P,1}$. Then, if N wind turbines in the wind farm experienced the same wind, the total wind farm production would be $P_N = NP_1$ and the standard deviation of the wind farm electrical power output would be $\sigma_{P,N} = N\sigma_{P,1}$. Usually, however, the wind at an individual wind turbine is not well correlated with the wind at any other turbine and, thus, the wind turbines do not all experience the same wind. It can be shown that if N wind turbines experience wind with the same mean wind speed and uncorrelated turbulence with the same statistical description, then the mean power output of the N turbines is still $P_N = NP_1$, but the standard deviation of the resulting aggregated power is just:

$$\sigma_{P,N} = \frac{N\sigma_{P,1}}{\sqrt{N}} \tag{9.8}$$

Thus, the fluctuation of the total power from the wind farm is less than the fluctuation of the power from individual wind turbines. This effect is termed power smoothing.

In reality, the wind at two different turbine sites in a wind farm is neither perfectly correlated nor perfectly uncorrelated. The degree of correlation depends on the distance between the two locations and on the spatial and temporal character of the wind field. An expression for the variance in wind farm output power as a function of the turbulent length scale and the number of and distance between machines is developed here. The analysis assumes that all of the turbines experience the same mean wind speed and that the power from each machine can be assumed to be linear with wind speed about the mean power output. The analysis builds on the material in Chapter 2.

The temporal character of the wind field is expressed by a power spectrum, which measures the variance of the fluctuating winds at one specific location as a function of frequency. As explained in Chapter 2, in the absence of a power spectrum based on actual data collected at a site, atmospheric turbulence is often characterized by the von Karman power spectrum (Fordham, 1985). The von Karman power spectrum, $S_1(f)$ is defined by:

$$\frac{S_1(f)}{\sigma_U^2} = \frac{4\frac{L}{U}}{\left[1 + 70.8\left[\frac{Lf}{U}\right]^2\right]^{5/6}} \tag{9.9}$$

where $S_1(f)$ is the single point power spectrum, L is the integral length scale of the turbulence, U is the mean wind speed, and f is the frequency (in Hz).

The spatial character of the wind can be expressed by a coherence function, which is a measure of the magnitude of the power spectrum at one location with respect to the power

spectrum at another location. When using the von Karman spectrum, an expression for the coherence in terms of Bessel functions is, strictly speaking, the most appropriate. That expression is significantly more complex than the exponential coherence function approximation for atmospheric turbulence which is often used in micrometeorology (see Beyer *et al.*, 1989), which is given by:

$$\gamma_{ij}^2(f) = e^{-a\frac{x_{ij}}{U}f} \tag{9.10}$$

where $\gamma_{ij}^2(f)$ is the coherence between the power spectra at points i and j, a is the coherence decay constant, taken to be 50, x_{ij} is the spacing between points i and j, U is the mean wind speed, and f is the frequency (in Hz). The coherence decay constant of 50 is most appropriate to the case where the turbines are in a line, perpendicular to the prevailing wind direction (see Kristensen *et al.*, 1981). Equation (9.10) illustrates that the similarity in the wind experienced by turbines at different locations decreases with distance between the turbines and the frequency of turbulent fluctuations. At low frequencies (long time periods) and close distances, the winds are similar, but at high frequencies (short time scales) and long distances, they are very different.

The spectrum of the total variance in the wind at N turbine locations, $S_N(f)$, is (Beyer *et al.*, 1989):

$$S_N(f) = S_1(f)\frac{1}{N^2}\sum_{i=1}^{N}\sum_{j=1}^{N}\gamma_{ij}(f) \tag{9.11}$$

The term $1/(N^2)\sum_{i=1}^{N}\sum_{j=1}^{N}\gamma_{ij}(f)$ is known as the 'wind farm filter.'

The variance of the fluctuating wind speed is given by the integral of the power spectrum over all frequencies. Note that the total variance is the same value that may be found from time series data in the usual way:

$$\sigma_U^2 = \int_0^{\infty} S_1(f)\,df \tag{9.12}$$

If the standard deviation of the power from each of the wind turbines at the mean power level can be assumed to be k multiplied by the standard deviation in the wind speed (that is, if $\sigma_P = k\sigma_U$), then the variance of the fluctuating power from one wind turbine is given by:

$$\sigma_{P,1}^2 = k^2\int_0^{\infty} S_1(f)df \tag{9.13}$$

The variance of the total fluctuating power is given by:

$$\sigma_{P,N}^2 = N^2 k^2 \int_0^{\infty} S_N(f)df = k^2 \int_0^{\infty} \left\{ S_1(f)\int_{i}^{N}\int_{j}^{N}\gamma_{ij}(f) \right\}df \tag{9.14}$$

and using the von Karman spectrum:

$$\sigma_{P,N}^2 = k^2 \int_0^\infty \left\{ \frac{4\frac{L}{U}}{\left[1 + 70.8\left(\frac{Lf}{U}\right)^2\right]^{5/6}} \sum_{i=1}^N \sum_{j=1}^N \exp\left(\frac{-25x_{ij}f}{U}\right) \right\} df \qquad (9.15)$$

Thus, the variability of the total power from a wind farm decreases as the distance between turbines increases. Also, the lack of correlation between the wind at higher frequencies contributes more to the decrease in total variability than do the relatively correlated winds at low frequencies. It is easy to verify, using Equations (9.10) and (9.14), that, if the wind at the turbines is completely correlated ($x_{ij} = 0$ for all i, j), then the turbines all act as one large turbine. Similarly, if the wind at N turbines is completely uncorrelated ($x_{ij} = 0$ when $i = j$ and is otherwise infinite), then Equation (9.8) applies.

As an example, Figure 9.12 illustrates the effect of spacing for two and ten wind turbines, assumed to be equally spaced along a line perpendicular to the wind direction. For this example, $L = 100$ m and $U = 10$ m/s. The figure shows the fractional reduction in power variability as a function of crosswind spacing. The absolute levels of power fluctuations will depend on the operating conditions of the wind turbines. For variable-speed wind turbines operating at rated power, k, the ratio of the magnitudes of the power fluctuations to those of the wind is close to zero and the power fluctuations will be low regardless of turbulence intensity. For operation below rated power in turbulent wind conditions, fluctuations of power from each individual wind turbine might be very high and the reduction due to the aggregation of power from all of the turbines in a wind farm might be very large.

As described above, the wind turbines in a wind farm often do not experience the same mean wind or turbulence of the same statistical description, but the power-smoothing effect can nevertheless be seen in wind farm data. Thus, wind farms with a large number of wind turbines can reduce the voltage fluctuations and other problematic effects caused by the power fluctuations of individual wind turbines (see Section 9.5).
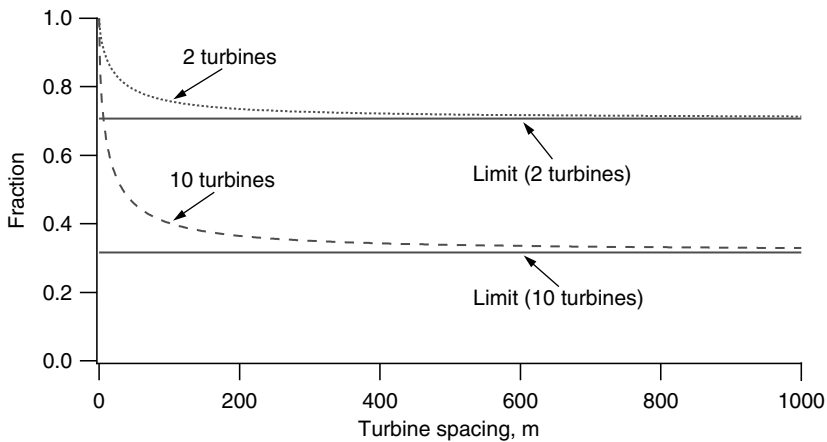
Figure 9.12 Fraction of wind farm power variability as a function of turbine spacing

9.5 Wind Turbines and Wind Farms in Electrical Grids

Wind turbines supply power through large electrical grids, which are often characterized as 'stiff;' that is to say, totally unaffected by connected loads or generation equipment. In reality, grid characteristics can affect and are affected by wind turbines connected to them. To help understand these effects, a brief description of electrical grids and grid connection equipment is provided. This is followed by a summary of the electrical behavior of turbines in grids and the types of grid–turbine interactions that can affect wind turbine installations.

9.5.1 Electrical Grids

Electrical grids can be divided into four main parts: generation, transmission, distribution, and supply feeders (see Figure 9.13). The generation function has historically been provided by large synchronous generators powered by fossil or nuclear fuel or hydroelectric turbines. These generators respond to load variations, keep the system frequency stable, and adjust the voltage and power factor at the generating station as needed. Generators in large, central power plants produce power at high voltage (up to 25 000 V). These generators feed current into the high-voltage transmission system (110 kV to 765 kV) used to distribute the power over large regions. The transmission systems use high voltage to reduce the losses in the power transmission lines. The local distribution system operates at a lower voltage (10 kV to 69 kV), distributing the power to neighborhoods. Locally, the voltage is reduced again and the power is distributed through feeders to one or more consumers. Industrial loads in the United States typically consume 480 V power while commercial and residential consumers in the United States and much of the rest of the world connect to 120 or 240 V systems. In Europe, industrial loads generally connect at 690 V and residential loads use 230 V power.

The term electrical load is used to describe a sink for power or a specific device that absorbs power. The total electrical load on the transmission system is the sum of the many fluctuating end loads. Fluctuations in these end loads are mostly uncorrelated, resulting in a fairly steady load on transmission lines that varies according to the time of day and season. The distribution
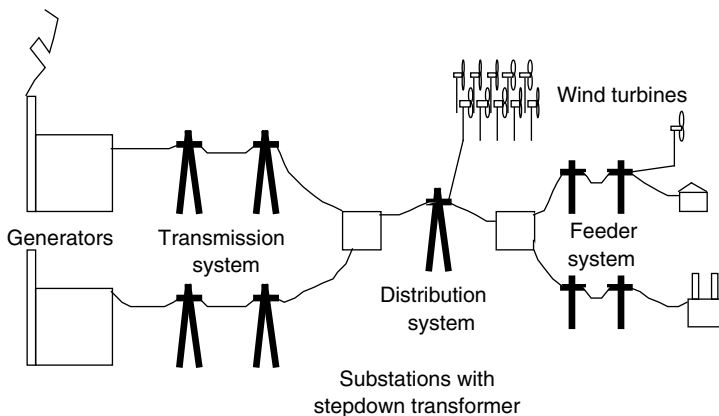
Figure 9.13 Electrical grid system schematic

and supply systems are closer to consumer loads, far from the large generators, and, thus, increasingly affected by these changing loads.

The locations of usable wind resources do not always allow wind turbines to be easily tied into the high-voltage transmission system. Wind turbines are most often connected to the distribution system or, in the case of smaller wind turbines, into the feeder system.

Most generators in electrical networks are synchronous generators (see Chapter 5) that are driven by prime movers such as steam, hydroelectric, or gas turbines or diesel engines. System operators attempt to control the grid frequency and voltage to be within a narrow range about the nominal system values. Frequency in large electrical grids in industrialized countries is maintained at less than $\pm$ 0.1% of the desired value. Depending on the country, voltages at distribution points are allowed to fluctuate from $\pm$ 5% to up to $\pm$ 7% of the nominal value, but allowable customer-induced voltage variations are often less (Patel, 1999).

The grid frequency is controlled by the power flows in the system. The torque on the rotor of any given generator consists of the torque of the prime mover, Q_{PM}, the electrical torques due to loads in the system, Q_L, and other generators in the system, Q_O. The equation of motion for the generator, with rotating inertia J, and speed ω, can be written:

$$J\frac{\mathrm{d}\omega}{\mathrm{d}t} = Q_{PM} + Q_L + Q_O \tag{9.16}$$

Each of the generators in the system is synchronized with the other generators in the system. Thus, this same equation of motion can represent the behavior of the system as a whole if each term represents the sum of all of the system inertias or loads.

Recognizing that power is just the product of torque and speed, one can derive the following equation:

$$\frac{\mathrm{d}\omega}{\mathrm{d}t} = \frac{1}{J\omega}(P_{PM} + P_L + P_O) \tag{9.17}$$

where P_{PM} is the prime mover power, P_L is the power from electrical loads, and P_O is the power from other generators.

Here, changes in the rotational speed of the generators (which is proportional to grid frequency) are expressed as functions of the input power from the prime movers, the system load, and any power flows from other connected equipment. If the system load changes, then the power from the prime movers is adjusted to compensate and keep the system frequency stable.

The system voltage is regulated by controllers on the field excitation circuits of each of the generators. Changing the field excitation changes both the terminal voltage and the power factor of the power delivered to the load. When the fields are controlled to stabilize system voltage, the power factor is determined by the connected loads. Voltage is controlled, in this manner, at each generating station.

Electrical grids, like other electrical circuits, provide an impedance to current flow that causes voltage changes between the generating station and other connected equipment. This can be illustrated by considering a wind turbine generator connected to a grid system (see Figure 9.14) with a line-to-neutral voltage, V_S, that is assumed to be the same as the voltage at the generating station. The voltage at the wind turbine, V_G, is not necessarily the same as V_S. The difference in voltage is caused by the electrical collection system impedance, which consists of the collection system resistance, R, that causes voltage changes primarily because
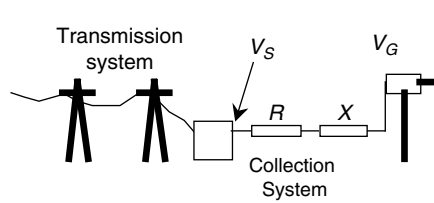
Figure 9.14 Collection system schematic: R, resistance; X, reactance; V_S and V_G, grid and wind turbine voltage respectively

of the real power flowing in the system and collection system reactance, X, that causes voltage changes because of the reactive power flowing in the system (see Chapter 5 for a definition of electrical terms). The magnitudes of R and X, which are functions of the distribution system, and the magnitudes of the real generated power, P, and reactive power requirements, Q, of the wind turbine or wind farm will determine the distribution system voltage at the wind turbine.

The voltage at the generator can be determined from Equation (9.18) (Bossanyi *et al.*, 1998):

$$V_G{}^4 + V_G{}^2[2(QX{-}PR){-}V_S{}^2] + (QX{-}PR)^2 + (PX{-}QR)^2 = 0 \qquad (9.18)$$

In lightly loaded circuits, the voltage change can be approximated by Equation (9.19):

$$\Delta V = V_G{-}V_S = \frac{PR{-}QX}{V_S} \qquad (9.19)$$

It can be seen that the voltage increases due to the real power production (P) in the system. However, the voltage decreases when reactive power (Q) is consumed by equipment in the system.

These voltage changes can be significant. Transformers equipped for automatic voltage control (AVR) are used to provide reasonably steady voltages to end-users. These transformers have multiple taps on the high-voltage side of the transformer. Current flow is switched automatically from one tap to another as needed. The different taps provide different turn ratios and therefore different voltages (for more information, see Rogers and Welch, 1993).

The same cable resistance that causes voltage fluctuations also dissipates energy. The electrical power losses in the collection system, P_{LO}, can be expressed as:

$$P_{LO} = \frac{(P^2 + Q^2)R}{V_S^2} \qquad (9.20)$$

Finally, grid 'strength' or stiffness is characterized by the fault level, M, of the distribution system. The fault level at any location in the grid is the product of the system voltage and the current that would flow if there were a short circuit at that location. Using the example above, if there were a short circuit at the wind turbine, the fault current, I_F, would be:

$$I_F = \frac{V_S}{\left(R^2 + X^2\right)^{1/2}} \qquad (9.21)$$

and the fault level (in volt-amperes), M, would be:

$$M = I_F V_S \tag{9.22}$$

This fault level is an indication of the strength of the network, with higher fault levels indicating stronger networks.

9.5.2 Turbine–Distribution System Interactions

On the one hand, the introduction of wind turbines into a distribution grid can, at times, lead to problems that limit the magnitude of the wind power that can be connected to the grid. On the other hand, depending on the grid and the turbines, the introduction of turbines may help support and stabilize a local grid. Turbine–grid interactions depend on the electrical behavior of (1) the turbines under consideration and (2) the electrical grids to which the turbines are connected. Important aspects of these have been explained above. Interconnection issues include problems with steady state voltage levels, flicker, harmonics, and grid capacity limits. This section focuses mainly on interactions that affect the local system voltages and currents on medium- to short-term time scales. Larger questions related to overall system control are discussed in Sections 9.5.4 and 9.5.5.

9.5.2.1 The Behavior of Wind Turbines Connected to Electrical Grids

Wind turbine operation results in fluctuating real and reactive power levels and may result in voltage and current transients or voltage and current harmonics. These may contribute to turbine–grid interactions, as explained in Section 9.5.4. This section builds on the material in Chapter 5 and addresses those aspects of turbine operation that may be significant for turbine–grid interactions.

Constant-speed turbines connected to electrical grids generally use induction generators. Induction generators provide real power (P) to the system and absorb reactive power (Q) from the system. The relationship of real to reactive power is a function of the generator design and the power being produced. Both real and reactive power are constantly fluctuating during wind turbine operation. Low-frequency real power fluctuations occur as the average wind speed changes. Reactive power needs are approximately constant or increase slowly over the operating range of the induction generator. Thus, low-frequency reactive power fluctuations are usually smaller than low-frequency real power fluctuations. Higher frequency fluctuations of both real and reactive power occur as a result of turbulence in the wind, tower shadow, and dynamic effects from drive train, tower, and blade vibrations.

Wind turbines with synchronous generators operate in a different manner than those with induction generators. When connected to a large electrical network with a constant voltage, the field excitation of the synchronous generators on wind turbines can be used to change the line power factor and to control reactive power, if desired.

Variable-speed turbines usually have a power electronic converter between the generator and the grid. These systems can control both the power factor and voltage of the delivered power. Power electronic converters connected to induction generators also need to supply reactive power to the turbine generator. This is done, in effect, by circulating reactive current through the generator coils to support the magnetic field in the generator. The converter

components connected to the grid can usually provide current to the grid at any desired power factor. This capability may be used to improve grid operation, if desired.

When generators are connected or disconnected from a power source, voltage fluctuations and transient currents can occur. As explained in Chapter 5, connecting an induction generator to the grid results in a momentary starting current as the magnetic field is energized. Also, if the generator is used to speed up the rotor from speeds far from synchronous speed (high slip operation), significant currents can occur. These high currents can be limited, but not eliminated, with the use of a 'soft-start' circuit, which limits the generator current. When induction generators are disconnected from the grid, voltage spikes can occur as the magnetic field decays. Turbines with synchronous generators, in contrast, generally have no starting current requirements. Normally they must be accelerated up to operating speed by the turbine rotor before grid connection can occur. Nevertheless, voltage transients may still occur on connection and disconnection as the stator field is energized and de-energized.

9.5.2.2 Steady State Voltages

Changes in the mean power production and reactive power needs of a turbine or a wind farm can cause quasi-steady state voltage changes in the connected grid system. These changes occur over numerous seconds or more and are explained above. The X/R ratio of the distribution system and the generator operating characteristics (the amount of real and reactive power at typical operating levels) determine the magnitude of the voltage fluctuations. It has been found that an X/R ratio of about 2 results in the lowest voltage fluctuations with typical fixed-speed turbines with induction generators. The X/R ratio is typically in the range of 0.5 to 10 (Jenkins, 1995).

The weaker the grid is, the greater are the voltage fluctuations. 'Weak' grids that can cause problematic turbine–grid interactions are those grid systems in which the wind turbine or wind farm rated power is a significant fraction of the system fault level. Studies suggest that problems with voltage fluctuations are unlikely with turbine ratings of 4% of the system fault level (Walker and Jenkins, 1997). Germany limits renewable power generator ratings to 2% of the fault level at the POC, and Spain limits them to 5% (Patel, 1999).

Power factor correction capacitors are installed at the grid connection to reduce system voltage fluctuations and the reactive power needs of the turbine. Power factor correction capacitors need to be chosen carefully to avoid self-excitation of the generator. This occurs when the capacitors are capable of supplying all of the reactive power needs of the generator and the generator becomes disconnected from the grid. In this case the capacitor–inductor circuit, consisting of the power factor correction capacitors and the generator coils, can resonate, providing reactive power to the generator and resulting in possibly very high voltages.

9.5.2.3 Flicker

Flicker is defined as disturbances to the network voltage that occur faster than steady state voltage changes and which are fast enough and of a large enough magnitude that lights noticeably change brightness. These disturbances can be caused by the connection and disconnection of turbines, the changing of generators on two-generator turbines, and by

torque fluctuations in fixed-speed turbines as a result of turbulence, wind shear, tower shadow, and pitch changes. The human eye is most sensitive to brightness variations around frequencies of 10 Hz. The blade-passing frequency in large wind turbines is usually closer to 1–2 Hz or less, but even at these frequencies the eye will detect voltage variations of $\pm 0.5\%$ (Walker and Jenkins, 1997). The magnitude of the flicker due to wind turbulence depends on the slope of the real vs. reactive power characteristics of the generator, the slope of the power vs. wind speed characteristics of the turbine, and the wind speed and turbulence intensity. Flicker is, in general, much less of a problem for constant-speed, stall-regulated machines than pitch-regulated machines (Gardner *et al.*, 1995). Variable-speed system power electronics usually do not impose rapid voltage fluctuations on the network, but still may cause flicker when turbines are connected or disconnected. Flicker does not damage equipment connected to the grid, but in weak grids, where the voltage fluctuations are greater, it may become an annoyance to other consumers. Numerous countries have standards for quantifying flicker and limits for allowable flicker and step changes in voltage (see, for example, CENELEC, 1993).

9.5.2.4 Harmonics

Power electronics in variable-speed wind turbines introduce sinusoidal voltages and currents into the distribution system at frequencies that are multiples of the grid frequency (see Chapter 5). Because of the problems associated with harmonics, utilities have strict limits on the harmonics that can be introduced into the system by power producers such as wind turbines.

The usual measure of the degree of waveform distortion at any point in a system is total harmonic distortion (THD). THD is a function of the magnitude of the fundamental frequency and of the harmonics in the voltage waveform. The instantaneous voltage, v, can be expressed as the sum of the fundamental voltage, v_F (a sinusoidal voltage at the fundamental frequency) and a superimposed harmonic voltage, v_H. The harmonic voltage is the sum of the numerous harmonics, v_n, of order n, $(n > 1)$:

$$v_H = \sum_{n=2}^{\infty} v_n \tag{9.23}$$

The individual harmonic voltages, v_n, consist of the cosine and sine harmonic components defined in Chapter 5:

$$v_n = a_n \cos\left(\frac{n\pi t}{L}\right) + b_n \sin\left(\frac{n\pi t}{L}\right) \tag{9.24}$$

where n is the harmonic number, t is time, L is half the period of the fundamental frequency, and a_n and b_n are constants. These harmonics can be expressed as sine functions with amplitudes, c_n, and phases, φ_n:

$$v_n = c_n \sin\left(\frac{n\pi t}{L} + \varphi_n\right) \tag{9.25}$$

where:

$$c_n = \sqrt{a_n{}^2 + b_n{}^2} \tag{9.26}$$

and where the phase is defined by:

$$\sin\varphi_n = \frac{a_n}{c_n}, \quad \cos\varphi_n = \frac{b_n}{c_n} \tag{9.27}$$

The harmonic distortion caused by the nth harmonic of the fundamental frequency, HD_n, is defined as the ratio of the rms value of the harmonic voltage of order n over some time T (an integral number of periods of the fundamental) to the rms value of the fundamental voltage, v_F, over the same time T:

$$HD_n = \frac{\sqrt{\dfrac{1}{T}\displaystyle\int_0^T v_n^2 dt}}{\sqrt{\dfrac{1}{T}\displaystyle\int_0^T v_F^2 dt}} \tag{9.28}$$

The THD can be expressed as (see also Stemmler, 1997 and Phipps $et\ al.$, 1994):

$$\text{THD} = \frac{\sqrt{\displaystyle\sum_{n=2}^{\infty}\dfrac{1}{T}\displaystyle\int_0^T v_n^2 dt}}{\sqrt{\dfrac{1}{T}\displaystyle\int_0^T v_F^2 dt}} = \sqrt{\sum_{n=2}^{\infty}(HD_n)^2} \tag{9.29}$$

In both the United States and Europe, many power companies use the IEEE 519 Standard (ANSI/IEEE, 1992) to determine allowable THD at the point of common coupling (PCC). Minimizing problems at this point minimizes problems for other electrical customers. The allowable THDs of the voltage waveform according to IEEE 519 are detailed in Table 9.2. Similar restrictions on current harmonics, which depend on the ratio of maximum demand load current to maximum short circuit current at the PCC, can be found in IEEE 519.

9.5.2.5 Grid Capacity Limitations

There may be times when the current-carrying capacity of the grid is limited, possibly due to outages of a line or hot weather when the grid capacity needs to be de-rated. Under these

Table 9.2 Maximum allowable total harmonic distortion (THD) of voltage at the point of common coupling (PCC)

PCC voltage	Individual harmonic, %	THD, %
2.3–69 kV	3.0	5.0
69–138 kV	1.5	2.5
>138 kV	1.0	1.5

conditions, if it is windy, turbines may be required by the local utility to curtail their output. This might be accomplished by operating only some wind turbines or by operating all of the wind turbines at a reduced power level.

9.5.3 Grid Connection Equipment

The turbine–grid connection consists of equipment to connect and disconnect the turbine or wind farm from the larger grid, equipment to sense problems on the grid or the turbine side of the connection, and transformers to transfer power between different voltage levels. This equipment is in addition to the electrical equipment associated with each wind turbine that is described in Chapter 5.

- **Switchgear.** Switchgear to connect and disconnect wind power plants from the grid usually consists of large contactors controlled by electromagnets. Switchgear should be designed for fast automatic operation in case of a turbine problem or grid failure.
- **Protection equipment.** Protection equipment at the point of connection needs to be included to ensure that turbine problems do not adversely affect the grid and vice versa. This equipment must include provision for rapid disconnection in case of a short circuit or over-voltage situation in the wind farm. The wind farm should also be disconnected from the grid in case of a deviation of the grid frequency from the rated frequency due to a grid failure or a partial or full loss of one of the phases in a three-phase grid (see Chapter 5). The protection equipment consists of sensors to detect problem conditions. Outputs from these sensors control contactor magnets or additional solid state switches such as silicon-controlled rectifiers (SCRs). The ratings and operation of protection equipment should be coordinated with that of other local equipment to ensure that no problems occur. For example, in the case of a momentary grid failure, the disconnect at the wind farm should react fast enough to prevent currents from flowing into the grid fault and should remain off long enough to ensure that reconnection only occurs after the other grid faults have been cleared (Rogers and Welch, 1993).
- **Electrical conductors.** Electrical conductors (cables) for connecting wind farms to the grid are usually made of aluminum or copper. The electrical conductors used for transformers and grid connections dissipate power because of their electrical resistance. These losses reduce system efficiency and can cause damage if wires and cables get too hot. Cable resistance increases linearly with distance and decreases linearly with the cross-sectional area of the conductor. Economic considerations tend to dictate the resistive losses allowable, given the increased cost of larger cables.
- **Transformers.** Transformers at the substation are used to connect electrical circuits at different voltage levels. The details of transformer operation are covered in Chapter 5. Usually, these transformers have automatic voltage control to help maintain the system voltage.
- **Grounding.** Turbines, wind farms, and substations need grounding systems to protect equipment from lightning damage and short circuits to ground. Providing a conductive path for high currents to the earth can be a significant problem in locations with exposed bedrock and other non-conductive soils. Lightning strikes or faults can result in significant differences in ground potential at different locations. These differences can disrupt grid protection equipment and pose a danger to personnel.

9.5.4 Grid Operation and Control

As the number of wind turbines connected to grids increases, their effect on grid operation and control increases. Relevant aspects of typical grid operation are described in this section and the effects of the large-scale integration of wind turbines into grid systems are described in Section 9.5.5.

9.5.4.1 Load and Generator Characteristics

As described above, utilities need to deliver electrical power at the nominal system voltage to all of the system loads. A number of large prime movers are used to provide mechanical power, including steam, gas, and hydroelectric turbines to the generators. Ideally, generators closely follow the fluctuating load and so minimize voltage and frequency fluctuations. The electrical demand (the load that must be supplied) on the generators in a power system fluctuates on daily and seasonal scales. The load generally increases in the morning and decreases in the evening with similar patterns each day. The daily load pattern may change with changes in seasons and on weekends and holidays. Figure 9.15 shows an example of what the load pattern of a large grid system might look like. The magnitude of the loads or its average may also change over these time scales. As can be seen in Figure 9.15, the system load is never zero and fluctuates over a specific range of loads which is only infrequently exceeded.

A load duration curve of this theoretical regional power system is shown in Figure 9.16. The figure shows the percentage of time that loads greater than a given magnitude occur. It can be seen that there is a load of at least 8 GW at all times. This is referred to as the base load. The intermediate load range covers the range over which a significant amount of energy must be supplied at a range of power levels. It corresponds to the range of the typical daily fluctuations seen in Figure 9.16. Finally, peak loads are those which occur rarely or infrequently, perhaps on hot days in the summer. In this example, the peak loads, those over 20 GW, occur only 1.5% of the time.
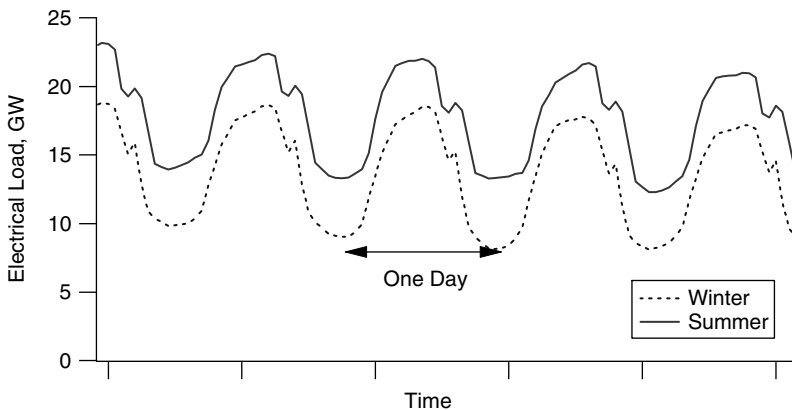
Figure 9.15 Sample utility load curve for a utility with different load levels in winter and summer
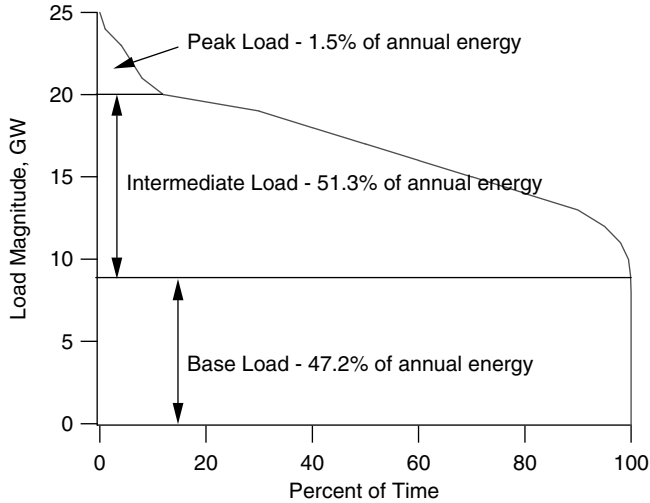
Figure 9.16   Sample load duration curve for a utility

Generators with different characteristics are used to supply power at these different power levels. Nuclear and coal-fired power plants do not respond quickly to changing loads and may need a significant warm-up and cool-down period. These types of plants are used for base-power stations. Intermediate-power stations use technologies that can change generation levels more rapidly. Hydropower stations are well suited for this. Peak-power stations need to be able to be ramped up very quickly and are used only rarely. Diesel generators, gas turbine generators, and pumped storage hydropower plants often serve as peak-power stations. Peak-power stations may only operate for an hour a day and only in some seasons. It can be seen that each power system must have a mix of generators that, together, can supply any load that may occur and whose dynamics allow control of the system voltage and frequency on sufficiently fast time scales.

9.5.4.2 Grid Control

The power being consumed in the grid must be balanced by the power that is being generated. In order to maintain that power balance and, thus, the frequency of the grid, the grid operator must have some generation capacity that is dedicated to load following: varying power output to match the load as closely and quickly as possible. There are three major mechanisms by which power is balanced: regulation or primary control, load following or secondary control, and scheduling or unit commitment. For more information, see Ackerman (2005) and Weedy and Cory (1998).

As the load changes during the day, generators are brought online, but large prime movers may take a while to prepare for generation. Thus, a certain amount of unused generation capacity, called 'spinning reserve,' is kept online ready to respond to rapid load fluctuations.

Power plants used for primary control or regulation are the first to be called on to increase or decrease output when there is a mismatch between the load and the power generated. These units can respond within seconds to minutes. In this category are generators that are kept

on spinning reserve. These machines are run at minimum or very low output, where they are quite inefficient, ready to ramp up output when conditions call for it. Regulation is usually tied to grid frequency, increasing power output when the frequency begins to fall, and decreasing output when frequency rises.

Load following or secondary control generation capacity also helps to balance the load and the generation, but has a slower reaction time. Generators in this category might have response times of tens of minutes to hours. For example, load-following generators are called upon when the average power demand is increasing, in order to free up plants performing regulation to follow rapid fluctuations in load. The capabilities of load-following units will be most challenged during times when the energy demand is changing most rapidly. The most rapid increase that a power system is likely to experience in a given year is called the maximum ramp rate, usually measured in megawatts per minute. The higher this rate, the more control capacity is needed to cover potential load increases. Load following can also be difficult during times of rapid decreases in load. In order to prevent an unacceptable increase in frequency, generation must be decreased to match demand at times when energy use is decreasing. Under these circumstances, control generators must be producing enough power at any given time that they can cover a decrease in load by decreasing their power output. It is possible that during a sustained drop in load or a grid fault, there might be an insufficient margin for decrease in generation to maintain power balance.

Scheduling or unit commitment is the process of scheduling base-load, intermediate-load, and peak-load generators so they will be available when needed in the upcoming hours or days. Utilities also try to ensure that there is enough reserve power to cover the load after the loss of the largest single generator in the power system. Thus, the outage of any one plant would not require the disconnection of customers. In vertically integrated utilities, scheduling is performed by the utility. Within power systems that are not vertical monopolies – that is, in which the system operator does not own the generation – power producers enter into contracts with the system operator for power production over various time scales. There are day-ahead and week-ahead markets in which producers agree to produce energy at particular times in the coming day or week for a particular rate. Hour-ahead markets mediate deviations from the expected power consumption during the day. Some power systems, including in Australia and some US states, have sub-hourly markets in which the system operators make bids every 15 or 30 minutes for energy in the next 15 or 30 minutes. Sub-hourly markets are a form of load-following control.

9.5.5 Integration of Wind Turbines into Electrical Grids

The integration of wind power into electrical grids affects grid control, costs for spinning reserves, and unit commitment. These costs can be reduced by advances in wind turbine and wind farm control capabilities, the use of wind forecasts, the creation of large balancing areas, and the use of energy storage.

9.5.5.1 Effects on Control

When wind turbines supply a significant fraction of an electrical system's requirement, the difference between the load and the wind energy is known as the net load. This net load must be supplied by conventional generators. The net load may fluctuate significantly due to variations

in wind as well as in the load itself. If the wind and the load are uncorrelated and if the standard deviation of the system load over any given time period is σ_{load} and the standard deviation of the wind generation is σ_{wind}, then the standard deviation of the net load, σ_{net}, is:

$$\sigma_{net} = \sqrt{\sigma_{load}^2 + \sigma_{wind}^2} \qquad (9.30)$$

Not only does variability of the net load increase due to the variability of wind power, but the uncertainty of the net load in the future increases. Unit commitment decisions must be made based on projections of the load and of the available wind power, and of the uncertainties of those contributing factors. This increase in the variability and uncertainty of the net load requires the commitment of additional spinning reserve to handle larger increases and decreases in net load from one hour or one minute to the next than would otherwise be needed.

The effect of wind's variability on system operation costs depends on the mix and characteristics of the conventional generators in the system, fuel costs, the nature of the wind resource, the characteristics and geographical dispersion of the wind power plants, and the regulatory environment. Numerous studies of the cost of the inclusion of large amounts of wind power into grid systems have been completed (see DOE, 2008 for a summary). The effects depend on which grid system is being considered. These studies have generally shown that having wind energy capacities up to 20% of the system load increases system operating costs by less than \$0.005/kWh. Most of these costs are for committing additional generating stations. Load following and regulation costs are usually a small proportion of the total cost.

Energy balancing occurs within control regions. When balancing regions are large and wind farms are widely distributed, the fluctuation of the total wind energy is reduced, reducing the impact on control decisions. For example, studies of European power systems with large amounts of installed wind power have shown that additional control capacity is not required to support wind power when the average energy produced by wind is less than 20% of the average load and the wind generation is geographically diverse. Having turbines spread over a large area has a significant smoothing effect on their power output (as explained in Section 9.4). Wind farms of 200 MW have had measured ramp rates of 20 MW/min, whereas 1000 MW of wind generation comprised of 10 to 20 MW farms might have a maximum ramp rate of only 6.6 MW/min (Ackermann, 2005).

Increasingly sophisticated controls are being included in grid-scale wind turbines. These have the possibility of taking some of the control load off conventional regulation and load-following generators in a grid system in which wind farm control is integrated into the grid control system. Such control options include the ability to limit ramp rates or operate with reserve capacity by operating at reduced aerodynamic efficiency as the wind increases or in higher winds, respectively.

9.5.5.2 Forecasting of Wind Power Production

Wind energy forecasts are increasingly being integrated into the control systems of grids with large amounts of installed wind power. These predictions are important on several time scales. Short-term forecasting of loads can give regulation control equipment a head-start on covering increases or decreases in load. Day-ahead or two-day-ahead forecasts of grid conditions allow system operators to plan unit commitment.

System operators routinely forecast the load on their system based on detailed statistics of past power demand. Successful prediction of load includes knowledge of seasonal variations such as heating and lighting demands and how these change with weather conditions, daily variations in residential and industrial power use, and small but statistically significant short-term variations such as television use during the Super Bowl.

Wind power forecasts for 6 to 36 hours in the future generally use mesoscale numerical weather models (NWP) to predict wind speeds and then use information on the installed wind turbines in the region and historical and recent wind power generation to predict overall wind power generation over the balancing area. These predictions are complicated by a number of factors:

- NWP models may not have the spatial and time resolution to accurately predict the timing or magnitude of wind speed changes of fast-moving weather systems or systems with large changes in wind conditions over short distances.
- NWP models may have difficulty predicting wind speed and direction variations over complex terrain and at specific geographic locations.
- NWP model results become more uncertain as the time horizon increases and different NWP models may provide different predictions.
- Generation levels depend on wake losses which may be sensitive to wind direction.
- Low wind turbine availability, power curtailments due to transmission constraints, and energy losses due to icing, high-speed cut-out hysteresis, direction sector management, or other control actions may limit power.
- Power generation changes with air density.
- Power levels are very sensitive to wind speeds below rated.
- It may be difficult to obtain operational information about all of the wind turbines or wind farms in a region, and predictions may be based on a sample of the total population of wind turbines.
- Future turbine availability may be unknown.

For these reasons, forecasting systems often employ methods for incorporating current operating data, historical operating data, relationships between historical NWP predictions and measured wind speeds and directions or measured generation at each wind farm and density corrections to power curves, or relationships between wind speed and power.

Of most value to grid operators are predictions of the exact magnitude and timing of sudden changes in generation levels. These are difficult to provide, given the spatial and temporal resolution of NWP models. A technique known as ensemble forecasting is sometimes used to provide better estimates of generation and the uncertainty of generation levels or the timing of fronts moving through the region. Ensemble forecasting consists of integrating two or more forecast methods to mitigate the shortcomings of individual methods. Especially when the different forecast methods are quite different, and their errors are uncorrelated, this method can yield significantly better results than the individual methods that are its constituents. When combining the predictions, the individual predictions can also be weighted based on their performance over time. These weights might change depending on the season, the characteristics of the input data, or the time horizon for the prediction.

9.5.5.3 Grid Penetration Issues

The concept of grid penetration is used to characterize the contribution of wind to a grid system. Wind power grid penetration can be defined in a variety of ways. Capacity penetration is defined as the ratio of the installed wind power to the maximum grid connected load (approximately equal to the total connected generation). Instantaneous penetration is the ratio of the wind power at a given time to the electrical load at the same time. Energy penetration is the fraction of consumed energy (kWh) generated by wind power over a period of time. For example, while the capacity penetration of wind in Denmark is about 10%, the average energy penetration is about 20%. High levels of energy penetration can be achieved if wind power plants are integrated into the grid control system, as described above, and if there are adjacent control areas that can use excess energy or if grid-scale energy storage is available. For example, in Denmark, the instantaneous energy penetration is at times as great as 100% during periods of low load and high winds. This was possible because power could be transferred to neighboring countries. Energy storage technologies are described in Chapter 10.

References

Ackerman, T. (Ed.) (2005) *Wind Power in Power Systems*. John Wiley & Sons, Ltd, Chichester.

Ainslie, J. F. (1985) Development of an eddy-viscosity model for wind turbine wakes. *Proc. 7th British Wind Energy Association Conference*. Multi-Science Publishing Co, London.

Ainslie, J. F. (1986) Wake modelling and the prediction of turbulence properties. *Proc. 8th British Wind Energy Conference*, Cambridge, pp. 115–120.

ANSI/IEEE (1992) *IEEE Recommended Practices and Requirements for Harmonic Control in Electrical Power Systems*. ANSI/IEEE Std 519–1992.

AWEA (2008a) *Wind Energy Siting Handbook*. American Wind Energy Association, Washington, DC. Available at www.awea.org/sitinghandbook.

AWEA (2008b) *AWEA Third Quarter 2008 Market Report*. American Wind Energy Association, Washington, DC.

Baker, R. W. (1999) Turbine energy shortfalls due to turbulence and dirty blades. *Proc. of the 1999 American Wind Energy Association Conference,* Burlington, VT.

Beyer, H. G., Luther, J. and Steinberger-Willms, R. (1989) Power fluctuations from geographically diverse, grid coupled wind energy conversion systems. *Proc. of the 1989 European Wind Energy Conference,* Glasgow, pp. 306–310.

Bossanyi, E., Saad-Saoud, Z. and Jenkins, N. (1998) Prediction of flicker produced by wind turbines. *Wind Energy*, **1**(1), 35–55.

Bossanyi, E. A., Maclean, C., Whittle, G. E., Dunn, P. D., Lipman, N. H. and Musgrove, P. J. (1980) The efficiency of wind turbine clusters. *Proc. Third International Symposium on Wind Energy Systems,* Lyngby, DK.

CENELEC (1993) Flickermeter – functional and design specifications. European Norm EN 60868: 1993 E: IEC686:1986 + A1: 1990. Brussels.

Crespo, A. and Herandez, J. (1986) A numerical model of wind turbine wakes and wind farms. *Proc. of the 1986 European Wind Energy Conference,* Rome.

Crespo, A. and Herandez, J. (1993) Analytical correlations for turbulence characteristics in the wakes of wind turbines *Proc. of the 1993 European Community Wind Energy Conference,* Lübeck.

Crespo, A., Manuel, F. and Herandez, J. (1990) Numerical modelling of wind turbine wakes. *Proc. of the 1990 European Wind Energy Conference,* Madrid.

Crespo, A., Manuel, F., Moreno, D., Fraga, E. and Herandez, J. (1985) Numerical analysis of wind turbine wakes. *Proc. of the Workshop on Wind Energy Applications,* Delphi.

Derrick, A. (1993) Development of the measure–correlate–predict strategy for site assessment. *Proc. of the 1993 European Community Wind Energy Conference,* Lübeck, pp. 681–685.

DOE (2008) *20% Wind Energy by 2030*, Report DEO/GO-102008-2567. US Department of Energy, Washington, DC.

EWEA (2008) *Delivering Energy and Climate Solutions, EWEA Annual Report 2007*. European Wind Energy Association.

Fordham, E. J. (1985) Spatial structure of turbulence in the atmosphere. *Wind Engineering*, **9**, 95–135.

García-Rojo, R. (2004) Algorithm for the estimation of the long-term wind climate at a meteorological mast using a joint probabilistic approach, *Wind Engineering*, **28**(2), 213–223.

Gardner, P., Jenkins, N., Allan, R. N., Saad-Saoud, Z., Castro, F., Roman, J. and Rodriguez, M. (1995) Network connection of large wind turbines. *Proc. of the 17th British Wind Energy Conference,* Warwick, UK.

Hassan, U., Taylor, G. J. and Garrad, A. D. (1988) The impact of wind turbine wakes on machine loads and fatigue. *Proc. of the 1998 European Wind Energy Conference,* Herning, DK, pp. 560–565.

Hiester, T. R. and Pennell, W.T. (1981) *The Meteorological Aspects of Siting Large Wind Turbines*. U.S. DOE Report No. PNL-2522.

Jenkins, N. (1995) Some aspects of the electrical integrations of wind turbines. *Proc. of the 17th BWEA Conference,* Warwick, UK.

Joensen, A., Landberg, L. and Madsen, H. (1999) A new measure–correlate–predict approach for resource assessment. *Proc. of the 1999 European Wind Energy Conference,* Nice, pp. 1157–1160.

Johnson, C. (2008) *Summary of Actual vs. Predicted Wind Farm Performance – Recap of WINDPOWER 2008*, Presentation at 2008 AWEA Wind Resource Assessment Workshop, Portland, OR. American Wind Energy Association, Washington, DC.

Katić, I., Højstrup, J. and Jensen, N. O. (1986) A simple model for cluster efficiency *Proc. of the 1986 European Wind Energy Conference,* Rome.

Kristensen, L., Panofsky, H. A. and Smith, S. D. (1981) Lateral coherence of longitudinal wind components in strong winds *Boundary Layer Meteorology* **21**(2), 199–205.

Landberg, L. and Mortensen, N. G. (1993) A comparison of physical and statistical methods for estimating the wind resource at a site. *Proc. 15th British Wind Energy Conference,* York, pp. 119–125.

Lissaman, P. B. S. and Bates, E. R. (1977) *Energy Effectiveness of Arrays of Wind Energy Conversion Systems*. AeroVironment Report AV FR 7050. Pasadena, CA.

Lissaman, P. B. S., Zaday, A. and Gyatt, G. W. (1982) Critical issues in the design and assessment of wind turbine arrays. *Proc. 4th International Symposium on Wind Energy Systems,* Stockholm.

Lutgens, F. K. and Tarbuck, E. J. (1998) *The Atmosphere, An Introduction to Meteorology*. Prentice Hall, Upper Saddle River, NJ.

Mortimer, A. A. (1994) A new correlation/prediction method for potential wind farm sites. *Proc. of the 1994 British Wind Energy Association Conference*.

NREL (2007) Puerto Rico and U.S. Virgin Islands. 50 m wind power, National Renewable Energy Laboratory, U.S. Dept. of Energy. Available at http://www.windpoweringamerica.gov/pdfs/wind_maps/pr_vi_50m.pdf

NWCC (2002) *Permitting of Wind Energy Facilities, A Handbook*. Prepared by the NWCC Siting Subcommittee, National Wind Coordinating Committee, Washington, DC.

Patel, M. R. (1999) Electrical system considerations for large grid-connected wind farms. *Proc. of the 1999 American Wind Energy Association Conference,* Burlington, VT.

Pennell, W. R. (1982) *Siting Guidelines for Utility Application of Wind Turbines*. EPRI Report: AP-2795.

Petersen, E. L. and Troen, I. (1986) The European wind atlas. *Proc. of the 1986 European Wind Energy Conference,* Rome.

Petersen, E. L., Troen, I. and Mortensen, N. G. (1988) The European wind energy resources *Proc. of the 1998 European Wind Energy Conference, Herning,* DK, pp. 103–110.

Phipps, J. K., Nelson, J. P. and Pankaj, K. S. (1994) Power quality and harmonic distortion on distribution systems, *IEEE Transactions on Industry Applications*, **30**(2), 476–484.

Putnam, P. C. (1948) *Power from the Wind.* Van Nostrand Reinhold, New York.

Rogers, W. J. S. and Welch, J. (1993) Experience with wind generators in public electricity networks. *Proc. of BWEA/RAL Workshop on Wind Energy Penetration into Weak Electricity Networks*. Rutherford Appleton Laboratory, Abington, UK.

Rogers, A. L., Rogers, J. W. and Manwell, J. F. (2005) Comparison of the performance of four measure–correlate–predict algorithms. *Journal of Wind Engineering and Industrial Aerodynamics*, **93**(3), 243–264.

Smith, D. and Taylor, G. J. (1991) Further analysis of turbine wake development and interaction data. *Proc. of the 13th British Wind Energy Association Conference,* Swansea.

Sørensen, J. N. and Shen, W. Z. (1999) Computation of wind turbine wakes using combined Navier–Stokes actuator-line methodology. *Proc. of the 1999 European Wind Energy Conference,* Nice, pp. 156–159.

Stemmler, H. (1997) High power industrial drives. In Bose, B.K. (Ed.), *Power Electronics and Variable Frequency Drives, Technology and Applications*. IEEE Press, New York.

Troen, I. and Petersen, E. L. (1989) *European Wind Atlas*. Risø National Laboratory, Roskilde, DK.

Vermeulen, P. E. J. (1980) An experimental analysis of wind turbine wakes. *Proc. Third International Symposium on Wind Energy Systems,* Lyngby, DK, pp. 431–450.

Voutsinas, S. G., Rados, K. G. and Zervos, A. (1993) Wake effects in wind parks. A new modelling approach. *Proc. of the 1993 European Wind Energy Conference,* Lübeck, pp. 444–447.

Wade, J. E. and Hewson, E. W. (1980) *A Guide to Biological Wind Prospecting*. U.S. DOE Report: ET-20316, NTIS.

Walker, J. F. and Jenkins, N. (1997) *Wind Energy Technology*. John Wiley & Sons, Ltd, Chichester.

Weedy, B. M. and Cory, B. J. (1998) *Electric Power Systems*. John Wiley & Sons, Ltd, Chichester.

Wegley, H. L., Ramsdell, J. V., Orgill, M. M. and Drake, R. L. (1980) *A Siting Handbook for Small Wind Energy Conversion Systems*. Battelle Pacific Northwest Lab., PNL-2521, Rev. 1, NTIS.

WWEA (2008) *World Wind Energy Report 2008*. World Wind Energy Association, Bonn.

10

Wind Energy Applications

10.1 General Overview

Previous chapters have focused on wind turbines that are connected to conventional electrical grids under 'typical' conditions. The presumption in these discussions was also that the presence of wind turbines had relatively little impact on the grid itself. Wind turbines may also be used in other situations, where they may supply a large fraction of the total energy requirement. In addition, as more and more wind turbines are added to conventional networks, attention must be given to the best way to make use of the energy they can contribute. This chapter considers a number of those situations. These include distributed generation, hybrid power systems, offshore wind energy, installations in severe climates, special purpose applications, energy storage, and fuel production.

Distributed generation refers to situations in which generators such as wind turbines are connected to a utility's relatively low voltage distribution system. This topic is discussed briefly in Section 10.2.

Wind turbines may be connected to smaller, isolated electrical grids or may supply a large fraction of the power in a weak grid. When these systems contain other generators, storage or power converters, they are known as hybrid power systems. In these systems the wind power, other power sources, and any system loads may strongly influence each other. The characteristics of the components in such situation need to be understood in order to design the complete system. These issues are covered in Section 10.3.

Offshore wind turbines have a whole host of unique issues. The most significant differences between land-based and offshore wind turbines are their support structures and the factors that must be considered in their design. Other important differences include undersea electrical transmission, installation, operation, and maintenance. Environmental issues, siting, and permitting are also quite different offshore than on land. Offshore wind energy is covered in Section 10.4.

Issues related to operation in severe climates are covered separately in Section 10.5. These include cold weather, high temperatures, and lightning.

Special purpose applications include water pumping, sea water desalination, space or water heating, and ice making. These are the subject of Section 10.6.

There are a wide variety of energy storage options. These include batteries, pumped hydroelectric, flywheels, and compressed air, among others. These four storage options are discussed in Section 10.7.

Wind energy can be used to make fuel or to enhance a lower energy fuel. Two of the possibilities, hydrogen and ammonia, are discussed in Section 10.8.

10.2 Distributed Generation

Distributed generation refers to situations in which generators such as wind turbines are connected to a utility's relatively low voltage distribution system. As discussed in Chapter 9, distribution systems' voltages are typically on the order of 15 kV or less. These systems are designed to accept power flow in one direction. When large amounts of wind generation are added, the remainder of the supply from the local utility can become more variable, and in some cases generation may be sufficient to send power in the other direction. Adjustments may need to be made to the electrical system to allow this to take place smoothly and also to protect the system in case of an electrical fault. This topic is discussed in more detail by Masters (2004). Issues associated with distributed generation often have some similarity to those of hybrid power systems, which are the subject of the next section.

10.3 Hybrid Power Systems

Many wind turbines are connected not to large electrical grids, but to small, independent, diesel-powered grids, in which wind generators may be a large fraction of the total generating capacity. Such systems are referred to as wind/diesel power systems (Hunter and Elliot, 1994). Sometimes other renewable generators are added to complement the power from the wind. Power systems that include conventional generation and one or more renewable energy sources are more generally called hybrid power systems. The integration of wind turbines into these hybrid power systems presents unique system design issues. This section provides an overview of the most significant of those issues.

Wind turbines are sometimes integrated into weak grids (those in which the voltage or frequency may not be able to remain relatively constant under all conditions). To help stabilize these grids, additional components may be added, similar to what is done in isolated networks. Much of the following section is applicable to those situations as well.

Numerous communities in isolated locations, islands, and developing countries are connected to small, independent electrical grids powered by diesel generators. They may range in size from relatively large island grids of many megawatts down to systems with a capacity of a few kilowatts. Isolated and island grids vary significantly. Some isolated grids powered by diesel generators provide power for only a part of the day to conserve fuel. Some have large voltage swings due to the effect of one or two significant loads on the system, such as a saw mill or a fish-processing plant. Large isolated grids provide power at stable voltages and constant frequency. In general, isolated grids are weak grids in which voltage and frequency are susceptible to disruption by interconnected loads and generation.

Wind turbines and other renewable power sources (including wind, solar, biomass, or hydropower) can be integrated into these small electrical grids. As in larger stable grids, the

terms 'wind penetration' and 'renewables penetration' are used to characterize the magnitude of the wind or renewable power in the system compared to the rated load. In typical grid-connected wind turbine applications, turbine–grid interactions are limited to part of a distribution system. In contrast, wind turbines in isolated grids may significantly affect the operation of the entire network. In high wind penetration hybrid systems, the wind turbines might, at times, produce more power than the instantaneous system load. This could require the conventional generator to be shut off completely or cause additional loads to be turned on to absorb the extra power. Because of the significant effects of introducing renewable power into such a grid, these hybrid systems must be designed and analyzed as a complete interacting system.

In this section a number of issues related to hybrid power systems will be considered. The section includes:

- a review of issues related to diesel-powered grids;
- an overview of hybrid system design issues;
- a description of the components of a complete hybrid power system;
- information on computer models for hybrid systems.

10.3.1 Independent Diesel-powered Grids

Independent diesel-powered electrical grids include the diesel generators, a power distribution system, electrical loads, and some form of system supervision.

10.3.1.1 Diesel Generators

Generators in independent power systems are normally diesel engines directly coupled to synchronous generators. The frequency of the AC power is maintained by a governor on the engine or on one of the engines in a multi-diesel application. The real and reactive power in a conventional AC system is supplied by the synchronous generator. This is done in conjunction with the voltage regulator on the generator. DC grids typically use a diesel-powered AC generator with a dedicated rectifier.

Figure 10.1 illustrates fuel consumption (including a linear fit to the data) for a typical small diesel generator set that might be used in an existing hybrid grid. It can be seen that the no-load
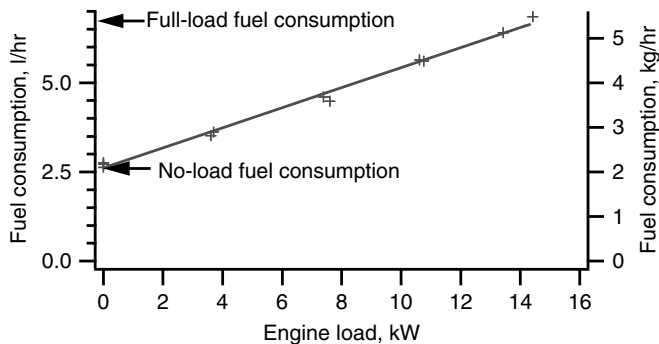
Figure 10.1 Sample diesel engine fuel consumption with linear fit

fuel consumption may be a fairly high fraction of the full-load fuel consumption. Large modern diesels have somewhat lower relative no-load fuel consumption than in this example, but still consume a significant amount of fuel at low loads. Obviously, substantial fuel savings could be achieved if a lightly loaded diesel generator could be shut down.

Diesel fuel at remote locations is often expensive. These diesels often operate at low load and with poor fuel efficiency. Reducing the load or shutting off diesels reduces fuel costs. This may be the goal of the introduction of renewable power, but it also has negative consequences. Reducing the load on a diesel engine can increase engine maintenance requirements, increase engine wear, and, consequently, decrease engine life. Frequent starts and stops significantly increase engine wear. To improve total system economics, a minimum diesel load is often required while the diesel is running and a minimum diesel run time may be specified. Each of these measures increases fuel consumption compared to operation with frequent starts and stops and operation at no load, but these measures are designed to improve overall system economics by reducing diesel overhaul and increasing replacement intervals.

10.3.1.2 Electrical Loads

Electrical loads in independent AC systems are primarily of two types: resistive or inductive. Resistive loads include incandescent light bulbs, space and water heaters, etc. Devices with electric motors are both resistive and inductive. They are a major cause of the need for a source of reactive power in AC systems. DC sources can only supply resistive loads. DC loads may have an inductive component, but this only causes transient voltage and current fluctuations during changes in system operation.

10.3.1.3 System Supervision

System supervision in conventional diesel-powered systems may be automated, but usually consists of a system operator turning diesel generators on and off as the anticipated load changes, synchronizing them with the other operating diesels, and performing engine maintenance when needed.

10.3.2 Overview of Hybrid System Design Issues

The design of hybrid power systems depends on the specifics of the existing power system and on the match of the load and the available renewable resource. Given these constraints, there are numerous options including the wind turbine design, the amount of wind penetration, the inclusion of other renewable power sources, the amount of any energy storage, and the nature of any load management. A review of the issues related to hybrid power system design follows.

10.3.2.1 Match of Electrical Load and Resource

A determining factor in hybrid power system design is the interdependence of the system electrical load and the power produced by the hybrid system. Over short time frames, the load needs to equal the power produced to ensure system stability. To provide a consistent energy

supply over long time periods, a hybrid system may need either longer term energy storage or backup conventional generation.

To maintain system stability, power flows need to be balanced over short time frames. The frequency regulation of an electrical system is a function of the rotating inertia in the system, the fluctuating load, and the responsiveness of the prime mover and its control system. The faster the prime mover can respond to changing power flows, the better the frequency regulation. In high-penetration systems, the prime mover may not have the capability to respond to changing power flows. In that case, additional controllable sources or sinks for power need to be used to control the system frequency. These may be loads that can be switched on to balance power flows, subsystems for the short-term storage and production of power (with a few minutes to an hour of storage), or additional generators that can be brought online. In high-penetration systems, the conventional generators may be turned off when the renewable power can supply the entire load. In that case, the system has fairly low inertia and, without another rapidly controllable power source to control frequency, the system frequency can deviate significantly from its set-point.

Power or energy flows also needs to be balanced over longer time frames. If the load peaks in the daytime and the wind blows only at night, then the wind can be used neither to supply energy to the daytime load nor to save fuel. In such a case, the addition of longer-term energy storage (systems with a few hours to a day of storage) would allow the wind energy to be stored and used later. Long periods of lack of renewable power would deplete any energy storage and require the use of conventional generation, which would need to be capable of supplying the whole load.

Based on the considerations above, it is apparent that a hybrid system might benefit from the addition of energy storage and/or controllable loads. Energy storage could provide power for periods when the wind power is less than the load. When the wind power is greater than the load, energy storage and controllable loads could provide sinks for excess power. With multiple sources and sinks for power, a hybrid power system would also need a system supervisory controller (SSC) to manage power flows to and from system components.

10.3.2.2 System Design Constraints

A number of factors affect the specifics of the design of a hybrid system, including the nature of the load, the characteristics of the diesel generators and electrical distribution system, the renewable resource, fuel costs, availability of maintenance personnel, and environmental factors.

- **Electrical load.** The magnitude and temporal profile of the local load affect the rated system capacity, energy storage needs, and control system algorithm.
- **Diesel generation and electrical distribution system.** In existing power systems, the fuel consumption and electrical characteristics of any existing power generation system affect the economics of the hybrid system, equipment selection, and the control system design. Fuel costs are one important factor in determining system operating cost. In new systems, the generation and distribution systems can be designed in conjunction with the design of the hybrid components.

- **Renewable resource.** The magnitude, variability, and temporal profile of the renewable resource, whether it is wind, solar, hydropower, and/or biomass affect the choice of renewable power system, the control strategy, and storage requirements.
- **Maintenance infrastructure.** The availability of trained operating and maintenance personnel affects the long-term operability of the system, operating costs, and installation costs.
- **Site conditions.** Site constraints such as the nature of the terrain, local severe weather conditions, and the remoteness of the site affect the ability to get equipment to the site, equipment design requirements, and operating system requirements.

In projects with an existing generation and distribution system, the system design objective is usually the minimization of the cost of energy by reducing fuel consumption and the increase of overall system capacity to enable continued local economic development. New systems are often implemented as an alternative to other options such as grid extension.

10.3.2.3 Hybrid Power System Design Rules

There are many factors affecting the design of a high-penetration hybrid power system and many choices of components that need to be considered to optimize system cost and efficiency. Design choices include the type, size, and number of wind turbines, solar panels, etc., the instantaneous and long-term energy storage capacity, the size of dump loads, possibilities for other load management strategies, and the control logic needed to decide when and how to use each of the system components. Thus, the problem becomes one of designing a complicated power system with multiple controllable power sources and sinks. The possibilities for controllable loads will depend on the fit of any given load management approach with the daily needs of the local community. Evaluating all of the parameters is most easily done with a computer model intended for hybrid system design (see Section 10.3.4).

Typically, hybrid power systems have been developed by introducing renewable power into existing isolated grids in order to reduce high fuel costs and to provide increased energy. In trying to predict the performance of a hybrid power system, it is worth considering the limiting possibilities. In an ideal diesel grid, the diesel fuel consumption would be exactly proportional to the power generated. Thus, the fuel use would be proportional to the load. When renewables are added, the effect is to reduce the load that must be served by the diesel generators. If there were a perfect match between the load and renewable power, the diesel load could be reduced to zero. All the renewable power produced (up to the amount of the load) would be used, but any power produced in excess of that would have to be dumped or otherwise dissipated. If there were a temporal mismatch between the load and the available renewable power, even less of the latter would be used. This gives rise to the following rules:

Rule 1: The maximum renewable energy that can be used is limited by the load.
Rule 2: The use of renewable energy will be further limited by temporal mismatch between the load and the renewables.

The introduction of energy storage increases the use of the renewable resource when there is a temporal mismatch between the load and the renewable resource. Based on Rules 1 and 2,

the maximum possible improvement in the use of renewable energy afforded by use of storage is limited by the mismatch between its availability and the load.

In practice, the fuel use of diesel generators never varies in exact proportion to the load. Diesel generator efficiency virtually always decreases with decreasing load. However, a diesel generator system which includes storage may be optimized to improve its performance. This gives rise to two more rules:

Rule 3: The maximum possible benefit with improved controls or operating strategies, without using renewables, is a system approaching the fuel use of the ideal diesel generator – fuel use proportional to the diesel-served load.

Rule 4: The maximum fuel savings arising from the use of renewables in an optimized system is never greater than the fuel savings of an ideal generator supplying the proportional reduction in load resulting from the use of renewables.

10.3.3 Hybrid Power System Components

A hybrid system includes diesel generators, renewable generators, a system supervisory controller, and possibly controllable loads and energy storage. Note that storage is actually both a source and a load. To make all of the subsystems work together, one may also include power converters or a 'coupled diesel' system. A schematic of the possibilities for a hybrid system is illustrated in Figure 10.2. The operation of each of these components and the interactions between components is described below.
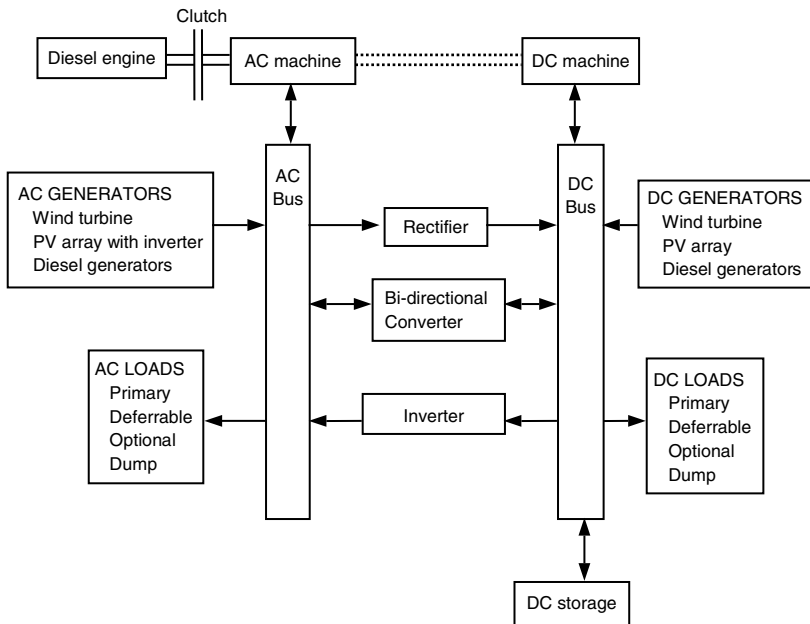
Figure 10.2   Hybrid power system configuration options

Larger systems, usually above 100 kW, typically consist of AC-connected diesel generators, renewable sources, and loads, and occasionally include energy storage. Below 100 kW, combinations of both AC- and DC-connected components are common, as is the use of energy storage.

The components in DC systems may include diesel generators, renewable sources, and storage. Small hybrid systems serving only DC loads, typically less than 5 kW, have been used commercially for many years at remote sites for telecommunications repeater stations and other low-power applications.

The remainder of this section provides more detail on many of these components. Note, however, that batteries are discussed later in this chapter, in Section 10.7.

10.3.3.1 Diesel Generators in Hybrid Systems

In a conventional AC power system, there must always be at least one diesel generator connected to the network in order to set the grid frequency and to supply reactive power. It is possible to modify the system so that the diesel generator is not always required, but in that case other components must be added. These other components could include an inverter, a rotary converter, a synchronous condenser, a clutch, or another power producer such as a wind turbine with a synchronous generator. As described in Chapter 5, an inverter is a device (typically a solid state electronic device) that provides AC power from a DC source. A rotary converter is sometimes used as an electromechanical inverter. In that case, it requires a separate controller to set the frequency. A synchronous condenser is a synchronous electrical machine connected to the network and allowed to spin at a speed determined by the grid frequency. Operating in conjunction with a voltage regulator, it supplies reactive power to the network but does not control grid frequency. Reactive power production may also be achieved with a synchronous generator connected to a wind turbine.

10.3.3.2 Wind Turbines in Hybrid Systems

Wind turbines used in larger isolated AC electrical systems typically have a capacity of 10 kW to 500 kW. Most of the wind turbines in this size range are fixed-speed turbines that use induction generators and so require an external source of reactive power. Thus, in hybrid power systems they can operate only when at least one diesel generator is operating or in systems that have separate sources for reactive power. The starting current of turbines with induction generators also needs to be supplied by the system. Some wind turbines use synchronous generators. If they have pitch control, they may be able to be used to control grid frequency and to provide reactive power. In such cases, these turbines could operate without any diesel generators being online. Other turbines use power electronic converters. Such machines may also be able to run without the presence of a diesel generator.

There are a number of wind turbines that supply DC power as their principal output. These machines are typically in the smaller size range (10 kW or less). With suitable controls or converters they may operate in conjunction with AC or DC loads.

As components in a hybrid power system, control of the wind turbines would need to be integrated into the system supervisory controller.

10.3.3.3 Photovoltaic Panels in Hybrid Systems

Photovoltaic (PV) panels may provide a useful complement to wind turbines in some hybrid power systems. PV panels provide electrical power directly from incident solar radiation. PV panels are inherently a DC power source. As such, they usually operate in conjunction with storage and a separate DC bus. In larger systems they may be coupled with a dedicated inverter and thus act as a *de facto* AC power source.

PV panels provide fluctuating power. Variations of the solar resource on annual and diurnal scales, as well as on the time scales of front-driven weather patterns and the passage of clouds, complicate the design of hybrid systems.

The power generated by PV panels is determined by the solar radiation level on the panel, the panel characteristics, and the voltage of the load to which it is connected. Figure 10.3 shows the current–voltage characteristics of a typical PV panel at a given temperature and solar insolation level. It can be seen that the range of voltages over which a given panel performs effectively is fairly limited. To increase the output voltage, multiple panels are connected in series. To increase the current (and power at a given voltage), multiple panels are connected in parallel. The power produced from a PV panel depends strongly on the load to which it is connected. In particular, the terminal voltage and current of the panel must equal those of the load. In general, photovoltaic panels and loads have different current–voltage relations. At any given operating condition, there is normally only one operating point where both the panel and load have the same voltage and current. This occurs where the panel and load current–voltage curves cross, as illustrated in Figure 10.3.

The power from the panel is equal to the product of the current and the voltage. The maximum power point, where the power is the greatest, occurs at a voltage somewhat less than the open circuit voltage (which is the highest voltage). For the PV panels to be most effective when used with batteries, the nominal battery voltage should be close to the maximum power point voltage. It is sometimes useful to use power-conditioning equipment (maximum power point trackers or MPPT) to match the load with the characteristics of the PV panel. These power electronic converters can adjust the PV array voltage for maximum PV power and
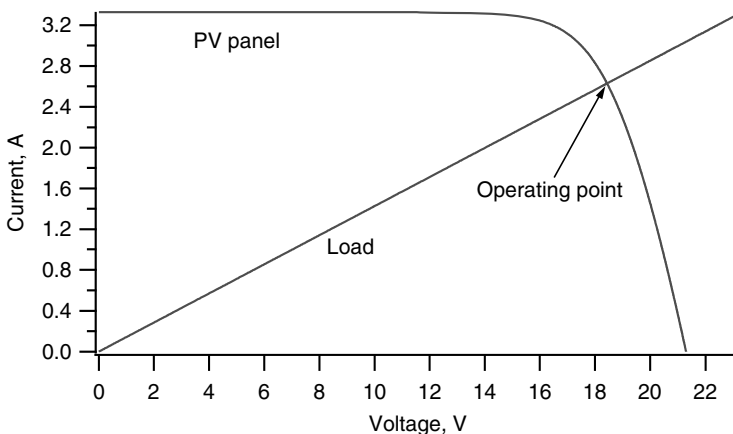
Figure 10.3   Load matching for a photovoltaic PV panel with a given insolation level

convert that resulting PV power so that its voltage is that required by the DC load or the AC grid. The purpose of such a converter is to maximize the power conversion in the electrical parts of the system, whatever the radiation.

10.3.3.4 Controllable Loads

One component which may be required in hybrid power systems, but which is uncommon in conventional isolated systems, is a 'dump load'. A dump load is used to dissipate excess electrical power in the network. Such an excess could arise during times of high renewable contribution and low load. Excess energy could lead to grid instability. The dump load may be based on power electronics or switchable resistors. In some cases, dissipation of excess power may be accomplished without the use of a dump load. An example is the dissipation of excess wind power using blade pitch control.

Load management can also be used in hybrid power systems to augment or take the place of storage or to supplant dump loads. For example, optional loads are those that provide a use for surplus power that would otherwise go to waste. An example would be excess energy that was directed toward space heating that would reduce the need for other fuels. Deferrable loads are those which must be supplied at some time, but for which the exact time is flexible. Consider, for example, a water storage tank that needs to be refilled at least once a day. The pumping is a load that needs to be met, but the exact timing may not matter. In this case, excess energy could be used for water pumping. If there were no excess energy in a day, then energy from battery storage or the diesel generators would need to be used to make sure that the water tank was full at the end of the day.

10.3.3.5 Power Converters

There are two types of power conversion functions of particular significance for hybrid power systems: rectifying and inverting (see Chapter 5). Rectifiers are commonly used to charge batteries from an AC source. Inverters are used to supply AC loads from a DC source, such as batteries and photovoltaic panels.

As mentioned in Chapter 5, most electronic inverters are of one of two types: line-commutated or self-commutated. Line-commutated inverters require the presence of an external AC line. Thus they cannot set the grid frequency if, for example, all of the diesel generators in a hybrid power system are turned off. Self-commutated inverters control the frequency of the output power based on internal electronics. They do not normally operate together with another device that also sets the grid frequency. There are inverters that can operate either in a line-commutated or a self-commutated mode. These are the most versatile, but presently they are also the most expensive.

A rotary converter is an electromechanical device than can be used as either a rectifier or an inverter. It consists of an AC machine (usually synchronous) directly coupled to a DC machine. Each electrical machine can act as either a motor or a generator. When one machine functions as a motor, the other is a generator and vice versa. The advantages of a rotary converter, compared to a solid state power converter, include that it is a well-developed piece of equipment and is normally quite rugged. The main disadvantages are that the efficiency is lower and the cost is greater than solid state devices.
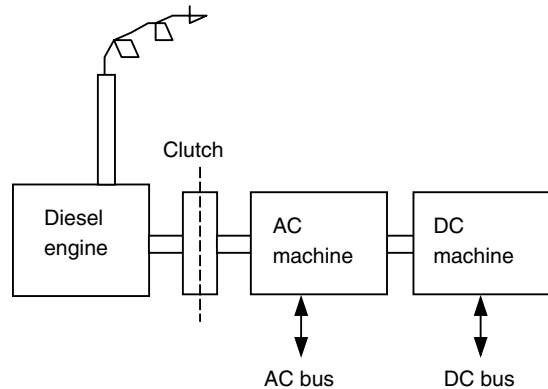
Figure 10.4 Diesel engine coupled to a rotary converter

10.3.3.6 Coupled Diesel

In some hybrid power systems the diesel generator is modified and is then referred to as a 'coupled diesel'. In this arrangement, the engine and AC generator are not permanently connected. Rather, they are coupled by a clutch. The clutch can be engaged or disengaged as required. When the clutch is engaged, the generator is driven by the diesel in the normal way. When it is disengaged, the diesel engine stops, but the generator will continue to turn if it is still electrically connected to the network and there is another source of electrical power in the system. In this case the AC generator may serve as a synchronous condenser, supplying reactive power. This concept is most useful when the other source of electrical power is an induction generator, which requires a reactive power source.

In a variant of the coupled diesel, the diesel engine is coupled by clutch to a rotary converter (see Figure 10.4). The advantage of this concept is that it provides a more efficient means of incorporating a rotary converter than would be the case if the diesel engine were associated only with its own generator and there were a separate rotary converter.

10.3.3.7 System Supervisory Control

Most hybrid power systems incorporate numerous forms of control. Some control functions are carried out by dedicated controllers that are integral to the system components. Typical examples include the governor on a diesel, the voltage regulator on a synchronous generator, the supervisory controller on a wind turbine, or the charge controller in a battery bank. Overall system control is accomplished by the system supervisory control (SSC). The system supervisory control might control some or all of the components indicated in Figure 10.5. This control is usually thought of as automatic, but in reality some of the functions may be carried out by an operator. Specific functions of the system supervisory controller may include turning diesel generators on and off, adjusting their power set points, charging batteries, and allocating power to a controllable load. Supervisory control may also be integrated into a component recognition and communication system ('plug and play') such as described by Abdulwahid *et al.* (2007).
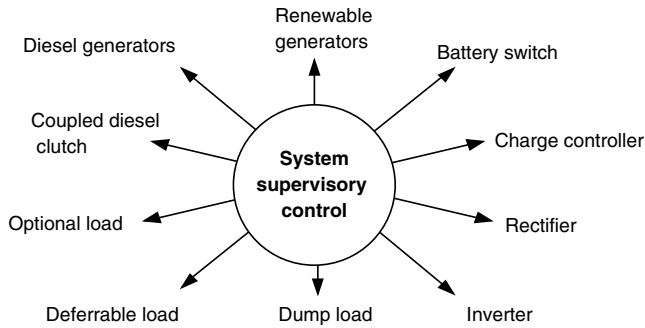
Figure 10.5   Functions of system supervisory control

10.3.4 Hybrid System Modeling

Many simulation models have been developed for hybrid power system design. See, for example, articles by Infield *et al.* (1990) and Manwell *et al.* (1997). Generally, one can classify these models into two broad categories: logistical and dynamic models.

Logistical models are used primarily for long-term performance predictions, component sizing, and for providing input to economic analyses. Generally, they can be divided into the following three categories:

- **Time series (or quasi-steady state).** This type of model requires the long-term time series input of variables such as wind speed, solar insolation, and load.
- **Probabilistic.** Models of this type generally require a characterization of long-term load and resource data (e.g. monthly or seasonal) as inputs. The analytical model is based on the use of statistical modeling techniques.
- **Time series and probabilistic.** As the name implies, models in this category are based on the use of a combined time series and statistical approach.

Some examples of widely used logistical models are Hybrid2 (University of Massachusetts), HOMER (National Renewable Energy Laboratory), and RETScreen (National Resources Canada).

Dynamic models are used primarily for component design, assessment of system stability, and determination of power quality. They are generally used for hybrid power systems with no storage capability, or systems with minimal storage, such as a flywheel. Depending on the time step size and the number of modeled components, they can be divided into the following three categories:

- **Dynamic mechanical model.** This type of model is based on the mechanical equations of motion and power balances. It can be used to get a first approximation of the dynamic behavior of a system and to find such long-term effects as the start–stop behavior of the diesel engine component.
- **Dynamic mechanical, steady state electrical model.** This class of model is based on the mechanical equations of motion and the steady state equations of the electrical components of the system. It can give a first approximation of the electrical behavior of the system.

- **Dynamic mechanical and electrical model.** Models of this type are based on the dynamic equations of motion of the mechanical and electrical components of the system. They are intended to investigate the electrical stability of the system (millisecond scale) and mechanical vibrations.

A variety of dynamic wind/diesel system simulation codes have been developed over the years. Typically, these have been specific to an application and have not been widely used beyond the application for which they have been developed. An example of one of these models is RPM-SIM (National Renewable Energy Laboratory).

10.4 Offshore Wind Energy

Offshore wind energy, as the name implies, refers to electricity produced by wind turbines that are installed offshore and implicitly in the ocean (or in lakes). The last twenty years has seen a great deal of interest in this technology. The primary impetus for this has been the lack of available land with a good wind resource for new turbines, particularly in northern Europe.

This section will review the history, current technology, and state of the art of offshore wind energy. Similar to land-based wind systems, the topic of offshore wind energy is quite broad and encompasses technology, environmental issues, economics, etc.

10.4.1 History of and General Considerations for Offshore Wind Energy

The first concepts of offshore wind turbines were developed by Hermann Honnef in Germany in the 1930s (Dörner, 2009). Extensive offshore wind farms off the coast of Massachusetts were proposed in the early 1970s (Heronemus, 1972), but they were never built. The first actual offshore wind turbine was installed in Sweden in 1991 and the first real offshore wind farm was constructed in 1992 in shallow (2–5 m) water off the coast of Denmark near the town of Vindeby. The Vindeby wind farm, which is still operating, consists of eleven 450 kW machines approximately 3 km from the shore. Since then, offshore wind turbines have been installed in the Netherlands, the United Kingdom, Sweden, Ireland, Germany, and China. In 2002 and 2003, the first large, utility-scale offshore farms were commissioned. The Horns Rev and Nysted wind farms, both in Denmark, were the first farms built with capacities exceeding 100 MW. As of the end of 2008, there was over 1000 MW of installed offshore wind capacity, most of it in Europe.

Offshore wind energy has several promising attributes. These include:

- greater area available for siting large projects;
- proximity to cities and other load centers;
- generally higher wind speeds compared with onshore locations;
- lower intrinsic turbulence intensities;
- lower wind shear.

There are some challenges as well, most notably:

- higher project costs due to a necessity for specialized installation and service vessels and equipment and more expensive support structures;
- more difficult working conditions;

- more difficult and expensive installation procedures;
- decreased availability due to limited accessibility for maintenance;
- necessity for special corrosion prevention measures.

  The main considerations in offshore wind energy are the following:

- wind resource;
- offshore wind turbines themselves;
- external design conditions;
- characteristics of prospective sites;
- offshore wind farm design and layout;
- offshore wind farm operation and maintenance;
- offshore environmental issues;
- offshore wind energy economics.

10.4.2 Offshore Wind Turbines and their Support Structures

The basic component of an offshore wind energy project is the offshore wind turbine itself. It is defined as 'a wind turbine with a support structure which is subject to hydrodynamic loading' (IEC, 2009). This type of wind turbine consists of the following components (see also Figure 10.6.)
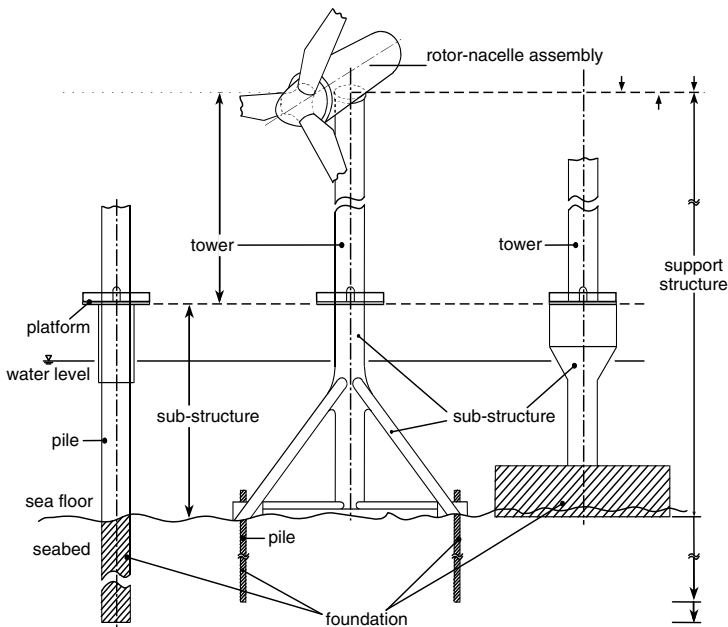
Figure 10.6 Components of an offshore wind turbine (GL, 2005). Reproduced by permission of Germanischer Lloyd

- **Rotor-nacelle assembly (RNA).** This is the part of a wind turbine carried by the support structure. It includes:
  - o **rotor** – part of a wind turbine consisting of the blades and hub;
  - o **nacelle assembly** – part of a wind turbine consisting of all the components above the tower that are not part of the rotor. This includes the drive train (shafts, couplings, gearbox, generator(s), and brakes), bed plate, yaw system, and the nacelle enclosure.
- **Support structure.** This consists of the tower, substructure, and foundation:
  - o **tower** – part of the support structure which connects the substructure to the rotor-nacelle assembly;
  - o **substructure** – part of the support structure which extends upwards from the seabed and connects the foundation to the tower;
  - o **foundation** – part of the support structure which transfers the loads acting on the structure into the seabed.

10.4.2.1 Support Structure Options for Offshore Wind Turbines

A number of different support structure designs may be considered for offshore installations. Three of these designs were illustrated in Figure 10.6. The most common type of support structure is the monopile. Monopiles are steel tubes in the range of 2.5–4.5 m in diameter. Monopiles are most often driven 10–20 m into the seabed, but in harder soils or rock, drilling may be necessary. No seabed preparation is normally needed, although heavy-duty pile-driving equipment is required. Monopiles may not be suitable in a seabed with large boulders.

The second most common option is the gravity structure. Gravity structures achieve stability through their total weight (including ballast) and large base area. The base area is able to help counter the overturning moment of the wind turbine by passively varying the distribution of loads transmitted to the sea floor – the same way a wine glass achieves stability. A gravity structure consists of a circular base 12–18 m in diameter and weighing between 500–1000 tonnes. An inner structure which will connect to the tower is situated in the center of the circular base. This inner section may be fabricated together with the outer part, or it may be separate. Sections must be separate if the outer part is to be floated to the site of installation. Most often the gravity structure is constructed of reinforced concrete, but steel structures have also been proposed. In some cases, the top of the structure is conical in shape so as to break up floating ice. Rip-rap is often placed around the circumference of the base to protect against erosion due to currents. The total ballasted weight of a concrete gravity structure may be well over 1000 tonnes. The actual weight will depend on the specifics of the wind turbine and the site. The weight of a concrete gravity structure will also increase more than linearly with water depth, so such structures are often less attractive for deeper water. The sea floor must be prepared before the gravity structure is lowered into place. This consists essentially of making the location where the structure will go uniform and level. Dredging is typically used for this activity.

Steel gravity structures could be made of an upright cylindrical steel tube placed on a flat steel box on the seabed. These structures would be lighter than corresponding concrete structures; they would be filled with dense ballast, however, once placed in their intended location. They may be applicable for deeper water than concrete structures since their unballasted weight would not increase as rapidly with depth. They would also be easier to transport because of their lower weight.
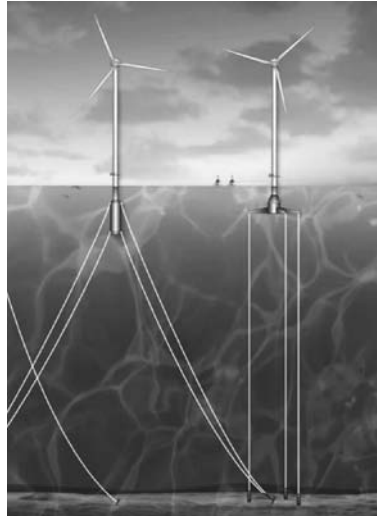
Figure 10.7 Conceptual wind turbines supported by spar buoy (left) and TLP (right) (National Renewable Energy Laboratory)

Multimember support structures typically are fabricated from three or four angled tubular members welded to a central tubular member, and then via even smaller members to each other. Additional, shorter tubing provides guides for relatively small pilings that are used to hold the structure in place. One type of multimember support structure is the tripod, such as was illustrated in Figure 10.6. Another type of multimember structure is the 'jacket'. This is the four-legged structure commonly used in the offshore oil and gas industry. Multimember structures need minimal site preparation and are suitable for greater water depths.

For deeper seas, floating wind turbines have been proposed using spar buoys to support one or more individual turbines (Heronemus, 1972). A spar buoy is a closed cylinder which floats upright in the water. Stability is maintained by counterbalancing the weight of the RNA and the thrust loads with ballast at the bottom of the spar. The buoy is kept in place by catenary mooring lines and anchors. Another concept is the tension leg platform (TLP), which is used by the offshore oil and gas industry for deeper waters. A TLP consists of a floating platform, which is kept in place by tendons under tension. The tendons are attached to anchors on the ocean floor as well as to the bottom of the platform. Wind turbines mounted on a spar buoy and TLP are illustrated in Figure 10.7.

10.4.2.2 Design Considerations for Offshore Wind Turbines

The detailed design of the rotor-nacelle assembly of offshore wind turbines is at present similar to that of onshore turbines, but there are significant differences as well. These differences relate primarily to the very different external conditions which the turbines experience in the marine environment. These conditions are the subject of Section 10.4.4. The design of the support structure is quite different from that of onshore turbines, however. Bottom-mounted support structures must resist wave action, while floating support structures must also be

designed to minimize interactions between the periodic excitation by the waves and turbine dynamics. The primary considerations in the design of the support structures for bottom-mounted offshore wind turbines are the water depth, the sub-bottom soil characteristics, and the meteorological/oceanographic ('metocean') design conditions. Finally, the turbine tower needs to be high enough to provide clearance between the blades and the highest expected sea, including waves and high tides.

Further discussion of the support structures themselves for offshore wind turbines is outside the scope of this text. The reader is referred to the IEC offshore wind turbine design standards (IEC, 2009) and the many PhD dissertations from the Technical University of Delft and other universities for more in-depth discussion. These include Kühn (2001), Cheng (2002), van der Tempel (2006), and Veldkamp (2006).

10.4.3 The Offshore Wind Resource

The wind resource offshore is one of the key factors that make offshore wind energy attractive. Winds over open water are invariably higher, exhibit less shear, and are intrinsically less turbulent than over adjoining land. In addition, the average wind speed increases with distance from shore (up to approximately 50 km). At the same time, the wind shear and turbulence intensity decrease. For example, Figure 10.8 illustrates the average wind speeds and average wind power density for the coast of Massachusetts. As can be seen, average wind speeds increase from less than 7 m/s onshore to 7.5 m/s near shore and over 9 m/s in the open ocean.
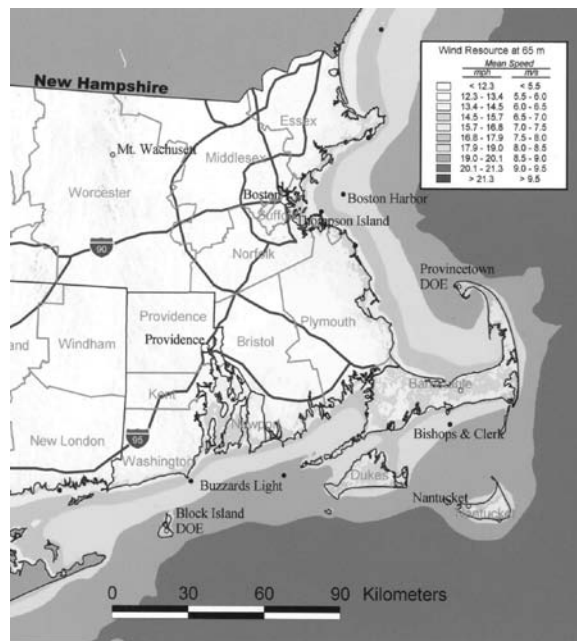
Figure 10.8 Wind resource off the coast of Massachusetts (Massachusetts Technology Collaborative)

The higher wind speeds result in higher productivity. For example, all other things being equal, a typical MW scale wind turbine which has a capacity factor of approximately 29% in a 7 m/s average wind regime, would produce 28% more energy in an 8 m/s average wind and 53% more in a 9 m/s average wind.

Lower wind shear also means that, in general, tower height can be lower offshore than is often necessary on land. This reduced tower height can, to some degree, compensate for the substantially greater support structure which is required below the water level.

The effect of reduced offshore turbulence is generally beneficial, but not completely so. On the positive side, wind turbines generally perform better in less turbulent winds. On the other hand, less turbulence means that downstream wakes take longer to recover than when the winds are more turbulent. Thus, spacing between wind turbines may need to be greater offshore than it would be on land. This whole matter is also further complicated by the turbulence which is generated within the wind farm by the motion of the rotors.

Higher wind speeds, lower wind shear, and lower turbulence are related phenomena, and arise because the water surface is so much smoother than the land. This smoothness appears in the physics of the wind through the lower surface roughness, which is on the order of 0.0002 m. See, for example, Barthelmie *et al.* (1996). In contrast to the land, however, surface roughness of the water may change with time, particularly as a function of wave height. This is discussed in more detail below.

The following provides an overview of some of the characteristics of the wind that are unique to offshore.

10.4.3.1 Offshore Wind Shear

The variation in wind speed with height (wind shear) over water is typically modeled with the logarithmic equation introduced in Chapter 2. To a first approximation, a homogeneous surface with neutral stability may be assumed. The mean wind speed, $U(z)$, at a height z is then described by:

$$U(z) = \frac{U_*}{\kappa} \ln\left(\frac{z}{z_0}\right) \tag{10.1}$$

where U_* is the friction velocity (see Chapter 2), κ is the von Karman constant ($\kappa = 0.4$), and z_0 is the roughness length. If the wind speed at a reference height, z_r, is known, then the logarithmic wind shear model, discussed in Chapter 2, may be used.

At any given time, the water surface roughness length varies with wave height and so is a function of wind speed and fetch (distance from shore). Consistent with this, Lange and Højstrup (1999) have shown that roughness length of the Baltic Sea increases with wind speed over the range of wind speeds typically used for power production.

The Charnock model is often used for modeling the change in sea surface roughness length as a function of wind speed:

$$z_0 = A_C \frac{U_*^2}{g} \tag{10.2}$$

where g is the gravitational constant and A_C is the Charnock constant. A_C is often assumed to be 0.018 for coastal waters. The friction velocity was defined in Chapter 2 as $U_* = \sqrt{\tau_0/\rho}$ where

τ_0 is the surface shear stress. The shear stress is, in turn, related to the wind speed and, for offshore, to the height of the waves.

Another, more direct, method to estimate roughness length (see Hsu, 2003) as a function of wave parameters is Equation (10.3):

$$\frac{z_0}{H_s} = 1200\left(\frac{H_s}{L_P}\right)^{4.5} \tag{10.3}$$

where H_s = significant wave height and L_p = peak period wavelength (see Section 10.4.5)

10.4.3.2 Offshore Turbulence

Turbulence intensity is lower offshore than on land because of the lower surface roughness and lower vertical temperature gradients. The temperature gradients are lower because of the high specific heat of water, which results in relatively constant water temperature. In addition, sunlight penetrates several meters into water, whereas on land it only hits the uppermost layer of soil, concentrating the heat near the surface. Offshore turbulence intensity also decreases with height.

As noted previously, however, although the intrinsic turbulence intensity at offshore sites may be lower than at sites on land, once a wind farm has been built the average turbulence intensity may increase significantly. This is due to the operation of the turbines and the wakes that result.

10.4.4 Meteorological-oceanographic (Metocean) External Design Conditions

For the design of wind turbines on land, the primary external condition to consider is the wind itself. Offshore, however, waves can be of comparable importance. They are of particular relevance to the design of the support structure. Wind conditions as they affect turbine design were discussed in Chapter 7. This following section focuses on waves. Other factors may also be significant. Some of these are discussed briefly below as well.

10.4.4.1 Waves

First of all, it should be noted that most waves originate as a result of the wind. The shear force due to the wind along the surface of the sea causes some of the water to move. This motion ultimately becomes periodic and manifests itself as waves. In deep water and under the influence of relatively low wind speeds, the wave motion is quite regular. In the presence of higher wind speeds the motion can become quite complex.

Some terminology is useful here. The term 'sea' describes a situation in which waves are being formed; 'sea state' refers to characteristics of the sea in terms of wave height, period, and direction; 'fully developed sea state' indicates that power in from the wind equals power being dissipated in breaking waves.

Waves are typically classified into one of three categories: (1) regular waves, (2) irregular waves, (3) random waves. The easiest waves to describe are regular waves. These are also
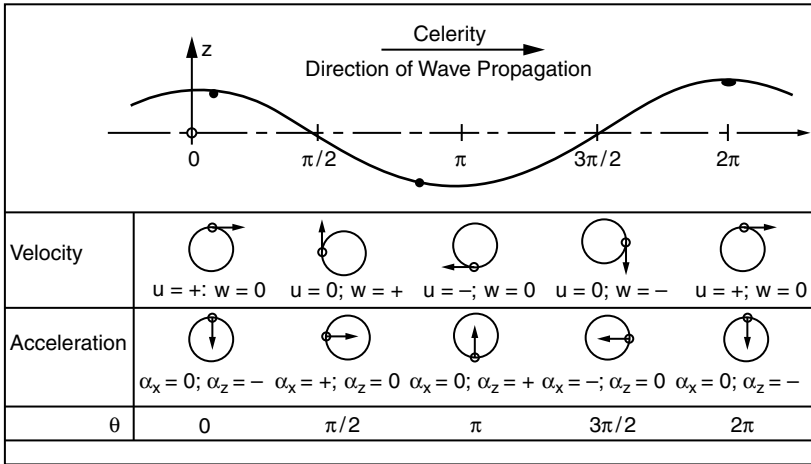
Figure 10.9   Particle motion in Airy waves (USACE, 2002)

known as first order, small-amplitude, or Airy waves. Their behavior was first described by
G. B. Airy (Airy, 1845).

The following is a summary of the most important features of waves. More information
on waves may be found in such sources as the Coastal Engineering Manual (USACE, 2002)
or Ochi (1998).

Regular (Airy) Waves

The Airy model is most applicable to deep water swell, but it provides a useful and elegant
starting point for discussion of more complex wave behavior as well. The motion of the water
in the Airy model is illustrated in Figure 10.9.

Some of the key parameters of the Airy model are the following:

- the wave profile is defined by $\zeta = \hat{\zeta}\cos(kx - \omega t)$ where $\hat{\zeta}$ is the amplitude of the waves
  (1/2 the height, H);
- the wave number, k, is $k = 2\pi/L$ where $L =$ wavelength;
- the angular frequency is $\omega = 2\pi/T$ where $T =$ wave period;
- the water particle trajectories are circular orbits with radius $= \hat{\zeta}\, e^{kz}$, where z is the distance up
  from mean water level;
- the pressures at the wave's crest and trough are, respectively, $p_c = \rho_w g\hat{\zeta}\, e^{kz} - \rho_w gz$ and
  $p_t = -\rho_w g\hat{\zeta}\, e^{kz} - \rho_w gz$, where ρ_w is the density of water and d is the water depth to mean
  water level;
- the wave celerity, c, is the speed at which the wave crest moves.

The assumptions of the Airy model include the following:

- water is homogeneous and incompressible;
- surface tension is neglected;
- coriolis effects are neglected;

- the pressure at the free surface is constant;
- viscosity is neglected;
- waves do not interact with other water motions;
- the flow is irrotational;
- there is no velocity at the seabed;
- the amplitude is small and the waveform is invariant in time and space;
- the wave is long-crested (two-dimensional).

According to the Airy model, wave motion can be described in terms of a velocity potential, Φ, which may be shown to be the following:

$$\Phi(x, z, t) = \frac{\hat{\zeta} \, g}{\omega} \frac{\cosh(k(z-d))}{\cosh(kd)} \cos(\omega \, t - kx) \tag{10.4}$$

Using the velocity potential it may further be shown that the wavelength, L, is given by:

$$L = \frac{gT^2}{2\pi} \tanh\left(\frac{2\pi \, d}{L}\right) \tag{10.5}$$

For many situations, the wavelength may be approximated as:

$$L = \frac{gT^2}{2\pi} \sqrt{\tanh\left(\frac{4\pi^2 d}{T^2 g}\right)} \tag{10.6}$$

Equation (10.6) above is convenient because the wavelength only appears on one side.

The forward speed of the wave (its celerity, c) is given by:

$$c = L/T \tag{10.7}$$

There are some additional approximations for wavelength, but there are differences according to water depth. In deep water, for example, the following relation holds:

$$L = \frac{gT^2}{2\pi} = \frac{9.8}{2\pi} T^2 \approx 1.56 \, T^2 \tag{10.8}$$

The actual motion of the water particles also changes according to depth. In deep water the path is circular; the path becomes more oval when the depth is shallower.

The velocity and acceleration of the water are often useful, particularly for the calculation of forces. For Airy waves, the horizontal components of these, U_w and $\dot{U}_w$, are:

$$U_w = \frac{H}{2} \frac{gT}{L} \frac{\cosh[2\pi(z+d)/L]}{\cosh(2\pi d/L)} \cos(\theta) \tag{10.9}$$

$$\dot{U}_w = \frac{H}{2} \frac{gT}{L} \frac{\sinh[2\pi(z+d)/L]}{\cosh(2\pi d/L)} \sin\theta \tag{10.10}$$

Other Types of Waves

There are other types of waves and wave models as well. In some cases, waves appear to be nearly regular Airy waves, as described above, but they do not have a sinusoidal cross-section.
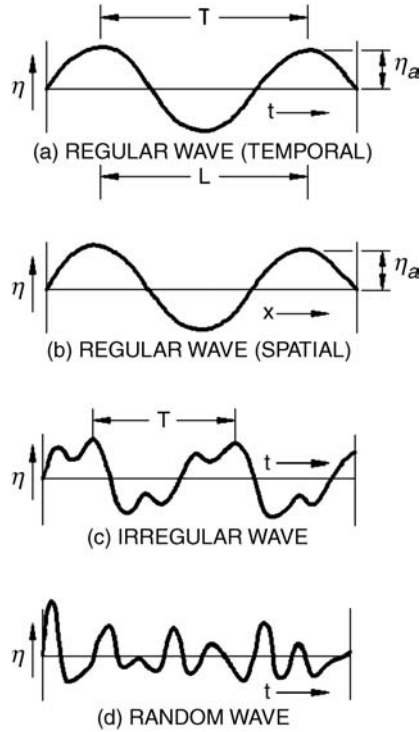
Figure 10.10   Various types of waves (USACE, 2002)

Approaches to modeling them include Stokes waves (of various orders), Cnoidal waves, and Boussinesq waves. Also of interest are: (1) irregular waves, (2) random waves, (3) breaking waves, and (4) extreme waves. Irregular waves are those which do not have a single wavelength and uniform height. Random waves are non-repeating irregular waves. A breaking wave is one whose base is unable to support the peak, causing it to collapse. An extreme wave is a wave that is relatively high but relatively rare. Figure 10.10 illustrates the cross-sections of some of the types of waves. Random waves are discussed in some detail below; breaking waves and extreme waves are described briefly. Detailed discussion of the other wave models is outside the scope of this text.

(i) Random Waves

Waves from different directions, distances, and sources combine to produce random waves, as illustrated in Figure 10.11. Random waves are important in offshore wind energy because they may have a significant effect on the design of the support structure. In particular, the relation between the frequency of the waves and the natural frequencies of the structure needs to be considered. Random waves are unlike regular waves in that within any given wave train there are waves with different heights and wavelengths. This is illustrated in Figure 10.12.
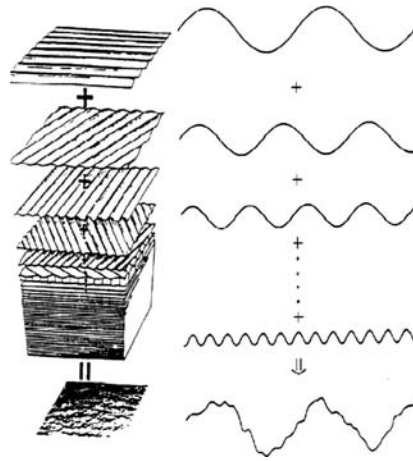
Figure 10.11   Formation of random waves (USACE, 2002)

The important considerations in characterizing a random sea state are the following:

- significant wave height;
- peak period;
- distributions of wave heights.

Analysis of the random sea is carried out using statistical and spectral methods (see Appendix C). The fundamental characterization of a sea state is the significant wave height, H_s. Historically, this was estimated by sailors as the average of the highest third of the waves that could be seen from their ship. Nowadays, it is taken to be four times the standard deviation of the sea surface height. This standard deviation is, in turn, based on the spectral description of the waves, as is discussed below.
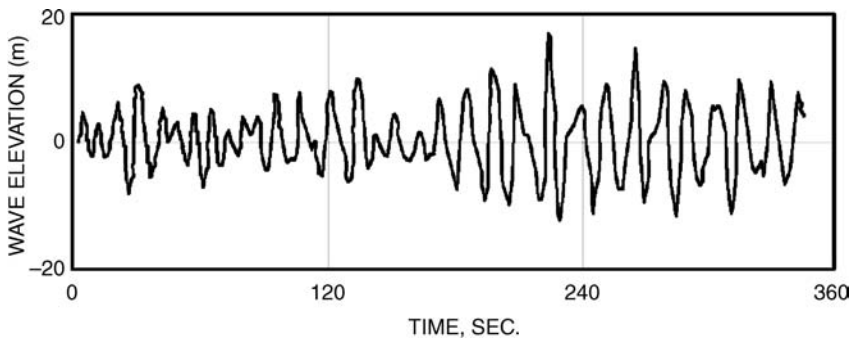
Figure 10.12   Typical wave train (USACE, 2002)

The peak period, T_P, is the wave period associated with the most energetic waves. Strictly speaking, it is the inverse of the frequency, f_p, at which the wave spectrum reaches its maximum value (see below). The peak wavelength, L_p, is that wavelength associated with the peak period.

The spectral method assumes that the sea state can be characterized by a spectrum. Wave spectra, $S(f)$, are energy densities in terms of frequency. They relate the energy in the waves (based on the square of the displacement of the sea surface from the mean water level) to the wave frequency. As is standard with spectra, the integral over all frequencies is equal to the variance, σ_H^2, as illustrated in Equation (10.11).

$$\sigma_H^2 = \int_0^{H_{\max}} S(f)\mathrm{d}f \tag{10.11}$$

where $H_{\max}$ = the maximum wave height.

The significant wave height is then defined by:

$$H_s = 4\sigma_H = 4\sqrt{\int_0^{H_{\max}} S(f)\mathrm{d}f} \tag{10.12}$$

The most common wave spectrum used is known as the Pierson–Moskowitz (PM) spectrum. It is most applicable to deep water, but it is often used for other situations as well. The Pierson–Moskowitz spectrum is given by:

$$S_{PM}(f) = 0.3125 \cdot H_s^2 \cdot f_p^4 \cdot f^{-5} \cdot \exp\left(-1.25\left(\frac{f_p}{f}\right)^4\right) \tag{10.13}$$

where:

H_s = significant wave height, m
f_p = peak frequency ($=1/T_p$), Hz
f = frequency, Hz

Figure 10.13 illustrates the PM spectrum for a sea state with H_s equal to 2.25 m and T_p equal to 7.13 s.

Another commonly used spectrum is the JONSWAP. This spectrum is a modification of the Pierson–Moskowitz. It is more applicable to a developing sea in a fetch-limited situation. The spectrum accounts for a higher peak and a narrower spectrum in a storm situation for the same total energy as compared with the PM spectrum. The JONSWAP spectrum is therefore often used for extreme event analysis. More discussion of this spectrum may be found in USACE (2002).

(ii) Breaking Waves

So far, we have only considered non-breaking waves. For some applications, particularly in shallow water, breaking waves are likely. A breaking wave is one whose base can no longer support its top, causing it to collapse. Waves will break in shallow water when the height of the wave is greater than 0.78 times the water depth. See Barltrop and Adams (1991) for more detail on this. The forces resulting from a breaking wave can be considerably higher than from a non-breaking wave of equivalent height. This phenomenon is examined in detail by Wienke (2001).
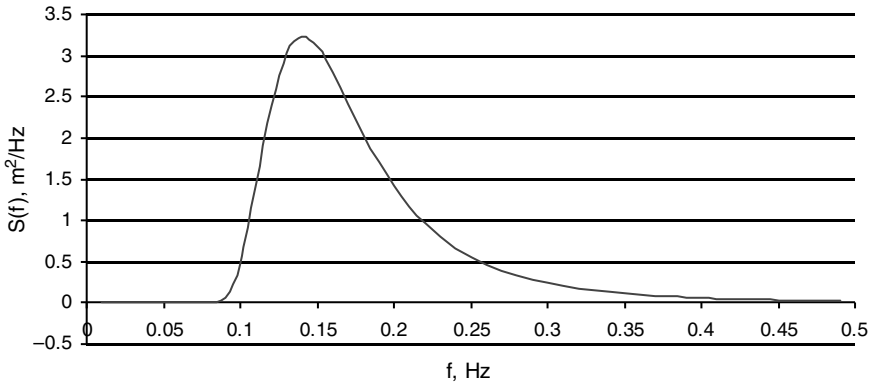
Figure 10.13   Example of Pierson–Moskowitz spectrum

(iii) Extreme Waves

As discussed in Chapter 2, it is important to have an estimate of the highest expected wind speeds when designing the rotor and other major components of a wind turbine. Similarly, it is necessary to know what the maximum wave height is likely to be at a given site over an extended time period. Such estimates are relevant to the design of the support structure. Maximums of particular interest include: (1) the highest wave within a sea state, (2) the highest wave over some longer period of time, such as one year or 50 years. Maximum wave heights may be estimated by considering wave trains in the time domain. The Rayleigh distribution (see Chapter 2) may be used to model the frequency of occurrence of waves of different heights within a sea state. One can estimate the total number of waves (based on the mean wave period), then use the cumulative probability to estimate the highest wave. For example, if there were 1000 waves in the sea state, then the highest wave would be that value which was exceeded 0.1% of the time. For longer periods, such as 50 years, the extreme wave height can be estimated by applying the Gumbel distribution to the occurrences of high waves over a shorter period (at least a year, preferably longer) and applying a similar process. See Chapter 2 or Gumbel (1958) for more discussion of this distribution.

Forces from Waves

When waves impinge on a structure they produce both viscous drag and inertia forces on that structure. Morison's equation is commonly used for the calculation of those forces. Morison's equation for a cylindrical member is:

$$\hat{F} = \frac{1}{2} C_d \rho_w D |U_w| U_w + C_m \rho A \dot{U}_w \tag{10.14}$$

where:

$\hat{F} =$ force per unit length of the member
$C_d =$ drag coefficient
$C_m =$ inertia coefficient
$\rho_w =$ density of water

D = member diameter
A = cross-sectional area of the member
U_w = velocity of the water, resolved normal to the member
$\dot{U}_w$ = acceleration of the water, resolved normal to the member

(ii) Wave Loads on a Monopile

It is of interest to consider the forces and moments due to Airy waves on a slender monopile, because closed-form equations may be developed to describe them. In general, calculations of forces and moments are not so simple.

According to the Airy model, the maximum inertial and drag forces due to waves on a monopile of diameter D in water of depth d are as follows (see van der Tempel, 2006):

$$F_I = \rho_w g \frac{C_m \pi D^2}{4} \hat{\zeta} \tanh(kd) \tag{10.15}$$

$$F_D = \rho_w g \frac{C_d D}{2} \hat{\zeta}^2 \left[\frac{1}{2} + \frac{kd}{\sinh(2kd)} \right] \tag{10.16}$$

Similarly, the moments at the sea floor due to the inertial and drag forces are:

$$M_I = \rho_w g \frac{C_m \pi D^2}{4} \hat{\zeta} \, d \left[\tanh(kd) + \frac{1}{kd} \left(\frac{1}{\cosh(kd)} - 1 \right) \right] \tag{10.17}$$

$$M_D = \rho_w g \frac{C_d D}{2} \hat{\zeta}^2 \left[\frac{d}{2} + \frac{2(kd)^2 + 1 - \cosh(2kd)}{4k \sinh(2kd)} \right] \tag{10.18}$$

10.4.4.2 Wind/Wave Correlations

As previously noted, wind and waves are the primary external conditions to be considered in the design of offshore wind turbines. It is also important to understand the coincidence of wind and wave events. The simplest assumption to make is that the highest waves occur simultaneously with the highest winds. This assumption may be misleading, however. It is preferable to characterize the joint probability of wind and wave occurrences over all likely conditions. Characterizations may be facilitated by the use of scatter diagrams, as illustrated in Figure 10.14.

Statistical models may be used to describe wind/wave correlations. One method is illustrated in Equation (10.19), which shows an expression for the joint probability of occurrences of wind speed, U, significant wave height, H_s, and peak period, T_p.

$$f_{U,H_s,T_p}(u, h, t) = f_U(u) f_{H_s|U}(h|u) f_{T_p|H_s,U}(t|h, u) \tag{10.19}$$

In other words, the joint probability density function of wind speed, wave height, and peak period is given by the product of the probability density function of wind speed and the conditional probability density function of wave height, given the wind speed, multiplied by the conditional probability density function of the wave period, given the wave height and peak period. Assuming appropriate functions can be found for all of the above density functions on

Wave Height H_s [m]	NOAA Buoy #44013 1984–2004						
	Wind Speed [m/s]						
	0–5	5–10	10–15	15–20	20–25	>25	sum
0–1	5 3235	4 8019	5518	92	1	0	10 6865
1–2	7041	1 3319	8063	660	9	0	2 9092
2–3	815	2502	2446	310	4	0	6077
3–4	69	413	1058	240	5	0	1785
4–5	13	55	302	206	9	0	585
5–6	1	10	74	144	16	1	246
6–7	0	0	11	62	17	0	90
7–8	0	0	0	20	6	0	26
8–9	0	0	0	1	1	0	2
>9	0	0	0	0	1	0	1
sum	6 1174	6 4318	1 7472	1735	69	1	14 4769

Figure 10.14 Occurrences of significant wave heights and mean wind speed at NOAA buoy 44013

the right side of Equation (10.19), then an expression for the joint probability density function of wind speed, wave height, and peak period is at hand. Note that the probability of an occurrence of wind speed between U_1 and U_2, wave height between $H_{s,1}$ and $H_{s,2}$ and wave period between $T_{P,1}$ and $T_{P,2}$ is given by the integral in Equation (10.20):

$$P(U_1 < u \le U_2, H_{s,1} < h \le H_{s,2}, T_{P,1} < t \le T_{P,2}) = \int_{U_1}^{U_2} \int_{H_{s,1}}^{H_{s,2}} \int_{T_{P,1}}^{T_{P,2}} f_{U,H_s,T_P}(u, h, t) \quad (10.20)$$

Further discussion of these methods is outside the scope of this text. It should also be noted, however, that the distribution of structural loads may not follow the distribution of wind and wave events, due to the nonlinearity in the response of the wind turbine to the external forces. For more information on this see Cheng (2002).

10.4.4.3 Other Metocean Design Conditions

The previous discussion has focused on wind and waves insofar as they affect the design of offshore wind turbines, especially their support structures. In addition, one must also take into account currents, tides, floating ice, water salinity, temperature, and a variety of other factors. See IEC (2009) for more information on these topics.

10.4.4.4 Offshore Metocean Data Collection

Gathering of wind, wave, and other metocean data offshore is an extensive topic unto itself, but it is beyond the scope of this text. For an overview of some of the relevant issues, see Manwell *et al.* (2007).

10.4.5 Offshore Electrical Power Transmission

Underwater electrical power cables are required to bring to shore the electricity generated by the offshore wind turbines. Underwater power transmission requires careful attention to

numerous technical and economic issues including:

- transmission voltage;
- power losses;
- cable electrical characteristics and costs;
- cable burial technologies and costs.

Power transmission cables, if not designed properly, can result in significant energy losses. For short distances, medium-voltage AC cables are suitable. Long-distance power transmission requires large conductors and higher voltages. For especially long distances, high-voltage direct-current (HVDC) transmission has been proposed. For example, studies have shown that a three-phase AC power transmission system might have losses of 30% over transmission distances of 50 km. The transmission losses for a comparable HVDC transmission system would be only 13% over the same distance (Westinghouse Electric Corp., 1979).

The power system designer needs to consider the cost of switchgear, transformers, and cable for different transmission voltages, the most cost-effective type of cable insulation and cable capacitance. Offshore transmission voltages may be limited to 33 kV within the wind farm by switchgear and transformer size and cost, which increase rapidly above that size (Gardner *et al.*, 1998). Cable voltages to shore may be as high as 150 kV, if there is a separate transformer platform. Some possible cable insulation technologies include cross-linked polyethylene (XPLE), ethylene propylene rubber (EPR), and self-contained fluid-filled insulation (SCFF). XPLE is in widespread use on land (and is thus less expensive) but needs a moisture barrier under water. EPR does not require a metal sheath and can be designed for underwater use (Grainger and Jenkins, 1998). High-voltage SCFF cable has a copper conductor surrounded by an oil duct and a wood pulp paper insulation layer that is surrounded by wire and rubber sheaths for protection (Fermo *et al.*, 1993). Finally, the capacitance of power lines may be significant enough to provide some reactive power or to cause the self-excitation of turbine generators and needs to be considered.

Careful planning for the installation of power cables is very important to minimize the lifetime cost of the cables. Cable-laying ships and equipment are very expensive and cables are subject to damage. The greatest hazards are from anchors and trawling, so cables should ideally be buried at least 1 m under the sea floor. Another danger is mobile sand waves. These can uncover buried cable in a few weeks. Cables may need to be buried 2–3 m deep to avoid wave action. Where abrasion on rock is a problem, armored cable, buried cable, or a combination may be needed.

A good cable design must balance expensive cable installation and burial costs with the cost of down time and repair. Burial methods include ploughing, air-lifting, water jetting, excavating, and rock-sawing. There are many types of burial machines: towed, free-swimming, and tracked remotely operated vehicles (ROVs). Generally, ploughs are used on long flat routes with clay-based sediments. Jetting tools work best on sands and are less expensive for short runs. Some machines can change tools for changing seabed conditions. Cables may be laid directly on the seabed (not buried), laid and buried simultaneously, or laid and buried later (post-lay burial). The choice of cable-laying and burial method will depend on the length of the run, water depth, soil characteristics, and equipment available. Cable-laying vessels will need a good mooring and control system, a deck area for cable, and equipment and accommodation for personnel. One project may need different vessels for different technologies and areas. A special purpose vessel may be needed for some projects. A good design will be based on an

assessment and survey of the route and contingency plans for bad weather. Finally, the system and routes will need to be designed to allow for economical repairs. Cables must be laid so that any damaged section can be identified and located easily and can be jointed in a marine environment. Martínez de Alegría *et al.* (2009) present a summary of some of the key issues regarding cables for offshore wind systems.

10.4.6 Offshore Wind Farm Design Issues

Offshore wind farm siting requires the consideration of a variety of issues including permitting requirements, shipping lanes, fishing areas, fish, mammal and bird breeding and feeding habits, existing underwater communication and power cables, visual concerns (for near-shore wind farms), storm tides and seas, seabed properties, underwater currents, underwater archaeological sites, designated marine sanctuaries, competing uses (recreation, defense), the available infrastructure and staging areas for construction (cable-laying vessels, facilities for foundation fabrication, barges for installation), and transportation for maintenance.

The layout of wind turbines in an offshore wind farm will have a significant effect on the economics. Economic issues are discussed in detail in Chapter 11, but they are intertwined with productivity, which is also related to the layout. For example, when turbines are spaced close together, wake effects will reduce the total energy production. On the other hand, the cables will be longer and hence the cost of the electrical network within the wind farm will be higher when the turbines are spaced farther apart. Similarly, if the turbines are sited farther from shore, the wind speeds and hence energy production will be relatively high. Counteracting that benefit, the installed costs will be higher because the transmission cable to shore will be longer and the water depths are likely to be greater, so the support structures will be more expensive. For more information on this topic see Elkinton (2007).

10.4.7 Offshore Wind Farm Site Investigation

Before an offshore wind farm can be built, there is normally an extensive feasibility study and permitting activity. These require significant investigations. In addition to measurements of metocean conditions, many or all of the following may be required:

- bathymetry;
- sea floor imaging;
- acoustic sub-bottom profiling;
- magnetometry;
- vibracores;
- soil borings.

Bathymetry is the measurement of water depth. A device called an echosounder may be used for this purpose. The results of these measurements should be more accurate than information available from nautical charts.

Sea floor imaging is done using side scan SONAR. The purpose is to determine what is visible on the sea floor, such as shipwrecks, which could affect the placement of turbines.

Acoustic sub-bottom profiling is used as part of the preliminary geophysical investigations to ascertain the nature of the soil beneath the sea floor. In particular, it can help identify the
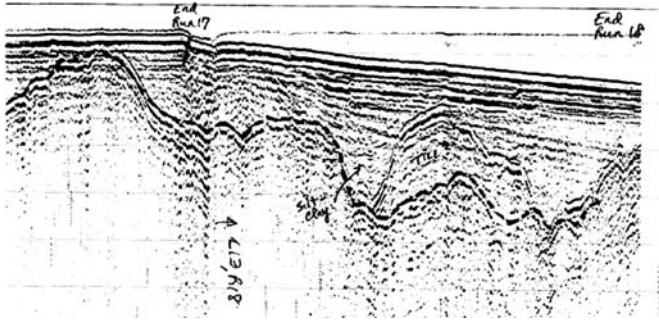
Figure 10.15   Typical sub-bottom profile

nature and depth of transition zones between different types of material, such as between sand and rock. As the name implies, the method is based on sound waves. The sound is produced by a 'boomer' which is towed behind a boat. The sound penetrates soil to various depths; some of it is returned. The returned sound signal is then processed to provide information about soil. A typical profile is shown in Figure 10.15.

Magnetometry is used to determine if there is any magnetic material in the area of interest. Such metal could come from shipwrecks or unexploded ordnance.

Vibracoring is a method of retrieving undisturbed core samples of sub-bottom sediment. The samples obtained using this method are from relatively close to the seabed, on the order of a few meters. Vibracore samples are used to study the proposed paths for the electrical cables.

Soil samples will be needed to finalize the design of the support structure. These are obtained with an offshore drilling rig. The rig will bore holes and obtain samples over the full length of the anticipated structure if possible and at least as far as the bedrock.

10.4.8 Other Considerations for Offshore Wind Energy

Other factors to consider for offshore wind energy include operation and maintenance, economics, and environmental issues. Operation and maintenance is quite significant, in that it can involve the issue of specialized vessels and other equipment, and that the costs can be quite significant. This topic is outside the scope of this text, however. Some aspects of offshore wind economics are discussed in Chapter 11 and some of the environmental issues are presented in Chapter 12.

More information on offshore wind energy technology may be found in a variety of sources, such as Musial (2007) and Twidell and Gaudiosi (2009).

10.5 Operation in Severe Climates

Operation in severe climates imposes special design considerations on wind turbines. Severe climates may include those with unusually high extreme winds, high moisture and humidity, very high or low temperatures, and lightning.

High temperatures and moisture in warm climates cause a number of problems. High temperatures can thin lubricants, degrade the operation of electronics, and may affect motion in mechanical systems that expand with the heat. Moisture and humidity can corrode metal and degrade the operation of electronics. Moisture problems may require the use of desiccants, dehumidifiers, and improved sealing systems. All of these problems can be solved with site-specific design details, but these should be anticipated before the system is installed in the field.

Operation in cold temperatures also raises unique design considerations. A number of wind turbines have been installed in cold weather regions of the globe, including Finland, northern Quebec, Alaska, and other cold regions of Europe and North America and in Antarctica. Experience has shown that cold weather locations can impose significant design and operating requirements on wind turbines because of sensor and turbine icing, material properties at low temperatures, permafrost, and snow.

Turbine icing is a significant problem in cold climates. Ice comes in two main forms: glaze ice and rime ice. Glaze ice is the result of rain freezing on cold surfaces and occurs close to $0\,°C$. Glaze ice is usually transparent and forms sheets of ice over large surfaces. Rime ice results when supercooled moisture droplets in the air contact a cold surface. Rime ice accumulation occurs in temperatures colder than $0\,°C$. Ice accumulation on aerodynamic surfaces degrades turbine performance and, on anemometers and wind vanes, results in either no information from these sensors or misleading information. Ice can also result in rotor imbalance, malfunctioning aerodynamic brakes, downed power lines, and a danger to personnel from falling ice. Attempts to deal with some of these problems have included special blade coatings (Teflon®, black paint) to reduce ice build-up, heating systems, and electrical or pneumatic devices to dislodge accumulated ice.

Cold weather also affects material properties. Cold weather reduces the flexibility of rubber seals, causing leaks, reduces clearances, reduces fracture strength, and increases lubricating oil viscosity. Each of these can cause mechanical malfunctions or problems in everything from solenoids to gearboxes. Most turbines designed for cold weather operation include heaters on a number of critical parts to ensure correct operation. Materials also become more brittle in cold climates. Component strengths may need to be de-rated for cold climate operation or special materials may be required for the correct operation of components in cold weather or to ensure adequate fatigue life.

Wind turbine installation and operation may be affected by cold weather climate conditions. Wind turbine access may be severely limited by deep snows. This may result in longer down times for turbine problems, or delayed and expensive maintenance. In installation in permafrost, the turbine installation season may be limited to the winter when the permafrost is fully frozen and transportation is easier.

More information on wind turbine operation in cold weather may be found in the proceedings of the seven (so far) BOREAS conferences. These are conferences which have a particular focus on wind energy in cold climates. The conferences are held periodically in northern Europe. Many of the papers from these conferences are available on the Internet.

Finally, many regions have frequent occurrences of lightning. Lightning can damage blades and mechanical and electrical components as it travels to ground. Designing for lightning protection includes providing very low impedance electrical paths to ground that bypass important turbine components, protecting circuitry with voltage surge protectors, and designing a low impedance grounding system (IEC, 2002).

10.6 Special Purpose Applications

Wind energy has historically been used for a wide range of special applications, ranging from grinding grain to sawing wood, and including many others as well. More recently, at least four special purpose applications have been used or investigated. These include: water pumping, desalination, heating, and ice making. These four are discussed in this section.

10.6.1 Wind Water Pumping

There are millions of people throughout the world who do not have access to water for all of their needs. In many of these situations, water is available in wells or aquifers, but it must be pumped from those sources for it to be usable. Wind has been used for water pumping for many hundreds of years, and it still has a role to play for that purpose today. Historically, wind pumps were purely mechanical devices. Nowadays, mechanical pumps are still a viable option, but there are other possible arrangements as well. These include wind/electric water pumps and conventional water pumps in a hybrid power system.

There are four main types of applications for wind water pumping. These are: (1) domestic use, (2) irrigation, (3) livestock watering, and (4) drainage. Another possibility is high pressure pumping for use in sea water desalination. That topic, however, is discussed in Section 10.6.2.

A basic introduction to wind water pumping may be found in Manwell (1988). A comprehensive discussion of the topic may be found in Kentfield (1996). More details on pumps in general may be found in Fraenkel (1997). In the 1980s there was a considerable effort in the Netherlands devoted to developing and investigating 'fast-running' mechanical water-pumping windmills. The group that carried out this work was the Consultancy for Wind Energy in Developing Countries (CWD). Some of the results of that work are still readily available (see Lysen, 1983). The following provides a summary of the key issues.

10.6.1.1 Mechanical Water Pumping

The most commonly imagined type of water pumping is completely mechanical. The wind water pump includes at least the following components: (1) the wind rotor, (2) the tower, (3) a mechanical pump, (4) mechanical linkage, (5) a well or other water source, and (6) a water delivery system (piping). Frequently, some form of water storage also accompanies the wind water pump. Tanks, ponds, or reservoirs may be used for storage, depending on the application. A schematic of a typical mechanical water pump is shown in Figure 10.16.

The key considerations in mechanical wind water pump design include (1) selecting or designing the rotor, (2) selecting the pump, (3) matching of the rotor to the pump, and (4) safe operation and then shutdown or furling in high winds. These tasks are undertaken with reference to the likely nature of the wind resource.

Windmill pumps have historically been of the piston type. These are relatively simple devices that serve the purpose adequately and are straightforward to service. Some early pump designs have used Archimedes screws and more recently progressive cavity pumps have been used in some wind pump applications. Centrifugal pumps have historically not been used with mechanical water pumps due to their intrinsically high operating speeds.

Wind water pumping, by its nature, typically requires fairly high torques and low pump operating speeds. Accordingly, wind turbine rotors are generally designed to have their
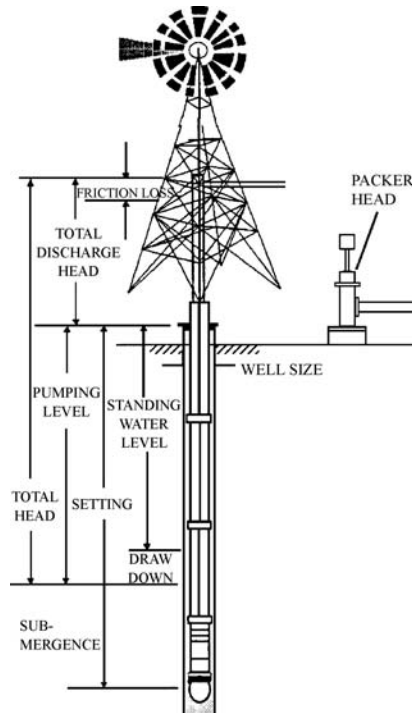
Figure 10.16   Mechanical water pumping windmill (Manwell, 1988)

maximum power coefficients at relatively low tip speed ratios. That means that the rotor will have a fairly high solidity. Due to the low speeds, drag will not pose a major limitation on the performance of the rotor, so the airfoil can be of a simple shape.

Water Requirements

Water may be needed for domestic use or agriculture. Pumping may also be needed for drainage.

Domestic water use will depend a great deal on the amenities available. A typical villager in a rural community in much of the world may use from 15–30 liters per day. When indoor plumbing is available, water consumption may be substantially higher. For example, a flush toilet consumes 6–25 liters (depending on the design) with each use, and a shower may take 100 liters or more.

Agricultural water use includes livestock and irrigation. Basic livestock requirements range from about 0.2 liters a day for chickens or rabbits to 135 liters per day for a milking cow. Estimating irrigation requirements is more complex and depends on a variety of meteorological factors as well as the types of crops involved. The amount of irrigation water needed is approximately equal to the difference between that needed by the plants and that provided by rainfall. Various techniques may be used to estimate evaporation rates, due for example to wind and sun. These may then be related to plant requirements at different stages during their growing cycle. By way of example, in one semi-arid region, irrigation requirements varied

from 35 000 liters per day per hectare for fruits and vegetables to 100 000 liters per day per hectare for cotton (Manwell, 1988).

Drainage requirements are very site dependent. Typical daily values might range from 10 000 to 50 000 liters per hectare.

In order to make the estimate for the water demand, each user's consumption is identified and summed to find the total. It is desirable to do this on a monthly basis so that the demand can be conveniently related to the wind resource.

Water-pumping Power

The power required to pump water is proportional to its density (approximately 1000 kg/m³), the acceleration of gravity, the total pumping head (m), and the volume flow rate of water (m³/s). Power is also inversely proportional to the pump efficiency. Note that 1 cubic meter equals 1000 liters. Expressed as a formula, pumping power, P_p, (W) is given by:

$$P_p = \frac{\rho_w g \, z \, \dot{V}}{\eta_{pump}}$$
(10.21)

where: $\rho_w =$ density of water, $g =$ acceleration of gravity, $z =$ pumping head, $\dot{V} =$ water volumetric flow rate, and $\eta_{pump} =$ pump mechanical efficiency.

Coupling the Pump to the Rotor

For any given wind speed, the power from the rotor must match the pumping power. Therefore:

$$C_P \frac{1}{2} \rho \, \pi \, R^2 U^3 = \frac{\rho_w g \, z \, \dot{V}}{\eta_{pump}}$$
(10.22)

The pump flow, $\dot{V}$, is a function of the stroke volume (stroke length multiplied by the pump area) and the pump speed (stroke length multiplied by the pump crank angular speed), multiplied by the volumetric efficiency of the pump:

$$\dot{V} = \eta_{vol} s_{pump} \frac{\pi}{4} D_{pump}^2 \frac{\Omega}{2\pi \, g_r}$$
(10.23)

where: $\eta_{vol} =$ volumetric efficiency of the pump, $s_{pump} =$ stroke of the pump, $D_{pump} =$ pump diameter, $g_r =$ the ratio between the speed of the rotor and that of the pump crank.

Expressed in terms of the tip speed ratio, wind speed, and rotor radius:

$$\dot{V} = \eta_{vol} \frac{s_{pump}}{8} D_{pump}^2 \frac{\lambda \, U}{g_r R}$$
(10.24)

The design wind speed may then be found:

$$U_d = \frac{\eta_{vol} s_{pump} D_{pump}^2 \lambda_d \rho_w g \, z}{4 C_{P,max} \eta_{pump} \rho \, \pi \, R^3 g_r}$$
(10.25)

Some convenient mathematical expressions for the behavior of a wind pump may also be developed, using the assumptions that the pump torque is constant and that the tip speed ratio vs. torque coefficient relation is linear. See Lysen (1983) for more information on this.

Starting Torque

An important consideration in the design of a wind water pump is the starting torque of the rotor. For a piston pump, the operating torque, including that required for starting, varies with the force on the piston and the length and position of the crank associated with raising and lowering of the piston rod. The force on the piston, F_p, is due to the weight of the water and the piston's area:

$$F_p = \rho_w g \, \pi \, \frac{D_{pump}^2}{4} z \qquad (10.26)$$

The maximum torque occurs when the crank is perpendicular to the pump rod, so that:

$$Q_{p,\max} = \frac{s_{pump}}{2} F_p = \frac{s_{pump}}{2} \rho_w g \, \pi \, \frac{D_{pump}^2}{4} z \qquad (10.27)$$

The maximum torque turns out to be π multiplied by the average torque.

Control and High Wind Protection

There are two major control issues to be considered in the design of mechanical water pumping windmills: (1) yaw control and (2) protection in high winds. Most mechanical water-pumping windmills use a tail vane to yaw the wind rotor into the wind. The vane is mounted perpendicular to the plane of the rotor. The vane accomplishes its intended purpose through the action of a moment due to drag on the side of the vane, after the wind direction has changed. Protection in high winds involves yawing the rotor out of the wind. This is an action which must override the normal tendency of the tail vane to do the opposite. The protection effect is often accomplished by offsetting the rotor from the yaw axis. Thrust on the rotor in high winds will tend to push the rotor parallel to the tail vane, and thus parallel to the wind, reducing the overall loads. To keep the rotor where it belongs in normal winds, a spring or gravity mechanism is incorporated into the design. Some of the possibilities are illustrated in Le Gouriérès (1982).

10.6.1.2 Wind Electric Water Pumps

In a number of situations where water is needed, mechanical water pumping may not be suitable. A wind electric pump might be more appropriate. This may be the case, for example, when the wind resource at the site of the well is low, but there may be a site with good exposure to the wind not too far away.

In the wind electric water pump, the wind turbine could be an essentially conventional wind electric wind turbine used for remote applications. Rather than have its generated power used to charge batteries or be integrated into an AC grid, the power can be used directly by an electrically driven water pump.

The wind turbines used in wind electric water-pumping applications typically have permanent magnet AC generators. Water pumps here are of the centrifugal type, driven by a conventional induction motor. The wind turbine's generator is generally directly connected to the pump motor. Batteries or power converters such as inverters are not used in this arrangement. Pressure and/or float switches and possibly a microcontroller are used for control purposes. With suitable controls, the turbine and pump can operate over a range of speeds. Some wind electric pumping systems have even been configured to provide both

water pumping and electrification. More details on one approach to wind electric pumping are given in Bergey (1998).

10.6.1.3 Hybrid Grid Water Pump

Water may also be pumped with wind energy in a hybrid power system. In this case the technical aspects of the pumping are essentially the same as they are in a conventional utility network. The one distinction is that the water pumping may be done in conjunction with water storage so as to assist in load management, and thereby make more effective use of the available wind resource.

10.6.2 Wind-powered Desalination

Much of the world does not have access to potable water. In many locations, however, there is brackish or salt water which could be converted into drinking water by desalination. Desalination is an energy-intensive process, and often there is no attractive conventional source of energy to power a desalination process. In many of these situations, the wind is a plausible source of that energy.

Desalination is most often accomplished through either a thermal process or a membrane process. The most common methods are reverse osmosis (RO) or vapor compression systems. Advances in membrane technology over the last few decades have been making reverse osmosis progressively more attractive for desalination, regardless of the energy source. The following section discusses RO-based desalination.

10.6.2.1 Principles of Reverse Osmosis Desalination

Reverse osmosis is a filtration process in which a semi-permeable membrane is used to allow water to pass through while rejecting salts. Osmosis is a naturally occurring phenomenon that can be explained by statistical thermodynamics. If a partially permeable membrane separates a volume of pure water and a salt solution, the result is a gradual flow of freshwater to the salt solution. When mechanical pressure is applied to the salt solution, however, water can be forced the other way through the membrane. The result is that pure water (the 'permeate') can be collected on the other side. This is the reverse of the normal osmosis process, hence the origin of the name reverse osmosis.

The pressure required to force a solution through a semi-permeable membrane is called the osmotic pressure. For low concentration solutions, the osmotic pressure, p_π, (Pa) can be calculated by the following equation (also known as the Morse equation):

$$p_\pi = iS\rho_w R_u T/M \qquad (10.28)$$

where $i =$ the van't Hoff factor (here, approximately 1.8), S is the salinity (g/kg), ρ_w is the density of water (kg/m^3), R_u is the universal gas constant (8.31447 m^3 Pa/mol K), T is the absolute temperature (K), and M is the molecular weight of salt (58.5 g/mol).

The salinity of seawater varies depending on the location. A typical value is 35 g salt per kg of water. By way of example, this salinity value would correspond to an osmotic pressure of approximately 2.7 MPa, assuming seawater density and temperature of 1020 kg/m^3 and 20 °C

respectively. This means that the feed water pressure must be more than 26 times atmospheric before any water can permeate the membrane.

The power required to desalinate water is primarily a function of the pressure required to force water through the membrane and the desired flow rate of the permeate. Approximately 7% of the water entering the system passes through the membrane as permeate. The remainder continues through the system and leaves as concentrated brine. Power is required to pump the brine as well as the permeate, so the pressure across the membrane must be higher than the osmotic pressure to ensure a reasonable flow rate. Typically this is at least twice the osmotic pressure. Common values are in the range of 5–7 MPa (Thompson, 2004). The result is a greater total power expended per unit of permeate than might be expected based on just the permeate flow rate and the osmotic pressure. The total specific work, $w_{desal,tot}$ (in kWh/m^3), can be determined from the following equation:

$$w_{desal,tot} = \frac{(\Delta p_{L,1} + \Delta p_{L,2} + \Delta p_H) + \Delta p_{RO} f_p + \Delta p_B (1 - f_p)}{(f_p)(3600)} \quad (10.29)$$

where: $\Delta p_{L,1}, \Delta p_{L,2}, \Delta p_H =$ pressure rise in first and second low-pressure feed pumps and high-pressure feed pump; $\Delta p_{RO} =$ pressure drop across membrane (approximately twice the osmotic pressure); $\Delta p_B =$ pressure rise across brine pump, $f_p =$ permeate fraction. (All pressures are in kPa. The 3600 converts kJ/m^3 to kWh/m^3.) See also Figure 10.17.
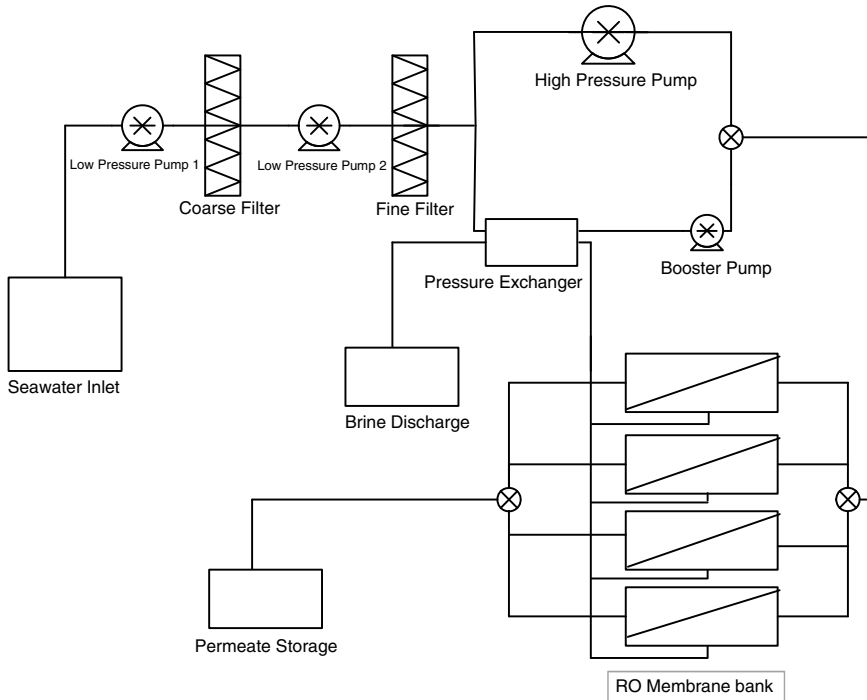
Figure 10.17   Seawater desalination

The net practical effect is that a typical reverse osmosis system nowadays consumes between 3 and 5 kWh/m^3 of pure water produced (assuming input salinity of 35 g salt/kg water), depending on the design of the system. This is at least four times as much energy as would be expected, considering only the osmotic pressure.

10.6.2.2 Applications for Wind/Desalination Systems

Wind-powered desalination may be applied in one of four types of applications: (1) within a large central electrical grid, (2) on the distribution system of a central electrical grid, (3) in a hybrid power system network, or (4) in a direct-connected system.

Systems in the first category are physically essentially the same as conventional, grid-connected desalination systems. Insofar as the wind turbines are assumed to be at transmission level voltage, they will, in general, be located some distance from the desalination plant. If the desalination plant were located close to the generators, then they could have some characteristics of distribution level desalination systems (see below). Otherwise, there are few, if any, issues of substance distinguishing these systems from conventional desalination systems.

Distribution Level Desalination Systems
Systems in this category are those in which the wind turbines and the desalination plant are all connected to the distribution system, and at a distribution voltage (typically 13 kV or less). In these systems there could be technical issues associated with the amount of generation that could be connected, and so there could be, in effect, an upper limit imposed on the amount of generation that could be installed, or on the amount of power that could be exported from the system during times of high generation and low loads. In practice, limitations could be regulatory as well as technical. Economic factors could also be significant in these systems. In principle at least, a community in this category could, at times: (1) purchase or sell electricity, (2) produce water by desalination, (3) purchase or sell water, (4) distribute water immediately, (5) store or release water. At any given time, decisions would need to be made regarding which of these should be done.

Wind Hybrid Desalination Systems
Systems in this category include those on islands and those in isolated communities. There could be significant technical issues in such systems, affecting both the electrical stability of the network and satisfactory operation of the desalination system. Maintenance of the electrical stability may be facilitated by use of equipment common to wind/diesel or hybrid power systems. These could include a supervisory control system, dump loads, power-limiting of the generators (e.g. pitch control on wind turbines), and electrical energy storage.

Load control, particularly of the desalination plant, is also an option. This would presumably be done in RO systems with multiple modules, such that one or more modules would be turned on or off, as called for by the situation. It should be noted, however, that cycling would be done relatively slowly so as not to adversely affect the module membranes. It is also expected that, with the exception of varying the number of operating modules, an RO unit would be run as it normally is. That is, the pressures would remain essentially constant, as would the flow rates within each module. The effect of short-term fluctuations of the renewable energy generator would, in general, be compensated by a

conventional generator (typically diesel in these situations) or through some type of power-smoothing storage.

A number of analytical investigations or demonstration projects have involved wind-driven reverse osmosis systems for autonomous or non-grid connected situations. The economics of such systems can be strongly affected by the coincidence of the water requirement and the availability of energy. A recent example of a study of such a system is one undertaken at Star Island in New Hampshire (Henderson *et al.*, 2009).

Direct Connected Wind/Desalination Systems
The fourth category of system is the free-standing, direct-coupled renewable generator-desalination system. These are typically smaller systems, and in some ways the most problematic, in that short-term power fluctuations and their possible impact on the desalination system must be dealt with directly. These are technically very interesting, but they are beyond the scope of this text. Discussion of various aspects of such systems may be found, however, in articles or reports by Miranda and Infield (2002), Thompson and Infield (2002), Fabre (2003), and Carta *et al.* (2003). Adapting RO to work directly with wind turbines was also investigated in the 1980s by Warfel *et al.* (1988).

10.6.2.3 Desalination Plant Description

A schematic of a typical desalination plant is shown in Figure 10.17. As can be seen, it includes a number of pumps, filters, heat exchangers, and a bank of reverse osmosis modules. Each module contains a wound semi-permeable membrane. Pure water passes through the membrane. The remainder continues to the brine discharge.

The majority of seawater RO system designs are single stage with from five to eight membrane elements per pressure vessel (Wilf and Bartels, 2005). There is an obvious cost advantage in the increased number of elements per vessel. For a typical configuration, an RO system with six elements per pressure vessel requires 33% more vessels than one with eight elements per vessel. The actual number of membrane elements that can be 'stacked' in a pressure vessel is a unique characteristic of each membrane.

RO membranes are particularly susceptible to failure and excessive fouling when the inlet water is not properly filtered. Accordingly, a pretreatment system with cartridge-type filters is usually installed upstream of the membranes. Low-pressure pumps are used to push water through the filters. The purpose of these filters is to remove any substance that could otherwise damage the membranes. Cartridge filters are not effective in removing pollutants such as oil, however.

In order to reduce the energy requirements of a desalination system, an energy recovery device may be incorporated. Some RO systems include a Pelton water turbine that is connected to an electrical generator which, in turn, delivers power to a high-pressure pump. Another approach uses a pressure exchanger. This device allows the high-pressure brine discharge to be directly used to pressurize the inlet feedwater (Andrews *et al.*, 2006).

10.6.3 Wind-powered Heating

Wind energy can be used for space heating, domestic hot water, or other similar purposes. One version of the concept, which originated in the 1970s, was known as the Wind Furnace

(Manwell and McGowan, 1981). In this arrangement, a dedicated, specially designed wind turbine was used to provide heat to a residence. The wind turbine's electricity was dissipated in resistance heaters, which were inside a water storage tank. Hot water was circulated from the storage tank to the rest of the house as needed. The purpose was to provide the heat directly, rather than to interconnect to the utility power lines. The advantage was that the turbine could run at constant tip speed ratio (and thus at maximum power coefficient) for its entire operating range between cut-in and rated wind speed, all without the need for intermediate power converters. A similar concept, known as the Windflower, was investigated in Denmark in the 1980s and at least one wind heating system was installed in Bulgaria in the 1990s. There has also been some work on the concept in Finland. In spite of these endeavors, wind heating based on dedicated wind turbines has not been widely used.

A variant of the wind heating concept has been more widely used, however, particularly in hybrid power systems. In these cases, a conventional wind turbine is used to supply regular electrical loads, and is also used to supply space or domestic hot water heating. In these situations, the heating is normally undertaken with some type of thermal storage, so the heating system serves a load management role. When there is excess energy from the wind turbine, some of it is used to heat up the thermal storage. When heat is needed, it is either taken directly from the wind turbine if there is sufficient available, or heat is taken from the storage. An example of a hybrid power system that utilizes wind energy in its supply of heat and electricity is that of Tanadgusix (TDX) Corporation on the island of St Paul, Alaska (Lyons and Goodman, 2004).

In wind heating systems with storage, the heat is typically either stored in water or in ceramics. One concept of a wind/diesel system with heating and ceramic thermal storage is described by Johnson *et al.* (2002). In this concept, distributed controllers were to be used to facilitate the match between the availability of wind-generated electricity and the requirement to recharge the storage.

One final point to bear in mind is that the conversion efficiency of electricity from the wind turbine to heat is essentially 100%. When heat is the desired product, wind-generated electricity is thus a plausible way to produce it. On the other hand, electricity has a very high availability (in the thermodynamic sense). Accordingly, electricity can be used to produce even more heat than it can by simple dissipation through the use of a heat pump. Just how much more heat can be produced will be a function of the temperature of the heat pump's heat source reservoir. The heat reservoir may be the air, the ground, or water from a well. Depending on the nature of the source, its temperature, and the design of the heat pump, the coefficient of performance (ratio of delivered heat to input electricity) will be in the range of 2.0–5.0. Including a heat pump in the system will thus clearly result in a more effective use of a wind turbine's electricity than just using resistors. Whether it makes economic sense to do so will depend on the cost of the heat pump and the total additional useful energy it will provide over the course of a year.

10.6.4 Wind-powered Ice Making

Wind energy can be used for ice making. The premise behind this concept is somewhat similar to others in which the wind energy is used directly to supply a particular requirement. Here, the requirement is for ice, or the cooling capacity that results from it.

The principle behind the wind-powered ice making concept is to use the electricity from a wind turbine to drive a conventional Rankine cycle-based freezer. The ice may be made in either a batch or continuous process. If a batch process is used, however, the process must be interrupted when the ice is removed. Ideally, both the wind turbine's rotor and the freezer's compressor should be able to turn at variable speed. This helps to maximize the efficiency of the conversion of wind energy to mechanical form and could obviate the need for maintaining a constant frequency of the electrical power.

As far as is known to the authors, the only wind-driven ice making systems that have been built were experimental. At least one such system was built in the United States (Holz *et al.*, 1998) and another one was built in the Netherlands in the 1980s.

10.7 Energy Storage

Energy storage can serve a very useful role in wind energy systems, particularly those in which the wind is to provide a large fraction of the total energy requirement. Energy storage can help to overcome mismatches between the availability of wind energy and the requirement for energy. There are many storage options to consider. These include batteries, compressed air, flywheels, and pumped hydroelectric, among others. Hydrogen can also be thought of as storage, but since it also has the properties of a fuel, it will be discussed in a later section. There are two characteristics of particular interest: (1) the quantity of energy that can be stored per unit cost and (2) the rate at which energy can be absorbed or delivered (i.e. the power). The time scale of the storage is also important – is it useful for dealing with fluctuations on the order of seconds, minutes, hours, or days? For example, pumped hydroelectric is typically used to cover daily variations in electrical load. Batteries are most effective for dealing with variations on the order of minutes to hours, and flywheels are used for smoothing power fluctuations on the order of seconds to minutes. At the present time, the most common storage medium for wind energy applications is batteries, and there has been renewed interest in compressed air energy storage and flywheels. Pumped hydroelectric also remains an attractive option for some situations. For that reason, the remainder of this section focuses on these four options. More information on energy storage may be found in Ibrahim *et al.* (2008) and Baxter (2006).

10.7.1 Battery Energy Storage

Battery energy storage is very common with smaller hybrid power systems and is occasionally used in larger electrical networks as well. Batteries have proven to be a popular energy storage medium, based primarily on their convenience and cost. Battery storage systems are modular, and multiple batteries can store large amounts of energy. Lead acid batteries are most prevalent, although nickel–cadmium batteries are occasionally used. Batteries are inherently DC devices. Thus, battery energy storage in AC systems requires a power converter.

An important aspect of batteries is their terminal voltage, which varies according to current and state of charge. Typical battery voltage during a discharge–charge cycle is illustrated in Figure 10.18. It can be seen that the terminal voltage drops as the battery is discharged. When charging is initiated, the terminal voltage jumps to a value above the nominal cell voltage. As the cell becomes fully charged, the terminal voltage increases even more before gassing occurs (the production of hydrogen gas in the cells) and the terminal voltage levels off.
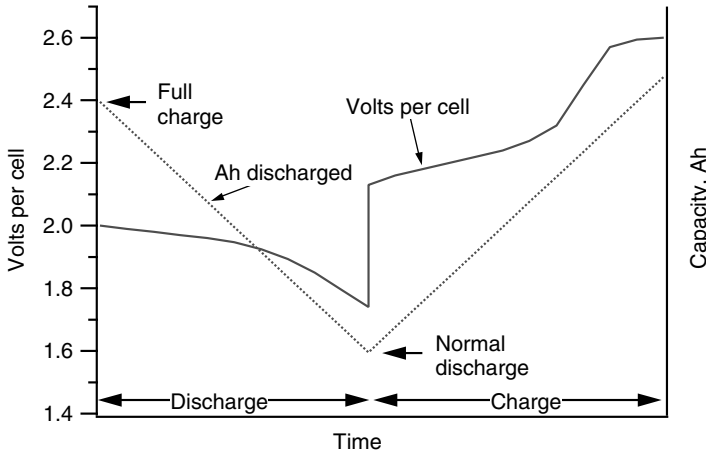
Figure 10.18 Typical battery voltage and capacity curve (Fink and Beaty, 1978). Reproduced by permission of McGraw-Hill Companies

A number of aspects of battery behavior affect their use in power systems (see Manwell and McGowan, 1994). These are summarized below. More details on some of these topics are provided subsequently.

- **Battery capacity.** Effective battery capacity is a function of current. Thus, the amount of available storage is a function of the rate at which the storage is used.
- **Terminal voltage.** Terminal voltage is a function of state of charge and current level. This affects the operation of the power transfer circuit between the battery storage and the rest of the system.
- **Efficiency.** Batteries are not 100% efficient. Battery losses can be minimized by intelligent controller operation, but most of the losses are due to differences in voltage during discharging and charging and are inherent to battery operation.
- **Battery life.** Batteries have a limited useful life. Battery life is a function of the number and depth of charge–discharge cycles, and is also related to the battery design.
- **Temperature effects.** Battery capacity and life are functions of temperature. Usable battery capacity decreases as the temperature decreases. Typically, battery capacity at $0\,^\circ$C is only half that at room temperature. Above room temperature, battery capacity increases slightly, but battery life decreases dramatically.

10.7.1.1 Battery Capacity and Voltage

Total battery capacity is expressed in Amp-hours (Ah), a unit of charge, or kWh. Rated battery capacity is considered to be the Ah discharged at the rated current until the voltage has dropped to 1.75 V per cell (10.5 V in a 12 V battery). Usable battery capacity depends on the charge or discharge rate. High rates of discharge result in early depletion of the battery. The voltage soon drops and no more energy is available. At low discharge rates, the battery can provide much more total energy before the voltage drops. High charge rates result in rapidly increasing terminal voltage after only a short while. Slower charging rates result in much more charge
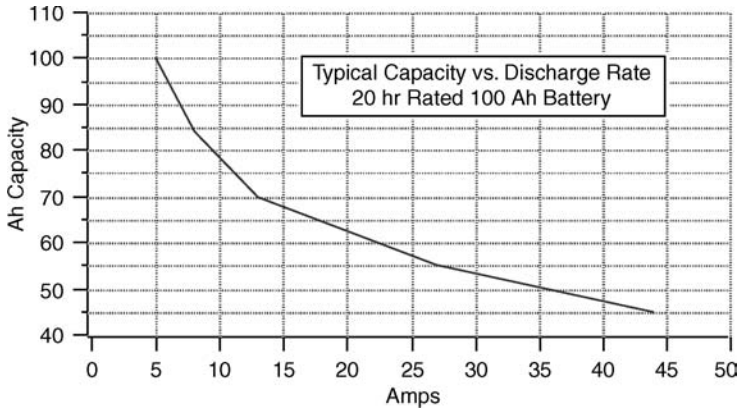
Figure 10.19   Battery capacity vs. discharge rate curve

being returned to the battery. Figure 10.19 illustrates this relationship between usable battery capacity and discharge rate. In this example the battery energy storage capacity changes by a factor of 2 over the range of currents illustrated.

Battery Capacity Modeling
As discussed above, battery capacity in both charging and discharging is known to decrease with increasing charge and discharge rates. This behavior can be modeled by assuming that some of the charge is 'available' (that is, immediately accessible) and some of it is 'bound.' The bound charge can be released, at a rate proportional to a rate constant, k. The Kinetic Battery Model embodies these assumptions and can be used to model battery capacity and voltage (Manwell and McGowan, 1993; 1994). In this model, the total charge, q, in the battery at any time is the sum of the available charge and bound charge. This model was developed originally for lead acid batteries, but it can be applied to other types of batteries as well. According to this model, the maximum apparent capacity, $q_{max}(I)$, at current I is given by:

$$q_{\max}(I) = \frac{q_{\max}\, kct}{1 - e^{-k\,t} + c(kt - 1 + e^{-k\,t})} \tag{10.30}$$

where:

$t =$ charge or discharge time, defined by $q_{\max}(I)/I$, hrs
$q_{\max} =$ maximum capacity (at infinitesimal current), Ah
$k =$ rate constant, hrs^{-1}
$c =$ ratio of available charge capacity to total capacity.

The three constants, $q_{\max}$, k, and c can be derived from manufacturer's or test data, as described by Manwell *et al.* (1997).

Battery Voltage Modeling
Battery terminal voltage, V, as a function of state of charge and current can be modeled using the equivalent circuit shown in Figure 10.20 and Equations (10.31) and (10.32).
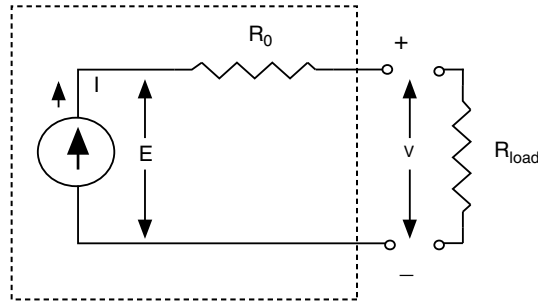
Figure 10.20   Battery equivalent circuit

Equation (10.31) describes the terminal voltage in terms of the internal voltage E_0 and the internal resistance, R_0. Equation (10.32) relates the internal voltage of the battery to its state of charge.

$$V = E - IR_0 \qquad (10.31)$$

$$E = E_0 + AX + CX/(D-X) \qquad (10.32)$$

where:

$E_0 =$ fully charged/discharged internal battery voltage (after any initial transient)

$A =$ parameter reflecting the initial linear variation of internal battery voltage with state of charge. 'A' will typically be a negative number in discharging and positive in charging.

$C =$ parameter reflecting the decrease/increase of battery voltage when the battery is progressively discharged/charged. C will always be negative in discharging and positive in charging.

$D =$ parameter reflecting the decrease/increase of battery voltage when the battery is progressively discharged/charged. D is positive and is normally approximately equal to 1.0.

$X =$ normalized capacity at the given current.

The normalized capacity, X, during charging is defined in terms of the charge in the battery by:

$$X = q/q_{max}(I) \qquad (10.33)$$

During constant current discharging, X is defined in terms of the charge removed by:

$$X = (q_{max}(I) - q)/q_{max}(I) \qquad (10.34)$$

10.7.1.2 Battery Efficiency

There are two measures of battery efficiency. Coulombic efficiency is the ratio of the charge delivered by the battery during discharging to the charge put into the battery during charging in one complete charge–discharge cycle. Typical coulombic efficiencies range from 90%

to 100%. Coulombic efficiency is higher with lower charging currents (and reduced gassing). The second measure of efficiency is energetic efficiency. Energetic efficiency is the ratio of the energy transferred from the battery to the energy provided to the battery in one complete charge–discharge cycle. Energetic efficiency reflects the lower voltages on discharge and the higher voltages required for charging. Energetic efficiencies are usually between 60% and 90%, depending on operating conditions.

10.7.1.3 Battery Life

Unlike other storage media, battery capacity decreases with use. Batteries are typically deemed to be exhausted when their capacity has dropped to 60% of the rated capacity. Battery life is often expressed as the number of charge–discharge cycles to a certain depth of discharge that one can get from the battery. Generally, for a given battery, the deeper the cycle depth of discharge, the shorter is the life of the battery. Cycle life also depends on battery construction. Long cycle life batteries last 1500–2000 deep discharge cycles whereas automotive batteries, for example, can only be deep discharged about 20 times. Battery life is sometimes modeled with techniques patterned after those developed for material fatigue. See Wenzl *et al.* (2005) for more information on battery life.

10.7.2 Compressed Air Energy Storage

Compressed air energy storage (CAES) uses an external electricity source, such as wind turbines, to power air compressors. The compressed air is then stored, for example in an underground storage chamber, and used subsequently in a turbine/generator to provide electricity back into the network. In principle, the compressed air could be used in an air turbine, but in all of the actually existing CAES systems, the compressed air is used to supply some or all of the air required by a natural gas turbine.

The central issues of compressed air energy storage can be illustrated by reference to the ideal gas law, which relates pressure, volume, and mass. For air, the equation is:

$$pV = mR_aT \tag{10.35}$$

where p = pressure (kPa), V = volume (m^3), m = mass (kg), R_a = gas constant for air (0.287 kPa m^3/kg K), and T = temperature (K).

Ideal compressors and turbines are adiabatic. That means that there is no heat transfer to or from them during the compression or expansion. (Strictly speaking, the ideal devices are actually isentropic, so the processes are reversible as well as adiabatic.) Equation (10.36) shows the relationship between temperatures and pressures in isentropic compression or expansion and Equation (10.37) gives the isentropic work out during the process (by convention, work in is negative).

$$T_{2s} = T_1 \left(\frac{p_2}{p_1}\right)^{(k-1)/k} \tag{10.36}$$

$$w_s = \frac{kR_aT_1}{k-1}\left[1-\left(\frac{p_2}{p_1}\right)^{(k-1)/k}\right] \tag{10.37}$$

where k is the ratio of constant pressure specific heat to constant volume specific heat (k is equal to 1.4 at room temperature and varies somewhat from that at other temperatures), w is the specific work out of the device (kJ/kg), and the subscripts 1 and 2 refer to the inlet and outlet of the device respectively. The subscript 's' signifies isentropic.

The thing to note is that the temperature of the air increases during compression and decreases during expansion. Once the air is compressed and the temperature has risen, however, the air begins to lose heat to the surroundings. If the heat transfer persists, the temperature will become equal to that of the surroundings. The resultant energy loss will be a significant fraction of the original energy imparted to the air during compression. This 'lost' energy will have to be replaced prior to expansion in the turbine, for example by burning natural gas to heat the air. The overall effect is one of significantly decreasing the round trip efficiency of the energy storage. There are methods to decrease the effect of the heat loss, such as using isothermal compressors and turbines (or approximations thereto, using multiple stages), thermal storage, and regenerators. In this concept, heat is removed from the compressor, stored temporarily, and then transferred to the air before the latter enters the turbine. This still entails losses and it also increases the complexity of the system. In very large air storage chambers, the surface area (where the heat loss occurs) is relatively small compared to the volume, so when the holding time is short, the effect of the heat loss is reduced.

In actually existing CAES systems, air is compressed and stored at night or other times when the value of the electricity is low. The compressed air is released and supplied to a gas turbine during the day or other times of higher demand for electricity. A typical gas turbine may use approximately 50% of the power it produces for running its own compressor. By being able to use the stored compressed air, the gas turbine will consume substantially less fuel for the same output.

Figure 10.21 is a schematic of a CAES system using an open cycle gas turbine. As can be seen, air enters the compressor (driven by an electric motor) at '1'. It is compressed up to a
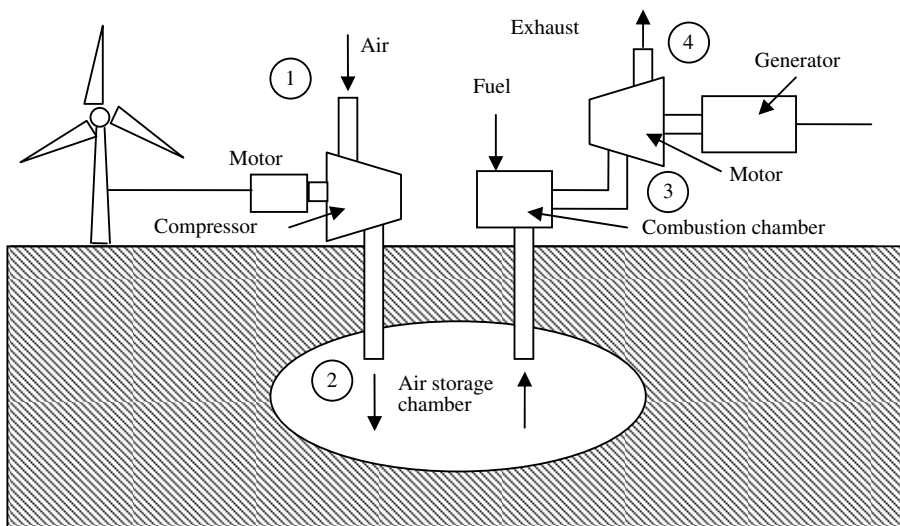
Figure 10.21   Schematic of CAES with gas turbine

higher pressure and temperature to state '2' and is stored in the air chamber. The air then enters the combustion chamber, together with the fuel (natural gas). The fuel is combusted, increasing the temperature at the inlet to the turbine, '3'. The turbine extracts much of the energy from the combustion gases in the form of shaft work. The pressure and temperature both drop during this part of the process, and the exhaust gases leave at '4'. Under conventional conditions (i.e. no wind turbine), much of the shaft work is used to drive the compressor. The remainder is used to turn the electrical generator.

For the ideal conventional (no CAES) gas turbine, the efficiency is a function of the ratio of the pressures at state points '3' and '4', as given in Equation (10.38).

$$\eta_{th,Brayton} = \frac{w_{net}}{q_{in}} = 1 - \left(\frac{p_3}{p_4}\right)^{\frac{k}{k-1}} \tag{10.38}$$

where w_{net} = net specific work out of the turbine; q_{in} = heat input from the combustion; P_3 and P_4 are the respective pressures at points 3 and 4.

The above discussion assumes an ideal Brayton cycle. In particular, that means that the compressor and the turbine are isentropic and that the heat transfer takes place at constant pressure. For practical pressure ratio ranges, the highest efficiency one might get from an ideal Brayton cycle is about 60%. Real gas turbines have lower efficiencies, typically in the range of 35–40%. For more details on this cycle, see a thermodynamics text such as Cengel and Boles (2006).

The net specific work may also be expressed as shown in Equation (10.39), which more clearly illustrates turbine work, w_{turb}, and compressor work, w_{comp}, (which is negative). Turbine and compressor efficiency (η_{turb} and η_{comp}) are also included. For the CAES system, the net specific work will increase, so the apparent efficiency will increase as well.

$$w_{net} = w_{comp} + w_{turb} = \frac{kR_aT_1}{\eta_{comp}(k-1)}\left[1-\left(\frac{p_2}{p_1}\right)^{\frac{k-1}{k}}\right] + \eta_{turb}\frac{kR_aT_3}{k-1}\left[1-\left(\frac{p_4}{p_3}\right)^{\frac{k-1}{k}}\right] \tag{10.39}$$

The first commercial scale compressed air energy storage facility was built in Huntorf, Germany in 1978. It has a capacity of 290 MW. The second one, a facility of 110 MW capacity, was constructed in McIntosh, Alabama in 1991. In this facility, the storage chamber is an abandoned salt cavern, with a capacity of 183,000 m^3, located 457 m underground. When full, the air pressure is 7.48 MPa, and when 'empty' the pressure is 4.42 MPa.

With present designs, the compression stage of the CAES process is actually far from isentropic, largely due to heat loss from the compressed air in the storage chamber (as discussed above). This lost heat needs to be compensated for by burning additional fuel. One approach to improving the efficiency of compressed air energy storage, by making the compression part of the process closer to isentropic, is discussed in Bullough *et al.* (2004).

10.7.3 Flywheel Energy Storage

Energy can be stored in a rotating flywheel by accelerating it, and can be recovered by decelerating it. A typical flywheel energy storage (FES) system is shown in Figure 10.22.

As shown in the figure, two power converters which can direct power either way are connected to an electrical machine, which is in turn connected to the flywheel. The electrical machine can run as either a motor or a generator, and so can either accelerate or decelerate the flywheel.
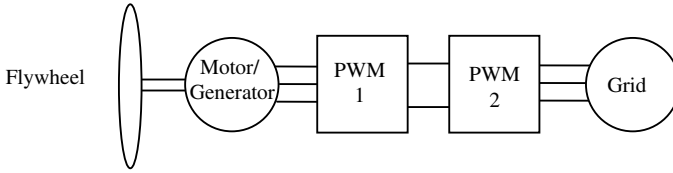
Figure 10.22   Flywheel energy storage system; PWM = converter using pulse width modulation

The total energy (J) stored in a flywheel is proportional to the mass moment of inertia, I_{Rot} (kg m^2) and the square of the rotational speed. The useful energy capacity, E, is limited by the range of allowable rotational speeds, Ω_{min} and Ω_{max} (rad/s), as shown in Equation (10.40). The round trip efficiency of FES is approximately 80–90%.

$$E = 0.5 I_{Rot}(\Omega_{max}^2 - \Omega_{min}^2) \tag{10.40}$$

Flywheels are typically made of composite materials. In order to minimize the amount of material in the flywheel itself, FES systems are designed so that the flywheel can run at speeds that are as high as practical. Rotational speeds may be on the order of 20 000 to 50 000 rpm. Flywheels are normally run in a near vacuum to minimize losses. One of the limiting factors is the high internal stress that arises during high rotational speeds.

Flywheel energy storage devices have been successfully applied in some wind/diesel systems, such as the one on Fair Isle, Scotland (Sinclair and Somerville, 1989). Subsequently, research on FES systems has been undertaken in Spain (Iglesias *et al.*, 2000).

10.7.4 Pumped Hydroelectric Energy Storage

Energy can be stored by pumping water from a lower reservoir to a higher one. The energy is recovered by allowing the water to return to the lower level, passing through a hydroelectric turbine in the process. The pump and turbine may actually be the same device, but able to function with water flowing in either direction. Round trip energy efficiency is in the range of 65–80%, depending on the details of the system. Figure 10.23 shows a schematic of a typical pumped hydroelectric energy storage system (PHS).
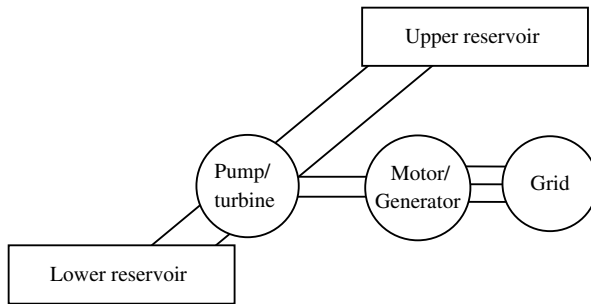
Figure 10.23   Pumped hydroelectric energy storage system

The energy, E (J), that may be stored in a reservoir of volume V (m^3) at an elevation z (m) above a reference elevation is:

$$E = V\rho_w g z \tag{10.41}$$

where ρ_w is the density of water (kg/m^3) and g is the gravitational constant (m/s^2).

Pumped hydroelectric energy storage has been employed in many locations for large-scale energy storage. For example, the pumped storage facility in Northfield, Massachusetts operates between the Connecticut River and a mountain top reservoir, 244 m higher, which is capable of holding 21.2 million m^3 of water. The effective energy storage capacity is approximately 14 000 MWh, and the facility can deliver up to 1080 MW of power. At least one pumped hydroelectric facility has been constructed to operate with a wind/diesel system. This was on the island of Foula, off the coast of Scotland (Somerville, 1989).

10.8 Fuel Production

10.8.1 Hydrogen

The electricity generated by a wind turbine can be used to produce hydrogen by the electrolysis of water. The fundamental relation is:

$$H_2O \rightarrow H_2 + \frac{1}{2}O_2, \Delta H = 286 \text{ kJ/mol } H_2O \tag{10.42}$$
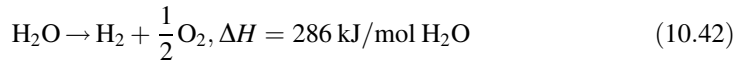
where: ΔH = change in enthalpy, and mol = gram molecular weight.

The hydrogen which has been produced can be stored in tanks, typically as a compressed gas, but sometimes as a liquid. The hydrogen can be used as a fuel, or it may be converted back to electricity at some later time. The energy content of hydrogen is theoretically the same as that required to electrolyze the water, i.e. 286 kJ/mol. Taking into account the molecular weight of hydrogen (2.016), this converts to 142 kJ/g (39.4 kWh/kg). On a weight basis, hydrogen has a very high energy density, but on a volume basis, the energy density is very low. Because the volume of a gas varies so much with changes in pressure or temperature, properties are typically referenced to 'normal' conditions, which are 0 °C and 1 atm (101 kPa). Under these conditions, the specific volume of hydrogen (i.e. the reciprocal of the density) is 11.11 Nm^3/kg, where Nm^3 means normal cubic meter. The energy content of the hydrogen at normal conditions is therefore 3.55 kWh/Nm^3. It is because the density of hydrogen is so low that hydrogen is compressed before being stored.

A schematic of a hydrogen production, compression, and storage process using a grid-connected wind turbine is illustrated in Figure 10.24. In this configuration, the wind turbine can supply electricity to the hydrogen system or to the utility grid. In addition, the grid can be used for the electricity supply as well. See also Bossel (2003) for discussion of hydrogen as an energy carrier.

10.8.1.1 Electrolysis of Water

In the electrolysis process, a DC voltage is applied to two electrodes immersed in a solution of water and an electrolyte. Typically potassium hydroxide is used as the electrolyte, although under some circumstances sodium hydroxide, sulphuric acid, or common salt (sodium
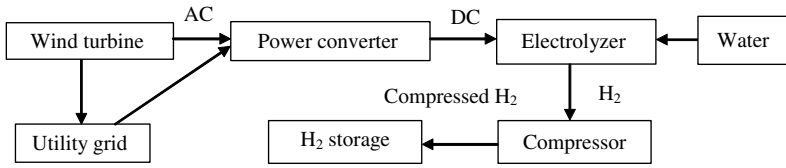
Figure 10.24   Wind/hydrogen production system

chloride) could be used. The electrolyte facilitates the flow of current through the solution. The electrodes are normally constructed from nickel, although other materials may be used. The voltage difference between the electrodes is on the order of a few volts. For example, in one case, the ideal voltage difference between the two electrodes is 1.23 V. In practice, it is actually higher, typically around 1.76 V. This increased voltage difference is one of the major reasons that the conversion efficiency of electricity to chemical energy is less than 100%. Presently, efficiencies of real electrolyzers are in the range of 65–75%.

During the electrolysis, the negative electrode (cathode) supplies electrons to positively charged hydrogen ions, resulting in the formation of H_2. Similarly, the positive electrode (anode) accepts electrons from the negatively charged hydroxyl ions, resulting in the production of O_2. The complete process involves a number of other steps as well, including maintaining separation of the hydrogen from the oxygen, separating the gases from the potassium hydroxide, and deoxidizing and drying the hydrogen. A typical electrolysis process, including some of the ancillary components, is illustrated in Figure 10.25.

10.8.1.2 Hydrogen Storage

The density of hydrogen is very low. Therefore, it is compressed for storage or transport. Storage tank pressures are in the range of 20–40 MPa. A significant amount of energy is required to compress the hydrogen. Just how much this is will depend on the type of process used and the efficiency of the compressor. The process will be between adiabatic and
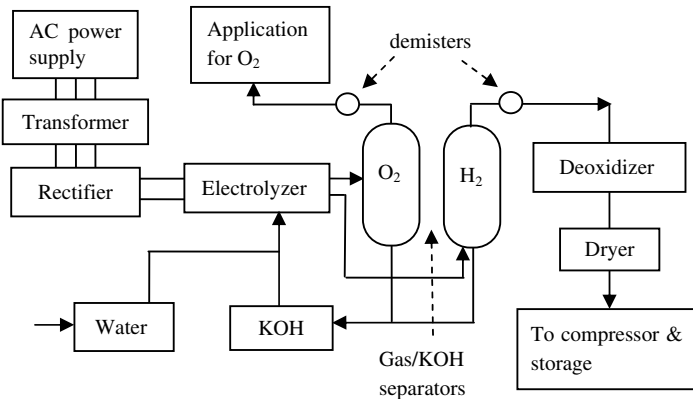
Figure 10.25   Hydrogen electrolysis process

isothermal. The specific work involved in the adiabatic compression, w_{comp} (kJ/kg), is:

$$w_{comp} = \frac{p_0 v_0 k/(k-1)}{\eta_{comp}} \left[\left(\frac{p_f}{p_0} \right)^{\frac{k-1}{k}} - 1 \right] \tag{10.43}$$

where:

p_0 = initial pressure, kPa
p_f = final pressure, kPa
k = ratio of constant pressure to constant volume specific heats (= 1.407 for hydrogen)
v_0 = initial specific volume of hydrogen, m^3/kg.
η_{comp} = compressor efficiency.

The specific work involved in isothermal compression, $w_{comp,iso}$, (kJ/kg) is:

$$w_{comp,iso} = \frac{p_0 v_0 \ln\left(\frac{p_f}{p_0} \right)}{\eta_{comp}} \tag{10.44}$$

By way of illustration, consider compression from 100 kPa to 40 MPa at 25 °C. The adiabatic specific work would be approximately 19.5 kJ/g, corresponding to about 14% of the energy in the hydrogen. Isothermal compression under the same conditions would consume approximately 7.4 kJ/g, or 5% of the energy.

Hydrogen could also be liquefied for storage, but this is not commonly done in a stationary application. This is because the energy required for the liquefaction is quite large, typically at least 30% of the energy in hydrogen.

Hydrogen could also be stored in metal hydrides, but at the present time this is not considered practical for stationary applications.

10.8.1.3 Uses of Hydrogen

Once it is produced, hydrogen may be used as an energy source. There are basically two main ways by which this may be done. The first is to use hydrogen as a transportation fuel. The second is to use it as a fuel for the generation of electricity. These are discussed below.

Hydrogen as a Transportation Fuel
There has been considerable interest over the last few years in the use of hydrogen as a transportation fuel. The intent is to use hydrogen as a replacement for fossil fuels. This implies that the hydrogen would be obtained from a non-fossil source, such as wind energy, so that the adverse effects of the carbon would not just be displaced elsewhere in the energy cycle. A detailed discussion of hydrogen as a transportation fuel is outside the scope of this book, so only a brief discussion will be given here.

At the present time, most of the activity regarding hydrogen as a transportation fuel has focused on public transport, particularly buses. This is because of hydrogen's low density and the need to carry it in pressurized tanks. For example, The Clean Urban Transport for Europe (CUTE) was a European Union project intended to demonstrate the use of hydrogen in buses in a number of European cities. Different hydrogen production and refueling infrastructures

were established in each of the cities. More information may be found at http://www.global-hydrogen-bus-platform.com/Home.

The hydrogen can be used in either a conventional internal combustion (IC) engine or it may be supplied to a fuel cell (see below). If an IC engine is used, then the bus is otherwise similar to conventional buses (except for the hydrogen storage tank). If a fuel cell is used, then the electricity from the fuel cell is used to power electric motors, which in turn drive the wheels.

Hydrogen for Stationary Electricity Generation

If hydrogen is used for stationary electricity generation, then the overall effect of the entire process is to use hydrogen as a reversible energy storage medium, similar to what might otherwise be done with batteries, pumped hydroelectric, or compressed air energy storage. As with the other energy storage options, the key questions have to do with overall round trip efficiency and the economics of the process. As will be seen below, the round trip efficiency of hydrogen storage is rather low, presently well under 30% (unless the hydrogen is combusted in a combined cycle power plant). The economics are also still not attractive at the present time.

There are essentially two methods by which hydrogen could be used to produce electricity: (1) gas turbine generators and (2) fuel cells.

(i) Gas Turbine Generators

Hydrogen could be used in a conventional gas turbine (perhaps with some modifications) in a similar way to the use of natural gas. The hydrogen could either be used straight or it could be mixed with natural gas. Gas turbines operate according to the Brayton cycle, which was discussed previously in Section 10.7.2. As also noted there, typical efficiencies of real gas turbines are on the order of 35–40%.

The round trip efficiency of the hydrogen energy storage when using a gas turbine generator, taking into account the electrolyzer (65–75%), the compression of the hydrogen (85–95%), the gas turbine (35–40%), and the electrical generator (95%), would be between 18% and 27%. Higher efficiencies could be obtained if the hydrogen were combusted in a combined cycle power plant. Such a plant could have an efficiency as high as 60%, resulting in an overall efficiency of 31–41%. The round trip efficiency is thus, even in the best of cases, quite low. It is therefore apparent that both the capital costs of the complete system and the value of electricity during the time of hydrogen production would also have to be low for this to be an economically attractive method of storing energy.

(ii) Fuel Cells

Fuel cells are devices that can be used to directly convert hydrogen into electricity. Conceptually, they may be thought of as the reverse of electrolyzers. In reality, fuel cells come in a variety of different designs. The types of hydrogen fuel cells available today are the following: (1) proton exchange membrane (PEM), (2) phosphoric acid, (3) molten carbonate, (4) alkaline, (5) solid oxide. The efficiency of conversion of hydrogen energy into electricity may be on the order of 50–60%, depending on the type of fuel cell and the details of its operation. Use of a fuel cell instead of a gas turbine generator in the previous example would result in round trip efficiencies of 28–43%, which would be a distinct improvement. In-depth discussion of fuel

cells is outside the scope of this book, so the reader should consult other sources, such as Larminie and Dicks (2003), for more information on this subject.

10.8.2 Ammonia

Ammonia is another possible fuel which could be produced using the wind as the energy source. The process would involve the conversion of hydrogen, produced as described above, into ammonia by the following reaction:

$$3H_2 + N_2 \rightarrow 2NH_3 \tag{10.45}$$

Ammonia has some properties that make it more convenient than hydrogen. For example, it can be liquefied at lower pressures and higher temperatures, such as as 1 MPa and ambient temperature or 100 kPa at $-28\,^{\circ}$C. As a liquid it has approximately 50% greater volumetric energy density than liquid hydrogen and twice the volumetric energy density of hydrogen at 70 MPa. In many ways ammonia is comparable to propane.

Ammonia can be burned directly in internal combustion engines or can be used directly in alkaline fuel cells. It can also be used as a source of hydrogen when that is desired, such as for supply to PEM fuel cells.

Ammonia can be made from hydrogen using the Haber–Bosch process, which was invented in Germany early in the 20th century. Basically, the process involves passing hydrogen gas and nitrogen gas over an iron catalyst.

The process to produce the ammonia is exothermic; thus the excess energy must be disposed of and will also result in a decrease in overall efficiency. The reaction releases 30.8 kJ of energy for every mol of hydrogen (H_2) converted. This amounts to approximately 10% of the energy in the hydrogen. In addition, the nitrogen gas must have been previously separated from the air. This part of the process is not as energy intensive as others, but it does need to be considered.

Ammonia also has some disadvantages. For example, it is toxic when released into the air. It is also readily absorbed into water, and this property must be considered in the design of equipment to handle and store the ammonia.

More details on ammonia as a possible fuel source may be found in Leighty and Holbrook (2008) and Thomas and Parks (2006).

References

Abdulwahid, U., Manwell, J. F. and McGowan, J. G. (2007) Development of a dynamic control communication system for hybrid power systems. *Renewable Power Generation*, **1**(1), 70–80.

Airy, G. B. (1845) On tides and waves. *Encyclopedia Metropolitana*, **5**, 241–396.

Andrews, W. T., Shumway, S. A. and Russell, B. (2006) *Design of a 10,000 cu-m/d Seawater Reverse Osmosis Plant on New Providence Island, The Bahamas*. DesalCo Limited.

Barltrop, N. D. P. and Adams, A. J. (1991) *Dynamics of Fixed Marine Structures*. Butterworth Heinemann, Oxford.

Barthelmie, R. J., Courtney, M. S., Højstrup, J. and Larsen, S. E. (1996) Meteorological aspects of offshore wind energy: observations from the Vindeby wind farm. *Journal of Wind Engineering and Industrial Aerodynamics*, **62**(2–3), 191–211.

Baxter, R. (2006) *Energy Storage: A Non-Technical Guide*. Penwell Books, Tulsa.

Bergey, M. (1998) Wind electric pumping systems for communities. *Proc. First International Symposium on Safe Drinking Water in Small Systems,* Washington (also available at http://www.bergey.com/School/NSF.Paper.htm).

Bossel, U. (2003) The physics of the hydrogen economy. *European Fuel Cell News*, **10**(2), 1–16 (Also available from http://www.efcf.com/reports/E05.pdf.)

Bullough. C., Gatzem, C., Jakiel, C., Koller, A., Nowi, A. and Zunft, S. (2004) Advanced adiabatic compressed air energy storage for the integration of wind energy. *Proc. of the 2004 European Wind Energy Conference,* London (also available at http://www.ewi.uni-koeln.de/ewi/content/e266/e283/e3047/EWECPaperFinal2004_ger.pdf).

Carta, J. A., González, J. and Subiela, V. (2003) Operational analysis of an innovative wind powered reverse osmosis system installed in the Canary Islands. *Solar Energy*, **75**(2), 153–168.

Cengel, Y. and Boles, M. (2006) *Thermodynamics: An Engineering Approach*, 6th edition. McGraw Hill, New York.

Cheng, P. W. (2002) *A Reliability Based Design Methodology for Extreme Responses of Offshore Wind Turbines.* PhD dissertation, Delft University of Technology.

Dörner, H. (2009) *Milestones of wind energy utilization 1.* Available at: http://www.ifb.uni-stuttgart.de/~doerner/ewindenergie1.html. Note: a better reference (but harder to find and in German) is: Honnef, H. (1932) *Windkraftwerke*. Friedr. Vieweg & Sohn Akt.-Ges., Braunschweig.

Elkinton, C. N. (2007) *Offshore Wind Farm Layout Optimization*. PhD dissertation, University of Massachusetts, Amherst.

Fabre, A. (2003) Wind turbines designed for the specific environment of islands case study: experience of an autonomous wind powered water desalination system on the island of Therasia, Greece. *Proc. International Conference RES for Islands, Tourism, and Desalination,* Crete, Greece.

Fermo, R., Guida, U., Poulet, G., Magnani, F. and Aleo, S. (1993) 150 kV system for feeding Ischia Island. *Proc. Third Conference on Power Cables and Accessories, 10 kV–500 kV,* London, UK.

Fink, D. and Beaty, H. (1978) *Standard Handbook for Electrical Engineers*. McGraw-Hill.

Fraenkel, P. (1997) *Water-Pumping Devices: A Handbook for Users and Choosers*. Intermediate Technology Press, Reading.

Gardner, P., Craig, L. M. and Smith, G. J. (1998) Electrical systems for offshore wind farms. *Proc. 1998 British Wind Energy Association Conference.* Professional Engineering Publishing Limited, UK.

GL (2005) *Guidelines for the Certification of Offshore Wind Turbines*. Germanischer Lloyd, Hamburg.

Grainger, W. and Jenkins, N. (1998) Offshore wind farm electrical connection options. *Proc. British Wind Energy Association Conference.* Professional Engineering Publishing Limited, UK.

Gumbel, E. J. (1958) *Statistics of Extremes*. Columbia University Press, New York.

Henderson, C. R., Manwell, J. F. and McGowan, J. G. (2009) A wind/diesel hybrid system with desalination for Star Island, NH: feasibility study results. *Desalination*, **237**, 318–329.

Heronemus, W. E. (1972) Pollution-free energy from offshore winds. *Proceedings of 8th Annual Conference and Exposition, Marine Technology Society,* Washington, DC.

Holz, R., Drouihlet, S. and Gevorgian, V. (1998) Wind-electric ice making investigation, NREL/CP-500-24622. *Proc. 1998 American Wind Energy Association Conference,* Bakersfield, CA.

Hsu, S. A. (2003) Estimating overwater friction velocity and exponent of power-law wind profile from gust factor during storms. *Journal of Water, Port, Coastal and Ocean Engineering*, **129**(4), 174–177.

Hunter, R. and Elliot, G. (Eds) (1994) *Wind–Diesel Systems*. Cambridge University Press, Cambridge, UK.

Ibrahim, H., Ilincaa, A. and Perron, J. (2008) Energy storage systems – characteristics and comparisons. *Renewable and Sustainable Energy Reviews*, **12**, 1221–1250.

IEC (2002) *Wind Turbines – Part 24: Lightning Protection, IEC 61400-24 TR* 1st edition. International Electrotechnical Commission, Geneva.

IEC (2009) *Wind Turbines – Part 3: Design Requirements for Offshore Wind Turbines, 61400-3*. International Electrotechnical Commission, Geneva.

Iglesias, I. J., Garcia-Tabares, L., Agudo, A., Cruz, I. and Arribas, L. (2000) Design and simulation of a stand-alone wind-diesel generator with a flywheel energy storage system to supply the required active and reactive power. *Proc. IEEE Power Electronics Specialists Conference.* IEEE Power Electronics Society, Washington (also available from: http://www.cedex.es/ceta/cetaweb/info_fisicas/almacenador_-pesc00.pdf)

Infield, D. G., Lundsager, P., Pierik, J. T. G, van Dijk, V. A. P., Falchetta, M., Skarstein, O. and Lund, P. D. (1990) Wind diesel system modelling and design. *Proc. 1990 European Wind Energy Conference*, pp. 569–574.

Johnson, C., Abdulwahid, U., Manwell, J. F. and Rogers, A. L. (2002) Design and modeling of dispatchable heat storage in remote wind/diesel systems. *Proc. of the 2002 World Wind Energy Conference,* Berlin. WIP-Munich.

Kentfield, J. (1996) *The Fundamentals of Wind-Driven Water Pumpers*. Gordon and Breach Science Publishers, Amsterdam.

Kühn, M. (2001) *Dynamics and Design Optimisation of Offshore Wind Energy Conversion Systems*. PhD dissertation, Delft University of Technology, Delft.

Lange, B. and Højstrup, J. (1999) The influence of waves on the offshore wind resource. *Proc. 1991 European Wind Energy Conference,* Nice.

Larminie, J. and Dicks, A. (2003) *Fuel Cell Systems Explained*, 2nd edition. John Wiley & Sons, Ltd, Chichester.

Le Gouriérès (1982) *Wind Power Plants: Theory and Design*. Pergamon Press, London (now Elsevier, Amsterdam).

Leighty, W. and Holbrook, J. (2008) Transmission and firming of GW-scale wind energy via hydrogen and ammonia. *Wind Engineering*, **32**(1), 45–65.

Lyons, J. and Goodman, N. (2004) TDX Power: St Paul Alaska operational experience. *Proc. 2004 Wind-Diesel Workshop,* Anchorage (available from http://www.eere.energy.gov/windandhydro/windpoweringamerica/pdfs/workshops/2004_wind_diesel/operational/st_paul_ak.pdf).

Lysen, E. H. (1983) *Introduction to Wind Energy*. Consultancy Wind Energy in Developing Countries, Amersfoort, Netherlands (also available at http://www.uce-uu.nl/?action=25&menuId=4).

Manwell, J. F. (1988) *Understanding Wind Energy for Water Pumping*. Volunteers in Technical Assistance, Arlington, VA, (also available at http://www.fastonline.org/CD3WD_40/VITA/WINDWATR/EN/WINDWATR.HTM).

Manwell, J. F. and McGowan, J. G. (1981) A design procedure for wind-powered heating systems. *Solar Energy*, **26**(5), 437–445.

Manwell, J. F. and McGowan, J. G. (1993) Lead acid battery storage model for hybrid energy systems. *Solar Energy*, **50** (5), 399–405.

Manwell, J. F. and McGowan, J. G. (1994) Extension of the Kinetic Battery Model for Wind/Hybrid Power Systems. *Proc. 1994 European Wind Energy Conference,* Thessaloniki.

Manwell, J. F., Elkinton, C., Rogers, A. L. and McGowan, J. G. (2007) Review of design conditions applicable to offshore wind energy in the United States. *Renewable and Sustainable Energy Reviews*, **11**(2), 183–364.

Manwell, J. F., Rogers, A., Hayman, G., Avelar, C. T. and McGowan, J. G. (1997) *Hybrid2–A Hybrid System Simulation Model, Theory Summary*. NREL Subcontract No. XL-1-11126-1-1. Dept. of Mechanical and Industrial Engineering, University of Massachusetts, Amherst.

Martínez de Alegría, I., Martín, J. L., Kortabarria, I., Andreu, J. and Ereño, P. I. (2009) Transmission alternatives for offshore electrical power. *Renewable and Sustainable Energy Reviews*, **13**, 1027–1038.

Masters, G. (2004) *Renewable and Efficient Electric Power Systems*. Wiley-IEEE Press, Chichester.

Miranda, M. S. and Infield, D. (2002) A wind powered seawater reverse-osmosis system without batteries. *Desalination*, **153**, 9–16.

Musial, W. (2007) Offshore wind electricity: a viable energy option for the coastal United States. *Marine Technology Society Journal*, **41**(3), 32–43.

Ochi, M. K. (1998) *Ocean Waves – The Stochastic Approach*. Cambridge University Press, Cambridge.

Sinclair, B. A. and Somerville, W. M. (1989) Experience with the wind turbine flywheel combination on Fair Isle. *Proc. 1989 European Wind Energy Conference,* Glasgow.

Somerville, W. M. (1989) Wind turbine and pumped storage hydro generation in Foula. *Proc. 1989 European Wind Energy Conference,* Glasgow.

Thomas, G. and Parks, G. (2006) *Potential Roles of Ammonia in a Hydrogen Economy*. USDOE Hydrogen Energy Program, available from http://www.hydrogen.energy.gov/pdfs/nh3_paper.pdf.

Thompson, A. M. (2004) *Reverse-Osmosis Desalination of Seawater Powered by Photovoltaics Without Batteries*. PhD dissertation, Loughborough University.

Thompson, M. and Infield, D. (2002) A photovoltaic-powered seawater reverse-osmosis system without batteries. *Desalination*, **153**, 1–8.

Twidell, J. and Gaudiosi, G. (2009) *Offshore Wind Power*. Multi-Science Publishing Co. Ltd, Brentwood, UK.

USACE (2002) *Coastal Engineering Manual, CEM M 1110-2-1100*. US Army Corps of Engineers (USACE), Washington (also available from http://chl.erdc.usace.army.mil/chl.aspx?p=s&a=PUBLICATIONS;8).

van der Tempel, J. (2006) *Design of Support Structures for Offshore Wind Turbines*. PhD dissertation, Delft University of Technology, Delft.

Veldkamp, D. (2006) *Chances in Wind Energy: A Probabilistic Approach to Wind Turbine Fatigue Design*. PhD dissertation, Delft University of Technology, Delft.

Warfel, C. G., Manwell, J. F. and McGowan, J. G. (1988) Techno-economic study of autonomous wind driven reverse osmosis desalination systems. *Solar and Wind Technology*, **5**(5), 549–561.

Wenzl, H., Baring-Gould, I., Kaiser, R., Liaw, B. Y., Lundsager, P., Manwell, J. F., Ruddell, A. and Svoboda, V. (2005) Life prediction of batteries for selecting the technically most suitable and cost effective battery. *Journal of Power Sources*, **144**(2), 373–384.

Westinghouse Electric Corp. (1979) *Design Study and Economic Assessment of Multi-unit Offshore Wind Energy Conversion Systems Application.* DOE WASH-2830-78/4.

Wienke, J. (2001) *Druckschlagbelastung auf Schlanke Zylindrische Bauwerke durch Brechende Wellen.* PhD dissertation, TU Carolo-Wilhelmina zu Braunschweig, Braunschweig.

Wilf, M. and Bartels, C. (2005) Optimization of seawater RO systems design. *Desalination*, **173**, 1–12.

11

Wind Energy System Economics

11.1 Introduction

In the previous chapters, the main emphasis has been on the technical and performance aspects of wind turbines and their associated systems. As discussed there, in order for a wind turbine to be a viable contender for producing energy, it must: (1) produce energy, (2) survive, and (3) be cost effective.

Assuming that one has designed a wind energy system that can reliably produce energy, one should be able to predict its annual energy production. With this result and the determination of the manufacturing, installation, operation and maintenance, and financing costs, the cost effectiveness can be addressed. As shown in Figure 11.1, in discussing the economic aspects of wind energy, it is also important to treat the costs of generating wind energy and the market value of the energy produced (its monetary worth) as separate subjects. The economic viability of wind energy depends on the match of these two variables. That is, the market value must exceed the cost before the purchase of a wind energy system can be economically justified.

The economic aspects of wind energy vary, depending on the application. Grid-connected wind turbines will probably make a larger contribution to the world energy supply than turbines on isolated networks (EWEA, 2004). Thus, the primary emphasis in this chapter will be on wind systems supplying electricity to consumers on the main grid. Much of the material here, however, can be used for small to medium-sized wind energy installations that are isolated from a large electrical grid.

This chapter concentrates on the economics of larger wind energy systems, first introducing the subjects shown in Figure 11.1. Next, details of the capital, operation, and maintenance cost of wind energy systems are summarized in Sections 11.3 and 11.4. Sections 11.5 and 11.6 discuss the value of wind energy and the variety of economic analysis methods that can be applied to determine the economic viability of wind energy systems. These methods range from simplified procedures to detailed life cycle costing models. The chapter concludes with a section reviewing wind energy system market considerations.
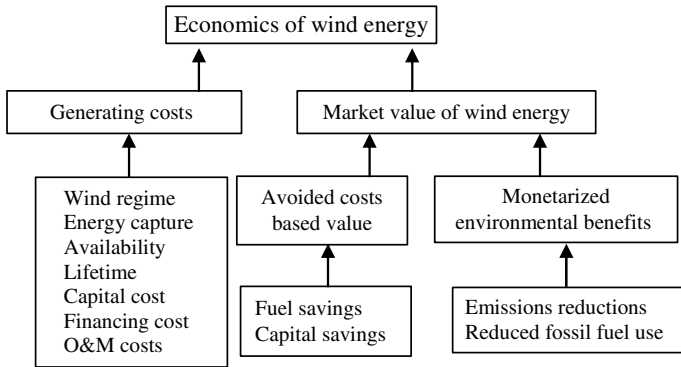
Figure 11.1   Components of wind system economics

11.2 Overview of Economic Assessment of Wind Energy Systems

This section discusses the overall economics of wind energy systems, covering the topics shown in Figure 11.1.

11.2.1 Generating Costs of Grid-connected Wind Turbines: Overview

The total generating costs for an electricity-producing wind turbine system are determined by the following factors:

- wind regime;
- energy capture efficiency of the wind turbine(s);
- availability of the system;
- lifetime of the system;
- capital costs;
- financing costs;
- operation and maintenance costs.

The first two factors have been addressed in detail in previous chapters. The remaining factors are summarized below. As pointed out in Chapter 2, variation in the long-term wind resource can cause uncertainty in the production and resulting generation costs (Raftery *et al.*, 1999). Thus, these topics should be considered in more detailed economic analyses.

11.2.1.1 Availability

The availability is the fraction of the time that the wind turbine is able to generate electricity. The times when a wind turbine is not available include downtime for periodic maintenance or unscheduled repairs. Reliable numbers for availability can be determined only if data for a large number of turbines over an operation period of many years are available. By the mid 1990s, only the United States and Denmark had enough data to provide this information.
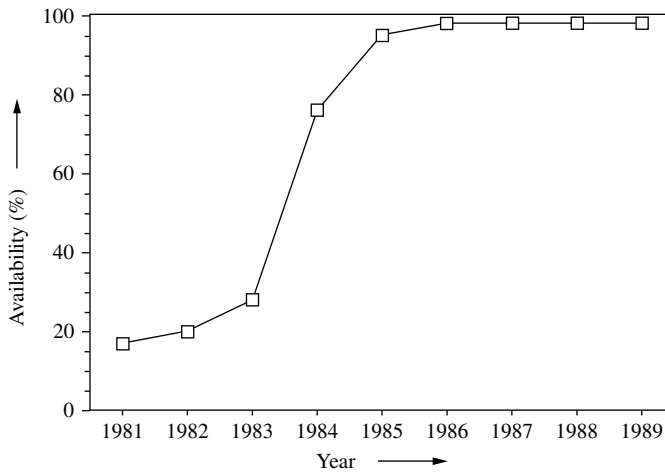
Figure 11.2 Availability of the best wind turbines in California (WEC, 1993). Reproduced by permission of the World Energy Council, London

For example, as shown in Figure 11.2, at the end of the 1980s, the best wind turbines in the United States reached availability levels of 95% after five years of operation (WEC, 1993). Recent data indicate that availability is now on the order of 97–99% (EWEA, 2004).

11.2.1.2 Lifetime of the System

It is common practice to equate the design lifetime with the economic lifetime of a wind energy system. In Europe, a period of 20 years is often assumed for the economic assessment of wind energy systems (WEC, 1993). This follows the recommendations of the Danish Wind Industry Association (2006), which states that a 20-year design lifetime is a useful economic compromise that is used to guide engineers who develop components for wind turbines.

Following improvements in wind turbine design, an operating life of 30 years was used for detailed US economic studies (DOE/EPRI, 1997). This assumption requires that adequate annual maintenance be performed on the wind turbines and that ten-year major maintenance overhauls be performed to replace key parts.

11.2.1.3 Capital Costs

Details on the determination of the capital cost of wind energy systems are given in Section 11.3. The determination of the capital (or total investment) costs generally involves the cost of the wind turbine(s) and the cost of the remaining installation. Wind turbine costs can vary significantly. For example, Figure 11.3 gives the cost range (not including installation) for production of Danish wind machines (Danish Wind Industry Association, 2006). As shown, costs vary significantly for each rated generator size. This may be due to differing tower height and/or rotor diameter.

In generalized economic studies, wind turbine installed costs are often normalized to cost per unit of rotor area or cost per rated kW. Examples of both of these types of normalized wind
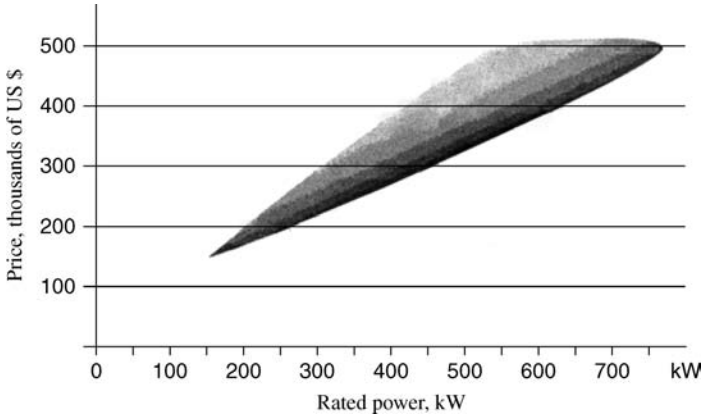
Figure 11.3 Cost (2006) of Danish wind turbines as a function of size: the 'price banana' (Danish Wind Industry Association, 2006). Reproduced by permission of the Danish Wind Industry Association

turbine costs are shown in Figures 11.4 and 11.5. Figure 11.4 gives the specific cost per unit of rotor area for commercial and early experimental utility scale machines in the United States and Europe (Harrison *et al.*, 2000). It should be noted that all of the prototype units have manufacturing costs that are significantly higher than those of commercial or mass-produced units.
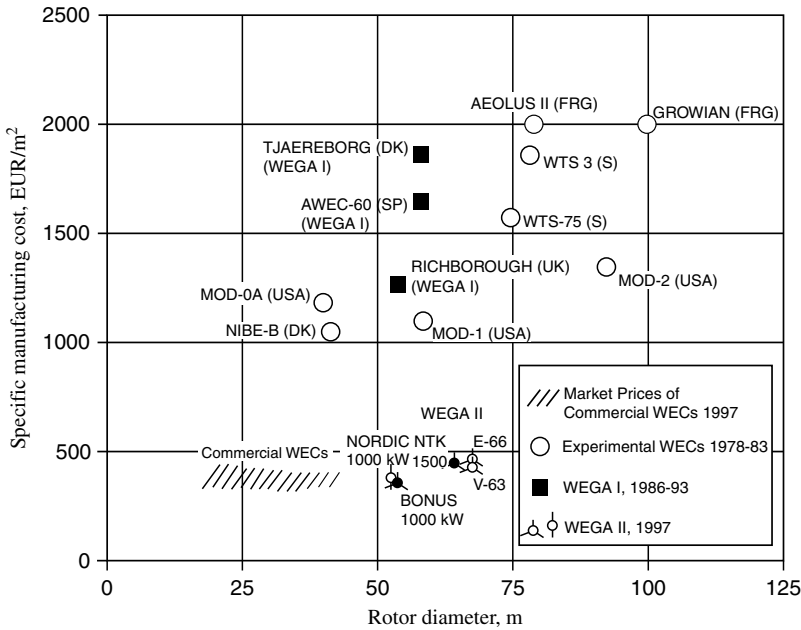
Figure 11.4 Large wind turbine costs per unit rotor area (Harrison *et al.*, 2000)
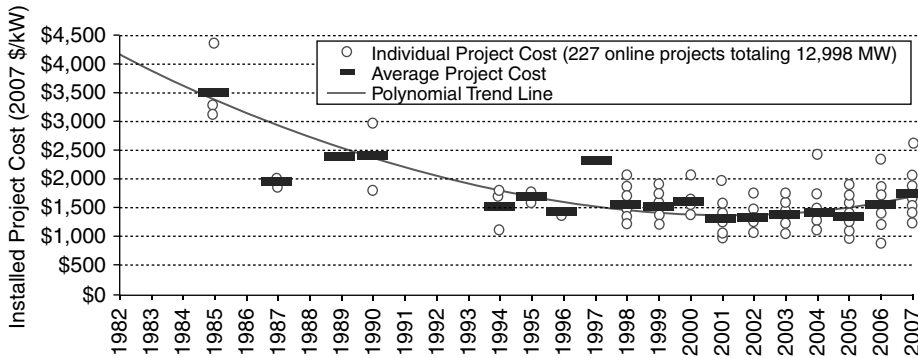
Figure 11.5 Wind turbine installed prices in the US (Wiser and Bolinger, 2008)

The normalization of wind turbine costs to installed cost per unit of rated power (e.g., $/kW) output follows conventional large-scale electrical generation practice and is often used. For commercial turbines used in wind farms there was a steady decrease in cost per unit power since the 1980s. Since 2003, however, the cost of wind turbines has increased, primarily due to higher materials and energy input prices (e.g., steel, aluminum, and copper). This point is illustrated in Figure 11.5, in which installed US wind turbine costs ($/kW) are given as a function of time (Wiser and Bolinger, 2008). According to a recent report from the European Wind Energy Association (EWEA, 2008), a steady decrease in wind turbine capital costs is expected to return in the near future.

Other investigators have projected capital cost data for large-scale wind farms from 1997 to 2030. For example, the US Department of Energy (DOE) and the Electric Power Research Institute (EPRI) projected costs in 1997 dollars (DOE/EPRI, 1997) to decrease from $1000/kW in 1997 to $635/kW in 2030.

As is discussed in Section 11.3.4, the costs of a wind farm installation include costs beyond those of the wind turbines themselves. For example, in developed countries of the world, the wind turbine represents only approximately 65% to 75% of the total investment costs. Wind farm costs also include costs for infrastructure and installation, as well as electrical grid connection costs. Costs per kW of single wind turbine installations are generally much higher, which is the reason for wind farm development in the first place.

11.2.1.4 Financing Costs

Wind energy projects are capital intensive, and the majority of the costs must be borne at the beginning. For that reason, the purchase and installation costs are largely financed. The purchaser or developer will pay a limited down payment (perhaps 10% to 20%) and finance (borrow) the rest. The source of capital may be a bank or investors. In either case, the lenders will expect a return on the loan. The return in the case of a bank is referred to as the interest. Over the life of the project, the cumulative interest can add up to a significant amount of the total costs. Other methods of financing are also used, but they are beyond the scope of this text.
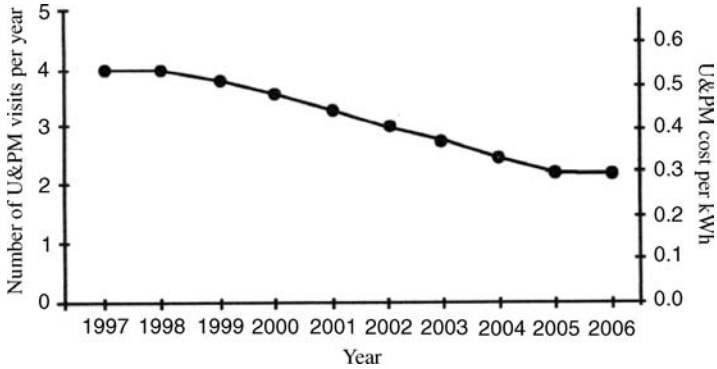
Figure 11.6 Predicted operation and maintenance costs (Chapman *et al.*, 1998); U&PM, unscheduled and preventive maintenance

11.2.1.5 Operation and Maintenance Costs

The Danish Wind Industry Association (2006) states that annual operation and maintenance (O&M) costs for wind turbines generally range from 1.5% to 3% of the original turbine cost. This organization also points out that regular service to the turbine constitutes most of the maintenance cost.

Many authors prefer to use a set cost per kWh of output for their operation and maintenance cost estimates. Figure 11.6 gives results from a US study (Chapman *et al.*, 1998) in which unscheduled and preventive maintenance (U&PM) costs are given as a function of time. Note that these costs were predicted to decline from 0.55 to 0.31 cents per kWh in the 1997 to 2006 time frame. Section 11.4 gives more details on the range of values for O&M costs.

11.2.2 Value of Grid-generated Wind Energy: Overview

The value of wind energy depends on the application and on the costs of alternatives to produce the same output. To determine value, one may try to figure 'what the market will bear'. For example, a manufacturer may ask a price and adjust it until he or she finds a buyer (negotiated price). Alternatively, a buyer, such as an electric utility, may ask for competitive bids to supply power and select those with the lowest prices that look qualified.

For a utility, the value of wind energy is primarily a function of the cost of the fuel that would not be needed or the amount of new system generating capacity that could be deferred. For society as whole, however, the environmental benefits can be quite significant. When these benefits are monetized, they can contribute significantly to the market value of the electricity. More details on the determination of wind energy's value (including monetized environmental benefits) are given in Section 11.5.

11.2.3 Economic Analysis Methods: Overview

A wind energy system can be considered to be an investment that produces revenue. The purpose of an economic analysis is to evaluate the profitability of a wind energy project

and to compare it with alternative investments. The alternative investments might include other renewable electricity producing power systems (photovoltaic power, for example) or conventional fossil fuel systems. Estimates of the capital costs and O&M costs of a wind energy system, together with other parameters which are discussed below, are used in such analyses.

In Section 11.6, the following three different types of overall economic analysis methods are described:

- simplified models;
- detailed life cycle cost models;
- electric utility economic models.

Each of these economic analysis techniques requires its own definitions of key economic parameters and each has its particular advantages and disadvantages.

11.2.4 Market Considerations: Overview

At the present time, the market for utility-scale wind energy systems is rapidly expanding. The world market demand has grown from about 200 MW/year in 1990 to more than 10 000 MW/year through 2008. In Section 11.7, the market considerations for wind systems are discussed. They include the following issues:

- the potential market for wind systems;
- barriers to expansion of markets;
- incentives for market development.

11.3 Capital Costs of Wind Energy Systems

11.3.1 General Considerations

The determination of the capital costs of a wind energy system remains one of the more challenging subjects in wind energy. The problem is complicated because wind turbine manufacturers are not particularly anxious to share their own cost figures with the rest of the world, or, in particular, with their competitors. Cost comparisons of wind turbine research and development projects are particularly difficult; that is, the development costs cannot be compared consistently. Also, costs other than the turbine may be site specific. This problem can further complicate capital cost estimates. This is especially true for offshore systems, in which installation costs may be large relative to the wind turbine costs.

In determining the cost of the wind turbine itself, one must distinguish between the following types of capital cost estimates:

- **Cost of wind turbine(s) today.** For this type of cost estimate, a developer or engineer can contact the manufacturer of the machine of interest and obtain a formal price quote.
- **Cost of wind turbine(s) in the future.** For this type of cost estimate (assuming present wind turbine state of the art), one has a number of tools that can be applied, namely: (1) historical trends, (2) learning curves (see next section), and (3) detailed examination of present designs (including the total machine and components) to determine where costs may be lowered.

- **Cost of a new (not previously built) wind turbine design.** This type of capital cost estimate is much more complex since it must first include a preliminary design of the new turbine. Price estimates and quotes for the various components must be obtained. The total capital cost estimate must also include other costs such as design, fabrication, testing, etc.
- **Future cost of a large number of wind turbines of a new design.** This type of cost estimate will involve a mixture of the second and third types of cost estimates.

It is assumed that one can readily obtain the first type of capital cost estimate. Accordingly, the following discussion concentrates on information that can be used for the last three types of cost estimates.

Recent worldwide experience with wind turbine fabrication, installation, and operation has yielded some data and analytical tools that can be used for capital cost estimates of wind turbines and/or of the supporting components that are required for a wind farm installation. For example, there have been numerous capital cost estimates for wind turbines based on various simplified scaling techniques. These usually feature a combination of actual cost data for a given machine and empirical equations for the cost of the key components based on a characteristic dimension (such as rotor diameter) of the wind turbine. The same type of generalized scaling analysis has been used to predict wind farm costs.

After a brief discussion of the use of learning curves to predict capital costs of wind turbines, a summary is presented showing how estimates can be made for the capital costs of wind turbines alone and wind turbines in combination with the other components that constitute a wind farm system.

11.3.2 Use of Experience (or Learning) Curves to Predict Capital Costs

One unknown in capital cost estimates is the potential reduction in costs of a component or system when it is produced in large quantities. One can use the concept of experience (or learning) curves to predict the cost of components when they are produced in large quantities. The experience curve concept is based on over 40 years of studies of manufacturing cost reductions in major industries (Johnson, 1985; Cody and Tiedje, 1996).

The experience curve gives an empirical relationship between the cost of an object $C(V)$ as a function of the cumulative volume, V, of the object produced. Functionally, this is expressed as:

$$\frac{C(V)}{C(V_0)} = \left(\frac{V}{V_0}\right)^b \tag{11.1}$$

where the exponent b, the learning parameter, is negative and $C(V_0)$ and V_0 correspond to the cost and cumulative volume at an arbitrary initial time. From Equation (11.1), an increase in the cumulative production by a factor of 2 leads to a reduction in the object's cost by a progress ratio, s, where $s = 2^b$. The progress ratio, expressed as a percentage, is a measure of the technological progress that drives the cost reduction.

A graphical example of this relationship is presented in Figure 11.7, which gives a plot of normalized cost $C(V_0) = 1$ for progress ratios ranging from 70% to 95%. As shown, given the initial cost and an estimate of the progress ratio, one can estimate the cost of the tenth, hundredth, or whatever unit of production of the object.

Experience has shown that s can range from 70% to 95%. For example, Johnson (1985) gives values of s of 95% for electrical power generation, 80% for aircraft assembly,
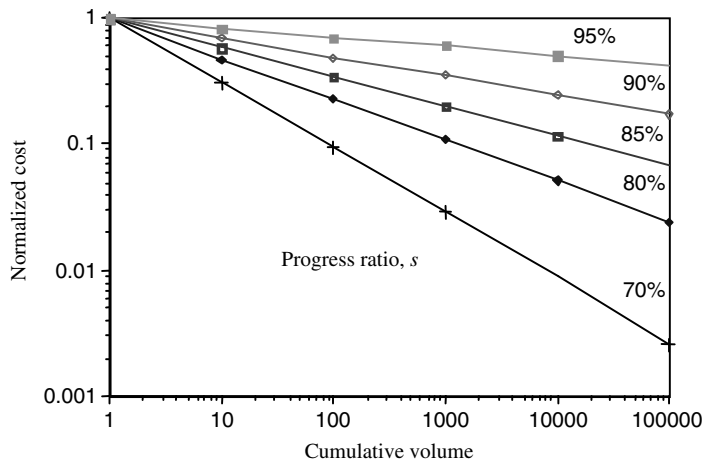
Figure 11.7   Normalized cost vs. cumulative volume for varying progress ratios

and 74% for hand-held calculators. Various parts of a wind turbine would be expected to have different progress ratios; that is, components such as the blades and hub that are essentially unique to wind turbines would have smaller values of s. Electrical generators, however, could represent a mature technology, with higher progress ratio values. For wind turbines, Neij (1999) gives a summary of progress ratios for various utility-scale machines. A more recent summary of global experience curves for wind farms is given by Junginger *et al.* (2005).

11.3.3 *Wind Turbine Costs*

11.3.3.1 Historical Overview

One way to estimate the capital costs of a new wind turbine is to use cost data for smaller existing machines normalized to a machine size parameter. Here, the usual parameters that are used are unit cost per kW of rated power or unit cost per area of rotor diameter. Although this methodology can be used for energy generation system or planning studies, it yields little information as to the details of a particular design and potential cost reduction for new designs of wind turbines.

   A more fundamental way to determine the capital cost of a wind turbine is to divide the machine into its various components and to determine the cost of each component. This method represents a major engineering task, however, and there are relatively few such studies documented in the open literature. Historically interesting examples here include US work on a conceptual 200 kW machine (NASA, 1979) and work on the MOD2 (Boeing, 1979) and MOD5A (General Electric Company, 1984) machines. More recent work, supported under the WindPact (Wind Partnerships for Advanced Component Technology) program sponsored by NREL (see http://www.nrel.gov/wind/advanced_technology.html) in the US, has produced a number of reports containing methods for the estimation of wind turbine component and total wind turbine costs (e.g., Fingersh *et al.*, 2006).

Table 11.1 Projected construction costs for large turbines (Johnson, 1985)

Specification or Cost	British design	Smith–Putnam	P.T. Thomas	NASA MOD-X
Specification				
Rotor diameter (m)	68.6	53.3	61	38.1
Rated power (kW)	3670	1500	7500	200
Rated wind speed (m/s)	15.6	13.4	15.2	9.4
Production quantity	40	20	10	100
Component Cost (%)				
Blades	7.4	11.2	3.9	19.6
Hub, bearings, main shaft, nacelle	19.5	41.5	5.9	15.2
Gearbox	16.7	9.5	2.3	16.5
Electric generator and installation	12.5	3.5	33.6	7.6
Controls	4.4	6.5	8.3	4.4
Tower	8.1	7.7	11.2	20.6
Foundation and site work	31.4	16.6	20.3	16.1
Engineering		3.6	14.5	

The results of such a detailed study depend strongly on the turbine, design assumptions, and method of economic analysis. As summarized in Table 11.1, some interesting historical comparisons between large wind turbine designs can be made if the component costs are expressed as percentages. Note that all these studies were based on horizontal axis wind machines over the time period of the 1950s through the 1980s.

The fourth numerical column summarizes the result of a 1980 NASA study of a 200 kW horizontal axis wind turbine (MOD-X) based on their experience with the MOD-0 and MOD-0A machines. This conceptual design featured two pitch-controlled blades, a teetered hub, and a free yaw system. The rotor was connected to the low-speed shaft of a three-stage parallel shaft gearbox, and a synchronous generator rated at 200 kW with a speed of 1800 rpm was used. A significant difference between the three earlier studies and the 1979 NASA study occurred in the area of improved technology in component hardware and analysis techniques.

To further illustrate the differences in component cost fractions for wind turbine designs, one can refer to the text of Hau *et al.* (1993). Based on this work, Figure 11.8 gives a capital cost breakdown for the main components of three large-scale European wind turbines. A wide variation in component cost fractions can be seen.

11.3.3.2 Detailed Capital Cost Model Example

In an effort to quantify the capital costs for horizontal axis wind turbines, a detailed cost model for horizontal axis wind turbines has been developed at the University of Sunderland (Hau *et al.*, 1996; Harrison and Jenkins, 1993; Harrison *et al.*, 2000). Starting with an outline specification of a proposed (two- or three-bladed) wind turbine, and using some basic design options, the computer code can provide a capital cost estimate of a specific wind turbine design. An overview of the key features of the (weight-based) model's operation is given in Figure 11.9.

Based on the input data, the model uses first principles to develop estimates of the most important influences on cost of the proposed machine. As shown in Figure 11.9, these are called
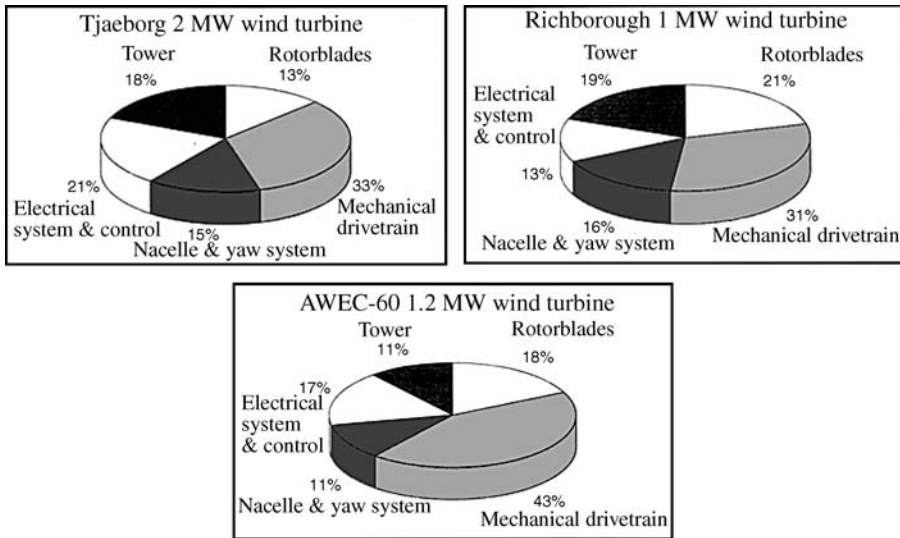
Figure 11.8 Manufacturing cost breakdown of 1990s European wind turbines (Hau *et al.*, 1993) Reproduced by permission of Springer-Verlag GmbH and Co.

'design drivers' and include such variables as the blade loadings, the horizontal thrust on the machine, gearbox requirements, and generator specifications. Next, the model estimates the loads on the major subsystems of the wind turbine, allowing the approximate sizes for the major components to be determined. For example, analytical expressions are used to estimate the low-speed shaft diameter such that the shaft will be able to carry both the torsional and axial loading exerted on it by the rotor. For more complex components, where analytical expressions are not sufficient, look-up tables relating component size to loadings are used. In certain cases, components are assigned a complexity rating in order to reflect how much work is involved in their manufacture.

Using the calculated size of each component, the weights of the components (assuming a known material density) are then determined. It should be noted that some of the weights are used to calculate loadings on other components, but their primary purpose is to allow the estimation of the wind turbine cost. The cost of each subsystem is then determined via the following expression:

$$\text{Cost} = \left(\begin{array}{c} \text{Calibration} \\ \text{coefficient} \end{array} \right) \times (\text{Weight}) \times \left(\begin{array}{c} \text{Cost per} \\ \text{unit weight} \end{array} \right) \times \left(\begin{array}{c} \text{Complexity} \\ \text{factor} \end{array} \right) \qquad (11.2)$$

The calibration coefficient is a constant for each subsystem. It is determined by a statistical analysis of existing wind turbine cost and weight data. The complexity factor is the value assigned during the component sizing phase to reflect the amount of work required for the subsystem's construction.

The total capital cost of the wind turbine is calculated from a sum of the cost estimates for each subsystem. To validate the model's cost prediction, the code has been used to predict the weight and capital cost of a wide range of actual wind turbines (Harrison *et al.*, 2000). Figure 11.10 gives a comparison between the model predictions of the relationship between
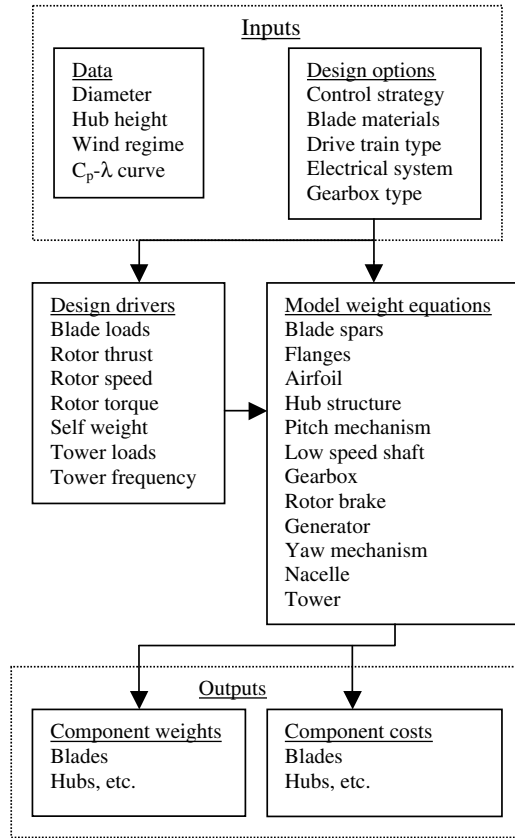
Figure 11.9   Flowchart of Sunderland cost model; C_p, power coefficient; λ, tip speed ratio
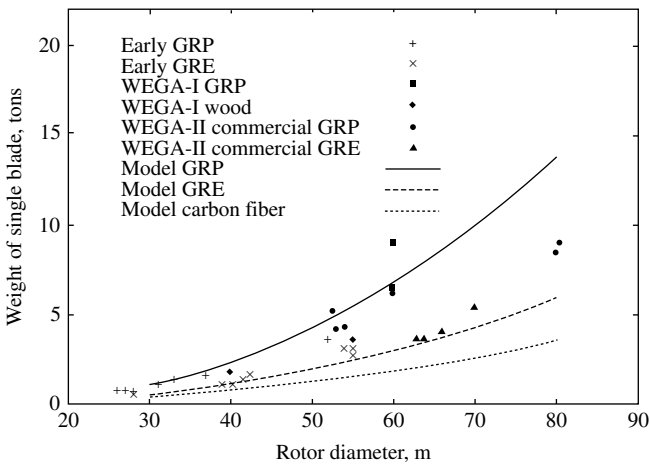
Figure 11.10   Validation of Sunderland cost model weight predictions (Harrison *et al.*, 2000)
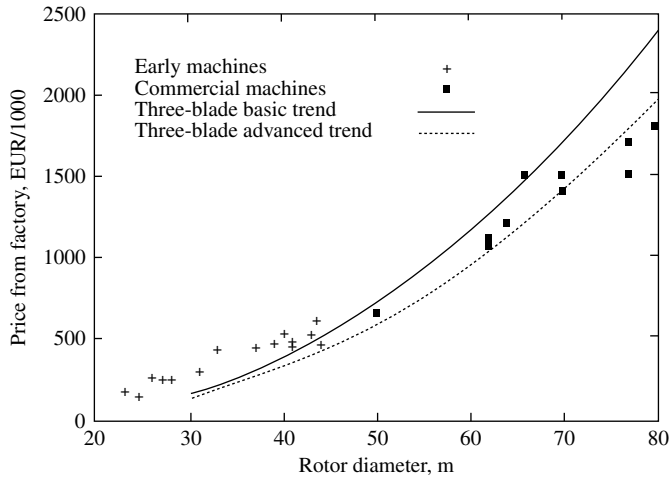
Figure 11.11   Validation of Sunderland wind turbine cost predictions (Harrison *et al.*, 2000)

blade weight and rotor diameter for three types of blade material (solid or dotted lines) and data from a number of operating wind turbines. (WEGA is an acronym for 'Wind Energie Grosse Anlagen'.) Figure 11.11 presents a comparison of total capital cost predictions (for three-bladed machines) and actual factory costs of early small machines and current large machines. Both graphs show good agreement between the model and actual weight and cost data.

11.3.3.3 Capital Costs for Offshore Wind Turbines

Capital costs for offshore wind turbines are invariably higher than those for land-based turbines. The Opti-OWECS project (Kühn *et al.*, 1998) defined a design methodology for the structural and economic optimization of offshore wind turbines. Their design methodology considered the correlation between the wind and wave loads to determine design strengths. The per kW cost difference has generally been in the range of 25% more to three times as much, depending on such factors as distance from shore, water depth, environmental conditions, soil type, maturity of the technology, and project size. It is anticipated, however, that capital costs for offshore wind turbines can be reduced by optimizing wind turbines for offshore use.

More details on the cost of offshore wind turbines and offshore wind farm systems can be found in a recent publication by the European Wind Energy Association (EWEA, 2009).

11.3.4 Wind Farm Costs

The determination of total system capital cost, or installed capital cost, involves more than just the cost for the turbines themselves. For example, the installed capital cost of a wind farm could include the following (NWCC, 1997):

- wind resource assessment and analysis;
- permitting, surveying, and financing;

- construction of service roads;
- construction of foundations for wind turbines, pad mount transformers, and substation;
- wind turbine and tower delivery to the site and installation;
- construction and installation of wind speed and direction sensors;
- construction of power collection system including the power wiring from each wind turbine to the pad mount transformer and from the pad mount transformer to the substation;
- construction of operations and maintenance facilities;
- construction and installation of a wind farm communication system supporting control commands and data flow from each wind turbine to a central operations facility;
- provision of power measurement and wind turbine computer control, display and data archiving facilities;
- integration and checkout of all systems for correct operation;
- commissioning and shakedown;
- final turnover to owner or operating agency.

A detailed discussion of the determination of each of these cost components is beyond the scope of this text. A few examples are presented below, however, that give an idea of how these costs are distributed for modern wind farms. A typical breakdown of costs (for a medium-sized onshore wind farm in Europe) is given in Table 11.2 (EWEA, 2009). In addition to the wind turbine (including tower), the major costs include the foundation installation and roads, the cost associated with the connection to the main electrical grid, and financial costs.

Another example (DOE/EPRI, 1997) is based on larger sized wind farms (on the order of 50 machines). The results for a 1997 base case design, normalized to \$/kW and as a percentage of total cost, are given in Table 11.3.

From these examples of wind farm costs, and other data on the subject, it is reasonable to assume that the cost of wind turbines and towers represents about 65% to 75% of the total capital costs for wind farms in the industrialized countries of the world. In developing countries, however, the relative cost breakdown is slightly different. According to data on the subject, about 30% to 50% of the total capital costs are for infrastructure, installation, and grid connection (WEC, 1993).

Fuglsang and Thomsen (1998) studied the possibility of reducing energy costs for offshore wind farms by optimizing the wind turbine design. They concluded that, by optimizing the turbine tower height, diameter, power rating, rotor speed, and turbine spacing, the energy

Table 11.2 Wind farm capital cost breakdown (EWEA, 2009)

Component	Percentage of total cost
Wind turbines	68 to 84
Foundation	1 to 9
Electric installation	1 to 9
Grid connection	2 to 10
Land	1 to 5
Financial costs	1 to 5
Road construction	1 to 5
Consultancy	1 to 5

Table 11.3 50-turbine wind farm capital cost breakdown (DOE/EPRI, 1997)

Component	Cost ($/kW)	Percentage of total
Rotor assembly	185	18.5
Tower	145	14.5
Generator	50	5.0
Electrical/electronics/controls/instrumentation	155	15.5
Transmission/drive train/nacelle	215	21.5
Balance of station	250	25.0
Total installed cost	1000	100.0

Table 11.4 Average investment costs related to offshore wind farms in Horns Rev and Nysted (EWEA, 2009)

Component	Cost [1000€/MW)	Percentage of total
Turbines (including transport and erection)	815	49.0
Transformer station and main cable to coast	270	16.0
Internal grid between turbines	85	5.0
Support structure	350	21.0
Design and project management	100	6.0
Environmental analysis	50	3.0
Miscellaneous	10	<1

costs for an offshore wind farm would only be about 10% greater than those of a comparable onshore stand-alone turbine. The installation costs were higher than those for onshore turbines, but the modeling showed that the offshore wind turbines would produce 28% more energy as a result of the better wind resource.

The main differences in costs between onshore and offshore wind farms are due to support structure and electrical connection issues (EWEA, 2009). For example, Table 11.4 gives a breakdown of the average investment costs for typical European offshore wind farms (Horns Rev and Nysted). As shown, the support structure and electrical connection cost components are each approximately 21% of the total, and are thus considerably more expensive than onshore sites.

11.4 Operation and Maintenance Costs

Next to the purchase and installation of the wind turbines, operation and maintenance (O&M) are the most significant sources of costs. It is especially important to project O&M costs if the owner of a wind farm seeks to refinance or sell the project. The operation costs can include a cost for insurance on the wind turbine, taxes, and land rental costs, while the maintenance costs can include the following typical components:

- routine checks;
- periodic maintenance;
- periodic testing;
- blade cleaning;

- electrical equipment maintenance;
- unscheduled maintenance costs.

For some time, the prediction of the operation and maintenance costs of installed wind turbines was regarded as somewhat speculative (Freris, 1990). Based on experience from the wind farms of California (Lynnette, 1986), and information from the Danish Wind Industry Association (2006) and from US studies (DOE/EPRI, 1997), this is less so today. However, as will be discussed below, the current data indicate that there still exists a wide range of O&M costs for wind turbines. This difference may depend on the size of the installed wind farm.

Operation and maintenance costs can be divided into two categories: fixed and variable. Fixed O&M costs are yearly charges unrelated to the level of plant operation. These must be paid regardless of how much energy is generated (generally expressed in terms of $/kW installed or percentage of turbine capital cost). Variable O&M costs are yearly costs directly related to the amount of plant operation (generally expressed in $/kWh). Probably the best estimates of O&M costs are a combination of these two categories.

One example of data on O&M costs is contained in a 1987 EPRI (Spera, 1994) study of California wind farm costs. This study estimated variable O&M costs, ranging from 0.008 to 0.012 $/kWh (in 1987 dollars). At the time of this study it was found that the variable O&M costs for small-scale machines (up to 50 kW) were higher than for medium-scale machines (up to 200 kW). The work also concluded that the O&M expenditure was approximately distributed as shown in Table 11.5.

The Danish Wind Industry Association (2006) compiled data on over 5000 machines installed in Denmark. They found that the newer generation of wind turbines have lower repair and maintenance costs relative to those of the older generation of wind turbines. Specifically, the older wind turbines (sized from 25 to 150 kW) have annual maintenance costs averaging about 3% of the original capital cost of the turbine(s). For the newer machines, the estimated annual O&M costs range from 1.5% to 2% of the original capital cost, or approximately $0.01/kWh. Germanischer Lloyd (Nath, 1998) reports the same trend with machine age in O&M costs. Their variation of O&M costs, however, is much larger, ranging from 2% to 16% of the price of the wind turbine. Other European investigators have stated that for large turbines, maintenance costs of less than $0.006/kWh are possible (Klein *et al.*, 1994).

Methods have been developed for the prediction of the increase in wind turbine maintenance costs with time (Vachon, 1996). Vachon used a statistical approach for modeling component failures (and maintenance costs) as a function of time. Based on actual field data, Table 11.6 gives results from a Danish Energy Association study (Lemming *et al.*, 1999) that show that

Table 11.5   Breakdown of O&M costs (Spera, 1994)

Cost component	Cost percentage
Labor	44
Parts	35
Operations	12
Equipment	5
Facilities	4

Table 11.6 Comparison of total O&M costs as a function of size and age of turbine (Lemming *et al.*, 1999)

Turbine size	Years from installation				
	1–2	3–5	6–10	11–15	16–20
150 kW	1.2	2.8	3.3	6.1	7.0
300 kW	1.0	2.2	2.6	4.0	6.0
600 kW	1.0	1.9	2.2	3.5	4.5

Note: O&M costs are expressed as a percent of total wind farm installation costs.

wind energy systems' O&M costs (expressed as a percentage of total wind farm installation cost) vary with turbine size and age. It is important to note the predicted rise in costs with turbine age.

O&M costs for offshore wind systems are substantially higher than for land-based installations. This subject is discussed in detail in recent technical publications by Eecen *et al.* (2007) and Rademakers *et al.* (2003).

11.5 Value of Wind Energy

11.5.1 Overview

The traditional way to assess the value of wind energy is to equate it to the direct savings that would result due to the use of the wind rather than the most likely alternative. These savings are often referred to as 'avoided costs'. Avoided costs result primarily from the reduction of fuel that would be consumed by a conventional generating plant. They may also result from a decrease in total conventional generating capacity that a utility requires. This topic is discussed in more detail in Section 11.5.2.

Given the cost reductions in wind turbines themselves over the last several decades, there are already some locations where wind may be the most economic option for new generation. Basing wind energy's value exclusively on the avoided costs, however, would result in many potential applications being uneconomic.

Equating wind energy's value exclusively to the avoided costs misses the substantial environmental benefit that results from its use. The environmental benefits are those which arise because wind generation does not result in any significant amount of air emissions, particularly oxides of nitrogen and sulfur and carbon dioxide. Reduction in emissions translates into a variety of health benefits. It also decreases the concentration of atmospheric chemicals that cause acid rain and global warming.

Converting wind energy's environmental benefits into monetary form can be difficult. Nonetheless, the results of doing so can be quite significant, because when that is done, many more projects can be economic.

The incorporation of environmental benefits into the market for wind energy is done through two steps: (1) quantifying the benefits and (2) 'monetizing' those benefits. Quantifying the benefits involves identifying the net positive effects on society as a result of wind's use. Monetizing involves assigning a financial value to the benefits. It allows a financial return to be captured by the prospective owner or developer of the project. Monetization is usually
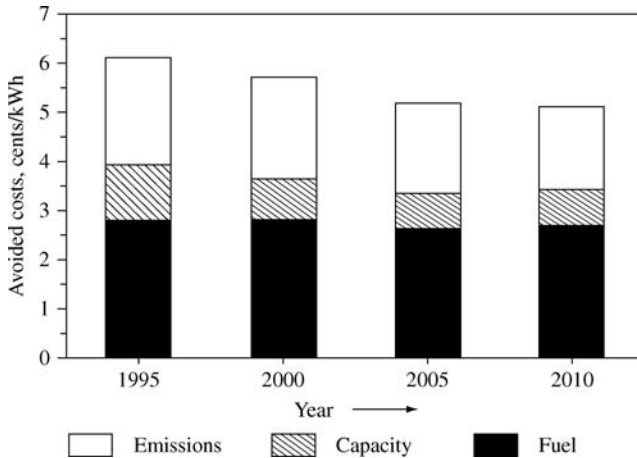
Figure 11.12 Avoided costs of wind energy for the Netherlands for 1995–2010 (WEC, 1993) Reproduced by permission of the World Energy Council, London

accomplished by government regulation. The process frequently considers the cost of alternative measures to reduce emissions (such as scrubbers on coal plants) to assign a monetary value to the avoided emissions. Section 11.5.3 provides more detail on the environmental benefits of wind energy, and the result of monetizing some of those benefits.

The effect of this method of incorporating environmental benefits is to create two categories of potential revenue for a wind project: (1) revenue based on avoided costs and (2) revenue based on the monetized environmental benefits. Figure 11.12 illustrates what the relative magnitude of these two revenue sources might be. In the cases shown, the effect of including the monetized environmental benefits ('avoided emissions') is to increase the total value by approximately 50% above that based on avoided fuel and capacity alone.

Because of the very real environmental benefits of wind energy, and because of the enormous impact that including these benefits in economic assessments could have, many countries have developed laws and regulations to facilitate the process. These are discussed in Section 11.7.4.

How revenues based on avoided costs and monetized environmental benefits may factor into an economic assessment of a particular project depends on what may be referred to as the 'market application' and the relation of the project or developer to that market application. Sections 11.5.4.1 and 11.5.4.2 describe various market applications and common types of owners or developers. Section 11.5.4.3 summarizes the most common sources of revenue that may be available to a wind energy project. After that, some hypothetical examples are presented to illustrate the difference in value that may result.

11.5.2 Avoided Cost-based Value of Wind Energy

As stated above, the traditional way of assigning value to wind energy, particularly to a utility, has been to base the value on calculations of avoided fuel and capacity costs. These are discussed in more detail below.
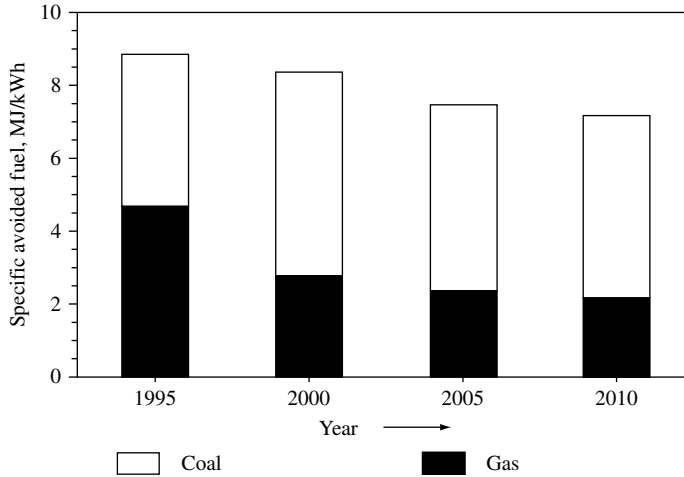
Figure 11.13 Specific avoided fuel consumption for the Netherlands (WEC, 1993) Reproduced by permission of the World Energy Council, London

11.5.2.1 Fuel Savings

The inclusion of wind turbines in an electricity producing system can reduce the demand for other generating plants that require a fossil fuel input. It might appear that the calculation of fuel saving would be quite straightforward, but this is not generally the case. The type and amount of fuel savings depends on such factors as the mix of different fossil fuel and nuclear plants in the electrical generating system, requirements for 'spinning reserves', and operating characteristics of the fossil fuel components (such as efficiency or heat rate as a function of component load).

The electrical system as a whole must be modeled in order to estimate the avoided consumption of fuel. For example, Figure 11.13 summarizes the results of a study for the Netherlands through the year 2010 (WEC, 1993). Here, the specific amount of avoided fossil fuel is expected to decrease because of an assumed increase in wind generating capacity and because of the higher generation efficiency of new fossil-fired power plants.

11.5.2.2 Capacity Value

The capacity value (or credit) of a wind system is simply defined as: 'the amount of conventional capacity which must be installed to maintain the ability of the power system to meet the consumers' demand if the wind power installation is deleted' (Tande and Hansen, 1991). In spite of the apparent simplicity of the concept, some authors (see Fox *et al.*, 2007) note that few topics generate more controversy than the determination of capacity value for wind energy systems.

At one extreme, if the utility were absolutely certain that a wind energy plant would produce its full rated power during peak demand hours, its capacity value would equal its rated power. At the other extreme, if the utility were certain that the wind energy plant would never operate

during peak hours, then its capacity value would be zero. For a utility, the higher the capacity value of wind power plants, the less new generation capacity is required. In practice, the capacity value of a wind generating plant is somewhere between zero and its average power generation during some time interval of high electrical demand in the system. Accordingly, the actual value will depend on the seasonal match of the wind resource to the utility's demand. There are two main methods for the calculation of capacity value (Walker and Jenkins, 1997):

1. The contribution of the wind system during peak demand on a utility is assessed over a period of years and the average power at these times is defined as the capacity value.
2. The loss of load probability (LOLP) or loss of load expectation (LOLE) is calculated, initially, with no wind generators in the system (Billinton and Allan, 1984). It is then recalculated with wind generation on the system, and then conventional plant capacity is subtracted until the initial level of LOLP is obtained. The subtracted conventional plant capacity is the capacity value of the wind.

Both methods give similar results. Also, for small penetration of wind systems, the capacity value is generally close to the average output of the wind system.

An example of the first method, using an analytical equation, is given in the work of Voorspools and D'haeseleer (2006). Most often, capacity value is calculated by the second method (generally using statistical techniques). For example, as shown in Figure 11.14, the capacity value of wind energy in the Netherlands has been determined by two separate studies (WEC, 1993), and can be found as a function of the total size of the wind contribution to the total power grid. For a 1000 MW rated wind capacity, the relative capacity credit is predicted to vary between 16% and 18% (equivalent to about 160 to 180 MW of conventional capacity).

Some studies have produced capacity values ranging from a few percent to values approaching 30–40%. In the middle are other researchers, who propose that renewables with
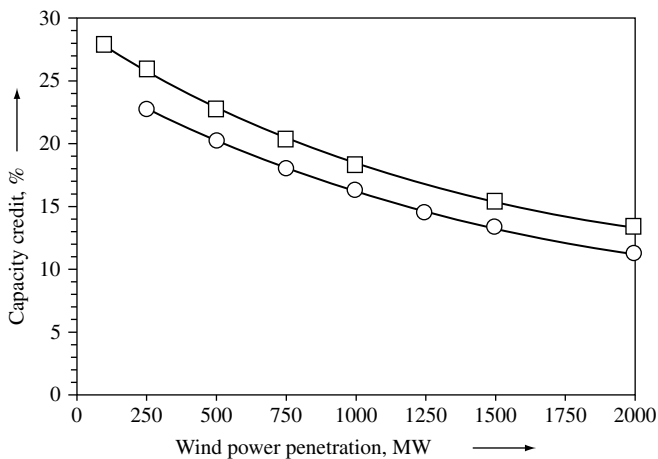
Figure 11.14 Capacity value (%) for the Netherlands vs. wind penetration (WEC, 1993) Reproduced by permission of the World Energy Council, London

somewhat predictable schedules deserve partial capacity payments (Perez *et al.*, 1997). Also, in the United States, as reviewed by Milligan and Porter (2005), the determination of capacity value of wind is a regional function and can vary considerably depending on the regional definition of capacity reserve requirements and capacity resource.

11.5.3 Environmental Value of Wind Energy

The primary environmental value of electricity generated from wind energy systems is that the wind offsets emissions that would be generated by conventional fossil fuel based power plants. These emissions include sulfur dioxide (SO_2), oxides of nitrogen (NO_x), carbon dioxide (CO_2), particulates, slag, and ash. The amount of emissions saved via the use of wind energy depends on the types of power plant that are replaced by the wind system, and the particular emissions control systems currently installed on the various fossil-fired plants. A detailed review of the external costs (costs that are not incorporated into the cost streams of a project) for utility-scale energy systems is given in a recent European Commission report (Bickel and Friedrich, 2005).

Numerous studies have been carried out to determine the emissions savings value of wind power systems (e.g., EWEA, 2004). In general, depending on the country and/or region, there are major differences in the amount of emissions that can be saved per unit of electricity generated. This depends mainly on the mix of conventional generating units and the emissions control status of the individual units. For example, in the US, each MWh of electricity generated results in the emission of about 1340 pounds of carbon dioxide, 7.5 pounds of sulphur dioxide, and 3.55 pounds of oxides of nitrogen (Reeves, 2003).

At the present time, there is no standard method for computing the emissions savings value of wind energy systems. Most methods, however, as noted above in Section 11.5.1, make some reference to the costs of alternative measures that could be applied to reduce emissions by the same amount.

There are also benefits associated with wind energy production other than the direct environmental ones. These include such indirect benefits as improved public health and political benefits that would accrue by reducing fossil fuel imports. All the benefits (and the corresponding costs) from all sources of energy production are often considered under the general topic of the 'social costs of energy production'. The earliest studies in this area were from Hohmeyer (1990) and reviewed by WEC (1993) and Gipe (1995). In general, the results show higher social or 'external' costs for conventional electrical power generation plants. As with the value of direct emissions reduction, there is, as yet, no agreement as to how to quantify the exact monetary value. In some countries, however, estimates of the external costs are considered in developing incentives for wind energy, such as renewable portfolio standards, tax credits, or guaranteed prices. These are discussed briefly in Section 11.7.4. The monetary results of those incentives are discussed below.

11.5.4 Market Value of Wind Energy

The market value of wind energy is the total amount of revenue one will receive by selling wind energy, or will avoid paying through its generation and use. The value that can be 'captured' depends strongly on three considerations: (1) the 'market application', (2) the project owner or developer, and (3) the types of revenues available.

The market application affects the type of project that might be built and the magnitude of the avoided costs. The relation of the owner to the market application will determine whether the avoided costs will be accounted for directly or indirectly in the sale of the electricity. The types of revenues are basically in two categories. The first category, which includes the sale of electricity and reduced purchases, relates to the market value of the energy itself. The second category includes those revenues which are based on monetized environmental benefits and derive from governmental policies. All of these topics are discussed briefly below.

11.5.4.1 Market Applications

The market application refers to the system in which the wind project is located. For example, European wind energy market development is summarized in Volume 5 of a recent European Wind Energy Association publication (EWEA, 2004). The most common market applications include: (1) traditional utilities, (2) restructured utilities, (3) customer-owned generation, (4) remote power systems, and (5) grid-independent applications. The relation between the market application and the person or entity that may own or develop the project has the important effect of determining whether the revenues appear in the form of savings in the costs of production or as sales of energy.

Traditional Utilities
Traditional electric utilities are entities that generate, transmit, distribute, and sell electricity. They may be privately or publicly owned. When privately owned, they are considered a 'natural monopoly' and are normally regulated by a state or national government. Although most traditional utilities generate at least some of the electricity they sell, many also purchase electricity from other utilities. Two publicly owned types of utilities are (1) municipal electric companies and (2) rural electric cooperatives. These utilities are owned and operated by cities or towns or by their customers (in the case of the coops). Frequently they buy most or all of their power from large publicly owned generating entities, such as the Tennessee Valley Authority in the southern United States.

Restructured Utilities
In recent years, many electric utilities have been 'restructured' or 'deregulated'. They have typically been broken into three parts: (1) a generating company, (2) a 'wires' company, and (3) a marketing company. The wires company only owns and maintains the transmission and distribution wires in a given service area. It does not own generation (at least for that service area). Generation is owned independently. The marketer of energy, not necessarily the utility itself, will purchase energy from a generator, 'rent' the wires for moving the electricity, and will sell the electricity to its customers. Customers are, in principle, free to choose their supplier (marketer). The marketer sometimes offers electricity 'products' with particular attributes that may be of interest to the customer. These might have to do with reliability, interruptability, or fuel source. The proper functioning of the system is maintained by an 'independent system operator' (ISO), which oversees the process of energy purchase and sale. The wires companies are normally still regulated.

Customer-owned Generation
Customers of utilities, whether traditional or restructured, may wish to generate some of their own electricity. In this case the customer may purchase a wind turbine and connect it to the local

distribution lines, normally on his or her side of the meter. For this reason, customer-owned generation is also known as 'behind-the-meter' generation. To what extent this is possible or economically worthwhile depends greatly on the specific laws and regulations that may be in place. In projects of this type, most of the energy is used to reduce purchases of electricity, but in some cases any excess generation may be sold into the electrical grid.

Remote Power Systems

Remote power systems are similar in many ways to larger utilities. The main differences are: (1) the type of generators that they use (normally diesel) and (2) their inability to exchange power with other utilities. When wind turbines are added to such systems, they result in a hybrid power system, as discussed in Chapter 10.

Grid-independent Systems

Grid-independent wind energy systems typically consist of a wind turbine, battery storage, a power converter, and electrical loads. They are normally relatively small and self-contained. They may be installed as an alternative to interconnecting to a utility or in lieu of a diesel or gasoline generator.

11.5.4.2 Wind Project Owners or Developers

The nature of the owner or developer, and his, her, or its relation to the market application, will have a significant impact on the type of revenues available. Types of owners or developers may include: (1) traditional utilities themselves, (2) independent power producers, (3) electricity consumers wishing to reduce their purchases, (4) entities responsible for isolated power systems, or (5) individuals needing energy in a grid-independent application.

Traditional Utilities

A traditional utility could develop and own its own wind generation capacity. The wind generation would save some fuel or reduce purchases of electricity from other utilities. The wind project might also provide some capacity value, as described in Section 11.5.2.2.

Independent Power Producers

Independent power producers (IPPs) own and operate their own generating facilities and sell the electricity to a utility. They may operate in either traditional or restructured utilities. Wind project IPPs are similar to other generators, except that they may suffer because wind generation is not dispatchable (that is, it cannot be turned on and off at will). However, they may benefit by being able to take advantage of incentives not offered to generators that use fossil fuels. They normally require a multi-year contract ('power purchase agreement' or PPA) to secure financing. The details of the PPA are often very important in determining whether or not a project is economically viable.

Customer Generators

The customer is normally (but not always) the owner and developer in a behind-the-meter wind energy project. Typical examples include residential customers, farmers, and small businesses.

11.5.4.3 Types of Revenue

As described above, there are basically two types of revenue that may be available: those based on avoided costs and those based on monetized environmental benefits. The first category

includes: (1) reduction in purchases of electricity, fuel, capital equipment, or other expenses (avoided costs themselves) and (2) sale of electricity (the price of which will reflect the avoided costs). The second category includes: (1) sale of renewable energy certificates, (2) tax benefits, (3) guaranteed, above-market rates, and (4) net metering.

Reduced Purchases

When the owner of the turbine is the same as the traditional generator, the revenue from the wind project is actually a saving. In the case of a traditional utility or the manager of a remote power system, the revenue would appear as reduced fuel or electricity purchases, reduced operation and maintenance costs on the other generators, and possibly reduced costs for replacements or upgrades to the other generators. The value of the saving (the 'avoided cost') would typically range from about $0.05/kWh to $0.08/kWh (2008), depending on the fuel source and type of conventional generators used. For a remote power system, the avoided cost would be in the range of $0.20–0.60/kWh. For the owner of a 'behind-the-meter' project, the value of the reduced purchases would be the retail price of electricity. This is much higher than the wholesale price (in the vicinity of $0.15/kWh in a conventional utility to $0.40/kWh or more in a remote power system).

Electricity Sale

An independent power producer would normally derive revenue by selling electricity into the grid. Ideally the rate would be set by a long-term contract. This rate is close to the expected 'avoided cost' of energy, as discussed previously, for the utility into which the electricity will be sold. The contract price is generally highest for generators which are dispatchable. A wind project operator may also gain a better price if production can be forecast to some extent. Electricity can also be sold on a day-to-day basis (the 'spot market'), but this generally brings the lowest price. In some cases, an IPP might be able to sell the energy as 'green power' to a customer willing to pay more to ensure that the electricity comes from an environmentally preferred source.

Renewable Energy Certificates

Over the last few years, new incentives have been developed to facilitate the introduction of more renewable energy into restructured utilities. One of these incentives is the renewable energy or 'green' certificate. In the system on which this incentive is based, the desired attribute of 'greenness' is assumed to be separated from the energy itself and is used to assign value to a certificate. The certificates then have value, typically in the range of a few cents US per kWh. Such certificates may be used to ensure compliance, for example, with mandates known as 'renewable portfolio standards' (RPS). The wind project will receive a quantity of certificates in proportion to the energy generated. The certificates can then be sold, and the proceeds will augment the revenue from the sale of the electricity itself. More details can be found in Section 11.7.4.

Tax Benefits

Over the years a number of types of tax credits have been used to foster the development of wind energy. At one time, the investment tax credit was widely used. This provides a source of revenue to the project developer based on the cost of the project, rather than its production. A more common incentive nowadays is the production tax credit. It is based on the actual energy produced, and typically amounts (in the US) to approximately $0.02/kWh.

Guaranteed, Above-market Rates

Some countries, such as Germany and Spain, provide for guaranteed, above-market rates for generators of wind energy. This scheme is known as a 'feed in tariff' (see Ringel, 2006 and Section 11.7.4). This arrangement functions similarly to the energy sale method described above. The difference is that the price is set by the government at a value higher than one could expect to receive by conventional sales into the electricity market. The rate for land-based wind energy in these situations has typically been close to the retail price.

Net Metering

The situation faced by a small behind-the-meter generator is actually a little more complicated than it first appears. Due to the variability of the wind and the load, it may frequently be the case that the instantaneous generation from a turbine is more than the electrical load, even if the average generation is well below the average load. Depending on the utility rules and type of metering, it is possible for an operator to receive little or no revenue from the energy that is produced in excess of the load. This could seriously affect the effective average value for the generation.

In an effort to address this situation, and to provide additional incentives to small generators, a number of states in the US have developed 'net metering' rules. Under these rules, the key consideration is the net energy that is produced, in comparison to the consumption, over some extended period of time (typically a month or more). As long as the net generation is less than the consumption, all the generation will be valued at retail. Any generation in excess of the consumption is subject to the same rules as would apply to an independent power producer. In 2009, more than 40 states and the District of Columbia had net metering programs that required utilities to purchase power from systems that qualified for the program. Net metering rules normally apply to relatively small generators (50 kW or less), although New Jersey has a much larger limit of 2 MW (see http://www.windustry.org).

11.5.4.4 Examples

It should be apparent that there is a wide range of revenue or value that might apply to a unit of wind-generated electricity, depending on the details of the application. The following are some hypothetical examples of this:

1. A private utility using coal-fired generators has a fuel cost of \$0.03/kWh and needs no new capacity. There are no monetized environmental benefits in the state in which it operates. The value of wind energy would thus be the avoided fuel costs, or \$0.03/kWh.
2. A wind energy project developer in a state with restructured utility can sell his energy into the grid for \$0.03/kWh. The state provides renewable energy certificates, which he can sell for \$0.035/kWh. He can also take advantage of a federal production tax credit, valued at \$0.019/kWh. The total value of his wind-generated electricity would be \$0.084/kWh.
3. A municipal electric utility buys all its electricity at a fixed rate of \$0.07/kWh. The value of wind energy would thus be the avoided energy purchase costs, or \$0.07/kWh.
4. A farmer is considering whether to install a 50 kW wind turbine to supply part of the farm's electricity. She presently pays \$0.15/kWh. She can take advantage of net metering and a production tax credit of \$0.019/kWh. The value of her wind-generated electricity would be \$0.169/kWh.

11.6 Economic Analysis Methods

As stated previously, a wind energy system can be considered to be an investment that produces revenue. An economic analysis is used to evaluate the profitability of a wind energy project and to compare it with alternative investments. Economic analysis methods can be applied for wind energy systems, assuming that one has a reliable estimate for the capital costs and O&M costs. The general purpose of such methods is not only to estimate the economic performance of a given design of wind energy system, but also to compare it with conventional and other renewable energy-based systems. Three different types of economic analysis method will be described in this section. They are:

- simplified models;
- life cycle cost models;
- electric utility economic models.

Each of these economic analysis techniques has its own definitions of key economic parameters and each has its particular advantages and disadvantages.

It is important to clarify who the owner or developer is, and what market value can be expected for the energy, as discussed in Section 11.5.4. Depending on the application, one or more of the economic evaluation methods discussed below may be appropriate.

11.6.1 Simplified Economic Analysis Methods

For a preliminary estimate of a wind energy system's feasibility, it is desirable to have a method for a quick determination of its relative economic benefits. Such a method should be easy to understand, free of detailed economic variables, and easy to calculate. Two methods that are often used are: (1) simple payback and (2) cost of energy.

11.6.1.1 Simple Payback Period Analysis

A payback calculation compares revenue with costs and determines the length of time required to recoup an initial investment. The payback period (in years) is equal to the total capital cost of the wind system divided by the average annual return from the energy produced. In its simplest form (simple payback period), it is expressed in equation form as:

$$SP = C_c/AAR \tag{11.3}$$

where SP is the simple payback period, C_c is the installed capital cost, and AAR is the average annual return. The latter can be expressed by:

$$AAR = E_a P_e \tag{11.4}$$

where E_a is the annual energy production (kWh/year), and P_e is the price obtained for electricity ($/kWh). Thus, the simple payback period is given by:

$$SP = C_c/(E_a P_e) \tag{11.5}$$

Consider the following example: $C_c = \$50\,000$, $E_a = 100\,000$ kWh/yr, $P_e = \$0.10$/kWh. Then $SP = 50\,000/(100\,000 \times 0.10) = 5$ years.

Note that the calculation of simple payback period omits many factors that may have a significant effect on the system's economic cost effectiveness. These include changing fuel and loan costs, depreciation on capital costs, O&M, variations in the value of delivered electricity, and lifetime of the system. Some authors attempt to include some of these variables in their calculations for a simple payback period. For example, one author (Riggs, 1982) divides the capital costs by the net annual savings to obtain simple payback.

11.6.1.2 Cost of Energy Analysis

The cost of energy, COE, is defined as the unit cost to produce energy (in \$/kWh) from the wind energy system. That is:

$$\text{Cost of energy} = (\text{Total costs})/(\text{Energy produced}) \qquad (11.6)$$

Based on the previous nomenclature, the simplest calculation of COE is given by:

$$COE = [(C_c \times FCR) + C_{O\&M}]/E_a \qquad (11.7)$$

where $C_{O\&M}$ is the average annual operation and maintenance cost and FCR is the fixed charge rate. The fixed charge rate is a term that reflects the interest one pays or the value of interest received if money were displaced from savings. For utilities, FCR is an average annual charge used to account for debt, equity costs, taxes, etc. (see Section 11.6.3).

Using the values from the previous numerical example, and assuming that $FCR = 10\%$ and $C_{O\&M} = 2\% \times C_c = \$1000/\text{yr}$:

$$COE = [(50\,000 \times 0.10) + 1000]/100\,000 = \$0.06/\text{kWh}$$

This simplified calculation is based on a number of key assumptions, most of which neglect the time value of money. They will be addressed in the next section.

11.6.2 Life Cycle Costing Methods

Life cycle costing (LCC) is a commonly used method for the economic evaluation of energy-producing systems based on the principles of the 'time value' of money. The LCC method summarizes expenditure and revenue occurring over time into a single parameter (or number) so that an economically based choice can be made.

In analyzing future cash flows one needs to consider the time value of money. An amount of money can increase in quantity by earning interest from some investment. Also, money can have a reduced value over time as inflation forces prices upward, making each unit of currency have lower purchasing power. As long as the rate of inflation is equal to the return on investment for a fixed sum of money, purchasing power is not diminished. As is usually the case, however, if these two values are not equal, then the sum of money can increase in value (if investment return is greater than inflation) or decrease in value (if the inflation rate is greater than investment return).

The concept of LCC analysis is based on accounting principles used by organizations to analyze investment opportunities. The organization seeks to maximize its return on investment (ROI) by making an informed judgment on the costs and benefits to be gained by the use of its capital resources. One way to accomplish this is via an LCC-based calculation of the ROI of the various investment opportunities available to the organization.

To determine the value of an investment in a wind power system, the principles of LCC costing can be applied to its costs and benefits; that is to say, its expected cash flows. The costs include the expenses associated with the purchase, installation, and operation of the wind system (see Sections 11.3 and 11.4). The economic benefits of a wind system include the use or sale of the generated electricity as well as tax savings or other financial incentives (see Section 11.5). Both costs and benefits may also vary over time. The principles of life cycle costing can take into account time-varying cash flows and refer them to a common point in time. The result will be that the wind system can be compared to other energy-producing systems in an internally consistent manner.

LCC methodology, as described in this section, takes the parameters of inflation and interest applied to money and uses a model based on the 'time value of money' to project a 'present value' for an investment at any time in the future. The important variables and definitions used in life cycle costing analysis follow.

11.6.2.1 Overview and Definition of Life Cycle Costing Concepts and Parameters

In LCC analysis, some key concepts and parameters include:

- the time value of money and present worth factor;
- levelizing;
- capital recovery factor;
- net present value.

A summary description of each follows.

Time Value of Money and Present Worth Factor
A unit of currency that is be to paid (or spent) in the future will not have the same value as one available today. This is true even if there is no inflation, since a unit of currency can be invested and bear interest. Thus its value is increased by the interest. For example, suppose an amount with a present value PV (sometimes called present worth) is invested at an interest (or discount) rate r (expressed as a fraction) with annual compounding of interest. (Note that in economic analysis the discount rate is defined as the opportunity cost of money. This is the next best rate of return which one could expect to obtain.) At the end of the first year the value has increased to $PV(1+r)$, after the second year to $PV(1+r)^2$, etc. Thus, the future value, FV, after N years is:

$$FV = PV(1+r)^N \tag{11.8}$$

The ratio PV/FV is defined as the present worth factor PWF, and it is given by:

$$PWF = PV/FV = (1+r)^{-N} \tag{11.9}$$

For illustration purposes, numerical values of PWF are given in Table 11.7.

Levelizing
Levelizing is a method for expressing costs or revenues that occur once or in irregular intervals as equivalent equal payments at regular intervals. A good way to illustrate this variable is by the following example (Rabl, 1985). Suppose one wants loan payments to be arranged as a series of equal monthly or yearly instalments. That is, a loan of present value

Table 11.7 Present worth factor for discount rate r and number of years N

Discount rate, r	Number of years, N					
	5	10	15	20	25	30
0.01	0.9515	0.9053	0.8613	0.8195	0.7798	0.7419
0.02	0.9057	0.8203	0.7430	0.6730	0.6095	0.5521
0.03	0.8626	0.7441	0.6419	0.5537	0.4776	0.4120
0.04	0.8219	0.6756	0.5553	0.4564	0.3751	0.3083
0.05	0.7835	0.6139	0.4810	0.3769	0.2953	0.2314
0.06	0.7473	0.5584	0.4173	0.3118	0.2330	0.1741
0.07	0.7130	0.5083	0.3624	0.2584	0.1842	0.1314
0.08	0.6806	0.4632	0.3152	0.2145	0.1460	0.0994
0.09	0.6499	0.4224	0.2745	0.1784	0.1160	0.0754
0.10	0.6209	0.3855	0.2394	0.1486	0.0923	0.0573
0.11	0.5935	0.3522	0.2090	0.1240	0.0736	0.0437
0.12	0.5674	0.3220	0.1827	0.1037	0.0588	0.0334
0.13	0.5428	0.2946	0.1599	0.0868	0.0471	0.0256
0.14	0.5194	0.2697	0.1401	0.0728	0.0378	0.0196
0.15	0.4972	0.2472	0.1229	0.0611	0.0304	0.0151
0.16	0.4761	0.2267	0.1079	0.0514	0.0245	0.0116
0.17	0.4561	0.2080	0.0949	0.0433	0.0197	0.0090
0.18	0.4371	0.1911	0.0835	0.0365	0.0160	0.0070
0.19	0.4190	0.1756	0.0736	0.0308	0.0129	0.0054
0.20	0.4019	0.1615	0.0649	0.0261	0.0105	0.0042

PV is to be repaid in equal annual payments A over N years. To determine the equation for A, first consider a loan of value PV_N that is to be repaid with a single payment F_N at the end of N years. With N years of interest on the amount PV_N, the payment is: $F_N = PV_N(1+r)^N$. In other words, the loan amount PV_N equals the present value of the future payment F_N; $PV_N = F_N(1+r)^{-N}$

A loan that is to be repaid in N equal installments can be considered as the sum of N loans, one for each year, the jth loan being repaid in a single instalment A at the end of the jth year. Thus, the value, PV, of the loan equals the sum of the present values of all loan payments:

$$PV = \frac{A}{1+r} + \frac{A}{(1+r)^2} + \dots + \frac{A}{(1+r)^N} = A\sum_{j=1}^{N}\frac{1}{(1+r)^j} \qquad (11.10)$$

Or, using an equation for a geometric series:

$$PV = A[1-(1+r)^{-N}]/r \qquad (11.11)$$

It should be noted that this equation is perfectly general and relates any single present value, PV, to a series of equal annual payments A, given the interest or discount rate, r, and the number of payments (or years), N. Also note that when $r=0$, $PV = A \times N$.

Capital Recovery Factor
The capital recovery factor, CRF, is used to determine the amount of each future payment required to accumulate a given present value when the discount rate and the number of

payments are known. The capital recovery factor is defined as the ratio of A to PV and, using Equation (11.11), is given by:

$$CRF = \begin{cases} r/[1-(1+r)^{-N}], & \text{if } r \neq 0 \\ 1/N, & \text{if } r = 0 \end{cases} \qquad (11.12)$$

The inverse of the capital recovery factor is sometimes defined as the series present worth factor, SPW.

Net Present Value

The net present value (NPV) is defined as the sum of all relevant present values. From Equation (11.8), the present value of a future cost, C, evaluated at year j is:

$$PV = C/(1+r)^j \qquad (11.13)$$

Thus, the NPV of a cost C to be paid each year for N years is:

$$NPV = \sum_{j=1}^{N} PV_i = \sum_{j=1}^{N} \frac{C}{(1+r)^j} \qquad (11.14)$$

If the cost C is inflated at an annual rate i, the cost C_j in year j becomes:

$$C_j = C(1+i)^j \qquad (11.15)$$

Thus, the net present value, NPV, becomes:

$$NPV = \sum_{j=1}^{N} \left(\frac{1+i}{1+r}\right)^j C \qquad (11.16)$$

As will be discussed in the next section, NPV can be used as a measure of economic value when comparing investment options.

11.6.2.2 Life Cycle Costing Analysis Evaluation Criteria

Earlier in this chapter, two economic parameters, simple payback and cost of energy, were introduced. These can be used for a preliminary economic analysis of a wind energy system. With LCC analysis, one can apply a number of other economic figures of merit or parameters to evaluate the feasibility of a wind energy system. Among others, these include net present value of cost or savings and the levelized cost of energy.

Net Present Value of Cost or Savings

The net present value of a particular parameter is generally used as a measure of economic value when comparing different investment options in a life cycle cost analysis. Note that it is important to define the NPV clearly, since various authors have used the term 'net present value' to define a wide variety of life cycle cost analysis parameters. First, one can define the savings version of net present value, NPV_s, as follows:

$$NPV_s = \sum_{j=1}^{N} \left(\frac{1+i}{1+r}\right)^j (S-C) \qquad (11.17)$$

where S and C represent the yearly gross savings and costs during a project's lifetime ($S-C$ is the yearly net saving).

In evaluating various systems using this criterion, one would look for the systems with the largest value of *NPVs*. In practice, a spreadsheet format can be used to evaluate the yearly gross savings (*S*) and cost (*C*), and to calculate the sum of the annual levelized values. As will be shown next, however, it is also possible to use closed form analytical expressions for the direct calculation of net present value. These expressions are valuable tools for use in generalized parametric studies of wind energy systems.

If only cost factors are considered, then a cost version of net present value, NPV_C, may be used. It is the sum of the levelized costs of the energy system. For this version of this parameter, when comparing a number of different systems, the design with the lowest NPV_C is desired.

As an example of costs for wind energy systems, the net present value of costs can be found by calculating the total costs of a system for each year of lifetime. The annual costs should then be levelized to the initial year, and then summed up. If one assumes that both the general and energy inflation rates are constant over the system life, and that the system loan is repaid in equal instalments, NPV_C may be found from the following equation:

$$NPV_C = P_d + P_a Y\left(\frac{1}{1+r}, N\right) + C_c f_{OM} Y\left(\frac{1+i}{1+r}, L\right) \tag{11.18}$$

where:

$P_d =$ downpayment on system costs
$P_a =$ annual payment on system costs $= (C_c - P_d)CRF$
$CRF =$ capital recovery factor, based on the loan interest rate, b, rather than r
$b =$ loan interest rate
$r =$ discount rate
$i =$ general inflation rate
$N =$ period of loan
$L =$ lifetime of system
$C_c =$ capital cost of system
$f_{OM} =$ annual operation and maintenance cost fraction (of system capital cost)

The variable $Y(k, \ell)$ is a function used to obtain the present value of a series of payments. It is determined from:

$$Y(k, \ell) = \sum_{j=1}^{\ell} k^j = \begin{cases} \dfrac{k - k^{\ell+1}}{1-k}, & \text{if } k \neq 1 \\ \ell, & \text{if } k = 1 \end{cases} \tag{11.19}$$

Levelized Cost of Energy

In its most basic form, the levelized cost of energy, COE_L, is given by the sum of annual levelized costs for a wind energy system divided by the annual energy production. Thus:

$$COE_L = \frac{\sum(\text{Levelized annual costs})}{\text{Annual energy production}} \tag{11.20}$$

This type of definition is generally used in a utility-based calculation for cost of energy. Sometimes, the levelized cost of energy is defined as the value of energy (units of $/kWh) that, if held constant over the lifetime of the system, would result in a cost-based net present value (such as the value calculated via Equation (11.18)). Using this basis, the COE_L is

given by:

$$COE_L = \frac{(NPV_C)(CRF)}{\text{Annual energy production}} \tag{11.21}$$

Note that the capital recovery factor, CRF, is here based on the lifetime of the system, L, and the discount rate, r. On this basis, the levelized cost of energy multiplied by the annual power production would equal the annual loan payment needed to amortize the net present value of the cost of the energy system.

Other Life Cycle Analysis Economic Parameters

There are a number of other economic performance factors that can be used for evaluating the life cycle based performance of an energy system. Two of the more common parameters are internal rate of return (*IRR*) and the benefit–cost ratio (*B/C*). They are defined by:

$$IRR = \text{Value of discount rate for } NPV_S \text{ to equal zero} \tag{11.22}$$

$$B/C = \frac{\text{Present value of all benefits (income)}}{\text{Present value of all costs}} \tag{11.23}$$

The *IRR* is often used by utilities or businesses in assessing investments and is a measure of profitability. The higher the *IRR* is, the better is the economic performance of the wind energy system in question.

Generally, systems with a benefit–cost ratio greater than one are acceptable, and higher values of the B/C value are desired.

11.6.3 Electric Utility-based Economic Analysis for Wind Farms

From a power-generating business or utility perspective, the previous definition of cost of energy can be used for a first estimate of utility generation costs for a wind farm system. In this application, *COE* can be calculated from:

$$COE = \frac{[(C_c)(FCR) + C_{O\&M}]}{\text{Annual energy production}} \tag{11.24}$$

where C_c is the capital cost of the system, FCR is the fixed charge rate (a present value factor that includes utility debt and equity costs, state and federal taxes, insurance, and property taxes), and $C_{O\&M}$ is the annual operation and maintenance cost.

In the United States, electric utilities and the wind industry commonly use either of two methods to estimate the *COE* from a utility-sized wind energy system (Karas, 1992): (1) the Electric Power Research Institute, Technical Analysis Group (EPRI TAG) method (EPRI, 1979; 1989) or, (2) a cash flow method (CFM). Summary details of each follow.

11.6.3.1 EPRI TAG Method

This method produces a levelized cost of energy (*COE*), and in its simplest form for wind energy systems, *COE* ($/kWh) is calculated from:

$$COE = FCR\left(\frac{\bar{C}_c}{8760 \times CF}\right) + \bar{C}_{O\&M} \tag{11.25}$$

where:

$\bar{C}_c$ = total cost of constructing the facility normalized by rated power (\$/kW)
CF = capacity factor
$\bar{C}_{O\&M}$ = cost of operation and maintenance normalized per unit of energy (\$/kWh)

Since this method produces a levelized energy cost it can be applied to a number of technologies, including conventional power plants (with the addition of fuel costs) for a useful comparison index. Some limitations of the EPRI TAG method include:

- it assumes a loan period equal to the life of the power plant;
- it does not readily allow for variable equity return, variable debt repayment, or variable costs.

The second limitation generally excludes the use of this method for independent power producers (IPPs), under which many wind farm projects fall.

11.6.3.2 Cash Flow Method (CFM)

The cash flow method is based on the use of an accounting type spreadsheet that requires an annual input of estimated income and expenses over the lifetime of the project. The cost of energy is calculated via the following operations:

- each cost component of the plant and operation is identified (e.g., plant construction, O&M, insurance, taxes, land, power transmission, administrative costs, etc.);
- a cost projection of each of the above components for each year of the plant's service life;
- an annual estimate of depreciation, debt services, equity returns, and taxes;
- discounting of the resulting cash flows to present values using the utility's cost of capital (as established by appropriate regulatory agency);
- levelizing the cost by determination of the equal payment stream (annuity) that has a present value equal to the results of the previous calculations.

The cash flow method allows for the real variations that can be expected in cost, operational, and economic data, such as price increases, inflation, and changing interest rates. A detailed description of several cash flow models used to assess the effects of ownership structure and financing on utility-scale wind systems is given by Wiser and Kahn (1996).

Karas (1992) notes that the *COE* estimates can be determined in a wide variety of ways. His examples show that wind energy system *COE*s are extremely sensitive to actual plant cost and operating assumptions, especially capacity factor and plant installation costs.

Regardless of the method used to calculate a levelized or other type of *COE*, it should be emphasized that one plant can have a number of equally valid *COE*s depending on the assumptions used. Thus, it is important that in the determination of any cost of energy for a wind system, the terminology, methods of parameter determination, and assumptions be made explicit.

11.6.4 *Economic Performance Sensitivity Analysis*

The previous sections have described a number of methods for the determination of economic performance parameters (such as cost of energy) that can be used to evaluate various wind

systems, or to compare their performance with other types of power system. In practice, however, one soon realizes that a large number of machine performance and economic input variables exist that can influence the desired parameter's value. In addition, the potential variation or range of uncertainty of many input parameters may be large.

A complete economic study of a wind energy system should include a series of sensitivity studies for calculation of the output variable of interest. Specifically, each parameter of interest is varied around some central or 'best estimate'. The desired figure of merit (such as cost of energy) is then calculated. The calculations are repeated for a range of assumptions. For example, the following economic and performance variables could be varied:

- plant capacity factor (or average wind speed at the site);
- turbine availability;
- operation and maintenance costs;
- capital or installed cost;
- lifetime of system and components;
- length of loan repayment;
- interest or discount rate.

With calculations of this type, the results are often summarized graphically. This can be accomplished via the use of a 'spider' or 'star' diagram, illustrated in Figure 11.15. It is intended to show how a percentage change in a given parameter changes the cost of energy, expressed as a percentage. This type of diagram readily shows the more important variables
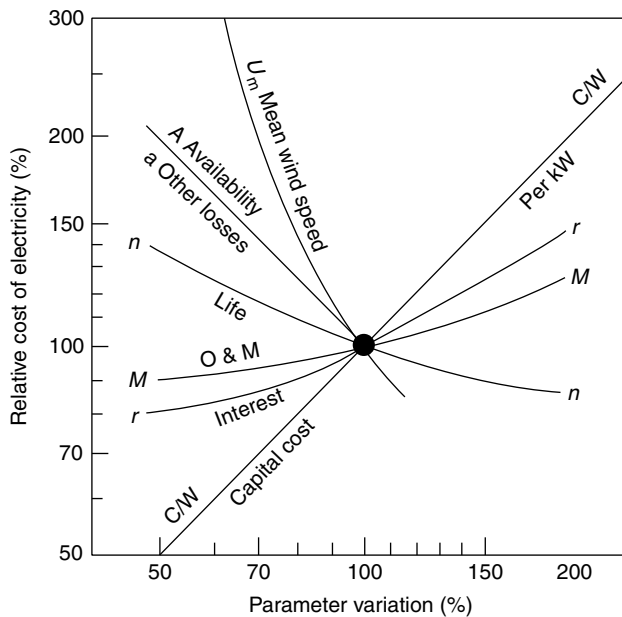
Figure 11.15 Sensitivity of cost of electricity to various parameters (Freris, 1990). Reproduced by permission of Pearson Education Limited

by lines with the steeper slopes. Note, however, that it may not be reasonable to vary all parameters by the same percentage amount, since some may be known quite accurately (Walker, 1993).

11.7 Wind Energy Market Considerations

11.7.1 Overview

There exists a large potential worldwide market for wind energy systems. In this section a review of market considerations for wind energy systems is presented. There are three major issues to consider:

1. Potential market for wind systems.
2. Barriers to expansion of markets.
3. Incentives for market development.

There are numerous technical publications on these subjects in the open literature. This is especially true for utility-scale or wind farm applications (e.g., OECD/IEA, 1997; EWEA, 2004). The potential market for small or dispersed wind hybrid systems has also been addressed (for example, see WEC, 1993). A summary of some of this work on the marketing issues (for utility-scale systems) follows.

11.7.2 The Market for Utility-scale Wind Systems

An overview of utility-scale market projections from an international and US perspective is presented in this section.

11.7.2.1 International Wind Energy Market

The prediction of long-term trends in worldwide installed wind power capacity is a complex issue. For example, work by the European Wind Energy Association (EWEA, 2004) has shown that predictions for wind power development in Europe have been significantly underestimated, even by wind power advocates. In recent times, a number of organizations have made detailed long-term predictions for the growth of wind power installations in the world at large and in Europe. A summary of predictions for the worldwide growth of wind power capacity is shown in Figure 11.16 (Molly, 2004). This summary includes information from the following organizations:

1. **BTM Consult.** This Danish consulting firm has a long record of making reasonable and accurate assessments of the future market for wind power in the world and in Europe (EWEA, 2004). A wind power capacity of about 235 000 MW was predicted at the end of 2013.
2. **DEWI (Deutsches Windenergie-Institut).** This German consulting firm has based its estimates on an annual survey of several hundred wind companies.
3. **HSH Nordbank.** This German consulting firm based its estimates on work completed in 2002 and 2004.
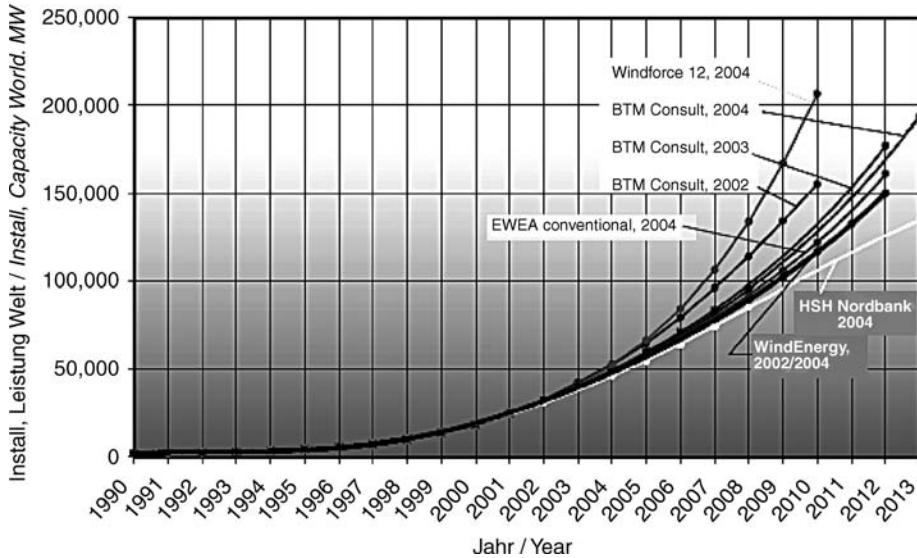
Figure 11.16   Predicted cumulative worldwide wind capacity (Molly, 2004). Reproduced by permission of DEWI magazine

4. **European Wind Energy Association (EWEA, 2004).** EWEA based its predictions on two different cases: (1) a conventional scenario and (2) an advanced scenario (from its Wind Force 12 study).

11.7.2.2 United States Wind Energy Market

A National Renewable Energy Laboratory study (Short *et al.*, 2004) on the impact of federal policies on the US wind market is a recent example of the predicted wind energy market for the US. In this work, projections for the market expansion of wind energy are made, considering three different technological improvement scenarios:

- a no R&D case (no improvement in turbine cost/performance);
- a base case (33% of projected cost improvements and 50% of capacity factor improvements);
- a full R&D case (maximum predicted improvement in turbine cost/performance).

The results are summarized in Figure 11.17 (the middle curve represents the base case). As can be seen, there is a significant variation in the predicted market for wind energy in the US. For example, the no R&D case predicts a 20 GW installed wind capacity in 2050 while the full R&D case predicts 310 GW installed capacity in 2050.

11.7.3 Barriers to Wind Energy Deployment

In spite of the potential for wind energy development, there are nonetheless a number of barriers that will slow the process. The barriers to the deployment of utility-scale wind energy
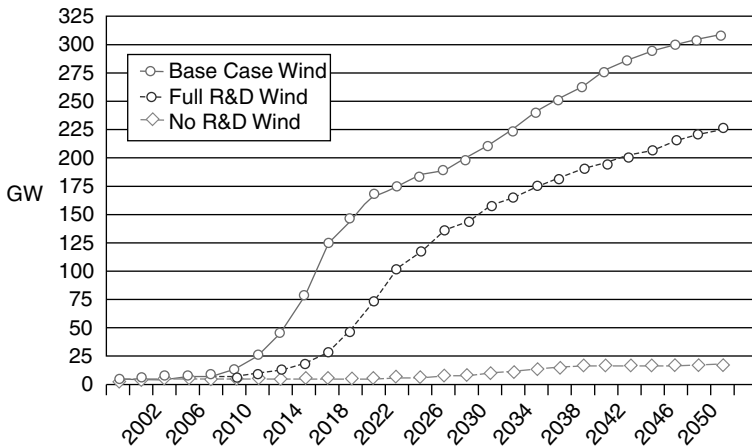
Figure 11.17 US wind energy capacity with varying degrees of technological improvement (Short *et al.*, 2004)

can be divided into the following areas:

- **Direct costs**. A general disadvantage of wind turbines is that their total cost is highly concentrated at the time of initial construction as a result of high capital costs.
- **System integration**. For low penetration systems, the integration of wind power into electrical power systems is readily accomplished with existing engineering tools, but there may be major costs involved.
- **Regulatory and administrative processes**. The responsibilities for approving the siting and other aspects of wind project implementation are usually assigned to existing bodies (i.e., local zoning boards) that have had little experience with wind power – with corresponding regulatory and administrative bottlenecks.
- **Environmental impacts**. All wind energy projects have effects on the environment (as will be discussed in Chapter 12) and resulting barriers that must be overcome.
- **Electricity system planning**. One barrier to the introduction of large-scale wind generation into some utility systems is their very novelty. Those utilities in particular may lack appropriate planning experience. Other utilities may already have wind generation in their service area, but have not yet addressed the issue of how much more wind generation they can absorb before they need to consider additional measures, such as forecasting or short-term energy storage.

More details on these potential barriers to wind energy development can be found in an OECD/IEA (1997) publication. The authors of this study conclude that barriers in the way of deployment of wind energy are comparatively low relative to market barriers facing some other renewable energy technologies. They also note that the key issue here remains the cost of wind energy relative to other energy sources.

11.7.4 Incentives to Wind Energy Development

The largest amount of wind energy generation has been installed in countries that have offered various incentives to its market deployment. These have either been in the form of financial incentives (e.g., capital tax credits, production tax credits, or guaranteed energy prices) or regulatory options (e.g., renewable portfolio standards and net metering). These are mechanisms that monetize the environmental benefits of wind energy, as discussed in Section 11.5. Countries where such incentives have made the largest impact have included some in Europe (Denmark, Germany, Spain, the Netherlands, and the United Kingdom) and the United States. A detailed discussion of the various incentives for the first three countries is included in an OECD/IEA (1997) publication.

A number of national support programs have been implemented in Europe. Many different incentives have been used and the level of economic support has differed considerably from country to country and with time. Some of the most common incentives for market stimulation follow (EWEA, 2004):

- public funds for R&D programs;
- public funds for demonstration projects;
- direct support of investment cost (% of total cost or based on kW installed);
- support through the use of guaranteed price of electricity from wind systems (i.e., feed-in tariff);
- financial incentives – special loans, favorable interest rates, etc.;
- tax incentives (e.g., production tax credit, favorable depreciation);
- the use of renewable energy or 'green' certificates.

Regulatory and institutional measures carried out recently in Germany are of particular note. The German system has provided a framework which has resulted in a rapid increase in the amount of installed wind generation. Among other things, the German system mandates a guaranteed, above-market rate for wind-generated electricity (feed-in tariff). See Gutermuth (2000) for more details on these measures. One interesting feature of the German feed-in tariff incentive is that two rates are provided over the life term of the project. The duration of the initial, higher, rate is a function of the energy production of the wind turbine. The rates are set such that a turbine will be economic in most locations in Germany. The effect of the two-rate tariff is that extensive site monitoring is not needed before the decision to proceed with the wind project is made. Also, in the European Union, both feed-in tariffs and green certificates have been used as incentives for renewable energy development (see Ringel, 2006).

In the US, significant wind energy development occurred in the California wind farms in response to federal and state legislation that provided a market and favorable tax incentives that attracted private capital. Incentives for wind farms were accomplished via three separate, yet coincidental, federal government actions and one act passed by the state of California. They were the Public Utilities Regulatory Policies Act (PURPA) of 1978, the Crude Oil Windfall Profits Act of 1980, the Economic Recovery Tax Act of 1981, and California state tax credits. These incentives were either in the form of investment or production tax credits.

At the present time, the major incentives for wind energy development in the United States are the production tax credits under the National Energy Policy Act and the planned

implementation of renewable portfolio standards (RPSs). An RPS is a policy mechanism to ensure a minimum level of renewable energy generation in the portfolios of power suppliers in an implementing jurisdiction (e.g., a state or nation). Rules for the implementation of renewable portfolio standards have been adopted by a number of states in the United States, several European countries, and Australia (see Berry and Jaccard, 2001). One feature which is being used in some states as a way to track and account for renewable electrical generation is the renewable energy or 'green' certificate. These certificates are issued to generators in an amount proportional to production and are tradable on a commodities exchange. One state that has adopted a certificate-based RPS is Massachusetts. Details can be found at http://www.state.ma.us/doer/rps/.

Feed-in tariffs are also being considered in Canada and some states in the US. See, for example, Rickerson *et al.* (2008).

References

Berry, T. and Jaccard, M. (2001) The Renewable Portfolio Standard: Design Considerations and an Implementation Survey. *Energy Policy*, **29**, 263–277.

Bickel, P. and Friedrich, R. (2005) *ExternE Externalities of Energy – Methodology 2005 Update*, European Commission Report EUR 21951.

Billinton, R. and Allen, R. (1984) *Reliability Evaluation of Power Systems*. Plenum Press, New York.

Boeing (1979) MOD-2 Wind Turbine System Concept and Preliminary Design Report. *Report No. DOE/NASA 0002-80/2*, Boeing Engineering and Construction Co.

Chapman, J., Wiese, S., DeMeo, E. and Serchuk, A. (1998) Expanding Windpower: Can Americans Afford It? *Renewable Energy Policy Project, Report No. 6*. Washington, DC.

Cody, G. and Tiedje, T. (1996) A learning curve approach to projecting cost and performance in thin film photovoltaics. *Proc. 25th Photovoltaic Specialists Conference. IEEE*, pp. 1521–1524.

Danish Wind Industry Association (2006) *Guided Tour on Wind Energy*. Available at: http://www.windpower.org/en/tour.htm.

DOE/EPRI (US Department of Energy/Electric Power Research Institute) (1997) *Renewable Energy Technology Characterizations*. EPRI Report: TR-109496, EPRI, Palo Alto, CA.

Eecen, P. J. *et al.* (2007) Estimating costs of operation and maintenance of offshore wind farms. *Proc. 2007 European Wind Energy Conference,* Milan.

EPRI (Electric Power Research Institute) (1979) *Technical Assessment Guide*, Vols 1–3. EPRI Report: EPRI-PS-1201-SR, EPRI.

EPRI (Electric Power Research Institute) (1989) *Technical Assessment Guide*, Vol 1, Rev. 6. EPRI Report: EPRI P-6587-L, EPRI.

EWEA (2004) *Wind Energy, The Facts*, Vols 1–5. European Wind Energy Association, Brussels.

EWEA (2008) *Pure Power: Wind Energy Scenarios up to 2030*. European Wind Energy Association, Brussels.

EWEA (2009) *The Economics of Wind Energy*. European Wind Energy Association, Brussels.

Fingersh, L., Hand, M. and Laxon, A. (2006) *Wind Turbine Design Cost and Scaling Model*. NREL Report: NREL/TP-500-40566. National Renewable Energy Laboratory, Golden, CO.

Fox, B. *et al.* (2007) *Wind Power Integration: Connection and System Operational Aspects*. The Institution of Engineering and Technology, London.

Freris, L. L. (1990) *Wind Energy Conversion Systems*. Prentice Hall, New York.

Fuglsang, P. and Thomsen, K. (1998) *Cost Optimisation of Wind turbines for Large-scale Off-shore Wind Farms*. Riso National Laboratory, Roskilde, Denmark.

General Electric Company (1984) *MOD-5A Wind Turbine Generator Program Design Report – Vol II, Conceptual and Preliminary Design*. Report No. DOE/NASA/0153-2, NTIS.

Gipe, P. (1995) *Wind Energy Comes of Age*. John Wiley & Sons, Inc., New York.

Gutermuth, P-G. (2000) Regulatory and institutional measures by the state to enhance the deployment of renewable energies: German experiences. *Solar Energy*, **69**(3), 205–213.

Harrison, R. and Jenkins, G. (1993) *Cost Modelling of Horizontal Axis Wind Turbines.* UK DTI Report ETSU W/34/00170/REP.

Harrison, R., Hau, E. and Snel, H. (2000) *Large Wind Turbines: Design and Economics.* John Wiley & Sons, Ltd, Chichester.

Hau, E., Langenbrinck, J. and Paltz, W. (1993) *WEGA Large Turbines.* Springer-Verlag, Berlin.

Hau, E., Harrison, R., Snel, H. and Cockerill, T. T. (1996) Conceptual design and costs of large wind turbines. *Proc. 1996 European Wind Energy Conference,* Göteborg, pp. 128–131.

Hohmeyer, O. H. (1990) Latest results of the international discussion on the social costs of energy – how does wind compare today? *Proc. 1990 European Wind Energy Conference,* Madrid, pp. 718–724.

Johnson, G. L. (1985) *Wind Energy Systems.* Prentice-Hall, Englewood Cliffs, NJ.

Junginger, M., Faaij, A. and Turkenburg, W. C. (2005) Global experience curves for wind farms. *Energy Policy*, **33**, 133–150.

Karas, K. C. (1992) Wind energy: what does it really cost? *Proc. Windpower '92*, American Wind Energy Association, Washington, DC, pp. 157–166.

Klein, H., Herbstritt, M. and Honka, M. (1994) Milestones of European wind energy development – EUROWIN in Western, Central, and Eastern Europe. *Proc. 1994 European Wind Energy Conference,* Thessaloniki, pp. 1275–1279.

Kühn, M., Bierbooms, W. A. A. M., van Bussel, G. J. W., Ferguson, M. C., Göransson, B., Cockerill, T. T., Harrison, R., Harland, L. A., Vugts, J. H. and Wiecherink, R. (1998) *Opti-OWECS Final Report*, Vol. 0–5. Institute for Wind Energy, Delft University of Technology, Report No. IW-98139R.

Lemming, J., Morthorst, P. E., Hansen, L. H., Andersen, P. and Jensen, P. H. (1999) O&M costs and economical lifetime of wind turbines. *Proc. 1999 European Wind Energy Conference*, pp. 387–390.

Lynnette, R. (1986) *Wind Power Stations: 1985 Performance and Reliability.* EPRI Report AP-4639, EPRI.

Milligan, M. and Porter, K. (2005) *Determining the Capacity Value of Wind: A Survey of Methods and Implementation.* NREL/CP-500-38062. National Renewable Energy Laboratory, Golden, CO.

Molly, J. P. (2004) Market prognosis 2008, 2012, and 2030. *DEWI Magazine*, **25** (August), 33–38.

NASA (1979) *200 kW Wind Turbine Generator Conceptual Design Study.* Report No. DOE/NASA/1028-79/1, NASA Lewis Research Center, Cleveland, OH.

Nath, C. (1998) *Maintenance Cost of Wind Energy Conversion Systems.* Germanischer Lloyd, available at: http://www.germanlloyd.de/Activities/Wind/public/mainten.html.

Neij, L. (1999) Cost dynamics of wind power. *Energy*, **24**, 375–389.

NWCC (1997) *Wind Energy Costs.* Wind Energy Series Report No. 11. National Wind Coordinating Committee, Washington, DC.

OECD/IEA (1997) *Enhancing the Market Deployment of Energy Technology: A Survey of Eight Technologies.* Organisation for Economic Co-Operation and Development, Paris.

Perez, R., Seals, R., Wenger, H., Hoff, T. and Herig, C. (1997) Photovoltaics as a long-term solution to power outages case study: the great 1996 WSCC power outage. *Proc. 1997 Annual Conference, American Solar Energy Society*, Washington, DC, pp. 309–314.

Rabl, A. (1985) *Active Solar Collectors and Their Applications.* Oxford University Press, Oxford.

Rademakers, L. W. M. M. *et al.* (2003) Assessment and optimisation of operation and maintenance of offshore wind turbines. *Proc. 2003 European Wind Energy Conference*, Madrid.

Raftery, P. *et al.* (1999) Understanding the risks of financing wind farms. *Proc. 1999 European Wind Energy Conference*, Nice, pp. 496–499.

Reeves, A. (2003) *Wind Energy for Electric Power: A REPP Issue Brief.* Renewable Energy Policy Project, Washington, DC.

Rickerson, W., Bennhold, F. and Bradbury, J. (2008) *Feed-in Tariffs and Renewable Energy in the USA: A Policy Update*. Heinrich Böll Foundation North America, Washington, DC.

Riggs, J. L. (1982) *Engineering Economics.* McGraw-Hill, New York.

Ringel, M. (2006) Fostering the use of renewable energies in the European Union: the race between feed-in tariffs and green certificates. *Renewable Energy*, **31**, 1–17.

Short, W., Blair, N. and Heimiller, D. (2004) *Projected Impact of Federal Policies on US Wind Market Potential.* NREL/CP-620-36052. National Renewable Energy Research Laboratory, Golden, CO.

Spera, D. (Ed.) (1994) *Wind Turbine Technology.* American Society of Mechanical Engineers, New York.

Tande, J. O. G. and Hansen, J. C. (1991) Determination of the wind power capacity value. *Proc. 1991 European Wind Energy Conference*, Amsterdam, pp. 643–648.

Vachon, W. A. (1996) Modeling the Reliability and Maintenance Costs of Wind Turbines Using Weibull Analysis. *Proc. Wind Power 96*, American Wind Energy Association, Washington, DC, pp. 173–182.

Voorspoools, K. R. and D'haeseleer, W. D. (2006) An analytical formula for the capacity credit of wind power. *Renewable Energy*, **31**, 45–54.

Walker, J. F. and Jenkins, N. (1997) *Wind Energy Technology*, John Wiley & Sons, Ltd, Chichester.

Walker, S. (1993) Cost and Resource Estimating. *Open University Renewable Energy Course Notes – T521 Renewable Energy*.

WEC (1993) *Renewable Energy Resources: Opportunities and Constraints 1990–2020.* World Energy Council, London.

Wiser, R. and Bolinger, M. (2008) *Annual Report on U.S. Wind Power Installation, Cost, and Performance Trends: 2007.* U.S. Department of Energy Report.

Wiser, R. and Kahn E. (1996) *Alternative Windpower Ownership Structures: Financing Terms and Project Costs.* Lawrence Berkeley National Laboratory Report: LBNL-38921.

12

Wind Energy Systems: Environmental Aspects and Impacts

12.1 Introduction

This chapter will review the environmental aspects associated with the deployment of a single wind turbine or a wind farm. Wind energy development has both positive and negative environmental impacts. On the positive side, wind energy is generally regarded as environmentally friendly, especially when the environmental effects of emissions from large-scale conventional electrical generation power plants are considered. For example, estimates of the total emissions (sulfur and nitrogen oxides, and carbon dioxide) of coal and gas-fired power plants (German energy mix) as compared to those of wind systems are shown in Table 12.1 (Ackerman and Soder, 2002). The average wind speed for the wind system was 6.5 m/s.

As shown in Table 12.1, the stack (or direct) emissions of wind systems are generally small (one or two orders of magnitude less than those of conventional power plants). Also, the indirect emissions associated with the actual production of wind turbines and the erection and construction of wind turbine systems and wind farms are small.

The determination of the overall cost to society of the various emission pollutants is difficult to measure and open to much debate. One way to calculate the environmental benefits of wind power is to determine the avoided emissions from other sources. These benefits generally come from the displacement of generation (MWh) as opposed to capacity (MW). The displacement of capacity does have its benefits, however, especially if extension of the fuel and water supply infrastructure can be avoided (Connors, 1996).

As emphasized in a comprehensive report by the Global Wind Energy Council and Greenpeace International (2006), a major driving force behind wind power expansion is the urgent need to combat global climate change. As stated in this reference: 'This is now accepted to be the greatest environmental threat facing the world. The UN's Intergovernmental Panel on Climate Change projects that average temperatures will increase by up to 5.8 °C over the

Table 12.1 Stack emissions of coal, gas, and wind power plants (kg/GWh, t/GWh for CO_2)

Pollutant	Conventional coal	Gas (CCGT)	Wind
Sulfur oxides	630–1370	45–140	2–8
Nitrogen oxides	630–1560	650–810	14–22
Carbon dioxide	830–920	370–420	10–17

coming century. This is predicted to result in a wide range of climatic shifts, including melting of the polar ice caps, flooding of low-lying land, storms, droughts and violent changes in weather patterns. Responsibility for climate change lies with the excessive build-up of greenhouse gases in the atmosphere, a trend encouraged by the world's growing industrialization. Within energy uses, the main culprit is fossil fuels, whose combustion produces carbon dioxide, one of the main greenhouse gases.'

In addition to the environmental aspects associated with power system emissions, the subject of the energy requirements related to the production and manufacture of materials for such systems has been a topic of recent interest. The determination of energy requirements for a wind turbine system requires a detailed analysis of the materials required for system construction, and their corresponding energy use. Extensive use has been made of life cycle analysis models (LCA) for this type of analysis. Examples of research using this type of model include the wind farm (land-based and offshore) analysis of Schleisner (2000) and the wind turbine analysis of Lenzen and Munksgaard (2002).

Many publications document the positive environmental aspects of wind power (see, for example, National Academy of Sciences, 2007; volume 4 of EWEA, 2004; and REPP, 2003). As more wind turbines and wind farm systems are planned or installed in the world, the importance of their environmental effects has increased. On the other hand, some negative environmental aspects have been shown to be especially important in populated or scenic areas. Here, a number of potential wind energy projects have been delayed or denied permits because of strong opposition based on some anticipated negative environmental effects of these systems.

This chapter will review the potential negative environmental aspects associated with the deployment of a single wind turbine or a wind farm (keeping the positive environmental aspects in mind). It should be noted that it ought to be one of the objectives of wind energy system engineers to maximize the positive impacts while, at the same time, minimizing the negative aspects. In addition to their importance in the siting process for wind systems, the potentially adverse environmental effects of wind turbines tie in directly with much of the wind turbine design material discussed in previous chapters. With appropriate design of the wind turbine and the wind energy system, these adverse environmental factors can be minimized.

The potential negative impacts of wind energy can be divided into the following categories:

- avian/bat interaction with wind turbines;
- visual impact of wind turbines;
- wind turbine noise;
- electromagnetic interference effects of wind turbines;
- land-use impact of wind power systems;
- other impact considerations.

For land-based wind systems, the first three topics include most of the major environmental issues affecting wind system deployment, but the other topics are also important and should be addressed. For example, a number of these subjects are related to the topic of public acceptance of wind power. A discussion of this subject is beyond the scope of this work. An overview of this important subject, however, is included in the work of Devine-Wright (2005) and Johansson and Laike (2007).

For offshore wind systems, one must also consider the environmental effects on the marine environment and the sea life (including vulnerable species). Thus, environmental aspects of birds, fish, marine mammals, and benthic plants and animals must be addressed for offshore wind farms. At the present time, published studies on the environmental impacts of offshore wind systems are limited, with the exception of some recent studies in Germany (see Köller *et al.*, 2006) and Denmark (Operate A/S, 2006). In the Danish work, a comprehensive study of two Danish offshore wind farms, it was concluded that there were negligible environmental effects on birds, fish, and mammals.

In the next sections the emphasis will be on land-based systems. It should also be noted, however, that there are many similarities with environmental assessments for offshore wind systems.

In this chapter, the following general topic areas are considered for each environmental impact:

- problem definition;
- source of the problem;
- quantification or measurement of the problem;
- environmental assessment examples;
- reference resources or tools that address the problem.

Many of these subjects have to be addressed in the permitting phases of a wind project. Furthermore, depending on the particular site's environmental assessment regulations, one or more of these areas may require detailed investigation and/or an environmental impact statement. The scope of this chapter does not permit a full summary of the various regulations and laws on this subject, but, where possible, the reader will be referred to the appropriate literature on the subject.

12.2 Avian/Bat Interaction with Wind Turbines

12.2.1 Overview of the Problem

The environmental problems associated with avian interaction with wind systems surfaced in the United States in the late 1980s. For example, it was found that some birds, especially federally protected Golden Eagles and Red-tailed Hawks, were being killed by wind turbines and high voltage transmission lines in wind farms in California's Altamont pass. This information caused opposition to Altamont Pass wind energy development among many environmental activists and aroused the concern of the US Fish and Wildlife Service, which is responsible for enforcing federal species protection laws.

Work on this subject in the US addressed the question of how the number of wind turbine-caused bird deaths compared to the number of other anthropogenically caused bird deaths in the

United States (National Academy of Sciences, 2007). With several important reservations, they did note that bird deaths caused by wind turbines are a minute fraction of the total anthropogenic bird deaths – less than 0.003% in 2003. Their reservations emphasized the importance of local and temporal factors in evaluating the effects of wind turbines on bird populations, including a consideration of local geography, seasonal bird abundances, and the species at risk.

Another way to consider the effect of wind turbines on birds is in terms of fatalities per kWh. This is particularly relevant as the total amount of wind energy increases and begins to significantly affect the amount of electricity produced from other sources. This topic has been considered by Sovacool (2009). That study considered all aspects of the energy production change, from mining, through construction to plant operation. According to that study, there are approximately 0.3–0.4 fatalities per kWh due to wind turbines. In comparison, the fatalities due to nuclear power are approximately the same, but the fatalities associated with fossil fuel based electricity generation are much higher, approximately 5.2 fatalities per kWh. The implication is that as wind energy displaces progressively more fossil fuel based electricity, the overall effect on avian populations will be positive.

There are two primary concerns related to the adverse effects of wind turbines on birds: (1) effects on bird populations from the deaths caused either directly or indirectly by wind turbines, and (2) violations of the Migratory Bird Treaty Act, and/or the Endangered Species Act. These concerns, however, are not confined to the United States alone. Bird kill problems have surfaced at other locations in the world. For example, in Europe, major bird kills have been reported in Tarifa, Spain (a major point for bird migration across the Mediterranean Sea), and at some wind plants in Northern Europe. Wind energy development can adversely affect birds in the following manners (Colson, 1995):

- bird electrocution and collision mortality;
- changes to bird foraging habits;
- alteration of migration habits;
- reduction of available habitat;
- disturbance to breeding, nesting, and foraging.

Conversely, the same author states that wind energy development has the following beneficial effects on birds:

- protection of land from more dramatic habitat loss;
- provision of perch sites for roosting and hunting;
- provision and protection of nest sites on towers and ancillary facilities;
- protection or expansion of prey base;
- protection of birds from indiscriminate harassment.

At the present time, the long-term implications of the bird issue on the wind industry are not clear. Problems may arise in areas where large numbers of birds congregate or migrate, as in Tarifa, or where endangered species are affected, as in Altamont Pass (NWCC, 2002). This could include a large number of locations, however, since some of the traits that characterize a good wind site also happen to be attractive to birds. For example, mountain passes are

frequently windy because they provide a wind channel through a mountain range. For the same reason, many times they are the preferred routes for migratory birds.

Environmental problems with bats surfaced in the United States in the late 1990s with reported bat kills at Appalachian Mountain ridge top turbines. Since that time, a limited number of research studies considering this problem have been carried out in the US and Europe (e.g., AWEA/Audubon, 2006; Rodriques *et al.*, 2006). These studies have identified the following research needs regarding the environmental effects of wind turbines on bats:

- methodology development;
- mortality and population effects;
- migration and/or avoidance;
- collision;
- disturbance, barrier effect.

In the previously mentioned report of the Global Wind Energy Council and Greenpeace International (2006), it is noted that, despite publicity given to bat deaths around wind farms (mainly in the US), studies have shown that wind turbines do not pose a significant threat to bat populations. It should pointed out, however, that similar to avian studies, bat studies are often recommended or required in the planning and siting process for wind farms.

The key factors of the environmental effect on birds will be reviewed next. This includes the characterization of the problem, mitigation concepts, and available resources that can be used to assess the problem. It should be noted that following section considers effects on birds, but much of what is presented there applies to bats as well.

12.2.2 Characterization of the Problem

There is a close correlation between a locality and its bird fauna. Many bird species are very habitat-specific and often particularly sensitive to habitat changes. Furthermore, there is a correspondingly close correlation between the site and the location of the wind turbines, which is especially dependent on the wind conditions. In European (Clausager and Nohr, 1996) and US studies (Orloff and Flannery, 1992) the impact on birds is generally divided into the following two categories: (1) direct impacts, including risk of collision, and (2) indirect impacts, including other disturbances from wind turbines (e.g., noise). Such effects may result in a total or partial displacement of the birds from their habitats and deterioration or destruction of the habitats.

The risk of collision is the most obvious direct effect, and numerous studies have focused on it. These studies include the estimation of the number of birds that collide with the rotor or associated structures, and they have concentrated on the development of methods for the analysis of the extent of the collisions. There are also indirect effects. They include:

- disturbance of breeding birds;
- disturbance of staging and foraging birds;
- disturbing impact on migrating and flying birds.

12.2.3 Mitigation Concepts and Case Studies

12.2.3.1 Mitigation Concepts

A number of recent studies have addressed a number of measures for the minimization of the impact of wind turbine systems on birds. The most detailed work has taken place in California and has been supported by the California Energy Commission and the American Wind Energy Association. Typical mitigation measures from some of these studies (Colson, 1995; Wolf, 1995) include the following:

- **Avoid migration corridors.** Major bird migration corridors and areas of high bird concentrations should generally be avoided when siting wind facilities unless there is evidence that because of local flight patterns, low bird usage of the specific area, or other factors, the risk of bird mortality is low.
- **Fewer, larger turbines.** For a desired energy capacity, fewer large turbines may be preferred over many smaller turbines to reduce the number of structures in the wind farm.
- **Avoid micro habitats.** Microhabitats or fly zones should be avoided when siting individual wind turbines.
- **Alternate tower designs.** Where feasible, tower designs that offer few or no perch sites should be employed in preference to lattice towers with horizontal members that are suitable for perching. Unguyed meteorological and electrical distribution poles should be used over guyed structures. Also, existing lattice towers should be modified to reduce perching opportunities.
- **Remove nests.** With agency approval, raptor nests found on structures should be moved to suitable habitat away from wind energy facilities.
- **Prey base management.** Where appropriate, prey base management should be investigated as an option. A humane program, such as live trappings should be established to remove unwanted prey from existing wind farms.
- **Bury electrical lines.** Electrical utility lines should be underground when feasible. New overhead electrical distribution systems should be designed to prevent bird electrocutions. Existing facilities should employ techniques that significantly reduce bird electrocutions.
- **Site-specific mitigation studies.** The cause and effect of bird interactions with wind energy facilities should be examined to determine the manner in which collisions occur, and appropriate mitigation identified and employed.
- **Conservation of alternative habitats.** Habitat conditions that will benefit affected species should be maintained to protect them from other, more damaging land uses.

12.2.3.2 Case Studies

Numerous technical reports and papers exist that have focused on the potential or actual environmental effects of wind turbine systems on birds at a specific site. Although it is beyond the scope of this text to review them in detail, a few of the more appropriate ones (and their particular applications) are listed below:

- **US studies.** A review of this subject, as applied to the wind farms in Altamont Pass and Solano County, is contained in a technical report by the California Energy Commission (Orloff and Flannery, 1992). Sinclair (1999) and Sinclair and Morrison (1997) give

an overview of the US avian research program through 1999. Also, Goodman (1997) presents a summary of the avian studies (and other environmental issues) carried out for a 6 MW wind farm in Vermont. An NREL sponsored study covering an assessment of bird and bat use and fatalities at the US National Wind Technology Center site is given by Schmidt *et al.* (2003).

- **European studies.** Gipe (1995) presents an overview of bird-related environmental impact studies in Europe up to 1995. In addition, representative examples of European environmental impact studies of birds (especially for Denmark and the UK) are given in the technical papers of Clausager and Nohr (1996) and Still *et al.* (1996). A report by Birdlife International (2003) reviews numerous European case studies (including some offshore wind farms) on the subject of the effects of wind farms on birds.

12.2.4 Resources for Environmental Assessment Studies of Avian Impacts

A review of the previously referenced case studies regarding the environmental impacts of wind systems on birds reveals that such studies can require specialized expertise, be very detailed, and can add to the cost and deployment time of a potential wind site. Summaries of such types of studies can be found for the US (e.g., NWCC, 2001) and for Europe (e.g., Birdlife International, 2003). As mentioned previously, a representative example of this process is given in the technical report of the California Energy Commission (Orloff and Flannery, 1992). In general, this type of work can be divided into two parts: (1) a complete definition of the study area and (2) an assessment of bird risk.

The first part primarily consists of a detailed definition of the site topography and machine siting layout of the wind farm. In addition, when different types of wind turbines and towers are used, it is important to group them into categories. For example, Figure 12.1 illustrates the eight categories of wind turbines that were installed at the Altamont Pass in California in the 1980s. Another part of this phase of the work involves the selection of sample sites where detailed bird–wind turbine interaction data are to be collected.

The second, and much more detailed part of this type of study, the assessment of bird risk, generally involves a comprehensive methodology for accomplishing this task. In the United States, a number of sponsors including the National Renewable Energy Laboratory (NREL) and the National Wind Coordinating Committee (NWCC) Avian subcommittee have recently worked to develop this type of methodology. This work has focused on the development of a standardized method for determination of the factors responsible for avian deaths from wind turbine facilities, and scientific methods that can be used to reduce fatalities. The following summary presents some examples of the methods, measurements, and relationships (metrics) that have been used for this type of work (Anderson *et al.*, 1997; NWCC, 1999):

1. **Bird utilization counts.** Under this part of a study, an observer notes the location, behavior, and number of birds using an area. This is done in repeatable ways, using standard methods, so that results can be compared with bird utilization counts from other studies. Bird behavior to be noted includes: flying, perching, soaring, hunting, foraging, and actions close (50 meters or less) to wind farm structures.
2. **Bird utilization rate.** The bird utilization rate (based on bird utilization counts) is defined as the number of birds using the area during a given time or time and area. Two definitions of

Turbine type:	Three-blade Lattice (downwind)	Three-blade Lattice (upwind)	Three-blade Guyed-Pipe Tower
Tower height:	60–80 feet	45–80 feet	40–60–80 feet
Rotor diameter:	59 feet	50–56 feet	33–80 feet
Description:	Downwind, free yaw	Upwind	Downwind
Number:	3,359 (1989)	248	1,559
	3,640 (1990)		

Turbine type:	Two-blade Lattice (downwind)	Medium Tubular	Large Tubular
Tower height:	80 feet	100–150 feet	82 feet
Rotor diameter:	54 feet	50–82 feet	102 feet
Description:	Downwind, free yaw	Upwind	Upwind
Number:	346	1,421	135

Turbine type:	Vertical Axis	Windwall
Tower height:	90–106 feet	140 feet
Rotor diameter:	56–62 feet	59 feet
Description:	–	Downwind, free yaw
Number:	169	103

Figure 12.1   Eight categories of wind turbines in the Altamont pass (Orloff and Flannery, 1992)

the bird utilization rate follow:

$$\text{Bird utilization rate} = \frac{\text{No. of birds observed}}{\text{Time}} \qquad (12.1a)$$

or

$$\text{Bird utilization rate} = \frac{\text{No. of birds observed}}{\text{Time} \times \text{area}} \qquad (12.1b)$$

3. **Bird mortality.** The bird mortality is defined as the number of observed deaths, per unit search area (again, this is based on the bird utilization count). Therefore:

$$\text{Bird mortality} = \frac{\text{No. of dead birds}}{\text{Defined search area}} \qquad (12.2)$$

4. **Bird risk.** Bird risk is a measure of the likelihood that a bird using the area in question will be killed. It is defined as follows:

$$\text{Bird risk} = \frac{\text{Bird mortality}}{\text{Bird utilization rate}} = \frac{\text{No. of dead birds/defined area}}{\text{No. of birds observed/time or time and area}} \qquad (12.3)$$

Bird risk can be used to compare risk differences for many different variables: i.e., distances from wind facilities; species, type, and all birds observed; seasons; and turbine structure types. It can be used to compare risks between wind resource areas and with other types of facilities such as highways, power lines, and TV and radio transmission towers.

5. **Rotor swept area metrics.** Under this category, two measurements that consider the effects of different wind turbine sizes and designs have been defined. The first, rotor swept hour is defined as:

$$\text{Rotor Swept Hour} = [\text{Rotor swept area}(m^2)] \times (\text{Hours of operation}) \qquad (12.4)$$

This parameter combines the size of the area of the rotor with the time it operates. The second parameter, rotor swept hour risk (RSHR) allows for a comparison of risks associated with different rotor swept areas, or turbine sizes, in relation to the time they operate. It is defined by:

$$\text{Rotor Swept Hour Risk} = \frac{1}{\text{Rotor Swept Hour}} \times \text{Bird risk} \qquad (12.5)$$

A detailed discussion of the example use of these metrics is beyond the scope of this work. It is expected that many of them will be used in future research studies aimed at developing methods to measure the risk to birds not only from wind systems, but also from other human-created hazards such as buildings and highways (NWCC, 2001; 2002).

As in the US, European researchers have mainly concentrated on onshore investigations into the effects of wind turbines on birds. Some recent studies, however (see Köller *et al.*, 2006) have considered the effects of offshore wind farms on various species of birds. This work also summarizes the results of a variety of new techniques that can be used to study bird migration near wind farms. They include: radar, thermal imaging, use of video cameras, and microphone

techniques. Similar to land-based wind farms, Köller *et al.* note that the following measures can be used to mitigate the effects of offshore wind turbines on birds:

- abandonment of wind farms in zones with dense migration corridors;
- alignment of turbines in rows parallel to the main migration direction;
- several kilometer wide free migration corridors between wind farms;
- no construction of wind farms between resting and foraging areas;
- shutdown of turbines at night with bad weather/visibility and high migration intensity;
- refraining from large-scale continuous illumination;
- measures to make wind turbines generally more recognizable to birds.

In summary, it should be pointed out that even if the initial research indicates that a wind energy project is unlikely to seriously affect bird populations, further studies might be needed to verify this conclusion. These could include monitoring baseline bird populations and behavior before the project begins, then simultaneously observing both a control area and the wind site during construction and initial operation. In certain cases, operational monitoring might have to continue for years. As an example, the National Academy of Sciences (2007) discusses quantitative tools for the prediction of bird and bat fatalities at proposed and existing wind energy facilities.

12.3 Visual Impact of Wind Turbines

12.3.1 Overview

Aesthetic issues are often a primary reason for concern about wind energy projects. As pointed out by the National Academy of Sciences (2007), however, few regulatory processes adequately address aesthetic issues. One of wind power's perceived adverse environmental impact factors, and a major concern of the public, is its visibility (Gipe, 1995; Pasqualetti *et al.*, 2002). Compared to the other environmental impacts associated with wind power, the visual impact is the least quantifiable. For example, the public's perceptions may change with knowledge of the technology, location of wind turbines, and many other factors. Although the assessment of a landscape is somewhat subjective, professionals working in this area are trained to make judgments on visual impact based on their knowledge of the properties of visual composition and by identifying elements such as visual clarity, harmony, balance, focus, order, and hierarchy (Stanton, 1996).

Wind turbines need to be sited in well-exposed sites in order to be cost effective. It is also important for a wind engineer to realize that the visual appearance of a wind turbine or a wind farm must be considered in the design process at an early stage. For example, the degree of visual impact is influenced by such factors as the type of landscape, the number and design of turbines, the pattern of their arrangement, their color, and the number of blades.

12.3.2 Characterization of the Problem

Visual or aesthetic resources refer to the natural and cultural features of an environmental setting that are of visual interest to the public. An assessment of a wind project's visual compatibility with the character of the project setting can be based on a comparison of the

setting and surrounding features with simulated views of the proposed project. In this light, the following parameters and questions can be considered:

- **Viewshed alteration**: – will the project substantially alter the existing project setting (generally referred to as the 'viewshed'), including any changes in the natural terrain or landscape?
- **Viewshed consistency**: – will the project deviate substantially from the form, line, color, and texture of existing elements of the viewshed that contribute to its visual quality?
- **Viewshed degradation**: – will the project substantially degrade the visual quality of the viewshed, affect the use or visual experience of the area, or intrude upon or block views of valuable visual resources?
- **Conflict with public preference**: – will the project be in conflict with directly identified public preferences regarding visual and environmental resources?
- **Guideline compatibility**: – will the project comply with local goals, policies, designations, or guidelines related to visual quality?

The scope of a visual impact assessment depends on whether a single or a number of wind turbines are to be sited in a particular location. Visual impact is not directly proportional to the number of turbines in a wind farm development. It will, however, vary a great deal between a single turbine and a wind farm. That is, a single wind turbine has only a visual relationship between itself and the landscape, but a wind farm has a visual relationship between each turbine as well as with the landscape (Stanton, 1996).

An important task here is the characterization of the location where the proposed wind system is to be sited. As one example of this process, the work of Stanton (1994) as applied to wind farms in the UK uses the design principles shown in Figure 12.2. It should be noted that although this visual impact study is based on widely known and accepted principles (such as those summarized in Figure 12.2), the judgments made are subjective in nature.

12.3.3 Design of Wind Systems to Minimize Visual Impact

In the United States and Europe, there are numerous publications that suggest potential designs for wind systems that minimize visual impact (e.g., see Ratto and Solari, 1998; Schwartz, 2005). In many cases, the subjective nature of this topic appears and there are major differences of opinion between researchers. An example of this problem includes the choice of turbine colors (Aubrey, 2000). Two examples of previous design strategies (one from the United States and the other European) for the reduction of the visual impact of wind energy systems follow.

12.3.3.1 Visual Impact Mitigation Design Strategies for US Sites

From work carried out in the US (see National Academy of Sciences, 2007), a number of design strategies for reducing the environmental impact of wind systems have been proposed. They include the following:

- Using the local land form to minimize visibility of access and service roads, and to protect land from erosion. Use of low-profile and unobtrusive building designs to minimize the urbanized appearance or industrial character of projects located in rural or remote regions.
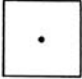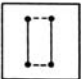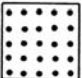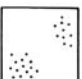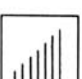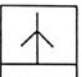
	HARMONY & CLARITY	• Clarity - The eye seeks clarity in a visual pattern. That is the eye must be able to tell what a design is trying to say • Harmony - Refers to a feeling of restful completeness, creating a feeling of balance where opposite forms and forces compensate
	ORDER	• Order is achieved when the 'pushes and pulls' within a composition can be clearly understood by the eye, when there is no doubt about the direction in which a form is moving or the nature of its relationship to an ideal shape or position
	A POINT	• Points have traditionally been used to mark a position in space, eg obelisk • A point has no length, width or depth and is therefore static, directionless and centralised • At the centre of its environment, a point is stable and at rest, organising surrounding elements about itself and dominating its field
	A LINE & EDGE	• Two points describe a line that connects them. Although the points give a line finite length, the line can be considered a segment of an infinitely larger axis • A line, in describing the path of a point in motion, is capable of expressing movement, direction and growth • A line joins, links, supports and intersects other visual elements. It gives shape and articulation to the surface of planes and describes edges. Edges are linear elements which form the boundaries between two phases. They may be barriers, more or less penetratable, which close one region from another; or they may be seams, lines along which two regions are related and joined together. These edge elements are important organising features, particularly in the role of holding together generalised areas, as in the outline of a city by water or wall
	PARALLEL LINES	• Two parallel lines have the ability to visually describe a plane. A transparent spatial membrane can be stretched between them to acknowledge their visual relationship. The closer these lines are to each other, the stronger will be the sense of place they convey
	GRID	• The grid encourages the viewer to divide their attention equally over an entire surface • The grid in 3 dimensions, generates a spatial network of points and lines. Within this modular framework, any number of forms and spaces can be visually organised • The organising power or a grid results from the regularity and continuity of its pattern that parades the elements it organises. It establishes a constant set of field of reference points, so features dissimilar in size, form and function relate
	CLUSTERS/ GROUPS	• Grouping - Used to organise and structure pieces of visual information into graspable visual patterns, depending on proximity • Clustering - Can consist of forms equivalent in size, shape and function, ordered into coherent non-hierarchial organisation by proximity and similarity of visual properties • Lacking introverted nature and geometrical regularity of centralised forms, clustering is flexible enough to incorporate various forms, shapes, sizes and orientation
	RHYTHM & REPETITION	• Rhythm refers to the regular or harmonious reoccurrence of lines, shapes, forms or colours. It incorporates the fundamental notion of repetition as one of the most effective devices to create unity in a composition, organising forms and spaces • Within repetition, the elegance of proportions and the reassuring expectancy of each element has a hypnotic regularity, the whole unified by the sameness of shape and interval, whilst remaining interesting in the visual changes that occur with distance
	SHAPE	• A geometric shape looks absolute, uncontaminated by accidents, outside of any style and universally understandable. Even geometric shapes in nature such as crystals, have a timeless look, giving an impression of creation rather than growth • Similar shapes have a structure easily grasped by the eye. The simple shape will have a clear order to its parts, angles and directions, that can be remembered at a close glance and will have an easy to see quality • The more vertical or horizontal the position of the shape, the more static or permanent it will appear. If a shape lies on a diagonal, it will seem in motion, temporary and dynamic • A radial form combines the aspects of linearity and centrality into a single composition. The core is either the symbolic or functional centre of the organisation

Figure 12.2 Summary of fundamental design principles significant to wind farm development (Stanton, 1994). Reproduced by permission of Mechanical Engineering Publications Ltd.

• Use of uniform color, structure types, and surface finishes to minimize project visibility in sensitive areas with high open spaces. Note, however, that the use of non-obtrusive designs and colors may conflict with efforts to reduce avian collisions and may be in direct conflict with aircraft safety requirements for distinctive markings.
• Selecting the route and type of support structures for above-ground electrical facilities as well as the method, mode, and type of installation (below- vs. above-ground). Where multiple generation units are to be sited close together, consolidation of electrical lines and roads into a single right of way, trench, or corridor will cause fewer impacts than providing separate access to each unit.

- Controlling the placement and limiting the size, color, and number of label markings placed on individual turbines or advertising signs on fences and facilities.
- Prohibiting lighting, except where required for aircraft safety, prevents light pollution in otherwise dark settings. This may incidentally minimize collision by nocturnal feeders which prey on insects attracted to lights.
- Controlling the relative location of different turbine types, densities, and layout geometry to minimize visual impacts and conflicts. Different turbine types and those with opposing rotation can be segregated by buffer zones. Mixing of types should be avoided or minimized.

12.3.3.2 European Wind Farm Visual Impact Design Characteristics

The assessment of the visual impact of a proposed wind farm development is an important design step in recent European work. One example of this type of work is summarized by the following list of wind farm design characteristics quoted from Stanton's (1994; 1996) UK studies:

- wind turbine form;
- blade number;
- turbine nacelle and tower;
- turbine size;
- wind farm size;
- spacing and layout of wind turbines;
- color.

Note that this work complements Stanton's previously described landscape character types. Again, the subjective nature of this example should be emphasized.

Other representative European-based visualization studies are given in the following technical papers:

- Möller (2006): Denmark;
- Hurtado *et al.* (2004): Spain;
- Bishop and Miller (2007): offshore wind farms.

12.3.4 Resources for Visual Impact Studies

In both the US and Europe there are numerous references and handbooks in which one can find design guidelines for minimizing the visual environmental impact of wind turbines and wind farms (e.g., see Ratto and Solari, 1998; Schwartz, 2005). A summary of some of the most representative examples follows.

12.3.4.1 US Visual Impact Resources

A good resource on the subject is contained in a handbook for the permitting of wind energy facilities (NWCC, 1998; 2002). In addition, this reference contains much additional information of potential use in this and many other phases of environmental impact

assessment. For example, the authors point out that a valuable process tool for the assessment of potential project impacts to sensitive visual resources is the preparation and use of visual simulations.

Goodman (1997) gives another good source of information on visual resources. This paper documents the environmental impacts of a wind farm installation in rural Vermont, and summarizes the methods used to minimize the environmental impact of a 6 MW wind farm.

An excellent review of visual assessment methods is given by the National Academy of Sciences (2007). In this work the authors summarize the steps involved and the basic visual principles that form the basis of aesthetic impact assessment. For example, the basic steps include the following:

- project description;
- project visibility, appearance, and landscape context (includes visual simulations);
- scenic-resource values and sensitivity levels;
- assessment of aesthetic impacts;
- mitigation techniques;
- determination of acceptability or undue aesthetic impacts.

12.3.4.2 European Visual Impact Resources

As discussed in numerous publications on the subject, the visual impact of wind turbines and wind farms has been under significant study in many European countries. A great deal of this work has been carried out in the UK. For example, the visual impact assessment work of Stanton (1994; 1996) has already been mentioned.

In Europe, a number of investigators have developed some very sophisticated and useful techniques that can be used to illustrate the visual intrusion of a potential wind farm installation. Furthermore, many of these have been successfully used in actual wind farm development projects (see Ratto and Solari, 1998). For example, one uses digital computer techniques based on topographical information and wind turbine design characteristics. With this type of technique it is possible to plot 'zones of visual impact' on a map to illustrate the locations where the development might be seen. One disadvantage to this technique is that it takes no account of local screening, e.g., by buildings or trees, so it is a worst case scenario. An example of the use of this type of technique, using geographical information systems (GIS), is given by Kidner (1996).

Another method (see Taylor and Durie, 1995) is based on the use of photomontages. Here, use is made of panoramic photographs taken from certain key locations of varying distances from the proposed site, and superimposing suitably scaled wind turbines in the photographs. A limitation to this technique is that the visibility of a wind system will change with time of day, season, and with certain weather conditions – especially when the turbine blades are rotating.

A third method attempts to overcome some of these disadvantages by creating a video montage of a proposed site and then superimposing rotating wind turbines on the scene (Robotham, 1992). While this creates a most effective visual presentation, its major disadvantage is its high cost compared to the other two methods. Today, a number of commercial software packages include all or some of these capabilities.

12.4 Wind Turbine Noise

12.4.1 Overview of the Problem

The problem associated with wind turbine noise has been one of the more studied environmental impact areas in wind energy engineering. Noise levels can be measured, but, as with other environmental concerns, the public's perception of the noise impact of wind turbines is a partly subjective determination.

Noise is defined as any unwanted sound. Concerns about noise depend on the level of intensity, frequency, frequency distribution, and patterns of the noise source; background noise levels; terrain between emitter and receptor; and the nature of the noise receptor. The effects of noise on people can be classified into three general categories:

- subjective effects including annoyance, nuisance, dissatisfaction;
- interference with activities such as speech, sleep, and learning;
- physiological effects such as anxiety, tinnitus (ringing in the ears), or hearing loss.

In almost all cases, the sound levels associated with environmental noise produce effects only in the first two categories. Workers in industrial plants and those who work around aircraft can experience noise effects in the third category. Whether a noise is objectionable will depend on the type of noise (see the next section) and the circumstances and sensitivity of the person (or receptor) who hears it. Mainly because of the wide variation in the levels of individual tolerance for noise, there is no completely satisfactory way to measure the subjective effects of noise, or of the corresponding reactions of annoyance and dissatisfaction.

Operating noise produced from wind turbines is considerably different in level and nature than most large-scale power plants, which can be classified as industrial sources. Wind turbines are often sited in rural or remote areas that have a corresponding ambient noise character. Furthermore, while noise may be a concern to the public living near wind turbines, much of the noise emitted from the turbines is masked by ambient or the background noise of the wind itself.

The noise produced by wind turbines has diminished as the technology has improved. For example, with improvements in blade airfoils and turbine operating strategy, more of the wind energy is converted into rotational energy, and less into acoustic noise. Even a well-designed turbine, however, can generate some noise from the gearbox, brake, hydraulic components, or even electronic devices.

The significant factors relevant to the potential environmental impact of wind turbine noise are shown in Figure 12.3 (Hubbard and Shepherd, 1990). Note that sound technology is based on the following primary elements: noise sources, propagation paths, and receivers. In the following sections, after a short summary of the basic principles of sound and its measurement, a review of noise generation from wind turbines, its prediction, and propagation, as well as noise reduction methods is given.

12.4.2 Noise and Sound Fundamentals

12.4.2.1 Characteristics of Sound and Noise

Sound is generated by numerous mechanisms and is always associated with rapid small-scale pressure fluctuations (which produce sensations in the human ear). Sound waves are
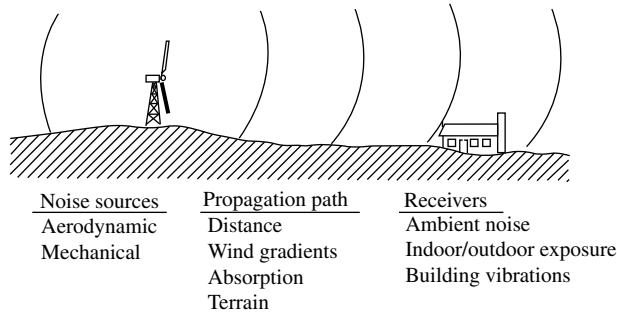
Figure 12.3   Wind turbine noise assessment factors (Hubbard and Shepherd, 1990)

characterized in terms of their wavelength, λ, frequency, f, and velocity of sound, c, where c is related to λ and f by:

$$c = f \lambda \tag{12.6}$$

The velocity of sound is a function of the medium through which it travels, and it generally travels faster in denser media. The velocity of sound is about 340 m/s in atmospheric air.

Sound frequency determines the 'note' or pitch that one hears, which, in many cases, corresponds to notes on the musical scale (Middle C is 262 Hz). An octave denotes the frequency range between sound with one frequency and one with twice that frequency. The human hearing frequency range is quite wide, generally ranging from about 20 Hz to 20 kHz (about ten octaves). Sounds experienced in daily life are usually not a single frequency, but are formed from a mixture of numerous frequencies from numerous sources.

Sound turns into noise when it is unwanted. Whether sound is perceived as a noise depends on the response to subjective factors such as the level and duration of the sound. There are numerous physical quantities that have been defined which enable sounds to be compared and classified, and which also give indications for the human perception of sound. They are discussed in numerous texts on the subject (e.g., for wind turbine noise see Wagner *et al.*, 1996) and are reviewed in the following sections.

12.4.2.2 Sound Power and Pressure Measurement Scales

It is important to distinguish between *sound power level* and *sound pressure level*. Sound power level is a property of the source of the sound. It gives the total acoustic power emitted by the source. Sound pressure level is a property of sound at a given observer location and can be measured there by a single microphone. In practice, the magnitude of an acoustical quantity is given in logarithmic form, expressed as a level in decibels (dB) above or below a zero reference level. For example, using conventional notation, a 0 dB sound power level will yield a 0 dB sound pressure level at a distance of 1 m.

Because of the wide range of sound pressures to which the ear responds (a ratio of 10^5 or more for a normal person), sound pressure is an inconvenient quantity to use in graphs and tables. In addition, the human ear does not respond linearly to the amplitude of sound pressure, and, to approximate it, the scale used to characterize the sound power or pressure amplitude of sound is logarithmic (see Beranek and Ver, 1992).

The sound power level of a source, L_W, in units of decibels (dB), is given by:

$$L_W = 10 \log_{10}(W/W_0) \tag{12.7}$$

where W is the source sound power and W_0 is a reference sound power (usually 10^{-12} W).

The sound pressure level of a noise, L_p, in units of decibels (dB), is given by:

$$L_p = 20 \log_{10}(p/p_0) \tag{12.8}$$

where p is the instantaneous sound pressure and p_0 a reference sound pressure (usually 20×10^{-5} Pa).

Low-frequency noise has been of some interest to the wind industry in the past and can be defined as follows: low-frequency pressure vibrations are typically categorized as *low-frequency sound* when they can be heard near the bottom of human perception (10–100 Hz) and *infrasound* when they are below the common limit of human perception. Sound below 20 Hz is generally considered infrasound, even though there may be some human perception in that range. This is also the type of noise that presents the most difficulties in its measurement and assessment (BWEA, 2005).

Infrasound is always present in the environment and stems from many sources including ambient air turbulence, ventilation units, waves on the seashore, distant explosions, traffic, aircraft, and other machinery. Infrasound propagates further (i.e., with lower levels of dissipation) than higher frequencies. Some characteristics of the human perception of infrasound and low-frequency sound are:

- Low-frequency sound and infrasound (2–100 Hz) are perceived as a mixture of auditory and tactile sensations.
- Lower frequencies must be of a higher magnitude (dB) to be perceived. (e.g., the threshold of hearing at 10 Hz is around 100 dB, whereas at 50 Hz it is 40 dB).
- Tonality cannot be perceived below around 18 Hz.
- Infrasound may not appear to be coming from a specific location, because of its long wavelengths.

The primary human response to perceived infrasound is annoyance, with resulting secondary effects. Annoyance levels typically depend on other characteristics of the infrasound, including intensity, variations with time, such as impulses, loudest sound, periodicity, etc. Infrasound has three annoyance mechanisms:

- a feeling of static pressure;
- periodic masking effects in medium and higher frequencies;
- rattling of doors, windows, etc. from strong low-frequency components.

For sound effects in general, Figure 12.4 gives some examples for various sound pressure levels on the decibel scale. The threshold of pain for the human ear is about 200 Pa, which corresponds to a sound pressure level of 140 dB.

12.4.2.3 Measurement of Sound or Noise

Sound pressure levels are measured via the use of sound level meters. These devices make use of a microphone, which converts pressure variations to a voltage signal, which is then recorded
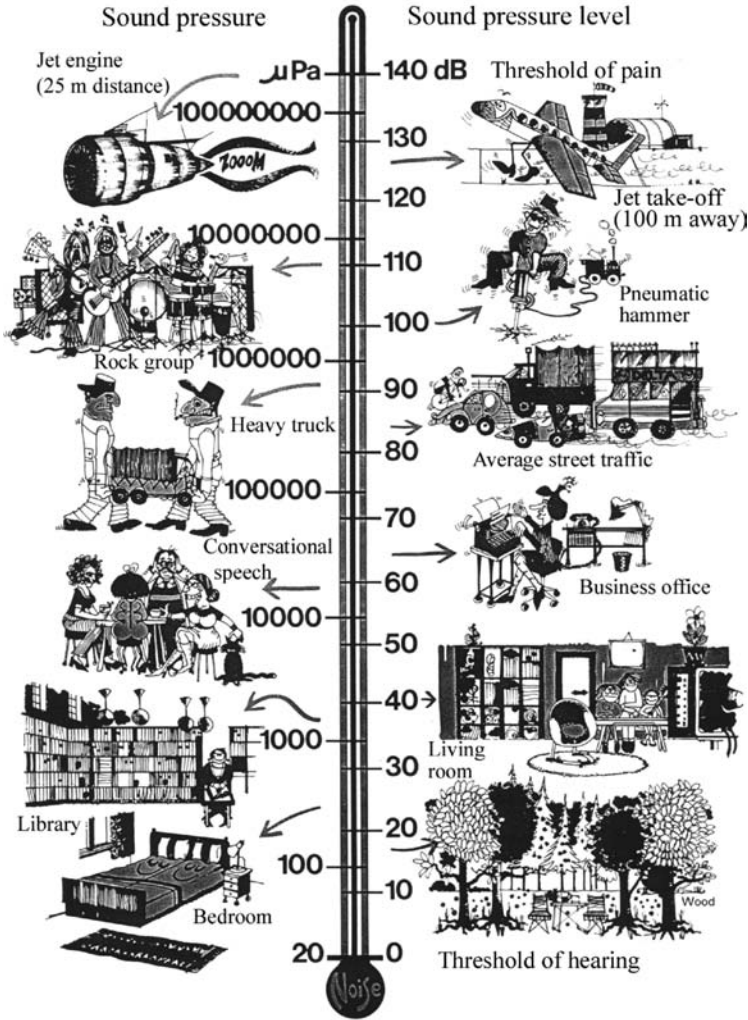
Figure 12.4 Sound pressure level (SPL) examples. Reproduced by permission of Bruel and Kjaer Instruments

on a meter (calibrated in decibels). The decibel scale is logarithmic and has the following characteristics (NWCC, 2002):

- Except under laboratory conditions, a change in sound level of 1 dB cannot be perceived.
- Outside of the laboratory, a 3 dB change in sound level is considered a barely discernible difference.
- A change in sound level of 5 dB will typically result in a noticeable community response.
- A 10 dB increase is subjectively heard as an approximate doubling in loudness, and almost always causes an adverse community response.
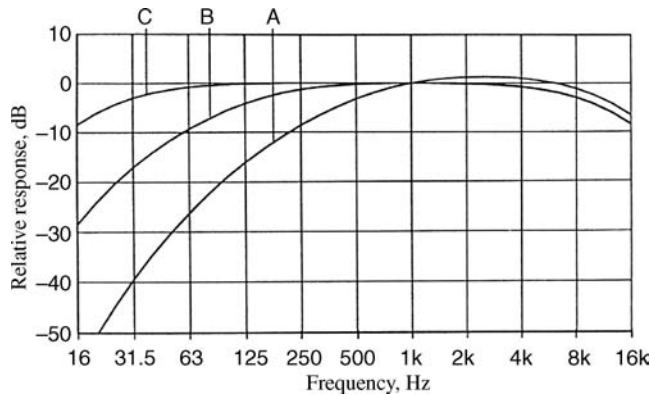
Figure 12.5 Definition of A, B, and C frequency weighting scales (Beranek and Ver, 1992)

A sound level measurement that combines all frequencies into a single weighted reading is defined as a broadband sound level (see Section 12.4.3). For the determination of the human ear's response to changes in noise, sound level meters are generally equipped with filters that give less weight to the lower frequencies. As shown in Figure 12.5, there are filters (referenced as A, B, and C) that accomplish this. There is also a G weighting scale specifically designed for infrasound (BWEA, 2005). The most common scale used for environmental noise assessment is the A scale. Measurements made using this filter are expressed in units of dB(A). Beranek and Ver (1992) discuss details of these scales.

Once the A-weighted sound pressure is measured over a period of time, it is possible to determine a number of statistical descriptions of time-varying sound and to account for the greater sensitivity to night-time noise levels. Common descriptors include:

- L_{10}, L_{50}, L_{90}. These represent the A-weighted noise levels that are exceeded 10%, 50%, and 90% of the time, respectively. During the measurement period L_{90} is generally taken as the background noise level.
- L_{eq} *(equivalent noise level).* The average A-weighted sound pressure level which gives the same total energy as the varying sound level during the measurement period of time.
- L_{dn} *(day–night noise level).* The average A-weighted noise level during a 24-hour day, obtained after addition of 10 dB to levels measured at night between 10 p.m. and 7 a.m.

12.4.3 Noise Mechanisms of Wind Turbines

There are four types of noise that can be generated by wind turbine operation: tonal, broadband, low-frequency, and impulsive. These are described below:

- **Tonal.** Tonal noise is defined as noise at discrete frequencies. It is caused by wind turbine components such as meshing gears, nonlinear boundary layer instabilities interacting with a rotor blade surface, by vortex shedding from a blunt trailing edge, or unstable flows over holes or slits.

- **Broadband.** This is noise characterized by a continuous distribution of sound pressure with frequencies greater than 100 Hz. It is often caused by the interaction of wind turbine blades with atmospheric turbulence, and is also described as a characteristic 'swishing' or 'whooshing' sound.
- **Low-frequency.** This describes noise with frequencies in the range of 20 to 100 Hz mostly associated with downwind turbines. It is caused when the turbine blade encounters localized flow deficiencies due to the flow around a tower, wakes shed from other blades, etc.
- **Impulsive.** Short acoustic impulses or thumping sounds that vary in amplitude with time characterize this noise. They may be caused by the interaction of wind turbine blades with disturbed air flow around the tower of a downwind machine, and/or the sudden deployment of tip breaks or actuators.

The causes of noise emitted from operating wind turbines can be divided into two categories: (1) aerodynamic and (2) mechanical. Aerodynamic noise is produced by the flow of air over the blades. The primary sources of mechanical noise are the gearbox and the generator. Mechanical noise is transmitted along the structure of the turbine and is radiated from its surfaces. A summary of each of these noise mechanisms follows. A more detailed review is included in the text of Wagner *et al.* (1996).

12.4.3.1 Aerodynamic Noise

Aerodynamic noise originates from the flow of air around the blades. As shown in Figure 12.6 (Wagner *et al.*, 1996), a large number of complex flow phenomena generate this type of noise. This type of noise generally increases with tip speed or tip speed ratio. It is broadband in character and is typically the largest source of wind turbine noise. When the wind is turbulent, the blades can emit low-frequency noise as they are buffeted by changing winds. If the wind is disturbed by flow around or through a tower before hitting the blades (on a downwind turbine design), the blade will create an impulsive noise every time it passes through the 'wind shadow' of the tower.
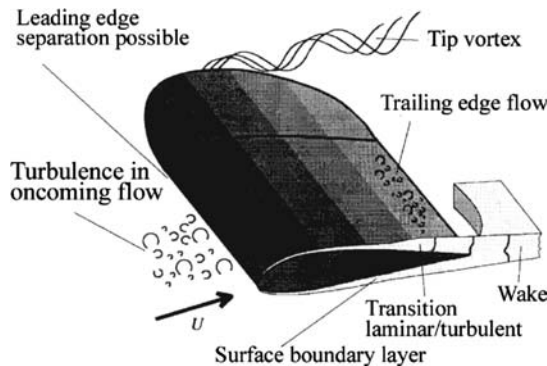
Figure 12.6   Schematic of flow around a rotor blade (Wagner *et al.*, 1996); *U*, wind speed. Reproduced by permission of Springer-Verlag GmbH and Co.

Table 12.2 Wind turbine aerodynamic noise mechanisms (Wagner *et al.*, 1996). Reproduced by permission of Springer-Verlag GmbH and Co.

Type or indication	Mechanism	Main characteristics and importance
Low-frequency noise		
Steady thickness noise; steady loading noise	Rotation of blades or rotation of lifting surfaces	Frequency is related to blade passing frequency, not important at current rotational speeds
Unsteady loading noise	Passage of blades through tower velocity deficit or wakes	Frequency is related to blade passing frequency, small in cases of upwind turbines/possibly contributing in case of wind farms
Inflow turbulence noise	Interaction of blades with atmospheric turbulence	Contributing to broadband noise; not yet fully quantified
Airfoil self-noise		
Trailing-edge noise	Interaction of boundary layer turbulence with blade trailing edge	Broadband, main source of high-frequency noise ($770\,\text{Hz} < f < 2\,\text{kHz}$)
Tip noise	Interaction of tip turbulence with blade tip surface	Broadband; not fully understood
Stall, separation noise	Interaction of turbulence with blade surface	Broadband
Laminar boundary layer noise	Nonlinear boundary layer instabilities interacting with the blade surface	Tonal, can be avoided
Blunt trailing edge noise	Vortex shedding at blunt trailing edge	Tonal, can be avoided
Noise from flow over holes, slits and intrusions	Unstable shear flows over holes and slits, vortex shedding from intrusions	Tonal, can be avoided

The various aerodynamic noise mechanisms are shown in Table 12.2 (Wagner *et al.*, 1996). They are divided into three groups: (1) low-frequency noise, (2) inflow turbulence noise, and (3) airfoil self-noise. A detailed discussion of the aerodynamic noise generation characteristics of a wind turbine is beyond the scope of this work.

12.4.3.2 Mechanical Noise

Mechanical noise originates from the relative motion of mechanical components and the dynamic response that results. The main sources of such noise include:

- gearbox;
- generator;
- yaw drives;
- cooling fans;
- auxiliary equipment (e.g., hydraulics).

Since the emitted noise is associated with the rotation of mechanical and electrical equipment, it tends to be tonal (of a common frequency) in character, although it may have
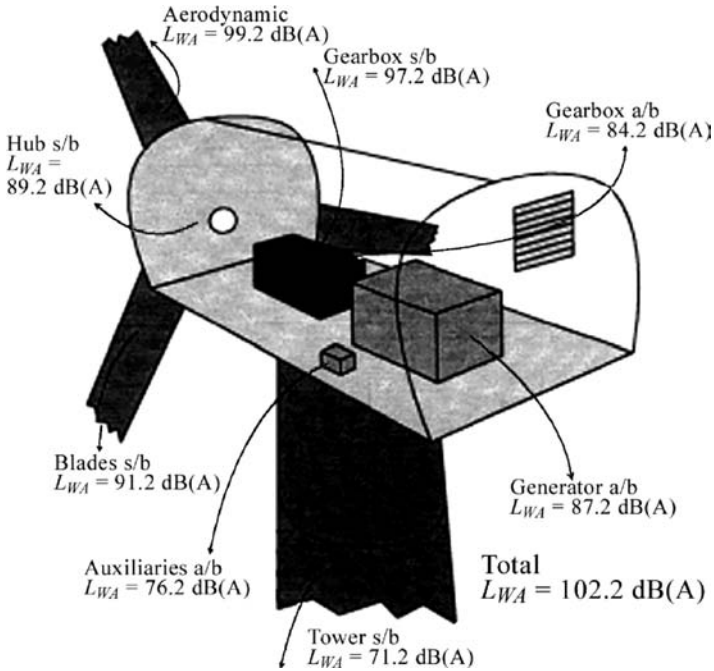
Figure 12.7   Components and total sound power level for wind turbine (Wagner *et al.*, 1996); L_{WA}, predicted A-weighted sound power level; a/b, air-borne; s/b, structure-borne. Reproduced by permission of Springer-Verlag GmbH and Co.

a broadband component. For example, pure tones can be emitted from the rotational frequencies of shafts and generators, and the meshing frequencies of the gears.

In addition, the hub, rotor, and tower may act as loudspeakers, transmitting the mechanical noise and radiating it. The transmission path of the noise can be air-borne (a/b) or structure-borne (s/b). Air-borne means that the noise is directly propagated from the component surface or interior into the air. Structure-borne noise is transmitted along other structural components before it is radiated into the air. For example, Figure 12.7 shows the type of transmission path and the sound power levels for the individual components determined at a downwind position (115 m) for a 2 MW wind turbine (Wagner *et al.*, 1996). Note that the main source of mechanical noise was the gearbox that radiated noise from the nacelle surfaces and the machinery enclosure.

12.4.4 Noise Prediction from Wind Turbines

12.4.4.1 Single Wind Turbines

The prediction of noise from a single wind turbine under expected operating conditions is an important part of an environmental noise assessment. Considering the complexity of the problem, this is not a simple task and, depending on the resources and time available, can be

quite involved. To complicate matters, wind turbine technology and design has steadily improved through the years, so prediction techniques based on experimental field data from operating turbines may not reflect state-of-the-art machines.

Despite these problems, researchers have developed analytical models and computational codes for the noise prediction of single wind turbines. In general, these models can be divided into the following three classes (Wagner *et al.*, 1996):

- **Class 1.** This class of models gives a simple estimate of the overall sound power level as a function of basic wind turbine parameters (e.g., rotor diameter, power, and wind speed). Models in this class represent rules of thumb and are simple and easy to use.
- **Class 2.** These consider the three types of noise mechanisms previously described, and represent current turbine state of the art.
- **Class 3.** These models use refined models describing the noise-generation mechanisms and relate them to a detailed description of the rotor geometry and aerodynamics.

For the Class 1 models, there are empirical equations that have been used to estimate the sound power level. For example, based on turbine technology up to about 1990, Bass (1993) states that a useful rule of thumb is that wind turbines radiate 10^{-7} of their rated power as sound power. Examples of three other Class 1 models for the prediction of sound power level are summarized in Equations (12.9) to (12.11).

$$L_{WA} = 10(\log_{10} P_{WT}) + 50 \qquad (12.9)$$

$$L_{WA} = 22(\log_{10} D) + 72 \qquad (12.10)$$

$$L_{WA} = 50(\log_{10} V_{Tip}) + 10(\log_{10} D) - 4 \qquad (12.11)$$

where L_{WA} is the overall A-weighted sound power level, V_{Tip} is the tip speed at the rotor blade (m/s), D is the rotor diameter (m), and P_{WT} is the rated power of the wind turbine (W).

The first two equations represent the simplest (and least accurate today, since they were developed for older machines) methods to predict the noise level of a given turbine based on either its rated power or rotor diameter. The last equation illustrates a rule of thumb that aerodynamic noise is dependent on the fifth power of the tip speed.

The complexity of the Class 2 and 3 models is illustrated in Table 12.3, where the input required for both models is summarized. A detailed discussion of all these models is beyond the scope of this section and is given in the text of Wagner *et al.* (1996).

12.4.4.2 Multiple Wind Turbines

Intuitively, one would expect that doubling the number of wind turbines at a given location would double the sound energy output. Since the decibel scale is logarithmic, the relation to use for the addition of two sound pressure levels (L_1 and L_2) is given as:

$$L_{total} = 10 \log_{10}(10^{L_1/10} + 10^{L_2/10}) \qquad (12.12)$$

Table 12.3 Typical inputs for Class 2 and 3 noise prediction models (Wagner et al., 1996). Reproduced by permission of Springer-Verlag GmbH and Co.

Group	Parameter	Class 2	Class 3
Turbine configuration	Hub height	X	X
	Type of tower (upwind or downwind)		X
Blades and rotor	Number of blades	X	X
	Chord distribution	(X)	X
	Thickness of trailing edge	(X)	X
	Radius	X	X
	Profile shape	(X)	X
	Shape of blade tip	(X)	X
	Twist distribution	(X)	X
Atmosphere	Turbulence intensity	X	X
	Ground surface roughness	X	X
	Turbulence intensity spectrum		X
	Atmospheric stability conditions		X
Turbine operation	Rotational speed	X	X
	Wind speed, alternatively: rated power, rated wind speed, cut-in wind speed	X	X
	Wind direction		X

This equation has two important implications:

- Adding sound pressure levels of equal value increases the noise level by 3 dB.
- If the absolute value of $L_1 - L_2$ is greater than 15 dB, the addition of the lower level has negligible effects.

This relation can be generalized for N noise sources:

$$L_{total} = 10 \log_{10} \sum_{i=1}^{N} 10^{L_i/10} \tag{12.13}$$

12.4.5 Noise Propagation from Wind Turbines

In order to predict the sound pressure level at a distance from a source with a known power level, one must consider how the sound waves propagate. Details of sound propagation in general are discussed in Beranek and Ver (1992). For the case of a stand-alone wind turbine, one might calculate the sound pressure level by assuming spherical spreading, which means that the sound pressure level is reduced by 6 dB per doubling of distance. If the source is on a perfectly flat and reflecting surface, however, then hemispherical spreading has to be assumed, which leads to a 3 dB reduction per doubling of distance.

Furthermore, the effects of atmospheric absorption and the ground effect, both dependent on frequency and the distance between the source and observer, have to be considered. The ground effect is a function of the reflection coefficient of the ground and the height of the emission point.

Wind turbine noise also exhibits some special features (Wagner *et al.*, 1996). First, the height of the source is generally higher than conventional noise sources by an order of magnitude, which leads to less importance of noise screening. In addition, the wind speed has a strong influence on the generated noise. The prevailing wind directions can also cause considerable differences in sound pressure levels between upwind and downwind positions.

The development of an accurate noise propagation model generally must include the following factors:

- source characteristics (e.g., directivity, height, etc.);
- distance of the source to the observer;
- air absorption;
- ground effect (i.e., reflection of sound on the ground, dependent on terrain cover, ground properties, etc.);
- propagation in complex terrain;
- weather effects (i.e., change of wind speed or temperature with height).

A discussion of complex propagation models that include all these factors is beyond the scope of this work. A discussion of work in this area is given by Wagner *et al.* (1996). For estimation purposes, a simple model based on hemispherical noise propagation over a reflective surface, including air absorption, is given as:

$$L_p = L_W - 10 \log_{10}(2\pi R^2) - \alpha R \qquad (12.14)$$

where L_p is the sound pressure level (dB) a distance R from a noise source radiating at a power level L_W (dB) and α is the frequency-dependent sound absorption coefficient.

This equation can be used with either broadband sound power levels and a broadband estimate of the sound absorption coefficient [$\alpha = 0.005$ dB(A) m^{-1}] or more preferably in octave bands using octave band power and sound absorption data.

12.4.6 Noise Reduction Methods for Wind Turbines

Turbines can be designed or retrofitted to minimize mechanical noise. This can include special finishing of gear teeth, using low-speed cooling fans, mounting components in the nacelle instead of at ground level, adding baffles and acoustic insulation to the nacelle, using vibration isolators and soft mounts for major components, and designing the turbine to prevent noise from being transmitted into the overall structure. Also, as pointed out by NWCC (2002), the limited number of downwind machines that have been developed or sold recently have been engineered to reduce low-frequency noise (e.g., increasing the distance of the rotor from the tower).

If a wind turbine has been designed using appropriate design procedures (as described in Chapters 6 and 7), it is likely that new noise-reducing airfoils will have been used, and mechanical noise emissions will not be a problem. In general, designers trying to reduce wind turbine noise even more must concentrate on the further reduction of aerodynamic noise. It has been previously noted that the following three mechanisms of aerodynamic noise generation are important for wind turbines (assuming that tonal contributions due to slits, holes, trailing

edge bluntness, control surfaces, etc., can be avoided by proper blade design):

- trailing edge noise;
- tip noise;
- inflow turbulence noise.

A review of work in these three areas is beyond the scope of this text and here the reader is again referred to the text of Wagner *et al.* (1996). It should be noted that noise has been reduced in modern turbine designs via the use of lower tip speed ratios, lower blade angle of attack, upwind designs, and, most recently, by using specially modified blade trailing edges.

12.4.7 Noise Assessment, Standards, and Regulations

An appropriate noise assessment study should contain the following four major types of information:

- An estimation or survey of the existing ambient background noise levels.
- Prediction (or measurement) of noise levels from the turbine(s) at and near the site.
- Identification of a model for sound propagation (sound modeling software will include a propagation model).
- An assessment of the acceptability of the turbine(s) noise level via comparison of calculated sound pressure levels from the wind turbine(s) with background sound pressure levels at the location of concern.

There are standards for measuring sound power levels from utility-scale wind turbines as well as national and local standards for acceptable noise power levels. At the present time, there are no sound measurement standards for small wind turbines, but both the International Electrotechnical Commission (IEC) and the American Wind Energy Association (AWEA) are working on future standards.

The internationally accepted standard used to measure utility-scale wind turbine sound power levels is the IEC Standard: 61400-11: Wind turbine generator systems – part 11: Acoustic noise measurement techniques (IEC, 2002). This reference defines:

- the quality, type, and calibration of instrumentation to be used for sound (and corresponding wind speed) measurements;
- locations and types of measurements to be made;
- data reduction and reporting measurements.

This standard requires measurements of broadband sound, sound levels in one-third octave bands, and tonality. These measurements are all used to determine the sound power level of the wind turbine at the nacelle, and the existence of any specific dominant sound frequencies. Measurements are to be made when the wind speeds at a height of 10 m are 6, 7, 8, 9, and 10 m/s. Manufacturers of IEC compliant wind turbines can provide sound power level measurements at these wind speeds as measured by certified testing agencies. Measurements of noise directivity, low-frequency noise (20–100 Hz), and infrasound (< 20 Hz) are optional.

Table 12.4 Noise limits of equivalent sound pressure levels, L_{eq} [dB(A)]: European countries (Gipe, 1995)

Country	Commercial	Mixed	Residential	Rural
Denmark			40	45
Germany				
day	65	60	55	50
night	50	45	40	35
Netherlands				
day		50	45	40
night		40	35	30

At the present time, there are no common international noise standards or regulations for sound pressure levels. In most countries, however, noise regulations define upper bounds for the noise to which people may be exposed. These limits depend on the country and are different for daytime and night time. In Europe, as shown in Table 12.4, fixed noise limits are the standard (Gipe, 1995).

In the United States, although no formal federal noise regulations exist, the US Environmental Protection Agency (EPA) has established noise guidelines. Many states do have noise regulations, and many local governments have enacted noise ordinances. Examples of such ordinances (California) for wind turbines are given in the first edition of *Permitting of Wind Energy Facilities: A Handbook* (NWCC, 1998).

It should also be pointed out that imposing a fixed noise level standard might not prevent noise complaints. This is due to the relative level of broadband background turbine noise compared to changes in background noise levels (NWCC, 1998). That is, if tonal noises are present, higher levels of broadband background noise are needed to effectively mask the tone(s). Accordingly, it is common for community noise standards to incorporate a penalty for pure tones, typically 5 dB(A). Therefore, if a wind turbine meets a sound power level limit of 45 dB(A), but produces a strong whistling, 5 dB(A) are subtracted from the limit. This forces the wind turbine to meet a real limit of 40 dB(A).

A discussion of noise measurement techniques that are specific to wind turbine standards or regulations is beyond the scope of this text. Reviews of such techniques are given in Hubbard and Shepherd (1990), GL (1994), and Wagner *et al.* (1996).

12.5 Electromagnetic Interference Effects

12.5.1 Overview of the Problem

Electromagnetic interference, EMI, is an electromagnetic disturbance that interrupts, obstructs, or degrades the effective performance of electronics or electrical equipment. Through EMI, wind turbines can have negative impacts on a number of signals important to human activities such as television, radio, microwave/radio fixed links, cellular telephones, and radar (see National Academy of Sciences, 2007).
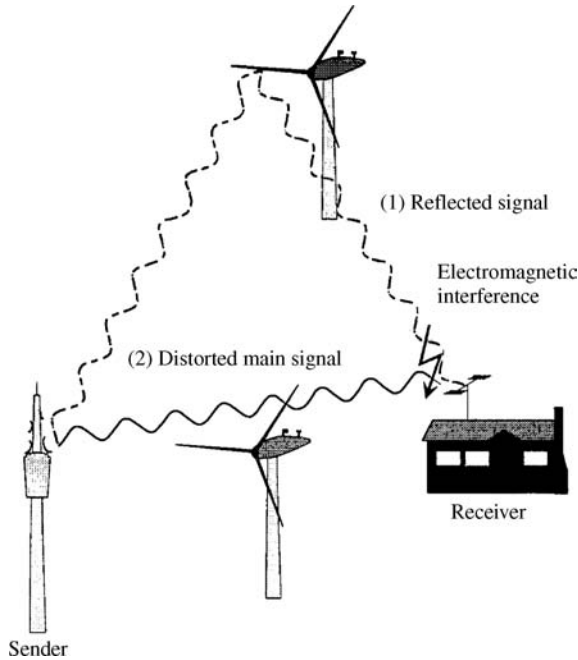
Figure 12.8   Scattering of electromagnetic signals by a wind turbine (Wagner *et al.*, 1996). Reproduced by permission of Springer-Verlag GmbH and Co.

Wind turbines can present an obstacle for incident electromagnetic waves, which may be reflected, scattered, or diffracted by the wind turbine. As shown schematically in Figure 12.8 (Wagner *et al.*, 1996), when a wind turbine is placed between a radio, television, radar, or microwave transmitter and receiver, it can sometimes reflect portions of the electromagnetic radiation in such a way that the reflected wave interferes with the original signal arriving at the receiver. This can cause the received signal to be significantly distorted.

Some key parameters that influence the extent of electromagnetic interference (EMI) caused by wind turbines include:

- type of wind turbine (i.e., horizontal axis wind turbine or vertical axis wind turbine);
- wind turbine dimensions;
- turbine rotational speed;
- blade construction material;
- blade angle and geometry;
- tower geometry.

In practice, the blade construction material and rotational speed are key parameters. For example, older HAWTs with rotating metal blades have caused television interference in areas near the turbine. Today, EMI from wind turbines is less likely because most blades are now made from composite materials. Most modern machines, however, have lightning protection on the blade surfaces, which can result in some electromagnetic interference.

12.5.2 Characterization of Electromagnetic Interference from Wind Turbines

12.5.2.1 Mechanism of Electromagnetic Interference

Electromagnetic interference from wind turbines is generated from multiple path effects. That is, as shown in Figure 12.8, in the vicinity of a wind installation, two transmission paths occur linking the transmitter to the receiver. Multiple paths occur on many electromagnetic transmissions (caused by large buildings or other structures). The feature unique to wind turbines, however, is blade rotation, which causes changes, over short time intervals, in the length of the secondary or scattered path. Thus, the receiver may acquire two signals simultaneously, with the secondary signal causing EMI because delay or distortion of the signal varies with time.

In the context of wind energy projects, it has been noted (National Academy of Sciences, 2007) that EMI is often considered in relation to the following telecommunications facilities:

- television broadcast transmissions (approximately 50 MHz–1 GHz);
- radio broadcast transmissions (approximately 1.5 MHz [AM] and 100 MHz [FM]);
- microwave/radio 'fixed links' (approximately 3–60 GHz);
- mobile phones (approximately 1 or 2 GHz);
- radar.

Effects of the signal variation change depend on the modulation scheme; that is, the manner in which the received information is coded. For example, for amplitude modulated (AM) signals, the variation in signal level can be highly undesirable. Interference may also be produced in frequency modulated (FM) signals. Furthermore, the Doppler shift caused by rotation of the blades may interfere with radar and, for digital systems, the signal variation can increase the bit error rate (Chignell, 1986).

12.5.2.2 Wind Turbine Parameters

A wind turbine may provide a number of different electromagnetic scattering mechanisms. The turbine blades in particular can play a significant role in generating electromagnetic interference. They may scatter a signal directly as they rotate and they may also scatter signals reflected from the tower. The degree of EMI caused by wind turbines is influenced by numerous factors, including:

- the wide frequency range of radio signals;
- the variety of modulation schemes;
- the wide variation in wind turbine parameters.

There are many possible ways whereby a wind turbine can modulate the electromagnetic signal and cause interference. Situations have either been reported or postulated where almost every design parameter of the wind turbine system may be critical to a specific service. The following general comments on the most important design variables can be made (Chignell, 1986):

1. **Type of machine.** Different waveforms have been observed in the interference generated by horizontal and vertical axis machines. Most work in this area has concentrated on television interference (TVI) effects.

2. **Machine dimensions.** The overall dimensions, particularly the diameter of the rotor, are important for establishing the radio frequency bands where interference may occur. Specifically, the larger the machine, the lower the frequency above which radio services may be affected. That is, a large machine will affect HF, VHF, UHF, and microwave bands, while a small machine may degrade only UHF and microwave transmissions.

3. **Rotational speed.** The rotational speed of the wind turbine and the number of blades determine the modulation frequencies in the interfering radio or telecommunications signal. If one of these coincides with a critical parameter in the radio or telecommunications receiver, the interference is increased.

4. **Blade construction.** The blade cross-section and material can be significant here. For example, the following general observations have been made:
   - The geometry of the blade should be simple; ideally a combination of simple curves which avoid sharp corners and edges.
   - In general, scattering from fiberglass or wooden blades is less than from a comparable metal structure. Fiberglass is partially transparent to radio waves whereas wood absorbs them, not allowing energy to be scattered.
   - The addition of any metallic structure such as a lightning conductor or a metal blade root to a fiberglass blade may negate the material advantages, with the composite structure scattering more effectively than an all-metal blade. To avoid this problem, the metallic components should avoid sharp edges and corners.

5. **Blade angles and geometry.** In larger machines, and with microwave signals, the angles defining the area where interference occurs become so narrow that small changes in the yaw, twist, and pitch of the blades become important along with the tilt, cone, and teeter angles.

6. **Tower.** The tower may also scatter radio waves and, as the wind machine rotates, the blades can 'chop' this signal. The geometry of the tower should be kept simple, but if a complicated lattice is essential, a careful choice of angles may reduce the problem. Note, however, that Sengupta and Senior (1994) have not found the tower to be a significant source of EMI.

12.5.2.3 Potential Electromagnetic Interference Effects of Wind Turbines

For electromagnetic interference generated by a wind turbine to disturb an electromagnetic (EM) signal, the following conditions must be satisfied:

- An electromagnetic transmission must be present.
- The wind system must modify the EM signal.
- An EM receiver must be present in the volume affected by the wind system.
- The EM receiver must be susceptible to the modified signal.

Based on EMI experiments, field experience, and analytical modeling in the United States (Sengupta and Senior, 1994) and Europe (Chignell, 1986), a summary of the effects of wind

turbine EMI on various electromagnetic transmissions is as follows:

- **Television interference.** Most reports of electromagnetic interference from wind turbines concern television service. Television interference from wind turbines is characterized by video distortion that generally occurs in the form of a jittering of the picture that is synchronized with the blade passage frequency (rotor speed multiplied by the number of blades). A significant amount of work on this subject has been carried out in the United States and Europe to quantify this effect.
- **FM radio interference.** Effects on FM broadcast reception have only been observed in laboratory simulations. They appear in the form of a background 'hiss' superimposed on the FM sound. This work concluded that the effects of wind turbine EMI on FM reception were negligible except possibly within a few tens of meters from the wind turbine.
- **Interference to aviation navigation and landing systems.** The effects on VOR (VHF omnidirectional ranging) and LORAN (a long-range version of VOR) systems have been studied via analytical models. Results from the VOR studies indicate that a stopped wind turbine may produce errors in the navigational information produced by the VOR. When the wind turbine is operating, however, the potential interference effects are significantly reduced. Note that existing Federal Aviation Authority rules prevent a structure the size of many wind turbines being erected within 1 km of a VOR station. For LORAN systems, which operate at very low frequencies, no degradation in communication performance is likely to occur. This assumes that a wind turbine is not in close proximity to the transmitter or receiver.
- **Interference to radar.** Aviation and/or air defense radar interference has recently emerged as an issue with regards to the siting of wind turbines (e.g., see US Department of Defense, 2006). Work in this area has shown that, at some wind farm sites, wind turbines can interfere with civilian or military aviation radar via direct or Doppler interference.
- **Interference to microwave links.** Analytical work has indicated that electromagnetic interference effects tend to smear out the modulation used in typical microwave transmission systems.
- **Interference with cellular telephones.** Since cellular radio is designed to operate in a mobile environment, it should be comparatively insensitive to EMI effects from wind turbines.
- **Interference with satellite services.** Satellite services using a geostationary orbit are not likely to be affected because of the elevation angle in most latitudes and the antenna gain.

12.5.3 Prediction of Electromagnetic Effects from Wind Turbines: Analytical Models

12.5.3.1 General Overview

A summary of the most detailed and general models for the analysis of radio signals with electromagnetic interference from wind turbines is given by Sengupta and Senior (1994). In this report, the authors summarize over 20 years of work directed toward this subject, focusing on large-scale wind turbine systems. Specifically, they have developed a general analytical model for the mechanism by which a wind turbine can produce electromagnetic interference. Their model is based on the schematic system shown in Figure 12.9, which illustrates the field conditions under which a wind turbine can cause EMI. As shown, a transmitter, *T*, sends a direct signal to two receivers, *R*, and a wind turbine, *WT*. The rotating blades of the wind turbine
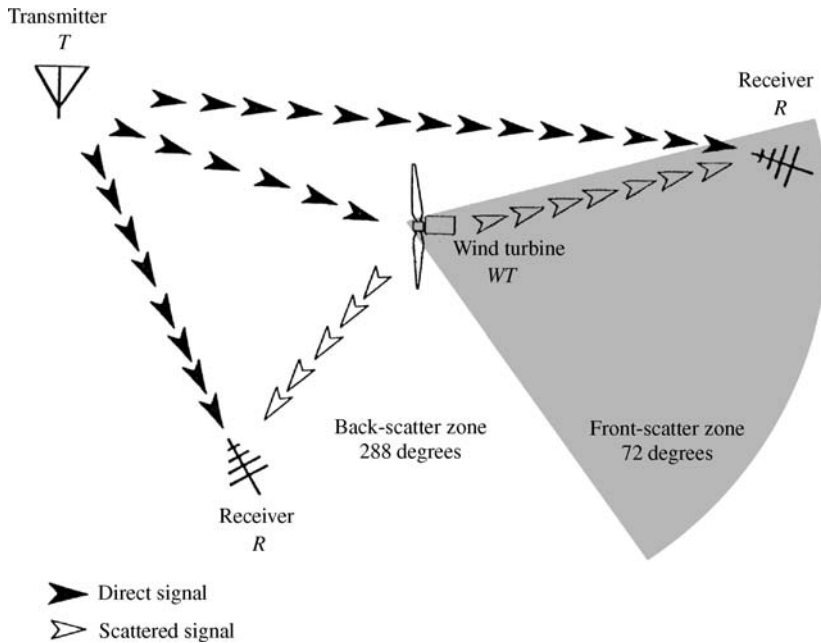
Figure 12.9 Model configuration for electromagnetic interference due to a wind turbine (Sengupta and Senior, 1994). Reproduced by permission of the American Society of Mechanical Engineers

both scatter a signal and transmit a scattered signal. Therefore, the receivers may acquire two signals simultaneously, with the scattered signal causing the EMI because it is delayed in time or distorted. Signals reflected in a manner analogous to mirror reflection are defined as back-scattered (about 80% of the region around the wind turbine). Signal scattering that is analogous to shadowing is called forward-scattering and represents about 20% of the region around a turbine.

For more details of this analysis, the reader is referred to Sengupta and Senior (1994), where analytical expressions are developed for the signal power interference (expressed in terms of a modulation index) and the signal scatter ratio, important EMI parameters. This work also summarizes their analytical scattering models for various wind turbine rotors. Their approach here was to develop simplified, idealized models of HAWT and VAWT rotors and to compare the model predictions of signal scattering with measured scattering. This approach is used to illustrate the basic principles of EMI from wind turbines and to provide useful equations for estimating the magnitude of potential interference in practical situations. An example of this is contained in their reports designed to assess TV interference from large and small wind turbines (Senior and Sengupta, 1983; Sengupta et al., 1983).

12.5.3.2 Simplified Analysis

At the present time, the general, and even specialized, models developed by US researchers that have been previously described are not readily usable by wind system designers. Simplified models, however, can be used to predict potential EMI problems from a wind turbine.

$L_1 + A_1$: Path loss transmitter–receiver (C-signal)
$L_2 + A_2$: Path loss transmitter–obstacle
$L_r + A_r$: Path loss obstacle–receiver (I-signal)
C/I : Signal to Interference ratio at receiver
τ : Time delay at receiver
σ_b : Bistatic radar cross-section of obstacle
ΔG : Signal discrimination of receiving aerial
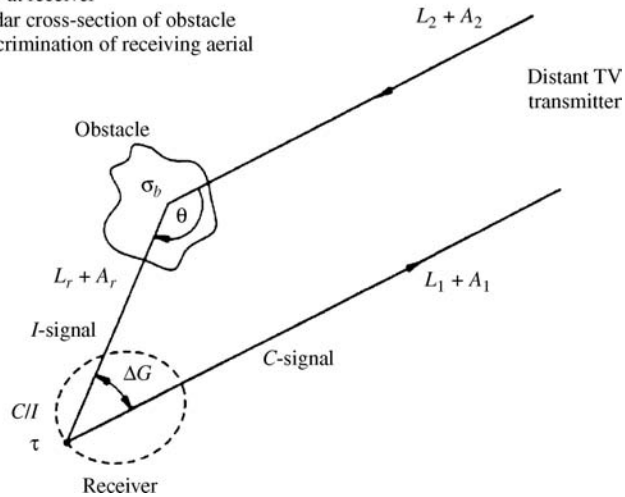
Figure 12.10 Geometry for interference of the electromagnetic path by an obstacle (Van Kats and Van Rees, 1989). Reproduced by permission of the Institution of Electrical Engineers

For example, Van Kats and Van Rees (1989) developed a simple EMI interference model for wind turbines that could be used to predict their impact on TV broadcast reception. As summarized below, results from this model produce a calculated value for the signal-to-interference ratio (C/I) for UHF TV broadcast reception in the area around the wind system that can be used to evaluate TV picture quality.

The general geometry and definition of terms for the model are given in Figure 12.10. This model is based on the assumption that the wind turbine behaves as an obstacle for incident electromagnetic waves, serving as a secondary source of radiation.

In this model, the spreading of this secondary field over its environment is determined by the following factors:

- size and shape of the obstacle with respect to signal wavelength, λ;
- dielectric and conductive properties of components of the wind turbine;
- position of the blades and the structure of the wind turbine with respect to the polarization of the incident wave.

Because the wind turbine blades are in continuous motion, the impact of the reflected and scattered fields is complex. Thus, the calculation of these fields requires empirical correlation. To approximate the behavior of the system, the model is based on radar technology, where an obstacle is characterized by its (bistatic) radar cross-section, σ_b. (This variable is defined as the imaginary surface of an isotropic radiator from which the received power corresponds to

the actual power received from the obstacle.) In general, σ_b is a function of the dielectric properties and geometry of the obstacle and the signal wavelength.

When the impact of a wind turbine on radio waves is modeled using σ_b, an expression for the signal-to-interference ratio, C/I, can be found in the area around the wind turbine. It should be noted that for each specific radio service (e.g., TV, mobile radio, microwave links, etc.) a different C/I ratio will be required for reliable operation. Using the assumed geometry and nomenclature shown in Figure 12.10, the C/I ratio at a distance r from the turbine can be determined by separately calculating the strength of the desired signal, C, and the strength of the interference signal, I. The desired signal is given by:

$$C = P_t + (L_1 + A_1) + G_r \qquad (12.15)$$

where P_t is the transmitter power, L_1 is the free space path loss between the transmitter and the receiver, A_1 is the additional path loss between the transmitter and the receiver, and G_r is the receiver gain. In a manner similar to acoustic measurements, signal strength is expressed in decibels (here, dBW or dB above 1 W). The undesired signal, I, is given by:

$$I = P_t - (L_2 + A_2) + 10 \log(4\pi\sigma_b/\lambda^2) - (L_r + A_r) + G'_r \qquad (12.16)$$

where L_2 is the free space path loss between the transmitter and the obstacle, A_2 is the additional path loss between the transmitter and the obstacle, L_r is the free space path loss between the obstacle and the receiver, A_r is the additional path loss between the obstacle and the receiver, and G'_r is the receiver gain (obstacle path).

Next, assume that $L_1 = L_2$ when the distance of the wind turbine and the receiver to the TV transmitter is large. In this equation, the free space loss, L_r (in dB), can be calculated from:

$$L_r = 20 \log(4\,\pi) + 20 \log(r) - 20 \log(\lambda) \qquad (12.17)$$

If one defines the antenna discrimination factor, G, as:

$$\Delta G = G_r - G'_r \qquad (12.18)$$

then, the C/I ratio (in dB) becomes:

$$C/I = 10 \log(4\pi) + 20 \log(r) - 10 \log(\sigma_b) + A_2 - A_1 + A_r + \Delta G \qquad (12.19)$$

From this equation, it follows that C/I can be improved by:

- decreasing σ_b (reducing the effect of the wind turbine);
- increasing ΔG (better directivity of the antenna);
- increasing the additional loss $A_2 + A_r$ on the interference path;
- decreasing the additional loss A_1 in the direct path.

The control of these parameters depends strongly on the location of the receiver to the wind system. In general, two alternative situations can be distinguished:

1. A significant delay time between the desired signal (C) and the undesired signal (I). The receiver is located in an area between the wind turbine and the transmitter. In this area the undesired signal is dominated by reflection and scatter from the wind turbine (back-scatter region).

2. No delay time between the desired signal (C) and the undesired signal (I). This phenomenon occurs in places where the receiver is behind the wind turbine, as seen from the transmitter. In this area the undesired signal can only be the result of scatter or refraction at the wind turbine (forward-scatter region).

In Equation (12.19), the distance r from the wind turbine to the receiver can be considered as a variable. When the factors A_1, A_2, and A_r are assumed constant, $\Delta G = 0$, and σ_b of the wind turbine is known, then $r = f(C/I)$ can be calculated.

When C/I is defined as that signal-to-interference ratio required for a specific radio service, a curve with radius r around a wind turbine can be drawn. This will define an area within which the required C/I will not be satisfied. Thus, using this method, criteria for the siting of a particular design of wind turbine with respect to its electromagnetic interference on TV reception can be produced, provided that:

- The C/I required for TV reception is known (experimentally determined examples of this ratio are presented in the original reference).
- The bistatic cross-section, σ_b, of the wind turbine is known (again, experimentally determined examples of this parameter for both the forward- and back-scattering regions are presented in the original reference).

12.5.4 Resources for Estimation and Mitigation Measures

As can be seen from the previous discussion, at present it is impossible to provide a wind system designer with complete technical guidance on the subject of EMI. Thus, problems have to be addressed on a site-by-site basis. In Europe, the International Energy Agency (IEA) Expert Group recommended an interim assessment procedure for identifying when electromagnetic interference may arise at a particular site. This procedure can be regarded as a means of warning when a problem may arise, but, at present, it does not make a recommendation for dealing with such situations.

For an initial step, one must establish what radio services are present in the volume occupied by the wind system – this means identifying the radio transmitters. Ideally, in each location there would be a central register of all transmitters that the wind system designer could access, but this is not usually the case. The IEA recommends that this should include approaches to radio regulatory agencies, visual observations at the site and on appropriate maps, and a site survey to monitor the radio transmissions that are actually present. Also, the survey should be long enough to include services that are only present on a part-time basis and should note the requirements of mobile users including emergency services, aircraft, shipping, and public utilities.

Once the radio services present have been identified and the transmitters have been marked on a map, the interference zones should be determined. This may be the most complex part of the process, as only the detailed analytical or experimental measurement techniques described by Sengupta and Senior (1994) are presently available. The next part of the procedure is to determine if any receivers for that service will be present in the interference zone. For television broadcasting, this essentially means establishing if there are any dwellings in the zones. If receivers exist, further advice should be sought. Note that the presence of such a receiver does not necessarily mean that an EMI problem will arise. It also depends on whether the radio service is robust to major changes in its signal level.

For the case of aviation radar systems, at present, the only means identified to completely eliminate the effects of wind turbines on radar, when they occur, are (US Department of Defense, 2006):

- move the wind turbines;
- lower the wind turbines' height;
- relocate the affected radar.

According to this reference, however, a variety of technical modifications are presently available that would result in a more comprehensive solution. They include:

- software upgrades to existing radar;
- processing filters related to signature identification;
- replacing aging radar.

Recent research in this area (see Watson, 2007) has demonstrated that the potential effects of turbines on radar systems can be modeled using a variety of techniques. In addition to the technical modifications mentioned above, this work has shown that there are a number of new techniques for minimizing the radar effects of wind turbines (e.g., shielding optimization, data fusion, stealth blades, and advanced processing systems).

12.6 Land-Use Environmental Impacts

12.6.1 Overview

There are a number of land-use issues to be considered when siting wind turbines. Some of them involve government regulations and permitting (such as zoning, building permits, and approval of aviation authorities). Others may not be subject to regulation, but do have an impact on public acceptance. The following are some of the major land-use issues:

- actual land required per energy output or capacity per unit of land area;
- amount of land potentially disturbed by a wind farm;
- non-exclusive land-use and compatibility;
- rural preservation;
- turbine density;
- access roads and erosion and/or dust emissions.

It is beyond the scope of this text to go into the extensive details of these factors. Gipe (1995) presents an overview of them (and other land-use considerations). The next sections present a summary of the most general land-use considerations for wind energy systems, and potential strategies that can be used to minimize the environmental problems associated with wind turbine land use.

12.6.2 Land-use Considerations

Compared to other power plants, wind generation systems are sometimes considered to be land intrusive rather than land intensive. The major intrusive effects, via visual impacts, were

addressed in Section 12.3. On the extent of land required per unit of power capacity, wind farms require more land than most energy technologies. On the other hand, while wind energy system facilities may extend over a large geographic area, the physical 'footprint' of the actual wind turbine and supporting equipment only covers a small portion of the land.

In the United States, for example, wind farm system facilities may occupy only 3–5% of the total acreage, leaving the rest available for other uses. In Europe, it has been found that the percentage of land use by actual facilities is less than the US wind farms in California. For example, UK wind farm developers have found that typically only 1% of the land covered by a wind farm is occupied by the turbines, substations, and access roads. Also, in many European projects, farm land is cultivated up to the base of the tower. When access is needed for heavy equipment, temporary roads are placed over tilled soil. Thus, European wind farms only occupy from 1–3% of the available land.

When one determines the actual amount of land used by wind farm systems, it is also important to note the influence of the wind turbine spacing and placement. Wind farms can occupy from 4 to 32 hectares (10 to 80 acres) per megawatt of installed capacity. The dense arrays of the California wind farms have occupied from about 6 to 7 hectares (15 to 18 acres) per megawatt of installed capacity. Typical European wind farms have the wind turbines spread out more and generally occupy 13 to 20 hectares (30 to 50 acres) per megawatt of installed capacity (Gipe, 1995).

Since wind generation is limited to areas where weather patterns provide consistent wind resources over a long period, the development of wind power in the US has occurred primarily in rural and relatively open areas. These lands are often used for agriculture, grazing, recreation, open space, scenic areas, wildlife habitat, and forest management. Wind development is generally compatible with the agricultural or grazing use of a site. In Europe, due to higher population densities, there are many competing demands for land, and wind farms have tended to be of a smaller total size.

The development of a wind farm may affect other uses on or adjacent to a site. For example, some parks and recreational uses that emphasize wilderness values and reserves dedicated to the protection of wildlife (e.g., birds) may not be compatible with wind farm development. Other uses, such as open space preservation, growth management, or non-wilderness recreational facilities may be compatible depending on set-back requirements, and the nature of on-site development.

In general, the variables that may determine land-use impacts include:

- site topography;
- size, number, output, and spacing of wind turbines;
- location and design of roads;
- location of supporting facilities (consolidated or dispersed);
- location of electrical lines (overhead or underground).

12.6.3 Mitigation of Land-use Problems

A wide range of actions is available to ensure that wind energy projects are consistent and compatible with most existing and planned land uses. Many of these involve the layout and design of the wind farm. For example, where wind energy development is located in or near recreational or scenic open space, some permitting agencies have established requirements

intended to 'soften' the industrial nature of the project. As summarized in the first version of the National Wind Coordinating Committee Permitting handbook (NWCC, 1998), these include the following (again, note that many are a result of visual impact considerations):

- selecting equipment with minimal structural supports, such as guy wires;
- requiring electrical lines to be placed underground;
- requiring maintenance facilities to be off-site;
- consolidating equipment on the turbine tower or foundation pad;
- consolidating structures within a wind farm area;
- requiring the use of more efficient or larger turbines to minimize the number of turbines required to achieve a specific level of electrical output;
- selecting turbine spacing and types to reduce the density of machines and avoid the appearance of 'wind walls';
- using roadless construction and maintenance techniques to reduce temporary and permanent land loss;
- restricting most vehicle travel to existing access roads;
- limiting the number of new access roads, width of new roads, and avoiding or minimizing cut and fill;
- limiting placement of turbines and transmission towers in areas with steep, open topography to minimize cut and fill.

From a land-use viewpoint, this complete list is really a goal for a 'perfect' wind site, and permitting agencies should consider the following points when determining which of these should be applied to a particular site:

- cost associated with a particular strategy;
- type and level of impact;
- land-use objectives of the community;
- significance of any potential land-use inconsistency or incompatibility;
- available alternatives.

Many of the previous requirements have been used in wind energy projects in Europe. Here, such projects are often located in rural or agricultural areas, and have tended to consist of single dispersed units or small clusters of wind turbines. In several European countries, wind turbines have been placed on dikes or levees along coastal beaches and jetties, or just offshore. Wind turbines sited in farming areas have also been located to minimize disturbances to planting patterns, and the permanent subsystems have been consolidated within a single right of way on field edges, in hedgerows, or along farm roads. Often, no access roads have been constructed and erection or periodic maintenance is carried out with moveable cushioned mats or grating.

In the United States, other land-use strategies associated with wind farm sites include the use of buffer zones and setbacks to separate the project from other potentially sensitive or incompatible land uses. The extent of this separation varies, depending on the area's land-use objectives and other concerns such as visual aspects, noise, and public safety. Also, on some wind farm projects, the resource managers for adjacent properties have established lease or permit conditions such that wind farm development on one site does not block the use of the wind resource on adjacent sites.

12.7 Other Environmental Considerations

This section will summarize some topics that should be considered when assessing the environmental impact of a wind energy system. These include safety, general impacts on flora and fauna, and shadow flicker.

12.7.1 Safety

12.7.1.1 The Problem

Safety considerations include both public safety and occupational safety. Here, the discussion will be centered on the public safety aspects (although some occupational safety issues will be included as well). A review of occupational safety in the wind industry is contained in the work of Gipe (1995).

In the public safety area, the primary considerations associated with wind energy systems are related to the movement of the rotor and the presence of industrial equipment in areas that are potentially accessible to the public. Also, depending on the site location, wind energy system facilities may also represent an increased fire hazard. The following aspects of public safety are important:

- **Blade throw.** One of the major safety risks from a wind turbine is that a blade or blade fragment may be thrown from a rotating machine. Wind turbines that have guy wires or other supports could also be damaged. Turbine nacelle covers and rotor nose cones can also blow off machines. In actuality, these events are rare and usually occur in extreme wind conditions, when other structures are also susceptible. The distance a blade, or turbine part, may be thrown depends on many variables (e.g., turbine size, height, size of broken part, wind conditions, topography, etc.). Examples of blade throw calculations are given by Larwood (2005) and Madsen *et al.* (2005).
- **Falling ice or thrown ice.** Safety problems can occur when low temperatures and precipitation cause a build-up of ice on turbine blades. As the blades warm, the ice melts and either falls to the ground, or can be thrown from the rotating blade. Falling ice from nacelles or towers can also be dangerous to people directly under the wind turbine. This problem was reviewed in an NWCC siting research meeting (NWCC, 2005) and a detailed technical review of the safety aspects of this problem is summarized by Bossanyi and Morgan (1996).
- **Tower failure.** The complete failure of wind turbine towers or guy wires usually brings the entire wind turbine to the ground if the rotor is turning, or if the problem is not detected immediately. High ice loads, poor tower or foundation design, corrosion, and high winds can increase this potential safety risk.
- **Attractive nuisance.** Despite their usual rural location, many wind energy system sites are visible from public highways, and are relatively accessible to the public. Because the technology and the equipment associated with a wind turbine site are new and unusual, it can be an attraction to curious individuals. Members of the public who attempt to climb towers or open access doors or electrical panels could be subject to injuries from moving equipment during operation, electrical equipment during operation, or numerous other hazardous situations.

- **Fire hazard.** In arid locations, site conditions that are preferable for development of wind sites such as high average wind speeds, low vegetation, few trees, etc., may also pose a high fire hazard potential during the dry months of the year. Particularly vulnerable sites are those located in rural areas where dry land grain farming occurs or the natural vegetation grows uncontrolled and is available for fuel. In these types of locations fires have started from sparks or flames as a result of numerous causes, including: substandard machine maintenance, poor welding practices, electrical shorts, equipment striking power lines, and lightning.
- **Worker hazard.** For any industrial activity, there is the potential for injury or the loss of life to individuals. At the present time there are no statistics that can be used to compare wind facility work with work at other energy-producing facilities. There have, however, been several fatalities associated with wind turbine installation and maintenance (see Gipe, 1995).
- **Electromagnetic fields.** Electrical and magnetic fields are caused by the flow of electric current through a conductor, such as a transmission line. The magnetic field is created in the space around the conductor, and its field intensity decreases rapidly with distance. In recent years, some members of the public have been concerned regarding the potential for health effects associated with electromagnetic fields.

12.7.1.2 Mitigation of Public Health Safety Risks

The following summarizes how the public health safety risks previously mentioned can be mitigated:

- **Blade throw.** The most appropriate method for reducing the blade throw potential is the application of sound engineering design combined with a high degree of quality control. Today, it is expected that blade throw should be rare. For example, braking systems, pitch controls, and other speed controls on wind turbines should prevent design limits from being exceeded. Because of safety concerns with blade throw and structural failure, many permitting agencies have separated wind turbines from residences, public travel routes, and other land uses by a safety buffer zone or setback. Examples of typical regulations for the United States are contained in the first edition of the permitting handbook of the National Wind Coordinating Committee (NWCC, 1998).
- **Falling ice or thrown ice.** To reduce the potential for injury to workers, discussion of blade throw and ice throw hazards should be included in worker training and safety programs. Also, project operators should not allow work crews near the wind turbines during very windy and icy conditions.
- **Tower failure.** Complete failure of the structure should be unlikely for turbines designed according to modern safety standards (see Section 7.4). Additional security may be obtained by locating the turbine a distance at least equal to the height of the tower plus the radius of the rotor away from inhabited structures.
- **Attractive nuisance.** Many jurisdictions require fencing and posting at wind project boundaries to prevent unauthorized access to the site. On the other hand, other jurisdictions prefer that the land remains unfenced, particularly if located away from well-traveled public roads, so that the area appears to remain open and retains a relatively natural character. Many jurisdictions require the developer to post signs with a 24-hour toll-free emergency

phone number at specified intervals around the perimeter if the area is fenced, and throughout the wind site if it is unfenced. Also, liability concerns dictate that access to towers and electrical equipment be locked, and that warning signs be placed on towers, electrical panels, and at the project entrance.

- **Fire hazard.** The single most effective fire hazard avoidance measure is to place all wiring underground between the wind turbines and the project substation. In fire-prone areas, most agencies establish permit conditions for the project which address the potential for fire hazard, and a fire control plan may be required. In addition, most agencies require fire prevention plans and training programs to further reduce the potential for fires to escape the project and spread into surrounding areas.
- **Worker hazard.** To minimize this hazard, the wind energy project should follow well-established worker protection requirements for the construction and operation of wind energy sites.
- **Electromagnetic fields.** Given the rural nature of most wind farm sites, and the relatively low power levels transmitted in a typical site, this safety problem may not represent a major public safety hazard. In the United States, a few states have sought to limit field exposure levels to the levels from existing transmission lines by specifying limits on field strengths, either within or at the edge of the rights-of-way for new lines.

12.7.2 Impact on Flora and Fauna

12.7.2.1 The Problem

Since wind turbine sites are typically located in rural areas that are either undeveloped or used for grazing or farming, they have the potential to directly and indirectly affect biological resources (the effects on birds were discussed in Section 12.2). For example, since the construction of wind farms often involves the building of access roads and the use of heavy equipment, it is most probable that there will be some disturbance to the flora and fauna during this phase of the project.

It should also be noted that the biological resources of concern include a broad variety of plants and animals that live, use, or pass through an area. They also include the habitat that supports the living resources, including physical features such as soil and water, and the biological components that sustain living communities. These range from bacteria and fungi through the predators on top of the food chain.

The effects on, or conflicts with, flora and fauna, if any, will depend on the plants and animals present, and the design and layout of the wind energy facility. In some cases, permitting agencies have discouraged or prevented development because of likely adverse consequences on these resources. In cases where sensitive resources are not present, or where adverse effects could be avoided or mitigated, development has been permitted to proceed.

12.7.2.2 Mitigation Measures

An important consideration regarding the flora and fauna that are found at a site is the potential loss of habitat. Many species are protected by state or national laws. It may therefore be useful to consult with ecological or biological specialists early in the planning stages of a project, in order to make sure that sensitive areas are not disturbed, and so that suitable mitigation

measures are taken. Any survey work should be carried out at the appropriate time of the year in order to take account of the seasonal nature of some of the potential biological effects.

The wind system developer needs to meet with the local zoning or planning authority, and relevant ecological/biological consultants, in order to discuss the timing of construction and the placement of wind turbines and access roads to avoid at-risk species or habitats. In addition, there may be requirements for on-going monitoring or an overall ecological management plan during the construction period and during the lifetime of the wind system.

12.7.3 Shadow Flicker and Flashing

12.7.3.1 The Problem

Shadow flicker occurs when the moving blades of the wind turbine rotor cast moving shadows that cause a flickering effect, which could annoy people living close to the turbine. In a similar manner, it is possible for sunlight to be reflected from gloss-surfaced turbine blades and cause a 'flashing' effect. This effect has not surfaced as a real environmental problem in the United States. It has been more of a problem in Northern Europe, because of the latitude and the low angle of the sun in the winter sky, and because of the close proximity between inhabited buildings and wind turbines. Shadow flicker (and shadow calculation for the topography) may be analytically modeled and there are several commercial packages available for this purpose (see National Academy of Sciences, 2007).

For example, Figure 12.11 shows the results of calculations to determine the annual duration of the shadow flicker effect for a location in Denmark (EWEA, 2004). In this figure there are two houses marked as A and B that are respectively 6 and 7 hub heights from the turbine in the
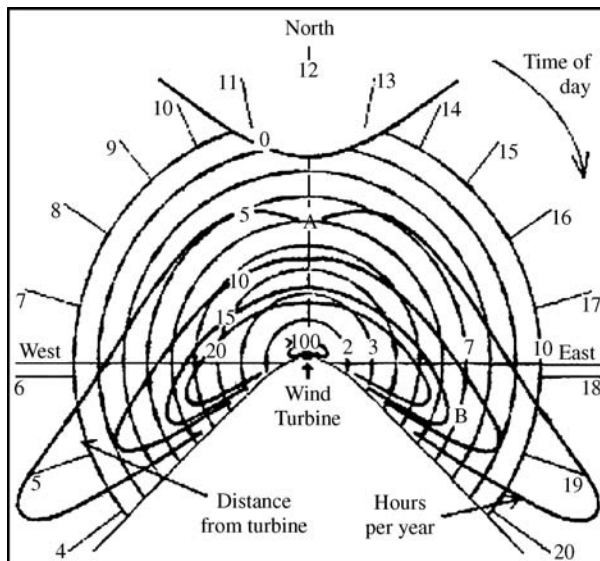
Figure 12.11   Diagram of shadow flicker calculation (EWEA, 2004); A, B are house locations

center of the diagram. This figure shows that house A will have a shadow from the turbine for five hours per year. House B will have a shadow for about 12 hours per year. Note that the results for this type of calculation vary for different geographical regions due to different allowances for cloud cover and latitude.

12.7.3.2 Mitigation Measures

In the worst cases, flickering will only occur for a short duration (on the order of 30 minutes a day for 10–14 weeks of the winter season). In Europe, one proposed solution is to not run the turbines during these short time periods, while another is to site machines carefully, taking account of the shadow path on nearby residences. Flashing can be prevented by the use of non-reflective, non-gloss blades, and also by careful siting.

A common guideline used in Denmark is to have a minimum distance of 6 to 8 rotor diameters between the wind turbine and the closest neighbor. Houses located at a distance of 6 rotor diameters (about 250 meters for a 600 kW machine) from a wind turbine in any of the sectors shown in Figure 12.11 will be affected for two periods each of five weeks' duration per year (EWEA, 2004).

References

Ackerman, T. and Soder, L. (2002) An overview of wind energy – status 2002. *Renewable and Sustainable Energy Reviews*, **6**, 67–128.

Anderson, R.L., Kendall, W., Mayer, L.S., Morrison, M.L., Sinclair, K., Strickland, D. and Ugoretz, S. (1997) Standard metrics and methods for conducting avian/wind energy interaction studies. *Proc. 1997 American Wind Energy Association Conference,* Austin, pp. 265–272.

Aubrey, C. (2000) Turbine colors…do they have to be grey? *Wind Directions*, March, 18–19.

AWEA/Audubon (2006) Understanding and resolving bird and bat impacts. *Workshop Proceedings,* January.

Bass, J. H. (1993) Environmental aspects – noise. In course notes for *Principles of Wind Energy Conversion*, L. L. Freris (Ed.), Imperial College, London.

Beranek, L.L. and Ver, I.L. (1992) *Noise and Vibration Control Engineering: Principles and Applications*, John Wiley & Sons, Ltd, Chichester.

Birdlife International (2003) *Wind farms and Birds: An Analysis of the Effects of Wind farms on Birds, and Guidance on Environmental Assessment Criteria and site Selection Issues.* Council of Europe Report T-PVS/Inf (2003) 12.

Bishop, I. D. and Miller, D.R. (2007) Visual assessment of off-shore wind turbines: The influence of distance, contrast, movement and social variables *Renewable Energy*, **32**(5), 814–835.

Bossanyi, E.A. and Morgan, C.A. (1996) Wind turbine icing – its implications for public safety *Proc. 1996 European Union Wind Energy Conference,* Göteborg, pp. 160–164.

BWEA (2005) *Low Frequency Noise and Wind Turbines Technical Annex*. British Wind Energy Association, London.

Chignell, R.J. (1986) Electromagnetic interference from wind energy conversion systems – preliminary information. *Proc. 1986 European Wind Energy Conference,* Rome, pp.583–586.

Clausager, I. and Nohr, H. (1996) Impact of wind turbines on birds. *Proc. 1996 European Union Wind Energy Conference,* Göteborg, pp. 156–159.

Colson, E. W. (1995) Avian interactions with wind energy facilities: a summary. *Proc. Windpower '95,* American Wind Energy Association, Washington, pp. 77–86.

Connors, S. R. (1996) Informing decision makers and identifying niche opportunities for windpower: use of multi-attribute trade off analysis to evaluate non-dispatchable resources. *Energy Policy*, **24**(2), 165–176.

Devine-Wright, P. (2005) Beyond NIMBYism: towards an integrated framework for understanding public perceptions of wind energy. *Wind Energy*, **8**, 125–139.

EWEA (2004) *Wind Energy, The Facts*, Vols. 1–5. European Wind Energy Association, Brussels.

Gipe, P. (1995) *Wind Energy Comes of Age*. John Wiley & Sons, Ltd, Chichester.

GL (1994) *Regulation for the Certification of Wind Energy Conversion Systems*, supplement to the 1993 edition, Germanischer Lloyd, Hamburg.

Global Wind Energy Council and Greenpeace International (2006) *Global Wind Energy Outlook 2006*.

Goodman, N. (1997) The Environmental impact of windpower development in Vermont: a policy analysis. *Proc. 1997 American Wind Energy Association Conference,* Austin, pp. 299–308.

Hubbard, H. H. and Shepherd, K. P. (1990) *Wind Turbine Acoustics.* NASA Technical Paper 3057 DOE/NASA/20320-77.

Hurtado, J.P. *et al.* (2004) Spanish method of visual impact evaluation in wind farms. *Renewable and Sustainable Energy Reviews*, **8**, 483–491.

IEC (2002) *Wind Turbines – Part 11: Acoustic noise measurement techniques, IEC 61400-11*, 3rd edition. International Electrotechnical Commission, Geneva.

Johansson, M. and Laike, T. (2007) Intention to respond to local wind turbines: the role of attitudes and visual perception. *Wind Energy*, **10**, 435–451.

Kidner, D. B. (1996) The visual impact of Taff Ely wind farm – a case study using GIS. *Wind Energy Conversion 1996*, British Wind Energy Association, London, pp. 205–211.

Köller, J, Köppel, J. and Peters, W. (2006) *Offshore Wind Energy Research on Environmental Impacts*. Springer, Berlin.

Larwood, S. (2005) *Permitting Setbacks for Wind Turbines in California and the Blade Throw Hazard.* California Wind Energy Collaborative Report: CWEC-2005-01, Sacramento.

Lenzen, M. and Munksgaard, J. (2002) Energy and CO_2 life-cycle analyses of wind turbines – review and applications. *Renewable Energy*, **26**, 339–362.

Madsen, K.H., Frederiksen, S.O., Gjellerup, C. and Skjoldan, P.F. (2005) Trajectories for detached wind turbine blades. *Wind Engineering*, **29**(2), 143–154.

Möller, B. (2006) Changing wind-power landscapes: regional assessment of visual impact on land use and population in Northern Jutland, Denmark. *Applied Energy*, **83**(5), 477–494.

National Academy of Sciences (2007) *Environmental Impacts of Wind-Energy Projects*. National Academic Press, Washington.

NWCC (1998) *Permitting of Wind Energy Facilities: A Handbook*. RESOLVE, National Wind Coordinating Committee, Washington. Available at: http://www.nationalwind.org/publications/siting/nwcch1.pdf.

NWCC (1999) *Studying Wind Energy/Bird Interactions: A Guidance Document*. RESOLVE, National Wind Coordinating Committee, Washington.

NWCC (2001) *Avian Collision with Wind Turbines: A Summary of Existing Studies and Comparison to Other Sources of Avian Collision Mortality in the United States*. RESOLVE, National Wind Coordinating Committee, Washington.

NWCC (2002) *Permitting of Wind Energy Facilities: A Handbook*. RESOLVE, National Wind Coordinating Committee, Washington.

NWCC (2005) *Proceedings: Technical Considerations in Siting Wind Developments*. RESOLVE, National Wind Coordinating Committee, Washington.

Operate A/S (2006) *Danish Offshore Wind: Key Environmental Issues*. Report for DONG Energy, Vattenfall, Danish Energy Authority, and Danish Forest and Nature Agency.

Orloff, S. and Flannery, A. (1992) *Wind Turbine Effects on Avian Activity, Habitat Use, and Mortality in Altamont Pass and Solano County Wind Resource Areas: 1989–1991*. Report No. P700-92-001, California Energy Commission, Sacramento.

Pasqualetti, M.J., Gipe, P. and Righter, R.W. (2002) *Wind Power in View: Energy Landscapes in a Crowded World*. Academic Press, San Diego.

Ratto, C.F. and Solari, G. (1998) *Wind Energy and Landscape*. A.A. Balkema, Rotterdam.

REPP (2003) *Wind Energy for Electric Power: A REPP Issue Brief*. Renewable Energy Policy Project Report, Washington.

Robotham, A.J. (1992) Progress in the Development of a Video Based Wind Farm Simulation Technique. *Proc. Wind Energy Conversion 1992,* British Wind Energy Association, London, pp. 351–353.

Rodriques, L. *et al.* (2006) Wind turbines and bats: guidelines for the planning process and impact assessment. EUROBATS Report: Doc.EUROBATS.MoPoP5.12.Rev.3.Annex1, September.

Schleisner, L. (2000) Life cycle assessment of a wind farm and related externalities. *Renewable Energy*, **20**, 279–288.

Schmidt, E. *et al.* (2003) *National Wind Technology Center Site Environmental Assessment: Bird and Bat Use and Fatalities – Final Report*. National Renewable Energy Laboratory Report: NRER/SR-500-32981, NTIS.

Schwartz, S. S. (Ed.) (2005) Technical considerations in siting wind developments. *Proceedings of NWCC Siting Technical Meeting*. RESOLVE, National Wind Coordinating Committee, Washington.

Sengupta, D.L. and Senior, T.B.A. (1994) Electromagnetic interference from wind turbines, Chapter 9 in *Wind Turbine Technology*, Spera, D. A. (Ed.) ASME, New York.

Sengupta, D. L., Senior, T. B. A. and Ferris, J. E. (1983) *Study of Television Interference by Small Wind Turbines: Final Report*. SERI/STR-215-1881, Solar Energy Research Institute, NTIS.

Senior, T. B. A. and Sengupta, D. L. (1983) *Large Wind Turbine Handbook: Television Interference Assessment*. SERI/STR-215-1879, Solar Energy Research Institute, NTIS.

Sinclair, K.C. (1999) Status of the U.S. Department of Energy/National Renewable Energy Laboratory avian research program. *Proc. 1999 American Wind Energy Association Conference*.

Sinclair, K.C. and Morrison, M.L. (1997) Overview of the U.S. Department of Energy/National Renewable Energy Laboratory avian research program. *Proc. 1997 American Wind Energy Association Conference*, pp. 273–279.

Sovacool, B.J. (2009) Contextualizing avian mortality: A preliminary appraisal of bird and bat fatalities from wind, fossil-fuel, and nuclear electricity. *Energy Policy*, **37**(6), 2241–2248.

Stanton, C. (1994) The visual impact and design of wind farms in the landscape *Proc. Wind Energy Conversion 1994,* British Wind Energy Association, London, pp. 249–255.

Stanton, C. (1996) *The Landscape Impact and Visual Design of Windfarms*. Landscape Publication No. LP/9603, School of Landscape Architecture, Heriot-Watt University, Edinburgh.

Still, D., Painter, S., Lawrence, E.S., Little, B. and Thomas, M. (1996) Birds, wind farms, and Blyth Harbor. *Proc. Wind Energy Conversion 1996,* British Wind Energy Association, London, pp. 175–183.

Taylor, D.C. and Durie, M.J. (1995) Wind farm visualisation. *Proc. Wind Energy Conversion 1995*, British Wind Energy Association, London, pp. 413–416.

US Department of Defense (2006) *Report to the Congressional Defense Committees: The Effect of Windmill Farms on Military Readiness.* Available at: http://www.defenselink.mil/pubs/pdfs/WindFarmReport.pdf.

Van Kats, P. J. and Van Rees, J. (1989) Large wind turbines: a source of interference for TV broadcast reception, Chapter 11 in *Wind Energy and the Environment*, D. T. Swift-Hook (Ed.), Peter Peregrinus, London.

Wagner, S., Bareib, R. and Guidati, G. (1996) *Wind Turbine Noise.* Springer, Berlin.

Watson, M. (2007) The effects of wind turbines on radar systems and technical mitigation developments. *Proc. 2007 European Wind Energy Conference,* Milan.

Wolf, B. (1995) Mitigating avian impacts: applying the wetlands experience to wind farms. *Proc. 1995 American Wind Energy Association Conference*, pp. 109–116.

Appendix A

Nomenclature

A.1 Note on Nomenclature and Units

This text includes material from many different engineering disciplines (e.g. aerodynamics, dynamics, controls, electromagnetism, acoustics). Within each of these disciplines commonly accepted variables are often used for important concepts. Thus, for acoustics engineers, α denotes the sound absorption coefficient, in aerodynamics it denotes the angle of attack, and in one common model for wind shear it is the power law exponent. In this text, an effort has been made to ensure that concepts that are found in multiple chapters all have the same designation, while maintaining common designations for generally accepted concepts. Finally, in an effort to avoid confusion over multiple definitions of one symbol, the nomenclature used in the text is listed by chapter.

Throughout this text units are, in general, not stated explicitly. It is assumed, however, that a consistent set of units is used. In SI units, then, for example, length is in m, speed is in m/s, mass is in kg, density is in kg/m^3, weight and force are in N, stress and pressure are in N/m^2 (Pa), torque is in Nm, power is in W. When other forms are in common usage, such as power in kW or kPa, those units are stated. Energy is also expressed in Wh or kWh, rather than in J or kJ, and angles are assumed to be in radians, except where explicitly stated otherwise. There are two possible sources of confusion: rotational speed and frequency. In this text, when referring to rotational speed, n is always in revolutions per minute (rpm) and Ω is in radians/second. With regards to frequency, f is always in cycles per second (Hz) while ω is always in radians/second. Finally, in other cases where the units are specific to a variable, they are indicated below.

A.2 Chapter 2

A.2.1 English Variables

A	Area
c	Weibull scale factor

c_P	Specific heat at constant pressure
C_f	Capacity factor
C_P	Power coefficient
CC	Capture coefficient
D	Rotor diameter
E_w	Wind machine energy (Wh)
f	(i) Coriolis parameter
f	(ii) Frequency (Hz)
f_i	Number of occurrences in each bin
$F()$	Cumulative distribution function
F_c	Coriolis force
F_p	Pressure force
g	Gravitational acceleration
h	Enthalpy
i	Index or sample number
k	(i) Weibull shape factor
k	(ii) von Karman constant
K_e	Energy pattern factor
ℓ	Mixing length
L	Integral length scale
m	Mass
m_i	Midpoint of bins
n	Direction normal to lines of constant pressure
N	Number of long-term data points
N_B	Number of bins
N_s	Number of samples in short-term averaging time
p	Pressure
$p()$	Probability density function
P	Power
P_R	Rated wind turbine power
$P_w(U)$	Wind turbine power as a function of wind speed
$\bar{P}/A$	Average wind power density
$\bar{P}_w$	Average wind turbine power
q	Heat transfer
r	Lag
R	(i) Gas constant
R	(ii) Radius of curvature
R	(iii) Radius of wind turbine rotor
$R(r\,\delta t)$	Autocorrelation function
$S(f)$	Power spectral density function
t	Time
T	Temperature
TI	Turbulence intensity
u	Internal energy
$\tilde{u}$	Fluctuating wind velocity about short-term mean
u_i	Sampled wind speed
$u(z,t)$	Instantaneous longitudinal wind speed

U	Mean wind speed (mean of short-term data)
U_c	Characteristic wind velocity
U_e	Extreme wind speed
U_g	Geostrophic wind speed
U_{gr}	Gradient wind speed
U_i	Wind speed average over period i
U^*	Friction velocity
$\overline{U}$	Long-term mean wind speed (mean of short-term averages)
v	Specific volume
$v(z,t)$	Instantaneous lateral wind speed
w_i	Width of bins
$w(z,t)$	Instantaneous vertical wind speed
x	Dimensionless wind speed
z	Elevation
z_i	Inversion height
z_o	Surface roughness
z_r	Reference height

A.2.2 Greek Variables

α	Power law exponent
Γ	Lapse rate
$\Gamma(x)$	Gamma function
δt	Sampling period
Δt	Duration of short-term averaging time
η	Drive train efficiency
λ	Tip speed ratio
ρ	Air density
σ_e	Standard deviation of data set
σ_u	Standard deviation of short-term data (turbulence)
σ_U	Standard deviation of long-term data
τ	Shear stress
τ_0	Surface value of shear stress
τ_{xz}	Shear stress in the direction of x whose normal coincides with z
φ	Latitude
ω	Angular speed of earth
Ω	Angular velocity of rotor

A.3 Chapter 3

A.3.1 English Variables

a	Axial interference or induction factor
a'	Angular induction factor
A	Projected airfoil area (chord $\times$ span), surface area, rotor swept area
B	Number of blades
c	Airfoil chord length

C_d	Two-dimensional drag coefficient
$C_{d,0}$	Constant drag term
$C_{d,\alpha 1}$	Linear drag term
$C_{d,\alpha 2}$	Quadratic drag term
C_D	Three-dimensional drag coefficient
C_l	Two-dimensional lift coefficient
$C_{l,0}$	Lift coefficient at zero angle of attack
$C_{l,\alpha}$	Slope of lift coefficient curve
C_L	Three-dimensional lift coefficient
C_m	Pitching moment coefficient
C_p	Pressure coefficient
C_P	Power coefficient
C_T	Thrust coefficient or local thrust coefficient
d_1	Variable for determining angle of attack with simplified method
d_2	Variable for determining angle of attack with simplified method
dr	Thickness
F	Tip loss correction factor
F_D	Drag force
$\tilde{F}_D$	Force per unit height
F_L	Lift force
F_N	Normal force, force normal to plane of rotation (thrust)
F_T	(i) Force tangential to circle swept by blade section
$\tilde{F}_T$	(ii) Force tangential per unit height
H	Height
k	Index of blade element closest to hub
l	Length or span of airfoil
L	Characteristic length, lift force
m	Mass
$\tilde{m}$	Mass flow rate per unit height
M	Pitching moment
N	Number of blade elements
p	Pressure
P	Power
q_1	Variable for determining angle of attack with simplified method
q_2	Variable for determining angle of attack with simplified method
q_3	Variable for determining angle of attack with simplified method
Q	Torque
r	Radius
r_h	Rotor radius at the hub
r_i	Radius at the midpoint of a blade section
R	Outer blade radius
Re	Reynolds number
T	Thrust
u	Velocity in direction of air flow
U	Characteristic velocity, mean air flow velocity
U_∞	Free stream air flow velocity

v	Velocity perpendicular to direction of air flow
y	$\lambda/(1-a)$
z	Vector describing offset circle

A.3.2 Greek Variables

α	Angle of attack
Γ	Circulation
ε	Surface roughness height
ζ	Vorticity
η_{mech}	Mechanical efficiency
η_{out}	Overall output efficiency
$\eta_{overall}$	Overall efficiency
θ_p	Section pitch angle
$\theta_{p,0}$	Blade pitch angle at the tip
θ_T	Blade twist angle
λ	Tip speed ratio
λ_h	Local speed ratio at the hub
λ_r	Local speed ratio
μ	Coefficient of viscosity
v	Kinematic viscosity
ξ	Locus of transformed points
ρ	Air density
σ	Rotor solidity
σ'	Local rotor solidity
φ	Angle of relative wind
ϕ	Angle between wind and quarter chord of a vertical axis airfoil
ω	Angular velocity of the wind
Ω	Angular velocity of the wind turbine rotor

A.4 Chapter 4

A.4.1 English Variables

a	(i) Acceleration
a	(ii) Axial induction factor
a	(iii) Offset of center of mass of gyroscope
A	(i) Area
A	(ii) Constant in Euler beam equation
A	(iii) Axisymmetric flow term $= (\Lambda/3) - (\theta_p/4)$
A_3	Axisymmetric flow term $= (\Lambda/2) - (2\theta_P/3)$
B	(i) Number of blades
B	(ii) Gravity term $= G/2\,\Omega^2$
c	(i) Maximum distance from neutral axis
c	(ii) Chord
c	(iii) Damping coefficient

c	(iv) Amplitude of sinusoid
c_c	Critical damping coefficient
C	Constant
$C_{l\alpha}$	Slope of angle of attack line
C_l	Lift coefficient
C_P	Power coefficient
C_Q	Torque coefficient
C_T	Thrust coefficient
$\bar{d}$	Normalized yaw moment arm $= d_{yaw}/R$
d_{yaw}	Yaw moment arm
D	(i) Determinant
D	(ii) Damage
e	Non-dimensional hinge offset
E	(i) Modulus of elasticity
E	(ii) Energy
F	External force
F_c	Centrifugal force
F_g	Gravitational force
$\tilde{F}_N$	Normal force per unit length
$\tilde{F}_T$	Tangential force per unit length
g	Gravitational constant
G	Gravity term $= g\,M_B\,r_g/I_b$
h	Height
$\boldsymbol{H}$	Angular momentum
H_{op}	Operating hours/yr
I	Area moment of inertia
I_b	Area or mass moment of inertia of a single blade
J	Polar mass moment of inertia
k	(i) Spring constant
k	(ii) Number of cyclic events per revolution
k_θ	Rotational stiffness
K	(i) Rotational spring constant
K	(ii) Flapping inertial natural frequency, $K = 1 + \varepsilon + K_\beta/I_b\Omega^2$
K_β	Spring constant in flapping direction
K_{vs}	Vertical wind shear constant
L	Length
$\tilde{L}$	Lift force per unit length
m	Mass
m_B	Mass of blade
m_i	Mass of ith section of beam
M	Moment
$\boldsymbol{M}$	Moment, vector
M_c	Flapping moment due to centrifugal force
M_f	Flapping moment due to flapping acceleration inertial force
M_g	Flapping moment due to gravity
M_i	Moment applied to ith lumped mass

M_{max}	Maximum moment
M_s	Flapping moment due to spring
$M_{X'}$	Yawing moments on tower
$M_{Y'}$	Backwards pitching moments on tower
M_{yaw}	Flapping yaw moment
$M_{Z'}$	Rolling moment on nacelle
M_β	Flapping moment
n	(i) Gear train speed-up ratio
n	(ii) Number of cycles
n_{rotor}	Rotational speed of rotor (rpm)
N	(i) Number of teeth on a gear
N	(ii) Cycles to failure
P	Power
q	Yaw rate (rad/s)
$\bar{q}$	Normalized yaw rate $= q/\Omega$
Q	Torque
r	Radial distance from axis of rotation
r_g	Radial distance to center of mass
R	(i) Radius of rotor
R	(ii) Stress ratio
S	Shear force
S_β	Flapwise shear force
S_ζ	Edgewise shear force
t	Time
T	Thrust
U	Free stream wind velocity
U_h	Wind velocity at height h
U_P	Perpendicular component of wind velocity
U_R	Relative wind velocity
U_T	Tangential component of wind velocity
$\bar{U}$	Normalized wind velocity $= U/\Omega R = 1/\lambda$
V_0	Cross-wind velocity
$\bar{V}$	Non-dimensional total cross flow, $\bar{V} = (V_0 + q\, d_{yaw})/(\Omega R)$
$\bar{V}_0$	Non-dimensional cross flow, $\bar{U}_0 = U_0/\Omega R$
w	Loading per unit length
W	Total load or weight
x	Distance (linear)
y_i	Deflection of beam
Y	Years of operation
Z	Non-dimensional difference between squares of rotating and non-rotating blade natural frequency

A.4.2 Greek Variables

α	(i) Angular acceleration of rotor $= \dot{\Omega}$
α	(ii) Angle of attack (radians)

α	(iii) Power law exponent
β	(i) Term used in vibrating beam solution
β	(ii) Flapping angle (radians)
$\dot{\beta}$	Flapping velocity (radians/s)
$\ddot{\beta}$	Second time derivative of flapping angle (radians/s^2)
β_0	Collective flapping coefficient (radians)
β_{1c}	Cosine flapping coefficient (radians)
β_{1s}	Sine flapping coefficient (radians)
β'	Azimuthal derivative of flap angle $= \ddot{\beta}/\Omega^2$ (radians^{-1})
β''	Azimuthal second derivative of flap angle $= \dot{\beta}/\Omega$
γ	Lock number $= \rho\, c\, C_{L\alpha} R^4 / I_b$
$\Delta U_{P,crs}$	Perpendicular velocity perturbation due to yaw error
$\Delta U_{P,vs}$	Perpendicular velocity perturbation due to wind shear
$\Delta U_{P,yaw}$	Perpendicular velocity perturbation due to yaw rate
$\Delta U_{T,crs}$	Tangential velocity perturbation due to yaw error
$\Delta U_{T,vs}$	Tangential velocity perturbation due to wind shear
$\Delta U_{T,yaw}$	Tangential velocity perturbation due to yaw rate
ε	Offset term $= 3e/[2(1-e)]$
η	Ratio, r/R
θ	Arbitrary angle (radians)
θ_p	Pitch angle (positive towards feathering) (radians)
Θ	Steady state yaw error (radians)
λ	Tip speed ratio
λ_i	Length between sections of beam
Λ	Non-dimensional inflow $= U(1-a)/\Omega R$
ξ	(i) Damping ratio
ξ	(ii) Aerodynamic damping ratio $= \gamma\Omega/16\omega_\beta$
ρ	Density of air
$\tilde{\rho}$	Density per unit length
σ	Stress
σ_a	Stress amplitude
σ_e	Stress endurance limit
σ_m	Mean stress
$\sigma_{\max}$	Maximum stress
$\sigma_{\min}$	Minimum stress
σ_u	Ultimate stress
$\sigma_{\beta,\max}$	Maximum flapwise stress
ϕ	(i) Angle of relative wind (aerodynamics)
ϕ	(ii) Phase angle (vibrations)
ψ	Azimuth angle, $0 =$ down
ω	(i) Frequency of oscillation
ω	(ii) Rate of precession of gyroscope
$\boldsymbol{\omega}$	Rate of precession (vector)
ω_d	Natural frequency for damped oscillation
ω_i	Frequency of oscillation of ith mode
ω_n	Natural frequency (radians/s)

ω_{NR}	Natural flapping frequency of non-rotating blade
ω_R	Natural flapping frequency of rotating blade
ω_β	Flapping frequency
Ω	Angular velocity ($=\dot{\psi}$)
$\boldsymbol{\Omega}$	Angular velocity vector

A.4.3 Subscripts

ahg	Axial flow, hinge spring, and gravity (blade weight)
cr	Cross wind
max	Maximum
min	Minimum
vs	Vertical wind shear
yr	Yaw rate
1, 2	Different heights or ends of a gear train

A.5 Chapter 5

A.5.1 English Variables

a	(i) Real component in complex number notation
a	(ii) Turns ratio of the transformer
a_n	Coefficient of cosine terms in Fourier series
A	Area
A_c	Cross-sectional area of coil
A_g	Cross-sectional area of gap
A_m	Magnitude of arbitrary phasor
$\hat{A}$	Arbitrary phasor
b	Imaginary component in complex number notation
b_n	Coefficient of sine terms in Fourier series
B	Magnitude of magnetic flux density (scalar)
B	Magnetic flux density (vector)
C	(i) Capacitance (F)
C	(ii) Constant
C_m	Magnitude of arbitrary phasor
$\hat{C}$	Arbitrary phasor
e_m	Stored magnetic field energy per unit volume
E	(i) Energy (J)
E	(ii) Induced electromotive force EMF (V)
E	(iii) Synchronous generator field-induced voltage
E_m	Stored energy in magnetic fields
E_1	Primary voltage in transformer
E_2	Secondary voltage in transformer
$\hat{E}$	EMF phasor
f	Frequency of AC electrical supply (Hz)
F	Force (vector)

g	Air gap width
$\boldsymbol{H}$	Magnetic field intensity (vector) (A-t/m)
H_c	Field intensity inside the core (A-t/m)
i	Instantaneous current
I	Mean current
I_a	Synchronous machine's armature current
I_f	Field current (a.k.a. excitation)
I_L	Line current in three-phase system
I_M	Magnetizing current
$I_{\max}$	Maximum value of current (AC)
I_P	Phase current in three-phase system
I_R	Rotor current
I_{rms}	Root mean square (rms) current
I_S	Induction machine stator phasor current
$\hat{\boldsymbol{I}}$	Current, phasor
j	$\sqrt{-1}$
J	Inertia of generator rotor
k_1	Constant of proportionality in synchronous machine (Wb/A)
k_2	Constant of proportionality (V/Wb-rpm)
ℓ	Path length (vector)
ℓ_c	Length of the core at its midpoint
L	(i) Inductance (H)
L	(ii) Length of coil
L	(iii) Half the period of the fundamental frequency
L	(iv) Length of face of pole pieces
n	(i) Actual rotational speed (rpm)
n	(ii) Harmonic number
n_s	Synchronous speed (rpm)
N	Number of turns in a coil
N_1	Number of coils on primary winding
N_2	Number of coils on secondary winding
NI	Magnetomotive force (MMF) (A-t)
$N\Phi$	Flux linkages (Wb)
P	(i) Real power
P	(ii) Number of poles
P_g	Air gap power in induction machine
P_{in}	Mechanical input power input to induction generator
P_{loss}	Power lost in induction machine's stator
$P_{mechloss}$	Mechanical losses
P_{out}	Electrical power delivered from induction generator
P_1	Power in one phase of a three-phase system
PF	Power factor
Q	(i) Reactive power (VA)
Q	(ii) Torque
Q_e	Electrical torque
Q_m	Mechanical torque

Q_r	Applied torque to generator rotor
r	(i) Radial distance from center of toroid
r	(ii) Radius
r_i	Inner radius of coil
r_o	Outer radius of coil
R	(i) Equivalent induction machine resistance
R	(ii) Reluctance of magnetic circuit (A-t/Wb)
R	(iii) Resistance
R_M	Resistance in parallel with mutual inductance
R'_R	Rotor resistance (referred to stator)
R_S	(i) Synchronous generator resistance
R_S	(ii) Stator resistance
R_X	External resistance
Re{}	Real part of complex number
s	Slip
S	Apparent power (VA)
t	Time
v	Instantaneous voltage
V	(i) Voltage in general
V	(ii) Electrical machine terminal voltage
V_{LL}	Line-to-line voltage in three-phase system
V_{LN}	Line-to-neutral voltage in three-phase system
V_{max}	Maximum voltage
V_{rms}	Root mean square (rms) voltage
V_1	(i) AC voltage filter input voltage
V_1	(ii) Terminal voltage in primary winding
V_2	(i) AC voltage filter output voltage
V_2	(ii) Terminal voltage in secondary winding
$\hat{V}$	Voltage, phasor
X	Equivalent induction machine reactance
X_C	Capacitive reactance
X_L	Inductive reactance
X'_{LR}	Rotor leakage inductive reactance (referred to stator)
X_{LS}	Stator leakage inductive reactance
X_M	Magnetizing reactance
X_S	Synchronous generator synchronous reactance
Y	'Wye' connected three-phase system
Y''	Admittance in resonant filter
$\mathbf{Z}_1$	Series impedance in resonant filter
$\mathbf{Z}_2$	Parallel impedance in resonant filter
$\hat{\mathbf{Z}}$	(i) Impedance in general
$\hat{\mathbf{Z}}$	(ii) Induction machine equivalent impedance
$\hat{\mathbf{Z}}_C$	Capacitive impedance
$\hat{\mathbf{Z}}_i$	Impedance with index i
$\hat{\mathbf{Z}}_L$	Inductive reactance
$\hat{\mathbf{Z}}_P$	Parallel impedance

$\hat{\boldsymbol{Z}}_R$	Resistive impedance
$\hat{\boldsymbol{Z}}_s$	(i) Series impedance
$\hat{\boldsymbol{Z}}_s$	(ii) Synchronous impedance
$\hat{\boldsymbol{Z}}_Y$	Impedance of Y-connected circuit
$\hat{\boldsymbol{Z}}_\Delta$	Impedance of Δ-connected circuit

A.5.2 Greek Variables

δ	Synchronous machine power angle
Δ	Delta-connected three-phase system
η_{gen}	Overall efficiency (in the generator mode)
θ	(i) Power factor angle
θ	(ii) Rotation angle
λ	Flux linkage $= N\Phi$
μ	Permeability, $\mu = \mu_r \mu_0$ (Wb/A-m)
μ_0	Permeability of free space, $4\pi \times 10-7$ (Wb/A-m)
μ_r	Relative permeability
ϕ	(i) Phase angle
ϕ	(ii) Power factor angle
ϕ_a	Phase angle of arbitrary phasor **A**
ϕ_b	Phase angle of arbitrary phasor **B**
Φ	Magnetic flux (Wb)
ω_r	Speed of generator rotor

A.5.3 Symbols

$\angle$	Angle between phasor and real axis
μF	MicroFarad (10^{-6} Farad)
Ω	Ohms

A.6 Chapter 6

A.6.1 English Variables

b	Width of gear tooth face
B	Constant in composites *S–N* model
c	Exponent in Goodman's Rule
d	Pitch diameter
D	(i) Dynamic magnification factor
D	(ii) Damage
D_{Ring}	Diameter of ring gear
D_{Sun}	Diameter of sun gear
D_y	Damage over a year
E	Modulus of elasticity
f_e	Excitation frequency

f_n	Natural frequency
F_b	Bending load applied to gear tooth
F_t	Tangential force on gear tooth
F_U	Fraction of time wind is in certain range
h	Height of gear tooth
H_{op}	Operating hours per year
I	Moment of inertia
k	Number of cyclic events per revolution
k_g	Effective spring constant of two meshing gear teeth
L	(i) Distance to the weakest point on gear tooth
L	(ii) Height of tower
m_{Tower}	Mass of tower
$m_{Turbine}$	Mass of turbine
n	(i) Rotational speed (rpm)
n	(ii) Number of cycles applied
n_{HSS}	Rotational speed of high-speed shaft (rpm)
n_{LSS}	Rotational speed of low-speed shaft (rpm)
n_{rotor}	Rotor rotational speed (rpm)
N	(i) Number of gear teeth
N	(ii) Number of cycles
p	Circular pitch of gear
P	Power
P_{rotor}	Rotor power
Q	Torque
R	Reversing stress ratio
U	Wind speed
V_{pitch}	Gear pitch circle velocity
y	Form factor (or Lewis factor)
Y	Years of operation

A.6.2 Greek Variables

δ	Logarithmic damping decrement
δ_3	Delta-3 angle
ξ	Damping ratio
σ	Cyclic stress amplitude
σ_a	Stress amplitude
σ_{al}	Allowable stress amplitude
σ_b	Allowed bending stress in gear tooth
σ_e	Zero mean alternating stress for desired life
σ_{el}	Endurance limit
σ_m	Mean stress
$\sigma_{\max}$	Maximum stress
$\sigma_{\min}$	Minimum stress
σ_u	Ultimate strength

A.7 Chapter 7

A.7.1 English Variables

A_c	Cross-sectional area
c	Chord length
C_P	Rotor power coefficient
E	Modulus of elasticity
f_d	Design values for materials
f_k	Characteristic values of the materials
F_c	Centrifugal force
F_d	Design values for loads
F_k	Expected values of the loads
g	(i) Gravitational constant
g	(ii) Gearbox ratio
I	Moment of inertia
I_{15}	Turbulence intensity at 15 m/s
M	Moment
M_A	Aerodynamic moment
Mg	Moment due to gravity
n	Rotational speed (rpm)
n_{rated}	Rotational speed of generator at rated power (rpm)
n_{rotor}	Rotor rotational speed (rpm)
n_{sync}	Synchronous rotational speed of generator (rpm)
P	Power
$P_{generator}$	Generator power
P_{rated}	Rated generator power
P_{rotor}	Rotor power
Q	Torque
r_{cg}	Distance to center of gravity
R	(i) Radius
R	(ii) Reversing stress ratio
$R(f_d)$	Resistance function, normally design stress
$S(F_d)$	Expected 'load function' for ultimate loading, normally expected stress
t	Thickness
T	Thrust
U	Wind speed
U_{e1}	1 year extreme wind speed
U_{e50}	50 year extreme wind speed
U_{gust50}	50 year return period gust
U_{hub}	Hub height wind speed
U_{ref}	Reference wind speed
W	Blade weight
z	Height above ground

A.7.2 Greek Variables

β_i	Constants in vibrating beam

γ	Safety factor
γ_f	Partial safety factor for loads
γ_m	Partial safety factor for materials
γ_n	Consequence of failure safety factor
η	Overall efficiency of drive train
ρ	Density of air
ρ_b	Mass density of blade
$\tilde{\rho}$	Mass density per unit length
σ	Stress due to aerodynamic loading
σ_b	Maximum blade root bending stress
σ_c	Tensile stress due to centrifugal force
σ_c	Stress due to gravity
σ_x	Standard deviation of the turbulence in the direction of the mean wind
ω	Frequency
ω_n	Natural frequency
Ω	Rotor rotational speed

A.8 Chapter 8

A.8.1 English Variables

A	Rotor swept area
B	Viscous friction coefficient
C	Capacitance
C_P	Rotor power coefficient
$C_{P,\max}$	Maximum rotor power coefficient
$e(t)$	Error
$g(t)$	Controller output
i	Index
J	Total rotating inertia
J_r	Rotor inertia
k	Slope of the torque voltage curve of a motor
K	Spring constant
K_D	Differential controller constant
K_I	Integral controller constant
K_p	Proportional controller constant
m	Slope of the torque speed curve for a motor/pitch mechanism
n	Gearbox gear ratio
p	Number of generator poles
P_{el}	Electrical power
P_r	Rotor power
Q_p	Pitching moment
$Q_p(s)$	Laplace transform of pitching moment
R	(i) Rotor radius
R	(ii) Resistance, Ohms
s	Complex frequency in Laplace transforms
s_i	Sample at time i

t	Time
U	Mean wind speed
$v(t)$	Voltage applied to pitch motor terminals

A.8.2 Greek Variables

η	Drive train efficiency
θ_p	Blade position
$\Theta_p(s)$	Laplace transform of blade position
λ	Tip speed ratio
λ_{opt}	Optimum tip speed ratio
ρ	Air density
ω	Frequency
ω_n	Nyquist frequency
Ω	Rotor speed
Ω_{el}	Generator speed

A.8.3 Subscripts

cut-in	(Wind speed) at turbine low-wind cut-in
cut-out	(Wind speed) at turbine high-wind cut-out
el	Electrical
i	Index
max	Maximum
opt	Optimum
p	Pitch
r	Rotor
rated	Rated (wind speed)
ref	Desired or commanded control input
0	Initial, at time $t = 0$
1	Reference to specific circuit element
2	Reference to specific circuit element

A.9 Chapter 9

A.9.1 English Variables

a	(i) Non-dimensional velocity deficit (axial induction factor)
a	(ii) Slope of linear fit
a	(iii) Coherence decay constant
a_n	Coefficient of cosine term in Fourier series
b	Offset of linear fit
b_n	Coefficient of sine term in Fourier series
c_n	Magnitude of harmonic voltage of order n
C_T	Turbine thrust coefficient
D	Turbine diameter

D_X	Wake diameter at a distance X downstream of the rotor
f	Frequency, Hz
HD_n	Harmonic distortion caused by the nth harmonic
I_F	Fault current
J	Rotating inertia
k	Wake decay constant
L	(i) Half the period of the fundamental frequency
L	(ii) The integral length scale of the turbulence in meters
M	Fault level
n	Harmonic number
N	Number of wind turbines
P	Real power
$P()$	Probability
$\hat{P}()$	Estimated probability
P_L	Power from electrical loads
P_{LO}	Electrical losses in collector system
P_O	Power from other generators
P_{PM}	Prime mover power
Q	Reactive power
Q_L	Torques from electrical loads
Q_O	Torques from other generators
Q_{PM}	Prime mover torque
R	Resistance
$S_1(f)$	The single point power spectrum
$S_N(f)$	Spectra of the total variance in the wind at N turbine locations
t	Time
T	Time period
u_c	Wind speed at candidate site
u_r	Wind speed at reference site
$\hat{u}_c$	Estimated wind speed at candidate site
U	The mean wind speed
U_0	Free stream velocity
U_X	Velocity in the wake at a distance X downstream of the rotor
$U_{X,1}$	Velocity in the wake at a distance X downstream of the rotor 1
$U_{X,2}$	Velocity in the wake at a distance X downstream of the rotor 2
v	Instantaneous voltage
v_F	Sinusoidal voltage at the fundamental frequency
v_H	Harmonic voltage
v_N	Harmonic voltage of order I, $(n>1)$
V	Mean voltage
V_G	Wind turbine voltage
V_S	Grid system voltage
x_{ij}	The spacing between points i and j (meters)
X	(i) Distance downstream of the rotor
X	(ii) Reactance

A.9.2 Greek Variables

$\gamma_{ij}^2(f)$	The coherence between the power spectrums at points i and j
θ_c	Mean hourly direction at the candidate site
θ_r	Mean hourly direction at reference site
μ_c	Mean wind speed at candidate site
μ_r	Mean wind speed at reference site
σ	Standard deviation
σ_c	Standard deviation of mean wind speed at candidate site
σ_{load}	Standard deviation of electrical system load
σ_{net}	Standard deviation of net load
$\sigma_{P,1}$	Standard deviation of power from one wind turbine
$\sigma_{P,N}$	Standard deviation of power from N wind turbines
σ_r	Standard deviation of mean wind speed at reference site
σ_u	Standard deviation of wind speed
σ_{wind}	Standard deviation of wind generation
φ_n	Phase of harmonic voltage of order n
ω	Rotational speed, rad/s

A.10 Chapter 10

A.10.1 English Variables

A	(i) Cross-sectional area
A	(ii) Initial battery voltage parameter
A_C	Charnock constant
c	(i) Ratio of available charge capacity to total capacity
c	(ii) Wave celerity
C	Second battery voltage parameter
C_d	Drag coefficient
C_m	Inertia coefficient
C_P	Power coefficient
d	Water depth
D	(i) Diameter
D	(ii) Third battery voltage parameter
D_{pump}	Pump diameter
E	(i) Useful energy (kJ) stored in a flywheel
E	(ii) Internal battery voltage
E_0	Fully charged/discharged internal battery voltage
f	Frequency at which the wave spectrum reaches is maximum value
f_p	Permeate fraction
$f_{U,H_s,T_P}()$	Joint probability density function of wind speed, wave height, and peak period
F_D	Drag force due to waves
F_I	Inertial force per unit length due to waves
F_p	Pump force
$\hat{F}$	Force per unit length

g	Gravitational constant
g_r	Ratio between the speed of the rotor and that of the pump crank
H_{max}	Maximum wave height
H_s	Significant wave height
i	Van't Hoff factor
I	Current
I_{Rot}	Mass moment of inertia
k	(i) Battery rate constant
k	(ii) Wave number $= 2\pi/L$
k	(iii) Ratio of constant pressure to constant volume specific heats
L	Wavelength
L_P	Wavelength associated with the peak period
m	Mass
mol	Gram molecular weight
M	Molecular weight of salt
M_D	Moment at the sea floor due to wave drag forces
M_I	Moment at the sea floor due to wave inertial forces
p	Pressure
p_c	Pressure under wave crest
p_f	Final pressure
p_t	Pressure under wave trough
p_0	Initial pressure
p_π	Osmotic pressure
P_p	Pumping power
q_{in}	Heat input from the combustion
q_{max}	Maximum battery capacity (at infinitesimal current)
$q_{max}(I)$	Maximum battery capacity at current I
$Q_{p,max}$	Maximum pump torque
R_0	Internal resistance
R_a	Gas constant for air ($0.287\,\text{kPa}\,\text{m}^3/\text{kg K}$)
R_u	Universal gas constant ($0.0831447\,\text{m}^3\,\text{Pa/mol K}$)
s_{pump}	Stroke of pump
S	Salinity (g/kg)
$S(f)$	Wave spectrum
$S_{PM}(f)$	Pierson–Moskowitz wave spectrum
t	Charge or discharge time, hrs
T	(i) Absolute temperature
T	(ii) Wave period
T_P	Wave period associated with the most energetic waves
U	Wind speed
U_w	Velocity of water
$\dot{U}_w$	Acceleration of water
U_*	Friction velocity
v_0	Initial specific volume of hydrogen, kg/m^3
V	(i) Battery terminal voltage
V	(ii) Volume

$\dot{V}$	Volumetric flow rate
w	Specific work
$w_{comp,iso}$	Specific work involved in isothermal compression
$w_{desal,tot}$	Specific work for desalination, kWh/m^3
w_{net}	Net specific work out of turbine
X	Normalized capacity at the given current
z	Height or elevation difference
z_0	Surface roughness

A.10.2 Greek Variables

ΔH	Change in enthalpy
Δp	Pressure rise or drop
ζ	Wave profile
$\hat{\zeta}$	Amplitude of wave
η_{comp}	Compressor efficiency
η_{pump}	Mechanical efficiency of pump
$\eta_{th,Brayton}$	Brayton cycle efficiency
η_{vol}	Volumetric efficiency of pump
κ	Von Karman constant
ρ	Density of air
ρ_w	Density of water
σ_H	Standard deviation of water surface elevation
τ_0	Shear stress
Φ	Velocity potential
ω	(i) Angular velocity
ω	(ii) Wave frequency
Ω_{max}	Maximum rotational speeds
Ω_{min}	Minimum rotational speeds

A.11 Chapter 11

A.11.1 English Variables

A	Installment
AAR	Average annual return
b	Learning parameter
B/C	Benefit–cost ratio
C	Cost
C_c	Capital cost of system
$\bar{C}_c$	Capital cost of system normalized by rated power
$C_{O\&M}$	Average annual operation and maintenance (O&M) costs
$\bar{C}_{O\&M}$	Direct cost of operation and maintenance per unit of energy
$C(V)$	Cost of an object as a function of volume
$C(V_0)$	Cost of an object as a function of initial volume
COE	Cost of energy (cost/kWh)

COE_L	Levelized cost of energy
CRF	Capital recovery factor
E_a	Annual energy production (kWh)
f_{OM}	Annual operation and maintenance (O&M) cost fraction
F_N	Payment at end of N years
FC	Capacity factor
FCR	Fixed charge rate
FV	Future value
i	General inflation rate
IRR	Internal rate of return
j	Index for year
L	Lifetime of system
N	Number of years or instalments
NPV	Net present value
NPV_C	Net present value of costs
NPV_S	Net present value of savings
P_a	Annual payment
P_d	Downpayment
P_e	Price obtained for electricity
PV	Present value
PV_N	Present value of future payment in year N
PWF	Present worth factor
r	Discount rate
ROI	Return on investment
s	Progress ratio
S	Savings
SP	Simple payback (years)
SPW	Series present worth factor
V	Volume of object produced
V_0	Initial cumulative volume
$Y(k, \ell)$	Function to obtain present value of a series of payments; k, ℓ: arguments

A.12 Chapter 12

A.12.1 English Variables

A_1	Additional path loss between the transmitter and the receiver
A_2	Additional path loss between the transmitter and the obstacle
A_r	Additional path loss between the obstacle and the receiver
B	Number of blades
c	Velocity of sound
C	Signal strength
C/I	Signal to interference ratio
D	Rotor diameter
E	Electric field strength ($\mathrm{mV\,m^{-1}}$)
f	Frequency

G_r	Receiver gain
G'_r	Receiver gain (obstacle path)
i	Noise source index
I	Interference length
L_{dn}	Day–night noise level (dB)
L_{eq}	Equivalent noise level (dB)
L_p	Sound pressure level (dB)
L_r	Free space loss (dB)
L_{total}	Total sound power level (dB)
L_w	Sound power level (dB)
L_{WA}	Predicted sound power level (dB)
L_x	A-weighted noise level exceeded $x\%$ of the time (dB)
L_1	Free space path loss (transmitter–receiver)
L_2	Free space path loss (transmitter–obstacle)
p	Sound pressure
P	Sound power
P_t	Transmitter power
P_{WT}	Rated power of wind turbine
r	Receiver distance from turbine
R	Distance from noise source
t	Time delay between desired and undesired signal
U	Wind speed
V_{Tip}	Blade tip speed velocity
W	Source sound power
W_0	Reference source sound power

A.12.2 Greek Variables

α	Sound absorption coefficient (dB m^{-1})
ΔG	Antenna discrimination factor (dB)
λ	Wavelength
Π	Relative position (spherical coordinates)
σ	Radar cross-section
σ_b	Bistatic radar cross-section of obstacle
τ	Time delay of signal to receiver
ω	Frequency of transmitted signal (rad s^{-1})
Ω	Turbine rotor speed (rad s^{-1})

A.13 Abbreviations

a/b	Air-borne
A/D	Analog-to-digital
AC	Alternating current
AM	Amplitude modulated

AVR	Automatic voltage control
BEM	Blade element momentum
CAES	Compressed air energy storage
CFD	Computational fluid dynamic
CFM	Cash flow method
CPU	Computer processing unit
D/A	Digital-to-analog
DC	Direct current
ECD	Extreme coherent gust with change in direction
ECG	Extreme coherent gust
EMF	Electromagnetic field
EMI	Electromagnetic interference
EOG	Extreme operating gust
EPA	Environmental Protection Agency, US
EPR	Ethylene propylene rubber
EPRI	Electric Power Research Institute
EPRI TAG	Electric Power Research Institute, Technical Analysis Group
EWM	Extreme wind speed
EWS	Extreme wind shear
FAA	Federal Aviation Authority
FES	Flywheel energy storage
FM	Frequency modulated
GIS	Geographical information system
GRP	Fiberglass reinforced plastic
GTO	Gate turn off thyristor
HAWT	Horizontal axis wind turbine
HF	High frequency
HVDC	High-voltage direct-current
I/O	Input–output
ID	Inner diameter
IEC	International Electrotechnical Commission
IGBT	Insulated gate bipolar transistor
IPP	Independent power producer
LCC	Life cycle costing
LOLE	Loss of load expectation
LOLP	Loss of load probability
LORAN	Long-range version of VOR
MCP	Measure–correlate–predict
MMF	Magnetomotive force
MOSFET	Metal-oxide semiconductor field-effect transistor
NREL	National Renewable Energy Laboratory
NTM	Normal turbulence model
NWCC	National Wind Coordinating Committee
NWP	Normal wind profile
O&M	Operation and maintenance
OD	Outer diameter

PCC	Point of common coupling
pdf	Probability density function
pf	Power factor
PI	Proportional–integral
PID	Proportional–integral–derivative
PNL	Pacific Northwest Laboratories
POC	Point of contact
PPA	Power purchase agreement
psd	Power spectral density
PURPA	Public Utilities Regulatory Policies Act (US)
PV	Photovoltaic
PWM	Pulse width modulation (inverter)
rms	Root mean square
RNA	Rotor nacelle assembly
RO	Reverse osmosis
ROI	Return on investment
ROV	Remotely operated vehicle
rpm	Rotations per minute
rps	Rotations per second
RPS	Renewable portfolio standards
RSHR	Rotor swept hour risk
s/b	Structure-borne
SCADA	Supervisory control and data acquisition
SCFF	Self-contained fluid-filled
SCR	Silicon-controlled rectifier
SERI	Solar Energy Research Institute
SODAR	Sonic detection and ranging acoustic Doppler sensor system
SPL	Sound pressure level
SSC	System supervisory controller
TALA	Tethered aerodynamic lifting anemometer
TEFC	Totally enclosed, fan cooled
THD	Total harmonic distortion
TLP	Tension leg platform
TVI	Television interference
U&PM	Unscheduled and preventive maintenance
UHF	Ultrahigh-frequency
VAR	Volt–Amperes reactive
VAWT	Vertical axis wind turbine
VHF	Very high frequency
VOR	VHF omnidirectional ranging
WEST	wood–epoxy saturation technique
XLPE	Cross-linked polyethylene

Appendix B

Problems

B.1 Problem Solving

Most of the problems in this text can be completed without reference to additional material beyond what is in the text. In some cases, new information is introduced in the problem statement to extend the reader's knowledge. It may also be helpful to refer to textbooks on fundamental engineering principles.

In some cases data files may be needed. These are available on the website of the Wind Energy Center at the University of Massachusetts (http://www.umass.edu/windenergy/). This site also contains the Wind Engineering MiniCodes that have been developed at the University of Massachusetts at Amherst. A number of these codes may be useful in solving problems and, in some cases, may be needed to solve problems. The Wind Engineering MiniCodes are a set of short computer codes for examining wind energy related issues, especially in the context of an academic setting.

B.2 Chapter 2 Problems

2.1 Based on average speed data only, estimate the annual energy production from a horizontal axis wind turbine with a 12 m diameter operating in a wind regime with an average wind speed of 8 m/s. Assume that the wind turbine is operating under standard atmospheric conditions ($\rho = 1.225 \, \text{kg/m}^3$). Assume a turbine efficiency of 0.4.

2.2 A 40 m diameter, three-bladed wind turbine produces 700 kW at a wind speed (hub height) of 14 m/s. The air density is 1.225 kg/m^3. Find:

(a) The rotational speed (rpm) of the rotor at a tip speed ratio of 5.0.
(b) What is the tip speed (m/s)?
(c) If the generator turns at 1800 rpm, what gear ratio is needed to match the rotor speed to the generator speed?

(d) What is the efficiency of the wind turbine system (including blades, transmission, shafts, and generator) under these conditions?

2.3 (a) Determine the wind speed at a height of 40 m over surface terrain with a few trees, if the wind speed at a height of 10 m is known to be 5 m/s. For your estimate use two different wind speed estimation methods.

(b) Using the same methods as part (a), determine the wind speed at 40 m if the trees were all removed from the terrain.

2.4 A 30 m diameter wind turbine is placed on a 50 m tower in terrain with a power law coefficient (α) of 0.2. Find the ratio of available power in the wind at the highest point the rotor reaches to that at its lowest point.

2.5 Find the size of a wind turbine rotor (diameter in m) that will generate 100 kW of electrical power in a steady wind (hub height) of 7.5 m/s. Assume that the air density is 1.225 kg/m^3, $C_p = 16/27$ and $\eta = 1$.

2.6 From an analysis of wind speed data (hourly interval average, taken over a one-year period), the Weibull parameters are determined to be $c = 6$ m/s and $k = 1.8$.

(a) What is the average velocity at this site?
(b) Estimate the number of hours per year that the wind speed will be between 6.5 and 7.5 m/s during the year.
(c) Estimate the number of hours per year that the wind speed is above 16 m/s.

2.7 Analysis of time series data for a given site has yielded an average velocity of 6 m/s. It is determined that a Rayleigh wind speed distribution gives a good fit to the wind data.

(a) Based on a Rayleigh wind speed distribution, estimate the number of hours that the wind speed will be between 9.5 and 10.5 m/s during the year.
(b) Using a Rayleigh wind speed distribution, estimate the number of hours per year that the wind speed is equal to or above 16 m/s.

2.8 Estimate the annual production of a 12 m diameter horizontal axis wind turbine operating at standard atmospheric conditions ($\rho = 1.225$ kg/m^3) in an 8 m/s average wind speed regime. You are to assume that the site wind speed probability density is given by the Rayleigh density distribution.

2.9 Assuming a Rayleigh distribution, a researcher (see Masters, 2004 *Renewable and Efficient Electric Power Systems.* John Wiley & Sons, Ltd) has proposed the following simple relationship for the capacity factor (CF) of a wind turbine:

$$CF = 0.87\bar{U} + \frac{P_R}{D^2}$$

where $\bar{U}$ is the average wind speed at the hub, P_R is the rated power (kW), and D is the rotor diameter (m). Furthermore, this researcher claims that this equation is accurate to within 10%

for capacity factors between 0.2 and 0.5. Your problem is to check out this equation for a selection of (say five) commercial wind turbines.

2.10   A wind turbine with a rotor diameter of 55 m is rated at 1 MW at a hub height wind speed of 14 m/s. It has a cut-in speed of 4 m/s and a cut-out speed of 25 m/s. Assume that this machine is located at a site where the mean wind speed is 10 m/s and that a Rayleigh wind speed distribution can be used. Calculate the following:

(a) The number of hours per year that the wind is below the cut-in speed.
(b) The number of hours per year that the machine will be shut down due to wind speeds above the cut-out velocity.
(c) The energy production (kWh/year) when the wind turbine is running at rated power.

2.11   Based on the spreadsheet (*MtTomData.xls*) which contains one month of data (mph) from Holoyke, MA, determine:

(a) The average wind speed for the month.
(b) The standard deviation.
(c) A histogram of the velocity data (via the method of bins – suggested bin width of 2 mph).
(d) From the histogram data develop a velocity duration curve.
(e) From above, develop a power duration curve for a given 25 kW turbine at the Holyoke site.

For the wind turbine, assume:

$$P = 0\,\text{kW} \qquad 0 < U \le 6 \text{ (mph)}$$
$$P = U^3/625\,\text{kW} \quad 6 < U \le 25 \text{ (mph)}$$
$$P = 25\,\text{kW} \qquad 25 < U \le 50 \text{ (mph)}$$
$$P = 0\,\text{kW} \qquad 50 < U \text{ (mph)}$$

(f) From the power duration curve, determine the energy that would be produced during this month in kWh.

2.12   Using results from Problem 2.11, carry out the following:

(a) Determine Weibull and Rayleigh velocity distribution curves and normalize them appropriately. Superimpose them on the histogram of Problem 2.11.
(b) Determine the Weibull and Rayleigh velocity duration and power duration curves and superimpose them on the ones obtained from the histogram.
(c) Using the Weibull distribution, determine the energy that would be produced by the 25 kW machine at the Holyoke site.
(d) Suppose the control system of the 25 kW machine were modified so that it operated as shown in Figure B.1 (and as detailed in Table B.1) How much less energy would be produced at Mt Tom with the modified machine? Find a fourth order polynomial fit to the power curve. Use the Weibull distribution to calculate the productivity (in any manner you choose). Plot the power duration curve using the modified power curve and the cubic power curve from Problem 2.11(e).
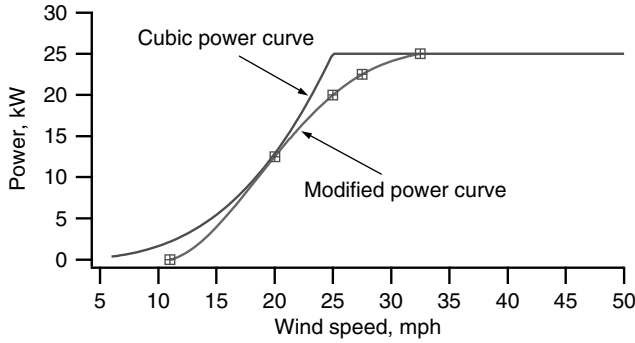
Figure B.1 Power curves for Problems 2.11 and 2.12

Table B.1 Power curve below rated power for Problem 2.12(d)

Wind speed (mph)	Power (kW)
11	0
20	12.5
25	20
27.5	22.5
32.5	25

2.13   Similar to Equation (2.27) in the text, the following empirical expression has been used to determine the power spectral density (psd) of the wind speed at a wind turbine site with a hub height of z. The frequency is f (Hz), and n ($n = fz/U$) is a non-dimensional frequency.

$$\frac{f\,S(f)}{(2.5U^*)^2} = \frac{11.40\,n}{1 + 192.4\,n^{5/3}}$$

where

$$U^* = \frac{0.4[U(z)]}{\ln\left(\frac{z}{z_0}\right)}$$

Determine the power spectral density of the wind at a site where the surface roughness is 0.05 m (z_0) and the hub height is 30 m, and the mean wind speed is 7.5 m/s.

2.14   This problem uses the power spectral density (psd) to examine variance in the wind. A time series of hourly wind speeds (mph) from Mt Tom for approximately one year is included in the data *MtTomWindUM.txt*. Routines to perform psd analysis are included with the UMass Wind Engineering MiniCodes. When the psd is graphed vs. the frequency it is hard to see features of interest. For this reason it is common to graph $f\,S(f)$ on the y axis vs. $\ln(f)$ on the x axis. When doing this the area under the curve between any two frequencies is proportional to the total variance associated with the corresponding range of frequencies.

(a) Use the MiniCodes to calculate the psd for the Mt Tom wind data. Focus on the variations in wind over time periods of less than one month by using a segment length of 512.

(b) Show from the results that the total variance as given by the integral of the psd $S(f)$ vs. f is approximately the same as what would be obtained in the normal way.

(c) Show by equations that the area under the curve in a plot of $f S(f)$ vs. $\ln(f)$ is the same as it would be for a plot of $S(f)$ vs. f.

(d) Plot $f S(f)$ vs. $\ln(f)$.

(e) Find the amount of variance associated with diurnal fluctuations. Use frequencies corresponding to cycle times from 22 hours to 27 hours. How much variance is associated with higher frequency variations and how much with lower frequency variations?

2.15 A variety of techniques is available for creating data sets that have characteristics similar to that of real data. The Wind Engineering MiniCodes include a few of these methods. In the ARMA technique (see Appendix C) the user must input long-term mean, standard deviation, and autocorrelation at a specified lag. The code will return a time series with values that are close to the desired values. (Note: a random number generator is used in the data synthesis routines, so any given time series will not be exactly the same as any other.)

(a) Find the mean, standard deviation, and autocorrelation for the Mt. Tom data: MtTom7Hzms.txt. This data, in m/s, is collected at a 25 m height, with a sampling frequency of 7.4 Hz. Plot a time series of the data. Determine the autocorrelation for a lag of up to 2000 points.

(b) Using the ARMA code with the autocorrelation at a lag of one time step, synthesize and plot a time series of 10,000 data points with equivalent statistics to those found in part a. Show a time series graph of the synthesized data.

(c) Find the autocorrelation for a lag of up to 2000 points for the synthetic data and plot the autocorrelations of both the real and the synthesized on the same graph.

(d) Comment on any similarities or differences between the two plots.

B.3 Chapter 3 Problems

3.1 The blades of a wind turbine are ready to be installed on a turbine on top of a ridge. The horizontal blades are supported at each end by saw horses, when a storm front arrives. The turbine crew huddles in their truck as the rain starts and the wind picks up, increasing eventually to 26.82 m/s (60 mph). Realizing that the wind coming up the western slope of the ridge roughly follows the 10 degree slope, the field engineer performs a quick calculation and drives his truck upwind of the blades to disrupt the air flow around the blades, preventing them from being lifted by the wind and damaged.

The blades are 4.57 m (15 feet) long, 0.61 m (2 feet) wide, and have a mass of 45.36 kg (100 lbm). As the front arrives the temperature drops to 21.2 °C (70 °F). Assume that the blades are approximately symmetric airfoils (the engineer remembered that potential flow theory predicts that, prior to stall, the lift coefficient of a symmetric airfoil is approximately $C_l = 2\pi \sin\alpha$). Assume that the center of both the lift and the drag force is concentrated over the center of mass of the blade and that the leading edge is facing into the direction of the wind. Assume the air density is 1.20 kg/m^3.

(a) Was there a reason to be concerned? At what wind speed will the blades be lifted by the wind, assuming that there is no drag?

(b) If they are lifted by a 26.82 m/s (60 mph) wind, how fast will they be accelerated horizontally if the blade's lift to drag ratio, C_d/C_l, is 0.03?

3.2   An inventor proposes to use a rotating cylinder to produce lift in a new wind energy device. The cylinder will be $D = 0.75$ m in diameter and will be $H = 7.5$ m high. It will rotate with a speed of $n = 60$ rpm.

(a) Recall that circulation around a cylinder is the integral of the tangential velocity about its perimeter. Show that the circulation is given by:

$$\Gamma = \frac{\pi^2 D^2 n}{60}$$

Hint: this is easiest done by using polar coordinates.
(b) Find an expression for the lift per unit height around a rotating cylinder in terms of the free stream wind velocity, U (m/s), the rotational speed, n (rpm), and the diameter, D (m), of the cylinder.
(c) Find the lift force produced by the cylinder in the inventor's device in a 10 m/s wind.

3.3   The operating conditions found at two different points of a blade on a wind turbine are shown in Table B.2.

Table B.2

Location r/R	Wind velocity at blade (m/s)	Wind velocity at blade (ft/s)	Chord (m)	Chord (ft)	Angle of attack (degrees)
0.15	16.14	52.94	1.41	4.61	4.99
0.95	75.08	246.32	0.35	1.15	7.63

These conditions were determined at $0\,°C$ ($32\,°F$), for which the kinematic viscosity is 1.33×10^{-5} m^2/s. What are the Reynolds numbers found at each blade section?

3.4   (a) Find θ, θ_p, θ_T, and c for one blade section from $r/R = 0.45$ to $r/R = 0.55$ (centered on $r/R = 0.50$) for an ideal blade (assume $C_d = 0$, $a' = 0$). Assume $\lambda = 7$, $B = 3$, $R = 5$ m, and $C_l = 1.0$ and the minimum C_d/C_l occurs at $\alpha = 7$ degrees.
   (b) Assume that C_d/C_l actually equals 0.02 for the above blade section and that the free stream wind speed, U, equals 10 m/s. Find $U_{rel}, dF_{L1}, dF_{D1}, dF_{N1}, dF_{T1}, dQ_1$ for the blade section. Don't forget to consider that the wind velocity is slowed down at the rotor. Use $a = 1/3$, $a' = 0$. Assume the air density is 1.24 kg/m^3 (20 °C).
   (c) For the same blade section find C_l, α, and a using the general strip theory method (including angular momentum). Also find C_l, α, and a if the rpm is increased such that $\lambda = 8$. Ignore drag and tip loss. Use a graphical approach. Assume that the empirical lift curve is $C_l = 0.1143\alpha + 0.2$ (α in degrees): i.e. $C_l = 0.2$ at $\alpha = 0$ degrees, $C_l = 1.0$ at $\alpha = 7$ degrees.

3.5 (a) Find θ, θ_p, θ_T, and c at all ten locations ($r/R = 0.10, 0.20, \ldots, 1.0$) for the Betz optimum blade. Assume $\lambda = 7$, $B = 3$, $R = 5$ m, and $C_l = 1.0$ and the minimum C_d/C_l occurs at $\alpha = 7$.

(b) Sketch the shape (planform) of the blade, assuming that all the quarter chords lie on a straight line.

(c) Illustrate the blade twist by drawing plausible airfoils with properly proportioned chord lengths, centered at the quarter chord chords for $r/R = 0.10, 0.50, 1.0$. Be sure to show where the wind is coming from and what the direction of rotation is.

3.6 Blades for a two-bladed wind turbine with a 24 m diameter have been designed for a tip speed ratio of 10. The 12-meter blades have the geometric and operational parameters listed in Table B.3 for operation at the design tip speed ratio. The rotor was designed assuming $C_l = 1.0$, $a' = 0$, no drag, and $a = 1/3$ using the methods outlined in the text for the design of an ideal rotor.

We want to know the rotor power coefficient for two assumed conditions: $C_d = 0$ and $C_d = 0.02$. Note that the two equations that have been derived do not serve our purpose here. Equation (3.90) requires a non-zero value for a' and Equation (3.91) has also been derived using relationships between a and a' that require non-zero values of a'.

(a) Starting with the definitions of the blade forces and the definition of C_P:

$$C_P = P/P_{wind} = \frac{\int_{r_h}^{R} \Omega \, dQ}{\frac{1}{2}\rho\pi R^2 U^3}$$

derive as simple an equation as you can for the power coefficient, C_P, of an ideal Betz limit rotor. The equation should include both lift and drag coefficients and tip speed ratio, and should assume that $a = 1/3$. Ignore tip losses.

(b) Using the above equation find the rotor C_P at the design tip speed ratio assuming that there is no drag ($C_d = 0$). How does this compare with the Betz limit?

Table B.3

Section radius r/R	Section radius (m)	Section pitch, θ_p degrees	Angle of relative wind, φ (degrees)	Section twist (degrees)	Chord, c (m)
0.05	0.60	46.13	53.13	49.32	4.02
0.15	1.80	16.96	23.96	20.15	2.04
0.25	3.00	7.93	14.93	11.12	1.30
0.35	4.20	3.78	10.78	6.97	0.94
0.45	5.40	1.43	8.43	4.61	0.74
0.55	6.60	− 0.09	6.91	3.10	0.60
0.65	7.80	− 1.14	5.86	2.04	0.51
0.75	9.00	− 1.92	5.08	1.27	0.45
0.85	10.20	− 2.52	4.48	0.67	0.39
0.95	11.40	− 2.99	4.01	0.20	0.35

(c) For a first approximation of the effect of drag on rotor performance, find the C_p for the same rotor at the design tip speed ratio assuming the more realistic conditions that C_d/C_l actually equals 0.02. Assume that the drag has no effect on the aerodynamics and that the operating conditions assumed for the ideal rotor without drag apply. What effect does drag have on the rotor C_P, compared to the C_P assuming that $C_d = 0$?

3.7 The Better Wind Turbine Company wants to start marketing wind turbines. The plans call for a 20 meter in diameter, three-bladed wind turbine. The rotor is to have its peak power coefficient at a tip speed ratio of 6.5. The airfoil to be used has a lift coefficient of 1.0 and a minimum drag to lift ratio at an angle of attack of 7 degrees.

   You, as the new blade designer, are to come up with two blade shapes as a starting point for the blade design. One shape assumes that there are no losses and that there is no wake rotation. The second design is based on the optimum rotor shape assuming that there is wake rotation (but still no losses).

   Find the chord length, pitch, and twist at ten stations of the blade, assuming that the blade extends right to the center of the rotor. How do the chord lengths and the twists compare at the tip and at the inner three blade stations?

3.8 The Better Wind Turbine Company wants to start marketing wind turbines. Their plans call for a turbine that produces 100 kW in a 12 m/s wind at a cold site ($-22.8\,^{\circ}\text{C}$, $-9\,^{\circ}\text{F}$) with an air density of 1.41 kg/m^3. They have decided on a 20 meter in diameter, three-bladed wind turbine. The rotor is to have its peak power coefficient at a tip speed ratio of 7 in a 12 m/s wind. The airfoil to be used has a lift coefficient of 1.0 and a minimum drag to lift ratio at an angle of attack of 7 degrees.

(a) You, as the new blade designer, are to come up with the blade shape as a starting point for the blade design. The design is to be based on the optimum rotor shape assuming that there is wake rotation (but no drag or tip losses). Find the chord length, pitch, and twist at nine stations of the blade (each 1 m long), assuming that the hub occupies the inner tenth of the rotor.
(b) Determine the rotor C_P assuming $C_d = 0$. Again determine the power coefficient assuming that the drag coefficient is 0.02, and that the aerodynamics are the same as the condition without any drag. How much power is lost due to drag? Which part of the blade produces the most power?
(c) Does it look like the chosen design is adequate to provide the power that the Better Wind Turbine Company wants?

3.9 A two-bladed wind turbine is designed using one of the LS-1 family of airfoils. The 13 m long blades for the turbine have the specifications shown in Table B.4.

   Assume that the airfoil's aerodynamic characteristics can be approximated as follows (note, α is in degrees):

For $\alpha < 21$ degrees:

$$C_l = 0.42625 + 0.11628\,\alpha - 0.00063973\,\alpha^2 - 8.712 \times 10^{-5}\alpha^3 - 4.2576 \times 10^{-6}\alpha^4$$

Table B.4 LS-1 airfoil blade geometry

r/R	Section radius (m)	chord (m)	twist (degrees)
0.05	0.65	1.00	13.000
0.15	1.95	1.00	11.000
0.25	3.25	1.00	9.000
0.35	4.55	1.00	7.000
0.45	5.85	0.87	5.000
0.55	7.15	0.72	3.400
0.65	8.45	0.61	2.200
0.75	9.75	0.54	1.400
0.85	11.05	0.47	0.700
0.95	12.35	0.42	0.200

Note: $\theta_{p,0} = -1.97$ degrees (pitch at tip)

For $\alpha > 21$: $C_l = 0.95$

$$C_d = 0.011954 + 0.00019972\,\alpha + 0.00010332\,\alpha^2$$

For the *midpoint* of section 6 ($r/R = 0.55$) find the following for operation at a tip speed ratio of 8:

(a) angle of attack, α
(b) angle of relative wind, θ
(c) C_l and C_d
(d) the local contributions to C_P.

Ignore the effects of tip losses.

3.10 This problem is based on the blades used for the UMass wind machine WF-1. Refer to Table B.5 for the blade geometry at specific locations along the blade. There is no airfoil below $r/R = 0.10$

In addition, note that for the NACA 4415 airfoil: for $\alpha < 12$ degrees: $C_l = 0.368 + 0.0942\alpha$, $C_d = 0.00994 + 0.000259\,\alpha + 0.0001055\,\alpha^2$ (note, α is in degrees). Radius: 4.953 m (16.25 ft); no. of blades: 3; tip speed ratio: 7; rated wind speed: 11.62 m/s (26 mph). The pitch at the tip is: $\theta_{p,0} = -2$ degrees.

(a) Divide the blade into ten sections (but assume that the hub occupies the innermost 1/10). For the *midpoint* of each section find the following: (i) angle of attack, α; (ii) angle of relative wind, φ; (iii) C_l and C_d; (iv) the local contributions to C_P and thrust. Include the effects of tip losses.
(b) Find the overall power coefficient. How much power would the blades produce at 11.62 m/s (26 mph)? Include drag and tip losses. Assume an air density of 1.23 kg/m³.

Table B.5 WF-1 airfoil geometry

r/R	Radius (ft)	Radius (m)	Chord (ft)	Chord (m)	Twist (degrees)
0.10	1.63	0.495	1.35	0.411	45.0
0.20	3.25	0.991	1.46	0.455	25.6
0.30	4.88	1.486	1.26	0.384	15.7
0.40	6.50	1.981	1.02	0.311	10.4
0.50	8.13	2.477	0.85	0.259	7.4
0.60	9.75	2.972	0.73	0.223	4.5
0.70	11.38	3.467	0.63	0.186	2.7
0.80	13.00	3.962	0.55	0.167	1.4
0.90	14.63	4.458	0.45	0.137	0.40
1.00	16.25	4.953	0.35	0.107	0.00

3.11   A two-bladed wind turbine is designed using one of the LS-1 family of airfoils. The 13 m long blades for the turbine have the specifications listed previously in Table B.4.

Assume that the airfoil's aerodynamic characteristics can be approximated as follows (note, α is in degrees):

For $\alpha < 21$ degrees:

$$C_l = 0.42625 + 0.11628\,\alpha - 0.00063973\,\alpha^2 - 8.712 \times 10^{-5}\alpha^3 - 4.2576 \times 10^{-6}\alpha^4$$

For $\alpha > 21$: $C_l = 0.95$

$$C_d = 0.011954 + 0.00019972\,\alpha + 0.00010332\,\alpha^2$$

For the *midpoint* of the outermost section of the blade ($r/R = 0.95$) find the following for operation at a tip speed ratio of 8:

(a) angle of attack, α, with and without tip losses
(b) angle of relative wind, θ
(c) C_l and C_d
(d) the local contributions to C_P
(e) the tip loss factor, F, and the axial induction factor, a, with and without tip losses.

How do tip losses affect aerodynamic operation and the local contribution to C_P at this outermost section?

3.12   A two-bladed wind turbine is operated at two different tip speed ratios. At 8.94 m/s (20 mph) (tip speed ratio = 9) one of the blade sections has an angle of attack of 7.19 degrees. At 16.09 m/s (36 mph) (tip speed ratio = 5) the same 1.22 m (4 ft) section of the blade is starting to

stall, with an angle of attack of 20.96 degrees. Given the following operating conditions and geometric data, determine the relative wind velocities, the lift and drag forces, and the tangential and normal forces developed by the blade section at the two different tip speed ratios. Determine, also, the relative contribution (the fraction of the total) of the lift and drag forces to the tangential and normal forces developed by the blade section at the two different tip speed ratios.

How do the relative velocities and the lift and drag forces compare? How do the tangential and normal forces compare? How do the effects of lift and drag change between the two operating conditions (operating conditions are listed in Table B.6)?

Table B.6 Operating conditions

λ	α	φ	a
5	20.96	22.21	0.070
9	7.19	8.44	0.390

This particular blade section is 1.22 m (4 ft) long, has a chord length of 0.811 m (2.66 ft), and has a center radius of 5.49 m (18 ft). The following lift and drag coefficients are valid for $\alpha < 21$ degrees, where α is in degrees:

$$C_l = 0.42625 + 0.11628\,\alpha - 0.00063973\,\alpha^2 - 8.712 \times 10^{-5}\alpha^3 - 4.2576 \times 10^{-6}\alpha^4$$

$$C_d = 0.011954 + 0.00019972\,\alpha + 0.00010332\,\alpha^2$$

3.13 Assume a VAWT operates with an axial induction factor of 0.3 and with a tip speed ratio of 12. Equations (3.147) and (3.149) can be used to determine the ratio of U_{rel} to U and the angle of attack. Equations (3.148) and (3.150) can be used to estimate those same quantities for high tip speed ratios. What is the maximum percentage deviation of the estimates of these quantities from the exact values as the blade of the VAWT makes one full rotation? If the blades are replaced and now the turbine operates at a tip speed ratio of 20 and the same axial induction factor?

3.14 Determine the operating axial induction factor of a vertical axis wind turbine with straight blades using Equation (3.156). Guess an 'input' axial induction factor and solve the right-hand side of the equation. Using the quadratic equation, solve the left side for the value of the axial induction factor that is less than 0.5. If the two do not agree, adjust the input value until it does. The resulting axial induction factor is the solution. Assume the following input conditions and that the lift coefficient as a function of the angle of attack is the same as that for a flat plate (Equation 3.51):

Number of blades	B	3
Radius	R	6
Chord	c	0.1
Tip speed ratio	λ	15

B.4 Chapter 4 Problems

4.1 A wind turbine rotor turning at 60 rpm is brought to a stop by a mechanical brake. The rotor inertia is $13\,558\,\text{kg m}^2$.

(a) What is the kinetic energy in the rotor before it is stopped? How much energy does the brake absorb during the stop?
(b) Suppose that all the energy is absorbed in a steel brake disc with a mass of 27 kg. Ignoring losses, how much does the temperature of the steel brake disc rise during the stop? Assume a specific heat for steel of 0.46 kJ/kg C.

4.2 A wind turbine has a rotor with polar mass moment of inertia, J, of $4.2 \times 10^6\,\text{kg m}^2$. It is operating in steady winds at a power of 1500 kW and a rotational speed of 20 rpm. Suddenly the connection to the electrical network is lost and the brakes fail to apply. Assuming that there are no changes in the aerodynamic forces, how long does it take for the operating speed to double?

4.3 A cantilevered 2 m long main shaft of a wind turbine holds a 1500 kg hub and rotor at its end. At rated power, the turbine develops 275 kW and rotates at 60 rpm. The shaft is a 0.15 m in diameter cylindrical steel shaft.

(a) How much does the shaft bend down at its end as a result of the load of the rotor and hub?
(b) How much does the shaft twist when the turbine is operating at rated power? What is the maximum shear stress in the shaft?

4.4 A wind turbine on a 24.38 m (80 ft) tower is subject to a thrust load of 26.69 kN (6000 lbf) during operation at 250 kW, the rated power of the turbine. In a 44.7 m/s (100 mph) hurricane, the thrust load on the stopped turbine is expected to be 71.62 kN (16 100 lbf).

(a) If the tower is a steel tube 1.22 m (4 ft) in outer diameter (OD) with a 0.0254 m (1 in) thick wall, how much will the top of the tower move during rated operation and in the hurricane force winds?
(b) Suppose the tower were a three-legged lattice tower with the specifications given in Figure B.2, how much will the top of the tower move during rated operation and in the hurricane force winds? Ignore any effect of cross bracing on the tower.

4.5 The wind turbine rotor shown in Figure B.3 has a rotor rotation velocity, Ω, of 1 Hz (60 rpm) and is yawing at an angular velocity, ω, of 10 degrees per second. The polar mass moment of inertia of the rotor is $13\,558\,\text{kg m}^2$ ($10\,000\,\text{slug ft}^2$). The rotor weighs 1459 kg (100 slugs) and is 3.05 m (10 feet) from the center of the bed plate bearing support. Centered over the bed plate bearing support are the bearings holding the main shaft. These bearings are 0.91 m (3 ft) apart. The directions of positive moments and rotation are indicated in the figure.

(a) What are the bearing loads when the turbine is not yawing?
(b) What are the bearing loads when the turbine is yawing?
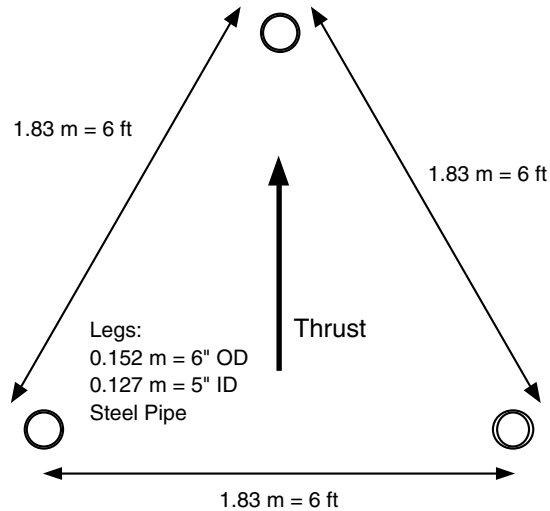
Figure B.2 Lattice tower cross-section; ID, inner diameter; OD, outer diameter
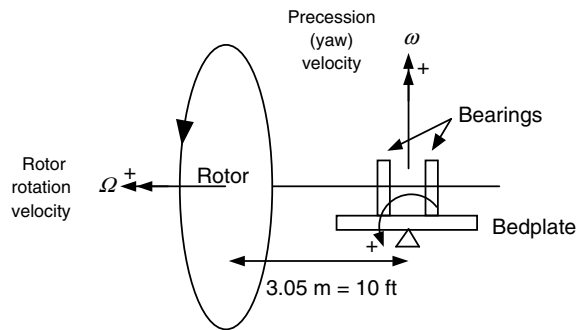
Figure B.3 Rotor configuration for problem 4.5

4.6 A three-bladed wind turbine has a rotor diameter of 38.1 m. The blade chord is constant and equal to 1.0 m. Each blade has a non-rotating natural frequency of 1.67 Hz. In operation, rotating at 50 rpm, each blade has a natural frequency of 1.92 Hz. The pitch angle of the blade is 1.8 degrees. (The hub is sufficiently small that it can be ignored.) The turbine is operating in a wind of 8 m/s. The airfoil lift curve slope is equal to 2π. Air density is 1.225 kg/m^3. If the blade has a mass of 898 kg, what (a) hinge–spring stiffness, (b) moment of inertia, and (c) offset would be used to model the blade dynamics with the hinge–spring blade model?

4.7 Consider the wind turbine rotor used in Problem 4.6. Using the hinge–spring blade model, find the flapping angle during these conditions. How far is the tip of the blade from the plane of rotation?

Hint: In solving this, there are a number of intermediate calculations that need to be made. It may be helpful to confirm your results with the MiniCodes. In any case, check the units of all parameters carefully.

4.8   Blade bending moments are being measured on a research wind turbine on a day with mean hub height winds of 9.14 m/s (30 ft/s), but a wind shear results in winds of 12.19 m/s (40 ft/s) at the top of the blade tip path and 6.09 m/s (20 ft/s) at the bottom of the blade tip path. A gust of wind has started the wind turbine yawing at a steady rate of 0.1 radians per second in the $+X'$ direction (see Figure 4.17 in the text). Meanwhile a wind direction change results in a crosswind of $+0.61$ m/s (2.0 ft/s). The 24.38 m (80 ft) diameter turbine starts with a flap hinge angle, β, of 0.05 radians and, at the moment that measurements are being made, the rate of change of the flap hinge angle is 0.01 rad/s. The rotor is 3.05 m (10 ft) from the yaw axis on this fixed-speed turbine that rotates at a speed of 1 Hz. The very efficient turbine is operating with an axial induction factor of 1/3.

   Ignoring tower shadow and transient effects, if these operating conditions were to persist for one revolution of the rotor, what would the perpendicular and tangential wind as a function of azimuth angle be half way out on the blades? What would the magnitude of the contributions to the perpendicular wind be from yaw rate, shear, crosswind, and blade flapping? How would the angle of attack vary at this part of the blade as the azimuth changes? Assume that the blade pitch angle, θ_p, is 0.05 radians (2.86 degrees).

4.9   When only blade rotation and the hinge–spring and offset are included in the calculation of the flap angle, the only non-zero term is the steady state flap angle, β_0.

(a) What is the derivative of the steady state flap angle with respect to wind velocity? Assume that the axial induction factor is also a function of wind velocity.
(b) Assuming that the Lock number is positive, what would the effect of a negative value of da/dU be on the steady state flap angle?
(c) Suppose $a = 1/3$ and $da/dU = 0$. In this case, what is the expression for the derivative of the steady state flap angle with respect to wind velocity?
(d) What is the derivative of the steady state flap angle with respect to blade pitch?

4.10   Just as the flap angle can be represented by the sum of a constant term, a sine term, and a cosine term, the lead–lag angle in the simplified dynamics model can be represented by the sum of a constant term, a sine term, and a cosine term:

$$\zeta \approx \zeta_0 + \zeta_{1c} \cos(\psi) + \zeta_{1s} \sin(\psi)$$

The following matrix equation for the solution of the lead–lag motion can be derived by substituting this solution into the lead–lag equations of motion (note that flap coupling terms have been omitted for simplicity):

$$
\begin{bmatrix}
2B & (K_2 - 1) & 0 \\
0 & 0 & (K_2 - 1) \\
K_2 & B & 0
\end{bmatrix}
\begin{bmatrix}
\zeta_0 \\
\zeta_{1c} \\
\zeta_{1s}
\end{bmatrix}
=
\begin{bmatrix}
-\dfrac{\gamma}{2}\left[K_{vs}\bar{U}A_4 - \dfrac{\theta_P \Lambda}{2}(\bar{V}_0 + \bar{q}\bar{d}) \right] \\[2ex]
-2B - \dfrac{\gamma}{2}\bar{q}A_4 \\[2ex]
\dfrac{\gamma}{2}\Lambda A_2
\end{bmatrix}
$$

where:

$K_2 = $ inertial natural frequency (includes offset, hinge–spring) $= \varepsilon_2 + \frac{K_\zeta}{I_b \Omega^2} = \left(\frac{\omega_\zeta}{\Omega}\right)^2$

$A_2 = $ axisymmetric flow term (includes tip speed ratio and pitch angle) $= \frac{\Lambda}{2} + \frac{\theta_p}{3}$

$A_4 = $ axisymmetric flow term (includes tip speed ratio and pitch angle) $= \frac{2}{3}\Lambda - \frac{\theta_p}{4}$

The other terms are all defined in the text.

(a) Write the matrix equation for lead–lag motion, including the terms for the steady mean wind and the hinge spring model, but assuming that gravity is zero and that other aerodynamic forcing functions are zero.
(b) Solve the equations and find the expression for the steady state lead–lag angle as a function of the Lock number, the non-dimensional wind speed, the lead–lag natural frequency, and the blade pitch.
(c) Suppose the pitch were 5.7 degrees, the rotor speed were 50 rpm, and the diameter were 9.14 m (30 ft). By what factor would the steady state lead–lag angle increase if the wind speed increased from 7.62 m/s (25 ft/s) to 15.24 m/s (50 ft/s)? Assume that the axial induction factor decreases from 0.30 to 0.25 as the speed increases to 15.24 m/s (50 ft/s).

4.11   Using the lead–lag equations described in Problem 4.10:

(a) Write the matrix equation for lead–lag motion if all of the terms are ignored except those that have to do with steady winds and vertical wind shear.
(b) Solve the equations and find the expression for the lead–lag angle with steady winds and vertical shear. What is the effect of vertical wind shear on each term of the lead–lag angle in the absence of yaw rate, gravity, and crosswind?

4.12   Consider the data file, *Flap1.txt*. This data represents ten minutes of blade bending moment data taken from an operating wind turbine. The turbine has a nominal operating speed of 60 rpm. The data was sampled at 40 Hz. Find the psd of the data. What are the predominant frequencies? What do you suspect that these frequencies might be caused by?

4.13   Consider the following turbine. The tower is 50 m high, has diameter of 2 m at the top and 3.36 m at the bottom. The mass of the nacelle and rotor is 20 400 kg. The wall thickness is 0.01384 m. Assume that the density of steel is 7700 kg/m^3 and that its modulus of elasticity is 160 GPa. The problem considers a number of approaches (successively improving) to estimate the natural frequency (1st mode) of the turbine.

(a) Assume that the tower is not tapered, but has a constant diameter of 2 m. What is the natural frequency using the simple equation, but ignoring the mass of the rotor nacelle assembly (RNA) on the top of the tower.
(b) Repeat (a) using the Euler method. Do this directly or with the MiniCodes.
(c) Repeat (a) using the Myklestad method. Use the MiniCodes.
(d) Repeat (a), taking into account the weight of the RNA the top, using the simple equation.

(e) Repeat (d), using the Myklestad method. This will require some approximations to account for the weight of the RNA.

(f) Repeat (e), but take into account the actual taper of the tower.

B.5 Chapter 5 Problems

5.1   A 48 V DC wind turbine is hooked up to charge a battery bank consisting of four 12 V batteries in series. The wind is not blowing, but the batteries must supply two loads. One is a light bulb, rated at 175 W at 48 V; the other is a heater, rated at 1000 W at 48 V. The loads are in parallel. The batteries may be considered to be constant 12 V voltage sources, with an internal series resistance of 0.05 Ohm each. How much power is actually supplied to the loads? How does that power compare to that which is expected? (Ignore the effect of temperature on resistance of filament and heating elements.)

5.2   An electromagnet is used to hold a wind turbine's aerodynamics brakes in place during operation. The magnet supplies 30 lbs (133.4 N) of force to do this. The magnet is supplied by a 60 V DC source. The coil of the electromagnet draws 0.1 A. The core of the electromagnet is assumed to have a relative permeability of 10^5. The diameter of the core is 3 in (7.62 cm).

Find the number of turns in the coil and the wire size. Assume that the relation between force, magnetic flux, and area of the core is given by $F = 397\,840\,B^2\,A_c$:

where: F = force (N), B = magnetic flux (Wb/m²), A_c = area of core (m²). Also, assume that the length of each turn is equal to the circumference of the core. The resistivity of copper is $\rho = 1.72 \times 10^{-6}\,\Omega\,cm$.

5.3   Consider the following phasors: $\hat{\mathbf{X}} = 10 + j14$, $\hat{\mathbf{Y}} = -4 + j5$. Find the following, and express in both rectangular and polar form: $\hat{\mathbf{X}} + \hat{\mathbf{Y}}$, $\hat{\mathbf{X}} - \hat{\mathbf{Y}}$, $\hat{\mathbf{X}}\hat{\mathbf{Y}}$, $\hat{\mathbf{X}}/\hat{\mathbf{Y}}$.

5.4   Show that the magnitude of the line-to-neutral voltage in a balanced, Y-connected three-phase system (V_{LN}) is equal to the line-to-line voltage (V_{LL}) divided by the square root of 3, i.e.

$$V_{LN} = V_{LL}/\sqrt{3}.$$

The line feeding a Y-connected three-phase generator has a line-to-line voltage of 480 V. What is the line-to-neutral voltage?

5.5   A circuit has a resistance and inductance in series. The applied AC voltage is $240\angle O°$ V, 60 Hz. The resistance is $8\,\Omega$ and the induction is $10\,\Omega$. Find the current in the circuit.

5.6   An AC circuit has a resistor, capacitor, and inductor in series with a 120 V, 60 Hz voltage source. The resistance of the resistor is 2 Ohms, the inductance of the inductor is 0.01 Henry; the capacitance of the capacitor is 0.0005 Farads. Find the following: reactance of the capacitor and inductor, current, apparent power, real power, reactive power, power factor angle, and power factor.

5.7 A circuit has a resistor and an inductor in parallel. In addition, a second resistor is in series with a capacitor in parallel and the two of them are in parallel with the inductor and the first resistor. The resistance of the first resistor is $8\,\Omega$ and that of the second resistor is $12\,\Omega$. The impedance of the inductor is $j16\,\Omega$ and that of the capacitor is $-j22\,\Omega$. The applied voltage is 200 V. Find the apparent power, the power factor, and the real power.

5.8 A transformer rated at 120 V/480 V, 10 kVA has an equivalent circuit as shown in Figure B.4. The low-voltage side is connected to a heater, rated at 5 kW, 120 V. The high-voltage side is connected to a 480 V, 60 Hz, single-phase power line. Find the actual power transferred, the magnitude of the measured voltage across the heater, and the efficiency (power out/power in) of the transformer.
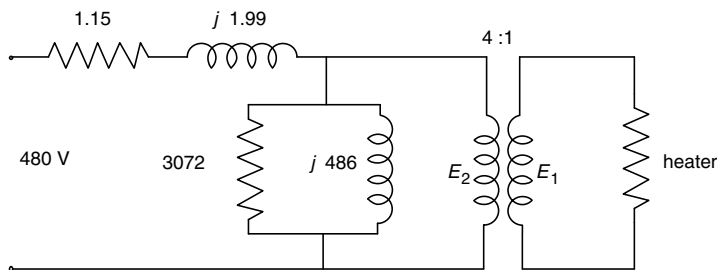
Figure B.4 Transformer equivalent circuit

5.9 A small wind turbine generator (single phase) produces a 60 Hz voltage at 120 V rms. The output of the generator is connected to a diode bridge full-wave rectifier, which produces a fluctuating DC voltage. What is the average DC voltage? A silicon-controlled rectifier (SCR) is substituted for the diode rectifier. Under one condition the SCRs are turned on at 60 degrees after the beginning of each half cycle. What is the average DC voltage in that case?

5.10 The parameters of an induction machine can be estimated from test data taken under a few specified conditions. The two key tests are the no-load test and blocked-rotor test. Under the no-load test, the rated voltage is applied to the machine and it is allowed to run at no load (i.e. with nothing connected to the shaft). In the blocked-rotor test, the rotor is prevented from turning and a reduced voltage is applied to the terminals of the machine. In both cases the voltage, current, and power are measured. Under the no-load test, the slip is essentially equal to 0, and the loop with the rotor parameters may be ignored. The magnetizing reactance accounts for most of the impedance and can be found from the test data. Under blocked-rotor conditions, slip is equal to 1.0 so the magnetizing reactance can be ignored, and the impedance of the leakage parameters can be found. A third test can be used to estimate the windage and friction losses. In this test the machine being tested is driven by a second machine but it is not connected to the power system. The power of the second machine is measured, and from that value is subtracted the latter's no-load power. The difference is approximately equal to the test machine's windage and friction.
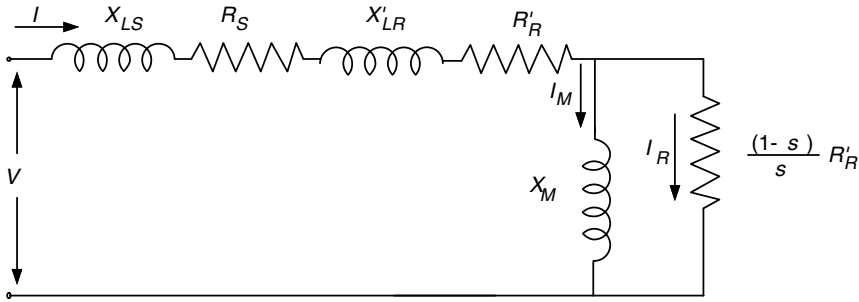
Figure B.5   Simplified induction machine equivalent circuit

In a simplified version of the analysis, all of the leakage terms may be assumed to be on the same side of the mutual inductance, as shown in Figure B.5. In addition, the resistance in parallel with the magnetizing reactance is assumed to be infinite, the stator and rotor resistances, R_S and R'_R, are assumed equal to each other and the leakage inductances are also assumed to be equal to each other.

The following test data are available for a Y-connected, three-phase induction machine:

  No-load test: $V_0 = 480$ V, $I_0 = 46$ A, $P_0 = 3500$ W
  Blocked-rotor test: $V_B = 70$ V, $I_B = 109$ A, $P_B = 5600$ W
  Windage and friction losses equal 3000 W.

Find the parameters for the induction generator model.

5.11   A four-pole induction generator is rated at 300 kVA and 480 V. It has the following parameters: $X_{LS} = X_{LR} = 0.15\,\Omega$, $R_{LS} = 0.014\,\Omega$, $R_{LR} = 0.0136\,\Omega$, $X_M = 5\,\Omega$. How much power does it produce at a slip of -0.025? How fast is it turning at that time? Also, find the torque, power factor, and efficiency. (Ignore mechanical losses.)

Suppose the generator is used in a wind turbine, and the torque due to the wind is increased to a value of 2100 Nm. What happens?

5.12   A resistive load of 500 kW at 480 V is supplied by an eight-pole synchronous generator connected to a diesel engine, and a wind turbine with the same induction generator as that in Problem 5.11. The synchronous machine is rated to produce 1000 kVA. Its synchronous reactance is 0.4 Ohms. A voltage regulator maintains a constant voltage of 480 V across the load and a governor on the diesel engine maintains a fixed speed. The speed is such that the grid frequency is 60 Hz. The power system is three-phase, and the electrical machines are both Y-connected. The power from the wind is such that the induction generator is operating at a slip of -0.01. At this slip, the power is 153.5 kW and the power factor is 0.888.

(a) Find the synchronous generator's speed, power factor, and power angle.
(b) Confirm that the power and power factor are as stated.
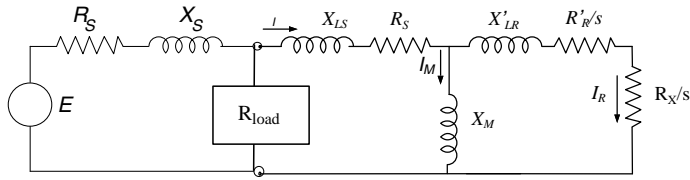
Figure B.6   System with synchronous generator and WRIG

5.13   A diesel engine driven synchronous generator and a wind turbine with a wound rotor induction generator (WRIG) are used to supply a resistive load as shown in Figure B.6. The power system is three-phase, and the electrical machines are both Y-connected.

The WRIG has four poles and is rated at 350 kVA and 480 V. It has the following parameters: $X_{LS} = X_{LR} = 0.15\,\Omega$, $R_S = 0.014\,\Omega$, $R'_R = 0.0136\,\Omega$, $X_M = 5\,\Omega$. The external resistor in the rotor circuit may be varied.

The resistive load consumes 800 kW at 480 V.

The synchronous generator is the same as in Problem 5.12. It has eight poles and is rated to produce 1000 kVA. Its synchronous reactance is 0.4 Ohms. A voltage regulator maintains a constant voltage of 480 V across the load and a governor on the diesel engine maintains a fixed speed. The speed is such that the grid frequency is 60 Hz.

All mechanical losses may be ignored.

The external resistance has been bypassed. The wind conditions are such that the WRIG is operating at a slip of -0.02.

(a) How fast (rpm) is the generator turning at this time?
(b) How much mechanical power is coming into the generator rotor from the wind turbine's rotor?
(c) What is the power factor of the WRIG?
(d) What is (i) the power from the synchronous generator; (ii) its power factor, (iii) the power angle; (iv) the generator speed (rpm) and the internal voltage, E?

5.14   This problem involves the same generator and load as in Problem 5.13, except now the external resistance of the WRIG is included and it may be varied as required. The wind speed has increased and the control system has responded such that the slip is now -0.42 but the stator currents are unchanged.

(a) What is the value (Ω) of the external resistance?
(b) What is the speed (rpm) of the generator?
(c) How much mechanical power from the turbine's rotor is now coming into the generator's rotor?
(d) How much electrical power is coming out of the stator windings?
(e) How much power is dissipated in the external resistance?

5.15   This problem involves the same situation as in Problem 5.14. Instead of an external resistor in the WRIG's rotor circuit, however, an ideal inverter has been inserted.
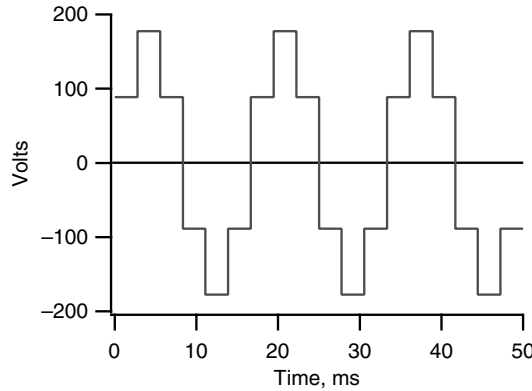
Figure B.7   Inverter staircase voltage

The inverter feeds the same power as was previously dissipated in the rotor resistance into the local network.

(a) How much total useful power is produced by the WRIG?
(b) What is the power and power factor of the synchronous generator?

5.16   A six-pulse inverter has a staircase voltage, two cycles of which are shown in Figure B.7. The staircase rises from 88.85 V to 177.7 V, etc. The frequency is 60 Hz.

(a) Show that the voltage can be expressed as the following Fourier series:

$$V_{inv}(t) = A\left[\sin(\omega t) + \frac{1}{5}\sin(5\omega t) + \frac{1}{7}\sin(7\omega t) + \frac{1}{11}\sin(11\omega t) + \ldots\right]$$

where $A = (3/\pi)(177.7)$ and $\omega = 2\pi f$.
(b) A series parallel resonance filter is connected across the terminals. The reactance of each component is the same, so that

$$f(n) = \left|n^2/\{(n^2 - 1) - n^2\}\right|.$$

Show how the filter decreases the harmonics. Find the reduction to the filter of the fundamental and at least the first three non-zero harmonics. Illustrate the filtered and unfiltered voltage waveform.

Hint: in general, a Fourier series for a pulse train (a square wave) can be expressed as:

$$V(t) = \frac{4}{\pi}H\left[\sin(\omega t) + \frac{1}{3}\sin(3\omega t) + \frac{1}{5}\sin(5\omega t) + \frac{1}{7}\sin(7\omega t) + \frac{1}{9}\sin(9\omega t) + \ldots\right]$$

where $\omega = 2\pi f$ and $H =$ the height of the square wave above zero.

B.6 Chapter 6 Problems

6.1 A wind turbine has a hollow steel shaft 5 m long. The outer radius is 1 m and the inner radius is 0.8 m. Find the area moment of inertia, I, and the polar mass moment of inertia, J. Assume that the density of steel, ρ_s, is 7800 kg/m^3.

6.2 The low-speed shaft of a wind turbine has a length, l, of 10 m and a diameter, D, of 0.5 m. It is made of steel with a modulus of elasticity of $E = 160$ GPa. It is rotating at 12.1 rpm and the turbine is generating 5 MW. Find:

(a) the applied rotor torque, assuming an overall drive train efficiency of 90%
(b) the angle of deflection
(c) the energy stored in the shaft
(d) the maximum stress in the shaft.

Hint: The rotational stiffness of a shaft, k_θ, is given by $k_\theta = IE/l$

6.3 For a helical coil spring, the spring constant, k, can be expressed in terms of the spring's dimensions and its material properties:

$$k = \frac{Gd^4}{64R^3 N_c}$$

where: $G =$ modulus of elasticity in shear, N/m^2 (lb/in^2); $d =$ diameter of wire, m (in); $R =$ radius of coil, m (in), and $N_c =$ number of coils. The average value of G for spring steel is 79.3×10^9 N/m^2 (11.5×10^6 lb/in^2). The coil radius is based on the distance from the longitudinal axis of the spring to the center of the wire making up the coil.

A spring is needed to return the aerodynamic brakes on a wind turbine blade to their closed position after deployment. The spring should exert a force of 653.9 N (147 lb) when extended 0.1524 m (6 in) (brake deployed) and a force of 111.2 N (25 lb) when the brake is closed. Space limitations dictate that the diameter of the spring be equal to 0.0381 m (1.5 inches). A spring of wire gage 7 (0.177 inches or 4.5 mm diameter) is available. How many coils would be required for this spring to have the desired force? How much would the spring coil weigh? Assume a weight density for steel of 76.815 kN/m^3 (498 lb/ft^3).

6.4 The basic rating load for ball bearings, L_R, is that load for which a bearing should perform adequately for at least one million revolutions. A general equation relates the basic rating load for ball bearings [with balls up to 1 inch (0.083 m diameter)] to a few bearing parameters:

$$L_R = f_c [n_R \cos(\alpha)]^{0.7} Z^{2/3} D^{1.8}$$

where $f_c =$ constant, between 3500 and 4500 (260 200 to 334 600 for ball diameter in m), depending on $D \cos(\alpha)/d_m$; $D =$ ball diameter, inches (m); $\alpha =$ angle of contact of the balls (often 0 deg); $d_m =$ pitch diameter of ball races [$=$(bore + outside diameter)/2]; $n_R =$ number of rows of balls; $Z =$ number of balls per row.

If two bearings are to operate for a different number of hours, the rating loads must be adjusted according to the relation:

$$L_2/L_1 = (N_1/N_2)^{1/3}$$

A bearing used on the output shaft of a wind turbine's gearbox has the following characteristics: OD $= 4.9213$ inches (0.125 m), ID (bore) $= 2.7559$ inches (0.07 m). The bearing has 13 balls, each 11/16 inches (0.01746 m) in diameter. Find the basic rating load of the bearing. Suppose that the gearbox is intended to run for 20 years, at 4000 hrs/yr. How does the bearing load rating change? Assume that $f_c = 4500$. The angle of contact of the balls is equal to zero. The shaft is turning at 1800 rpm.

6.5 A wind turbine is to be mounted on a three-legged truss tower 30 m high. The turbine has a mass of 5000 kg. The rotor diameter is 25 m. The tower is uniformly tapered and has a mass of 4000 kg. The tower legs are bolted in an equilateral pattern, 4 m apart, to a concrete foundation. Each leg is held in place by six $^3/_4$ inch bolts with coarse threads. The wind is blowing in line with one of the tower legs and perpendicular to a line through the other two legs (which are downwind of the single leg). The wind speed is 15 m/s. Find the torque in the bolts such that the upwind tower leg is just beginning to lift off the foundation. Assume that the rotor is operating at the maximum theoretical power coefficient. Hint: the torque in a bolt of this type can be approximately related to the load in the bolt by the following equation:

$$Q_B = 0.195dW$$

where $Q_B =$ bolt torque, Nm; $d =$ nominal bolt diameter, m; $W =$ load in bolt, N.

6.6 An inventor has proposed a multi-blade wind turbine. The downwind rotor is to have a diameter of 40 ft (12.2 m). Each blade is 17.6 ft (5.36 m) long, with a thickness of 3 inches (7.62 cm) and width of 8 inches (20.3 cm). Assume that the blades have a rectangular shape. The blades are to be made of wood, which can be assumed to have a modulus of elasticity of 2.0×10^6 lb/in^2 (1.38×10^{10} Pa) and a weight density of 40 lb/ft^3 (6280 N/m^3). The rotor turns at 120 rpm. Ignoring other potential problems, are any vibration problems to be expected? (Ignore rotational stiffening.) Explain.

6.7 A gearbox is to be selected for providing speedup to a generator on a new turbine. The turbine is to have a rotor diameter of 40 ft (12.2 m) and to be rated at 75 kW. The generator is to be connected to the electrical grid, and has a synchronous speed of 1800 rpm. A parallel shaft gearbox is being considered. The gearbox has three shafts (an input, intermediate, and output shaft) and four gears. The gears are to have a circular pitch of 0.7854 inches (1.995 cm). The characteristics of the gears are summarized in Table B.7. Find the diameter, rotational speed,

Table B.7 Gear teeth

Gear	Shaft	Teeth
1	1	96
2	2	24
3	2	84
4	3	28

and peripheral velocity of each gear. Find the tangential forces between gears 1 and 2 and between gears 3 and 4.

6.8 Plate clutches are often used as brakes on wind turbines. According to 'uniform wear theory', the load-carrying capability of each surface of a plate clutch can be described by the following equation for torque. The torque, Q, is simply the normal force multiplied by the coefficient of friction, μ, multiplied by the average radius, r_{av}, of the friction surface.

$$Q = \mu \frac{r_o + r_i}{2} F_n = \mu r_{av} F_n$$

where: r_o = outer diameter; r_i = inner diameter; μ = coefficient of friction; F_n = normal force.

A clutch-type brake is intended to stop a wind turbine at a wind speed 50 mph (22.4 m/s). The brake is to be installed on the generator shaft of the turbine. The turbine has the following characteristics: rotor speed = 60 rpm, generator power at 50 mph (22.4 m/s) = 350 kW, generator synchronous speed = 1800 rpm. The brake will consist of four surfaces, each with an outer diameter of 20 inches (0.508 m) and an inner diameter of 18 inches (0.457 m). The coefficient of friction is 0.3. The brake is spring applied. It is released when air at 10 lb/in² (68.95 kPa) is supplied to a piston which counteracts the springs. The effective diameter of the piston is 18 inches (0.457 m). What is the maximum torque that the brake can apply? Should that be enough to stop the turbine if the generator is disconnected from the grid? Ignore inefficiencies.

6.9 A cantilevered steel pipe tower, 80 ft (24.38 m) tall is being considered for a new wind turbine. The weight of the turbine is 12 000 lb (53.4 kN). The pipe under consideration has a constant outer diameter of 3.5 ft (1.067 m) and a wall thickness of 3/4″ (1.905 cm). The turbine is to have three blades. The nominal rotor is 45 rpm. Would the tower be considered stiff, soft, or soft–soft? Suppose that a tapered tower were being considered instead. How would the natural frequency be analyzed, using the methods discussed in this book? Assume that the density of steel is 489 lb/ft³ (76.8 kN/m³) and its elasticity is 30×10^6 lb/in² (206.9 MPa).

6.10 A wind turbine has a rotor with a polar mass moment of inertia, J, of 55 000 kg m². The equivalent stiffness of the drive train, k_θ, is 45 000 kNm/rad. The turbine is operating in high winds, such that the angular deflection, θ, in the drive train is 0.05 radians. Suddenly a brake is applied at the far end of the drive train, bringing it to a stop. What is the natural frequency of vibration (in Hz) of the rotor/drive train system as it 'rings' against the brake? Write the equation for the angular deflection as a function of time. Ignore any damping.

6.11 An operating turbine is having a problem. The emergency brake is applied, bringing the rotor to a stop in one second. The turbine has a rotor diameter of 80 m. The tower height is also 80 m. The mass of the rotor is 35 000 kg. The turbine is running at 20 rpm before being stopped.

Estimate the overturning moment at the base of the tower due to the application of the brake. Use the impulse-momentum theorem, and assume that all the mass is concentrated at a distance equal to one half of the radius from the center of the rotor.

B.7 Chapter 7 Problems

7.1 A turbine is being designed to operate in winds up to 15 m/s (at a hub height of 40 m). The turbine is to have a rotor diameter of $D = 45$ m. Consider an extreme operating gust which it

might be expected to experience at least once every 50 years. What is the wind speed at the peak of the gust? For how long would the wind speed exceed that of the nominal maximum operating wind speed? Graphically illustrate the hub height wind speed during the gust. Assume a higher turbulence site.

The IEC 50-year gust for turbines with hub heights greater than 30 m is defined by:

$$U(t) = \begin{cases} U - 0.37\, U_{gust50} \sin(3\pi t/T)[1 - \cos(2\pi t/T)], & \text{for } 0 \le t \le T \\ U, & \text{for } t < 0 \text{ and } t > T \end{cases}$$

where $T = 14\,$s and

$$U_{gust50} = 6.4\left(\frac{\sigma_x}{1 + 0.1(D/21)}\right).$$

7.2   The maximum hourly average wind speeds (m/s) recorded at Logan Airport over a sixteen year period are shown in Table B.8. Using this data, find the 50 yr and 100 yr expected maximum hourly wind speeds.

Table B.8   Annual maximum wind speeds

Year	Maximum
1989	17.0
1990	16.5
1991	20.6
1992	22.6
1993	24.2
1994	21.1
1995	19.0
1996	20.6
1997	18.5
1998	17.0
1999	17.5
2000	17.5
2001	17.0
2002	16.0
2003	17.0
2004	16.5

7.3   Show that maximum stresses due to flapping in a wind turbine blade are independent of size for turbines of similar design. For simplicity, assume a rectangular blade and an ideal rotor.

7.4   Derive the relationship for blade bending stiffness (EI) as a function of rotor radius (assuming that the tip speed ratio remains constant, the number of blades, airfoil, and blade material remain the same at different rotor radii, and that geometric similarity is maintained to the extent possible).

7.5 A wind turbine is being designed to supply power to a load which is not connected to a conventional electrical grid. This could be a water-pumping turbine, for example. This problem concerns the estimate of the power curve for this wind turbine–load combination.

The power coefficient vs. tip speed ratio of many wind turbine rotors can be described by the following simple third-order polynomial:

$$C_p = \left(\frac{3C_{p,\text{max}}}{\lambda_{\text{max}}^2}\right)\lambda^2 - \left(\frac{2C_{p,\text{max}}}{\lambda_{\text{max}}^3}\right)\lambda^3$$

where: $C_{p,\text{max}}$ = maximum power coefficient and λ_{max} = the tip speed ratio corresponding to the maximum power coefficient.

Using the assumptions that (a) the power coefficient = zero at a tip speed ratio of zero [i.e. $C_p(\lambda = 0) = 0)$], (b) the slope of the power coefficient curve is zero at, $\lambda = 0$ and (c) the slope of the power coefficient curve is also zero at tip speed ratio λ_{max}, derive the above relation.

The load the wind turbine is supplying is assumed to vary as the square of its rotational speed, N_L, which is related to the rotor speed by the gear ratio, g, so that $N_L = g\,N_R$. Using the rotor speed as reference, the load power is:

$$P_L = g^2\,k\,N_R^2$$

where k is a constant.

A closed-form expression can be derived for the power from the turbine to the load, as a function of rotor size, air density, wind speed, etc. Find that expression. Ignore the effect of inefficiencies in the turbine or the load.

For the following turbine and load, find the power curve between 5 mph (2.24 m/s) and 30 mph (13.4 m/s): $C_{p,\text{ max}} = 0.4$, $\lambda_{\text{max}} = 7$, $R = 5$ ft (1.524 m), gear ratio = 2:1 speed up, rated load power = 3 kW, rated load speed = 1800 rpm.

7.6 Assume that current 50 m blade designs have masses of 12 000 kg. Assume also that at the design aerodynamic load, the blade tip deflects in the flapwise direction 15 m from the blade root axis and the resulting root bending moment is 16 MNm. A new blade-testing laboratory is to be designed that will handle blades up to 85 m long. In order to design the new laboratory, the expected mass, tip deflection, and root bending moment of 85 m blades that will be designed in the future need to be estimated. Use the scaling relationships derived in the text or derive additional scaling relationships to estimate these quantities. Assume that the tip speed ratio remains constant, the number of blades, airfoil, and blade material remain the same at different rotor radii, and that geometric similarity is maintained to the extent possible. Assume that the blade has a uniform cross-section and a uniform distributed aerodynamic load of q. Note that in that case, the tip deflection, v, can be determined from:

$$v = \frac{qR^4}{EI}$$

7.7   The data file *ESITeeterAngleDeg50 Hz.xls* contains ten minutes of 50 Hz teeter angle data from a two-bladed 250 kW wind turbine with a downwind rotor.

(a) Determine the average, maximum, minimum, and standard deviation of the data.
(b) Graph the frequency distribution of the data (a histogram) in bins that are 0.5 degrees wide. If the hub includes dampers to damp teeter motion greater than 3.5 degrees, how many times in this ten-minute data set did the teetering hub contact the teeter dampers?
(c) Using the MiniCodes, generate and graph the power spectral density for the data using a segment length of 8192 data points. What is the dominant frequency of oscillation of the data?

7.8   The file *12311215Data.xls* includes data from full-scale testing of a 250 kW two-bladed constant-speed wind turbine with an induction generator. From kW and RPM data in *12311215Data.xls* determine the rated slip (in %) of the generator:

$$(RPM \text{ at rated kW} - Rated RPM)/(Rated RPM).$$

Rated RPM = 1800, rated kW = 250 kW

B.8 Chapter 8 Problems

8.1   Wind power has been used for centuries for productive purposes. One early yaw control system for windmills, invented by Meikle in about 1750, used a fan tail and gear system to turn the rotor into the wind. The windmill turret supported the rotor that faced into the wind. The fan tail rotor, oriented at right angles to the power-producing rotor, was used to turn the whole turret and rotor (see Figure B.8). The gear ratio between the fan tail rotor shaft rotation and the turret rotation was about 3000:1. Explain the operation of the yaw orientation system, including the feedback path that oriented the rotor into the wind.

8.2   A supervisory control system, as part of its tasks, is to monitor gearbox operation and the need for gearbox maintenance or repairs. What information should be collected by the supervisory controller and what information should be reported to the system operators?
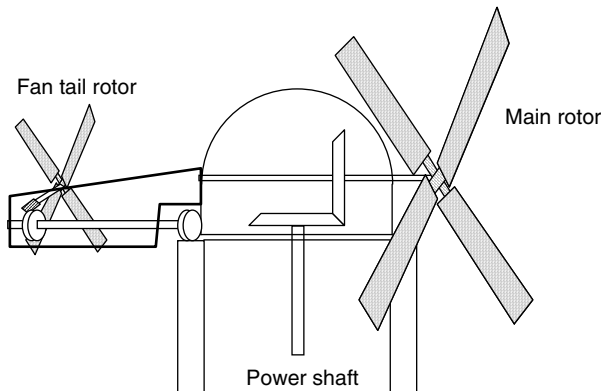
Figure B.8   Meikle yaw control

8.3 A variable-speed wind turbine control system uses blade pitch and speed variations to provide constant power to the grid. What are the tradeoffs between fluctuations in rotor speed and the time response of the pitch control system?

8.4 An accelerometer on an experimental wind turbine is used to measure tower vibration. Measurements indicate that the sensor is very sensitive to temperature variations. To complete a series of tests in cold weather, the test engineers rig up a quick electrical heating element and controller to keep the sensor's temperature constant. The system includes (1) a small electronic chip that provides a millivolt output that varies with temperature, (2) an electronic circuit, (3) a transistor, (4) a resistance heater, and (5) a housing to encase the chip, the heater, and the accelerometer. The electronic circuit provides a voltage output related to the difference between the voltages at the two inputs. A small current (milliamps) flows into the transistor that is a function of the circuit output voltage. The transistor uses that current to provide up to two amps of current to the heater. The heater maintains the temperature in the enclosure at 70 °F.

(a) What is the process that is being influenced by the control system?
(b) What elements play the roles of the sensor(s), the controller, the power amplifier, and the actuator?
(c) What, if any, are the disturbances in the system?

8.5 An accelerometer on an experimental wind turbine is used to measure tower vibration. Measurements indicate that the sensor is very sensitive to temperature variations. To complete a series of tests in cold weather, the test engineers rig up a quick electrical heating element and controller to keep the sensor's temperature constant. The closed loop transfer function of the system is:

$$\frac{T}{T_{ref}} = \frac{0.1}{s^2 + 0.5s + 0.1}$$

Plot the step response of the system to a step increase of the reference temperature of one degree F.

Hint: The step response is formed by multiplying the transfer function by $T_{ref} = 1/s$. The solution is determined by taking the inverse Laplace transform of the resulting equation:

$$T = \frac{0.1}{s^2 + 0.5s + 0.1}\left(\frac{1}{s}\right)$$

First it must be converted into a sum of terms, using the method of partial fraction expansion:

$$T = \frac{0.1}{s^2 + 0.5s + 0.1}\left(\frac{1}{s}\right) = \left(\frac{A}{s}\right) + \frac{Bs + C}{s^2 + 0.5s + 0.1}$$

Then the inverse Laplace transform of each of the terms can be determined. The fraction with the second order denominator may need to be broken into two terms to find the inverse Laplace transform.

8.6   The transfer function for a pitch control system is:

$$\frac{\Theta_m(s)}{\Theta_{m,ref}(s)} = \left(\frac{K}{s^3 + s^2 + s + K}\right)$$

The closed-loop system response to a step command to pitch the blades 1 degree is:

$$\Theta_m(s) = \left(\frac{K}{s^3 + s^2 + s + K}\right)\left(\frac{1}{s}\right) = \frac{K}{(s+a)(s^2 + bs + c)s}$$

(a) Calculate and plot the closed loop time domain system step response for $K = 0.5$, the initial choice of the designer. Comment on the closed loop system response, including damping, overshoot, and response time.
(b) For no good reason, the control system designer decides to increase the gain of the system, K. Calculate the closed loop time domain system step response for $K = 3$, the new choice of the designer.
(c) What differences are evident between the time responses, each with a different gain?

Hint: perform a partial fraction expansion of the general form of the closed loop response:

$$\frac{d}{(s+a)(s^2 + bs + c)s}$$

and find the inverse Laplace transform of each term, using the a, b, c, d variables. This symbolic form will be handy, as it will be used twice in the solution.

For parts (a) and (b), find the real root, a, of the denominator by graphing $s^3 + s^2 + s + d$, using the appropriate d. The value of s at the zero crossing is $-a$. The second order root is found using long division:

$$\frac{s^3 + s^2 + s + d}{(s+a)} = s^2 + (1-a)s + (1 - a + a^2)\,s$$

Thus, the roots of the denominator are s, $(s + a)$ and

$$s^2 + bs + c = s^2 + (1-a)s + (1 - a + a^2)$$

Insert the solutions for a, b, c, d into the general solution and plot the result.

8.7   A wind turbine manufacturer wants to design a yaw drive control system. To minimize wear on the drive gears the yaw is to be locked with a yaw brake until the ten-minute time-averaged yaw error is more than some specified amount (the 'yaw error limit'). At that point the yaw drive moves the turbine to face the previously determined ten-minute time-averaged wind direction.

(a) What consequences does the choice of yaw error limit and averaging time have on machine operation?
(b) What approach would you take to determining the quantitative tradeoffs between yaw error limit and other factors?

8.8 A pitch control system is being designed for a wind turbine. The response of the pitch control system to a unit step command has been determined to be:

$$\beta = \beta_{ref}[1 - 1.67e^{-1.6t}\cos(1.2t - 0.93)]$$

where θ_p is the pitch angle change and $\theta_{p,ref}$ is the magnitude of the commanded pitch angle change. In order to shut down the turbine in high winds the pitch must change by 16 degrees. This motion is opposed by three torques, those due to friction, the pitching moment, and inertia. The total friction torque, $Q_{friction}$, is assumed to be a constant 30 Nm, and the total pitching moment, $Q_{pitching}$, in high winds is assumed to be a constant 1000 Nm. Finally, the inertial torque is a function of the inertial moments: $Q_{inertia} = J\ddot{\beta}$. The total moment of inertia, J, of the blades is 100 kg m^2. The total power needed to pitch the blades is:

$$P_{total} = \dot{\beta}(J\ddot{\beta} + Q_{friction} + Q_{pitching})$$

What is the peak power required to pitch the blades 16 degrees (0.279 radians)?

8.9 The transfer function for the shaft torque, $Q_S(s)$, of a 250 kW grid-connected, fixed-pitch wind turbine with an induction generator as a function of the aerodynamic torque, $\alpha W(s)$, is:

$$\frac{Q_S(s)}{\alpha W(s)} = \frac{49(s + 96.92)}{(s + 97.154)(s^2 + 1.109s + 48.88)}$$

(a) This transfer function can be characterized as being the product of a first-order system, a second-order system, and a term of the form $K(s + a)$. The transfer function for second-order systems can be expressed as:

$$G(s) = \frac{\omega_n^2}{s^2 + 2\zeta\omega_n s + \omega_n^2}$$

where ω_n is the system natural frequency and ζ is the damping ratio. What is the natural frequency and damping ratio of the second-order system component?

(b) The transfer function for first-order systems can be expressed as:

$$G(s) = \frac{1/\tau}{s + 1/\tau}$$

where τ is the time constant of the first-order system. What is the time constant of the first-order system component?

8.10 A proportional–integral–derivative (PID) controller can be designed using the electrical circuit pictured in Figure B.9. The differential equation for the controller is:

$$g(t) = -\left[K_P e(t) + K_D \dot{e}(t) + K_I \int e(t)dt\right] = -\left[\left(\frac{R_2}{R_1} + \frac{C_1}{C_2}\right)e(t) + (R_2 C_1)\dot{e}(t) + \frac{1}{R_1 C_2}\int e(t)dt\right]$$

where $g(t)$ is the controller output, and R and C are the resistances and capacitances of the respective circuit elements, $e(t)$ is the error signal that is input to the controller, and the controller constants are K_P, K_I, and K_D.
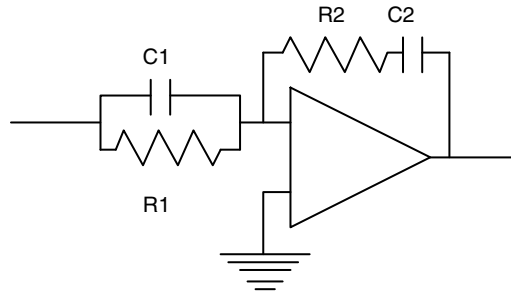
Figure B.9 PID controller

If R_1 is 10 000 Ohms, what values of R_2, C_1 and C_2 would be required for K_P, $= 10$, $K_I = 100$, and $K_D = 100$. Note resistances are in Ohms and capacitances are in Farads.

8.11 If it is required that a digital control system determine the system behavior at frequencies of at least 10 Hz

(a) What is the minimum sampling frequency that can be used?
(b) What cut-off frequency should be used to filter the input data?

8.12 The transfer function of a blade pitch controller meant to control the mean rotor power above rated on a constant speed wind turbine is approximated as:

$$\frac{\Theta}{\Theta_{ref}} = \frac{0.5}{s + 0.5}$$

Using partial fraction expansions, calculate the step response of the system. Thus, assume that:

$$\Theta_{ref} = \frac{1}{s}$$

What is the step response (the time for the blade pitch to get from 10% to 90% of the desired position)?

8.13 An engineer is studying the results of changing the blade pitch control loop gain in the controller that maintains the turbine rotor speed and generator power. The results of her simulations are provided in *WPControlNeg1.csv*, *WPControlNeg10.csv*, and *WPControl-Neg100.csv*. Note that the time steps for the case with a gain of -100 are less than in the other data sets. Determine the average and standard deviation of the blade pitch angle (degrees), the generator power (kW), and the rotor speed (rpm). Also determine the average and standard deviation of the blade pitch rate (deg/s). What difference do more negative gains make? What is happening when the gain is -100?

8.14 If the rotor speed controller on a variable-speed turbine can accurately maintain the rotor tip speed ratio at its optimum value, then the rotor C_P during constant tip speed

operation will always be at its maximum. In the real world, the control system cannot achieve this level of control. Suppose that the range of tip speeds over which the turbine operates during constant tip speed operation is described by a normal probability density distribution described by:

$$P(\lambda) = \frac{b}{\sqrt{2\pi}} e^{-\left[\frac{(b(\lambda - \lambda_0))^2}{2}\right]}$$

In this equation, b is a parameter that describes the width of the distribution of tip speed ratios. Suppose also that the $C_P(\lambda)$ within a reasonable distance from the optimum tip speed ratio can be described as:

$$C_P(\lambda) = -a(\lambda - \lambda_0)^2 + C_{P,\max}$$

In this equation, a is a parameter that determines the curvature at the top of the $C_P - \lambda$ curve. The average C_P that is described by this type of operation is then:

$$\int C_P(\lambda) P(\lambda) \mathrm{d}\lambda$$

Use Excel to numerically integrate the equation above to determine the average C_P and the percentage of optimum C_P when b is either 1 or 2 and when a is either 0.01 or 0.02. When a is fixed at 0.02, how much is the C_P improved when the distribution of the tip speeds is narrower? When b is fixed at 1, how much is the C_P improved when the top of the $C_P - \lambda$ curve has less curvature? Assume that $C_{P,\max} = 0.47$.

8.15 (a) Derive Equation (8.14) in the text. Hint, Power $=$ Torque*Speed.
(b) For a 5 MW turbine, with $R = 63$ m, $\lambda_{opt} = 8$, $C_{p,max} = 0.50$, and $\rho = 1.225 \, \text{kg/m}^3$ calculate the proportionality constant:

$$k = \frac{\rho \pi R^5 C_{p,\max}}{2(\lambda_{opt})^3}$$

B.9 Chapter 9 Problems

9.1 A wind farm is being considered for a ridge top site. Name ten or more issues that might be considered in evaluating this site.

9.2 Four identical wind turbines that are lined up in a row 12 rotor diameters apart are experiencing wind parallel to the row of wind turbines. Use Katić's wake model to determine the speed of the wind approaching each of the wind turbines. Assume that $k = 0.10$ and that the thrust coefficient is 0.7.

9.3 A wind farm developer has identified a site with unique winds. They blow all of the time from one direction and at one speed, 15 m/s. The site has enough room for two rows of turbines perpendicular to the prevailing winds. She is wrestling with which size of turbine and how

many to put in each row. All turbines being considered have the same hub height. She has developed two options:

Option 1 – this is an array of 24 1.5 MW turbines in two rows. The turbines just fit onto the site:

- Front row – 12 turbines, each with a rotor diameter of 60 m and a rated power output of 1.5 MW in 15 m/s wind speeds.
- Second row 500 m behind the first one (only 8.33 rotor diameters) – 12 turbines, each with a rotor diameter of 60 m and a rated power output of 1.5 MW in 15 m/s wind speeds.

Option 2 – this option includes slightly smaller turbines in the first row. This allows a few more turbines in the first row and reduces the velocity deficit in the second row because of the smaller rotor diameters in the first row. In addition, because of the reduced concerns of abutters, these smaller turbines can be moved 100 m closer to the front edge of the site, further reducing the wake effect. The second row is the same as in Option 1:

- Front row – 15 turbines, each with a rotor diameter of 50 m and a power output of 1.0 MW in 15 m/s wind speeds.
- Second row 600 m behind the first one – 12 turbines, each with a rotor diameter of 60 m and a power output of 1.5 MW in 15 m/s wind speeds.

To evaluate her options, the developer uses Katić's wake model to determine the wind speed behind the first row of turbines. She assumes that $k = 0.10$ and that the thrust coefficient is 8/9. She also assumes that in winds lower than the rated wind speed of 15 m/s, the power output of the turbines can be approximated by:

$$P = P_{rated}\left(\frac{U_X}{15}\right)^3$$

(a) For both options, what are the power production for each row and the total power production?
(b) If the turbines cost $800/installed kW, how much will each option cost to install (assume that no loans are needed)?
(c) If the developer's annual operation and maintenance (O&M) costs are 7% of the installed cost plus $10/MWh for maintenance, what are the total annual O&M costs?
(d) If the developer's income from the sale of energy is $30/MWh, what is her net income for a year (sales income – annual O&M costs)?
(e) If net income is the deciding factor, which option should she pursue?

9.4   A wind farm consists of two turbines, located 100 m from each other. They are operating in winds with a mean speed of 10 m/s and an integral time scale of 10 s.

(a) What does the graph of the von Karman spectrum look like (using log–log coordinates)?
(b) What is the function for the wind farm filter for these two turbines?
(c) Suppose that the spectrum of the local wind can be expressed by:

$$S_1(f) = \sigma_U^2 40e^{-40f}$$

Assume also that each wind turbine sees the same mean wind speed, U, and that the total average wind turbine power, P_N, can be expressed as $P_N = NkU$ where k is equal to 10 and N is the number of wind turbines. What is the standard deviation of the wind power from the two wind turbines? How does this compare to the standard deviation of the power from two wind turbines that experience exactly the same wind?

9.5 Consider a wind turbine generator connected to a grid system (see Figure B.10) with a line-neutral system voltage, V_S. The voltage at the wind turbine, V_G, is not necessarily the same as V_S. The distribution system resistance is R, and the distribution system reactance is X.
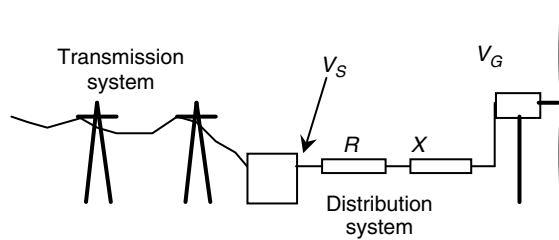
Figure B.10

The real generated power is P and the reactive power consumed by the wind turbine generator is Q. Suppose $R = 8.8\,\Omega$, $X = 4.66\,\Omega$, $Vs = 11\,kV$, $P = 313\,kW$, $Q = 162\,kVAr$, and the power factor at the generator is $pf = 0.89$. Determine the voltage difference between the grid and the generator, the voltage drop as a percentage of the grid voltage, the fault level at the generator, and the installed generator capacity as a percentage of the fault level.

9.6 A wind turbine is connected to an 11 kV distribution line. The magnitude of the harmonic voltages, c_n, at the point of common connection of the wind turbine and other grid users are listed in Table B.9.

Table B.9

n	1	2	3	4	5	6	7	8	9	10	11	12	13	14	15
c_n, Volts	11000	120	0	85	15	0	99	151	0	12	216	0	236	80	0

What is the harmonic distortion of each harmonic and the total harmonic distortion? Are these within the allowable IEEE 519 limits?

9.7 The data file '*Site1 v Site2 For MCP.csv*' includes five years of wind speed and direction data from Site 1 (the reference site) and Site 2 (the candidate or project site). Data that were determined to be incorrect (due to sensor icing or other problems, for example) are indicated by -999. Use these data to determine the appropriate variance MCP relationship between the two sites using three different years of concurrent data: 1999, 2001, and 2002. What are the slopes and offsets determined from these three different concurrent data sets? What is the data recovery of the data sets used for the analysis expressed as a percentage of a year's worth of data? What might be the cause of the difference between the results for different years?

9.8   A study determines that the maximum chord size in meters of blades can be expressed as:

$$c = 0.0005L^2 + 0.024L + 1.4$$

where L is the blade length and the mass of blades in kilograms can be approximated as

$$m = 9.043L^2 - 340L + 6300$$

The clearance under the bridges on the only road to a proposed project is 5.5 m and the trailer carrying the blades to the project must maintain a clearance between the blade and the road of 1 m. Additionally, the overpasses on the road are only rated for loads (tractor trailer plus cargo) of 36 000 kg. Note that the empty tractor trailer has a mass of 16 000 kg.

(a) If the underpass clearances are determined by the maximum blade chord, what is the largest blade that can be transported to the project that will fit under the road underpasses and over the bridges?
(b) Final access to the project is along a narrow dirt road. The minimum radius of curvature of the road, r, that will accommodate a blade of length L when the road width is w is:

$$r = \frac{\left(\frac{L}{2}\right)^2 - w^2}{2w}$$

What is the minimum radius of curvature that will accommodate the blade chosen in part (a) if $w = 8$ m?

9.9   A developer decides to install a 45 turbine offshore wind farm. The wind map of the proposed project is shown in the Figure B.11. The rows are 2 km apart in the north–south
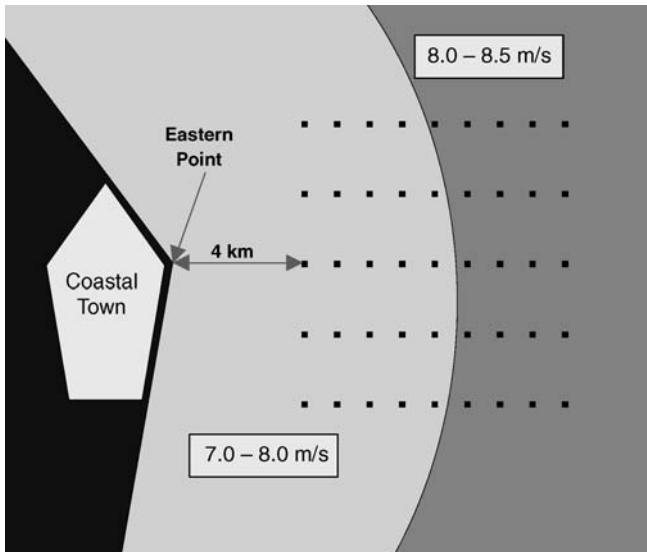
Figure B.11   Map of proposed project

direction and 1 km apart in the east–west direction. The closest turbine to land is 4 km to the east of Eastern Point.

The wind map shows the expected range of mean hub height wind speeds at the site in each shaded area. The Weibull shape factors found at this site are 2.4. As the permitting for the project moves forward, the developer realizes that he will need to eliminate four turbines in the higher wind speed region due to concerns at archeologically valuable shipwrecks nearby. He also decides to eliminate all turbines within 5.7 km of Eastern Point to avoid conflicts with lobstermen who are concerned about environmental damage to lobster beds. What is the expected range of average project capacity factors if the turbines that will be used have a rated power of 4.0 MW above 13 m/s and have a cubic power curve from 4 m/s to rated and a cut-out wind speed of 24 m/s? Assume array losses of 15%.

9.10   A proposed wind farm will have 18 wind turbines in a row. Each will be 8 rotor diameters apart. The wind speeds in each 30 degree direction bin are characterized in Table B.10. The turbine that will be used in this project generates rated power of 2.0 MW above 11 m/s and has a cubic power curve from 4 m/s to rated and a cut-out wind speed of 24 m/s. The array losses are assumed to be 15% when the wind is from the north or south (0 or 180 degrees) and 0% when the wind is from other directions. Additionally, it is assumed that other losses (downtime, electrical losses, weather conditions, etc.) will be 20%. Under these assumptions, what will the total project capacity factor of the wind farm be? After consulting the manufacturer, the developer learned that the wind turbine manufacturer would not honor the turbine warranty if the wind turbines were operated when the wind was directly along the row of the turbines (in direction sector bins of 0 and 180 degrees) due to excessive wake turbulence. Given this new information, how much can the developer expect the capacity factor at this wind farm to be to preserve the warranty on his turbines?

Table B.10   Wind speed and direction data

Direction bin center	Mean wind speed, m/s	Weibull shape factor	Percentage of time
0	7.9	2.0	8.0
30	7.0	2.1	6.0
60	6.7	2.0	4.0
90	5.6	2.1	10.0
120	6.9	2.3	8.0
150	7.2	2.1	7.0
180	8.8	2.2	7.0
210	9.2	2.1	10.0
240	9.0	2.0	8.0
270	8.3	2.1	14.0
300	8.4	2.1	12.0
330	7.6	2.2	6.0

9.11   The data file *HourlyLoadAndPowerOneYearGW.csv* contains average hourly electrical load (GW) in a utility control area and the wind power that is expected to be generated by future planned wind farms.

(a) Determine the total GWh, mean, maximum, minimum, and standard deviation of the grid load and the generated wind power. Graph the load duration curve of the utility with the existing load (before the installation of the wind plants).
(b) Determine the total GWh, mean, maximum, minimum, and standard deviation of the net load once the wind power plants are installed. Graph the load duration curve of the net load of the utility after the installation of the wind plants.
(c) How much does the mean electrical load decrease with the installation of the wind power plants? How much does the standard deviation of the load seen by the grid operators (the net load) increase with the inclusion of wind? How much does the peak net load change?

B.10 Chapter 10 Problems

10.1   An isolated power system serving the community of Cantgettherefromhere uses a 100 kW diesel generator. The community plans to add 60 kW of wind power. The hourly average load and power from the wind turbine over a 24-hour period are detailed in Table B.11. The diesel generator has a no-load fuel usage of 3 liters per hour and an additional incremental fuel use of 1/4 liter per kilowatt-hour.

For the day in question, using the hybrid system design rules, determine:

(a) The maximum renewable energy that can possibly be used in an ideal system.
(b) The maximum renewables contribution without storage, and the maximum with storage.
(c) The maximum fuel savings that can be achieved.
(d) The minimum diesel fuel use that can be achieved with intelligent use of storage and controls.

Table B.11   Diesel system load data

Hour	Load (kW)	Wind (kW)	Hour	Load (kW)	Wind (kW)
0	25	30	13	95	45
1	20	30	14	95	50
2	15	40	15	90	55
3	14	30	16	80	60
4	16	20	17	72	60
5	20	10	18	60	48
6	30	5	19	74	50
7	40	5	20	76	55
8	50	15	21	60	60
9	70	20	22	46	60
10	80	25	23	35	55
11	90	40			
12	85	45			

10.2 Based on the analysis in Problem 10.1 and other input, the community of Cantgetther-efromhere has upgraded its power system. The hybrid power system includes a 100 kW diesel generator, 100 kW of installed load, 60 kW of wind power, a 100 kW dump load, and energy storage with 100 kWh capacity. The hourly average load and power from the wind over a 24-hour period have remained the same and are listed in Table B.11.

Assume that the mean hourly data accurately describe the load and power from the wind and that fluctuations about the mean load are handled by the energy storage. Determine the hourly energy flows in the system for the following system control and operating approaches.

(a) Diesel-only system – in this baseline system, the diesel provides all of the power to the load. The diesel provides power down to 0 kW with no provision to ensure a minimum diesel load to avoid diesel engine wear.
(b) Minimum diesel – in this system minimizing diesel power takes priority, except that the diesel may not be shut off and must run at a minimum of 30 kW to ensure long diesel engine life. Thus, the system operates by the rules:
1. The minimum diesel power is 30 kW.
2. Only the minimum diesel power that is needed above 30 kW is used (no power above 30 kW is used to fill up the storage).
3. Storage can only be used between 20 and 95 kWh of capacity, to maximize storage efficiency and battery life.
4. Storage capacity starts at 50 kWh.
5. The sum of the energy into the power sources in the system (diesel, wind, battery) must equal the sum of the energy into the power sinks in the system (the load, dump load, and battery).
6. If there is excess energy in the system it is first stored, if possible, and dumped only if necessary.
(c) Diesel shut off – in this system a rotary inverter between the batteries and the grid provides reactive power and the diesel can be shut off. It shuts off whenever possible, but when running, needs to be at a minimum load of 30 kW. When running it is also used to fill up the storage to use the fuel most efficiently. The battery level is maintained between 20 and 90 kWh. This ensures that there is adequate capacity to handle fluctuating loads when there is no diesel in the system. Thus, the system operates by the rules:
1. The diesel can be shut off.
2. The minimum diesel power is 30 kW when the diesel is running.
3. When the diesel is running, the storage is also filled up if possible to improve diesel fuel efficiency.
4. Storage can only be used between 20 and 90 kWh of capacity, to maximize storage efficiency and battery life.
5. Storage capacity starts at 50 kWh.
6. The sum of the energy into the power sources in the system (diesel, wind, battery) must equal the sum of the energy into the power sinks in the system (the load, dump load, and battery).
7. If there is excess energy in the system it is first stored, if possible, and dumped only if necessary.

Specifically, for each operating approach, determine how much energy is supplied by the diesel over the 24-hour period and the reduction in diesel power compared to the diesel-only case.

10.3 This problem concerns a hypothetical island wind/diesel system. Wind and load data for the island for one year are in the files *Wind_TI.txt* and *Load_TI.txt*. Assume that the wind turbines available are (1) an AOC 15–50, (2) one with twice the output, or (3) one with four times the output. The power curves for these turbines are, respectively, *AOC_pc.csv*, *AOC_pc_x2.csv* and *AOC_pc_x4.csv*.
   The diesel to be considered is one rated at 100 kW, with no-load fuel consumption of 2 fuel units per hour and full-load fuel consumption of 10 units per hour.
   Using the MiniCodes, your job is to find: (1) the average wind power, (2) the useful wind power, (3) the average dumped power, and (4) the average fuel use for the three different turbine options , and for storage of 0 kWh, 100 kWh, and 1000 kWh.
   What do the results suggest about the usefulness of storage?

10.4 The ten-minute average wind speed at an offshore buoy is measured to be 8.5 m/s at an elevation of 10 m. The buoy is 10 km from land in the direction of the oncoming wind.

(a) If the surface roughness length is assumed to be 0.0002 m, what is the mean wind speed at 80 m?
(b) If the Charnock constant, A_C, is assumed to be 0.018 and $C_{D,10}$ is 0.0015, what is the mean wind speed at 80 m, assuming that the friction velocity is given by $U_* = U_{10}\sqrt{C_{D,10}}$?
(c) Assume that the water depth is 20 m, the wave height is 3 m, and the peak period of the waves is 9 s. What is the mean wind speed at 80 m in this case?

10.5 Derive the equation for total inertial force on a monopile (see Equation (10.15)). Note: the equation for the acceleration as a function of depth is: $\dot{U}_W(z) = \frac{g\pi H}{L}\frac{\cosh(k(z+d))}{\cosh kd}\cos(\theta)$ Assume that the depth is much greater than the wave height.

10.6 A wind turbine has rotor diameter of 90 m. It is installed on a monopile with a diameter of 4 m in water 15 m deep. The wind speed is 12 m/s and the wave height is 2 m. Estimate the force due to the wind and the maximum force due to waves. Use the Airy model for the waves and assume that the rotor thrust coefficient is the one corresponding to the Betz power coefficient. Assume that the inertia coefficient is 2.0 and the drag coefficient 1.5. (Assume that the maximum forces due to drag and inertia occur at the same time.)

10.7 A small community has 2000 residents and each of them consumes an average of 100 liters of water per day. They have access to an aquifer 100 m below ground level and are considering acquiring a wind electric water pump to bring the water to the surface. What would be the rated power of a wind turbine (kW) that would pump, on average, an amount of water equal to what the community uses? Assume that the capacity factor of the wind turbine is 0.25 and that the efficiency of the water pump is 80%.

10.8 An island community has 2000 residents and each of them consumes an average of 100 liters of water per day. The community is considering acquiring a wind-powered desalination

plant to produce pure water from sea water (density $= 1020\,\text{kg/m}^3$). The sea water is $20\,°\text{C}$ and has salinity of 38 g/kg. What size wind turbine would produce, on average, an amount of fresh water equal to what the community uses? Assume that the capacity factor of the wind turbine is 0.25, and that the desalination plant uses five times the minimum theoretical amount of power.

10.9 A lead acid battery has a nominal capacity of 200 Ahrs. The constant c is equal to 0.5 and the rate constant k is equal to 2.0. Find the apparent capacity of the battery (charge removed) and the corresponding current when it is discharged in (a) 1 hour and (b) 10 hours.

10.10 A bank of 12 lead acid batteries in series is being used to supply a resistive load with nominal power consumption of 1200 W at 120 V. The voltage constants for each battery (in discharging) are $E_0 = 12\,\text{V}, A = -0.05, C = -0.5, D = 1$. The internal resistance is $R_{int} = 0.1$ Ω. At a certain point the batteries are 70% discharged. Find the terminal voltage of the batteries and the actual power consumption at this point.

10.11 A natural gas-fired turbine operating on a Brayton cycle is used with a wind-powered compressed air storage facility. The cycle has the following characteristics: the temperature at the input to the compressor is $27\,°\text{C}$ and at the input to the turbine the temperature is $727\,°\text{C}$. The maximum pressure is 2 MPa and the minimum pressure is 100 kPa.

(a) Find the heat input from the natural gas if the net output of the gas turbine is 1 MW and the compressed air from the wind turbine is not being used.
(b) Now assume that the gas turbine's compressor is not being used, but the compressed air is coming from the compressed air storage. The compressed air storage is being continually recharged and the pressure remains constant at 2 MPa. All other things being the same, what would be the net power output of the gas turbine now? Assume that the constant pressure heat capacity of air is 1.005 kJ/kg K and that the ratio of c_p to c_v (i.e. k) is equal to 1.4.

10.12 An island community has 2000 residents, each of whom uses, on average, 8 kWh/day. The electricity is presently produced by a diesel generator, but they are considering acquiring a wind turbine. They would like to incorporate pumped water storage in their plans. An open spot on top of a hill could be dug out to form a circular reservoir. The reservoir could be 30 m in diameter and 5 m deep. The hill is 70 m above the town. A reservoir of similar size could be next at the same elevation as the town. How many hours could the upper reservoir supply the average electrical load of the community when discharging to the lower reservoir?

10.13 The famous dirigible Hindenburg had a volume of approximately 199 m^3. It was filled with hydrogen to give it buoyancy. Assume that the pressure inside was 100 kPa and that the temperature was $15\,°\text{C}$. How much hydrogen did the Hindenburg contain? How much energy (kWh) would it take to produce that hydrogen by electrolysis of water, assuming an electrolyzer efficiency of 65%? How long would it take to produce that hydrogen using a 1.5 MW turbine operating at full power?

10.14   A hydrogen-powered bus has four roof-top mounted storage cylinders with a total capacity of 1.28 m³. When full, the pressure is 45 MPa. How many times could the cylinders be refilled with the hydrogen that would fill the Hindenburg, as found in Problem 10.13? Assume that the cylinders are completely emptied before being refilled and assume that the ideal gas law is applicable.

B.11 Chapter 11 Problems

11.1   The first unit of a new wind turbine costs $100 000. The system is estimated to follow an $s = 0.83$ learning curve. What is the cost of the 100th unit?

11.2   Estimate the progress ratio (s) of modern utility-scale wind turbines. Use the time period of about 1980 to the present.

11.3   A small 50 kW wind turbine with an initial cost of $50 000 is installed in Nebraska. The fixed cost ratio is 15% and the annual operation and maintenance ($C_{O\&M}$) is 2% of the initial cost. This system produces 65 000 kWh/yr (AkWh). Determine the cost of energy (COE) for this system.

11.4   A small wind machine with a diameter of 6 m is rated at 4 kW in an 11 m/s wind speed. The installed cost is $10 000. Assuming Weibull parameters at the site to be $c = 8$ m/s and $k = 2.2$, it is claimed that the capacity factor is 0.38.

   The interest rate is 11%, the loan period is 15 years, the life is 20 years and the discount rate is 10%. Find the cost per unit area, per kW, and the levelized cost per kWh. You do not have to include factors such as inflation, tax credits, or operation and maintenance costs.

11.5   The estimated cost and savings from the purchase and operation of a wind machine over 20 years are given in Table B.12.

(a) Compare the total costs with the total savings.
(b) Find the present values of the cost and savings. Use an annual discount rate of 10%. Would this be a good investment?

Table B.12   Annual wind turbine costs

Year	Costs	Savings	Year	Costs	Savings
0	$9000		11	227	669
1	127	2324	12	241	719
2	134	1673	13	255	773
3	142	375	14	271	831
4	151	403	15	287	894
5	160	433	16	304	961
6	168	466	17	322	1033
7	180	501	18	342	1110
8	191	539	19	362	1194
9	202	579	20	251	1283
10	214	622			

(c) Determine the payback period for the wind machine.
(d) What is the breakeven cost of the machine?
(e) Estimate the cost of energy produced by the wind machine if it is expected to produce 9000 kWh annually.

11.6   Consider the application of a small 1 kW wind turbine with a capital cost of $2500. The installation and set-up cost raises its total installed cost to $4500. Assume that the $2500 capital cost is to be paid for with a 15-year, 7% loan. Also assume that O&M costs will be $200 per year. Estimate the (simplified) cost of energy) over the 15-year period if the capacity factor (CF) is 0.30.

11.7   A 2.4 MW wind turbine has an installed cost of 2.4×10^6. Assume that the annual operating and maintenance costs are 2% of the initial installed cost. The wind regime at this site results in a capacity factor (CF) of 0.35. It is also assumed that the lifetime of this turbine is 25 years and that the electrical output can be sold for $0.05/kWh. For a 5% discount rate calculate the following economic parameters for this system:

(a) Simple payback period.
(b) The net present value of the savings (NPV_S).
(c) The benefit–cost ratio (B/C)
(d) The internal rate of return (IRR)
(e) The levelized cost of energy (COE_L)

11.8   A proposed wind farm installation is based on the use of thirty 2 MW wind turbines. The installed capital cost is estimated at $1000/kW and the annual operation and maintenance costs are estimated to be 3% of the original capital cost. Financing for the project is to come from two sources: (1) A 20-year loan at 7% (75%), and (2) an equity investment that has a return of 15% (25%) . The average capacity factor of the wind farm is estimated to be 0.35. Determine the estimated cost of energy ($/kWh) from this proposed wind farm.

11.9   This problem is intended to assess the relative economic merits of installing a wind–diesel system rather than a diesel-only system at a hypothetical location. Assume that the existing diesel is due for replacement and that the annual system demand will remain fixed during the lifetime of the project.
   Your problem is to calculate the levelized cost of energy for the diesel-only and for the wind–diesel system. The following system and economic parameters hold:

System

Average system load	96 kW (841 000 kWh/yr)
Diesel rated power	200 kW
Mean diesel usage – no wind turbine generator	42.4 l/hr (371 000 l/yr)
Wind turbine rated power	100 kW
Average annual wind speed	7.54 m/s
Annual wind speed variability	0.47
Average wind turbine power	30.9 kW
Useful wind turbine power (based on 25% lower limit on diesel loading)	21.1 kW
Mean diesel usage with WTG	34.8 l/hr (305 000 l/yr)

Economics

Wind turbine cost	$1500/kW installed
Diesel cost	$350/kW installed
System life	20 yr
Initial payment	$30 000
Loan term	10 yr
Interest	10%
General inflation	5%
Fuel inflation	6%
Discount rate	9%
Diesel fuel cost	$0.50/l
Wind turbine O&M cost	2% of capital cost/yr
Diesel O&M cost	5% of capital cost/yr

B.12 Chapter 12 Problems

12.1   Despite its positive environmental attributes, not everyone is in favor of wind power development. Your assignment here is to perform an Internet search and summarize the view points of three different organizations that actively oppose wind projects in one way or another. Make sure that you list their objections. You should also comment on their technical validity.

12.2   Assume that you are planning the development of a small wind farm (say ten turbines of 500 kW) in a rural area. Describe how you would reduce the visual impact of this project. Also prepare a list of the tools that could be used for assessing the impact of this project on the surrounding environment.

12.3   Researchers from Spain (see Hurtado *et al.*, 2004 Spanish method of visual impact evaluation in wind farms. *Renewable and Sustainable Energy Reviews*, **8**, 483–491.) have developed a method that gives a numerical value for a factor that represents a coefficient of the affected population. Review this paper and give an evaluation of the use of this methodology.

12.4   Estimate the sound power level for a three-bladed, upwind wind turbine with the following specifications: rated power = 500 kW, rotor diameter = 40 m, rotor rotational speed 40 rpm, wind speed = 12 m/s.

12.5   Suppose the sound pressure level at a distance of 100 m from a single wind turbine is 60 dB. What are the sound pressure levels at a distance of 300, 500, and 1000 m?

12.6   Assuming the same turbine as in the previous problem, what are the sound pressure levels at a distance of 300, 500, and 1000 m for two, five, and ten turbines?

12.7   Two wind turbines emitting 105 dB (A) at the source are located 200 m and 240 m away from a location of interest. Calculate the sound pressure level (in dB(A)) at the point of interest from the combined acoustic effect of the two turbines. Assume a sound absorption coefficient of 0.005 dB(A)/m.

12.8 A wind turbine has a measured sound power level of 102 dB at 8 m/s. Plot the sound pressure level as a function of distance using both hemispherical and spherical noise propagation models. Do this for sound absorption coefficients of 0.0025, 0.005, and 0.010 (dB(A) m^{-1}).

12.9 For electromagnetic interference problems once the (bistatic) radar cross-section (σ_b) is known, the polar coordinate r can be calculated for a required interference ratio (C/I). For a TV transmitter operating in an urban environment, σ_b was experimentally determined to be 24 and 46.5 dBm^2 in the backscatter and forward scatter regions. Determine the value of r in both the backscatter and forward scatter regions for required values of C/I equal to 39, 33, 27, and 20 dB.

Appendix C

Data Analysis and Data Synthesis

C.1 Overview

This appendix concerns topics in the analysis or synthesis of time series data. Analysis is used to make sense of data from tests and other sources. Conversely, data are often synthesized for input to simulation models. The next two sections summarize some of the analysis and synthesis methods that are most commonly used in wind energy systems engineering.

C.2 Data Analysis

Much of the data encountered in wind energy engineering has random aspects and/or sinusoidal aspects. This is often the case with wind speed turbulence and its effects, structural vibrations, ocean waves, harmonics in electrical power systems, and noise. This section summarizes some of the methods used in analyzing these data.

Ideally, any data would be continuous and would be denoted by $x(t)$. In fact, real data files as used in wind energy applications are sampled time series rather than being continuous. A single time series is referred to as a data record. The expression for a data record corresponding to $x(t)$ is:

$$x_n = x(n\Delta t); n = 0, 1, 2, \ldots, N-1 \tag{C.1}$$

where:

N = number of points in data record
$\Delta t = T/N$ = sample interval
T = time length of period
n = index (point number)

Much of the discussion below is, strictly speaking, only applicable to data that are stationary and ergodic. This means that the data record is statistically similar over time and that any data

record is statistically similar to any other from the same process. To the extent that the data do not meet those criteria, the analytic results will be somewhat approximate. It should also be noted that, in general, data records should have their means subtracted out and any trends removed before the analysis described below is undertaken. A trend here refers to a relatively steady increase or decrease in the mean over the time interval of interest. Finally, all real data records have a finite length. This can result in artifacts appearing in the results. These artifacts can be largely eliminated through the use of 'windowing', which is also described below.

C.2.1 Autocorrelation Function

The autocorrelation function for sampled data is found by multiplying each value in the record by values in the same record, offset by a time 'lag', and then summing the products to find a single value for each lag. The resulting sums are then normalized by the variance to give values equal to or less than one. The normalized autocorrelation function for time series x_n with N points and variance σ_x^2 is given by:

$$R(r\Delta t) = \frac{1}{\sigma_x^2(N-r)} \sum_{n=1}^{N-r} x_n x_{n+r} \qquad (C.2)$$

where $r =$ lag number and $\Delta t =$ time interval between lags.

Note that the form of the autocorrelation function used here is sometimes referred to as the normalized autocorrelation function or autocorrelation coefficient. If it is not divided by the variance, then it is said to be unnormalized. An example of an autocorrelation function was given in Chapter 2 (Figure 2.16).

C.2.2 Cross Correlation Function

The cross correlation function provides a measure of how similar two records, x_n and y_n, are as they are shifted in time. The equation describing the cross correlation (Equation (C.3)) is similar to the autocorrelation, except that two data records are used instead of one.

$$R_{xy}(r\Delta t) = \frac{1}{\sigma_x^2(N-r)} \sum_{n=1}^{N-r} x_n y_{n+r} \qquad (C.3)$$

C.2.3 Power Spectral Density

Sinusoidally varying data are often analyzed in the frequency domain. The frequency domain is most often considered via the power spectral density (or 'psd') of a data file. The psd retains information regarding the magnitude of various frequency components, but eliminates the phase relations, which are usually irrelevant. In particular, psds are used to identify frequencies of interest and to see which frequencies are most prominent (i.e. have the most energy). With the help of a psd it is often relatively easy to see where there is an excitation or a natural frequency.

A psd may be found from time series data by applying a Fourier transform. Most commonly an algorithm known as the Fast Fourier Transform (FFT) is used. This method is described in detail in a variety of sources, such as Bendat and Piersol (1993). The following provides a summary.

The basis of this method is the observation that a time series may be expressed as a sum of sines and cosines, as shown in Equation (C.4).

$$x_n = A_0 + \sum_{q=1}^{N/2} A_q \cos\left(\frac{2\pi q n}{N}\right) + \sum_{q=1}^{(N/2)-1} B_q \sin\left(\frac{2\pi q n}{N}\right) \tag{C.4}$$

The coefficients (known as Fourier coefficients) are found as follows:

$$A_0 = \sum_{n=1}^{N} x_n = \bar{x} = 0$$

$$A_q = \frac{2}{N} \sum_{n=1}^{N} x_n \cos\left(\frac{2\pi q n}{N}\right) \quad q = 1, 2, \ldots, \frac{N}{2} - 1$$

$$A_{N/2} = \sum_{n=1}^{N} x_n \cos(n\pi) \tag{C.5}$$

$$B_q = \sum_{n=1}^{N} x_n \sin\left(\frac{2\pi q n}{N}\right) \quad q = 1, 2, \ldots, \frac{N}{2} - 1$$

Equation (C.4) is actually the discrete inverse Fourier transform of $X(f)$, which is discussed below. Equation (C.4) can also be written more succinctly using complex notation as shown in Equation (C.6).

$$x_n = \frac{1}{N} \sum_{k=1}^{N} X_k \exp\left[j\frac{2\pi k n}{N}\right] \tag{C.6}$$

where X_k are Fourier coefficients corresponding to the As and Bs above. They are explained in more detail below.

The general equation for the Fourier transform, $X(f)$, of a continuous real or complex valued function, $x(t)$, over an infinite range for some frequency, f, is:

$$X(f) = \int_{-\infty}^{\infty} x(t)e^{-j2\pi ft} dt \tag{C.7}$$

The Fourier transform over some time period, T, is:

$$X(f, T) = \int_{0}^{T} x(t)e^{-j2\pi ft} dt \tag{C.8}$$

The discrete form of Equation (C.8) is a Fourier series:

$$X(f, T) = \Delta t \sum_{n=0}^{N-1} x_n e^{-j2\pi fn\Delta t} \tag{C.9}$$

Selecting discrete frequencies, $f_k = k/T = k/(N\,\Delta t)$, where $k = 1, 2, \ldots, N-1$, results in the following expression for the Fourier coefficients:

$$X_k = \frac{X(f_k)}{\Delta t} = \sum_{n=0}^{N-1} x_n e^{-j\frac{2\pi k n}{N}} \tag{C.10}$$

The classical method to calculate the Fourier coefficients would be to apply Equations (C.5). This process would involve approximately N^2 multiplications and additions. To speed up the process, the Fast Fourier Transform (FFT) has been developed to calculate the coefficients.

The FFT is far faster than the standard Fourier transform, but it does have some limitations. The most significant of these is that FFTs can only be carried out on data files which are powers of two in length. This could consist of files that have 256, 512, 1024, etc. points. Accordingly, any file that is not that length must be truncated (or sometimes augmented) to have an acceptable length.

The equations for the FFT will not be presented here. It is sufficient to note that they may be found in a number of sources (Bendat and Piersol, 1993, for example), and in particular the equations have been incorporated in a number of software packages, such as Microsoft Excel and MatLab®, among others.

With the Fourier transform at hand, the psd may be readily calculated. The psd of real-valued data, denoted $S_{xx}(f)$, can be obtained from the FFT by multiplying the transform by its complex conjugate, $X^*(f,T)$, and normalizing it as follows:

$$S_{xx}(f) = \frac{1}{T}|X(f,T)|^2 = \frac{1}{T}X(f,T)X^*(f,T) \tag{C.11}$$

Often the data are divided into multiple segments in order to help eliminate spurious results. When the data have been divided into multiple segments, an FFT is performed on each segment. The psd is found by averaging the values obtained from each segment:

$$S_{xx}(f) = \frac{1}{n_d T}\sum_{i=1}^{n_d}|X_i(f,T)|^2 \tag{C.12}$$

where n_d = number of segments into which the data have been divided.

When the psd is calculated with the FFT, half of the points are actually redundant. In particular, $S(f) = S(N-f)$. Therefore, the second half of the points are eliminated from further consideration.

It is also important to note that some software packages do not apply standard normalization to the FFT, which should result in the integral of the psd being equal to the variance. In those situations, the FFT must be normalized separately. For example, the FFT obtained from Excel must be divided by the number of points.

It is also worth noting that the power spectrum is equal to the Fourier transform of the unnormalized autocorrelation function.

C.2.3.1 Side Lobe Leakage and Windowing

All real data time series have a finite length. A result of this is that the Fourier transform will introduce additional energy into certain frequencies. These spurious contributions can be largely eliminated through the use of windowing.

The origin of the problem can be seen as follows. A finite length time series over time T can be considered to be an infinitely long time series, $v(t)$, multiplied by a rectangular window $u(t)$ which is equal to one or zero, as shown in Equation (C.13):

$$u(t) = \begin{cases} 1 & 0 \le t < T \\ 0 & \text{otherwise} \end{cases} \tag{C.13}$$
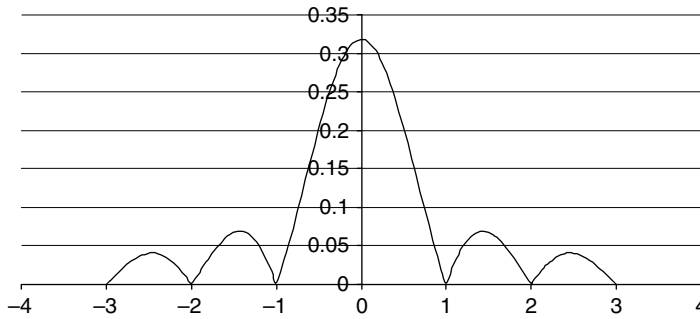
Figure C.1 Magnitude of Fourier transform of rectangle

According to this formulation, the time series of interest, $x(t)$, is given by:

$$x(t) = u(t)v(t) \tag{C.14}$$

It can be shown that the Fourier transform of $x(t)$, $X(f)$, is given by the convolution of the Fourier transforms of $u(t)$ and $v(t)$, $U(f)$ and $V(f)$, as shown in Equation (C.15) (where α is an integrating variable).

$$X(f) = \int\limits_{-\infty}^{\infty} U(\alpha)V(f-\alpha)\mathrm{d}\alpha \tag{C.15}$$

The Fourier transform of a rectangle can readily be shown to be as given in Equation (C.16). The absolute value of Equation (C.16) is illustrated in Figure C.1.

$$U(f) = T\left(\frac{\sin(\pi fT)}{\pi ft}\right)e^{-j\pi fT} \tag{C.16}$$

The 'lumps' on either side of the -1 and 1 are known as 'side lobes'. It is these side lobes which introduce spurious effects (artifacts) in the psd. Specifically, they cause greater energy to appear at certain frequencies than should actually be the case. These effects can be largely eliminated with specially shaped windows. The windows can take a variety of forms. The basic approach is to taper the time series data near the beginning and end so as to decrease the magnitude of the side lobes. A common window is the cosine squared, or Hanning, window described in Equation (C.17).

$$u_h(t) = \begin{cases} 1-\cos^2\left(\dfrac{\pi t}{T}\right) & 0 \leq t \leq T \\ 0 & \text{otherwise} \end{cases} \tag{C.17}$$

C.2.3.2 Graph Formats for Power Spectra

Power spectra may be plotted simply as the spectrum vs. frequency with conventional axes. In that case the units on the y axis are (original units)^2/Hz and the x axis units are Hz. In addition,

the area under the graph between any two frequencies corresponds to the amount of variance associated with that frequency range. Using that method in some situations, such as with wind data, however, most of the variance is concentrated in a small portion of the graph. In such cases, the spectrum is often plotted with a log x axis and sometimes with a log y axis as well. Another common method of depicting the spectrum is to plot the frequency multiplied by the psd on the y axis vs. the natural log of the frequency on the x axis. This method is useful because the areas on the graph between any two frequencies are again equal to the variance associated with that range of frequencies.

C.2.4 Cross Spectral Density

The cross spectral density provides a measure of the energy at various frequencies of two different records. It is given by:

$$S_{xy}(f_k) = \frac{1}{N\Delta t}\left[X^*(f_k)Y(f_k) \quad k = 0, 1, 2, \ldots, N-1\right] \tag{C.18}$$

where $X(f)$ and $Y(f)$ are the Fourier transforms of $x(t)$ and $y(t)$ and f_k are the discrete frequencies.

C.2.4.1 Coherence

The coherence function is the square of cross spectral density normalized by the product of the psds of the two data records:

$$\gamma_{xy}^2(f_k) = \frac{\left|S_{xy}(f_k)\right|^2}{S_{xx}(f_k)S_{yy}(f_k)} \tag{C.19}$$

An exponential decay function for coherence is often assumed, as was the case for wind speed in Chapter 9 (Equation (9.10)).

C.2.5 Aliasing

Aliasing is the result of digitally sampling data at frequencies slower than the frequency of the information in the data. Aliasing can result in the representation of higher frequency data as lower frequency data. For example, Figure C.2 shows a 2 Hz sinusoid that represents information to be measured and the resulting signals if it is sampled at less than 2 Hz. It can be seen that sampling the 2 Hz sinusoid at 1 Hz provides data that appear to be constant. Sampling the same 2 Hz sinusoid at frequencies near 1 Hz, but not exactly 1 Hz, provides data that appear to vary very slowly.

The effects of aliasing show up in frequency analysis of measured data also. Figure C.3 shows two spectra of an analog signal that includes two frequencies, one at 1 Hz and one at 1000 Hz. The original data were sampled at two different rates (312 Hz and 10 000 Hz) before the spectra were created. The spectrum of the data that have been sampled at 10 000 Hz clearly shows that there are variations at 1 and 1000 Hz. In the spectrum of the data that were sampled at 312 Hz, the content of the signal at 1000 Hz has been shifted to 63 Hz. In the later case, the signal has information at frequencies greater than half of the sampling frequency (156 Hz). That frequency, half of the sampling frequency, is called the Nyquist frequency and, in fact,
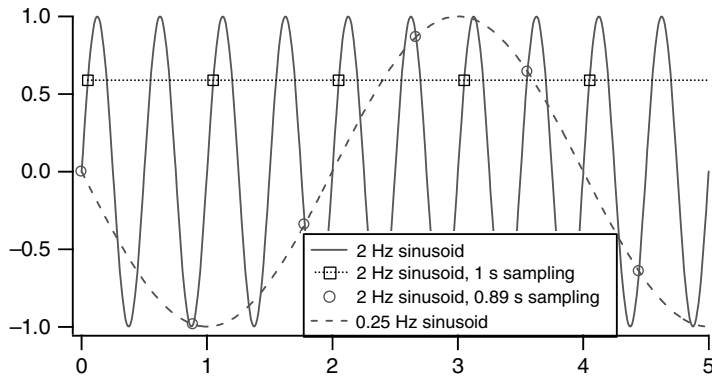
Figure C.2   Simple aliasing example

information at frequencies above the Nyquist frequency, f_N, cannot be correctly resolved. Furthermore, any information at frequencies higher than the Nyquist frequency appears as information at lower frequencies. Thus, all information at frequencies above the Nyquist frequency must be removed (or 'filtered,' see next section) from the data signal before digitization. Once the data have been collected, there is no way to correct the data.

C.2.6 Filtering

Filtering of physical phenomena is frequently observed in the wind energy field. For example, spatially separating multiple wind turbines has the effect of filtering out the large power fluctuations which would occur if a single, large turbine were used instead of the many smaller ones. Sometimes filtering is done intentionally, as when the output of a power electronic converter is filtered to remove frequencies above 50 or 60 Hz, so that the output more closely resembles utility grade electrical power, or where it is necessary to prevent aliasing, as noted in the previous section.

One of the conceptually simplest filters is the ideal low pass filter. This filter will remove all frequencies above a certain frequency (known as the cut-off frequency), and keep those below
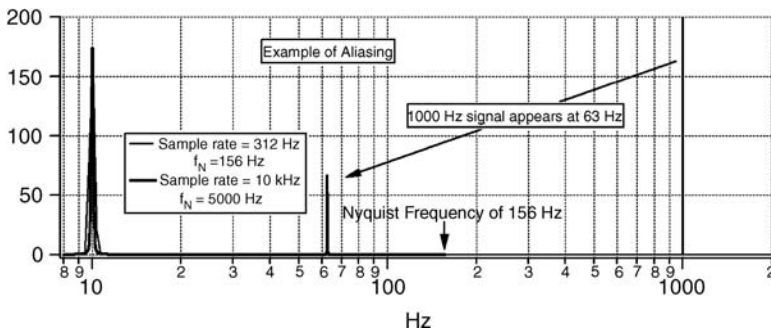
Figure C.3   Example of aliasing
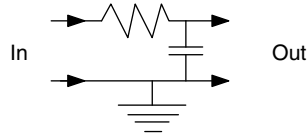
Figure C.4   Simple RC filter

that frequency. This filter looks like a rectangle in the frequency domain, with a value of 0 at frequencies above the cut-off frequency and 1 at lower (positive) frequencies.

Real low pass filters are more gradual than the ideal filter. Nonetheless, they do have the effect of reducing frequencies above the cut-off frequency and only marginally affecting lower frequencies. In electrical circuits, filtering is carried out by means of resistors, capacitors, and inductors. In mechanical systems, filtering is carried out by means of springs, masses, and dampers, and the allowance of some relative motion between various components.

A simple but real low pass filter is the RC filter, such as is illustrated in Figure C.4.

The RC filter has a cut-off frequency of $f_c = 1/(2\pi RC)$ Hz. Filters are also characterized by their time constant, τ, which for this case is given by $\tau = RC$. Filters are often realized in digital form. The digital expression for the RC filter, for example, is:

$$y_n = ax_n + (1-\alpha)y_{n-1} \tag{C.20}$$

where: $y_n =$ the output of the filter, $\alpha = \Delta t/(\tau + \Delta t)$ and $\Delta t =$ the time step of the data.

For example, Figure C.5 illustrates 10 min (600 s) of 1 Hz wind speed data. Superimposed on that is a smoother curve of that data filtered, with a filter whose cut-off frequency is 0.02 Hz (such that $RC = 7.9577$ s and $\alpha = 0.11164$).

The data above may also be examined in the frequency domain. Figure C.6 illustrates the psd of the original data and the psd of the filtered data superimposed on it for frequencies less than 0.1 Hz. For comparison, the psd of data filtered with an ideal low pass filter is also shown. The psds shown were obtained by truncating the original time series to 512 points, and dividing them into two segments of 256 points each before performing the FFTs. Note that the psd of the ideal filter follows that of the data exactly until the cut-off frequency is reached. The simple low pass filter, however, begins to attenuate frequencies well below the cut-off frequency.
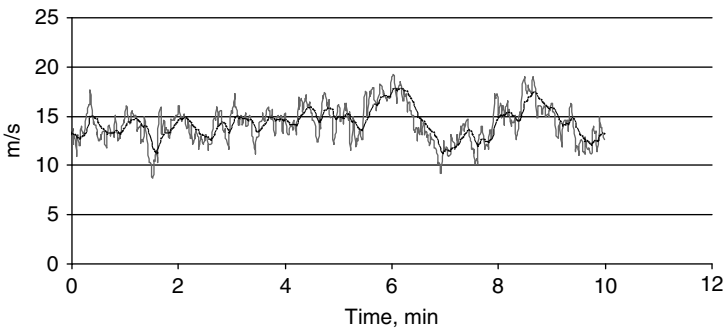
Figure C.5   Sample original and filtered time series data

PSD Comparison
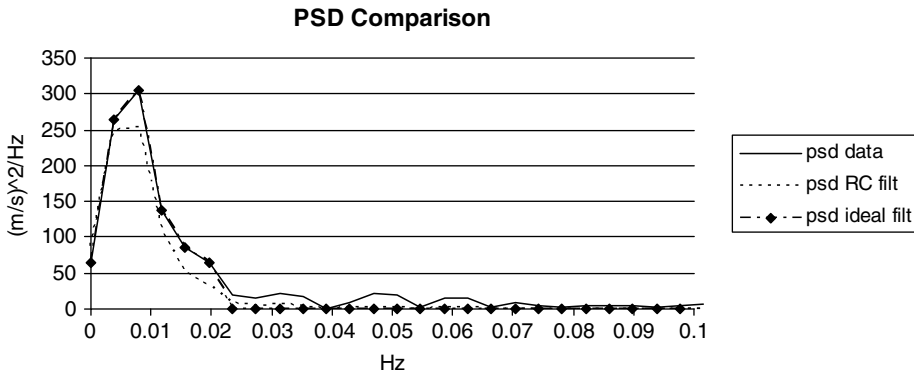
Figure C.6   Power spectral densities of original and filtered data

At higher frequencies, the attenuation increases substantially until there is very little contribution at frequencies higher than twice the cut-off frequency. This is as expected.

C.2.7 Rainflow Cycle Counting

The rainflow cycle counting technique was introduced in Chapter 6. A number of algorithms have been developed that can be incorporated into a computer code to actually do that counting. The essential features of one such algorithm are given below. This is a snippet of code, written in Visual Basic, based on the method suggested by Ariduru (2004). In this code, the vector *peakValleys*(.) contains the peaks and valleys of the data and *numberOfCycles*(.) is an output vector with the number of occurrences in ranges *binWidth* wide. The lowest range value bound is 0; the highest is large enough to incorporate all the data. The role of the other variables should be apparent from their names and context in the code. In this bit of code, any complete cycles are accounted for and then eliminated from the *peakValley*(.) data. The data are checked again for more complete cycles. Any half cycles are also identified and accounted for. This routine, as shown, only identifies cycle ranges, not their means, but it could be amended to do the latter as well. (Note that the function of the colon is to separate statements that could otherwise be on the next line.)

```
Sub RainFlow(maxRange, minRange, binWidth, nPeakValleyPoints%,
peakValleys(), numberOfCycles())
:
nRangeBins% = Int(1 + (maxRange − minRange) / binWidth) 'Determine #
range bins
remainingPoints% = nPeakValleyPoints%
'Initialize remainingPoints%
startPoint = peakValleys(1): i_point% = 1
'Initialize startPoint, i_point%

Step1:
'Check next peak or valley. If out of data, go to Step 6.
  If i_point% + 1 = remainingPoints% Then GoTo Step6
```

```
Step2:
'If there are fewer than three points, go to Step 6. Otherwise,
form ranges X 'and Y using the three most recent not yet
discarded peaks and valleys
  If remainingPoints% < 3 Then
    GoTo Step6
  Else
   X_range=Abs(peakValleys(i_point%+2)-peakValleys(i_point%+1))
   Y_range = Abs(peakValleys(i_point% + 1) - peakValleys(i_point%))
  End If
Step3:
  If Abs(X_range) < Abs(Y_range) Then
'No complete cycle found yet; advance to next point
    i_point% = i_point% + 1: GoTo Step1
  End If
Step4:
'If range Y_range contains the starting point, startPoint,
go to step 5 'otherwise, count Y_range as one cycle;
'discard the peak and valley of Y; and go to Step 2.

  If i_point% = 1 Then
    GoTo Step5
  Else
'Get rid of two points as cycle
    j% = Int(Y_range / binWidth)
    numberOfCycles(j%) = numberOfCycles(j%) + 1
    remainingPoints% = remainingPoints% - 2
    For i% = i_point% To remainingPoints%
      peakValleys(i%) = peakValleys(i% + 2)
    Next i%
'Go back to beginning of file
    startPoint = peakValleys(1): i_point% = 1: GoTo Step2
  End If
Step5:
'Count range Y_range as one-half cycle; discard first point
(peak or valley)
'in Y_range; move the starting point to next point in Y_range;
go to Step 2.

  j% = Int(Y_range / binWidth)
  numberOfCycles(j%) = numberOfCycles(j%) + 0.5
  remainingPoints = remainingPoints - 1
  For i% = i_point% To remainingPoints%
    peakValleys(i%) = peakValleys(i% + 1)
  Next i%
  GoTo Step2
```

```
Step6:
'Count each range that has not been previously counted as one-half
cycle.
  For i% = 1 To remainingPoints - 1
    j% = Int(Abs(peakValleys(i) - peakValleys(i + 1)) / binWidth)
    numberOfCycles(j) = numberOfCycles(j) + 0.5
  Next i%
End Sub
```

C.3 Data Synthesis

Data synthesis is the creation of artificial time series for some specific purpose. For example, hourly data may be needed for simulation models, but real hourly data may not be available. High-frequency, turbulent wind speed with certain specific characteristics may be needed as input to a structural dynamics code. Such high-frequency data are seldom available. The accepted way to obtain data for such purposes is through the application of a data synthesis algorithm.

The type of algorithm that is used for data synthesis depends on the application and the type of other data (if any) that may be available. Of the various methods available, three of the most commonly used are: (1) Auto-regressive moving average (ARMA), (2) Markov chains, and (3) the Shinozuka method. A fourth method, known as the Sandia method, is a variant of the Shinozuka. It is used to produce multiple, partially correlated time series.

C.3.1 Autoregressive Moving Average (ARMA)

The ARMA method is able to synthesize a time series which has the following specified characteristics: (1) mean, $\bar{x}$, (2) standard deviation, σ, and (3) autocorrelation at a particular lag. The ARMA model uses a random number generator and will have the same probability distribution as the random numbers do. The data do not have specified frequency domain characteristics.

Various forms of the ARMA method are available (see Box and Jenkins, 2008, for details.) The simplest, and most commonly used, method (ARMA 1), is defined, first of all, by the following equation for a normalized time series:

$$y_n = R(1)y_{n-1} + N(n) \tag{C.21}$$

where:

$N(n) =$ normally distributed noise term with zero mean and standard deviation, $\sigma_{noise} = \sqrt{(1 - R^2(1))}$
$R(1) =$ the value of the autocorrelation at a lag of 1

The final time series, x_n, with the prescribed mean $\bar{x}$ and standard deviation σ_x is then given by:

$$x_n = \sigma_x y_n + \bar{x} \tag{C.22}$$

C.3.2 Markov Chains

Wind data, especially long-term, hourly data, can be synthesized via Markov chains (see Kaminsky *et al.*, 1990 and Manwell *et al.*, 1999). The approach used is a two-step process: (1) generation of a transition probability matrix (TPM) and (2) use of the TPM, together with a random number generator.

The method assumes that any time series can be represented by a sequence of 'states.' The number of states is chosen not too few so that the generated time series does not appear too discontinuous, but not too many so that calculations are not too burdensome. The Markov TPM is a square matrix, whose dimension is equal to the number of states into which a time series is to be divided. The value in any given position in the matrix is the probability that the next point in the time series will fall (i.e. will make a transition) into the *j*th state, given that the present point is in the *i*th state. One feature of a TPM is that the sum of all the values in a given row should equal 1.0. This corresponds to the observation that any succeeding point must lie in one of the states. An additional consideration is that there must be a known relation between the state number and the value of that state. This value is normally the midpoint of the state. For example, suppose a time series with values between 0 and 50 were to be represented by ten states. The first state would be represented by 2.5, the second by 7.5, etc.

The most intuitive way, and most common, way to generate a Markov TPM is to start with a time series of data. Each successive pair of points is examined to see which states both points are in. By tallying these, the number of times, and hence probability, that there is a 'transition' from state *i* to state *j* can be determined. The result of this analysis for transitions from each state to each other state yields all the values needed to fill in a TPM.

Generating a TPM without using an initial time series is also possible, although it is considerably less intuitive. In addition, it is possible to do so in such a way that the probability density function of the data generated with use of the TPM will be equal (given a sufficient number of points) to a target probability density function. More information on this method may be found in McNerney and Richardson (1992).

In either case, the resulting TPM can be used to generate a time series which will have a mean, standard deviation, and probability density function close to that of the original data or the target pdf. (They will not be exactly the same, as discussed below.) The time series will have an exponentially decreasing autocorrelation, but will not necessarily be equal to that of the original data (or the target) for all lags.

A time series is generated by first assuming a starting value. This can be any number corresponding to a real state. A random number generator is then used to select the next point, based on weightings which are proportional to the probabilities in the row determined by the present state. For example, suppose a 5×5 TPM is being used, and that the state transition probabilities in the row of interest are 0, 0.2, 0.4, 0.3, and 0.1. Then, there would be no chance of the next number being in state 1, a 20% chance that it would be in state 2, a 40% chance it would be in state 3, etc. Subsequent points are generated in an analogous way.

In practice, when a finite length data set is synthesized, its mean and standard deviation may not be exactly equal to those of the original data or the target. Typically, scaling is then undertaken to produce a final time series with the expected summary statistics.

It is also the case that certain more deterministic characteristics in the final data set may be desired, such as seasonal or diurnal patterns in annual data. These patterns may be approximately accounted for by generating and then concatenating separate time series for

each month of the year and then adding the diurnal effect by suitable scaling of the resultant time series.

C.3.3 Shinozuka Method

The so-called Shinozuka method (Shinozuka and Jan, 1972) is often used to synthesize turbulent wind speed data, with a specified mean, standard deviation, and spectral characteristics corresponding to the specified psd. In this method, the range of frequencies of interest (between an upper value f_u and lower value f_l) in the psd is divided into N intervals, resulting in an interval between frequencies of $\Delta f = (f_u - f_l)/N$ and interval midpoint frequencies of f_i. Sine waves are generated at each midpoint frequency. The sine waves are then all weighted by the square root of the psd multiplied by Δf at that frequency to give the correct variance to the result. A random phase angle, ϕ_i, is used for each sine wave as well. The sum of all the sine waves results in a fluctuating time series with zero mean, $\tilde{x}_n$ as shown in Equation (C.23).

$$\tilde{x}_n = \sqrt{2\Delta f} \sum_{i=1}^{N} \sqrt{S(f_i)} \sin(2\pi f_i n + \phi_i) \tag{C.23}$$

The final result is the desired mean, $\bar{x}$, plus the fluctuating term, as shown in Equation (C.24).

$$x_n = \tilde{x}_n + \bar{x} \tag{C.24}$$

It should be noted that when the number of desired points exceeds the number of frequencies, the time series will begin to repeat itself. For that reason in their original formulation Shinozuka and Jan proposed to add a certain amount of noise, or 'jitter', given by $\alpha \Delta f$ to prevent the repetition. In that case the expression for the zero-mean time series is:

$$\tilde{x}_n = \sqrt{2\Delta f} \sum_{i=1}^{N} \sqrt{S(f_i)} \sin(2\pi(f_i + \alpha\Delta f)n + \phi_i) \tag{C.25}$$

This can suffice in some situations, but the psd is also changed. Ideally, the number of frequencies should equal the number of desired data points and there should be no need for jitter. See Jeffries *et al.* (1991) for more details.

C.3.4 Sandia Method for Partially Correlated Time Series

It is sometimes of interest to synthesize multiple turbulent wind speed time series that are partially correlated with each other. This is particularly the case when a field of time series across the rotor plane is desired. Such partial correlations can take into account the observation that slow variations in wind speed are often spatially rather large whereas rapid fluctuations tend to be rather small. Data of this type are needed as input to structural dynamics codes such as were discussed in Chapter 7.

One way to synthesize partially correlated time series data is with the Sandia method, which was proposed by Veers (1988). It is essentially an extension of the Shinozuka method described above. In the Sandia method, a coherence function is used to produce the appropriate correlation as a function of spacing between the time series. The time series are generated by linear combinations of independent sinusoids. The method uses a spectral matrix $\mathbf{S}(f_i)$ and

a triangular transformation matrix $\mathbf{H}(f_i)$, each of dimension $M \times M$ where M is the number of time series being produced. Matrix elements are updated for each frequency f_i being used. The elements of $\mathbf{S}(f_i)$ are derived from the target psd $S(f_i)$, which is the same for all the time series, and an assumed coherence function, γ_{jk}. These are shown in Equation (C.26).

$$\begin{aligned} S_{jj} &= S(f_i) \\ S_{jk} &= \gamma_{jk} S(f_i) \end{aligned} \tag{C.26}$$

The most convenient form of the coherence function is the exponential one, which was introduced in Chapter 9. The relation between the spectral matrix and the transformation matrix is shown in Equation (C.27). The matrix $\mathbf{H}(f_i)$ can be thought of as the matrix equivalent of the square root of $S(f_i)$ in Equation (C.23).

$$\mathbf{S}(f_i) = \mathbf{H}(f_i)\mathbf{H}^T(f_i) \tag{C.27}$$

The elements of the transformation matrix are found from a recursive relationship, as shown in Equation (C.28).

$$\begin{aligned} H_{11} &= S_{11}^{1/2} \\ H_{21} &= S_{21}/H_{11} \\ H_{22} &= (S_{22} - H_{21}^2)^{1/2} \\ H_{31} &= S_{31}/H_{11} \\ &\vdots \\ H_{jk} &= \left(S_{jk} - \sum_{l=1}^{k-1} H_{jl}H_{kl}\right)/H_{kk} \\ H_{kk} &= \left(S_{kk} - \sum_{l=1}^{k-1} H_{kl}^2\right)^{1/2} \end{aligned} \tag{C.28}$$

The transformation matrix is then used to produce the contribution of each frequency to each of the desired time series. The partial correlation is obtained through the phase angle of the sinusoids. In particular, the matrix $\mathbf{H}(f_i)$ is used to multiply an M-dimensional vector $\mathbf{X}$ of sine waves of frequency f_i with independent phase angles ϕ_i here $i \leq M$. The nth term of the M time series (corresponding to time $n\Delta t$) may be expressed as a vector $\tilde{\mathbf{x}}_n$, as shown in
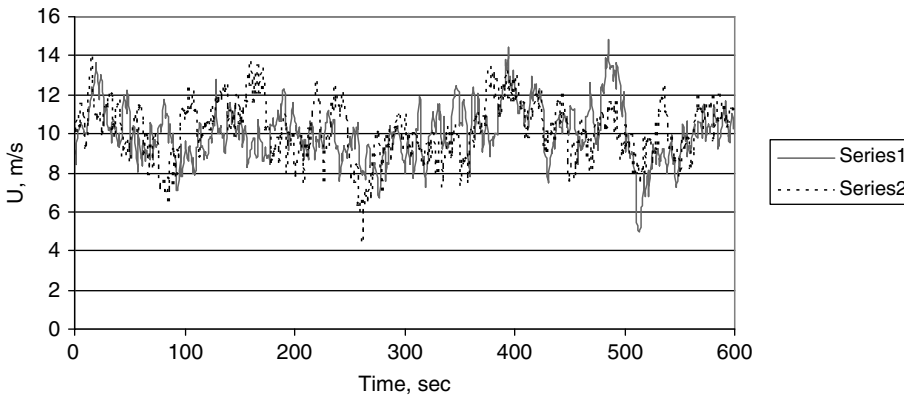
Figure C.7   Partially correlated, synthesized wind speed time series

Equation (C.29). The reader is referred to Veers (1988) for more details.

$$\tilde{\mathbf{x}}_n = \sqrt{2\Delta f} \sum_{j=1}^{N} \sum_{i=1}^{M} \mathbf{H}(f_i)\mathbf{X} \tag{C.29}$$

where:

$$\mathbf{X} = \begin{bmatrix} \sin(2\pi f_i n \Delta t + \phi_1) \\ \sin(2\pi f_i n \Delta t + \phi_2) \\ \vdots \\ \sin(2\pi f_i n \Delta t + \phi_M) \end{bmatrix}$$

For example, consider the synthesis of two 600 s (10 min) time series using a von Karman spectrum with the following characteristics: $\bar{U} = 10$ m/s, $\sigma_u = 0.15$, length scale $= 100$ m, separation between time series $= 30$ m, and coherence constant $A = 50$. The frequency range is 0.002 to 1 Hz, and 600 frequencies are used. The two time series are shown in Figure C.7. As expected, the two time series are generally similar, but are not identical. Changing the separation would result in time series that appear correspondingly more or less correlated, depending on the separation.

References

Ariduru, S. (2004) *Fatigue Life Calculation by Rainflow Cycle Counting Method.* MSc Thesis, Middle East Technical University, available at: www.nrel.gov/designcodes/papers.

Bendat, J. S. and Piersol, A. G. (1993) *Engineering Applications of Correlation and Spectral Analysis.* John Wiley & Sons, Ltd, Chichester.

Box, G. E. P. and Jenkins, G. M. (2008) *Time Series Analysis: Forecasting and Control*, 4th edition. John Wiley & Sons, Ltd, Chichester.

Jeffries, W. Q., Infield, D. and Manwell, J. F. (1991) Limitations and recommendations regarding the Shinozuka method for simulating wind data. *Wind Engineering*, **15**(3), 147–154.

Kaminsky, F. C., Kirchhoff, R. H. and Syu, C. Y. (1990) A statistical technique for generating missing data from a wind speed time series. *Proceedings of Wind Power '90,* American Wind Energy Assoc., Washington, DC.

Manwell, J. F., Rogers, A., Hayman, G., Avelar, C. T. and McGowan, J. G. (1999). *Hybrid2 – A Hybrid System Simulation Model: Theory Manual*. Department of Mechanical Engineering, University of Massachusetts, Amherst, MA.

McNerney, J. and Richardson, R. (1992) The statistical smoothing of power delivered from utilities by multiple wind turbines. *IEEE Transactions on Energy Conversion*, **7**(4), 644–647.

Shinozuka, M. and Jan, C.-M. (1972) Digital simulation of random process and its application. *Journal of Sound and Vibration*, **25**(1), 111–128.

Veers, P. (1988) *Three-Dimensional Wind Simulation.* Sandia National Laboratory Report SAND88-0152 UC-261.

Index